National Research Council Canada

Conseil national de recherches Canada

NRC·CNRC

Canadian Journal of Fisheries and Aquatic Sciences

Journal canadien des sciences halieutiques et aquatiques

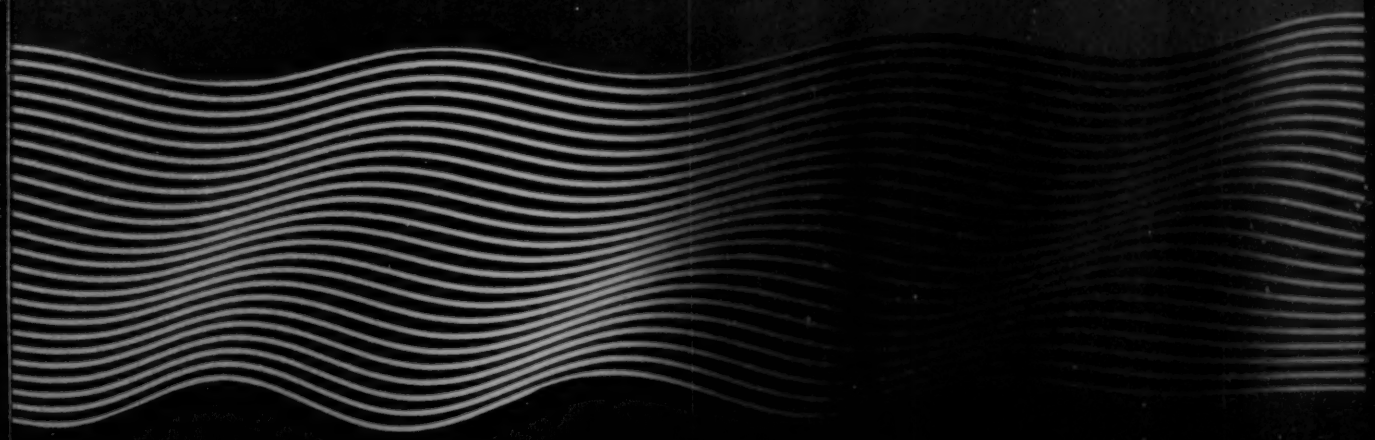

http://cjfas.nrc.ca

http://jcsha.cnrc.ca

ISSN 0706-652X / CJFSDX 59(5) 755–923 (2002)

The *Canadian Journal of Fisheries and Aquatic Sciences*, previously published as *Contributions to Canadian Biology* 1901–1925, *Contributions to Canadian Biology and Fisheries* 1926–1934, *Journal of the Biological Board of Canada* 1934–1937, and *Journal of the Fisheries Research Board of Canada* 1938–1979, is issued monthly to form annual volumes of 12 numbers plus supplements.

Editorial policy: The Journal publishes original research articles, perspectives (syntheses, critiques, re-evaluations), discussions (comment and reply), and rapid communications. Manuscripts may concern cells, organisms, populations, communities, ecosystems, or processes that affect aquatic systems. They may cover a range of disciplines including biology and ecology of marine and freshwater organisms, limnology, oceanography, physiology, toxicology, genetics, economics, disease, and management. Preference will be given to manuscripts that emphasize understanding of observed phenomena and interpretation of experimental results. The Journal encourages papers that lead from clearly stated purpose or rationale and from testable hypotheses, concepts, or questions to identifiable conclusions or syntheses. Such papers may amplify, modify, question, or redirect accumulated knowledge embodied in contemporary perceptions of a particular state of aquatic sciences. The Journal discourages papers that are essentially descriptive, except in emerging disciplines; have only site-specific or local applications (a certain year, place, taxon, chemical compound, etc.); only confirm previously established principles; or apply standard techniques without breaking new methodological ground.

Manuscripts for publication should be submitted to the Editors, *Canadian Journal of Fisheries and Aquatic Sciences*, Department of Zoology, University of Guelph, Guelph, ON N1G 2W1, Canada (519-824-4120 ext. 2646; fax: 519-767-9798; e-mail: cjfas@uoguelph.ca).

Submissions in either English or French are acceptable. The information must be original, that is, not copyrighted, published, or submitted elsewhere except in abstract form or unless by written consent of the Editor. NRC accepts no responsibility for statements or opinions expressed by a contributor. Acceptance of an advertisement, announcement, or other material does not imply endorsement by either the Journal's Editors or NRC. The use of proprietary names does not imply endorsement of the product or company.

Correspondence concerning accepted manuscripts and corrected proofs should be sent to NRC Research Press, National Research Council of Canada, Ottawa, ON K1A 0R6, Canada (fax: 613-952-7656; e-mail: research.press@nrc.ca).

Instructions to Authors are published once a year in the first issue of each volume. Copies are available from NRC Research Press or at http://cjfas.nrc.ca. The **Publication Policy** of NRC Research Press is available at http://cjfas.nrc.ca.

The National Research Council of Canada accepts no responsibility for statements or opinions expressed by a contributor. Acceptance of an advertisement, announcement, or other material does not imply endorsement by either the Journal's Editors or NRC.

Microfilm: Issues from 1934 through the current volume can be purchased on 16- or 35-mm microfilm. Photocopies of individual articles or issues can be purchased from University Microfilms International, 330 North Zeeb Road, Ann Arbor, MI 48106, U.S.A.

U.S. periodical postage paid at Champlain, N.Y., and at additional mailing offices. Attention U.S. POSTMASTER: Send address changes to **Canadian Journal of Fisheries and Aquatic Sciences**, c/o USACAN Media Distribution Center, P.O. Box 2888, Plattsburg, NY 12901, U.S.A.

Publié sans interruption depuis 1901, le *Journal canadien des sciences halieutiques et aquatiques* a paru sous plusieurs titres : *Contributions to Canadian Biology* 1901–1925, *Contributions to Canadian Biology and Fisheries* 1926–1934, *Journal of the Biological Board of Canada* 1934–1937, et *Journal of the Fisheries Research Board of Canada* 1938–1979. Le Journal paraît tous les mois, formant ainsi un volume de 12 numéros, et offre en plus jusqu'à deux suppléments par année.

Politique éditoriale : On publie, dans le Journal, des articles rendant compte de recherche originale, des perspectives (synthèses, critiques et réévaluations), des discussions (commentaires et réponses) et des communications rapides. Les documents peuvent porter sur les cellules, organismes, populations, communautés, écosystèmes ou processus qui affectent les systèmes aquatiques. Ils peuvent relever de divers domaines y compris la biologie et l'écologie des organismes marins et d'eau douce, la limnologie, l'océanographie, la physiologie, la toxicologie, la génétique, l'économie, la pathologie et la gestion. On accorde la préséance aux articles qui contribuent à la compréhension de phénomènes observés et à l'interprétation de résultats expérimentaux. On invite les auteurs à soumettre des articles ayant des objectifs précis ou relevant d'hypothèses, de concepts ou de questions vérifiables et se terminant par de solides conclusions ou d'utiles synthèses. Ces articles enrichissent, changent, mettent en question ou réorientent les connaissances acquises sur divers aspects des sciences aquatiques. On décourage toutefois la soumission d'articles simplement descriptifs (à moins qu'il ne s'agisse de nouvelles disciplines), d'application très limitée (applicables à une seule année, une seule région ou un seul taxon, portant sur un unique composé chimique, etc.); d'articles qui ne font que reprendre les principes énoncés dans des articles précédents; et d'articles rendant compte de l'application de normes sans gain de méthodologie.

Les auteurs voudront adresser leurs **manuscrits** aux directeurs scientifiques, *Journal canadien des sciences halieutiques et aquatiques*, Department of Zoology, University of Guelph, Guelph, ON N1G 2W1, Canada (519-824-4120 poste 2646; télécopieur : 519-767-9798; courriel : cjfas@uoguelph.ca).

Les contributions peuvent être en anglais ou en français. Elles doivent être originales, c.-à.-d. qu'elles ne doivent pas avoir fait l'objet d'un copyright, avoir été publiées ou soumises ailleurs, sauf sous forme abrégée ou avec le consentement du rédacteur. Le CNRC ne se tient en aucune façon responsable des opinions exprimées par un collaborateur ou des déclarations qui pourrait faire ce dernier. La publication d'annonces publicitaires, d'avis et autres n'implique pas l'endossement de leur contenu par les directeurs du Journal ou du CNRC. L'utilisation des noms de marques de commerce ne signifie aucunement une sanction du produit en question ou de la compagnie qui le fabrique.

La correspondance ayant trait aux manuscrits acceptés et les **épreuves corrigés** doivent être envoyées aux Presses scientifiques du CNRC, Conseil national de recherches du Canada, Ottawa, ON K1A 0R6, Canada (télécopieur : 613-952-7656; courriel : presses.scientifiques@cnrc.ca).

Les Recommandations aux auteurs sont publiées une fois par année dans le premier numéro de chaque volume. Des copies sont disponibles auprès du Bureau de la rédaction aux Presses scientifiques du CNRC ou au http://jcsha.cnrc.ca. **La Politique de publication** est disponible auprès des Presses scientifiques du CNRC ou au http://jcsha.cnrc.ca.

Le Conseil national de recherches du Canada ne se tient en aucune façon responsable des opinions exprimées par un collaborateur ou des déclarations que pourrait faire ce dernier. La publication d'annonces publicitaires, d'avis et autres n'implique pas l'endossement de leur contenu par les directeurs de la Revue ou du CNRC.

Microfilms : On peut acheter sur microfilms de 16 ou 35 mm tous les numéros depuis 1934. Des photocopies d'articles ou de numéros individuels sont aussi en vente auprès de University Microfilms International, 330 North Zeeb Road, Ann Arbor, MI 48106, É.-U.

This Journal is indexed or abstracted in / Cette revue est signalée ou résumée dans

ABSEARCH, Aquatic Sciences and Fisheries Abstracts, Biological Abstracts, Biological & Agricultural Index, CAB Abstracts, Chemical Abstracts, Current Contents, Elsevier BIOBASE, Environmental Abstracts, Environmental Periodicals Bibliography, GEOBASE, GeoRef, Internationale Bibliographie der Zeitschriftenliteratur, Life Sciences Collection, Meteorological and Geoastrophysical Abstracts, Oceanic Abstracts, PASCAL Database, and Science Citation Index.

Volume 59, Number 5, May 2002

Canadian Journal of Fisheries and Aquatic Sciences

Published by the National Research Council of Canada

Volume 59, numéro 5, mai 2002

Journal canadien des sciences halieutiques et aquatiques

Publié par le Conseil national de recherches du Canada

Editors / directeurs scientifiques John C. Roff and Moira M. Ferguson

Assistant to the Editors / adjointe aux directeurs scientifiques **Holly Foster**

Associate Editors / directeurs scientifiques associés

M.T. Arts, *Environment Canada, Burlington*
D. Boisclair, *Université de Montréal*
U. Borgmann, *Environment Canada, Burlington*
S.E. Campana, *DFO/MPO, Dartmouth*
R. Carignan, *Université de Montréal*
D.G. Dixon, *University of Waterloo*
A.E. Dizon, *National Marine Fisheries Service, La Jolla, Calif.*
J.J. Dodson, *Université Laval*
J.A. Downing, *Iowa State University*
K.T. Frank, *DFO/MPO, Dartmouth*
D.F. Houlihan, *University of Aberdeen, Aberdeen, Scotland*
F.A. Huntingford, *University of Glasgow*
J.A. Hutchings, *Dalhousie University*
G.S. Jamieson, *DFO/MPO, Nanaimo*
B. Jonsson, *Norwegian Institute for Nature Research, Oslo, Norway*
D.M. Mason, *NOAA-Great Lakes Environmental Research Laboratory, Ann Arbor, Mich.*
A. Mazumder, *University of Victoria*
D.L. Parrish, *Vermont Cooperative Fish and Wildlife Research Unit (USGS/BRD), University of Vermont*
P. Pepin, *DFO/MPO, St. John's*
T.M. Powell, *University of California, Berkeley, Calif.*
E.E. Prepas, *University of Alberta*
T.J. Quinn II, *University of Alaska–Fairbanks, Juneau, Alaska*
T.P. Quinn, *University of Washington*
R.D. Robarts, *Environment Canada, Saskatoon*
B. Sainte-Marie, *DFO/MPO, Mont-Joli*
D.W. Schindler, *University of Alberta*
S.J. Smith, *DFO/MPO, Dartmouth*
W.G. Sprules, *University of Toronto*
R.J. Thompson, *Memorial University of Newfoundland*
C.J. Walters, *University of British Columbia*
R.D. Ward, *CSIRO Marine Research, Australia*
C.M. Wood, *McMaster University*
B. de Young, *Memorial University of Newfoundland*

NRC Research Press / Presses scientifiques du CNRC

Editor-in-chief / directeur général **Bruce P. Dancik**

Assistant Editor-in-chief / directeur général adjoint **Iain E.P. Taylor**

Journals Program / Programme des revues

(Fax / télécopieur : 613-952-7656; e-mail / courriel : research.press@nrc.ca; URL: http://researchpress.nrc.ca)

Director / directrice **Aldyth Holmes**

Business Manager / gestionnaire des affaires **Paul McClymont**

Managing Editor / rédactrice administrative **Cecily M. Pearson (613-993-9099)**

Publication Officers / agentes de publication **Jennifer McColl and Lee Murphy**

Advertising / annonces publicitaires **Judy Gorman (613-993-0151)**

Reprints / tirés à part **Roxanne Landriault (613-990-2254)**

Subscriptions / abonnements **Helen Goulet (613-993-9084)**

© National Research Council of Canada 2002. World rights reserved.
No part of this publication may be reproduced, stored, or transmitted in any form or by any means, without the written permission of the publisher, except as stated below.

The National Research Council of Canada grants **permission*** to individuals to make single copies of articles for personal use. Any person may reproduce short excerpts from articles in the journal for any purpose that respects the moral rights of authors, provided that the source is fully acknowledged. As a courtesy, the consent of authors of such material should be obtained directly from the author.

Authorization to reproduce items for other than personal use, as stated above, is granted by the National Research Council of Canada provided that the copyright fee of $7.00 per copy is paid directly to CANCOPY, One Yonge Street, Suite 1900, Toronto, ON M5E 1E5, Canada.

*The above permission does not extend to other kinds of copying, such as copying for general distribution, for advertising, or promotional purposes, for creating new collective works, or for resale. For such copying, arrangements must be made with the publisher, National Research Council of Canada, Ottawa, ON K1A 0R6, Canada.

© Conseil national de recherches du Canada 2002. Tous droits réservés.
Il est interdit de reproduire, de sauvegarder ou de transmettre quelque partie de la présente publication dans quelque format ou de quelque façon sans le consentement écrit de l'éditeur, à l'exception des conditions suivantes.

Le Conseil national de recherches du Canada accorde aux particuliers le droit de faire des copies individuelles pour leur usage personnel. Toute personne peut reproduire de courts extraits des articles de la Revue pour autant que les droits moraux de l'auteur soient respectés et que la mention de provenance soit clairement indiquée. Il est de convenance de demander le consentement de l'auteur avant de faire mention de son travail.

On obtiendra l'autorisation de reproduire des articles à d'autres fins que l'usage personnel (tel qu'on l'a décrit ci-dessus) auprès du Conseil national de recherches du Canada pour autant que des redevances de droits d'auteurs de 7,00 $/copie soient versées au CANCOPY, 1, rue Yonge, bureau 1900, Toronto, ON M5E 1E5, Canada.

*La permission ci-dessus ne s'applique pas à la reproduction à grande échelle, telle que la reproduction aux fins de distribution générale, publicitaire ou promotionnelle, de compilation de nouveaux ouvrages collectifs ou de revente. Dans de tels cas, il faudra ratifier une entente particulière avec l'éditeur, le Conseil national de recherches du Canada, Ottawa, ON K1A 0R6, Canada.

Subscription information

The *Canadian Journal of Fisheries and Aquatic Sciences* (ISSN 0706-652X) is published monthly by the National Research Council of Canada. 2002 annual subscription rates (second class postage) for Canada are $732CAN institutional and $227CAN personal, for US & foreign $732US institutional and $227US personal. For air mail add $175US to foreign rate. Canadian customers please include 7% GST (business no. 12149 1807 RT 0275). Subscriptions are entered for the calendar year. Remittances should be made payable to the Receiver General for Canada credit NRC. Price for regular single issues: institutional, $95.00; personal, $30.00. Supplements will be priced separately. Special rates apply to members of Canadian scientific and engineering societies if they subscribe through their respective societies.

There are no refunds on cancelled subscriptions once delivery has begun. Claims for missing issues should be made within four months (N. America) or six months (outside N. America) following the date of publication. The publisher expects to supply missing issues only when losses have occurred in transit and when the reserve stock will permit. For change of address and subscription enquiries: Subscription Office, NRC Research Press, National Research Council of Canada, Ottawa, ON K1A 0R6, Canada; tel.: 613-993-9084; fax: 613-952-7656; e-mail: research.press@nrc.ca.

Microform backfiles are available from UMI, P.O. Box 1346, Ann Arbor, MI 48106-1346, U.S.A., and Micromedia Ltd., 20 Victoria St., Toronto, ON M5C 2N8, Canada.

All issues of the *Canadian Journal of Fisheries and Aquatic Sciences* since 1996 are available on the Web. Pricing information can be found at http://cjfas.nrc.ca.

Renseignements sur l'abonnement

Journal canadien des sciences halieutiques et aquatiques (ISSN 0706-652X) est une publication mensuelle du Conseil national de recherches du Canada. Le prix de l'abonnement annuel au Canada (courrier de deuxième classe) est de 732 $CAN pour les organismes et de 227 $CAN pour les particuliers. À l'étranger (y compris les É.-U.), le prix de l'abonnement est de 732 $US pour les organismes et de 227 $US pour les particuliers. L'expédition par avion exige des frais de 175 $US en sus du prix d'abonnement à l'étranger. Les clients du Canada doivent ajouter la TPS de 7% (numéro d'entreprise 12149 1807 RT 0275). Les abonnements sont pour l'année civile. Tout paiement doit être adressé au Receveur général du Canada, crédit du CNRC. Le prix par numéro est de 95 $ pour les organismes et de 30 $ pour les particuliers. Le prix des hors-série varie. Les membres des sociétés canadiennes de sciences et de génie bénéficient de taux préférentiels en s'abonnant via leurs sociétés respectives.

Aucun remboursement ne sera accordé ni aucune annulation acceptée une fois que les livraisons auront commencé. Les réclamations de numéros manquants devront être soumises dans les quatre mois (Amérique du Nord) ou dans les six mois (à l'extérieur de l'Amérique du Nord) suivant la date de publication. L'éditeur ne fournira de numéros manquants que si le document a été perdu pendant l'expédition et que si le stock le permet. Adressez tout changement d'adresse ou toute question quant à l'abonnement au : Bureau des abonnements, Presses scientifiques du CNRC, Conseil national de recherches Canada, Ottawa, ON K1A 0R6, Canada; téléphone : 613-993-9084; télécopieur : 613-952-7656; courriel : presses.scientifiques@nrc.ca.

On peut obtenir les fichiers rétrospectifs sur **microforme** auprès de UMI, P.O. Box 1346, Ann Arbor, MI 48106-1346, É.-U., et auprès de Micromedia Ltée, 20 rue Victoria, Toronto, ON M5C 2N8, Canada.

À partir de 1996, tous les numéros de *Journal canadien des sciences halieutiques et aquatiques* sont accessibles sur le Web. On trouvera des renseignements sur les tarifs à http://jcsha.cnrc.ca.

RAPID COMMUNICATION / COMMUNICATION RAPIDE

The economics of fishing down the food chain

Rögnvaldur Hannesson

Abstract: This paper uses a predator–prey model to discuss the fundamental economics of fishing down the food chain. Three regimes are compared: open access, global optimization, and partial optimization of rents from each stock. If the net price of prey species increases, fishing down the food chain would indeed be a desirable effect in economic terms. Under open access, however, fishing down the food chain could occur as a result of a higher net price of species higher up in the food chain. With partial optimization, there could be less fishing down the food chain than economically desirable.

Résumé : Un modèle prédateur–proie permet d'analyser les bases économiques de la pêche commerciale tout au long de la chaîne alimentaire. Trois régimes sont comparés, l'accès libre, l'optimisation globale et l'optimisation partielle des loyers pour chaque stock. Si le prix net des espèces de proies augmente, la pêche aux niveaux inférieurs de la chaîne alimentaire devient bénéfique en termes économiques. Dans un régime d'accès libre, la pêche aux niveaux inférieurs de la chaîne alimentaire pourrait, cependant, se produire en conséquence d'une augmentation des prix nets des espèces situées plus haut dans la chaîne. Dans un régime d'optimisation partielle, il pourrait y avoir moins de pêche dans les niveaux inférieurs de la chaîne alimentaire que ne l'exigerait l'économie.

[Traduit par la Rédaction]

Introduction

Recently, Pauly et al. (1998*a*) raised the question of whether we might be fishing down the food chain, starting with the top predators and then, as they become depleted, moving on to species one level below, and so on. They used the Ecopath model to assign a trophic level index to each species reported in the FAO (Food and Agricultural Organization of the United Nations) fish landings statistics and then analyzed how the composition of world landings of fish has changed over the period 1950–1994, finding that the average trophic level of fish landings has fallen over this period. This effect could be detected in the global catch, including inland fisheries, and in many different FAO-statistical areas, but it was most pronounced in the northern hemisphere. Caddy et al. (1998) agreed that a decline in the average trophic level of fish catches has most likely occurred but questioned whether this could be exclusively ascribed to fishing down the food chain.

Pauly et al. (1998*a*) were concerned that this pattern of exploitation might signal unsustainable fishing practices. To evaluate that, complex models of particular ecosystems are needed. The purpose of this article is not to develop any such approach. Instead we ask whether fishing down the food chain could be an appropriate response to market demand, and if it is not, why could it nevertheless happen? To investigate these issues we shall use a predator–prey model of the Lotka–Volterra type. The reason for choosing this model is its simplicity; it is adequate for a discussion of principles but woefully inadequate for applied work. It does not contain any age structure and so does not permit the analysis of complex interaction between species at different ages, or different age groups of the same species. Such age-structure specification might in fact reveal that, in a single-stock exploitation, "fishing down the age structure" would amount to fishing down the food chain. Furthermore, the analysis will be comparative-static and deterministic, comparing different long-term equilibria.

Received 8 March 2002. Accepted 30 April 2002. Published on the NRC Research Press Web site at http://cjfas.nrc.ca on 21 May 2002.
J16793

R. Hannesson. The Norwegian School of Economics and Business Administration, Helleveien 30, N-5045 Bergen, Norway (e-mail: rognvaldur.hannesson@nhh.no).

The model

The model to be used is from Larkin (1966) (see also Hannesson 1983)

$$(1a)\quad \frac{dS_1}{dt} = a_1 S_1 - b_1 S_1^2 + d_1 S_1 S_2 - Y_1 \equiv G_1(S_1, S_2) - Y_1$$

$$(1b)\quad \frac{dS_2}{dt} = a_2 S_2 - b_1 S_2^2 + d_2 S_1 S_2 - Y_2 \equiv G_2(S_1, S_2) - Y_2$$

S_i is the stock of species i, Y_i is the instantaneous catch of species i, a, b, and d are parameters, and $G_i(S_i, S_j)$ is the surplus growth function of species i. The sign of d_i determines what kind of interaction there is between the two species; in a predator–prey model the ds have opposite signs. Here, $d_1 < 0$ and $d_2 > 0$, so species 2 is the predator and species 1 is the prey.

If the model represents a self-contained system, species 2 could not exist without species 1, implying that $a_2 = 0$. The values assumed for the parameters in eq. 1, which are used

 DOI: 10.1139/F02-055 © 2002 NRC Canada

in the examples below, are summarized in Table 1. No deeper meaning should be attributed to these values; they only serve the purpose of using a numerical model for studying what happens when a certain variable changes. However, the parameter values have been selected to make some sense; it can be shown that the natural equilibrium is stable and the standing stock of the prey species in natural equilibrium is much larger than the stock of the predator species. This reflects the fact that there is a large loss of exploitable biomass in the transfer of nutrition up the food chain.

The economic assumptions pertain to prices and exploitation costs. The prices of the two species, denoted P_i (i = 1, 2), will be assumed to be independent of the amount of fish caught. This is, needless to say, a simplification. Note, however, that with prices being determined in a world market, which is not an unrealistic assumption for many fisheries, myopic fishermen, and even individual countries trying to optimize the yield from their fisheries, would have a limited to negligible impact on prices and are therefore likely to take them as given.

The unit cost of fish is assumed to be inversely proportional to the exploited stock

$$(2) \qquad c_i/q_iS_i$$

This is a somewhat strong assumption, but the essential thing is that the unit cost of fish must rise as the stock falls, to produce a viable economic equilibrium under open access. The above function is the simplest possible representation of this and is correspondingly popular in the fisheries economics literature.

Fishery regimes

Three fishery regimes will be compared: open access, optimal management, and a separate management of the two stocks. Despite all advances that have been made over the last quarter century or so, open access is still probably not a bad description of fishery regimes in many countries, particularly the poorer ones. Under optimal management, sustained rents from the fishery are maximized. (Rent is the difference between revenues and all costs, including capital costs. It can be considered as a payment for using a scarce, natural resource like a fish stock. The rationale for maximizing rents is that this is consistent with achieving efficiency in the economy overall.) For simplicity, the impact of discounting is ignored, as it is not likely to be qualitatively very significant in this context. The third regime is rent-maximizing management of each fish stock in isolation, ignoring the ecological relations among the species. Such a regime could result if the two stocks are managed by separate entities, either within a single jurisdiction or in two different jurisdictions. The latter could happen if the migratory patterns of the two stocks are such that they are primarily located within separate jurisdictions (one stock could be a highly migratory species, for example, while the other is largely confined to the exclusive economic zone). Within the same jurisdiction it is possible to envisage two interrelated stocks being managed by two different authorities trying to satisfy two distinct fisheries, each exploiting its "own" stock.

Table 1. Assumed values of the parameters in eq. 1, the natural equilibrium (S^*) produced, and maximum biomass at each ecological level.

	a_i	b_i	d_i	S_i^*	$S_i^{\max}$
Species 1	1	0.01	–0.05	50	100
Species 2	0	0.05	0.01	10	10

Open access

Under open access, each stock is fished down to the break-even level where the unit cost of fish is equal to the price

$$(3) \qquad P_i = c_i/q_iS_i$$

The sustainable yield is given by solving for S_i and substituting into the surplus growth eq. 1. We will assume that the cs are the same for both species and henceforth drop the subscripts of c.

Optimal management

Maximizing the sustained rent entails

$$(4) \qquad \max_{S_i} \sum (P_i - c/q_iS_i)G_i$$

The optimization is subject to the population dynamics (eqs. 1*a*, 1*b*) and non-negativity constraints on stock and catch levels. The pair of first-order conditions for maximum are

$$(5) \qquad \left(P_i - \frac{c}{q_iS_i}\right)\frac{\partial G_i}{\partial S_i} + \left(P_j - \frac{c}{q_jS_j}\right)\frac{\partial G_j}{\partial S_i} - \frac{cG_i}{q_iS_i^2} = 0$$

where $i, j = 1, 2; i \neq j$

Solving these equations, we get the optimal stock levels

$$(6) \qquad S_i^o = [2P_jb_j(P_ia_i + b_ic/q_i - d_jc/q_j) + (P_id_i + P_jd_j)(P_ja_j + b_jc/q_j - d_ic/q_i)]/[4P_iP_jb_ib_j - (P_id_i + P_jd_j)^2]$$

where $i, j = 1, 2; i \neq j$

Separate management of the stocks

Under this regime, each management authority controls only one stock. If they are able to cooperate, they could possibly achieve the globally optimal solution. If they cannot cooperate, or choose not to do so, the best each can do is to maximize the return from its stock for any given level of the other stock. The expressions to be maximized are, respectively, the two elements in eq. 4, but each agent controls only his own S. Hence, the first-order conditions for maximum are

$$(7) \qquad \left(P_i - \frac{c}{q_iS_i}\right)\frac{\partial G_i}{\partial S_i} - \frac{cG_i}{q_iS_i^2} = 0$$

where $i = 1, 2$

From this we can find mutually consistent solutions

$$(8) \qquad S_i^N = \frac{2P_jb_j(P_ia_i + b_ic/q_i) + P_id_i(P_ja_j + b_jc/q_j)}{4P_iP_jb_ib_j - (P_id_i + P_jd_j)^2}$$

where $i, j = 1, 2; i \neq j$

© 2002 NRC Canada

The superscript N indicates that these are non-cooperative Nash equilibrium stock levels. They will in general be different from the globally optimal levels, but it is not possible to make any unambiguous comparison as to which is highest (cf. eqs. 6 and 8). It is possible that the party fishing one of the stocks would obtain larger benefits in the non-cooperative Nash equilibrium than would be attributable to that party in the global optimum. In a case like that, cooperative equilibrium (global optimum) could not be achieved between two independent parties without side payments.

Comparison of regimes

To compare the regimes, we first normalize and set c/q = 1 for both stocks, focussing on the consequences of changes in the prices, one at a time, for each stock. Suppose, first, that $P_1 = 0.025$, whereas P_2 varies from 0.1 to 1. This means that it is worthwhile, but not very profitable, to exploit the prey species while it would not be profitable to exploit the predator at the lowest price (0.1), as its unit cost would be higher than 0.1 except in the natural equilibrium (see eq. 2).

In the optimal solution, the catch of the predator species rises towards the maximum sustainable yield as the price of that type of fish rises (Fig. 1). It is worthwhile to note that even at the lowest price shown (0.1), when exploitation of the predator is not profitable in isolation, it would nevertheless be exploited in the optimal solution, to improve the yields of the prey species. Under the two other regimes, the predator is not exploited at all at this price. The exploitation of the prey species ceases as the price of the predator exceeds a certain level; even if it would still be profitable in isolation, the prey are more valuable as feed for the predator (the price of the prey is held constant at 0.025).

In the open-access regime, the catches of the predator reach a maximum and then fall as its price rises. The catches of the prey species increase, on the other hand; as the stock of the predator is depleted the growth conditions for the prey stock improve, raising the catch of the prey. The non-cooperative Nash solution is in between the other two in that the catches of the predator continue to rise as its price rises but are always less that in the globally optimal solution. The reason lies in ignoring the ecological relationship between the two species; in the Nash solution there is still substantial fishing of the prey when it would be better to leave it in the sea as feed for the predator.

To illustrate "fishing down the food chain", a food chain index (Fig. 1) has been defined as $2 - G_1/(G_1 + G_2)$. This index is equal to 2 when only the predator is fished (level 2) and 1 when only the prey is fished (level 1). In the optimal solution this index rises to 2 as the price of the predator rises, as it becomes optimal to use the prey as feed for the predator fish, which are more valuable. In the two other solutions this index stays close to 1. For the lowest price of the predator, the index is equal to 1 because it is not profitable to catch the predator; the index then rises initially as the price of the predator rises, making it worthwhile to catch the predator. Beyond a certain point, however, the index falls in the open-access solution. Here we clearly see a perverse fishing down the food chain effect—as the price of predator fish rises, making prey fish less valuable, the catches of prey fish nevertheless rise, relative to the catches of predator fish.

Fig. 1. Catches of (*a*) prey and (*b*) predator fish, and (*c*) food chain index, as functions of the price of the predator (P_2), for a given price of the prey (P_1 = 0.025). Thin line, open access; thick line, optimal management; dashed line, non-cooperative Nash equilibrium.

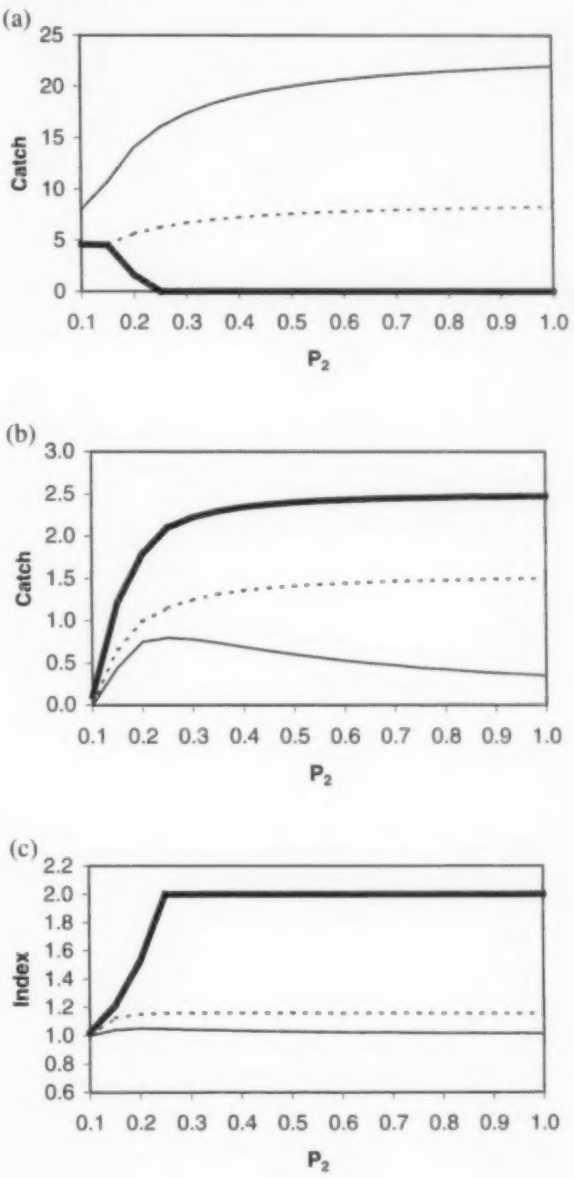

The reason is that higher prices of predator fish encourage overexploitation in the open-access regime and the catches of predator fish fall while the catches of prey fish rise.

In the non-cooperative Nash equilibrium solution, with prey and predator stocks being managed separately, the share of prey fish of the total catch remains high but fairly constant. What the Nash equilibrium solution fails to take into

© 2002 NRC Canada

Fig. 2. Catches of (*a*) prey and (*b*) predator fish, and (*c*) food chain index, as functions of the price of the prey (P_1), for a given price of the predator (P_2 = 0.2). Thin line, open access; thick line, optimal management; dashed line, non-cooperative Nash equilibrium.

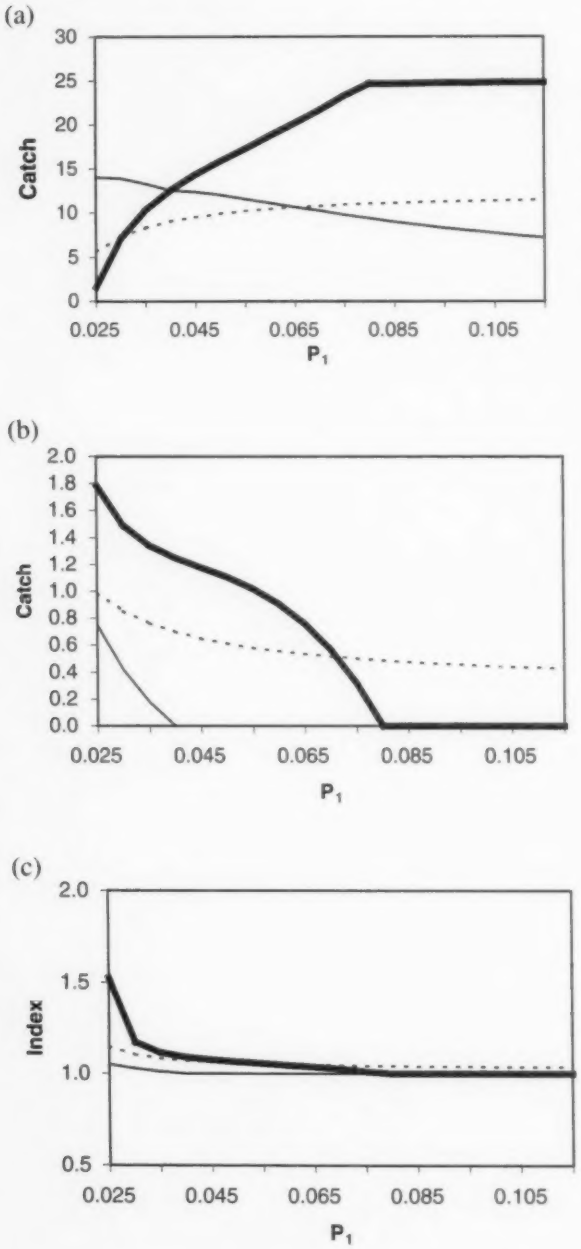

account is that prey fish become more valuable as feed for the predator as the price of predator fish rises.

Then consider what happens as a result of a rise in the price of the prey fish (Fig. 2). The price of predator fish was set at 0.2, so catching it is profitable for stock levels above 5, which is one half of the natural equilibrium level. In the optimal solution the catch of the predator fish falls uniformly as the price of the prey rises, and at a certain level it becomes economically optimal to eliminate the predator. At this point there is a kink in the curve showing how the catch of prey fish increases with its price.

In the open-access solution, the catches of the predator also fall to zero as the price of prey increases, but for a different reason; the predator stock is not eliminated but driven down by overfishing of the prey to such a low level that fishing of the predator becomes unprofitable. Owing to overfishing, the catches of the prey fall even as its price rises. As before, the non-cooperative Nash equilibrium represents an intermediate position. The catches of prey fish rise with its price, but less than in the global optimum. The predator fish is not eliminated and in fact gives positive yields throughout the price range. It is this higher standing stock of the predator that keeps down the yield of the prey, compared with the optimal solution.

The food chain index falls under all regimes as the price of prey rises (Fig. 2); i.e., the share of the total catch coming from the lower level in the food chain increases as the price of the prey species goes up.

Conclusion

Whether fishing down the food chain is detrimental or not depends, presumably, on the value of the various kinds of fish involved. If fish at a lower level in the food chain fetch a higher price (or can be caught more cheaply) than species at a higher level it would be desirable economically to increase the share of this type of fish in the total catch, for two reasons. (*i*) A higher net price of fish of a given type is a signal that more thereof is desired and should ordinarily be a signal to bring more forward, to the extent that the productivity of nature allows. (*ii*) It would make good sense economically to reduce stocks of predators to limit predation on stocks that are in high demand.

But there are cases where fishing down the food chain is encouraged despite prices and costs giving a signal in the opposite direction. This happens, unsurprisingly, under open access, which is well known for having perverse incentive effects. Under open access, a higher price of a predator species encourages overexploitation of the same, the yield falls, and the catches of prey fish increase because the growth conditions of this type of fish are improved.

References

Caddy, J.F., Csirke, J., Garcia, S.M., and Grainger, R.J.R. 1998. How pervasive is "fishing down marine food webs"? Science (Washington, D.C.), **282**: 1383*a*.

Hannesson, R. 1983. Optimal harvesting of ecologically interdependent fish species. J. Environ. Econ. Manag. **10**: 329–345.

Larkin, P. 1966. Exploitation in a type of predator–prey relationship. J. Fish. Res. Board Can. **23**: 349–356.

Pauly, D., Christensen, V., Dalsgaard, J., Froese, R., and Torres, F., Jr. 1998*a*. Fishing down marine food webs. Science (Washington, D.C.), **279**: 860–863.

Pauly, D., Froese, R., and Christensen, V. 1998*b*. Response. Science (Washington, D.C.), **282**: 1383*a*.

© 2002 NRC Canada

Effects of nutrient enrichment on recruitment of age-0 fathead minnows (*Pimephales promelas*): potential impacts of environmental change on the Boreal Plains

Susan C.H. Grant and William M. Tonn

Abstract: Eutrophication in lakes on the Canadian Boreal Plains is predicted to increase because of climate and land-use changes. The resulting increase in lake productivity might then increase recruitment of young fish via increased food availability, growth, and survival. To assess this hypothesis, we manipulated nutrient concentrations in experimental ponds and examined mechanisms influencing production and survival of age-0 fathead minnows (*Pimephales promelas*). Nutrient enrichment increased phytoplankton biomass (chlorophyll *a*) sevenfold in treatment compared to reference systems. In response, fish laid more eggs and survival of age-0 fish was enhanced, both of which contributed to a more than fivefold increase in total number of age-0 fish that survived to the end of the growing season in treatment versus reference systems. A complementary enclosure experiment suggested that enhanced growth and decreased susceptibility to starvation contributes to the greater survival of age-0 fish when food resources are increased. Furthermore, overwinter mortality of age-0 fathead minnows in experimental ponds was strongly size-selective; no fish smaller than 20 mm survived winter. Because of these effects on egg production and growth and survival of age-0 fish, environmental changes predicted for the Boreal Plains could significantly alter the dynamics of fish populations.

Résumé : On prédit l'eutrophisation croissante des lacs de la plaine boréale canadienne à cause des changements dans le climat et dans l'utilisation des terres. Il se peut alors que la productivité accrue des lacs augmente le recrutement des jeunes poissons à cause de la disponibilité plus grande de nourriture, de la croissance plus rapide et de la survie plus importante. Pour éprouver cette hypothèse, nous avons modifié les concentrations de nutriments dans des étangs expérimentaux et étudié les mécanismes qui influencent la production et la survie des têtes-de-boule (*Pimephales promelas*) d'âge 0. L'enrichissement en substances nutritives provoque un accroissement par un facteur de 7 de la biomasse du phytoplancton (chlorophylle *a*), par comparaison avec les témoins. En réaction, les poissons pondent plus d'oeufs et la survie des poissons d'âge 0 augmente, ce qui entraîne un accroissement de plus de 5 fois du nombre total de poissons d'âge 0 qui survivent jusqu'à la fin de la période de croissance dans les étangs traités. Une expérience complémentaire dans des enclos montre que la croissance accrue et le risque réduit d'exposition à la famine sont responsables de l'augmentation de la survie des poissons d'âge 0 lorsque les ressources alimentaires deviennent plus abondantes. De plus, la mortalité des poissons pendant l'hiver dans les étangs expérimentaux varie considérablement avec la taille et aucun poisson de taille inférieure à 20 mm ne survit à l'hiver. À cause de leurs effets sur la production d'oeufs et sur la croissance et la survie des poissons d'âge 0, les changements environnementaux que l'on prévoit dans les plaines boréales pourraient affecter la dynamique des populations de poissons de façon significative.

[Traduit par la Rédaction]

Introduction

Stages thought to be important in fish recruitment, and thus population dynamics, occur during early life history (Miller et al. 1988; Crowder et al. 1992). Because it is in these stages that the greatest numbers of individuals are found and the greatest mortality occurs (Sissenwine 1984), even small fluctuations in production or mortality should strongly influence the number of fish that ultimately recruit.

Body size and growth are key factors that influence egg production and survival of young fish. Fecundity is generally related to female body size (Wootton 1990). Because principal sources of mortality for larval and post-larval fish, predation and starvation, are both size dependent (Miller et al. 1988), faster growth will reduce the time a fish spends in smaller, more vulnerable size classes. In boreal regions, greater growth in the first summer should also reduce subsequent over-winter mortality, which is size dependent in young fish (Post and Ev-

Received 20 August 2001. Accepted 20 April 2002. Published on the NRC Research Press Web site at http://cjfas.nrc.ca on 31 May 2002.
J16495

S.C.H. Grant[1] and W.M. Tonn.[2] Department of Biological Sciences, University of Alberta, Edmonton, AB T6G 2E9, Canada.

[1]Present address: Department of Fisheries and Oceans, 100 Annacis Parkway, Unit 3, Delta, BC V3M 6A2, Canada.
[2]Corresponding author (email: bill.tonn@ualberta.ca).

 DOI: 10.1139/F02-054 © 2002 NRC Canada

ans 1989; Cargnelli and Gross 1996). Smaller individuals have lower energy reserves and higher mass-specific standard metabolic rates (Brett and Groves 1979; Shuter and Post 1990) and will deplete their energy reserves more quickly than larger fish.

In freshwater ecosystems, increased nutrient concentrations can significantly increase production of algae and zooplankton, the main food sources for many young fish (Stockner and Shortreed 1985) and adult minnows (Becker 1983), and therefore increase their growth, survival, and production (Stockner and MacIsaac 1996; Sandström and Karås 2002). Because a number of anthropogenic factors can increase nutrient concentrations in aquatic ecosystems, it is important to examine the effects of those increases on recruitment of young fish in regions where such increases are predicted. One such region is the Boreal Plains of western Canada, where global warming is predicted to increase eutrophication directly (Schindler 2001) and indirectly via effects of increased frequency of forest fires (Scrimgeour et al. 2001), and where increased agriculture and forestry can also result in increased nutrient inputs (Prepas et al. 2001).

To assess effects of eutrophication on recruitment of young fish in Boreal Plains lakes, we added nutrients to one side of divided ponds and compared in treatment and reference sides the production of age-0 fathead minnows (*Pimephales promelas*), which is often the most abundant or only fish present in small lakes in northern Alberta (Robinson and Tonn 1989). Our objectives were to test hypotheses that nutrient enrichment would increase (*i*) growth and survival of stocked fish, (*ii*) production and survival of eggs, and (*iii*) growth and survival of age-0 fish. In a complementary enclosure study, we assessed explicitly the effect of increased food resources on growth and survival of age-0 fish during summer. In a second pond study, we also examined if increased production and survival of age-0 fish during the summer would translate into increased recruitment as age-1 fish the following spring. In combination, these studies allowed us to explore mechanisms by which climate and land-use changes could affect recruitment in an important fish of Boreal Plains lakes.

Materials and methods

Study species

The fathead minnow is a short-lived (≤5 years), small-bodied fish that occurs throughout central North America. In boreal Alberta, their northwestern distributional limit (Scott and Crossman 1973), fathead minnow inhabits shallow lakes and ponds that often lack other fishes (Robinson and Tonn 1989).

Nutrient enrichment experiment

Research was conducted in three experimental ponds (25 × 13 m; maximum depth 1.5 m) at the Meanook Biological Research Station (MBRS) (54°37′N, 113°35′W). Each pond was divided in half with an impermeable polyvinyl curtain. All ponds had been initially drained and raked to remove potential spawning substrate. After filling, substrate (11 floating wooden boards, 0.2 × 1.5 m, covered by black tarpaulin and anchored with bricks) was added to each pond side.

Abiotic environment

Beginning on 13 June 1996, we added nutrients to one side of each pond and left the opposite side as an unmanipulated reference. Phosphoric acid (85% H_3PO_4) at 80 $\mu g \cdot L^{-1}$, and ammonium nitrate (NH_4NO_3 (34% N)) at 1200 $mg \cdot L^{-1}$, were added five times at ca. 2-week intervals to increase and maintain total phosphorus (TP) concentrations of treatment sides to ca. five times above reference sides and to maintain the ratio of total nitrogen (TN) to TP at ca. 20:1. The quantities added were based on TP and TN concentrations in the reference pond sides measured just prior to the addition of nutrients.

We collected water samples biweekly from all pond sides to monitor phosphorus and nitrogen concentrations. These samples were collected just prior to each addition of nutrients. On 24 July, water samples were also collected ca. 1 h after nutrient addition to determine if fertilization increased nutrient concentrations sufficiently (ca. 5 times) relative to reference pond sides. From each pond half, water was collected at mid-depth (0.75 m) with a 3.1-L Van Dorn bottle from inshore and offshore habitats, pooled into one composite sample, filtered, and stored. TP and total dissolved phosphorus (TDP) were determined in duplicate within 7 days using standard methods. A Technicon autoanalyzer was used to determine nitrates + nitrites (NO_2^- + NO_3^-) and ammonium (NH_4^+) concentrations, in triplicate, within 24 h of water collection. Total Kjeldahl nitrogen (TKN) concentrations were also measured in triplicate to calculate TN.

Additional water samples were collected biweekly at inshore and offshore sites and analyzed for dissolved oxygen. pH was measured biweekly from pond water collected near the pond surface and bottom using a Fisher Digital pH meter (model 109, Pittsburgh, Pa.). Temperature was measured and recorded hourly with data loggers submerged midway (0.75 m) down the water column.

Food availability

Water samples used to quantify phytoplankton biomass (measured as chlorophyll *a* (chl *a*)) were collected biweekly with a 3.1-L Van Dorn bottle at 0.75 m. A sample from an inshore and offshore site were pooled for each pond side, filtered, and stored. Chlorophyll *a* concentrations were determined in triplicate within two weeks of collection using an ethanol extraction and spectrophotometric procedure (Bergmann and Peters 1980). To sample zooplankton, 50 L of water from one inshore and one offshore site were collected and filtered through a 10-L Schindler–Patalas trap (45-μm mesh). Zooplankton were preserved in 4% sugar formalin and later sorted into coarse categories (rotifers, cladocerans, and copepods). To determine zooplankton dry mass, samples for three dates (26 June, 22 July, 19 Aug.) were first rinsed with distilled water, divided into three different size fractions (<153 μm, 153–500 μm, and >500 μm), filtered onto preweighed and predried Millipore 0.45-mm filters, oven-dried at 60°C for 24 h, cooled in a dessicator, and weighed on a Cahn microbalance (model C-31, Beverly, Mass.). Data for the three size fractions averaged from inshore and offshore sites on the three sampling dates were obtained for ponds one and two. Some samples from the treatment side of pond 2 and all samples from pond 3 were excluded because of high quantities of nonzooplankton organic and inorganic matter present in the samples.

© 2002 NRC Canada

Table 1. Mean (SE, standard error) nutrient concentrations, dissolved oxygen concentrations, and pH for the three experimental ponds (treatment and reference sides).

Variable	Mean (SE) $mg \cdot L^{-1}$		
	Treatment	Reference	$F_{1,2}$
Total phosphorus (n = 9)	47.5 (4.6)	21.2 (2.0)	15.4
Total dissolved phosphorus (n = 5)	20.0 (2.3)	7.0 (0.3)	32.9[a]
Total nitrogen (n = 2)	864.0 (142.0)	521.0 (32.7)	7.3
Ammonium (n = 8)	65.3 (15.0)	10.5 (1.4)	4.7
Nitrate + nitrites (n = 8)	277.0 (37.0)	4.2 (0.6)	19.3[a]
Dissolved oxygen (mg $O_2 \cdot L^{-1}$) (n = 9)	9.4 (0.6)	6.6 (0.7)	4.3
pH at surface (n = 6)	8.8 (0.1)	8.0 (0.1)	8.0
pH at bottom (n = 6)	8.8 (0.1)	7.9 (0.1)	5.2

Note: F value and significance of treatment for each variable are indicated, determined from repeated measures ANOVA. Sample size per pond side is also indicated for each variable.
[a]$P < 0.05$.

Fish

Fathead minnows were collected from a nearby natural pond and sorted into six categories: large (74–77 mm total length (TL)) and small (68–71 mm TL) adult males, large (68–71 mm TL) and small (62–65 mm TL) adult females, and large (52–59 mm TL) and small (40–47 mm TL) juveniles. Males, females and juveniles received batch-marks subcutaneously with acrylic paint for subsequent identification. Secondary sexual characteristics (Danylchuk and Tonn 2001) were used to distinguish males from females; juveniles were identified by their lack of secondary sexual characteristics.

On 15–16 June 1996, each pond side was stocked with fathead minnows at identical densities (1 $fish \cdot m^{-3}$) and proportions of life-history categories (0.16:0.20:0.14 of large males and females – small males and females – large and small juveniles), based on densities and proportions found in nearby natural populations (W.M. Tonn, unpublished data).

To monitor growth, condition, and densities of stocked fish, six Gee minnow traps were deployed overnight, biweekly, in each pond side. After sorting fish into the above life-history categories, they were measured (TL), weighed, and counted, and then returned to their respective pond sides.

To determine the total number of eggs laid in each pond side, fresh egg batches (stage-1 eggs, sensu Vandenbos 1996) were censused from 19 June to 6 Aug. during alternate-day surveys of nest boards; fates of these new eggs were determined from subsequent surveys. During these surveys we also scanned the ponds for any eggs laid elsewhere. We classified eggs as hatched if they disappeared after reaching the third (gold-eyed) stage, whereas egg batches that disappeared suddenly (and usually entirely) in the first and second stage were classified as cannibalized (Vandenbos 1996). Eggs infected by fungus were also recorded; these eggs would remain on the boards for a number of days but gradually disappeared.

To monitor growth and densities of age-0 fish, biweekly samples were collected from inshore (<1 m from shore) and offshore (>3 m from shore) habitats with an electrofishing unit and dipnet. During each sampling, five 1-m inshore sweeps and five 2-m offshore sweeps were conducted for each pond side; paired inshore and offshore samples were pooled, resulting in five samples per pond side. Captured fry were measured (TL), counted, and returned to their respective pond sides.

To determine end-of-season survival of all fish (stocked and age 0), ponds were drained on 7 Sept. to a maximum depth of 0.6 m and all surviving fish were removed by overnight minnow-trapping followed by repeated seining (until three consecutive seine hauls captured <2 fish). All fish were killed (anaesthetic overdose with MS 222), preserved in 95% ethanol, and counted to assess survival; a subsample from each pond side was measured (TL) and weighed.

Food addition experiment

We conducted an enclosure experiment to determine directly the effects of increased food levels on growth and survival of age-0 fathead minnows. Twelve enclosures (2.4 × 2.4 × 0.6 m), divided into three replicate blocks of four, were located within a large experimental pond at MBRS. Enclosure walls composed of impermeable polyvinyl tarpaulin, fastened onto wooden frames and buried into sandy sediment, prevented exchange of water and fish between enclosures. Duplicates of two treatments were randomly assigned to the four enclosures within each block. High-food (treatment) enclosures received a daily supplement of a ca. 300 mL concentrate of brine shrimp (*Artemia*) nauplii, which were cultured on site. Low-food (reference) enclosures received no supplemental food.

Fathead minnow eggs were collected from spawning substrata placed in a nearby natural pond. Eggs were transported to MBRS and incubated in the laboratory in buckets containing aerated well water. Once a large hatch occurred, 11 400 day-0 larvae were divided equally among 12 buckets to provide a stocking density of 0.27 $fish \cdot L^{-1}$, similar to the density of age-0 fish obtained in the nutrient addition experiment (S.C.H. Grant and W.M. Tonn, unpublished data). Prior to stocking fish into the enclosures, a subsample of 50 larvae from each bucket was measured (TL). Two blocks of enclosures were stocked on 9 July 1996, and the third block was stocked the following day.

After 45 days, all surviving fish were removed from each enclosure by electrofishing and preserved in 95% ethanol. These fish were later counted and a subsample of ca. 50 fish per enclosure was measured (TL) and weighed. Growth rates (G_L) ($mm \cdot day^{-1}$) were calculated as $G_L = (L_2 - L_1)/(T_2 - T_1)$

© 2002 NRC Canada

where L_1 and L_2 are the average initial and final lengths (mm), respectively, and T_1 and T_2 are the initial and final Julian dates, respectively, of the study period. During the first week, one high-food enclosure developed a hole in an externally facing wall and was dropped from analysis.

Overwinter mortality

In the spring of 1995, two of the experimental ponds used in 1996 for the nutrient-enrichment study were stocked with adult fathead minnows. Spawning substrate was provided and fish commenced spawning in late May. In September 1995, adult fish were removed by intensive minnow trapping. On 16 Sept. 1995, two weeks prior to ice-up (water temperature 6°C), we collected a sample of age-0 fish using an electrofishing unit and dip net. All fish collected were preserved in 95% ethanol, measured (TL), and weighed. On 2 May 1996, 1 week after ice-out (water temperature 5°C), each pond was drained to a depth of 0.6 m and seined repeatedly until two consecutive seine hauls produced fewer than two fish each. All captured fish were preserved in 95% ethanol, and samples from each pond were measured (TL) and weighed.

Results

Nutrient enrichment experiment

Abiotic environment

Nutrient concentrations in treatment pond sides were enhanced by nutrient addition, with significant increases observed for TDP and (NO_2^- + NO_3^-) (Table 1). Concentrations of TP averaged 2.2 times greater in treatment than reference pond sides; when water samples were collected 1 h after nutrient addition (24 July 1996), TP concentrations were 9 times greater in treatment than in reference pond sides ($\bar{x}$ = 238 $\mu g \cdot L^{-1}$ vs. 26.5 $\mu g \cdot L^{-1}$, respectively). Ratios of TN–TP were 18:1 for treatment pond sides and 24:1 for reference ponds sides. Neither dissolved oxygen nor pH differed between treatment and reference pond sides (Table 1). Between 6 June and 9 Sept., daily mean water temperature ranged from 12 to 23°C ($\bar{x}$ = 19°C) and did not differ between reference and treatment pond sides (paired t test, P = 0.5).

Food availability

Differences in chl *a* between the treatment and reference pond sides occurred as early as 26 June, within two weeks of the first nutrient application. Chlorophyll *a* concentrations were higher in the treatment pond sides throughout the season (repeated measures analysis of variance (ANOVA), P = 0.04) (Fig. 1), but differences between treatment and reference pond sides were more dramatic after 22 July (treatment 55.0 ± 9.2 $\mu g \cdot L^{-1}$ (mean ± standard error, SE); reference 6.75 ± 2.0 $\mu g \cdot L^{-1}$) than before (treatment 7.00 ± 2.0 $\mu g \cdot L^{-1}$; reference 1.9 ± 0.4 $\mu g \cdot L^{-1}$). Zooplankton composition was similar in all ponds, consisting primarily of calanoid and cyclopoid copepods, various cladocerans, and very few rotifers. Zooplankton biomass did not differ between the treatment and reference sides throughout the season for each size fraction (repeated measures ANOVA; small P = 0.28, medium P = 0.22, large P = 0.57), although small sample sizes limited the power of our tests. Zooplankton biomass was greatest on the first sampling date (26 June) and decreased subsequently.

Fig. 1. Chlorophyll *a* concentrations (mean ± standard error) in treatment (nutrient addition; ■) and reference (□) sides of three experimental ponds measured from June to August 1996. Arrows represent nutrient addition dates.

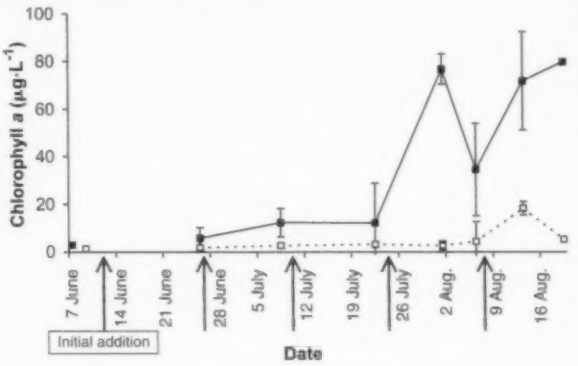

Fig. 2. (*a*) Number (mean ± standard error) of eggs laid in the first and second halves of the spawning season (19 June – 5 July and 6 July– 5 Aug., respectively) and the totals over the whole summer in treatment (nutrient addition; solid bars) and reference sides (open bars) of three experimental ponds in 1996. (*b*) Number (mean ± standard error) of eggs hatched in the first and second halves of the season and the totals over the whole summer in treatment (solid bars) and reference (open bars) sides.

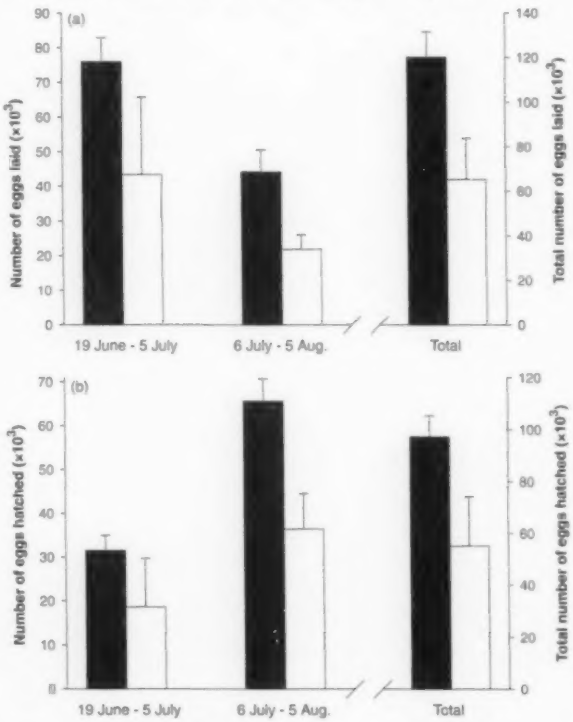

Fish

Lengths of stocked fish, which were initially similar be-

© 2002 NRC Canada

Fig. 3. Lengths (mean ± standard error) of age-0 fathead minnows for treatment (solid symbols) and reference (open symbols) sides of three experimental ponds during July–August 1996, and at the end of the season (8 Sept.).

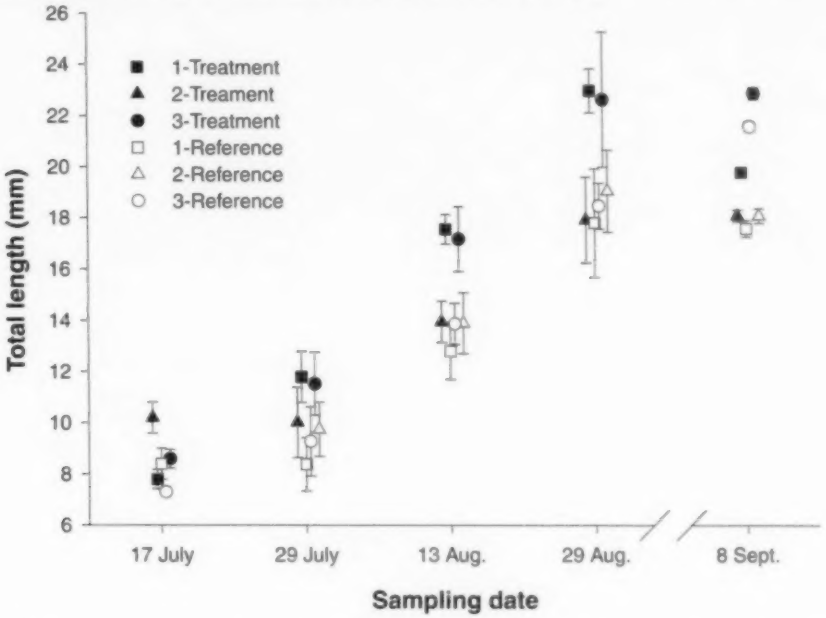

tween treatment and reference pond sides, began to diverge in late July. When compared at the end of the season (September 8), mean lengths were consistently larger in treatment (73.8, 68.8, and 62.6 mm for males, females, and juveniles, respectively) than in reference pond sides (72.5, 67.6, and 60.5 mm) (one-tailed paired t test, $P = 0.017$). Likewise, condition (100·mass·length^{-3}) of stocked fish began to diverge in late July and by the end of the season (8 Sept.), mean condition of males, females, and juveniles in treatment pond sides (1.27, 1.24, and 1.24, respectively) was consistently greater than in reference sides (1.16, 1.14, and 1.21) (one-tailed paired t test, $P = 0.04$).

Densities (measured as catch-per-unit-effort) of stocked fish declined in the first month after stocking, but stabilized subsequently (Kiesling 1999). Densities were similar in treatment and reference pond sides throughout the season (repeated measures ANOVA, $P = 0.95$). Survival of stocked fish (percentage of initial numbers present in the final removal) was lowest for males (40%); female and juvenile survivals were 59% and 57%, respectively. Overall, survival of stocked fish did not differ between treatment and reference pond sides (one-tailed paired t test, $P = 0.76$).

With the exception of one reference side, spawning commenced on 19 June, peaked between 29 June and 1 July, and tapered off to zero by 30 July. Hatching peaked between 5 and 7 July, and was completed by 5 Aug. Viable eggs were not laid in the reference side of pond 2, however, until early July.

The total number of eggs deposited on nest boards was 1.8 times greater in the treatment ($\bar{x}$ = 120 137 ± 11 425) than the reference ($\bar{x}$ = 65 264 ± 18 423) pond sides (Fig. 2). No eggs were observed on substrata other than the nest boards, and unused oviposition space was available on these boards throughout the spawning period. Because overall egg predation and disease was low and unaffected by treatment, the proportion of eggs surviving to hatch was similar (81.1% treatment; 81.2% reference). Consequently, the total number of eggs hatched was also 1.8 times greater in treatment ($\bar{x}$ = 97 215 ± 8096) versus reference ($\bar{x}$ = 55 089 ± 18 997) pond sides (Fig. 2). As with chl *a* concentrations, there was a temporal heterogeneity to the differences between treatments. In the first half of the spawning season (19 June – 5 July), the number of eggs laid (one-sided paired t test, $P = 0.14$) and hatched ($P = 0.22$) did not differ between treatment and reference pond sides (Fig. 2). In the second half, however, significantly more eggs were laid (one-sided paired t test, $P = 0.007$) and hatched ($P = 0.043$) in the treatment versus reference pond sides (Fig. 2).

Age-0 fish were consistently larger in treatment compared to reference sides for ponds 1 and 3 but not for pond 2 (Fig. 3). Similarly, final lengths of age-0 fish surviving to the end of the season were greater in the treatment sides of ponds 1 ($\bar{x}$ = 19.8 ± 0.2 mm) and 3 ($\bar{x}$ = 22.9 ± 0.3 mm), compared with their respective reference sides (pond 1, 17.6 ± 0.2 mm; pond 3, 21.6 ± 0.3 mm; ANOVAs: pond 1, $P < 0.001$; pond 3, $P = 0.002$). Because final lengths for pond 2 were similar between treatment and reference sides ($\bar{x}$ = 18.1 mm for both), the overall treatment effect was marginal (one-sided paired t test, $P = 0.10$).

Densities of age-0 fish fluctuated between 0.46 and 1.75 fish·L^{-1} throughout the season (17 July – 29 Aug.) in the treatment sides (Fig. 4). In the reference sides, densities were much lower (0.06–0.65 fish·L^{-1}) and decreased consistently after the initial sampling date (17 July; ponds 1 and 3) or following the first appearance of age-0 fish (29 July; pond 2). Numbers of age-0 fish in the final removal were nearly six times greater in the treatment ($\bar{x}$ = 11 113 ± 1423) versus reference ($\bar{x}$ = 1922 ± 412) pond sides (one-sided paired t

© 2002 NRC Canada

Fig. 4. Densities (mean ± standard error) (from 17 July to 29 Aug.) and final numbers (8 Sept.) of age-0 fathead minnows for treatment (solid bars) and reference (open bars) sides of (*a*) pond 1, (*b*) pond 2, and (*c*) pond 3.

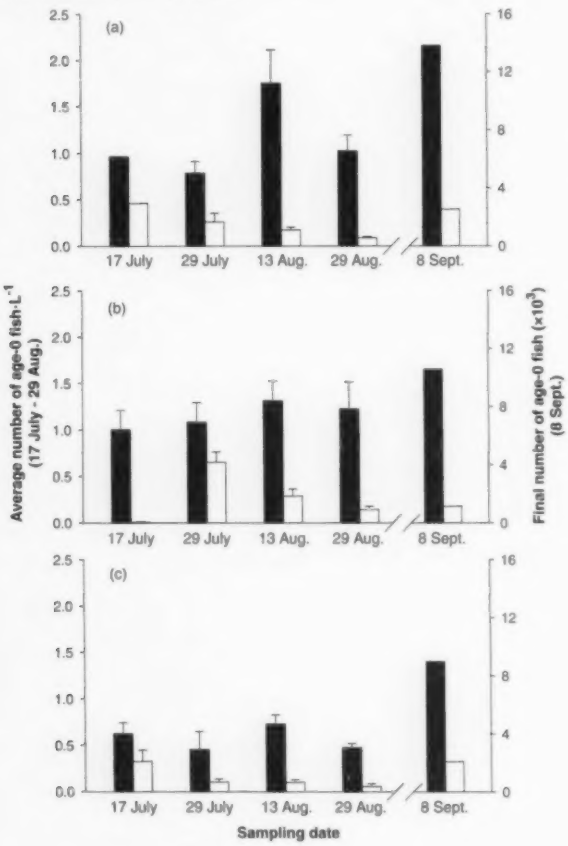

test, $P = 0.009$) (Fig. 4). In addition, a consistently greater proportion of age-0 fish survived from hatch to September in the treatment ($\bar{x} = 0.12 \pm 0.04$) than in the reference ($\bar{x} = 0.04 \pm 0.01$) pond sides (paired t test on arcsine square root transformed proportions, $P = 0.03$).

Food addition experiment

Average initial length of fish differed by < 0.01 mm between treatments (Table 2). Final length (1.9 times), mass (8 times), and growth rate (2.5 times) of surviving fish were all greater in the high-food versus the low-food treatments (ANOVAs, $P < 0.001$) (Table 2). Survival of age-0 fish was 1.7 times higher in the high-food versus the low-food treatments ($P = 0.001$; Table 2).

Overwinter mortality

In both ponds, length distributions differed between the fall (1995) and spring (1996) (K-S two sample tests, $P < 0.001$; Fig. 5). Mean lengths before ice-up, 19.7 ± 0.4 mm (SE) and 24.4 ± 0.6 mm for ponds 1 and 2, respectively, were less than lengths after ice-melt, 32.2 ± 0.3 and 31.0 ± 0.4 mm, respectively (ANOVAs, $P < 0.001$). No fish <20 mm survived the winter. Because of the loss of small fish, mean mass of individual fish was 4.2 times and 2.1 times greater after ice-up than before for pond 1 and 2, respectively ($P < 0.001$).

Discussion

Our data strongly supported the hypothesis that nutrient enrichment would increase recruitment of age-0 fathead minnows. Under enriched conditions, more eggs were produced and hatched, summer survival of age-0 fish was higher, and despite higher densities, growth was at least as great as in the unenriched reference pond sides. Because overwinter survival of age-0 fish was shown to be strongly size selective, the outcome of having higher densities yet comparable body sizes would be a larger cohort entering the yearling age-class under enrichment.

Production, growth, and survival

In our pond experiment, nutrient enrichment enhanced phytoplankton biomass, whereas zooplankton biomass was unaffected. Although important foods of adult and juvenile fathead minnow include both algae and zooplankton (Becker 1983), most studies of fathead minnow diets in Alberta indicate that the latter is more important (Price et al. 1991; Janowicz 1999). Because algae is low-quality food relative to zooplankton (Gerking 1994), it seems unlikely that the responses identified above could be fueled by increased algal production alone, and the similarities of the responses observed in the treatment ponds with those in the *Artemia*-enhanced enclosures further suggest that a bottom-up response to nutrient addition extended beyond the primary producers. We suggest that in the face of increased fish densities, the lack of observable differences in zooplankton biomass points to increased zooplankton production in treatment pond sides.

Spawning and nest guarding is energetically costly for fathead minnows and results in high post-reproductive mortality in adults, particularly males, which tend not to feed during these activities (Unger 1983). As well, the largest increases in food production (as evidenced by chl *a* concentrations) did not occur in the treatment pond sides until the second half of the summer, after the peak in reproductive activities. Therefore, it is not surprising that survival of stocked fish did not differ between treatment and reference sides and that increases in growth and condition were not observed in treatment sides until later in the season. Interestingly, the largest growth differential between treatment and reference stocked fish occurred in juveniles.

Because females feed during the reproductive season, allocation of extra food to reproduction in treatment sides would be expected (Wootton 1977); indeed, females laid nearly twice as many eggs in the treatment relative to the reference pond sides. This increased egg production in treatment sides was greater, however, only in the second half of the spawning season when the difference in chl *a* concentration between pond sides was greatest. Increased food supply for a multibatch spawning fish like fathead minnow can increase the number of times an individual female can spawn, decrease the time interval between successive spawnings, and increase batch fecundity (Wootton 1990; Reznick and Yang 1993). As well, part of the increased egg production in

© 2002 NRC Canada

Table 2. Numbers (mean, (standard error)) per enclosure (N), total lengths (TL), and masses of age-0 fathead minnows at the start (age: day 0) and end (age: day 45) of the food addition enclosure experiment for high- and low-food treatments and growth rates of fish during this period.

	Initial (July)		Final (August)			
Treatment	N	TL (mm)	N	TL (mm)	Mass (g)	Growth (mm·day^{-1})
High food[a]	950 (0)	5.2 (0.0)	308 (35)	29.0 (0.4)	0.16 (0.01)	0.5 (0.0)
Low food[b]	950 (0)	5.2 (0.0)	182 (26)	15.1 (1.0)	0.02 (0.00)	0.22 (0.0)

[a] n = 5 for each initial TL and final TL, mass, and growth.
[b] n = 6 for each initial TL and final TL, mass, and growth.

Fig. 5. Length–frequency distributions of age-0 fish just before ice-up (September 1995; solid bars) and the following spring (May 1996; open bars) for (*a*) pond 1 (n = 117 and 214, respectively) and (*b*) pond 2 (n = 115 and 68, respectively).

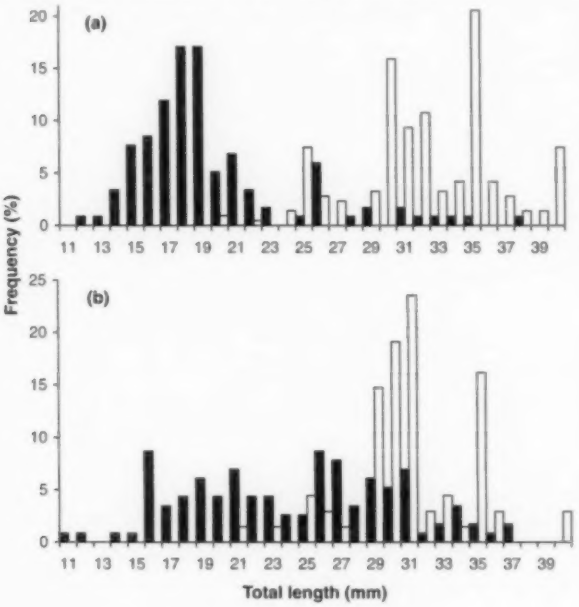

treatment pond sides later in the season may have come from accelerated maturation of juvenile stocked fish; although not quantified, secondary sexual characteristics began to develop in some juveniles in treatment pond sides later in the summer, with some females becoming noticeably gravid (S.C.H. Grant, personal observation).

The reference side of pond 2 exhibited little or no egg production in the first part of the spawning season. The few eggs that were observed at this time were not viable, and disintegrated upon contact. Interestingly, pond two had the lowest algal biomass (chl *a*) of all ponds throughout the season. Perhaps the initial amount of available food was so poor that females either resorbed many of their yolked oocytes or failed to produce vitellogenic eggs (Wootton 1990).

Addition of nutrients did not influence overall cannibalism of eggs by stocked fish. Mortality of eggs was similar (ca. 18%) in both treatment and reference pond sides. Using the same MBRS ponds, Vandenbos (1996) showed that egg cannibalism in fathead minnow is related to density of stocked (adult and juvenile) fish; at the density we used, Vandenbos (1996) observed a similar level of egg mortality (24%). Since the treatment had no effect on egg mortality, the increase in egg production accounted for the greater initial number of young fish in the treatment versus the reference pond sides.

Despite the intra-year-class competition that might be expected from such increased densities of age-0 fish (Vandenbos 1996), their survival to the end of the season was also greater in the treatment pond sides. This suggests that nutrient enrichment reduced starvation and (or) predation, the main mortality mechanisms usually acting on age-0 fish (Miller et al. 1988). Improved survival of age-0 fish under nutrient enhancement is generally attributed to bottom-up processes that increase food availability (Stockner and Shortreed 1985) and decrease starvation of young fish (Mills and Chalanchuk 1987; Fox et al. 1989). In addition, a positive feedback is expected whereby increased growth and size of age-0 fish that results from greater food resources, in turn, enhances the visual acuity (Blaxter 1986) and swimming performance (Frank and Leggett 1982; Rice et al. 1987) of age-0 fish, and therefore improves their ability to capture prey. In the enclosure experiment, where food supply was manipulated directly, both growth rates and survival of age-0 fathead minnows were greater in the treatment than in unenriched reference enclosures. Thus, larger body sizes of age-0 fish throughout the season in the treatment sides of ponds 1 and 3 suggest that nutrient enrichment did enhance food availability and growth rates (a suggestion supported by otolith microstructural analysis; S.C.H. Grant and W.M. Tonn, unpublished data), and thereby reduced starvation of the age-0 fish.

In addition to reducing their risk of starvation, faster growth rates and larger sizes should also decrease the susceptibility of age-0 fish to gape-limited predators (Miller et al. 1988); such predators would include adult fathead minnows in our pond experiment (Vandenbos 1996). Indeed, the presence of cannibalistic adults may have contributed to the greater difference in survival of age-0 fish between treatments in the pond experiment than in the enclosures, where no adults were present and the cost of slower growth was therefore less severe.

In pond 2, lengths of surviving fish did not differ between treatment and reference pond sides. Because most fish hatched after 5 July in the reference side, reference fish generally had a shorter time to grow. As a result, we expected reference fish to have been smaller than treatment fish. Chlorophyll *a* concentrations were exceptionally low in the reference side of pond 2, however, and survival of age-0 fish was low compared to treatment fish survival; therefore, we suggest that size-selective mortality explains this discrepancy.

© 2002 NRC Canada

Slower growing, smaller fish would likely have experienced greater mortality in the reference side, and as a result, survivors would have been the faster growing individuals.

Overwinter mortality

Increased growth of age-0 fish during the summer period and the resulting larger body sizes prior to freeze-up should strongly influence the intensity of size-selective starvation during the winter period. In our study, overwinter mortality of age-0 fish was strongly selective for smaller body sizes; no fish smaller than 20 mm survived the winter period. Because temperatures remained below (mostly well below) 6°C between the fall and spring sampling dates, these results should be primarily attributed to size-selective overwinter mortality rather than overwinter growth (Mann 1991). A comparison of maximum sizes sampled in fall versus spring suggest that growth might explain a 2- to 3-mm difference in size, but that amount of growth is insignificant relative to the differences actually observed.

Our results are consistent with field studies that have interpreted increases in mean lengths or changes in length–frequency distributions as evidence for size-selective overwinter mortality (Toneys and Coble 1979; Smith and Griffith 1994). Laboratory studies have also provided strong evidence of size-selective mortality in age-0 fish under simulated winter conditions (Post and Evans 1989). In the winter period, food availability is low and fish generally do not feed at colder temperatures (Shuter and Post 1990); therefore, smaller fish should deplete their energy reserves faster than larger fish (Brett and Groves 1979; Post and Evans 1989).

Our draining of the ponds in the fall of 1996 precluded a direct assessment of overwinter survival and recruitment to age 1 following our nutrient enrichment experiment. However, because lengths of age-0 fish in treatment sides were as large as or larger than those in reference sides, overwinter survival rate should also have been as high or higher in the former relative to the latter. Because nearly six times as many age-0 fish were present in treatment sides in the fall, we therefore suggest that total recruitment to age 1 under enriched conditions would far exceed that in unenriched systems.

In conclusion, fish populations on the Boreal Plains are expected to experience increased eutrophication as a result of regional and local changes in climate and land use. Increases in productivity can increase food availability for minnows that can lead to increased egg production, as well as increased growth and survival of age-0 fish during summer. This, in turn, should result in more age-0 fish surviving the winter period, unless increased primary and secondary production increases the frequency or severity of winterkill (A. Danylchuk and W.M. Tonn, unpublished data). Mechanistic studies of recruitment typically focus on characteristics of age-0 fish (e.g., Rice et al. 1987; Cargnelli and Gross 1996); rarely do such studies also include the potential influence of adult characteristics on the numbers of eggs produced (Wootton 1977, 1990) and predation on the early life-history stages (Crowder et al. 1992; Vandenbos 1996). Understanding the responses of both the adult and age-0 fish life-history stages to increased lake productivity and how these responses influence recruitment should improve our predictions of the effects of environmental change on fish populations.

Acknowledgments

This study was funded by a Challenge Grant in Biodiversity (Department of Biological Sciences, University of Alberta, and the Alberta Conservation Association) and a Boreal Alberta Research Grant (Canadian Circumpolar Institute) to S.C.H. Grant, and an NSERC (Natural Sciences and Engineering Research Council of Canada) Operating Grant to W.M. Tonn. Thanks to K. Vladicka, S. Boss, J. Rosnau, C. Herzog, J. McCormick, A. Danylchuk, and N. Grant for assistance, K. Gibson and K. Keglowitsch for logistics, and to N. Stacey, E. Macdonald, E. Prepas, M. Trudel, and three anonymous reviewers for comments on earlier versions of the manuscript.

References

Becker, G.C. 1983. Fishes of Wisconsin. University of Wisconsin Press, Madison, Wis.

Bergmann, M., and Peters, R.H. 1980. A simple reflectance method for the measurement of particulate pigment in lake water and its application to phosphorus–chlorophyll–seston relationships. Can. J. Fish. Aquat. Sci. **37**: 111–114.

Blaxter, J.H.S. 1986. Development of sense organs and behavior of teleost larvae, with special reference to feeding and predator avoidance. Trans. Am. Fish. Soc. **115**: 98–114.

Brett, J.R., and Groves, T.D.D. 1979. Physiological energetics. *In* Fish physiology. Vol. 10. *Edited by* W.S. Hoar, D.J. Randall, and J.R. Brett. Academic Press, New York. pp. 279–352.

Cargnelli, L.M., and Gross, M.R. 1996. The temporal dimension in fish recruitment: birth date, body size, and size-dependent survival in sunfish (bluegill: *Lepomis macrochirus*). Can. J. Fish. Aquat. Sci. **53**: 360–367.

Crowder, L.B., Rice, J.A., Miller, T.J., and Marschall, E.A. 1992. Empirical and theoretical approaches to size-based interactions and recruitment variability in fishes. *In* Individual-based approaches in ecology: concepts and individual models. *Edited by* D.L. DeAngelis and L.J. Gross. Chapman and Hall, New York. pp. 237–255.

Danylchuk, A.J., and W.M. Tonn. 2001. Effects of social behavior on reproductive activity in male fathead minnow (*Pimephales promelas*). Behav. Ecol. **12**: 482–489.

Fox, M.G., Keast, J.A., and Swainson, R.J. 1989. The effect of fertilization regime on juvenile walleye growth and prey utilization in rearing ponds. Environ. Biol. Fishes, **26**: 129–142.

Frank, K.T., and Leggett, W.C. 1982. Environmental regulation of growth rate, efficiency, and swimming performance in larval capelin (*Mallotus villosus*), and its application to the match/mismatch hypothesis. Can. J. Fish. Aquat. Sci. **39**: 691–699.

Gerking, S.D. 1994. Feeding ecology of fish. Academic Press, San Diego, Calif.

Janowicz, M.E. 1999. Trophic interactions in eutrophic boreal ponds in relation to fish predation pressure. M.Sc. thesis, University of Alberta, Edmonton, Canada.

Kiesling, S.C.H. 1999. Effects of nutrient enrichment on recruitment of age-0 fathead minnows (*Pimephales promelas*). M.Sc. thesis, University of Alberta, Edmonton, Canada.

Mann, R.H.K. 1991. Growth and production. *In* Cyprinid fishes: systematics, biology, and exploitation. *Edited by* I.J. Winfield and J.S. Nelson. Chapman and Hall, London. pp. 456–482.

© 2002 NRC Canada

Miller, T.J., Crowder, L.B., Rice, J.A., and Marschall, E.A. 1988. Larval size and recruitment mechanisms in fishes: toward a conceptual framework. Can. J. Fish. Aquat. Sci. **45**: 1657–1670.

Mills, K.H., and Chalanchuk, S.M. 1987. Population dynamics of lake whitefish (*Coregonus clupeaformis*) during and after the fertilization of Lake 226, the Experimental Lakes Area. Can. J. Fish. Aquat. Sci. **44**(Suppl. 1): 55–63.

Post, J.R., and Evans, D.O. 1989. Size-dependent overwinter mortality in young-of-the-year yellow perch (*Perca flavescens*): laboratory, in situ enclosure, and field experiments. Can. J. Fish. Aquat. Sci. **46**: 1958–1968.

Prepas, E.E., Pinel-Alloul, B., Planas, D., Methot, G., Paquet, S., and Reedyk, S. 2001. Forest harvest impacts on water quality and aquatic biota on the Boreal Plain: introduction to the TROLS lake program. Can. J. Fish. Aquat. Sci. **58**: 421–436.

Price, C.J., Tonn, W.M., and Paszkowski, C.A. 1991. Intraspecific patterns of resource use by fathead minnows in a small boreal lake. Can. J. Zool. **69**: 2109–2115.

Reznick, D., and Yang, A.P. 1993. The influence of fluctuating resources on life history: patterns of allocation and plasticity in female guppies. Ecology, **74**: 2011–2019.

Rice, J.A., Crowder, L.B., and Holey, M.E. 1987. Exploration of mechanisms regulating larval survival in Lake Michigan bloater: a recruitment analysis based on characteristics of individual larvae. Trans. Am. Fish. Soc. **116**: 703–718.

Robinson, C.L.K., and Tonn, W.M. 1989. Influence of environmental factors and piscivory in structuring fish assemblages of small Alberta lakes. Can. J. Fish. Aquat. Sci. **46**: 81–89.

Sandström, A., and Karås, P. 2002. Effects of eutrophication on young-of-the-year freshwater fish communities in coastal areas of the Baltic. Environ. Biol. Fishes, **63**: 89–101.

Schindler, D.W. 2001. The cumulative effects of climate warming and other human stresses on Canadian freshwaters in the new millennium. Can. J. Fish. Aquat. Sci. **58**: 18–29.

Scott, W.B., and Crossman, E.J. 1973. Freshwater fishes of Canada. Bull. Fish. Res. Board Can. No. 184.

Scrimgeour, G.J., Tonn, W.M., Paszkowski, C.P., and Goater, C. 2001. Benthic macroinvertebrate biomass and wildfires: evidence for enrichment of boreal subarctic lakes. Freshwater Biol. **46**: 367–378.

Shuter, B.J., and Post, J.R. 1990. Climate, population variability, and the zoogeography of temperate fishes. Trans. Am. Fish. Soc. **119**: 314–336.

Sissenwine, M.P. 1984. Why do fish populations vary? *In* Exploitation of marine communities. *Edited by* R.M. May. Springer-Verlag, Berlin. pp. 59–94.

Smith, R.W., and Griffith, J.S. 1994. Survival of rainbow trout during their first winter in the Henrys Fork of the Snake River, Idaho. Trans. Am. Fish. Soc. **123**: 747–756.

Stockner, J.G., and MacIsaac, E.A. 1996. British Columbia lake enrichment programme: two decades of habitat enhancement for sockeye salmon. Regul. Rivers Res. Manag. **12**: 547–561.

Stockner, J.G., and Shortreed, K.S. 1985. Whole-lake fertilization experiments in coastal British Columbia lakes: empirical relationships between nutrient inputs and phytoplankton biomass and production. Can. J. Fish. Aquat. Sci. **42**: 649–658.

Toneys, M.L., and Coble, D.W. 1979. Size-related first winter mortality of freshwater fishes. Trans. Am. Fish. Soc. **108**: 415–419.

Unger, L.M. 1983. Nest defense by deceit in the fathead minnow, *Pimephales promelas*. Behav. Ecol. Sociobiol. **13**: 125–130.

Vandenbos, R.E. 1996. Regulation of recruitment in fathead minnows (*Pimephales promelas*): multi-stage effects and consequences of size-variation. M.Sc. thesis, University of Alberta, Edmonton, Canada.

Wootton R.J. 1977. Effect of food limitation during the breeding season on the size, body components and egg production of female sticklebacks (*Gasterosteus aculeatus*). J. Anim. Ecol. **46**: 823–834.

Wootton, R.J. 1990. Ecology of teleost fishes. Chapman & Hall, London.

© 2002 NRC Canada

Increased metabolic cost of swimming and consequent alterations to circadian activity in rainbow trout (*Oncorhynchus mykiss*) exposed to dietary copper

H.A. Campbell, R.D. Handy, and D.W. Sims

Abstract: This study tests the hypothesis that rainbow trout (*Oncorhynchus mykiss*) compensate for the metabolic cost of dietary Cu exposure by reducing swimming activity at particular times during the diel cycle. Fish were exposed to excess dietary Cu for three months (726 mg Cu·kg^{-1} dry weight) and simultaneously oxygen consumption ($\dot{M}O_2$) and spontaneous swimming activity were measured. Rhythmicity in swimming activity was examined by videorecording fish behaviours for 48 h. Standard metabolic rate estimates (R_s) of 7.2 and 8.7 mmol O_2·kg^{-1}·h^{-1} (15°C) were measured for control and Cu-exposed fish, respectively. $\dot{M}O_2$ was higher in Cu-exposed fish at any chosen speed compared with control Cu-exposed trout, which decreased activity (mean speed) by at least 75%, spent more time at lower speeds, and lost circadian periodicity in these parameters compared with controls. Mean growth rates were normal, although Cu-exposed fish showed a narrower range of body weights and fewer mortalities than control groups, suggesting a suppression in social behaviour in Cu-exposed fish. Overall, the increased metabolic cost of swimming in Cu-exposed fish was fully compensated by a reduction in activity, particularly at night and dawn. However, this behavioural strategy suggests that spatial and temporal aspects of ecologically important social behaviours may be compromised in Cu-exposed fish.

Résumé : Nous voulons éprouver l'hypothèse selon laquelle la truite arc-en-ciel (*Oncorhynchus mykiss*) compense le coût métabolique d'une exposition au Cu alimentaire par une réduction de son activité de nage à des moments précis de son cycle journalier. Nous avons exposé des truites à du Cu alimentaire en excès (726 mg Cu·kg^{-1} de masse sèche) pendant 3 mois et mesuré leur consommation d'oxygène ($\dot{M}O_2$) et leur activité de nage spontanée. Des enregistrements vidéo de 48 h ont permis de déterminer la rythmicité du comportement de nage. Les estimations du métabolisme au repos (R_s) à 15°C sont de 7,2 mmol O_2·kg^{-1}·h^{-1} chez les poissons témoins et de 8,7 mmol O_2·kg^{-1}·h^{-1} chez les poissons traités. La consommation d'oxygène est plus grande chez les poissons exposés au Cu à toutes les vitesses de nage choisies. Par comparaison aux poissons témoins, les poissons exposés au Cu diminuent leur activité (vitesse de nage) d'au moins 75 %, ils passent plus de temps aux vitesses basses et ils perdent la périodicité circadienne de ces activités. Les taux moyens de croissance sont normaux, bien que les poissons exposés au Cu affichent une gamme réduite de masses corporelles et aient une mortalité plus faible, ce qui laisse croire à une suppression des comportements sociaux. De façon générale, le coût métabolique accru de la nage chez les poissons traités est complètement compensé par une réduction de l'activité, particulièrement durant la nuit et l'aurore. Toutefois, une telle stratégie comportementale de la part des poissons exposés au Cu peut probablement compromettre des aspects spatiaux et temporels de comportements sociaux de grande importance écologique.

[Traduit par la Rédaction]

Introduction

Bioenergetics explores the relationships between energy supply and expenditure that defines survival of individual organisms or populations (Kooijman et al. 1999). In essence, an organism may survive if energy intake in the long term equals energy expenditure. Energy intake or assimilation is the net energy acquired from food after digestion and absorption, whereas energy expenditure is associated with somatic maintenance, growth, and reproduction (Elliot and Hurley 1999; Kooijman et al. 1999). In juvenile trout, reproductive costs are negligible, hence most of the energy acquired from food is spent on growth and somatic maintenance (Ohta and Watanabe 1996). The latter includes repair and maintenance

Received 17 July 2001. Accepted 8 February 2002. Published on the NRC Research Press Web site at http://cjfas.nrc.ca on 31 May 2002.
J16451

H.A. Campbell[1,2] **and R.D. Handy.** Department of Biological Sciences and Plymouth Environmental Research Centre, University of Plymouth, Drake Circus, Plymouth PL4 8AA, U.K.
D.W. Sims. Marine Biological Association, The Laboratory, Citadel Hill, Plymouth PL1 2PB, U.K.

[1]Corresponding author (e-mail: h.a.campbell@bham.ac.uk).
[2]Present address: Department of Physiology, University of Birmingham, Edgbaston, Birmingham B15 2TT, U.K.

 DOI: 10.1139/F02-046 © 2002 NRC Canada

of internal organs, and scope for metabolic activities like swimming (Priede 1985; Kooijman et al. 1999). After the cost of standard metabolism (R_s, metabolic rate estimate, for maintenance of physiological systems in an unfed fish), daily energy is expended mostly on digestion and post-feeding activity (specific dynamic action, SDA) or locomotion (Priede 1985). In fact, juvenile trout expend a large portion of the daily energy budget on locomotion (e.g., 74%, Boisclair and Sirois 1993). This locomotor energy is used for behaviours that are vital for survival, such as efficiently searching for prey and avoiding predators.

The concept of a balanced energy budget has been applied to ecotoxicological problems to estimate the biological consequences of spending energy on avoiding exposure, metabolism, storage, or excretion of toxic substances (e.g., Cu, Waiwood and Beamish 1978; McGeer et al. 2000). For many invertebrates, the cost of pollutant exposure is generally met by reducing growth rate or reproductive capacity (e.g., Maltby and Naylor 1990). However, unlike many invertebrates, fish spend a large portion of their energy budget on swimming activities. Energy budgets are also dynamic and the cost of stress may be met by (*i*) increasing energy intake, (*ii*) reducing energy expenditure, and (or) (*iii*) re-allocation of existing energy. In the short term, fish appear to select the latter by making daily adjustments in swimming activity (e.g., Boisclair 1992). Ultimately, however, growth and fecundity of fish may become reduced in response to pollutant exposure (e.g., Cu, McKim and Beniot 1971), possibly as a result of a failed short-term strategy like decreased swimming activity.

Food route exposures to pollutants are of particular concern from a bioenergetic perspective because energy assimilation occurs via the gut, and population growth models are particularly sensitive to changes in energy flux through the food chain (Kooi et al. 1998). Indeed, the bioenergetics of pollutant accumulation and feeding are intimately related (Carlisle 2000) and trout are known to eat metal-contaminated prey in the wild (Dallinger and Kautzky 1985). Handy et al. (1999) showed that trout chronically exposed to dietary Cu appeared to meet the cost of exposure (e.g., tissue Cu accumulation, metallothionein induction) by sparing growth at the expense of lowering locomotor activity. There were also changes in the patterns of fat deposition in the liver of Cu-exposed fish, suggesting subtle changes in energy metabolism associated with the apparent trade-off. Increased mitochondrial density in the intestinal mucosa of dietary Cu-exposed fish (Kamunde et al. 2001) also support the notion of compensatory metabolic change.

In this paper we further explore these energy expenditure events in contaminated fish, by measuring oxygen consumption rates (MO_2, a relative measure of aerobic metabolic rate, Priede 1985) and spontaneous activity over the diel (24-h) cycle. We improve on previous attempts to relate MO_2 with activity (e.g., Waiwood and Beamish 1978; Wieser 1985) by simultaneously recording these parameters on individual free-swimming fish. Furthermore, because activity levels of trout normally change over the diel cycle (e.g., Sanchez-Vazquez and Tabata 1998), it is possible that the locomotor trade-off in response to Cu exposure occurs at particular times, rather than throughout the day. We therefore record diel activity patterns, and for the first time show depression of the diel rhythm of fish in response to aquatic contaminants. Finally, since swimming activity is vital for the establishment of normal social hierarchies during social feeding in trout, and dominant fish will receive the most food (McCarthy et al. 1992) and therefore greatest Cu exposure, we also follow the distribution of body size and mortality during the experiment.

Materials and methods

Dietary Cu exposure

Rainbow trout (*Oncorhynchus mykiss*) weighing 5 ± 0.2 g (mean ± standard error (SE), n = 200) were obtained from Hatchlands Fish Farm (Rattery, Devon). The fish were held for 14 days in stock aquaria (800 L) supplied with recirculating freshwater (in mmol·L^{-1}, means ± SE, n = 48: Ca, 0.48 ± 0.004; Mg, 0.13 ± 0.006; Na, 0.43 ± 0.008; K, 0.07 ± 0.004; Cu, <0.001; NH_3 0.024 ± 0.015; pH 6.8 ± 0.05; dissolved oxygen, 85% ± 4; temperature, 15°C ± 1.2), and were fed a control diet supplemented with a prophylactic antibiotic (oxylinic acid, 2 mg·kg^{-1} dry weight, dw, feed) for the first 10 days. The exposure aquarium consisted of six (185-L) tanks (33 fish per tank), with fresh water circulation via an 800-L biofilter. Fish were randomly distributed and allowed a further seven-day acclimation period, during which all fish were fed to satiation on a control diet (see below). After this period, three of these tanks were chosen at random and allocated to a Cu-contaminated diet containing a nominal 730-mg Cu·kg^{-1} dw feed; three tanks remained as controls (nominal 11-mg Cu·kg^{-1} dw feed). The Cu-contaminated diet was within the range found in invertebrates ingested by trout in chronically contaminated freshwater ecosystems (Dallinger and Kautzky 1985) and close to the maximum tolerable dietary Cu load for trout in terms of growth and normal haematology in aquaculture situations (Lanno et al. 1985). A 2% body weight ration was size-calculated and supplied to all tanks as a single meal at about 15:00 daily. Fish were observed during feeding to ensure that all food given was eaten. Pre- and post-feeding water quality analysis showed no rise in aqueous Cu levels, which remained <0.1 µmol·L^{-1} throughout the experiment. The experimental exposure was carried out from 1 Feb. 1999 to 19 April 1999 (84 days). The fish were held under a constant 12 h light : 12 h dark photoperiod during this time.

Diet formulation

Diets were formulated according to Handy et al. (1999), except the Cu-supplemented diet contained a nominal 730 mg·kg^{-1} dw feed. Cu was added as $CuSO_4$ dissolved in 300 mL water then mixed into the dry ingredients. Diets were extruded, pelleted, and dried at 40°C for 48 h. To prevent the oxidation of diets by Cu during storage, the food was frozen at –20°C and removed 2 h before feeding to defrost. Cu content of the Cu-exposure and control diets, determined by Inductively Coupled Plasma Atomic Emission Spectroscopy (ICPAES), were (mean ± SE, n = 5) 726 ± 1.6 and 23.3 ± 1.25 mg·kg^{-1} dw, respectively.

Blood biochemistry

A number of haematological and biochemical parameters were measured in control and Cu-exposed fish at the end of

© 2002 NRC Canada

the experiment (week 12). To confirm Cu exposure, tissue Cu concentrations (see below) as well as hepatic and intestinal metallothionein (MT) levels (Viarengo et al. 1997) were measured. Since Cu toxicity is known to cause haematological disturbances (e.g., Pilgaard et al. 1994), several blood parameters were therefore measured in caudal blood samples. These were haematocrit, red and white blood cell counts, serum protein, glucose, and triglycerides, according to Handy et al. (1999).

Trace metal analysis

Ion concentrations within individual organs were measured to confirm Cu exposure and to outline any major ionic disturbances in tissues collected from control and Cu-exposed fish at the end of the experiment (week 12). Fish were terminally anesthetized (buffered pH 7, MS 222, 0.5 $g \cdot L^{-1}$) and whole organs were sampled in the following order: muscle, gill, liver, heart, intestine, spleen, brain, and eyes. The tissue was rinsed in deionised water, dried to constant weight at 80°C for 48 h, weighed, and then digested in 0.5 mL 4-M HCl and 0.5 mL 4-M HSO_4. Ion analysis was carried out by ICPAES (Handy et al. 1999) for Ca, Cu, K, Mg, and Na. All ions were above detection limits (micromolar), except Cu, which was only detected in the liver and intestine (<0.96 $\mu mol \cdot L^{-1}$).

Computer-aided tracking of swimming activity

For analysis of swimming activity and associated behaviours an Ethovision Behavioural Tracking System (Tracksys Ltd., Nottingham, U.K.) was used. This consisted of a Sanyo CCD (charged coupled device) B/W videocamera suspended 1.5 m above the appropriate tanks. The camera was connected directly to a computer (Fujitsu Intel 80286), and the analogue image of the fish was translated into digital information by a TARGA+ frame-grabbing card (Truevision, The Netherlands), which enabled the fish to be tracked in real time at a rate of 4 frames$\cdot s^{-1}$. The computer software (Noldus software, U.K.) calculated the x–y co-ordinates of each fish's centre within defined arenas by comparing the fishes' contrast level with that of the white background (for details of tracking methodology see Winberg et al. 1993). From these point positions, the absolute movement of each fish between time intervals was determined. This software also calculated behavioural parameters, which included total distance moved (cumulative change in position of the fish between consecutive video images) and swimming speed (total distance moved per unit time). Each track was monitored visually during recording to ensure fish were tracked accurately. Tracks showing image interference >0.5% were discarded; overall, 10% of tracks were not included in the analyses for this reason.

Simultaneous MO_2 and swimming speed measurements

MO_2 was measured to indicate aerobic metabolic rate, and back extrapolation of MO_2 at zero swimming activity was used to calculate standard metabolism (Brett 1964). MO_2 and swimming speed of individual fish were recorded simultaneously. The respirometry chamber used was constructed out of opaque Perspex with a transparent lid (40 L × 20 W × 20 H cm), and water flow was set at 2 $cm \cdot s^{-1}$. Water quality parameters were maintained as above. Each week six fish were randomly selected (3 control, 3 Cu treated) and were individually placed (randomly) in one of seven independent respirometers arranged in parallel, with one respirometer remaining empty so bacterial oxygen demand during experiments could be calculated. After a 48-h acclimation period, all six fish were tracked simultaneously for 2 h using the Ethovision behavioural tracking system (as described above). Fish were not fed during the acclimation period or during tracking experiments. At the same time MO_2 was determined for each respirometer, using a flow system for which discrete water samples could be redirected from individual respirometer via a flow-cell containing a combined oxygen–temperature (WTW OX325) and a pH probe (WTW SenTix 41-3). The water was then returned back to the sampled respirometer via a peristaltic pump without disturbing the fish. Using this method, water from each respirometer could be sampled for oxygen concentration every 8 min. Fish tended to hold position in the current, thus swimming at 2 $cm \cdot s^{-1}$; additional forays around the respirometer chamber were, however, made by the fish and this spontaneous swimming was recorded via a camera above the chamber. At the end of respirometry and swimming speed measurements, fish were returned their appropriate tank. Triplicate tanks within the experimental design were sampled in rotation for respirometry. This ensured that fish had at least a three-week rest period before fish within each tank were sampled again (probability of selecting the same individual again <0.1%).

Weekly changes in specific swimming speed

Four fish from each treatment were removed at random from the exposure aquarium every seven days to assess long-term temporal changes in locomotor behaviour due to Cu exposure. The fish were placed separately into rectangular arenas (45 W × 70 L × 30 H cm), with arenas positioned side by side, to enable activity recording of all arenas simultaneously. Each arena contained 40 L of filtered, aerated water with quality identical to the exposure aquarium. The fish were given 48 h to acclimate to the arenas and their behaviour was then tracked for a 2-h period using the Ethovision behavioural recognition system (distance moved per unit time as described above). Fish were returned to their appropriate tanks in the exposure aquaria after video tracking.

Circadian behaviour after 12 weeks Cu exposure

After 12 weeks of Cu exposure (end of the experimental exposure), eight fish were chosen at random from each treatment for analysis of behavioural parameters over two consecutive 24-h (diel) periods. The arenas used and the locomotion parameters recorded were the same as the weekly locomotor measurements, except fish were each monitored for 48 h. Infrared battery lighting (Tracksys Ltd., Nottingham, U.K.) was used to illuminate the arenas during the hours of darkness. An infrared filter lens was fitted to the video camera to enable fish recognition by the computer in both dark and light regimes. Fish tracks were recorded for 30 min in each hour of the 48-h period. From these individual tracks of each fish, locomotory parameters were calculated using software for each hour of the two-day period to determine relative changes in activity of individual fish over the circadian cycle.

© 2002 NRC Canada

Growth

The total fish biomass in each tank was weighed fortnightly as a single group measurement, which reduced the possibility of handling stress, compared with individually measuring weight and length in individual fish. Individual measurements were, however, made at weeks 6 and 12 to give an indication of the variability in size distribution of fish within each treatment.

Statistical analysis

Data were analysed in a similar way to Handy et al. (1999) for tissue mineral content, haematology, biochemistry, and $\dot{M}O_2$ (triplicate tanks within treatments were compared and pooled prior to analysis), using the *t* test, or Mann–Whitney *U* test where appropriate for nonparametric data. Linear regression of $\dot{M}O_2$ against activity was used to determine metabolic rate (Brett 1964), and slopes of the regression lines were compared between treatments by analysis of covariance (ANCOVA). Swimming speed was expressed as specific swimming speed (body lengths, $BL \cdot s^{-1}$) to normalize the data for body length effects. Similarly, $\dot{M}O_2$ was corrected for weight-specific changes in metabolic rate to the exponential of 0.8 (Cech 1990).

Data only from the circadian rhythm experiments were analyzed as follows. The first approach employed periodogram analysis (Williams and Naylor 1978) to detect oscillations in time-series data. A computer program (Styrishave et al. 1995) was used to calculate the amplitude (standard deviation of the hourly means of activity) and confidence intervals (derived by randomizing data and performing periodogram analysis) for the given behavioural parameter. When plotted graphically, if true periodicity exists, the peak statistic produced by the assumed period length (24 h) will exceed the confidence interval on the plot ($P < 0.05$). Fish were tested for periodicity both as individuals and as group means for each treatment. Second, data for individual fish over the 48-h cycle were grouped into four time zones over the 24-h clock to compare differences in activity between control and Cu fish at different time periods. These groups were determined by mean relative changes in the control fish general activity (expressed as total distance moved). These were 12:00–18:00 (day), 18:00–00:00 (dusk), 00:00–06:00 (night), and 06:00–12:00 (dawn). To test the combined effects of Cu and photoperiod on activity, ANCOVA was used. In all the statistical analyses, differences at the $\alpha \leq 0.05$ level were considered significant.

Results

Tissue Cu levels and biochemistry

Cu-exposed fish showed higher Cu concentrations in the intestine and liver compared with controls (which were below detection <0.096 $\mu mol \cdot g^{-1}$ dw, Table 1). Cu concentrations within the gills and other organs (brain, spleen, heart, and striated red and white muscle) remained below detection regardless of treatment. MT levels were significantly elevated in liver (8-fold; *t* test, $t = -20.44$, $P < 0.0005$) and intestines (2-fold; $t = -6.04$, $P = 0.0005$) of Cu-exposed fish compared with controls (Table 1). Na, K, Ca, and Mg concentrations in most organs were not significantly different between treatments (*t* test, $P < 0.05$). For example, brain Na and K concentrations (mean ± SE, $n = 8$) were 283 ± 23 and 37.9 ± 4.1 $\mu mol \cdot g^{-1}$ dw, respectively, in Cu-exposed fish compared with 293 ± 34 and 36.3 ± 2.7 $\mu mol \cdot g^{-1}$ dw in controls. In striated muscle, Na and K concentrations were 71.6 ± 3.7 and 98 ± 12.9 $\mu mol \cdot g^{-1}$ dw, respectively, in Cu-exposed fish compared with 56.3 ± 5.6 and 76.36 ± 15.3 $\mu mol \cdot g^{-1}$ dw in controls. Thus, Na–K ratios in both brain (Na:K ~ 8) and muscle (Na:K = 0.7) were normal. Similar observations on Na and K concentrations were made for the heart. The spleens of Cu-exposed fish had lower levels of Ca (control, 198.0 ± 33.7 $\mu mol \cdot g^{-1}$ dw; exposed, 51.4 ± 1.9 $\mu mol \cdot g^{-1}$ dw, $n = 8$) and Mg (control, 92.5 ± 21.9 $\mu mol \cdot g^{-1}$ dw; exposed, below detection, <0.05 $\mu mol \cdot g^{-1}$ dw, $n = 8$). No disturbance to general haematology (haemoglobin, red and white cell counts, protein, or glucose) was observed at the end of the exposure period (Table 1).

$\dot{M}O_2$ measurements

The relationship between swimming speed and $\dot{M}O_2$ in control and Cu-exposed fish is shown in Fig. 1, and as expected, $\dot{M}O_2$ increases with swimming speed. However, Cu-exposed fish require more O_2 than control fish to maintain a given swimming speed. R_s was calculated by back extrapolation of the $\dot{M}O_2$ data to zero swimming speed. R_s was 7.17 and 8.69 mmol $O_2 \cdot kg^{-1} \cdot h^{-1}$ for control and Cu-exposed fish, respectively. These values of R_s were significantly different from each other, based on ANCOVA of the regression lines of the mean $\dot{M}O_2$ plots for each treatment (assuming unequal intercepts, $F = 46.7$, $P < 0.01$). $\dot{M}O_2$ rates in Cu and control fish are similar up to swimming speeds of about 0.065 $BL \cdot s^{-1}$. At higher levels of swimming activity, Cu-exposed fish required proportionally more O_2 to maintain a given speed, resulting in a significantly different aerobic scope between treatments (ANCOVA, assuming unequal slopes, $F = 5.91$, $P = 0.019$). Routine $\dot{M}O_2$ during spontaneous activity, determined by mean $\dot{M}O_2$ levels, irrespective of swimming speed, were significantly higher (Mann–Whitney *U* test $P < 0.05$) in the Cu-exposed fish (mean ± SE $n = 30$: control, 10.1 ± 0.4 mmol $O_2 \cdot kg^{-1} \cdot h^{-1}$; Cu exposed, 13.1 ± 0.7 mmol $O_2 \cdot kg^{-1} \cdot h^{-1}$).

Cu-exposed fish also showed a marked interindividual variability in metabolism compared to control fish. For example, R_s estimates for individual control fish were typically 7 mmol $O_2 \cdot kg^{-1} \cdot h^{-1}$, but values for Cu-exposed fish ranged from 7 to 11 mmol $O_2 \cdot kg^{-1} \cdot h^{-1}$ (mean ± SE $n = 30$–60 fish: control 7.1 ± 0.23 mmol $O_2 \cdot kg^{-1} \cdot h^{-1}$; Cu-exposed 8.6 ± 1.8 mmol $O_2 \cdot kg^{-1} \cdot h^{-1}$). Variances in spontaneous swimming activities of Cu-exposed fish were 3.7 times higher than controls for speeds up to 0.1 $BL \cdot s^{-1}$ (variance, controls 7.2, $n = 30$; Cu exposed, 26.7, $n = 60$), and 11 times higher than controls at speeds between 0.1 and 0.2 $BL \cdot s^{-1}$ (variance, controls 6.2, $n = 34$; Cu exposed, 69.2, $n = 24$). Only four Cu-exposed fish achieved speeds >0.2 $BL \cdot s^{-1}$, compared with 24 control fish.

Weekly changes in specific swimming speed

Cu-exposed fish showed a general decline in specific swimming speed compared with that of controls, which remained relatively constant during the 12-week Cu exposure (Fig. 2). The grand mean spontaneous swimming speed for control and Cu-exposed fish over the 12-week period was 0.31 ± 0.015 and 0.21 ± 0.015 $BL \cdot s^{-1}$ (mean ± SE, $n = 96$,

© 2002 NRC Canada

Table 1. Metal accumulation and biochemistry after 12 weeks dietary Cu exposure.

	Control diet (23 mg Cu·kg feed^{-1})	Cu diet (726 mg Cu·kg feed^{-1})
Liver [Cu] (Mmol·g^{-1} dw).	4.68 ± 0.65	17.37 ± 0.36*
Intestine [Cu] (μmol·g^{-1} dw)	<0.096	1.72 ± 0.07
Hepatic MT (μg·g^{-1} ww)	18.3 ± 1.8	143.9 ± 6.2*
Intestinal MT (μg·g^{-1} ww)	15.3 ± 2.8	30.8 ± 2.1*
Gill MT (μg·g^{-1} ww)	33.1 ± 1.1	27.2 ± 4.7
Red blood cells (10^6 mm^3)	0.74 ± 0.04	0.75 ± 0.03
White blood cells (10^3 mm^3)	11.9 ± 2.0	14.9 ± 2.5
Haemoglobin (g·dL^{-1})	7.19 ± 0.13	7.04 ± 0.10
Serum glucose (mmol·L^{-1})	6.4 ± 0.4	7.4 ± 0.4
Serum protein (g·L^{-1})	15.4 ± 2.4	13.0 ± 0.9

Note: Data are mean ± standard error (n = 8, except cortisol, n = 5). An asterisk (*) indicates Cu-exposed data that are significantly different from controls (t test, $P < 0.05$). ww, wet weight; dw, dry weight. Note that Cu levels were below detection (<0.096 μmol·g^{-1} dw) in all internal organs examined (brain, spleen, heart, and striated red and white muscle), except the liver and intestine above. Statistics are not shown for intestinal [Cu] because controls are below detection limit. MT, metallothionein.

Fig. 1. The relationship between voluntary spontaneous swimming speed and O_2 consumption rate (MO_2). Data are mean and standard error (SE) for individual fish (●, control; ○, exposed). The vertical error bar represents SE of MO_2 measurements made at 8-min intervals over a 2-h sampling period for each fish, and horizontal bars are SE for specific swimming speed over the 2-h period as determined by Noldus tracking software. Linear regression lines are fitted (Sigma-plot 4) for control ($y = 4.157x + 7.17$, $r^2 = 0.501$, $P < 0.001$, $n = 30$) and Cu-exposed fish ($y = 8.36x + 8.69$, $r^2 = 0.486$, $P < 0.001$, $n = 30$) with 95% confidence intervals for each regression line (ANCOVA of intercepts, $F = 46.7$, $P < 0.01$, and slopes $F = 5.91$, $P = 0.019$). Data were collected between weeks 4 and 12 of the experiment. Data were corrected for weight-specific changes in metabolic rate to the exponential of 0.8 (Cech 1990).

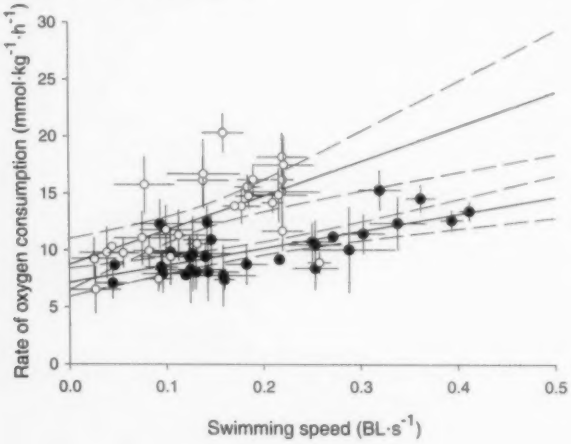

Fig. 2. Weekly changes in spontaneous net swimming speed over 12 weeks exposure to dietary Cu. Data are mean and standard error, n = 8 (●, control; ○, exposed). Net swimming speed of individual fish was recorded in 2-h sessions using the Ethovision tracking system every week. Data within treatment from each two-week period of the Cu exposure were pooled prior to analysis. Note that net swimming speed is an average of all swimming speeds observed from "stationary" position holding to voluntary burst swimming within the recording period. *, Cu-exposed fish significantly different from control at that time point (t test, $P < 0.05$); #, significantly different from data in first fortnight of the experiment (t test, $P < 0.05$).

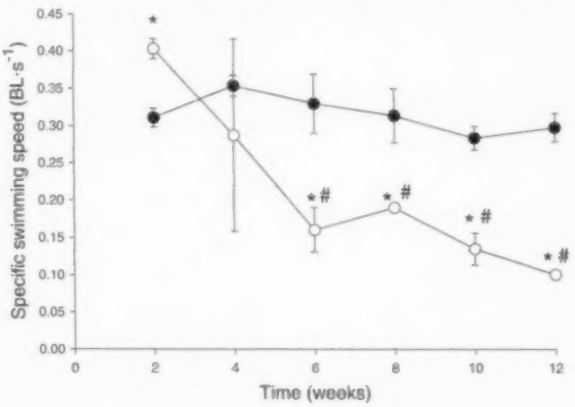

significantly different t test, $P < 0.05$), respectively. Cu-exposed fish displayed an initial period of hyperactivity, caused by them swimming 20% farther than controls. During weeks 3 and 4 there was a switch in the behaviour of Cu-exposed fish from hyperactivity to hypoactivity. The time lag of the switching response varied between individuals, producing a large variance in the Cu fish data in the pooled data for weeks 3–4 (Fig. 2). By week 6 the specific swimming speed of Cu-exposed fish was significantly lower (t test, $t = -1.24$, $P = 0.002$) than controls (50%), and by the end of the experiment this difference had increased to 66%.

Circadian behaviour after 12 weeks Cu exposure

Cu exposure had a dramatic effect upon the circadian behaviour of trout, substantially reducing the normally high nocturnal activity (Figs. 3 and 4). Control fish showed circadian rhythmicity in all behavioural parameters measured over a continuous 48-h period (periodogram analysis, S = 24 h, for mean swimming speed and maximum swimming speed). However, Cu-exposed fish showed a general loss of periodicity in behavioural parameters compared with con-

© 2002 NRC Canada

Fig. 3. Circadian swimming activity of control (●) and Cu-exposed (shaded triangles) fish over a 48-h period (n = 8) after 12 weeks Cu exposure. Data are normalized for the interanimal variability in basal activity by expressing each data point as a measured percent increase in activity over that individual's lowest recorded level of activity. The data points are fitted with a waveform line to visualize the general trend only and is not intended to imply statistically significant rhythmicity (see below). (*a*) Mean speed (control r^2 = 0.38; Cu r^2 = 0.249; $P < 0.001$ for both curve fits), (*b*) Maximum speed attained (control r^2 = 0.626; Cu r^2 = 0.477; $P < 0.001$ for both curve fits). Solid horizontal bars indicate periods of darkness. Each measured parameter has a graphical representation of the periogram statistic (S) performed on both control and Cu data sets (figure insert in each panel). Dotted and broken lines show confidence limits set by periogram analysis performed on randomization of the data set. Where S peaks above the upper confidence limit, periodicity is observed in the data. Duration of each period (h) is determined by the highest point of the peak.

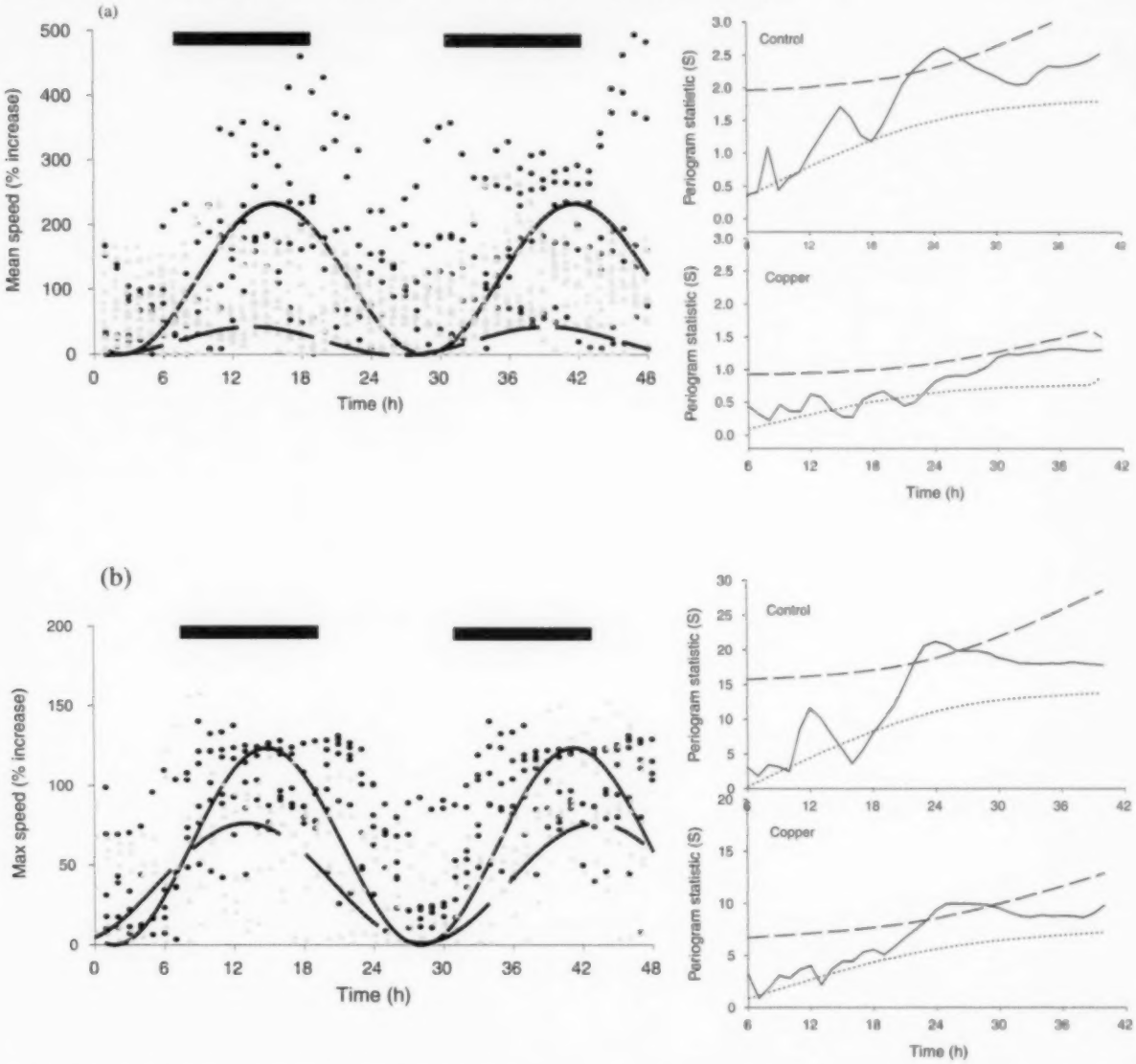

trols (Fig 3.), with only a statistically significant periodicity (S = 24 h) remaining in the maximum spontaneous swimming speed attained (Fig. 3*a*). Interestingly, whereas Cu-exposed fish showed periodicity in this maximum speed, it was not evident in the mean speed data (compare Figs. 3*a* and 3*b*). Since these latter parameters are calculated components of total distance moved, they therefore show that Cu-exposed fish spent proportionally more time at low speed (or resting) than control fish.

For further analyses of behavioural patterns, we divided the 24-h cycle into four equal time periods (day, dusk, night, dawn, see Fig. 4). During the 6-h continual daylight period (day), both control and Cu fish exhibited similar behaviour patterns, spending 55–60% of their time resting (<2 cm·s^{-1}),

© 2002 NRC Canada

Fig. 4. Mean changes in percent time (± standard error, $n = 16$) spent by (*a*) control and (*b*) Cu-exposed rainbow trout in four speed bins (<2, 2–10, 10–20, 20+ cm·s^{-1}) during a 24-h period after 12 weeks Cu exposure. In terms of BL·s^{-1}, these speed bins are <0.1, 0.1–0.5, 0.5–1.0, and >1.0, respectively (representing position holding, slow, medium, and high speeds). The 24-h clock has been divided into four time zones (day, dusk, dark, and dawn) each 6 h in length, and total darkness is represented by black horizontal bar. *, Cu data that is significantly ($P < 0.05$, *t* test) different from the equivalent speed bin in the control data set; + indicates a speed bin that is significantly different ($P < 0.05$, *t* test) from the speed bin in the previous time zone within treatment.

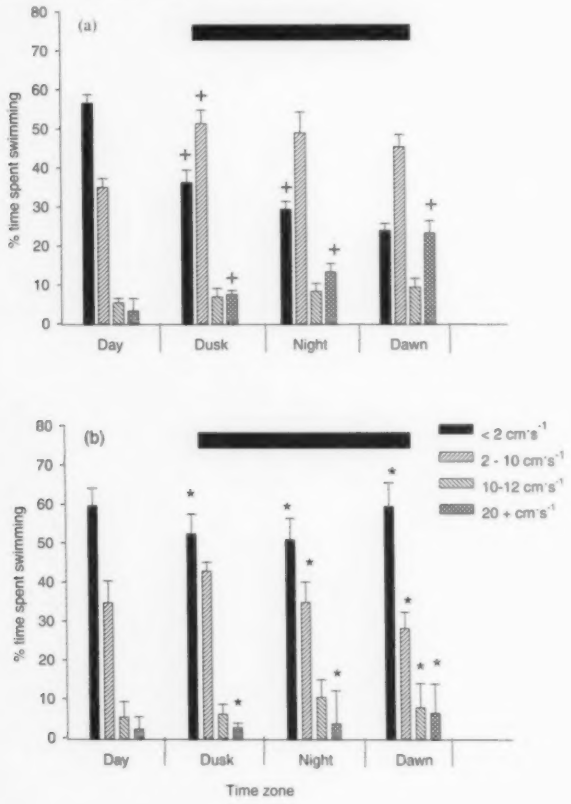

35% at low swimming speeds (2–10 cm·s^{-1}), 5–6% at medium speeds (10–20 cm·s^{-1}), and less than 2% of the time at high speeds. However, in the following period (dusk) when only 3 h of daylight occurred before dark, control fish altered their swimming patterns, resulting in an increase in overall activity. During this time, resting was reduced to 36%, low swimming activity was increased to 50%, and both medium and high swimming activity increased by 3–4%. Cu-exposed fish spent 10% more time swimming at slow speeds rather than resting, however, and spent significantly longer times resting in this period than controls (although their activity did increase slightly). Once into the period of full darkness (night), control fish continued to increase activity spending proportionally (30%) less time resting and at low speeds and more time (15%) at high speeds. This increase in activity was carried over into dawn where control fish spent 22% of their time swimming at a high speed and an equal amount of time resting. In contrast, Cu-exposed fish did not show similar increases in activity. Over the dark period they did not reduce their resting frequency but showed a reduction in low-speed swimming to 33%, whereas the time spent swimming at medium speeds increased to 12%. Once into the period of dawn where highest activity was exhibited by controls, there was an alteration in the behaviour of exposed fish, which increased the time spent resting and decreased swimming time at low and medium speeds, but spent 5% more time at high speeds. There was, however, still significantly less (Mann–Whitney *U* test, $U = 60$, $P = 0.0004$) than time spent high-speed swimming by control fish (22%).

Growth and variation in body size

There was no difference in the median growth rate of the control and Cu-exposed fish (Mann–Whitney *U* test, $U = 1182.5$, $P = 0.68$) at the end of the experiment (Fig. 5). Mean body weight (nonsignificant *t* test, $P > 0.05$) at the end of the experiment was 21.7 ± 9.0 g (control, $n = 44$ fish) and 18.4 ± 5.1 g (Cu exposed, $n = 47$ fish). However, the distribution of body weights within each tank differed between fish fed a control and Cu-contaminated diet (Fig. 5). These differences were not evident after six weeks of Cu exposure (data not shown). However, at week 12 (end of the experiment), the variability in individual fish weight for fish fed a control diet was significantly greater (variance 79.7, $n = 45$ fish) than in fish fed a Cu diet (variance 32.7, $n = 45$ fish). In control tanks, fish weight distribution became skewed towards larger body size as the number of outliers in the lower quartile was reduced and the upper quartile was extended owing to a small percentage of increasingly larger individuals. Control fish showed the normal aggressive behaviour of trout, and as expected, some mortalities occurred as the fish increased in size, whereas stocking density declined during the experiment because of sampling. The mortality within the total population was 9.6% and 4.0% for control and Cu treatments, respectively (Fig. 5). All mortalities in control tanks were of small fish below the group quartile size range for that treatment group (mean weights shown in Fig. 5). These small fish showed signs of social subordination with severe fraying of the dorsal and caudal fins—a condition typical of lower ranked individuals (Turnbull et al. 1998). In comparison, fewer mortalities occurred in the Cu-exposed fish with none occurring in the latter half of the experimental period. The dead fish were not of a size below the group median and did not show signs of physical damage, appearing to have died from causes other than interindividual aggression.

Discussion

Tissue Cu levels and biochemistry

The pattern of tissue Cu accumulation and MT induction is typical of chronic dietary Cu exposure, with increased levels of Cu and MT induction only in the intestine and (or) liver, and with no change in these parameters in the gills (Berntssen et al. 1999; Handy et al. 1999). The absence of tissue electrolyte disturbances, the normal haematology, and the absence of any effects on overall growth rate between

© 2002 NRC Canada

Fig. 5. Distribution plots of individually weighed fish from control (open boxes) and Cu-exposed (shaded boxes) fish from each of three tanks per treatment (n = 14–16 fish in each tank at week 12), and pooled data within treatment. Median value represented by vertical black line through box. Tails show 95% quartile. *, significantly different distribution of body size in each tank of Cu-treated fish compared with all control tanks ($P < 0.05$, Kolmogorov–Smirnov) from all control data. Tank 1 in the Cu treatment was different from control tanks 2 and 3 only. Initial fish weight was 5 g. At the end of experiment, fish had similar mean weights of around 20 g. Mortality rates for each tank are indicated, expressed as a percentage of the total cumulative mortality in the tank for the entire experiment. The mortality rate for pooled data is for all fish within treatment. Cont., control.

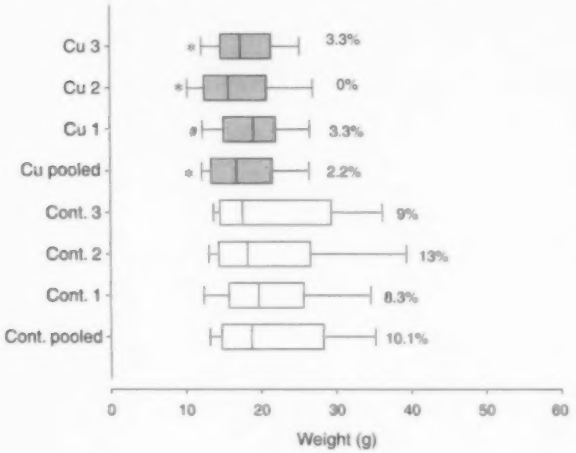

treatments suggest that fish remained generally healthy. These observations are consistent with our previous study (500 mg Cu·kg^{-1} diet for 12 weeks, Handy et al. 1999), despite the higher Cu dose used here (726 mg·kg^{-1} diet), and were similar to those of Kamunde et al. (2001) using a Cu exposure of 1000 mg Cu·kg^{-1} dw feed for four weeks. Lanno et al. (1985) reported reduced growth at the Cu concentration used here; this difference may be attributed to differences in Cu bioavailability in the feed formulations.

Effect of Cu on metabolic rate

The values for R_s were obtained by back extrapolation of $\dot{M}O_2$ to zero swimming activity using a well-established technique (Brett 1964). R_s values for control and Cu fish were 7 and 9 mmol O_2·kg^{-1}·h^{-1} (15°C), respectively. Such data derived from fish showing voluntary spontaneous swimming activity are rare, as most previous studies forced fish to exercise at a constant forward velocity in a tunnel respirometer (3.0 mmol O_2·kg^{-1}·h^{-1}, Skidmore 1970; 4.8 mmol O_2·kg^{-1}·h^{-1}, Webb 1971, at 15°C). The higher R_s values in our study reflect the higher metabolic cost of complex spontaneous swimming compared with simple linear swimming. For the latter, back-extrapolation of $\dot{M}O_2$ may underestimate R_s (Soofiani and Priede 1985; Forstner and Wieser 1990). The higher R_s estimates for Cu-exposed compared with control fish here are consistent with that of early reports for acute aqueous Cu exposure (R_s increasing from about 5 to 7 mmol O_2·kg^{-1}·h^{-1} during 40 μg·L^{-1} Cu exposure at 12°C, Waiwood and Beamish 1978), which implies additional maintenance costs (e.g., repair to damaged tissue). McGeer et al. (2000) reported a steeper slope on the $\dot{M}O_2$ versus swimming speed plot for trout chronically exposed to 75 μg·L^{-1} aqueous Cu compared with controls, suggesting a lower R_s in Cu-exposed fish. The reason for this difference in R_s between acute and chronic aqueous Cu exposure is unclear, given that McGeer et al. (2000) also report ionoregulatory disturbances that would tend to increase R_s. The biological significance of increased variance in $\dot{M}O_2$ in Cu-exposed fish compared with controls is uncertain, but has also been noted in trout at high swimming speeds following chronic aqueous Cu exposure (McGeer et al. 2000). In this study, R_a, active metabolic rate, was not measured directly; however, the increased $\dot{M}O_2$ recorded for Cu-exposed fish, while being more inactive than controls, suggests that R_a is diminished when feeding on a Cu-contaminated diet. The relationship between $\dot{M}O_2$ and swimming speed (BL·s^{-1}) in Cu-exposed fish compared with controls was not an artefact of the cost of swimming at different body sizes (growth during the experiment) because (*i*) $\dot{M}O_2$ data were corrected for weight-specific metabolic rate (0.8, Cech 1990) and change in this exponent is negligible over the body weight ranged used here (Bochdansky and Leggett 2001); and (*ii*) mean change in body weight and length over the experiment were the same for both treatments, thus mean power requirements for swimming in relation to body length were also the same.

Do long-term reductions in locomotor activity meet the extra cost of swimming in Cu-exposed fish?

On a daily basis, trout adopt a very conservative power-budgeting strategy for locomotion, with maximum power output in trout only occurring <1% of the time (Soofiani and Hawkins 1982; Priede 1985). This strategy ensures that the fish can carry out its normal functions while minimizing the probability of exceeding metabolic scope, and therefore potential mortality (Priede 1977). After an initial period of hyperactivity probably associated with avoidance behaviour (Scarfe et al. 1982), Cu-exposed trout decrease their specific swimming speed overall by 66% (from 0.29 BL·s^{-1} in week 4 to 0.1 BL·s^{-1} in week 12) compared with no change in the controls. If this decrease in swimming speed is related to $\dot{M}O_2$, then this equates to a routine metabolic saving of about 5 mmol O_2·kg^{-1}·h^{-1}. Even if the period of hyperactivity at the start of the experiment is included, this still equates to ~30% savings in the observed routine metabolic scope of Cu-exposed fish over the entire experiment. In fact, by the end of the experiment, the specific swimming speed of Cu-exposed fish decreased to around 0.1 BL·s^{-1}, so that their metabolic demands were similar to that of the control fish operating at around 0.3 BL·s^{-1}. Cu-exposed fish had almost fully compensated for the added cost of swimming by reducing swimming speed, and therefore matched their energy costs to the controls. Under these conditions, theoretically, the probability of long-term survival of both groups of fish is equal (Priede 1977).

Circadian locomotor activity

Most species of fish exhibit a diel pattern in activity (Boujard and Leatherland 1992). Salmonids can adopt a nocturnal, diurnal, or crepuscular rhythm in peak activity, and

© 2002 NRC Canada

these rhythms are responsive to variations in environmental temperature, light intensity, predation risk, and food availability (Heggenes et al. 1993; Metcalfe et al. 1999). In this laboratory study, control rainbow trout exhibited a circadian rhythm in mean and maximum swimming speed, with a periodicity of approximately 24 h (diel), where activity increased during the dark phase and peaked around dawn. Twelve weeks of chronic dietary Cu exposure abolished much of this rhythm in activity, with exposed fish swimming at a lower mean speed (covering less distance) compared with controls during darkness. To our knowledge, this is the first report of an aquatic pollutant disrupting the circadian locomotor rhythm of fish.

Similar to our previous findings recorded during daylight (11:00–13:00) using a lower Cu dose (500 mg Cu·kg^{-1} dw feed, Handy et al. 1999), Cu-exposed trout in the present study spend less time active, and spend proportionally more time at lower swimming speeds than controls. This reduction in activity of Cu-exposed fish, when compared with control fish, was much more prominent during the night, particularly in the period leading up to dawn when the swimming activity of control fish peaked.

We interpret the loss of circadian activity in Cu-exposed fish as a compensatory response to ensure the animal remains within metabolic scope over each 24-h period. To compensate for the relatively higher metabolic demands of swimming at high speed, Cu-exposed fish spend relatively more time at rest or at low swimming speeds, especially during the night. This behavioural strategy seems to work. If mean swimming speeds are calculated for the 24-h period, they are 0.46 ± 0.11 and 0.21 ± 0.07 BL·s^{-1} (mean ± SE, n = 8) for control and Cu fish, respectively. If these speeds are used to calculate routine metabolic rate, both treatments have very similar $\dot{M}O_2$ values of around 14 mmol·kg^{-1}·h^{-1}. In other words, over a 24-h period, the aerobic costs of control and Cu-exposed fish are the same.

Distribution of body size and growth rate

There were no overall differences in mean growth rates between treatments, which is in agreement with recent studies (e.g., Handy et al. 1999; Kamunde et al. 2001). However, there was a decreased range of body weight distribution in Cu-exposed fish compared with controls by the end of the experiment. This was not an artefact of tank position, because no differences were observed between tanks (populations) within treatments. The smallest fish in control treatments showed severe fraying of fins typical of subordinate fish (Turnbull et al. 1998). There was a background level of associated mortality, consistent with the normal aggressive social behaviour of trout, and the formation of a domination–subordination hierarchy with increased ranges of body mass within the social group (McCarthy et al. 1992). Cu-exposed fish showed none of these normal traits, and coupled with a relatively uniform distribution of body weights in each Cu-fed treatment, suggests reduced hierarchical behaviours. This apparent loss of aggressiveness is also consistent with reduced locomotor activity over the diel cycle in Cu-exposed fish.

Ecological implications

In this experiment, Cu-exposed trout appear to compensate for the proportionately higher Cu-induced metabolic costs at a given swimming speed compared with controls by reducing locomotor activity, and consequently, social interactions at night and dawn. This alternative behavioural strategy appears to offer Cu-exposed fish no long-term metabolic disadvantage compared with controls. Extrapolation of these laboratory observations to wild fish suggests that the social competitive ability of fish in the wild could decline during chronic, sublethal pollution scenarios. Intraspecific competitiveness is central to the natural selection processes of survival and reproduction (Dawkins 1995). In this study we have shown that Cu induced metabolic changes in fish, resulting in altered daily activity patterns. Any associated shifts in intraspecific competitiveness as a result of these changes may therefore have ecological implications not yet fully realized.

Acknowledgements

This work was supported by the University of Plymouth and a grant from the Wellcome Trust. Technical support at Plymouth University from S. McMahon, and J. Soane are gratefully acknowledged. We thank Dr. S. Davies for access to the fish nutrition unit at Plymouth University, and Professor M.H. Depledge for partial funding of the video tracking system.

References

Berntssen, M.H.G., Hylland, K., Wendelaar Bonga, SE, and Maage, A. 1999. Toxic levels of dietary copper in Atlantic salmon (*Salmo salar* L.) parr. Aquat. Toxicol. **46**: 87–99.

Bochdansky, A.B., and Leggett, W.C. 2001. Winberg revisited: convergence of routine metabolism in larval and juvenile fish. Can. J. Fish. Aquat. Sci. **58**: 220–230.

Boisclair, D. 1992. Relationship between feeding and actively foraging juvenile brook trout (*Salvelinus fontinalis*). Can. J. Fish. Aquat. Sci. **49**: 2566–2572.

Boisclair, D., and Sirios, P. 1993. Testing assumptions of fish bioenergetics models by direct estimation of growth, consumption and activity rates. Trans. Am. Fish. Soc. **122**: 784–796.

Boujard, T., and Leatherland, J.F. 1992. Circadian-rhythms and feeding time in fishes. Environ. Biol. Fishes, **35**: 109–131.

Brett, J.R. 1964. The respiratory metabolism and swimming performance of young sockeye salmon. J. Fish. Res. Board Can. **21**: 1183–1226.

Carlisle, D.M. 2000. Bioenergetic food webs as a means of linking toxicological effects across scales of ecological organisation. J. Aquat. Ecosyst. Stress Recovery, **7**: 155–165.

Cech, J.J. 1990. Respirometry. *In* Methods for fish biology. *Edited by* C.B. Schreck and P.B. Moyle. American Fisheries Society, Bethesda, Md. pp. 335–362.

Dallinger, R., and Kautzky, H. 1985. The importance of contaminated food for the uptake of heavy metals by rainbow trout (*Salmo gairdneri*): a field study. Oecologia (Berlin), **67**: 82–89.

Dawkins, M.S. 1995. Unravelling Animal Behaviour. Longman, Harlow, Essex, U.K.

Forstner, H., and Wieser, W. 1990. Patterns of routine swimming and metabolic rate in juvenile cyprinids at three temperatures: analysis with a respirometer-activity-monitor system. J. Comp. Physiol. B Biochem. Syst. Environ. Physiol. **160**: 71–76.

Handy, R.D., Sims, D.W., Giles, A., Campbell, H.A., and Musonda, M.M. 1999. Metabolic trade-off between locomotion and detoxi-

© 2002 NRC Canada

fication for maintenance of blood chemistry and growth parameters by rainbow trout (*Oncorhynchus mykiss*) during chronic dietary exposure to copper. Aquat Toxicol. **47**: 23–41.

Heggenes, J., Krog, O.M.W., Lindas, O.R., Dokk, J.G., and Bremnes, T. 1993. Homeostatic behavioural responses in a changing environment: brown trout (*Salmo trutta*) become nocturnal during winter. J. Anim. Ecol. **62**: 295–308.

Kamunde, C.N., Grosell, M., Lott, J.N.A., and Wood, C.M. 2001. Copper metabolism and gut morphology in rainbow trout (*Oncorhynchus mykiss*) during chronic sublethal dietary exposure. Can. J. Fish. Aquat. Sci. **58**: 293–305.

Kooi, B.W., Boer, M.P., and Kooijman, S.A.L.M. 1998. Consequences of population models for the dynamics of food chains. Math. Biosci. **153**: 99–124.

Kooijman, S.A.L.M., Kooi, B.W., and Hallam, T.G. 1999. The application of mass and energy conservation laws in physiologically structured population models of heterotrophic organisms. J. Theor. Biol. **197**: 371–392.

Lanno, R.P., Slinger, S.J., and Hilton, J.W. 1985. Maximum tolerable and toxicity levels of dietary copper in rainbow trout (*Salmo gaidneri* Richardson). Aquaculture, **49**: 257–268.

Maltby, L., and Naylor, C. 1990. Preliminary observations on the ecological relevance of the *Gammarus* 'scope for growth' assay: effect of zinc on reproduction. Funct. Ecol. **4**: 393–397.

McCarthy, I.D., Carter, C.G., and Houlihan, D.F. 1992. The effect of feeding hierarchy on individual variabilitiy in daily feeding of rainbow trout, *Oncorhynchus mykiss*. J. Fish Biol. **41**: 257–263.

McGeer, J.C., Szebedinszky, C., McDonald, D.G., and Wood, C.M. 2000. Effects of chronic sublethal exposure to waterborne Cu, Cd or Zn in rainbow trout. 1. Ionoregulatory disturbance and metabolic costs. Aquat. Toxicol. **50**: 231–243.

McKim, J.M., and Benoit, D.A. 1971. Effect of long-term exposure to copper on survival, growth, and reproduction of brook trout (*Salvelinus fontinalis*). J. Fish. Res. Board Can. **28**: 655–662.

Metcalfe, N.B., Fraser, N.H.C., and Burns, M.D. 1999. Food availability and the nocturnal vs. diurnal foraging trade-off in juvenile salmon. J. Anim. Ecol. **68**: 371–381.

Ohta, M., and Watanabe, T. 1996. Energy requirements for maintenance of body weight and activity, and for maximum growth in rainbow trout. Fish. Sci. **62**: 737–744.

Pilgaard, L., Malte, H., and Jensen, F.B. 1994. Physiological effects and tissue accumulation of copper in freshwater rainbow trout (*Oncorhynchus mykiss*) under normoxic and hypoxic conditions. Aquat. Toxicol. **29**: 197–212.

Priede, I.G. 1977. Natural selection for energetic efficiency and the relationship between activity level and mortality. Nature (London), **267**: 610–611.

Priede, I.G. 1985. Metabolic scope in fishes. *In* Fish energetics. *Edited by* P. Tytler and P. Calow. Croom Helm, London. pp. 33–64.

Sanchez-Vazquez, F.J., and Tabata, M. 1998. Circadian rhythms of demand-feeding and locomotor activity in rainbow trout. J. Fish Biol. **52**: 255–267.

Scarfe, A.D., Jones, K.A., Steele, C.W., Kleerekoper, H., and Corbett, M. 1982. Locomotor behaviour of four marine teleosts in response to sublethal copper exposure. Aquat. Toxicol. **2**: 335–353.

Soofani, N.M. and Hawkins, A.D. 1982. Energetic costs at different levels of feeding in juvenile cod, *Gadus morhua* L. J. Fish. Biol. **21**: 577–592.

Soofiani, N.M., and Priede, I.G. 1985. Aerobic metabolic scope and swimming performance in juvenile cod, *Gadus morhua* L. J. Fish. Biol. **26**: 127–138.

Styrishave, B., Rasmussen, A.D., and Depledge, M.H. 1995. The influence of bulk and trace metals on the circadian rhythm of heart rates in freshwater crayfish, *Astacus astacus*. Mar. Pollut. Bull. **31**: 87–92.

Turnbull, J.F., Adams, C.E., Richards, R.H., and Robertson, D.A. 1998. Attack site and resultant damage during aggressive encounters in Atlantic salmon (*Salmo salar* L.) parr. Aquaculture, **159**: 345–353.

Viarengo, A., Ponzano, E., Donodero, F., and Fabbri, R. 1997. A simple spectrophotometric method for metallothionein evaluation in marine organisms: an application to Mediterranean and Antartic molluscs. Mar. Environ. Res. **44**: 69–84.

Waiwood, K.G., and Beamish, F.W.H. 1978. Effects of copper, pH and hardness on the critical swimming performance of rainbow trout (*Salmo gairdneri* Richardson). Water Res. **12**: 611–619.

Webb, P.W. 1971. The swimming energetics of trout. (ii) Oxygen consumption and swimming efficiency. J. Exp. Biol. **55**: 521–540.

Wieser, W. 1985. Developmental and metabolic constraints of the scope for activity in young rainbow trout. J. Exp. Biol. **118**: 133–142.

Williams, J.A., and Naylor, E. 1978. A procedure for the assessment of significance of rhythmicity in time-series data. Int. J. Chronobiol. **5**: 435–444.

Winberg, S., Nilsson, G., Spruijt, B.M., and Höglund, U. 1993. Spontaneous locomotor activity in arctic charr measured by a computerised imaging technique: role of brain serotonergic activity. J. Exp. Biol. **179**: 213–232.

© 2002 NRC Canada

The response of planktonic phosphate uptake and turnover to ultraviolet radiation in Lake Erie

C.D. Allen and R.E.H. Smith

Abstract: The hypothesis that ambient ultraviolet radiation (UVR), at near-surface intensities, may diminish phosphorus availability to phytoplankton was tested in Lake Erie in July and August of 1998 and 1999. Relative to samples exposed to photosynthetically active radiation (PAR, 400–700 nm) only, those exposed to ultraviolet-B (UVB, 280–320) and (or) ultraviolet-A (UVA, 320–400 nm) in natural sunlight, or kept in darkness, had diminished phosphate uptake rates at elevated (1 μM P) dissolved phosphate concentrations. By contrast, the specific uptake rate of dissolved phosphate at ambient concentrations (turnover rate) was not significantly affected by UVR or darkness. Turnover was usually dominated by particles smaller than 0.8 μm, whereas uptake from elevated concentrations was dominated by larger particles. The size distribution of turnover and uptake activity was not affected by radiation treatment. Chlorophyll *a* concentrations were decreased by sufficient exposure to UVB and (or) UVA and increased by deprivation of PAR (dark controls), but the concentration of bacterial cells was unaffected. The results showed that UVR inhibited the phosphate uptake potential of larger, probably algal, plankton but did not change the apparent severity of phosphate limitation at ambient concentrations.

Résumé : L'hypothèse selon laquelle la radiation ultraviolette (UVR) ambiante, aux intensités qui prévalent près de la surface de l'eau, puisse diminuer la disponibilité du phosphore au phytoplancton a été mise à l'épreuve au lac Érié en juillet et août, en 1998 et 1999. Par comparaison à des échantillons exposés seulement à la radiation reliée à la photosynthèse (PAR, 400–700 nm), les échantillons exposés à l'ultraviolet-B (UVB, 280–320 nm) et (ou) à l'ultraviolet-A (UVA, 320–400 nm) sous un ensoleillement naturel, ou alors gardés à l'obscurité, affichent une diminution de l'incorporation du phosphate aux concentrations élevées (1 μM P) de phosphate dissous. En revanche, le taux spécifique d'incorporation de phosphate dissous aux concentrations ambiantes (le taux de renouvellement) n'est pas significativement affecté par la radiation UV ou par l'obscurité. Le renouvellement est dominé généralement par des particules de taille inférieure à 0,8 μm, alors que l'incorporation aux concentrations élevées l'est par des particules plus grandes. Les distributions de fréquence des tailles impliquées dans le renouvellement et l'incorporation ne sont pas modifiées par le traitement aux radiations. Les concentrations de chlorophylle *a* diminuent après une exposition suffisamment importante aux UVB et (ou) aux UVA et elles augmentent par pénurie de PAR (témoins gardés à l'obscurité), mais les concentrations de cellules bactériennes restent les mêmes. Nos résultats démontrent que la radiation UV inhibe le potentiel d'incorporation du phosphate du plancton de grande taille, sans doute essentiellement composé d'algues, mais elle ne change pas la gravité apparente de la pénurie de phosphate aux concentrations ambiantes.

[Traduit par la Rédaction]

Introduction

Ultraviolet radiation (UVR) effects on planktonic primary production have received considerable attention in recent years because of the vulnerability of microscopic phytoplankton to the increased surface-incident UVR resulting from stratospheric ozone depletion (e.g., Vincent and Roy 1991; Neale et al. 1998). The responses of short-term (<1 photoperiod) primary production to UVR are well documented for some marine plankton communities and are increasingly well defined for freshwater phytoplankton of the Laurentian Great Lakes (Gala and Geisy 1991; Furgal et al. 1998; Marwood et al. 2000). In both marine and freshwater communities, long-wavelength UVR (UVA, 320–400 nm) typically accounts for more inhibition of primary production than does UVB (280–320 nm). Daily losses of production due to UVR at ambient exposure levels have been estimated at 5–30% in both marine (e.g., Neale et al. 1998) and freshwater (Smith et al. 1998; Hiriart 2000) communities.

Less is known of UVR effects on inorganic nutrient cycling, even though primary production ultimately depends on a sufficient rate of inorganic nutrient acquisition. Nitrogen has been best studied. Nitrate and ammonium uptake by marine diatoms can be inhibited by UVB and (or) UVA (e.g., Döhler and Biermann 1987; Lohmann et al. 1998). The UVB effects on nitrate uptake may be due, at least in part, to specific effects on enzymes involved in nitrate reduction and are also dose and species specific (e.g., Döhler and Biermann 1987). Field (Behrenfeld et al. 1995) and mesocosm (Fauchot et al. 2000) studies of ammonium, nitrate, and urea uptake have confirmed that UVB at near-surface intensities can inhibit nitrogen uptake in marine plankton communities. The significance for nitrogen assimi-

Received 3 December 2001. Accepted 31 March 2002. Published on the NRC Research Press Web site at http://cjfas.nrc.ca on 7 June 2002.
J16647

C.D. Allen and R.E.H. Smith.[1] Biology Department, University of Waterloo, Waterloo, ON N2L 3G1, Canada.

[1]Corresponding author (e-mail: rsmith@sciborg.uwaterloo.ca).

 DOI: 10.1139/F02-050 © 2002 NRC Canada

lation over the mixed layer is not so clear (Fauchot et al. 2000).

UVB stimulates phosphate uptake by cultures of the green alga *Chlamydomonas reinhardtii* at low fluxes but inhibits uptake at higher fluxes (Hessen et al. 1995). UVB exposure can also reduce adenosine triphosphate contents of marine phytoplankton, suggesting problems with phosphorus (P) uptake or availability (Vosjan et al. 1990; Hessen et al. 1995). Despite the central role of P in the ecology of many lakes, there are no published reports of UVR effects on phosphate uptake in natural communities.

The P nutrition of phytoplankton in many lakes depends on a tight coupling between phosphate uptake and release processes (Hudson et al. 1999), with the ambient concentration of bioavailable orthophosphate typically at picomolar levels (Hudson et al. 2000). Consideration of UVR effects must then include regenerative processes, but no direct studies have yet been made. There is evidence that the activity of alkaline phosphatase may be increased by UVR exposure where organic complexation by humic compounds is appreciable (Boavida and Wetzel 1998). Bacterioplankton, which can act as both remineralizers and competitors with phytoplankton for phosphate (e.g., Currie 1990), are also affected by UVR at ambient exposure levels (e.g., Sommaruga et al. 1997; Wilhelm and Smith 2000). There is evidence that some of the bacterivorous plankton, which can be important remineralizers, are vulnerable to UVR (e.g., Sommaruga et al. 1996). In some waters, UVR may stimulate bacterial production indirectly, by promoting favourable changes in the quality of dissolved organic matter (e.g., Wetzel et al. 1995). Given the inherent complexities and fragmentary information currently available, the effects of UVR on P cycling are hard to predict.

Here we describe measurements of UVA and UVB effects on phosphate uptake and turnover in natural plankton communities. The experiments were done in Lake Erie, which has undergone great changes in trophic state and structure in recent years owing to P loading restrictions and invasion by dreissenid mussels (e.g., Charlton et al. 1999). With improved water clarity and diminished phytoplankton abundance, the earlier Lake Erie problem of eutrophication has been overtaken by concerns about the sustainability of the plankton-based food web (e.g., Johansson et al. 2000). Our experiments were designed to help test the hypothesis that increased UVR penetration might exert a negative feedback on plankton production by diminishing P availability to planktonic primary producers.

Materials and methods

Field sampling

All sampling and experimental work was performed aboard the CCGS *Limnos* in July and August of 1998 and 1999 in Lake Erie. Stations were occupied in both east central and west basins in 1998, but in the central basin only in 1999 (Table 1). Temperature profiles were measured with a Seabird SBE-19 profiler, and photosynthetically active radiation (PAR) profiles were measured with a LI-COR UWQ cosine collector quantum probe (Lincoln, Nebr.). The vertical attenuation coefficient for PAR was determined from the slope of ln(PAR) vs. depth. Water was taken from 5 m using a Niskin bottle on a rosette sampler and was screened through 100-μm nylon mesh to remove the larger zooplankton.

Incident UVR and PAR were measured with an Oriel Instaspec diode array spectroradiometer (Oriel Corp., Stratford, Conn., Smith et al. 1999) at all stations sampled in 1998. Measurements were taken at least twice an hour during experimental incubations. For stations sampled in July 1999, incident UVR data were provided by Environment Canada (National Water Research Institute) from their measurements taken aboard the *Limnos* with an Optronics spectroradiometer (Scully and Lean 1994). No direct measurements of incident UVR were available for stations sampled in August 1999. For those stations, we estimated the incident UVR from measurements of incident PAR, assuming the ratio of UVR to PAR to be the same as the average ratio that we observed in 1998 for similar sky conditions (i.e., clear) and dates.

Experimental design and radiation exposures

The experiments were designed to measure the effect of previous radiation exposure on phosphate uptake and turnover rates. Phosphate uptake was measured with a large addition of dissolved orthophosphate to estimate phosphate-saturated uptake rates (e.g., Lean et al. 1983, 1987). The specific uptake of phosphate at ambient concentration (turnover) was measured to gain an estimate of the demand to supply ratio for phosphate in the natural community (Lean et al. 1983; Hudson et al. 1999). Both uptake and turnover were measured in darkness following exposure to either full-spectrum sunlight, full spectrum minus UVB (PAR + UVA), PAR only, or darkness. Exposures were done in UVT (UV-transmitting) acrylic deck boxes (nominal 100% transmittance throughout UV and PAR, Hiriart et al. 2002), with circulating surface lake water to maintain temperatures within 2°C of ambient. The exposure vessels were 60-mL polystyrene flasks, transmitting approximately 30% UVB, 50% UVA, and 100% PAR (West et al. 1999). Deck boxes for full-spectrum treatments contained no additional spectral filters. Those for PAR + UVA treatments contained Mylar-D (50% transmission at 320 nm), and for PAR-only treatments, acrylic plastic (Cadillac Plastics grade UF3, 50% transmission at 405 nm). Exposures were for 4–5 h, centred on solar noon.

In 1998, a 50% transmission neutral-density filter was placed over each deck box. Although we term these for convenience as 50% exposures, the resulting maximum exposure (in the full-spectrum treatment) was approximately 50% PAR, 25% UVA, and 15% UVB when corrected for transmission through the polystyrene flasks. In 1998, we included 100% exposures (no screen), in which maximum exposures were approximately 100% PAR, 50% UVA, and 30% UVB. The actual spectral transmission of the deck boxes, filters, and flasks was confirmed in the field using the Oriel Instaspec spectroradiometer.

P cycling measurements

Phosphate turnover rates were measured in 50-mL samples in borosilicate glass tubes, spiked with 100 μL of carrier-free $H_3{}^{33}PO_4$ solution (ICN Pharmaceuticals Inc., Irvine Calif.; specific activity $>5.3 \times 10^{19}$ Bq·mmol^{-1}) to a final total activity of approximately 6×10^5 Bq·mL^{-1}. In 1998, 5-mL sam-

© 2002 NRC Canada

Table 1. Locations, dates and selected features of the stations sampled.

Station number	Sample date	Latitude (N)	Longitude (W)	Basin	Surface temperature (°C)	Station depth (m)	Mixed depth (m)	K_{PAR} (m^{-1})	Chl *a* ($\mu g \cdot L^{-1}$)	Bacterial density ($\times 10^6$ mL^{-1})
946	14 July 1998	42°10′03″	80°38′29″	EC	20.9	21	21	0.19	1.3	2.12
945	16 July 1998	42°24′01″	80°38′30″	EC	22.7	20	20	0.33	5.3	3.32
946	11 Aug. 1998	42°10′03″	80°38′29″	EC	23.6	21	21	0.28	2.6	3.55
961	13 Aug. 1998	41°54′30″	82°11′00″	EC	21.7	19	10.5	0.27	3.0	4.26
357	15 July 1998	41°49′35″	82°58′08″	W	24.0	9	9	0.36	2.1	4.07
337	12 Aug. 1998	41°41′42″	82°51′19″	W	24.8	6	6	0.63	4.0	4.38
84	11 July 1999	41°56′06″	81°39′30″	C	22.0	24	13	0.22	1.2	0.84
84	13 July 1999	41°56′06″	81°39′30″	C	21.9	24	13	0.23	1.6	0.56
84	14 July 1999	41°56′06″	81°39′30″	C	22.1	24	13	0.20	1.3	0.70
955	11 Aug. 1999	41°48′00″	81°26′30″	C	22.9	21	10	0.38	1.1	0.79
956	12 Aug. 1999	41°41′30″	81°26′30″	C	22.45	16	16	0.39	3.0	1.18

Note: Basins were EC, east central; W, west; C, central.

ples were removed and filtered through 0.2-μm cellulose acetate filters at 0, 1, 2.5, 5, 10, 30, and 60 min after isotope addition. Additional samples were filtered through 0.8-μm polycarbonate filters at 5 and 30 min after isotope addition. In 1999, samples were taken at 0, 1, 2.5, 5, 10, 15, and 20 min for the 0.2-μm filters and 0 and 5 min for the 0.8-μm filters.

Experiments to determine phosphate-saturated uptake rates were done by spiking 45-mL samples with unlabelled dipotassium phosphoric acid to a final concentration of 1.0 μmol $P \cdot L^{-1}$ before adding the carrier-free $H_3{}^{33}PO_4$ (Scott Millard, Fisheries and Oceans Canada, Canadian Centre for Inland Waters, Burlington, Ont., personal communication). Subsamples of 5 mL were filtered after 0, 120, 240, and 300 min through 0.2-μm filters, and after 0 and 300 min through 0.8-μm polycarbonate filters (0, 60, 120, 240, and 300 min on 0.2-μm filters and 0, 120, and 300 min on 0.8-μm filters in 1999).

At the end of each experiment, 100-μL samples were taken for total activity measurements. All filters were rinsed with 0.45-μm filtered lake water to remove unassimilated label. Samples were assayed by liquid scintillation counting in Ecolume scintillation cocktail (ICN Pharmaceuticals).

Phosphate turnover rates were derived by fitting the proportion of added label remaining in solution (i.e., passing the 0.2-μm filter) to a second-order polynomial function of incubation time and calculating the derivative at time zero (Currie 1986). Phosphate-saturated uptake rates were calculated from the rate of increase of activity on 0.2-μm filters, determined by linear regression, and the known specific activity of the added phosphate (e.g., Lean et al. 1987). The proportion of the total turnover or uptake rate by organisms >0.8 μm was estimated from the ratio of activities on 0.8- vs. 0.2-μm filters after 5 min (for turnover) or 300 min (for saturated uptake) of incubation.

Biological and chemical analyses

Samples of 20 mL were taken at the end of the experimental exposures, preserved to a final concentration of 1.5% gluteraldehyde, and refrigerated pending bacterial direct counts by the acridine orange method of Hobbie et al. (1977). We used 4-mL samples on 0.2-μm blackened polycarbonate filters and counted to a total of at least 350 cells at 1000× magnification. Samples for chlorophyll analysis (50–100 mL) were filtered onto glass fibre (GF/F, nominal pore size 0.8 μm) filters, which were frozen pending extraction with 90% acetone and quantification by fluorescence (Smith et al. 1999). Soluble reactive phosphorus (measured on GF/F filtrates) and total phosphorus (TP) were determined by the ascorbic acid – molybdate method before and after persulphate digestion, respectively (Furgal et al. 1998).

Results

Limnological conditions

The relatively shallow west basin displayed little or no thermal stratification, whereas the deeper central basin was usually stratified (Table 1). Three of the east central basin stations were unstratified when visited. Vertical attenuation coefficients for PAR were highest in the west and lower towards the east (Table 1). Chlorophyll *a* concentrations averaged 3.0 $\mu g \cdot L^{-1}$ for east central and west basin stations in 1998, and 1.9 $\mu g \cdot L^{-1}$ for the central basin stations in 1999 (Table 1). Bacterial numbers were 2.1–4.4 × 10^6 mL^{-1} at east central and west basin stations in 1998, and 0.56–1.2 × 10^6 mL^{-1} at central basin stations in 1999.

The concentrations of TP and soluble reactive P (SRP) were lowest at the east central basin stations, and the highest value was observed at a west basin station (Table 2). Some of the highest TP concentrations were observed at central basin stations in 1999. Much of the variation was expressed at one site (station number 84), a near mid-lake location occupied on successive days (Table 2).

Phosphorus cycling and uptake in the absence of UVR

Turnover or uptake rates did not differ significantly between the 50% and 100% PAR-only exposures (analysis of variance, ANOVA, $p > 0.05$), so the results for both treatments were averaged (Table 2). Of the 11 stations, nine had phosphate turnover rates at ambient concentration between 2.3 and 5.1% $\cdot min^{-1}$ (Table 2). The exceptions were one of the station 84 visits (0.1% $\cdot min^{-1}$) and station 956 (10.1% $\cdot min^{-1}$). Phosphate uptake with 1.0 μM added phosphate varied from 0.7 to 15.7 nmol $\cdot L^{-1} \cdot min^{-1}$ (Table 2).

© 2002 NRC Canada

Table 2. Phosphorus concentrations, turnover and uptake rates, and size distribution of turnover and uptake rates in samples exposed to photosynthetically active radiation only.

Station number	Sample date	Basin	SRP	TP	k_{PO_4}	V_{PO_4}	$\%k_{PO_4}$ > 0.8 μm	$\%V_{PO_4}$ > 0.8 μm
946	14 July 1998	EC	0.2	5.6	2.78±0.22	5.40±0.66	57.2±22.8	76.6±5.9
945	16 July 1998	EC	0.2	9.6	2.71±0.38	3.00±1.20	24.6±2.6	70.2±2.9
946	11 Aug. 1998	EC	0.2	6.9	3.10±0.09	10.41±1.83	28.3±1.6	100.4±5.2
961	13 Aug. 1998	EC	0.2	11.1	5.06±2.53	5.26±1.09	26.4±2.2	88.0±11.2
357	15 July 1998	W	4.0	11.2	2.74±1.30	1.11±0.65	34.8±1.1	94.6±38.3
337	12 Aug. 1998	W	0.9	17.7	2.60±0.18	3.38±0.66	26.4±1.6	90.9±2.0
84	11 July 1999	C	0.8	24.3	0.10±0.05	0.78±0.24	29.6±3.5	33.3±11.9
84	13 July 1999	C	0.7	21.2	3.07±1.82	3.29±0.61	45.4±12.0	68.9±10.8
84	14 July 1999	C	1.3	7.1	2.34±1.93	3.35±0.28	108.4±13.9	105.9±13.9
955	11 Aug. 1999	C	1.1	6.6	5.74±2.33	15.72±0.97	30.3±2.2	77.4±2.9
956	12 Aug. 1999	C	1.1	10.6	10.12±1.91	8.70±1.39	50.9±35.8	73.9±1.2

Note: Soluble reactive phosphorus (SRP) and total phosphorus (TP) are means of duplicates (μg P·L^{-1}). Turnover rate of orthophosphate, k_{PO_4} (%·min^{-1}), saturated uptake rate, V_{PO_4} (nmol·L^{-1}·min^{-1}), and their size distributions (% > 0.8 μm) are mean ± standard deviation for triplicates. Basins were EC, east central; W, west; C, central.

At ambient phosphate concentration, the 0.8-μm filters retained less than half as much radiophosphorus as the 0.2-μm filters at eight of 11 stations ($\%k_{PO_4}$ > 0.8 μm, Table 2). On one visit to station 84, the 0.8-μm filter retained 108% of the radiophosphorus retained on the 0.2-μm filter (i.e., 100% retention within limits of error). The average retention was 41.3% with this possibly erroneous value included, and 35.4% without. With 1.0 μM phosphate, more than 50% was retained on the 0.8-μm filter at 10 of 11 stations ($\%V_{PO_4}$ > 0.8 μm, Table 2), with an overall average retention of 80.0%.

UVR and PAR effects on chlorophyll and bacteria

All experimental radiation exposures were performed under mainly clear skies. The average instantaneous incident irradiance during each experimental exposure, in μW·cm^{-2}, varied from 24 475 to 35 593 for PAR, 2118 to 3753 for UVA, and 84 to 231 for UVB (Table 3). The incident radiation integrated over the duration of the experiments varied proportionately.

In both 1998 and 1999, experimental exposures were made under neutral density screening with 50% transmission. There was no significant effect of radiation treatment on bacterial cell concentrations ($p = 0.8363$, $n = 44$) or on chlorophyll *a* concentrations ($p = 0.2714$, $n = 44$) under the 50% screen, but variation among experiments was significant (ANOVA, $p < 0.01$). To help control for the variation in overall bacteria and chlorophyll concentrations among experiments, concentrations in each treatment were normalized to those in the PAR-only treatment. Normalized bacterial concentrations did not differ significantly from unity, indicating no significant average effect of UVR or darkness relative to PAR-only exposures (Fig. 1*a*). Normalized chlorophyll *a* concentrations in full-spectrum and PAR + UVA treatments were less than unity on average, but not significantly so (Fig. 1*a*). The dark treatment resulted in normalized chlorophyll *a* concentrations significantly greater than unity.

In 1999 only, additional exposures were done at 100% incident UVR. Bacterial concentrations varied significantly among experiments but not radiation treatments (ANOVA, $p < 0.01$). Bacterial cell concentrations normalized to those in the PAR-only treatment were not significantly different from unity, on average, for any of the treatments (Fig. 1*b*). Chlorophyll *a* concentrations were significantly affected by radiation treatment (ANOVA, $p = 0.0256$, $n = 26$), even without normalization. Normalized chlorophyll *a* concentrations averaged 1.4 in the dark treatment, but less than unity in both of the UV-exposed treatments (Fig. 1*b*; Table 4). Normalized chlorophyll *a* concentrations were more diminished in the PAR + UVA than in the full-spectrum treatment, although the ratios in the two treatments were not significantly different.

UVR and PAR effects on P cycling

Between-experiment effects dominated the total variation of phosphate uptake and turnover rates, so subsequent analysis was again based on rates normalized to those observed in the PAR-only treatments. Saturated phosphate uptake of the total plankton assemblage (>0.2 μm fraction), when so-normalized, was significantly affected by radiation treatment at both the 50% and 100% incident radiation levels (ANOVA, $p < 0.0001$). Normalized phosphate uptake was significantly diminished, on average, in the dark controls (Fig. 2). Average uptake rates were also diminished in the full-spectrum and PAR + UVA treatments, although the effect was significant only at the 100% incident exposure level. At the 100% exposure level, normalized uptake rates did not differ significantly among the full-spectrum, PAR + UVA, and dark control treatments. UVR effects under 100% incident exposure thus appeared to be due mainly to UVA and were comparable in magnitude to those produced by deprivation of PAR.

The size distribution of radiophosphorus incorporation at saturating phosphate (Table 2) suggested a predominance of larger, probably algal, particles. When biomass normalized to rates in the PAR-only treatment, chlorophyll-specific uptake rates (V^B) revealed significant responses to radiation treatment at both 50% and 100% incident exposure levels. On average, V^B was even more diminished by the dark treatment than was the volumetric uptake rate (Table 4). The full-spectrum and PAR + UVA treatments had smaller, but still significant, effects on V^B in the 100% incident exposures

© 2002 NRC Canada

Table 3. Incident radiation during the experimental exposures.

Station number	Sample date	E_{PAR}	E_{UVA}	E_{UVB}	H_{PAR}	H_{UVA}	H_{UVB}
946	14 July 1998	29 094.0	3112.0	149.9	2330.5	248.0	11.6
945	16 July 1998	35 592.8	3753.1	176.3	3177.8	329.9	16.6
946	11 Aug. 1998	31 204.3	3379.4	230.6	3628.4	393.0	26.4
961	13 Aug. 1998	28 775.6	3087.7	155.6	3578.9	381.2	19.5
357	15 July 1998	33 941.0	3576.7	175.8	3107.2	322.6	16.2
337	12 Aug. 1998	27 106.0	3076.2	158.0	2463.6	285.0	14.7
84	11 July 1999	24 475.4	2595.2	158.6	2265.4	243.0	12.8
84	13 July 1999	33 233.1	3378.1	189.4	2862.0	287.2	10.4
84	14 July 1999	29 673.2	3020.1	163.1	2433.4	244.6	8.6
955	11 Aug. 1999	32 226.5	3032.7	120.1	3073.9	286.22	11.9
956	12 Aug. 1999	24 603.0	2118.6	83.9	2147.4	199.9	8.3

Note: Instantaneous irradiance of photosynthetically active radiation (E_{PAR}), UVA (E_{UVA}), and UVB (E_{UVB}), all as $\mu W \cdot cm^{-2}$. Cumulative radiation during exposure (H_{PAR}, H_{UVA}, H_{UVB}) as $kJ \cdot m^{-2}$. UVA and UVB values for August 1999 were estimated from PAR as described in text.

(Table 4). As for volumetric uptake, V^B was not significantly diminished by UVR at the 50% incident exposure level.

Turnover rates of the >0.2 μm fraction, even when normalized to those in the PAR-only treatment, did not respond significantly to radiation treatment at either the 50% or 100% incident exposure levels (ANOVA, $p = 0.5525$). Unlike uptake rate, turnover rate was on average not significantly slower in dark controls than in samples exposed to PAR only (Figs. 2*c*, 2*d*). On average, full-spectrum and PAR + UVA treatments resulted in slightly faster normalized turnover rates at the 50% exposure level and slightly slower rates at the 100% level, but the differences were not significant (Figs. 2*c*, 2*d*).

The proportion of radiophosphorus appearing in the larger (>0.8 μm) size fraction may vary if plankton size, or bacteria vs. algal differences, is important in UVR response. We calculated the difference in percent >0.8 μm between each treatment and the PAR-only treatment and expressed the difference as a percentage of the value for the PAR-only treatment. For example, the full-spectrum treatment at the 50% incident exposure level produced an average increase of 14.5% in the proportion of saturated uptake in the >0.8 μm fraction ($V > 0.8$, Table 4). This was the only significant average effect of radiation treatment on size distributions.

Fig. 1. The mean values over all experiments for chlorophyll *a* (open bars) and bacterial cell concentrations (shaded bars) relative to those in treatments exposed to photosynthetically active radiation (PAR) only, with 95% confidence intervals: (*a*) 50% exposure; (*b*) 100% exposure.

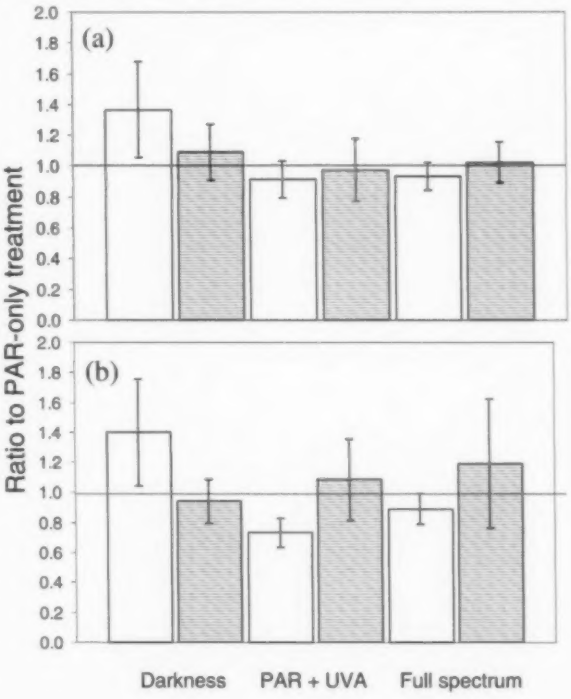

Discussion

Lake Erie is treated, for management purposes, as a P-limited lake. The phytoplankton biomass and chlorophyll concentration have varied with changes of total phosphorus concentration in recent decades (e.g., Charlton et al. 1999) and the summer plankton have historically revealed symptoms of phosphorus limitation (Lean et al. 1983). The current results revealed total phosphorus and SRP concentrations in the expected oligotrophic–mesotrophic range, and values for chlorophyll *a* concentration, PAR attenuation, and thermal structure within the range normally expected (e.g., Charlton et al. 1999; Johansson et al. 2000; Hiriart et al. 2002). The dissolved phosphate turnover rates we encountered, mostly 0.02–0.05 min^{-1}, were within the range observed in summer of 1979 (Lean et al. 1983) and would suggest a state of moderate P limitation in the plankton during our study period (Lean et al. 1987; Hudson et al. 2000). Despite the influences of dreissenid grazing and nutrient regeneration since 1988, the plankton thus appeared still to be P limited, at least at our relatively deep-water summertime stations. Changes in utilization or availability of phosphorus induced

© 2002 NRC Canada

Table 4. Average percentage changes, relative to photosynthetically active radiation (PAR) exposures, produced by darkness or PAR + UV exposures.

Treatment	V_{PO_4}	$V^B_{PO_4}$	k_{PO_4}	Chl *a*	Bacteria	$k > 0.8$	$V > 0.8$
Dark (vs. 50% PAR)	–35*	–44*	–3	+37*	+9	–2.7	–2.6
Dark (vs. 100% PAR)	–45*	–53*	+14	+40*	–6	+20.6	–1.4
50% PAR + UVA	+1	+21	+14	–9	–3	+4.5	+7.2
100% PAR + UVA	–46*	–18*	–11	–27*	+9	–15.2	–5.6
50% full spectrum	+1	+8	+20	–7	+2	–3.2	+14.5*
100% full spectrum	–52*	–43*	–10	–11*	+19	–3.0	–8.6

Note: V_{PO_4}, saturated phosphate uptake rate per volume of lake water (>0.2 µm); $V^B_{PO_4}$, uptake rate (> 0.2 µm) per chlorophyll *a* (Chl *a*); k_{PO_4}, phosphate turnover rate (> 0.2 µm); Bacteria, bacterial cell concentration; $k > 0.8$ and $V > 0.8$ are proportions of P uptake by large size fraction at ambient and elevated phosphate concentrations, respectively. Asterisks show values significantly different from zero ($p < 0.05$).

Fig. 2. Mean values and 95% confidence intervals over all experiments for saturated phosphate uptake rate (*a*, *b*) and phosphate turnover rate (*c*, *d*) of the >0.2 µm size fraction, relative to the values for treatments exposed to photosynthetically active radiation (PAR) only: (*a*) and (*c*), 50% exposure; (*b*) and (*d*), 100% exposure. ◇, mean for dark treatment; □, mean for PAR + UVA; △, mean for full spectrum; ×, means for individual experiments in each treatment.

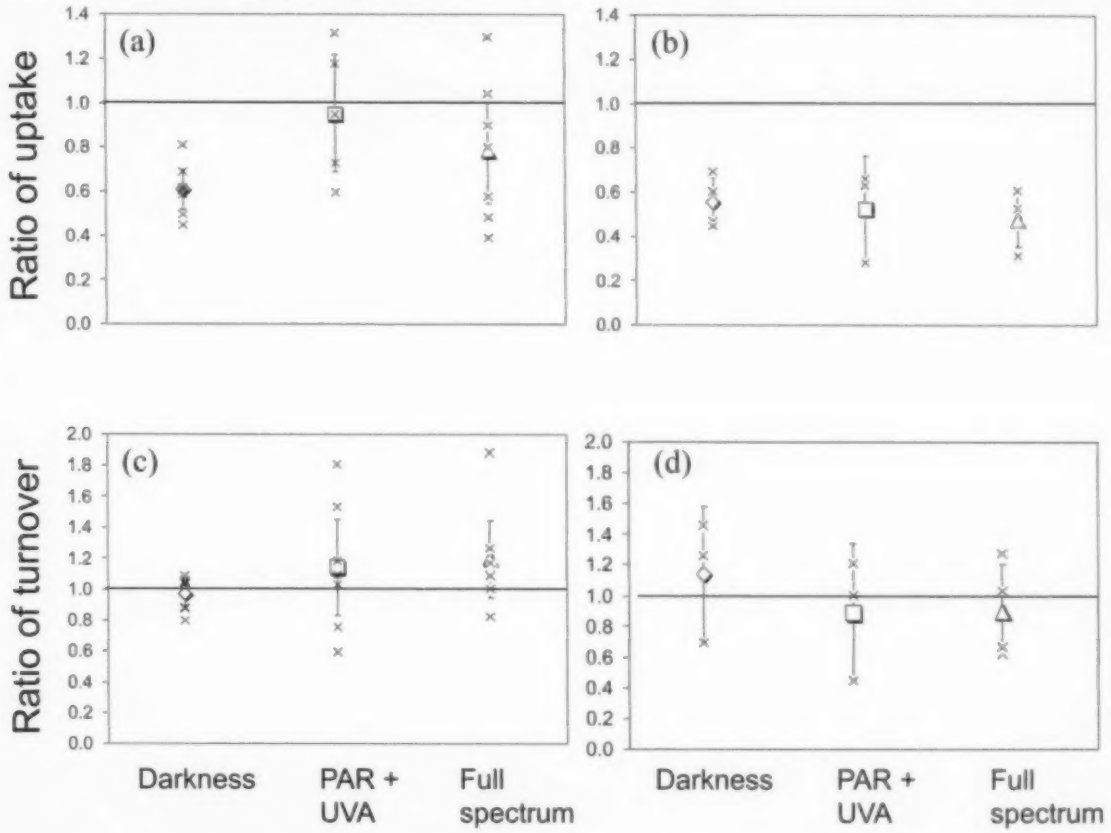

by UVR could therefore be expected to alter productivity in the lake.

The UVR exposures in our experiments were representative of near-surface conditions. The median attenuation coefficient for UVB at stations throughout Lake Erie in 1997 was 2.52 m^{-1} for 17 stations occupied in July and August (Smith et al. 1999). Approximately 30% of incident UVB was received by plankton in our most severe treatment, corresponding to a median depth of approximately 0.48 m, whereas the more moderate treatment (15%) corresponded to a median depth of 0.85 m. The equivalent depths for UVA exposure (median attenuation coefficient 1.50 m^{-1}, Smith et al. 1999) would be 0.46 m in the more severe exposure (50% of incident) and 0.94 m in the less severe exposure

© 2002 NRC Canada

(25%). Equivalent depths for UVB and UVA exposure were similar because the spectral attenuation of the polystyrene incubation containers (West et al. 1999) resembled that of Lake Erie water. Although approximate, these comparisons indicate that the UVR exposures were comparable to those received naturally in the upper metre of the water column, on predominantly sunny summer days. Impacts on the naturally circulating plankton will depend on the kinetics of response and details of the mixing regime (e.g., Neale et al. 1998; Smith et al. 1998), but our experiments should reveal the potential effects of prolonged near-surface exposures.

The more severe UVR exposure treatment caused a significant decrease in phosphate uptake at elevated dissolved phosphate concentrations and in chlorophyll *a* concentrations relative to samples exposed to PAR only. The elevated concentration of 1 μM should have been saturating for phytoplankton uptake, and we might also expect that phytoplankton would be the main agents of uptake at such concentrations (e.g., Currie and Kalff 1984; Lean et al. 1983, 1987). The >0.8 μm fraction, which should have contained almost all the phytoplankton, did dominate phosphate uptake at elevated concentration but would have included some bacteria. The small fraction, which should not have contained many algae, averaged 60–65% of the uptake at ambient phosphate concentration, but only 20% at elevated concentration. This suggests that uptake at elevated phosphate concentration was in fact dominated by phytoplankton, and that algal phosphate uptake potential (i.e., V_{max}, sensu Lean et al. 1987) was UVR sensitive, even if expressed relative to the (reduced) chlorophyll *a* concentrations under UVR stress.

UVR exposures of comparable severity also diminish photosynthetic carbon assimilation rates (Hiriart et al. 2002), photosynthetic electron transport (Marwood et al. 2000), and the rates of thymidine and leucine incorporation by bacterioplankton (Wilhelm and Smith 2000) in Lake Erie. UVA, rather than UVB, appears to be the predominant agent of inhibition for photosynthetic activity in the photic zone of lakes Erie and Ontario (Smith et al. 1998; Hiriart 2000) and other plankton systems (e.g., Neale et al. 1998). UVB might have appeared more important in the current study if we had included truly severe (and rather unrealistic) treatments with 100% exposure across the entire UVR spectrum, but under our experimental conditions, the results suggested that UVA caused most of the effect on saturated phosphate uptake. Furthermore, deprivation of PAR was equally effective as UVR in diminishing saturated phosphate uptake. The UVR effect may have been mediated largely by effects on photosynthesis, and thus on demand or energy availability for phosphate uptake.

In most assays of UVR effects on photosynthesis, responses are measured during exposure to the experimental radiation regimes. By contrast, our experimental design allowed some scope for recovery from UVR damage, in darkness, after the experimental radiation exposures. However, a similar protocol has been used in Lake Erie (Wilhelm and Smith 2000) and elsewhere (e.g., Sommaruga et al. 1997) to demonstrate UVR-dependent inhibition of bacterial production, with the argument that known recovery processes are relatively slow in darkness. Measurements in Lake Erie also indicated that dark recovery from UVR-dependent inhibition of photosynthetic electron transport by phytoplankton is negligible over several hours (Marwood et al. 2000). UVR effects were probably not greatly underestimated by our experimental procedure.

The specific uptake of phosphate at ambient concentrations (i.e., turnover) is a measure of the demand to concentration ratio for dissolved phosphate in the tightly coupled uptake-regeneration system typical of phosphorus-limited plankton communities (Lean et al. 1983; Hudson et al. 1999). In contrast to phosphate-saturated uptake rate, turnover rate was not significantly affected by UVR exposure or darkness. One possible reason is that different organisms were probably dominant in the two processes. The size distribution of labelled phosphate uptake at ambient concentrations suggested that bacterial uptake was dominant, consistent with experience in many other phosphorus-limited lakes (e.g., Currie 1990). Bacterial cell concentrations were not significantly affected by UVR exposure or darkness, so the lack of UVR effects on phosphate turnover may indicate that bacteria are more resistant than algae.

Comparisons of UVR effects on photosynthesis and bacterial production in Lake Erie (Hiriart 2000; Wilhelm and Smith 2000; Hiriart et al. 2002) do not show that bacterioplankton are less sensitive than phytoplankton to UVR, however. Limits imposed by cell size on the effectiveness of intracellular UV shading mechanisms suggest that smaller microorganisms should actually be more vulnerable to UVR than larger ones (e.g., Garcia-Pichel 1996). Among phytoplankton, a number of factors, including taxonomic composition and size, influence vulnerability to UVR (e.g., Laurion and Vincent 1998; Hiriart et al. 2002), but there is little reason to believe that bacterioplankton are intrinsically more resistant to UVR than are phytoplankton.

A major alternative possibility is that both the uptake rate and the ambient concentration of dissolved phosphate were diminished by UVR stress, such that the specific uptake rate did not change significantly. This could occur if, for example, the phosphate regeneration rate decreased more than the phosphate uptake rate. Bacteria and protists are probably the major phosphate regenerators in most phosphorus-limited lakes (e.g., Hudson and Taylor 1996), with viral lysis (e.g., Wilhelm and Smith 2000) and protistan bacterivory (e.g., Sommaruga et al. 1996) constituting important mechanisms of bacterial mortality and nutrient release. Both viruses and protists are sensitive to UVR (e.g., Sommaruga et al. 1996; Wilhelm and Smith 2000) and might have been severely inhibited in our simulated near-surface exposures.

Whatever the mechanism(s), and there are several other possibilities, the lack of response of turnover rate to UVR suggested that plankton (at least the bacteria) were not subject to increased difficulty in obtaining phosphate, relative to their needs, under UVR stress. There was no significant shift in size distribution of the incorporated phosphate either, suggesting no major effects of UVR on the sharing of phosphate between algae and bacteria, at either ambient or saturating phosphate concentrations. Further work to characterize the dynamics of the dissolved phosphate pool, and the longer-term acquisition of phosphorus by phytoplankton and bacterioplankton, is needed to fully elucidate the impacts of UVR on P cycling. The complexities of phosphorus cycling in plankton communities leave open the possibility that not

© 2002 NRC Canada

only the magnitude, but also the net direction, of UVR effects may vary as community composition and environmental conditions change. The statistical power of our individual experiments was insufficient to resolve such time-varying effects. The present results do show that phosphate uptake capacity of the plankton can be diminished by sufficient UVR stress but give little indication that the severity of phosphorus limitation is likely to be systematically increased with elevated UVR exposure.

Acknowledgements

The Natural Sciences and Engineering Research Council of Canada (NSERC) and Environment Canada supported this work. M.N. Charlton, B.M. Greenberg, C. Marwood, and V. Hiriart provided valuable assistance and consultation.

References

Behrenfeld, M.J., Lean, D.R.S., and Lee, H., II. 1995. Ultraviolet-B radiation effects on inorganic nitrogen uptake by natural assemblages of oceanic plankton. J. Phycol. **31**: 25–36.

Boavida, M.J., and Wetzel, R.G. 1998. Inhibition of phosphatase activity by dissolved humic substances and hydrolytic reactivation by natural ultraviolet light. Freshwater Biol. **40**: 285–293.

Charlton, M.N., Le Sage, M.N., and Milne, J.E. 1999. Lake Erie in transition: the 1990's. *In* State of Lake Erie, past present and future. *Edited by* M. Munawar, T. Edsall, and I.F. Munawar. Backhuys Publishers, Leiden, The Netherlands. pp. 97–124.

Currie, D.J. 1986. Does orthophosphate uptake supply sufficient phosphorus to phytoplankton to sustain their growth? Can. J. Fish. Aquat. Sci. **43**: 1482–1487.

Currie, D.J. 1990. Large-scale variability and interactions among phytoplankton, bacterioplankton and phosphorus. Limnol. Oceanogr. **35**: 1437–1455.

Currie, D.J., and Kalff, J. 1984. A comparison of the abilities of freshwater algae and bacteria to acquire and retain phosphorus. Limnol. Oceanogr. **29**: 298–310.

Döhler, G., and Biermann, I. 1987. Effect of UVB irradiance on the response of ^{15}N-nitrate uptake of *Lauderia annulata* and *Synedra planctonica*. J. Plankton Res. **9**: 881–890.

Fauchot, J., Gosselin, M., Levasseur, M., Mostajir, B., Belzile, C., Demers, S., Roy, S., and Zillegas, P.Z. 2000. Influence of UV-B radiation on nitrogen utilization by a natural assemblage of phytoplankton. J. Phycol. **36**: 484–496.

Furgal, J.A., Taylor, W.D., and Smith, R.E.H. 1998. Environmental control of photosynthate allocation in the phytoplankton of Georgian Bay (Lake Huron). Can. J. Fish. Aquat. Sci. **55**: 726–36.

Gala, W.R., and Giesy, J.P. 1991. Effects of ultaviolet radiation on the primary production of natural phytoplankton assemblages in Lake Michigan. Ecotoxicol. Environ. Saf. **22**: 345–361.

Garcia-Pichel, F. 1996. The absorption of ultraviolet radiation by microalgae; simple optics and photobiological implications. Sci. Marina, **60**: 73–79.

Hessen, D.O., Van Donk, E., and Andersen, T. 1995. Growth responses, P uptake and loss of flagellae in *Chlamydomonas reinhardtii* exposed to UV-B. J. Plankton Res. **17**: 17–27.

Hiriart, V.P. 2000. Ultraviolet radiation and primary production by Lake Erie phytoplankton communities. Ph.D. thesis, Biology Department, University of Waterloo, Waterloo, Ont., Canada.

Hiriart, V.P., Greenberg, B.M., Guildford, S.J., and Smith, R.E.H. 2002. Effects of ultraviolet radiation on rates and size distribution of primary production by Lake Erie phytoplankton. Can. J. Fish. Aquat. Sci. **59:** 317–328.

Hobbie, J.E., Daley, R.J., and Jasper, S. 1977. Use of Nuclepore filters for counting bacteria by fluorescence microscopy. Appl. Environ. Microbiol. **33**: 1225–1228.

Hudson, J.J., and Taylor, W.D. 1996. Measuring regeneration of dissolved phosphorus in planktonic communities. Limnol. Oceanogr. **41**: 1560–1565.

Hudson J.J., Taylor, W.D., and Schindler, D.W. 1999. Planktonic nutrient regeneration and cycling efficiency in temperate lakes. Nature (London), **400**: 659–661.

Hudson J.J., Taylor, W.D., and Schindler, D.W. 2000. Phosphate concentrations in lakes. Nature (London), **406**: 54–56.

Johansson, O.E., Dermott, R., Graham, D.M., Dahl, J.A., Millard, E.S., Myles, D.D., and LeBlanc, J. 2000. Benthic and pelagic secondary production in Lake Erie after the invasion of *Dreissena* spp. with implications for fish production. J. Gt. Lakes Res. **26**: 31–54.

Laurion, I., and Vincent, W.F. 1998. Cell size vs. taxonomic composition as determinants of UV sensitivity in natural phytoplankton communities. Limnol. Oceanogr. **43**: 1774–1779.

Lean, D.R.S., Abbott, A.P., Charlton, M.N., and Rao, S.S. 1983. Seasonal phosphate demand for Lake Erie plankton. J. Gt. Lakes Res. **9**: 83–91.

Lean, D.R.S., Abbot, A.A., and Pick, F.R. 1987. Phosphorus deficiency of Lake Ontario phytoplankton. Can. J. Fish. Aquat. Sci. **44**: 2069–2076.

Lohmann, M., Döhler, G., Huckenbeck, N., and Verdini, S. 1998. Effects of UV radiation of different wavebands on pigmentation, 15N ammonium uptake, amino acid pools and adenylate contents of marine diatoms. Mar. Biol. **130**: 501–507.

Marwood, C.A., Greenberg, B.M., Charlton, M.N., and Smith, R.E.H. 2000. Rapid ultraviolet radiation-dependent inhibition and partial recovery of photosynthesis in L. Erie phytoplankton. Can. J. Fish. Aquat. Sci. **57**: 371–79.

Neale, P.J., Davis, R.F., and Cullen, J.J. 1998. Interactive effects of ozone depletion and vertical mixing on photosynthesis of Antarctic phytoplankton. Nature (London), **392**: 585–589.

Scully, N.M., and Lean, D.R.S. 1994. The attenuation of ultraviolet radiation in temperate lakes. Arch. Hydrobiol. Beih. Ergebn. Limnol. **43**: 135–144.

Smith, R.E.H., Furgal, J.A., and Lean, D.R.S. 1998. The short-term effects of solar ultraviolet radiation on phytoplankton photosynthesis and photosynthate allocation under contrasting mixing regimes in Lake Ontario. J. Gt. Lakes Res. **24**: 427–44.

Smith, R.E.H., Furgal, J.A., Charlton, M.N., Hiriart, V., and Marwood, C. 1999. Attenuation of ultraviolet radiation in a large lake with low dissolved organic matter concentrations. Can. J. Fish. Aquat. Sci. **56**: 1351–61.

Sommaruga, R., Oberleiter, A., and Psenner, R. 1996. Effect of UV radiation on the bacterivory of a heterotrophic nanoflagellate. Appl. Environ. Microbiol. **62**: 4395–4400.

Sommaruga, R., Obernosterer, I., Herndl, G.J., and Psenner, R. 1997. Inhibitory effect of solar radiation on thymidine and leucine incorporation by freshwater and marine bacterioplankton. Appl. Environ. Microbiol. **63**: 4178–4184.

Vincent, W.F., and Roy, S. 1991. Solar ultraviolet-B radiation and aquatic primary production: damage, protection and recovery. Environ. Rev. **1**: 1–12.

Vosjan, J.H., Dohler, G., and Nieuwland, G. 1990. Effects of UV-B irradiation on the ATP content of microorganisms of the Weddell Sea, Antarctica. Neth. J. Sea Res. **25**: 391–394.

West, L.J., Greenberg, B.M., and Smith, R.E.H. 1999. Ultraviolet radiation effects on a microscopic green alga and the protective

© 2002 NRC Canada

effects of natural dissolved organic matter. Photochem. Photobiol. **69**: 536–544.

Wetzel, R.G., Hatcher, P.G., and Bianchi, T.S. 1995. Natural photolysis by ultraviolet irradiance of recalcitrant dissolved organic matter to simple substrates for rapid bacterial metabolism. Limnol. Oceanogr. **40**: 1369–1380.

Wilhelm, S.W., and Smith, R.E.H. 2000. Viruses and solar radiation influence bacterial production in L. Erie. Can. J. Fish. Aquat. Sci. **57**: 317–26.

© 2002 NRC Canada

Effects of temperature and salinity on survival of young-of-the-year Hudson River striped bass (*Morone saxatilis*): implications for optimal overwintering habitats

Thomas P. Hurst and David O. Conover

Abstract: We examined the role of salinity, body size, and energetic state in determining low temperature tolerance of young-of-the-year (YOY) striped bass (*Morone saxatilis*) and used this information to map optimal overwintering habitat in the Hudson River estuary. A long-term experiment compared survival at 15 ppt and 30 ppt. In additional experiments, winter-acclimated fish were exposed to temperature declines (2.3°C·day^{-1} to 1°C·week^{-1}) at salinities from 0 ppt to 35 ppt. Highest survival at low temperatures was consistently observed at intermediate salinities. These results suggest that the observed distribution of overwintering striped bass is related to physiological constraints on osmoregulatory ability at low temperatures. Low temperature tolerance appeared unrelated to body size and energetic state. Salinity profiles were used to describe the location and extent of optimal wintering habitats under various hydrographic regimes. The location of optimal habitats was displaced by over 27 km along the river axis because of variation in salinity regime. Changes in the availability of optimal habitat may be responsible for variation in recruitment to the Hudson River population. These results demonstrate the need to consider a holistic approach encompassing all seasons of the year in assessing habitat requirements of fishes.

Résumé : L'examen des rôles de la salinité, de la taille et du statut énergétique sur la tolérance à la température chez de jeunes bars rayés (*Morone saxatilis*) de l'année (YOY) a servi à cartographier l'habitat optimal d'hiver dans l'estuaire de la Hudson. Une expérience de longue durée a comparé la survie à 15 et à 30 ppt. Au cours d'expériences subséquentes, des poissons acclimatés à l'hiver ont été exposés à des déclins de température (2,3°C·jour^{-1} à 1°C·semaine^{-1}) à des salinités variant de 0 à 35 ppt. La survie maximale aux basses températures s'observe toujours aux salinités intermédiaires. Ces résultats laissent croire que la répartition des bars rayés observée pendant l'hiver dépend de contraintes physiologiques sur la capacité osmorégulatrice à basse température. La tolérance aux basses températures apparaît être sans relation avec la taille ou le statut énergétique. Des profils de salinité permettent de décrire l'emplacement et l'étendue des habitats optimaux d'hiver sous divers régimes hydrographiques. La position des habitats optimaux s'est déplacée de plus de 27 km le long de l'axe de la rivière à cause d'une variation dans le régime de salinité. Les changements dans la disponibilité de cet habitat optimal peuvent être responsables des variations dans le recrutement de la population de la Hudson. Ces résultats démontrent qu'il est nécessaire d'adopter une approche holistique qui couvre toutes les saisons de l'année pour évaluer les besoins en habitat des poissons.

[Traduit par la Rédaction]

Introduction

Estuaries are inhabited by many temperate fish species during one or more life stages and are considered an important nursery area for juveniles (Day et al. 1989; Able and Fahay 1998). Whether or not individual species are actually dependent on estuaries continues to be debated, as does the exact nature of the benefits offered to juvenile fishes. The terrestrial input of nitrogen and the vertical mixing of tides generate high rates of primary and secondary production in estuaries, promoting rapid growth and development of young fishes (Day et al. 1989). The shallow water and dominance of macrophyte vegetation common to estuaries may offer refuge from pelagic piscivores (Blaber and Blaber 1980; Paterson and Whitfield 2000). In addition, salinities near iso-osmotic to the blood of fish may minimize the

Received 31 July 2001. Accepted 17 April 2002. Published on the NRC Research Press Web site at http://cjfas.nrc.ca on 12 June 2002.
J16471

T.P. Hurst[1,2] **and D.O. Conover.** Marine Sciences Research Center, State University of New York, Stony Brook, NY 11794-5000, U.S.A.

[1]Corresponding author (e-mail: thomas.hurst@noaa.gov).
[2]Present address: Alaska Fisheries Science Center, National Marine Fisheries Service, NOAA, Hatfield Marine Science Center, Newport, OR 97365, U.S.A.

 DOI: 10.1139/F02-051 © 2002 NRC Canada

physiological costs of osmoregulation, allowing more energy to be allocated to growth, ultimately enhancing survival (Hettler 1976; Lankford and Targett 1994; Cardona 2000).

Most of the research evaluating the benefits of estuarine residency has been conducted in the summer, whereas the habitat value of estuaries in winter has yet to be evaluated. The abundance and diversity of fishes residing in many temperate estuaries is substantially reduced in winter, and there is often a major shift in community composition from summer to winter (Day et al. 1989; Able and Fahay 1998; Ishitobi et al. 2000). These shifts suggest that benefits to juvenile fish of summer residence in estuaries may not apply in winter. For example, in north temperate regions, estuarine water temperatures are lower than those in the coastal ocean during the winter (Bowman 1976). Low temperatures often disrupt ion exchange mechanisms in fishes, leading to osmotic stress (Hochachka 1988), potentially exacerbated by fluctuating salinities. In addition, the high mixing rates and flow velocities of estuaries may be detrimental to ectotherms in winter when locomotor abilities are reduced by low temperature (Bennett 1990). Hence, estuaries may be unsuitable habitat for many species in winter.

Recent work suggests that the first winter may be an important period in the life history of striped bass (*Morone saxatilis*), as size-dependent winter mortality of young-of-the-year (YOY) fish has been documented in two northern populations (Bradford and Chaput 1997; Hurst and Conover 1998). The selective removal of small fish in northern populations is believed to have led to the evolution of genetically based differences in growth rate among striped bass populations (Conover et al. 1997; Brown et al. 1998). Furthermore, recruitment rates of fish to age-1 in the Hudson River population were negatively correlated with the severity of winter that YOY fish experience, as cold winters tend to produce fewer age-1 fish than expected from the abundance of YOY fish in the previous summer (Hurst and Conover 1998). The causes of this mortality are still unknown, but potential factors include osmotic and thermal stress. Lower lethal temperatures have not been reported for this species. YOY striped bass are known to suffer a winter energy deficit that varies in severity among years. Energetic condition was related to survival in a laboratory experiment, but starvation did not appear to be the direct source of mortality (Hurst et al. 2000). These observations suggest an interaction between energetic and other stressors (Hurst et al. 2000).

Young-of-the-year striped bass in the Hudson River undergo a habitat shift from the principal summer nursery areas in the low salinity upper estuary to the lower estuary in winter (Lawler, Matusky and Skelly Engineers 1983; Dovel 1992). The distribution of YOY striped bass is also more restricted in winter than in summer. In summer, YOY striped bass are commonly found throughout the estuary and in the marine embayments along the north and south shores of western Long Island (Able and Fahay 1998). In contrast, during winter, the lower Hudson River estuary represents the only area where aggregations of YOY fish have been found (Dovel 1992). Trawling data from the winter of 1982–1983 illustrates the restricted distribution of striped bass in the Hudson River estuary (Fig. 1). Striped bass were markedly more abundant in the region adjacent to Manhattan (MAN) than in other regions. The reasons for this concentration at the onset of winter are unknown but may be related to the location of optimal conditions for overwinter survival.

In this study we determined how salinity, body size, and energetic state affect the survival of striped bass under rapidly and gradually decreasing temperatures. We also compared overwinter survival of fish held in the laboratory at mesohaline and polyhaline conditions. We then used salinity profiles through the Hudson River estuary to demonstrate how changes in the thermal and hydrographic regime interact to determine the location and extent of optimal overwintering habitats for YOY striped bass.

Methods

An overwinter simulation experiment evaluated the survival of striped bass maintained through the winter at two salinities (15 and 30 ppt) and ambient temperatures. This experiment was designed to examine responses to long-term exposure to a realistic environment and included fed and unfed treatments to examine the potential effect of energetic state on survival. Additional experiments were conducted to examine thermal and osmoregulatory stress under controlled conditions at a wide range of salinities. In these experiments, we exposed fish to declining temperatures at salinities ranging from 0 ppt to 35 ppt. Temperature decline rates ranged from 2.3°C·day^{-1} to 1°C·week^{-1}. The effect of energetic state on low temperature tolerance was assessed by prior manipulation of energy levels. We provide comparison of experimental conditions (Table 1), with details below.

Overwinter simulation

Wild YOY striped bass were collected from the Hudson River estuary in the vicinity of Croton Point, N.Y., in early November 1994, before their down-estuary migration. The fish were transported to the laboratory in river water and transferred to tanks of similar salinity. Salinity in the tanks was raised to that found in the overwintering area (approximately 25 ppt; Dovel 1992) over 3 days. Fish were given a prophylactic treatment of 15 ppm oxytetracycline for 7 days to reduce risk of mortality from infection. Temperatures during the acclimation period ranged from 5 to 9°C. Only fish appearing healthy and behaving normally were used in experiments. Fish were fed frozen adult *Artemia* sp. before experiments. Total lengths (TL) of experimental fish ranged from 67 mm to 128 mm and did not differ significantly among treatments or tanks ($p > 0.344$).

All fish were measured and randomly assigned to one of eight tanks on December 28, 1994. Salinities were changed from the acclimation salinity (~25 ppt) to test salinities (4 tanks each at 15 ppt and 30 ppt) over several days by partial water changes. Within each salinity treatment, tanks were randomly assigned to one of two feeding treatments. Half of the tanks were fed frozen adult brine shrimp, *Artemia* sp., ad libitum daily, while the remaining tanks had food withheld for the duration of the experiment. The tanks were housed in a greenhouse and exposed to ambient photoperiods and temperatures throughout the winter. The winter of 1994–1995 was one of the mildest on record in the region. Temperatures in the experiment were generally between 5°C and 10°C but fell below 3°C during a cold spell in early February. Tanks were checked at least twice daily and any mortalities were

© 2002 NRC Canada

Fig. 1. Map of lower Hudson River estuary and regional catch per unit effort (CPUE) of striped bass (*Morone saxatilis*). CPUE, salinity, and temperature data were drawn from Lawler, Matusky & Skelly Engineers (1983). CPUE data are presented as mean catch of striped bass per 10-min tow ± 1 standard error based on 8–42 samples per region per month. Fish were caught with a 30-ft. flat otter trawl with a 1/4-in. -mesh cod-end liner. NHB, north of Haverstraw Bay; SHB, south of Haverstraw Bay; STZ, south of Tappan Zee; MAN, Manhattan; HAR, harbor region.

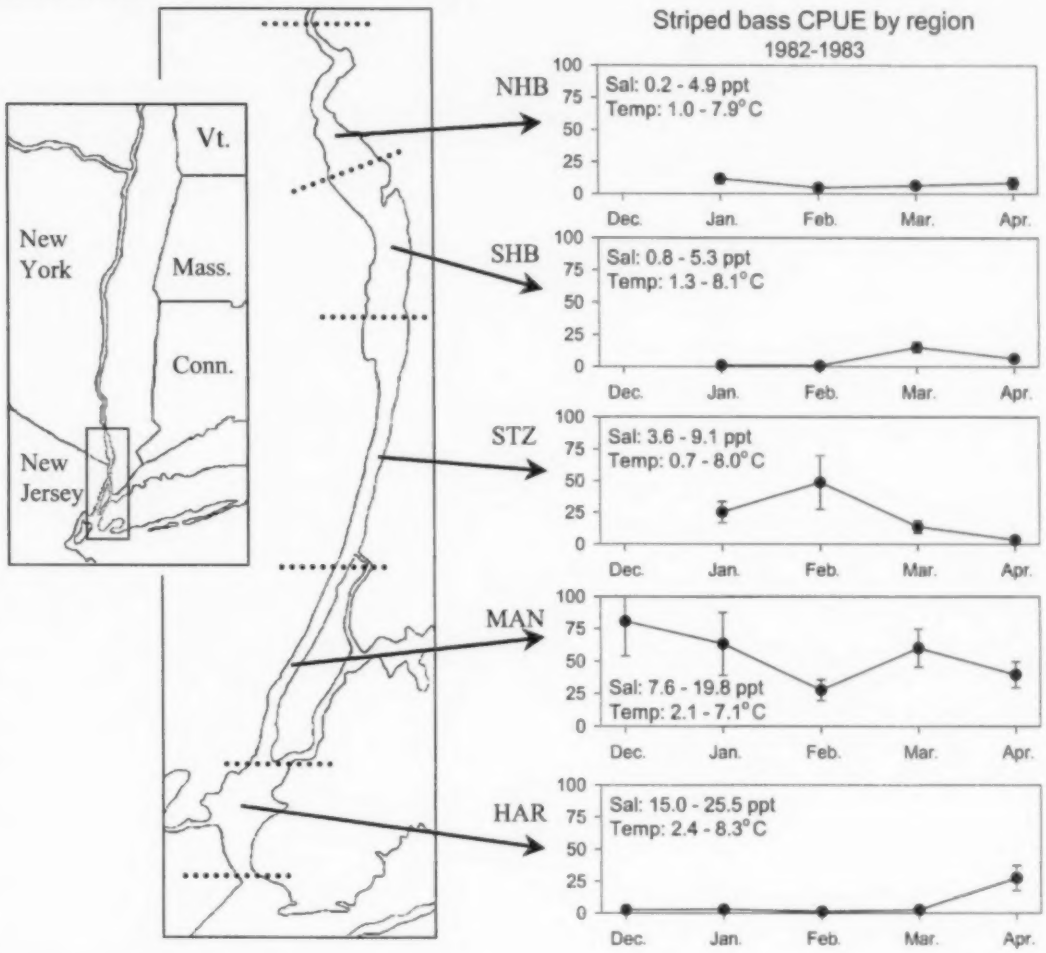

Table 1. Summary and comparison of experimental procedures.

Experiment	Timing	Salinities tested (ppt)	Thermal regime	Fish source	Fish size (mm TL)	Sample size	Energy analysis
Overwinter	Dec. 1994 – Mar. 1995	15, 30	Ambient 2–13°C	Wild	63–135	246	Fed + starved treatments
Decline 1	Jan. 1995	0, 5, 15, 30	2.3°C·day^{-1} decline	Lab-reared	91–130	40	None
Decline 2	Jan. 1997	0, 5, 15, 25, 35	1°C·day^{-1} decline	Wild	67–128	50	Prior manipulation
Decline 3	Feb. – Apr. 1997	5, 15, 25, 35	1°C·week^{-1} decline	Wild	72–126	40	Prior manipulation

Note: TL = total length.

measured (TL). The experiment was terminated on March 13, 1995, when all surviving fish were sacrificed with an overdose of anesthetic and measured.

Temperature decline experiments

Young-of-the-year striped bass were reared from eggs in the laboratory (decline 1) or collected from the Hudson River estuary in the vicinity of Croton Point, N.Y., in early November 1997 (declines 2 and 3). Laboratory rearing followed the procedures used in Fontes (1998). Laboratory-reared and wild-caught fish were acclimated to winter conditions in a greenhouse as describe above. Total lengths of fish used in the experiments ranged from 67 mm to 130 mm. Lengths did not differ significantly among treatments within

© 2002 NRC Canada

any experiment ($p > 0.123$), but laboratory-reared fish used in decline 1 were larger than wild-caught fish ($p < 0.001$).

Fish were transferred from the acclimation tanks to the experimental tanks and brought to a constant temperature of 7°C (5°C in decline 1). Fish were not fed in the experimental tanks. The salinity in the experimental tanks was then changed to the test salinity over several days by not more than 5 ppt·day^{-1}. Temperatures were reduced by 2.3°C·day^{-1} to –2°C in decline 1; by 1°C·day^{-1} to –1°C and held at –1°C for an additional week in decline 2; and by 1°C·week^{-1} to a minimum of 1°C in decline 3. These regimes were selected to represent the temperatures that YOY striped bass might be exposed to on the wintering grounds. Bottom water temperatures in the Hudson River rarely fall below 1°C for extended periods, but water temperature in shallow embayments can change rapidly, often falling below 0°C for several days (T. Hurst, personal observations). Fish unable to maintain orientation and coordinated swimming were removed from the tank, measured, and weighed. All fish remaining at the end of the experiment were removed, sacrificed with an overdose of anaesthetic, measured, and weighed. All fish from declines 2 and 3 were frozen for compositional analysis.

Experimental tanks (50 L) were submerged in a temperature-controlled water bath. Temperature in the bath was controlled with two recirculating water chillers and was generally within 0.5°C of the prescribed temperature. Each tank was aerated and water was changed periodically with water of the same salinity chilled to the temperature in the tanks. Photoperiod in the experiment was maintained at 10 h light (L) – 14 h dark (D) to mimic winter conditions.

Energy levels for fish used in declines 2 and 3 were manipulated before testing to generate increased variation. To accomplish this, fish were divided between two identical tanks on December 1, 1997. One group was fed frozen adult brine shrimp (*Artemia* sp.) daily until initiation of experiments (high lipid treatment), whereas the other group was fed a limited ration approximately once per week (low lipid treatment). To identify lipid treatment during experiments, fish from one group were marked with a clip of the ventral lobe of the caudal fin. The group receiving the mark was randomly determined for each experimental group. Subsequent analysis showed that this procedure for lipid level manipulation was highly successful: lipid levels differed significantly between the low lipid and high lipid treatments ($p < 0.001$), averaging 1.88% and 3.48% dry weight, respectively. Lipid content of individual fish was determined with standard extraction procedures. Details of our extraction procedures can be found in Hurst et al. (2000).

Statistical analysis

Data from the laboratory experiments were analyzed using survival analysis. This technique is applied when examining a time course of events where the event of interest (in this case mortality) does not occur in all subjects before termination of observations (end of experimental period; Miller 1981). This technique is preferable to comparisons of percent survival as it takes into account both the number and timing of mortalities. Feeding treatment and salinity were considered main effects in the analyses. Body length was used as a covariate in the analysis of all experiments to examine the effects of size in low temperature tolerance. In addition, lipid level measured at the end of the experiment was tested as a covariate in the analysis of experiments of declines 2 and 3.

Mapping of optimal habitats

Results from the laboratory experiments were combined with salinity profiles of the Hudson River estuary to describe the location and extent of optimal overwintering habitats for striped bass. Optimal salinities for overwintering YOY striped bass were estimated for warm and cold thermal regimes. A river temperature of 5°C represented warm conditions and 1°C represented severe conditions, based on observations of winter temperature cycling in the lower Hudson River estuary (Hurst and Conover 1998). Given that salinity in the Hudson River estuary can vary by up to 5 ppt during the tidal cycle (Oey 1985), we used conservative estimates of optimal salinities, such that habitats considered optimal offered high survival throughout the tidal cycle.

We used all available winter profiles to describe the variation in salinity structure in the Hudson River estuary. To be included, salinity profiles must have been conducted between October and May and have included the intersections of the 10 ppt and 25 ppt isohalines with the bottom. We found nine profiles of salinity structure that met these criteria (Olsen 1979; Hirschberg and Bokuniewicz 1991; and Bokuniewicz 1996). Regions with optimal salinities at the river bottom were then plotted on areal maps to illustrate changes in the location and extent of optimal habitats in warm and cold conditions.

Results

Overwintering experiment

Survival patterns were homogeneous among replicates within feeding treatments in the 15 ppt treatments ($p > 0.09$), but there were significant differences in survival among replicates in the 30 ppt treatments ($p < 0.01$; Fig. 2). Despite these differences among replicates, there was a clear effect of salinity on survival. Survival was high in all tanks at 15 ppt, ranging from 87% to 100%. One tank of fish at 30 ppt had similarly high survival (90%), whereas survival in the three remaining tanks ranged from 0% to 65%. Most mortality in the experiment (61% of 75 mortalities) occurred during a 12-day period when tank temperatures fell to 2°C and was largely restricted to tanks with 30 ppt water. Among the four tanks at 15 ppt, there was only a single mortality during this period. Survival in the overwintering experiment appeared unrelated to length ($p > 0.27$) or feeding treatment.

Decline 1

Survival of YOY striped bass was significantly affected by salinity in decline 1 (Fig. 3*b*). Fish held at 0 ppt had significantly lower survival than fish at all higher salinities ($p < 0.001$). At salinities between 5 ppt and 30 ppt, survival was high even at temperatures below 0°C. There were no differences in survival patterns between 5 ppt and 30 ppt ($p = 0.623$). Survival in decline 1 was independent of body size ($p = 0.267$).

Decline 2

There was no effect of lipid density on survival patterns of fish in decline 2. Survival patterns were homogeneous

© 2002 NRC Canada

Fig. 2. Temperature record (dotted line in *a*) and survival curves of young-of-the-year striped bass (*Morone saxatilis*) in overwintering simulation experiment: (*a*) fed treatments, (*b*) unfed treatments. Solid lines represent 15 ppt treatments, broken lines represent 30 ppt treatments.

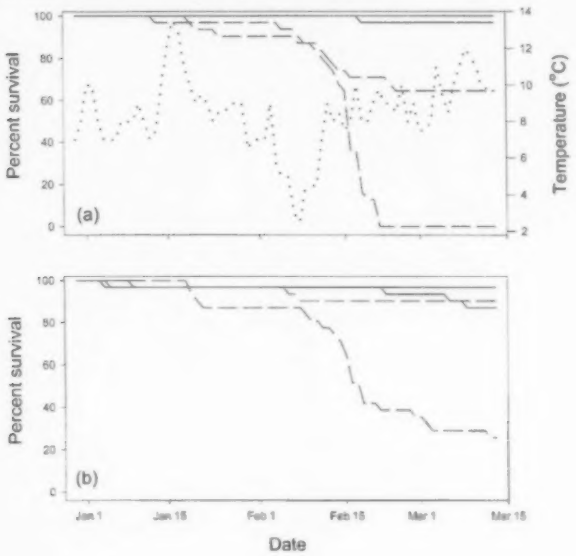

Fig. 3. Temperature records (*a*) and survival curves from (*b*) decline 1 and (*c*) decline 2 experiments. In *a*, the thick solid line represents temperatures in decline 1, the thin solid line and dotted line represent target and actual temperatures, respectively, recorded during decline 2. Note time scale in *b*.

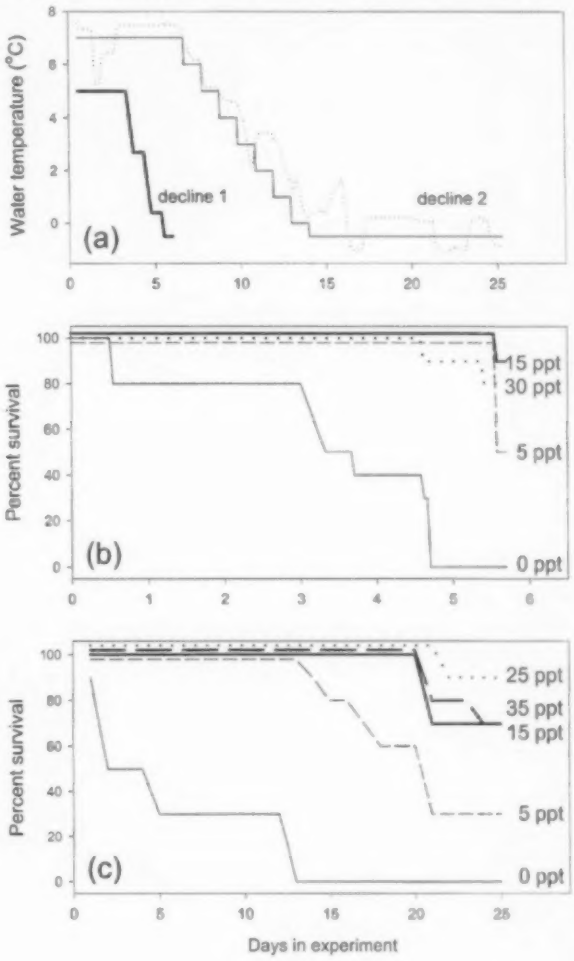

among fish from high lipid and low lipid treatments tested at the same salinity (all $p > 0.05$), allowing the lipid treatments to be combined for analysis of salinity effects. Survival was significantly affected by salinity ($p < 0.001$; Fig. 3*c*). Pairwise comparisons showed that survival in the 0 ppt treatment was significantly lower than at all higher salinities ($p < 0.001$). Survival at 5 ppt was significantly lower than survival at higher salinities ($p < 0.037$), but mortality in this treatment did not begin until temperatures fell below 1°C (Fig. 3*a*). There were no differences in survival among the 15, 25, and 35 ppt treatments (pairwise comparisons: $p > 0.222$). There was no effect of body length on survival (test of covariate: $p = 0.733$).

Decline 3

Because of the high mortality rate at 0 ppt salinity in the two previous experiments, we did not include a freshwater treatment in the decline 3 experiment. Survival was significantly affected by lipid level, with fish from the low lipid treatment dying before those from the high lipid treatment at all salinities ($p < 0.001$). Among the high lipid groups, there was a significant effect of salinity on survival rate ($p = 0.042$) owing to the higher survival of fish between 5 ppt and 25 ppt than at 35 ppt (Fig. 4). Among low lipid groups, survival patterns were nearly identical ($p = 0.639$) and independent of body length ($p = 0.112$). Again, survival was not affected by body length ($p = 0.431$).

Delineation of optimal habitats

Optimal salinities for overwintering YOY striped bass based on laboratory experiments were estimated to be from 5 to 35 ppt under warm conditions (5°C) and from 10 to 25 ppt under cold conditions (1°C). The lower end of the optimal salinity ranges is based on the observations of high mortality in freshwater at temperatures above 5°C and increasing mortality at 5 ppt as temperatures fell below 1°C in declines 1 and 2. The upper limit to optimal salinities under low temperatures is based on the observations of high midwinter mortalities in the overwinter simulation at 30 ppt and the higher mortality of the 35 ppt fed treatment fish in decline 3.

Based on these thresholds, we found substantial changes in the location and extent of optimal overwintering habitat for YOY striped bass (Fig. 5). In terms of salinity, most of the coastal ocean would provide suitable habitat for overwintering striped bass under warm conditions but not under cold conditions. The locations of intersections of the 10 ppt and 25 ppt isohalines with the river bottom (given as the distance in kilometres along the river axis, north from the Verrazano Narrows Bridge, river-kilometres (rkm)) var-

© 2002 NRC Canada

Fig. 4. Temperature record (*a*) and survival curves from decline 3 experiment. (*a*) The solid line represents the target temperature and the dotted line represents hourly temperatures recorded during experiment. (*b* and *c*) Survival curves of (*b*) high lipid and (*c*) low lipid treatments at different salinities. Line key is consistent across *b* and *c*.

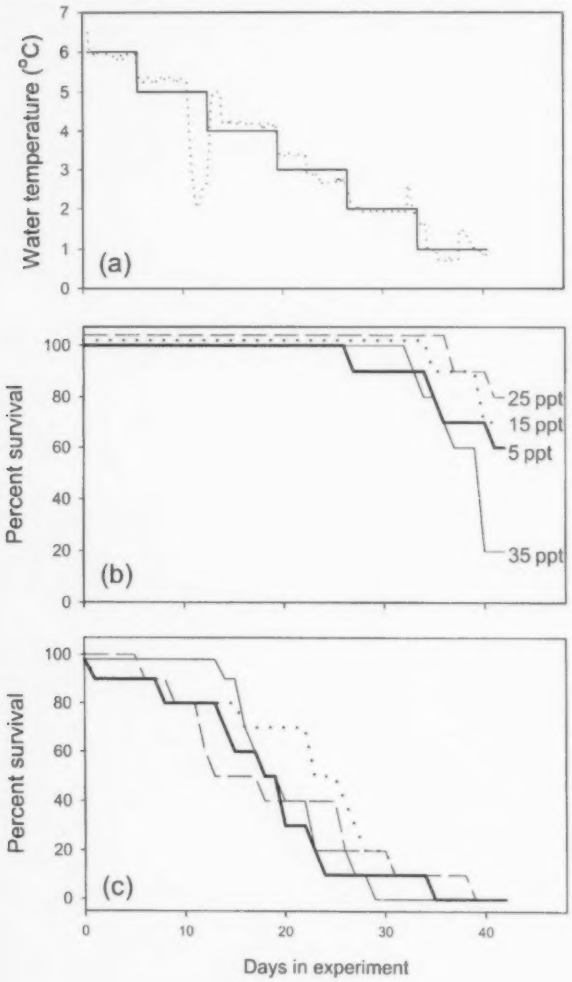

Fig. 5. Optimal overwintering habitats of young-of-the-year striped bass (*Morone saxatilis*) based on salinity transects through the Hudson River estuary: (*a*) January 1995, upriver habitat distribution; (*b*) May 1981, downriver habitat distribution; (*c*) May 1994, most restricted distribution of optimal habitats.

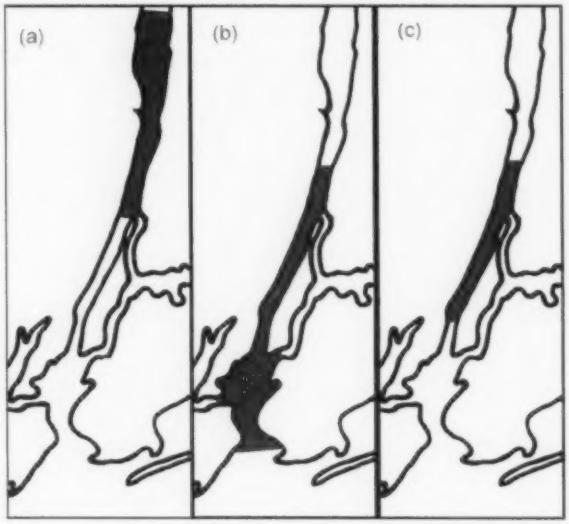

Table 2. Locations of 10 ppt and 25 ppt isoclines in the Hudson River estuary based on salinity profiles.

Date	25 ppt	10 ppt	Midpoint	Range
March 1977[a]	7	37	22	30
May 1981[b]	–5	47	21	52
May 1994[c]	15	37	26	22
October 1994[c]	15	67	41	52
December 1994[c]	5	44	24.5	39
January 1995[c]	29	67	48	38
March 1995[c]	25	60	42.5	35
April 1995[c]	20	65	42.5	45
May 1995[c]	20	53	36.5	33

Note: Locations are kilometres along river axis from Verrazano Narrows Bridge where isohalines intersect the substrate.
[a]From Olsen 1979.
[b]From Hirshberg and Bokuniewicz 1991.
[c]From Bokuniewicz 1996.

ied substantially in the available profiles (Table 2). Optimal habitats would be found furthest upriver (rkm 42–80) when the hydrography resembles that observed in January 1995, whereas the conditions observed in March 1977 led to the most downriver distribution of optimal habitats (rkm 20–50). The geographic extent of optimal wintering habitats was most restricted under the May 1994 hydrography (22 km). The locations of optimal habitats based on these salinities (Fig. 5) were consistent with the observed distribution of overwintering striped bass (Fig. 1).

Discussion

Previous work examining recruitment of YOY striped bass to the Hudson River population found a correlation between minimum winter temperatures and recruitment to age-1 (Hurst and Conover 1998). This correlation is apparently not directly due to the exposure to lethal temperatures during severe winters, as YOY striped bass exhibited high survival rates at temperatures below those likely encountered in the lower Hudson River estuary when held at intermediate salinities. However, low temperature tolerance was severely compromised at salinities approaching freshwater and full seawater, suggesting that salinity encountered in the wintering grounds plays an important role in determining habitat requirements and survival.

In laboratory experiments, YOY striped bass exposed to winter water temperatures consistently exhibited the highest survival at intermediate salinities. Fish were intolerant of low temperatures in freshwater, dying at significantly higher

© 2002 NRC Canada

temperatures than fish held at intermediate and high salinities in the decline 1 and decline 2 experiments. Striped bass survived brief exposure to rapidly declining temperatures at 5 ppt in these experiments but died after prolonged exposure to temperatures below 1°C in decline 2 (independent of feeding regime). Survival in longer duration experiments (>2 weeks; overwintering simulation and decline 3) was significantly lower at salinities of 30 ppt and 35 ppt than at 15 ppt. In both experiments, fish at high salinities began dying when temperatures were reduced to 2°C. The discrepancy between the survival of fish in 30–35 ppt water in the shorter trials at temperatures below those where fish in the longer term trials began dying is likely due to the cumulative effects of exposure. Based on these laboratory observations, it appears that although a wide range of salinities would offer high survival of YOY striped bass in warm winters, residence within a much narrower range appears to be required for high survival in cold winters.

A number of studies have documented the effects of salinity on physiological function (generally growth rate), implying that habitat suitability of estuarine fishes is determined in part by spatial and temporal patterns in salinity (Lankford and Targett 1994; Cardona 2000; Secor et al. 2000). Until recently there has been relatively little work examining the factors determining habitat suitability for overwintering marine and estuarine fishes. Lankford and Targett (2001) found that low temperature tolerance increased with salinity among Atlantic croaker (*Micropogonias undulatus*), indicating the importance of the lower estuary as an overwintering habitat. Here we demonstrate that survival of overwintering YOY striped bass is determined by the interaction of temperature and salinity such that the range of suitable salinities narrows as temperatures decrease.

Low temperature tolerance in fishes is generally governed by the ability to maintain ionic balances at both the cellular and organismal level (Maetz and Evans 1972; Toneys and Coble 1980; Hochachka 1988). Several studies have documented greater tolerances to low temperatures (Procarione 1986; Martin 1988) and reduced metabolic costs at intermediate salinities (Hettler 1976; Peterson-Curtis 1997), presumably owing to the reduction of the ion gradient across the gill membrane. Measurements of oxygen consumption among YOY striped bass at low temperatures were similar at 15 ppt and 30 ppt (T. Hurst, unpublished data), indicating that estuarine residency in winter is not likely related to metabolic efficiency. However, we did find that estuarine residency would confer a direct survival advantage to overwintering juvenile striped bass.

Valenti et al. (1976) observed low survival among YOY Hudson River striped bass overwintering in seawater, in agreement with our results. The effect of exposure history on osmoregulatory function is well documented in fish (Johnston and Cheverie 1985), suggesting that survival at extreme salinities could be improved by prolonged acclimation periods. For fish raised from the egg stage in freshwater, Harrell et al. (1988) and Kelly and Kohler (1999) found high survival of striped bass at winter temperatures. Although these observations may indicate that winter survival can be enhanced in a culture setting, our acclimation and testing procedures were developed to examine the mortality risk and habitat requirements of wild fish in the Hudson River population.

Previous work on overwintering striped bass in the Hudson River population has documented the occurrence of size-selective mortality against smaller fish in field collections and laboratory experiments, possibly related to thermal stress or the depletion of energy reserves (Hurst and Conover 1998; Hurst et al. 2000). Given the allometry of gill surface area to body mass we expected that small fish should be more vulnerable to temperature-induced osmotic stress than larger fish, a pattern seen in several studies (Allanson et al. 1971; Martin 1988). Moles et al. (1997) found that salinity tolerance of overwintering coho salmon (*Oncorhynchus kisutch*) was compromised by depleted energy levels, while Kelly and Kohler (1999) found that fatty acid composition affected cold tolerance in juvenile striped bass. In none of the experiments presented here, however, did we observe any effect of body size on temperature and salinity tolerance, indicating that the observed size selectivity of mortality among overwintering YOY striped bass (Hurst and Conover 1998) is not due solely to size-based differences in vulnerability to thermal and osmotic stress. Nor did we find any consistent effect of energetic status on low temperature tolerance. Although low lipid fish had lower survival than high lipid fish in the decline 3 experiment, this mortality appeared to result directly from starvation. Occupation of intermediate salinities did not prolong survival among low lipid fish as it did among high lipid fish.

Dovel (1992) reviewed the available data from a number of fisheries surveys conducted in the Hudson River to describe the movement patterns of juvenile striped bass. Young-of-the-year striped bass remain in the lower estuary through the winter, with the lower Hudson River estuary representing the only known aggregation area. Many species co-occurring with juvenile striped bass in the Hudson River and other mid-Atlantic Bight estuaries migrate offshore or southward for overwintering (Able and Fahay 1998). Offshore oceanic waters in the mid-Atlantic Bight remain warmer than estuarine waters through the winter (Bowman 1976), presumably offering a thermal refuge to these migratory species. Our experiments suggest that although coastal waters could be suitable for juvenile striped bass in warm winters, estuarine residency appears necessary in cold winters, as it offers a refuge from the osmotic stress associated with low temperatures and high salinities.

The available data on the overwintering distribution of striped bass coincides with those habitats deemed optimal based on salinity responses observed in our laboratory experiments (Dovel 1992). The trawl survey conducted during the winter of 1982–1983 covered a large portion of the lower estuary and found that striped bass were most abundant in the MAN region where salinities averaged 16.3 ppt. In addition, it appears that fish moved in response to changing river conditions. Catch rates in the region south of Tappan Zee (STZ) peaked in January when salinity was 9.1 ppt and fell as salinity declined to 3.6 ppt in April. Likewise, striped bass were rare in the harbor region (HAR) until April when salinities in the region fell below 20 ppt. Although there is insufficient field data available to empirically determine the response of YOY fish to various salinity regimes, combining physiological responses with hydrographic profiles of the Hudson River estuary suggests that the location and extent of optimal overwintering habitats likely varies among years.

© 2002 NRC Canada

For example, hydrographic conditions observed in January 1995 would cause experimentally determined optimal habitats to extend from rkm 29 to rkm 67. This region overlaps by only 8 km the location of optimal habitats based on conditions observed in March 1977 (rkm 7–37). In addition to the displacement of optimal habitats along the river axis, our results suggest dramatic differences in the extent of optimal habitats due to changes in salinity regime. The intermediate salinity waters optimal for survival (10–25 ppt) extended over a 52 km section of the Hudson River in the October 1994 profile, whereas these waters covered less than half that area (22 km) in the May 1994 profile. Further research would be required to establish the link between recruitment patterns and availability of overwintering habitat.

The salinity profiles that we used to describe the variation in salinity regime in the Hudson River estuary were gathered from the literature and did not include the adjacent water bodies of the Harlem River, East River, Long Island Sound, or Newark Bay. These habitats have not been extensively sampled in winter, although 1 year of sampling in the East River captured few striped bass (Lawler, Matusky and Skelly Engineers 1983). Therefore, although YOY striped bass may also inhabit these areas in winter, our descriptions of changes in the location and extent of optimal habitats, reflecting hydrographic changes in the mainstem Hudson River, should qualitatively apply to the potential use of adjacent water bodies.

There has been a recent initiative to determine essential fish habitats for species supporting commercial and recreational fisheries (Benaka 1999). The work presented here demonstrates the necessity of defining these habitats based on ecophysiological factors, incorporating multiple seasons and life stages. Habitat suitability is determined by a number of physical and biotic factors, such as temperature, salinity, oxygen content, prey availability, and predator abundance. Imposed on top of spatial and temporal patterns of variability in the environment are changing requirements associated with ontogeny. Habitats suitable for survival and growth for one life stage at one time of year may be unsuitable for other stages or in other seasons. For example, juvenile striped bass are commonly found throughout the estuary and in marine embayments in the summer but appear physiologically restricted to the intermediate salinity regions of the estuary in winter. In addition, this work demonstrates that conclusions drawn from physiological response experiments can vary depending on the time scale of exposure. When habitat values are based on laboratory experiments, they should consider the effects of exposure time scales, ontogenetic stage, and seasonal cycles.

Acknowledgments

Laboratory experiments were conducted with the assistance of A. Ehtisham, C. Knackal, J. Buckel, and J. Billerbeck. D. Fontes provided laboratory-reared striped bass for use in decline 1 experiments, and K. McKown of the New York State Department of Environmental Conservation assisted in collecting wild fish. This manuscript benefitted from thoughtful comments by D. Lonsdale, R. Cowen, R. Cerrato, E. Houde, and two anonymous reviewers. Funding for this research was provided by a Fellowship in Population Biology from the Electric Power Research Institute (T.P.H.) and a research grant from the Hudson River Foundation for Science and Environmental Research (D.O.C.). This is contribution number 1240 of the Marine Sciences Research Center, State University of New York, Stony Brook, N.Y.

References

Able, K.W., and Fahay, M.P. 1998. The first year in the life of estuarine fishes in the Middle Atlantic Bight. Rutgers University Press, New Brunswick, N.J.

Allanson, B.R., Bok, A., and van Wyk, N.I. 1971. The influence of exposure to low temperature on *Tilapia mossambica* Peters (Cichlidae). II. Changes in serum osmolarity, sodium and chloride ion concentrations. J. Fish. Biol. **3**: 181–185.

Benaka, L. (*Editor*). 1999. Fish habitat: essential fish habitat and rehabilitation. American Fisheries Society, Bethesda, Md.

Bennett, A.F. 1990. Thermal dependence of locomotor capacity. Am. J. Physiol. **259**: R253–R258.

Blaber, S.J.M., and Blaber, T.G. 1980. Factors affecting the distribution of juvenile estuarine and inshore fish. J. Fish. Biol. **17**: 143–162.

Bokuniewicz, H. 1996. Building the turbidity maximum in the Hudson River estuary. Special Data Report 115, Marine Sciences Research Center, State University of New York, Stony Brook, N.Y.

Bowman, M.J. 1976. Hydrographic properties. *In* MESA New York Bight Atlas Monograph. New York Sea Grant Institute, Albany, N.Y.

Bradford, R.G., and Chaput, G. 1997. Status of striped bass (*Morone saxatilis*) in the Gulf of St. Lawrence in 1996 and revised estimates of spawner abundance for 1994 and 1995. Department of Fisheries and Oceans, Canadian Stock Assessment Secretariat Research Document 97/16.

Brown, J.J., Ehtisham, A., and Conover, D.O. 1998. Variation in larval growth rate among striped bass stocks from different latitudes. Trans. Am. Fish. Soc. **127**: 598–610.

Cardona, L. 2000. Effects of salinity on the habitat selection and growth performance of Mediterranean flathead grey mullet *Mugil cephalus* (Osteichthys, Mugilidae). Estuar. Coast. Shelf Sci. **50**: 727–737.

Conover, D.O., Brown, J.J., and Ehtisham, A. 1997. Countergradient variation in growth of young striped bass (*Morone saxatilis*) from different latitudes. Can. J. Fish. Aquat. Sci. **54**: 2401–2409.

Day, J.W., Hall, C.A.S., Kemp, W.M., and Yanez-Arancibia, A. 1989. Estuarine ecology. John Wiley & Sons, New York.

Dovel, W.L. 1992. Movements of immature striped bass in the Hudson estuary. *In* Estuarine research in the 1980's. *Edited by* C.L. Smith. State University of New York Press, Albany, N.Y. pp. 276–300.

Fontes, D.S. 1998. Countergradient latitudinal variation in somatic growth rate of striped bass (*Morone saxatilis*): physiological mechanisms and implications. M.Sc. thesis, Marine Sciences Research Center, State University of New York, Stony Brook, N.Y.

Harrell, R.M., Meritt, D.W., Hochheimer, J.N., Webster, D.W., and Miller, W.D. 1988. Overwintering success of striped bass and hybrid striped bass held in cages in Maryland. Prog. Fish-Cult. **50**: 120–121.

Hettler, W.F. 1976. Influence of temperature and salinity on routine metabolic rate and growth of young Atlantic menhaden. J. Fish. Biol. **8**: 55–65.

© 2002 NRC Canada

Hirschberg, D., and Bokuniewicz, H.J. 1991. Measurements of water temperature, salinity and suspended sediment concentrations along the axis of the Hudson River estuary. Special Data Report 11, Marine Sciences Research Center, State University of New York, Stony Brook, N.Y.

Hochachka, P.W. 1988. Channels and pumps—determinants of metabolic cold adaptation. Comp. Biochem. Physiol. B, **90**: 515–519.

Hurst, T.P., and Conover, D.O. 1998. Winter mortality of young-of-the-year Hudson River striped bass (*Morone saxatilis*): size-dependent patterns and effects on recruitment. Can. J. Fish. Aquat. Sci. **55**: 1122–1130.

Hurst, T.P., Schultz, E.T., and Conover, D.O. 2000. Seasonal energy dynamics of young-of-the-year Hudson River striped bass. Trans. Am. Fish. Soc. **129**: 145–157.

Ishitobi, Y., Hiratsuka, J., Kuwabara, H., and Yamamuro, M. 2000. Comparison of fish fauna in three areas of adjacent eutrophic estuarine lagoons with different salinities. J. Mar. Syst. **26**: 171–181.

Johnston, C.E., and Cheverie, J.C. 1985. Comparative analysis of ionoregulation in rainbow trout (*Salmo gairdneri*) of different sizes following rapid and slow salinity adaptation. Can. J. Fish. Aquat. Sci. **42**: 1994–2003.

Kelly, A.M., and Kohler, C.C. 1999. Cold tolerance and fatty acid composition of striped bass, white bass, and their hybrids. N. Am. J. Aquacult. **61**: 278–285.

Lankford, T.E., and Targett, T.E. 1994. Suitability of estuarine nursery zones for juvenile weakfish (*Cynoscion regalis*): effects of temperature and salinity on feeding, growth and survival. Mar. Biol. **119**: 611–620.

Lankford, T.E., and Targett, T.E. 2001. Low-temperature tolerance of age-0 Atlantic croakers: recruitment implications for U.S. mid-Atlantic estuaries. Trans. Am. Fish. Soc. **130**: 236–249.

Lawler, Matusky and Skelly Engineers. 1983. 1982–1983 Westway winter sampling program. Vol. 1. Trawl data. Report to New York State Department of Transportation, Pearl River, N.Y.

Maetz, J., and Evans, D.H. 1972. Effects of temperature on branchial sodium exchange and extrusion mechanisms in the seawater-adapted flounder *Platichthys flesus* L. J. Exp. Biol. **56**: 565–585.

Martin, T.J. 1988. Interaction of salinity and temperature as a mechanism for spatial separation of three co-existing species of Ambassidae (Cuvier) (Teleostei) in estuaries on the south-east coast of Africa. J. Fish Biol. A, **33**: 9–15.

Miller, R.G. 1981. Survival analysis. John Wiley & Sons, Ltd., New York.

Moles, A., Korn, S., and Rice, S. 1997. Effects of low temperatures and starvation on resistance to stress in presmolt coho salmon. *In* Fish Ecology in Arctic North America. *Edited by* J. Reynolds. American Fisheries Society Symposium 19, Bethesda, Md. pp. 148–154.

Oey, L.Y., Mellor, G.L., and Hires, R.I. 1985. A 3-dimensional simulation of the Hudson–Raritan Estuary. 2. Comparison with observation. J. Phys. Oceanogr. **15**: 1693–1709.

Olsen, C.R. 1979. Radionuclides, sedimentation and accumulation of pollutants in the Hudson estuary. Ph.D. thesis, Columbia University, New York.

Paterson, A.W., and Whitfield, A.K. 2000. Do shallow-water habitats function as a refugia for juvenile fishes? Estuar. Coast. Shelf Sci. **51**: 359–364.

Peterson-Curtis, T.L. 1997. Effects of salinity on survival, growth, metabolism, and behavior in juvenile hogchokers, *Trinectes maculatus fasciatus* (Achiridae). Environ. Biol. Fishes, **49**: 323–331.

Procarione, L.S. 1986. Ultimate lower lethal temperature of red drum *Sciaenops ocellatus* as a function of temperature and salinity. M.S. thesis, Texas A & M University, College Station, Tex.

Secor, D.H., Gunderson, T.E., and Karlsson, K. 2000. Effect of temperature and salinity on growth performance in anadromous (Chesapeake Bay) and nonanadromous (Santee-Cooper) strains of striped bass *Morone saxatilis*. Copeia, 2000: 291–269.

Toneys, M.L., and Coble, D.W. 1980. Mortality, hematocrit, osmolality, electrolyte regulation, and fat depletion of young-of-the-year freshwater fishes under simulated winter conditions. Can. J. Fish. Aquat. Sci. **37**: 225–232.

Valenti, R.J., Aldred, J., and Liebell, J. 1976. Experimental cage culture of striped bass in northern waters. Proc. Annu. Meet. World Aquacult. Soc. **7**: 99–108.

© 2002 NRC Canada

Relationships of channel characteristics, land ownership, and land use patterns to large woody debris in western Oregon streams

Michael G. Wing and Arne Skaugset

Abstract: Regression tree analysis was used to test the relationship of channel and aquatic habitat characteristics from 3793 stream reaches in western Oregon State to the abundance of large woody debris (LWD). Stream reaches were drawn from diverse ownerships and land uses – land cover types over a broad geographic extent. When all land uses – land covers were considered, ownership and land use patterns were related to LWD abundance. When nonforested land uses were excluded, however, these factors became less important. In forested streams, LWD abundance was predicted primarily by stream gradient and bankfull channel width, with the volume, frequency, and size of LWD pieces decreasing as channel size increased. Within forested lands, stand age and forest distribution were related to LWD size but had small correlations with LWD volume and abundance. The strong relationship of stream gradient and bankfull channel width with LWD suggests that in forested areas, the most significant factor related to LWD counts is the geomorphology of stream reaches and their surrounding areas. Land managers in western Oregon who want to improve aquatic habitat quality may want to direct their efforts to increasing LWD in larger streams, which typically include smaller quantities of LWD.

Résumé : Des arbres de régression nous ont permis de tester la relation entre les caractéristiques du chenal et des habitats aquatiques et l'abondance des débris ligneux de grande taille (LWD) dans 3793 sections de cours d'eau de l'ouest de l'Oregon. Les sections de cours d'eau se retrouvent sur diverses sortes de propriétés et représentent une variété de types d'utilisation des terres et de couvertures végétales sur une large étendue géographique. Lorsque tous les types d'utilisation des terres et toutes les couvertures végétales sont prises en considération, il existe une relation entre le type de propriété et l'utilisation des terres, d'une part, et l'abondance des LWD, d'autre part. Cependant, si on exclut les zones qui n'ont pas de vocation forestière, ces facteurs deviennent moins importants. Dans les cours d'eau sous couvert forestier, l'abondance des LWD peut être prédite principalement à partir du gradient du cours d'eau et de la largeur du lit à pleins bords; le volume, la fréquence et la taille des pièces de LWD décroissent à mesure que s'élargit le chenal. Dans les zones forestières, l'âge et la répartition de la forêt sont en corrélation avec la taille des LWD, mais leur corrélation avec le volume et l'abondance des LWD est faible. La forte relation entre le gradient du cours d'eau et la largeur à plein bords du chenal, d'une part, et les LWD, d'autre part, laisse croire qu'en région forestière, le facteur explicatif le plus significatif de l'importance des LWD est la géomorphologie des sections de cours d'eau et des zones avoisinantes. Les gestionnaires du territoire désireux d'améliorer la qualité de l'habitat aquatique dans l'ouest de l'Oregon pourraient envisager d'augmenter la quantité de LWD dans les petits cours d'eau qui généralement en contiennent peu.

[Traduit par la Rédaction]

Introduction

The status of Pacific salmon stocks is uncertain in the Pacific Northwest (Botkin et al. 1995; Nehlsen 1997). Degradation of freshwater habitat is one of the leading causes of stock declines. Causes of habitat disturbance and reduction include dams, agriculture, logging, urbanization, grazing, and mining (Meehan 1991; Botkin et al. 1995). Many policy efforts suggest maintaining or restoring habitat areas so that high-quality conditions are present in streams (FEMAT 1993; ODF 1994). The identification of high-quality aquatic habitat for salmonids is challenging and reflects the complex life cycles of salmonids (see Groot and Margolis 1991). Common components in high-quality in-stream habitat include channel complexity, gravel beds, pools, undercut banks, riparian vegetation, low water temperature, and large woody debris (LWD) (Meehan 1991; NRC 1996). Of these components, LWD may be the most important because it can influence almost all other components (NRC 1996; Bilby and Bisson 1998). The contributions of LWD include reducing the power of streams (Beschta and Platts 1986), storing sediment in channels (Bilby and Bisson 1998), creating gravel bars (Abbe and Montgomery 1996), contributing organic matter (Bisson et al. 1987), and providing improved winter habitat (Tschaplinski and Hartman 1983).

LWD abundance has also been linked to the status of in-

Received 22 May 2001. Accepted 18 April 2002. Published on the NRC Research Press Web site at http://cjfas.nrc.ca on 14 June 2002.
J16365

M.G. Wing[1] and A. Skaugset. Department of Forest Engineering, Oregon State University, Corvallis, OR 97331, U.S.A.

[1]Corresponding author (e-mail: Michael.Wing@orst.edu).

 DOI: 10.1139/F02-052 © 2002 NRC Canada

stream pools. Pools are relatively deep portions of stream channels that can provide critical fish rearing habitat during low-flow conditions (Beschta and Platts 1986). Individual LWD pieces can dominate the formation of pools (Montgomery et al. 1995, 1996). Pool surface area and volume generally increase with increasing LWD counts and size (Bisson et al. 1987; Bilby and Ward 1989), whereas there are fewer pools and more riffle units in streams with low LWD abundance (Ralph et al. 1994). When LWD becomes less abundant, there may be fewer pools and less structural complexity (House and Boehne 1987). In general, as LWD decreases in streams, habitat quality and a stream's capacity for rearing salmon also decrease (Hicks et al. 1991). Thus, identifying the processes and landscape patterns that are related to LWD abundance is critical to understanding high-quality aquatic habitat.

Many different land uses and disturbances over the past 150 years have affected the amount and types of LWD available to streams in western Oregon. Activities such as logging, agriculture, grazing, and development have removed trees from riparian areas and reduced the amount and types of LWD potentially available to streams (Hicks et al. 1991; Meehan 1991). As early as the 19th century, large pieces of wood were removed from streams to maintain navigation routes and to allow transportation of large wood to downstream timber mills. In addition, splash damming was prevalent along smaller coastal streams until the early 1900s (Sedell and Luchessa 1982). Splash damming involved building dams and storing cut timber upstream of the dams. After streams filled the dammed area, the dam was broken, and the resulting rush of water carried the accumulated timber and other channel-bound wood downstream to be processed by mills. Stream cleaning was heavily practiced in western Oregon between the 1950s and 1970s. During this period, LWD was perceived as a barrier to anadromous salmonids on their spawning migration (Bilby and Bisson 1998). Consequently, LWD was actively removed from streams, thus destabilizing channels and creating large amounts of sediment that flowed downstream and threatened fish populations (Bisson et al. 1987).

In the Pacific Northwest, policies have encouraged monitoring aquatic habitat to establish baseline conditions for determining changes in habitat quality. Stream habitat classification techniques have been developed for estimating habitat quantity and quality (Rosgen 1994), and extensive stream surveys have been conducted during the past 10 years. Despite the extensive number of stream surveys conducted, there are few published studies examining the influences of land use and ownership on LWD abundance at broad spatial scales. Ralph et al. (1994) studied the influence of forest land management on aquatic habitat characteristics, including LWD, for 245 streams in western Washington State but did not study other land use types. There are, however, no published results that examine such relationships in Oregon. To this end, we analyzed an extensive spatial database of aquatic habitat conditions created for western Oregon using stream habitat classification techniques and a geographic information system (GIS) (Wing and Skaugset 1998). We used this database to identify factors related to LWD abundance in western Oregon streams. The database provides an unprecedented opportunity to use stream reach scale data to investigate LWD abundance over a large geographic area across multiple ownerships and land uses. Our overall objectives were to identify the database factors most strongly related to LWD abundance and to determine whether ownership and land use patterns are related to LWD abundance. We used an exploratory statistical technique called regression tree analysis to meet our study objectives.

Methods

Stream survey crews collected most of the data used for this analysis using protocols developed by the Oregon Department of Fish and Wildlife (ODFW) Aquatic Inventory Project (AIP). Since 1990, the ODFW has led Oregon efforts to collect aquatic habitat data and has developed a detailed method for stream habitat surveys (Moore et al. 1998). The method divides streams into discrete habitat units based on visual estimates of channel morphology and hydrology. Habitat units are typically no longer than the active channel width. Habitat features such as LWD, channel characteristics, and riparian vegetation are quantified for each unit by using both quantitative and qualitative approaches, with habitat unit data aggregated into reaches. Reaches are delineated by tributary junctions or major changes in stream channels, surrounding landforms, or vegetation. Following field collection, unit data are averaged for each reach. One consideration in working with AIP data is that streams are not selected for surveying through a random draw but through a number of criteria including developing baseline data for restoration activities, land owner interest, and to assess perceived alterations to habitat quality. The AIP has only recently (1999) implemented a systematic, statistically based sampling plan. We transferred all reach data collected between 1990 and 1996 into a GIS for data storage and analysis. This transformation allowed us to include geology, stream order, and ownership information in our GIS database (described by Wing and Skaugset 1998). The final spatial database contained data for 3793 reaches from 1370 streams and represented more than 5600 km of stream length (Fig. 1).

For analysis, we selected three LWD variables as response variables: LWD volume, the number of LWD pieces, and number of key LWD pieces. Following the AIP protocol (Moore et al. 1998), logs at least 0.15 m in diameter and 3 m in length were used to tabulate LWD volume and number of LWD pieces, whereas key LWD pieces were logs at least 0.60 m in diameter and 10 m long. Our response variables were based on average LWD quantities per 100 m of stream and were the primary LWD variables collected by field crews. For explanatory variables, we selected 16 measurements describing stream channel conditions and the land use – land cover types and ownership of areas surrounding streams (Table 1).

To test the relationships of explanatory variables on LWD abundance, we used a relatively new exploratory statistical technique known as regression tree analysis (Breiman et al. 1984), a powerful tool for identifying hierarchical structure in large databases. This technique is flexible in its ability to handle multiple explanatory variables; it can accommodate both categorical and continuous variables simultaneously. Although regression trees are relatively robust with regard to explanatory variables, continuous response variable distribu-

© 2002 NRC Canada

Fig. 1. Location of surveyed stream reaches in western Oregon, U.S.A.

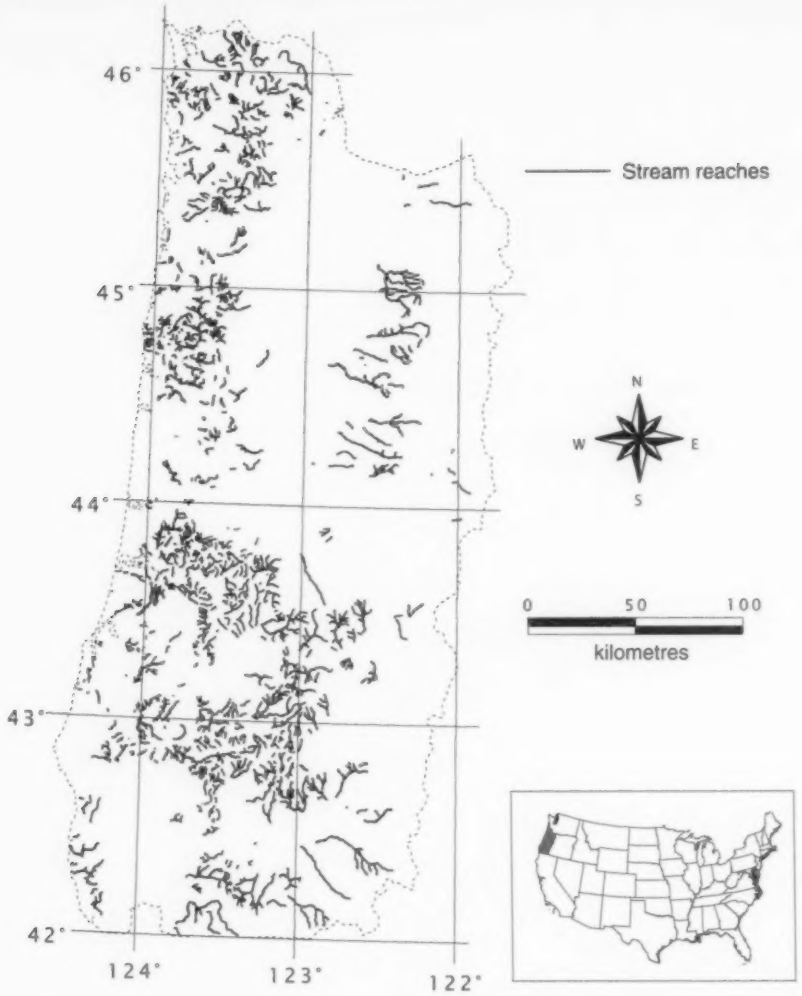

tions should approximate normality, and categorical response variables should be multinomial.

Regression trees are useful for revealing data structures, facilitating interpretation, and capturing nonadditive behavior (Clark and Pregibon 1993). Tree models are fit by using binary recursive partitioning that successively splits data into increasingly homogenous subsets. This process begins with the distributions of all predictor variables being considered as possible splits. For each possible split, the sum of squares of differences between observation response values and their means is calculated. The split associated with the smallest sum is selected as the first partition, which divides the response observations into two datasets. Each dataset continues to be partitioned in this manner until a tolerance defined by the operator is reached. The initial model term is called the root node. Partitioning of the dataset begins at the root node and successive partitions are referred to as splits or nodes with each split ending at a point known as a terminal node or leaf.

As with other statistical models, regression tree analysis may over-predict variation by over-fitting data and creating excessive subgroups or model terms (Rathert et al. 1999). Several techniques have been developed to assist in the optimal selection of model terms; the goal of these techniques is to "prune" or reduce the number of terminal nodes of a regression tree. We used a cross-validation technique that randomly divides a dataset into 10 subgroups and uses them to test the predictive ability of various-sized trees (Breiman et al. 1984). This method can be very effective in removing "noisy" variables from a final model (Therneau and Atkinson 1997) and suggests an optimum tree size. We took the median value of 10 separate cross-validation tests to assist in the pruning and final model selection.

After pruning a regression tree through cross-validation, it is helpful to examine the statistical significance of the final tree in describing variation in the dependent variable. One method for examining statistical significance is to compare the explained variance of the final pruned tree to a distribu-

© 2002 NRC Canada

Table 1. Explanatory variables and abbreviations for the regression tree analysis.

Name (abbreviation)	Description and category abbreviations
Channel constraint (Constraint)	Morphology of active channel
	Hillslope–bedrock (Hill–Bed)
	Terrace (Terr)
	Terrace–hillslope (Terr–Hill)
	Unconstrained (Uncon)
Geology	Lithology of stream channel
	Alluvium (Alluv)
	Basalt (Basalt)
	Cascades (Casc)
	Marine sedimentary (MarSed)
	Mesozoic sedimentary (MesSed)
	Metamorphic (Met)
Land use – land cover	Primary land use or land cover beyond the stream's riparian zone
	Forested—split into cover types
	Young timber, 15 cm dbh (YngTim)
	Second growth, 15–30 cm dbh (SecGrth)
	Large timber, 30–50 cm dbh (LgTim)
	Mature timber, 50–90 cm dbh (MatTim)
	Old growth, 90+ cm dbh (OldGr)
	Recent harvest (Harv)
	Rural residential (Rural)
	Agricultural (Agric)
	Grazing (Graz)
Ownership	Ownership of land surrounding the stream
	Private industrial (PI)
	Private nonindustrial (PNI)
	Bureau of Land Management (BLM)
	State
	United States Forest Service (USFS)
Riparian	Primary riparian vegetation within one active channel width
	Young conifer (YngCon)
	Mature conifer (MatCon)
	Young deciduous (YngDec)
	Mature deciduous (MatDec)
	Young mixed (YngMx)
	Mature mixed (MatMx)
	Grass–shrub (Gr–Shrub)
Bankfull channel width (Width)	Width of stream channel
Beaver dams (Beaver)	Presence or absence of beaver dams
Culverts (Culvert)	Presence or absence of culverts
Debris jams (Debris)	Presence or absence of debris jams
Gravel	Percent of gravel covering streambed
Large boulders (Boulders)	Number of large boulders ≥0.5 m diameter per 100 m channel length
Large conifers	Number of riparian conifers ≥90 cm dbh per 300 m of stream length
Mass failures (Failure)	Presence or absence of mass failures
Medium conifers	Number of riparian conifers ≥50 and <90 cm dbh per 300 m of stream length
Sand, silt, organics (Sand–organics)	Percent of sand, silt, organics covering streambed
Stream gradient (Gradient)	Percent slope for stream channel

Note: dbh, diameter at breast height.

tion of explained variances drawn from trees created from the same dataset but after randomly ordering the dependent variable (Rejwan et al. 1999). We followed this method by creating additional 2000 trees for each LWD variable, randomly ordering the dependent variable of each tree, and calculating the explained variance of the trees to create a variance distribution. We judged statistical analysis by examining whether the final pruned tree's explained variance was in the top 5% of the distribution of explained variances generated by the 2000 trees. If the final pruned tree's explained variance met this benchmark, the tree was judged to be statistically significant in describing variation in the LWD abundance.

This method of determining significance is more robust

© 2002 NRC Canada

than that used by standard regression analysis in which only the mix of variables in the final model are considered. By not considering all possible variables and their combinations, the standard regression approach can bias P values toward overestimating significance. In contrast, the tree-based significance test considers all possible combinations and correlations among independent variables in creating the final pruned tree and for the trees used for benchmark purposes.

We tested the correlations of several different sets of explanatory variables on the three LWD variables. Using the techniques described above, we created and pruned three separate regression trees for each of the LWD variables; they are referred to as Tree 1, Tree 2, and Tree 3. Tree 1 contained all 16 explanatory variables (Table 1), Tree 2 included all variables except land use – land cover and ownership, and Tree 3 included all 16 variables but excluded nonforested land use categories. Because reaches with missing variables were excluded from analysis, the final tree models included varying numbers of stream reaches. In addition, by eliminating nonforested land uses from analysis, the number of stream reaches analyzed was smaller for Tree 3 than it was for Tree 1 and Tree 2.

Stream reaches in the database were split among five ownerships and featured nine land use – land cover types (Table 2). About 38% of reaches were on land owned by private industrial (PI) owners and approximately 21% on land owned by private nonindustrial (PNI) owners (individual, family, or noncorporate); the remaining 41% of the reaches were split among public ownership (Bureau of Land Management (BLM), state of Oregon, and United States Forest Service (USFS)). Forested lands were segregated into land cover types defined by the average size of trees in stands as follows: second-growth timber (39%), mature timber (13%), large timber (12%), young timber (10%), recent harvests (7%), and old-growth timber (2%). Other stream reaches were in lands dominated by nonforested land uses, including rural residential (6%), agricultural (5%), and grazing (4%).

Previous studies have found relationships between stream size and LWD quantities (Frissel 1992; Ralph et al. 1994). We included two channel characteristics in the set of explanatory variables that others (Beschta and Platts 1986; Bilby and Ward 1989) have associated with stream size: bankfull channel width and stream gradient. Although we derived stream order for each stream using a network analysis technique within a GIS, the derived stream order results tended to underestimate actual stream order. Consequently, stream order was not included in the analysis, but stream order was correlated with bankfull channel width (Table 3).

Geologic age and lithology of stream channels were derived from broad-scale maps of Oregon geology (Walker and King 1967; Walker and MacLeod 1991). We split our study areas into six broad geologic types to represent the general lithology of streambeds and surrounding area. Approximately 47% of the stream reaches were in a marine sedimentary lithology, 18% in cascades, 17% in metamorphic, 12% in basalt, 6% in Mesozoic sedimentary, and less than 1% in alluvium.

Results

The final pruned tree models described 18 to 47% of the variation in the LWD variables (Table 4). Trends in the amount of variance explained by each tree model were similar for all three LWD variables: Tree 1 explained the most variance and Tree 3 the least. This implies that nonforested land uses were strongly related to variation in the LWD variables. In addition, the tree models explained the most variance for LWD volume and the least for key LWD pieces. All trees were found to explain a statistically significant amount of variance ($P < 0.001$).

The graphical output of regression trees can be substantial when there are large numbers of splits. For presenting results, only the seven splits that explained the most variation will be discussed. Although all trees contained more than seven splits, the first seven accounted for the majority of explained variance in all of the final tree models (Table 4). In Figs. 2, 3, and 4, first split begins under the root node. The amount of variance explained by each split is contained in parentheses. In addition, the length of the line or "stem" that extends between splits is used to represent the proportion of total variance explained by each split; longer stem lengths indicate greater importance (Figs. 2, 3, and 4 include an inset figure so that variances are more clearly displayed).

LWD volume

The most important predictor for LWD volume in Tree 1 was ownership, with PNI ownerships being split from BLM, PI, state, and USFS ownerships (Fig. 2*a*). Stream reaches in PNI ownerships contained on average 3.1 m^3 of LWD volume, whereas other ownerships averaged 17.4 m^3. This result was not surprising because stream reaches in PNI ownerships held a disproportionately large percentage of nonforested lands compared with lands held by the other ownership categories (Table 2). In Tree 2 (Fig. 2*b*), with land use – land cover and ownership information removed from the analysis, stream gradient was the most important split: reaches with gradients less than 2.3% averaged 5.8 m^3 LWD volume, and higher-gradient stream reaches averaged 17.9 m^3. Tree 3 (Fig. 2*c*) included land use – land cover and ownership information but excluded nonforested ownerships (rural residential, agricultural, and grazing) from analysis. As in Tree 2, stream gradient was the most important split for LWD volume; streams with gradients less than 4.7% averaged less than half (11.5 m^3) the LWD volume found in high-gradient reaches.

LWD pieces

Land use – land cover was the most important split for number of LWD pieces in Tree 1 (Fig. 3*a*). Nonforested land uses averaged 2.8 LWD pieces and forested land uses averaged 10 pieces. The primary split for Tree 2 (Fig. 3*b*) was gradient, with streams below 2.3% averaging fewer pieces (4.9) than higher gradient streams (10.7). Bankfull channel width was the main split for Tree 3 (Fig. 3*c*), with stream channels less than 12.2 m wide containing more LWD pieces (11.1) than larger channels (4.9).

Key LWD pieces

The primary split for key LWD pieces in Tree 1 was land use – land cover (Fig. 4*a*), with agricultural, grazing, and rural residential land uses predictably averaging fewer key LWD pieces (0.2) than forested land uses (0.7). Stream gradient was the most important split for Tree 2 (Fig. 4*b*), with

© 2002 NRC Canada

Table 2. Number and percent of all stream reaches in each of the ownership and land use – land cover categories.

	Ownership						
Land use – land cover	PI	PNI	BLM	State	USFS	Missing	Row total (%)
Young timber (15 cm dbh)							
N	242	35	54	36	15	8	390
% of row	62	9	14	9	4	2	10
% of column	17	4	7	9	5	7	
Second growth (15–30 cm dbh)							
N	740	136	332	167	59	49	1483
% of row	50	9	22	11	4	3	39
% of column	51	17	44	44	20	45	
Large timber (30–50 cm dbh)							
N	139	44	126	68	53	10	440
% of row	32	10	29	16	12	2	12
% of column	10	6	17	18	18	9	
Mature timber (50–90 cm dbh)							
N	107	49	126	76	105	12	475
% of row	23	10	27	16	22	3	13
% of column	7	6	17	20	35	11	
Old growth (90+ cm dbh)							
N	8	1	34	4	36	2	85
% of row	9	1	40	5	42	2	2
% of column	1	0	5	1	12	2	
Harvest (active harvest or clear cut)							
N	141	28	44	18	12	10	253
% of row	56	11	17	7	4	4	7
% of column	10	4	6	5	4	9	
Rural residential							
N	19	198	14	1	1	9	242
% of row	8	82	6	0	0	4	6
% of column	1	25	2	0	0	8	
Agricultural (includes dairy lands)							
N	31	150	5	2	3	3	194
% of row	17	78	3	1	2	2	5
% of column	2	19	1	1	1	3	
Grazing							
N	21	121	4	7	3	1	157
% of row	13	77	3	5	2	0	4
% of column	1	15	1	2	1	1	
Missing							
N	12	33	10	1	14	4	74
% of row	16	45	14	1	19	5	2
% of column	1	4	1	0	5	4	
Column total (%)	1460	795	1749	380	301	108	3793
	38	21	20	10	8	3	

Note: Abbreviations for ownership categories defined in Table 1. dbh, diameter at breast height.

reaches less than 4.8% averaging fewer key LWD pieces (0.4) than high-gradient reaches (0.9). The main split for Tree 3 (Fig. 4*c*) was also stream gradient, with reaches less than 4.9% slope averaging fewer key LWD pieces (0.5) than high-gradient reaches (0.9).

All LWD variables

In terms of variable importance, both ownership and land use – land cover were either primary or secondary splits for Tree 1 for all three LWD variables; gradient was prominent as a second- and third-level split. For Trees 2 and 3, gradient was the primary predictor for LWD volume and key LWD pieces, with bankfull width the primary predictor for number of LWD pieces. Trees 2 and 3 were similar in that geology, gradient, and debris jams were second-level splits for both LWD volume and LWD pieces. For key LWD pieces, stream gradient and the number of large conifers were second-level splits in Trees 2 and 3.

The Tree 3 models included geology as a second-, third-, or fourth-level split four times, with either stream gradient or bankfull width as the primary split. In three of these splits, Mesozoic sedimentary and metamorphic geologies, located in southern Oregon stream reaches, were grouped and split from basalt, cascade, and marine sedimentary geol-

© 2002 NRC Canada

Table 3. Mean bankfull channel widths by stream order.

Stream order	Mean bankfull channel width (m)	Number of stream reaches
1	5.3	1968
2	7.9	1194
3	13.9	511
4	22.9	120

Table 4. Explained variance for pruned regression trees and first seven splits of pruned regression trees.

	Tree 1	Tree 2	Tree 3
Pruned regression trees			
LWD volume	0.47	0.41	0.33
LWD pieces	0.45	0.41	0.33
Key LWD pieces	0.38	0.30	0.25
First seven splits of pruned regression trees			
LWD volume	0.40	0.29	0.24
LWD pieces	0.31	0.26	0.21
Key LWD pieces	0.30	0.25	0.18

Note: LWD, large woody debris.

ogies. In stream reaches in Mesozoic sedimentary and metamorphic geologies, the quantity of LWD was roughly half the amount found in other geologies. The only exception to this grouping was for LWD volume in larger stream reaches, where basalt and marine sedimentary geologies were grouped separately from all other geologies in a fourth-level split and contained more LWD volume.

Discussion

We found that the geomorphic qualities of stream channels play a more significant role than ownership or land use – land cover patterns in describing variation in LWD quantities in forested areas at the stream reach level of analysis. Within forested ownerships, stream gradient and bankfull channel width had the strongest correlation with LWD amounts. Although the amount of explained variance was greater in the tree models that incorporated all land use – land cover types, these increases were due to the wide disparity in LWD quantities between forested and nonforested lands. When nonforested land uses were removed from the analysis, the primary emphasis was related to the geomorphic characteristics of stream channels and surrounding landforms rather than to ownership and land use – land cover. This finding suggests that associating ownership or forested land cover categories with aquatic habitat quality may ignore other more dominant effects on LWD presence at the stream reach scale.

Previous research has shown that the quantity of LWD is strongly related to channel size (Swanson et al. 1982). Typically, larger channels are more likely than smaller channels to facilitate downstream movement of larger woody debris and to wash smaller pieces of woody debris out of channels (Bilby and Bisson 1998). Hence, although LWD numbers decrease in larger stream channels, LWD volume and size have generally been found to increase. Our results from forested lands were consistent with previous research in terms of LWD frequency (Bilby and Ward 1989).

An unexpected result was that the variables describing forest age (land use – land cover, riparian vegetation, and conifer counts) were significant predictors only for key LWD pieces. Stream gradient or bankfull channel width was a primary split in Tree 3 for all LWD measures. The primary split for key LWD pieces was stream gradient, but after gradient, ownership, geology, and land use – land cover were taken into account, all streams had more key LWD pieces where large conifers or mature forests were present. These findings differed somewhat from those of Ralph et al. (1994), who found that forest age-classes influenced LWD volume but not frequency, and that bankfull width was not related to LWD frequency. Our findings were more consistent with those of Bilby and Ward (1991) and Rot (1995). The differences between our results and those of Ralph et al. (1994) and previous research relating stream size and LWD size may involve several factors: the geographic distribution of stream reaches in this study, the different methods of gathering LWD data, the contrasting metrics used to quantify stream segment sizes, and the legacy of past management practices.

Past timber management practices in the U.S. Pacific Northwest included the active harvesting of riparian areas, stream channels being widened as they served as transportation corridors for timber, and removing fallen LWD from streams. Others (Bilby and Ward 1991) have noted that timber harvesting impacts are generally more pronounced in the years immediately following harvest but can have impacts that extend over many years, including reduced LWD abundance. Although information regarding historical management activities is not available in the AIP database, influences from past logging activities that affect LWD variable frequencies are without doubt present in stream data used in this study.

Confined channels with bedrock substrate typically contain about half the number of LWD pieces found in unconfined channels with finer channel composition (Bilby and Wasserman 1989). In the results for the Tree 3 models, geology appeared as a second-, third-, or fourth-level split four times, with stream gradient or bankfull width as a primary split. In three of these splits, the quantity of LWD in stream reaches associated with Mesozoic sedimentary and metamorphic geologies was about half the amount measured in other reaches. One explanation for this finding is that these geologies were in the southern portion of the study area. The southern portion of the study area is part of the Klamath Mountain physiographic province, western Oregon's oldest geology, which contains a mix of sedimentary, granitic, and volcanic rocks (Orr and Orr 1999). These materials may strengthen channel stability and reduce the input of LWD that could result from by stream bank cutting and erosion (Murphy and Koski 1989).

Salmonid populations are typically larger in LWD-rich streams than in LWD-depleted streams (Reeves et al. 1993; Bilby and Bisson 1998). Given that LWD presence tends to be greater in stream reaches in the upper portions of watersheds, land managers wishing to increase LWD and foster high-quality aquatic habitat may want to target efforts toward low-gradient, smaller streams in their jurisdictions. These efforts might include planning harvest operations in riparian and upland forest to ensure that larger conifers are

© 2002 NRC Canada

Fig. 2. Large woody debris (LWD) volume: best seven variable splits for (*a*) Tree 1, (*b*) Tree 2, and (*c*) Tree 3. Tree 1 contained all 16 explanatory variables, Tree 2 included all variables except land use – land cover and ownership, and Tree 3 included all 16 variables but excluded nonforested land use categories. Variance explained by each split is in parentheses. Root, solid rectangles; split, open circles; leaf, solid circles.

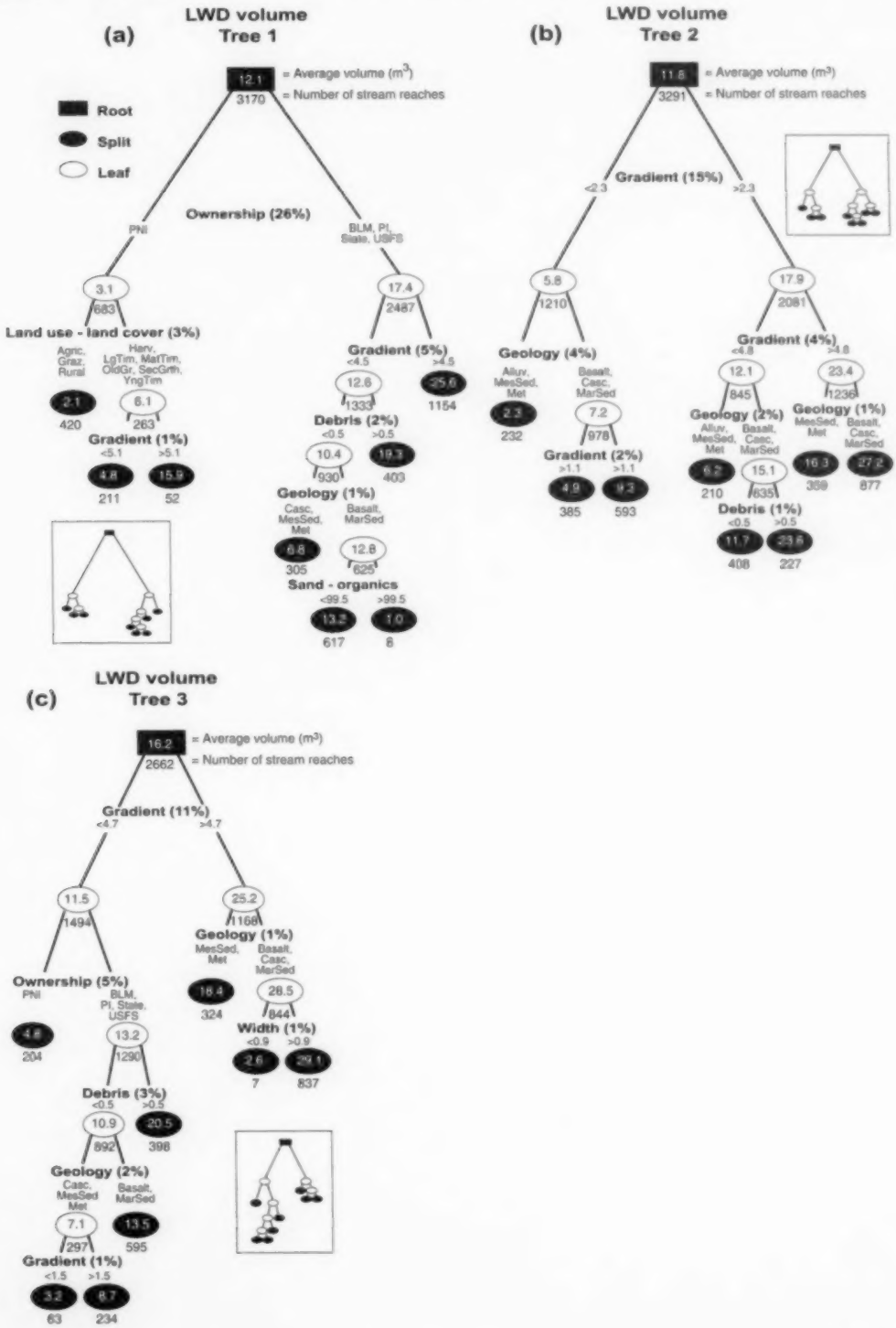

© 2002 NRC Canada

Fig. 3. Large woody debris (LWD) pieces: best seven variable splits for (*a*) Tree 1, (*b*) Tree 2, and (*c*) Tree 3. Tree 1 contained all 16 explanatory variables. Tree 2 included all variables except land use – land cover and ownership, and Tree 3 included all 16 variables but excluded nonforested land use categories. Variance explained by each split is in parentheses. Root, solid rectangles; split, open circles; leaf, solid circles.

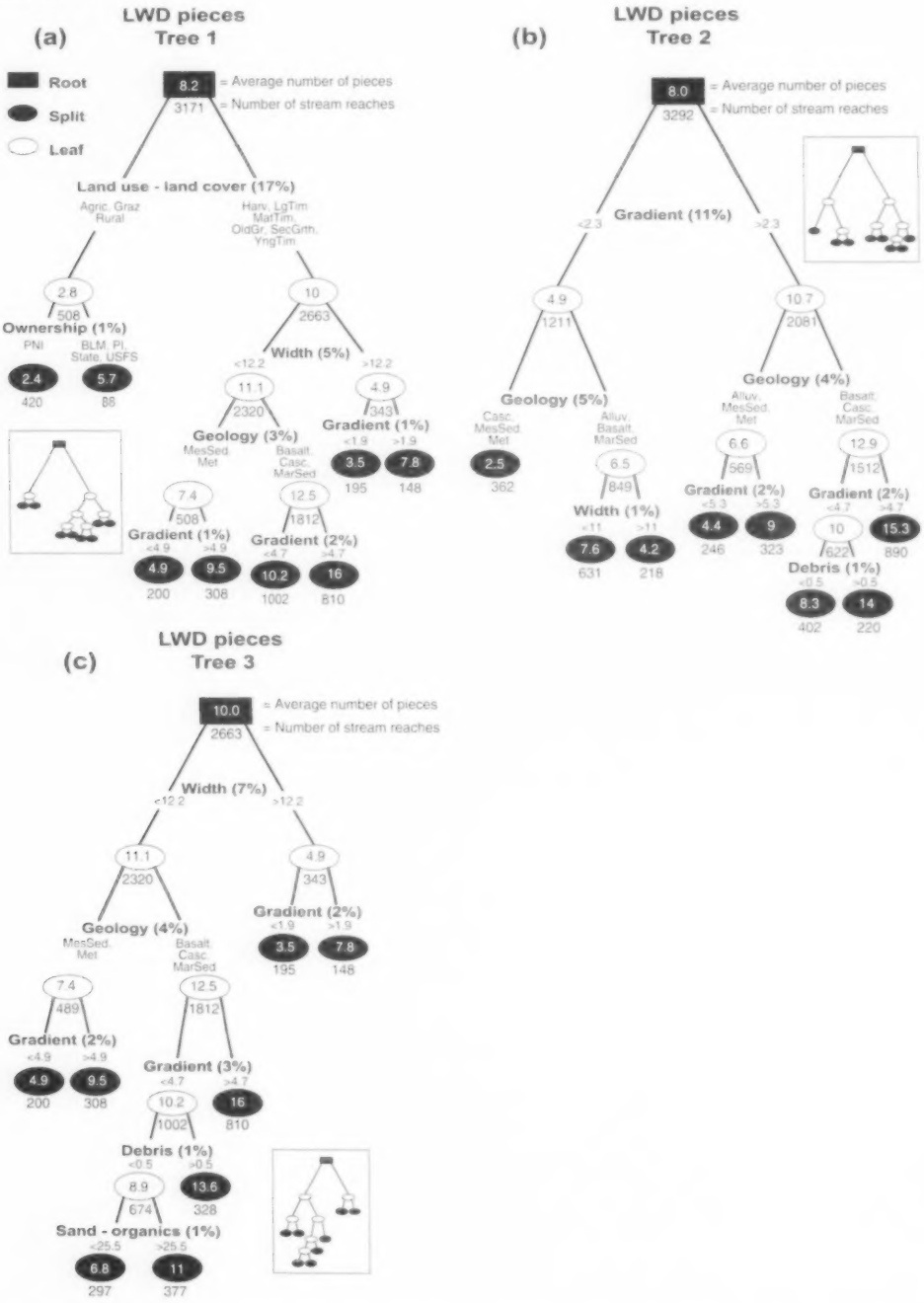

available as in-stream LWD recruits. They may also include more direct methods such as cabling or dragging fallen trees into the stream during harvest operations. Depending on the strategies and tree species used to introduce LWD into streams, active placement of trees into streams can lead to increased LWD abundance over time (Keim et al. 2000).

Ownership and land use patterns were related to LWD counts in some of our final pruned models. The relationships

© 2002 NRC Canada

Fig. 4. Key large woody debris (LWD) pieces: best seven variable splits for (*a*) Tree 1, (*b*) Tree 2, and (*c*) Tree 3. Tree 1 contained all 16 explanatory variables. Tree 2 included all variables except land use – land cover and ownership, and Tree 3 included all 16 variables but excluded nonforested land use categories. Variance explained by each split is in parentheses. Root, solid rectangles; split, open circles; leaf, solid circles.

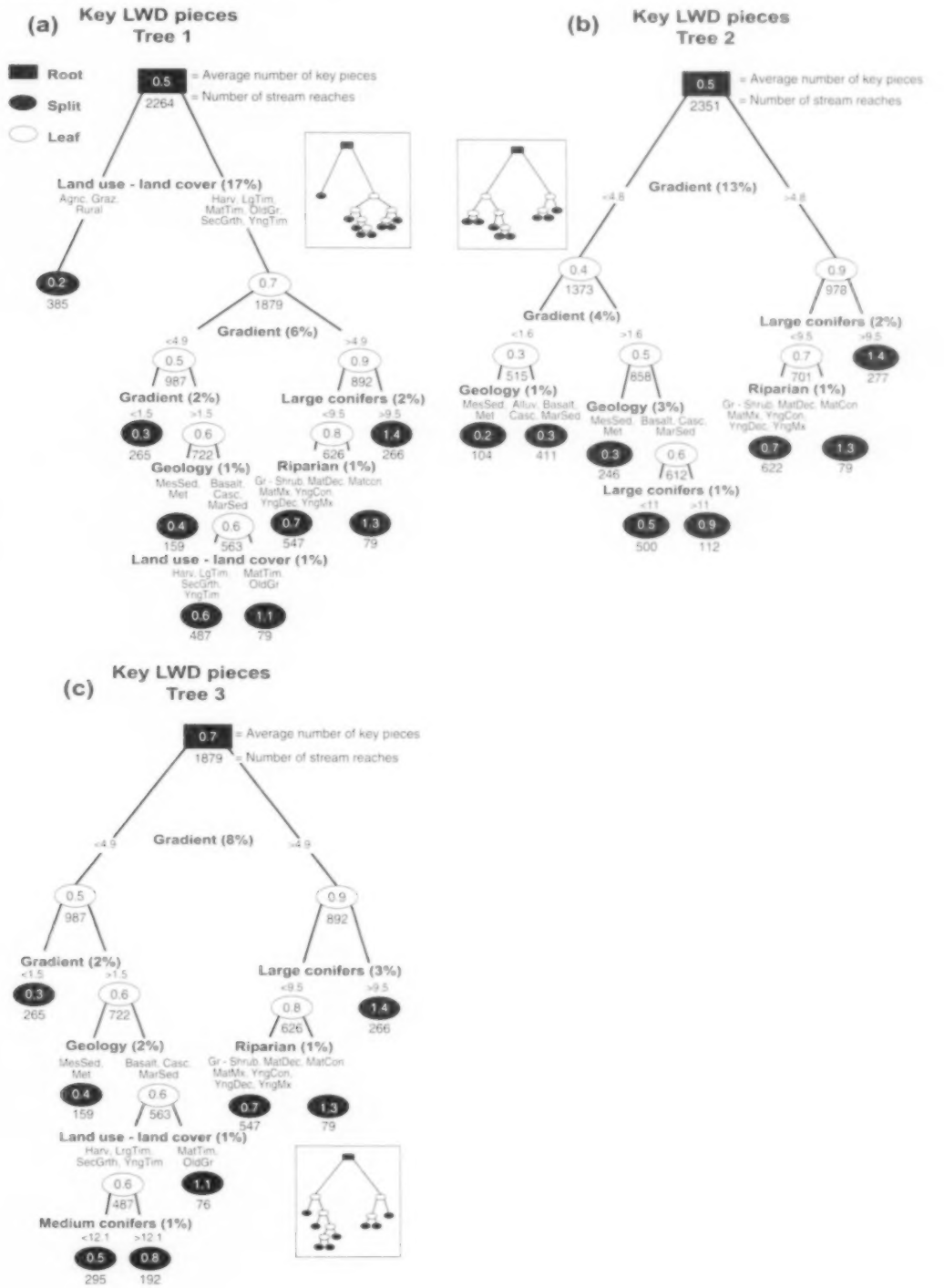

© 2002 NRC Canada

Fig. 3. Large woody debris (LWD) pieces: best seven variable splits for (*a*) Tree 1, (*b*) Tree 2, and (*c*) Tree 3. Tree 1 contained all 16 explanatory variables, Tree 2 included all variables except land use – land cover and ownership, and Tree 3 included all 16 variables but excluded nonforested land use categories. Variance explained by each split is in parentheses. Root, solid rectangles; split, open circles; leaf, solid circles.

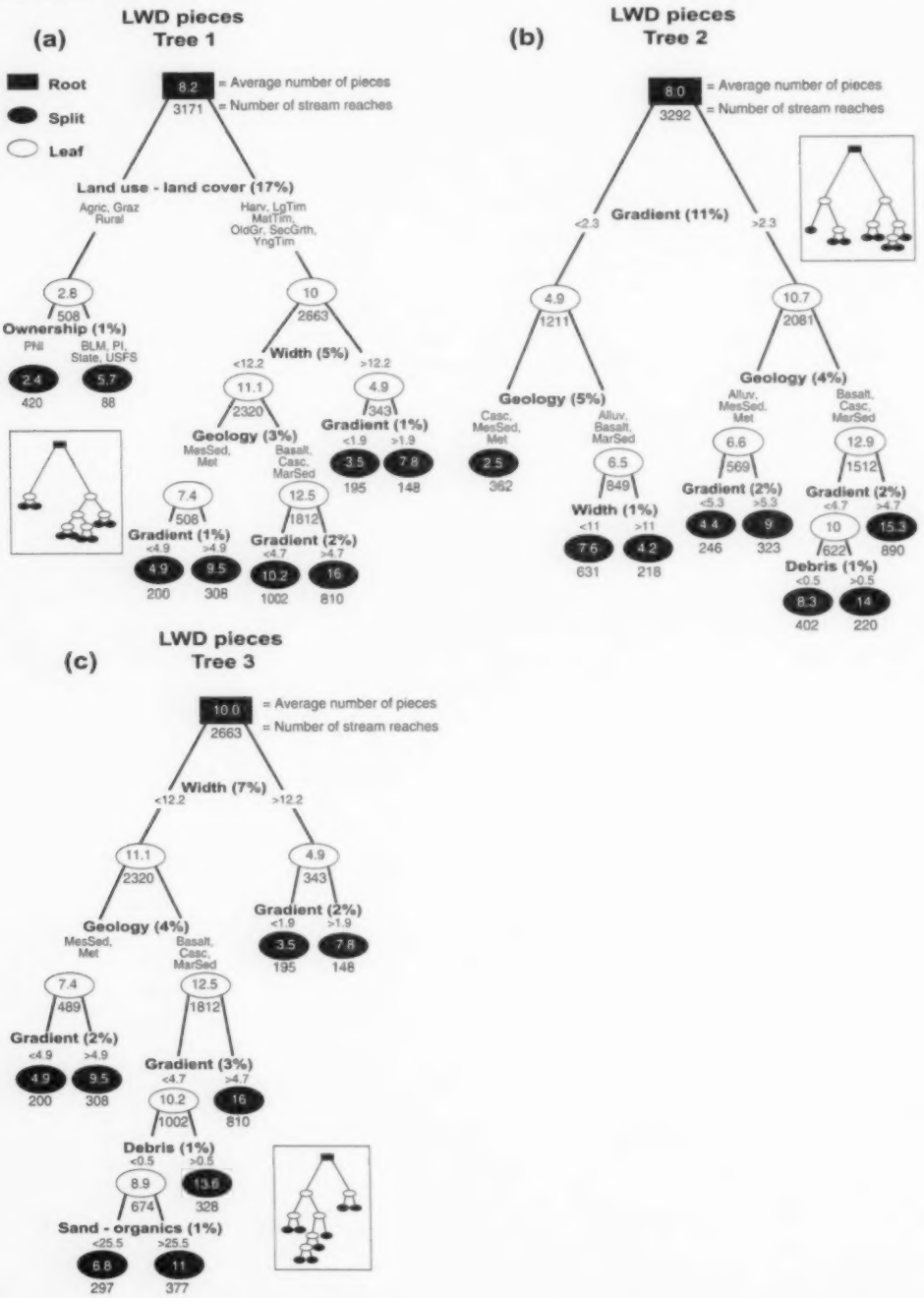

available as in-stream LWD recruits. They may also include more direct methods such as cabling or dragging fallen trees into the stream during harvest operations. Depending on the strategies and tree species used to introduce LWD into streams, active placement of trees into streams can lead to increased LWD abundance over time (Keim et al. 2000).

Ownership and land use patterns were related to LWD counts in some of our final pruned models. The relationships

© 2002 NRC Canada

Fig. 4. Key large woody debris (LWD) pieces: best seven variable splits for (*a*) Tree 1, (*b*) Tree 2, and (*c*) Tree 3. Tree 1 contained all 16 explanatory variables, Tree 2 included all variables except land use – land cover and ownership, and Tree 3 included all 16 variables but excluded nonforested land use categories. Variance explained by each split is in parentheses. Root, solid rectangles; split, open circles; leaf, solid circles.

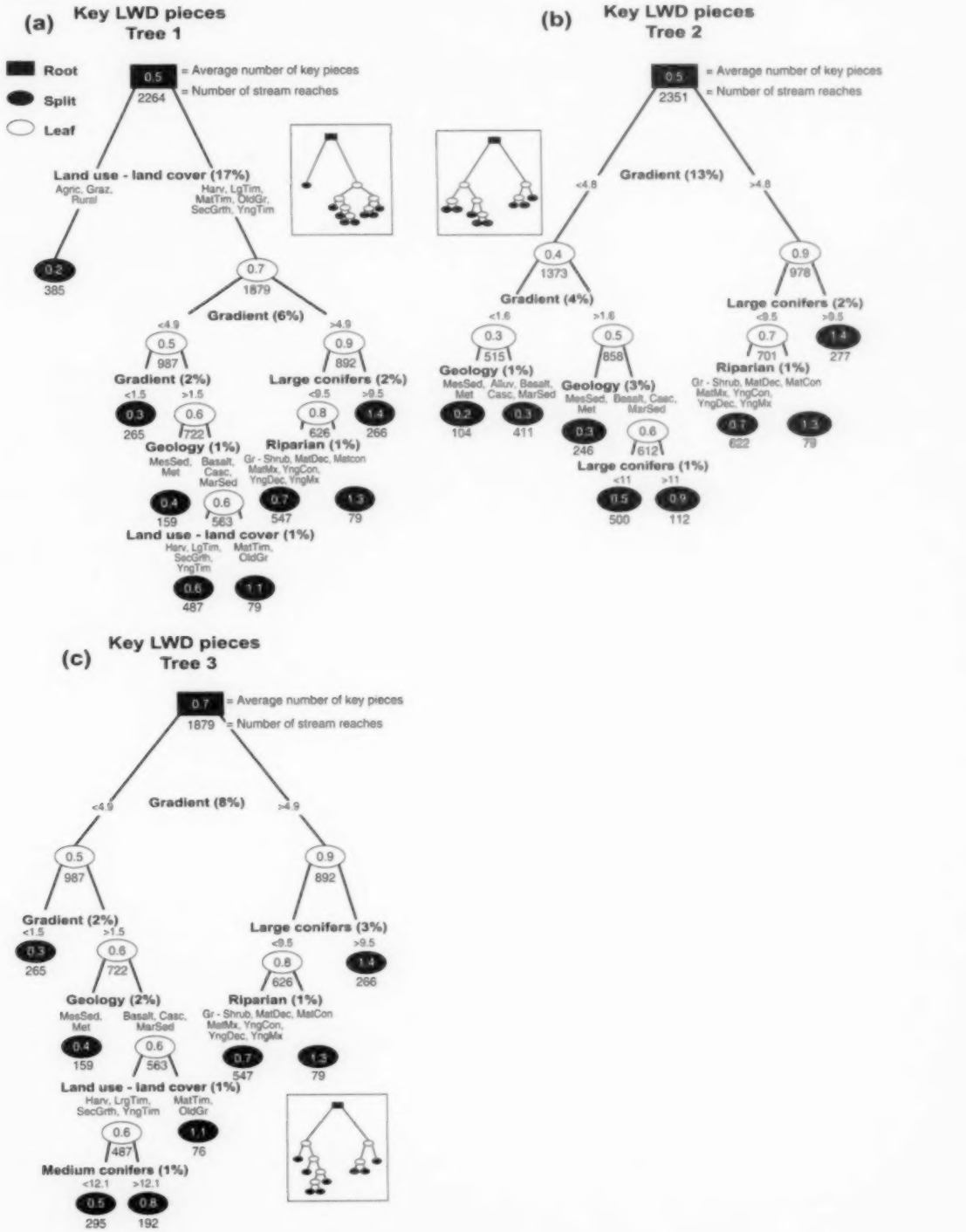

© 2002 NRC Canada

were strongest, however, when nonforested land uses and associated ownerships were accounted for in the tree models, representing the disparity between LWD inputs to forested and nonforested streams. In all ownership splits, BLM, PI, state, and USFS ownerships did not differ significantly from one another as predictors of LWD quantities. These results suggest that ownership patterns in forested land cover types were not significantly related to LWD quantities at the stream reach scale. The differences between PNI and all other ownerships in terms of LWD quantities probably reflect the diversity of activities and land management strategies that occur on PNI lands compared with those on other ownerships in this study, which focus primarily on timber production or resource conservation.

The results from Tree 3 showed strong patterns of geomorphic correlations with LWD abundance. Either stream gradient or bankfull width was the most important predictor for LWD abundance. These variables can be considered surrogates for stream size and describe the geomorphic qualities of steam reaches. Geology and debris jams each appeared at least twice as second- or third-level predictors; these variables were more strongly related to LWD abundance than any others.

The strong presence of stream gradient, geology, bankfull width, and debris jams therefore suggests that in forested areas, the most significant factor related to LWD abundance is the geomorphology of stream reaches and their surrounding areas. Geomorphology appears to be more strongly related than the age-class of surrounding forests. The findings may be due in part to a reliance on reach-scale averages; LWD counts were measured at a habitat-unit scale and averaged to give a broader, reach-scale representation of stream conditions, which may have limited the potential for detecting LWD differences resulting from ownership and land use – land cover patterns and other factors (Hicks et al. 1991). Performing the analysis on finer-scale stream segment data or on data that has been collected longitudinally may be a better method for determining factors that are significantly related to LWD abundance.

In general, we found that ownership and land use – land cover tended to correlate with LWD counts, but these effects were greatest when nonforested land uses were incorporated into the analyses. These results were not surprising; however, when we focused on LWD presence in forested stream reaches, we found that the impacts of forest age-classes and ownership patterns were overshadowed by the geomorphic characteristics of stream reaches—in particular, by stream gradient and bankfull width. The strong relationship of these factors to LWD presence emphasizes the need for researchers involved in broad-scale aquatic habitat research to stratify their stream data by channel size (Frissell 1992; Ralph et al. 1994). Otherwise, insight into other processes related to LWD presence and other habitat characteristics may be masked.

Acknowledgments

This is Paper 3430 of the Forest Research Laboratory, Oregon State University, Corvallis, OR 97331. Funding for this study was provided by the Forest Research Laboratory.

References

Abbe, T.B., and Montgomery, D.R. 1996. Large woody debris jams, channel hydraulics and habitat formation in large rivers. Regul. Rivers, **12**: 201–221.

Beschta, R.L., and Platts, W.S. 1986. Morphological features of small streams: significance and function. Water Resour. Bull. **22**: 369–379.

Bilby, R.E., and Ward, J.W. 1989. Changes in characteristics and function of woody debris with increasing size streams in western Washington. Trans. Am. Fish. Soc. **118**: 368–378.

Bilby, R.E., and Wasserman, L.J. 1989. Forest practices and riparian management in Washington state: data based regulation development. *In* Streamside management: forestry and fishery interactions. *Edited by* R.E. Gresswell, B.A. Barton, and J.L. Kershner. College of Forest Resources, University of Washington, Institute of Forest Resources. Contrib. No. 57. Seattle. pp. 87–94.

Bilby, R.E., and Ward, J.W. 1991. Characteristics and function of large woody debris in streams draining old-growth, clear-cut, and second-growth forests in southwestern Washington. Can. J. Fish. Aquat. Sci. **48**: 2499–2508.

Bilby, R.E., and Bisson, P.A. 1998. Function and distribution of large woody debris. *In* River ecology and management. *Edited by* R.J. Naiman and R.E. Bilby. Springer-Verlag, New York. pp. 324–346.

Bisson, P.A., Bilby, R.E., Bryant, M.D., Dolloff, C.A., Grette, G.B., House, R.A., Murphy, M.L., Koski, K.V., and Sedell, J.R. 1987. Large woody debris in forested streams in the Pacific Northwest: past, present, and future. *In* Streamside management: forestry and fishery interactions. *Edited by* E.O. Salo and T.W. Cundy. College of Forest Resources, University of Washington, Institute of Forest Resources Contrib. No. 57. Seattle. pp. 143–190.

Botkin, D.B., Cummins, K., Dunne, T., Regier, H., Sobel, M., Talbot, L., and Simpson, L. 1995. Status and future of salmon of western Oregon and northern California: overview of findings and options. Center for the Study of the Environment, Research Report 951002, Santa Barbara, Calif.

Breiman, L., Friedman, J.H., Olshen, R.A., and Stone, C.J. 1984. Classification and regression trees. Wadsworth and Brooks/Cole Advanced Books and Software, Monterey, Calif.

Clark, L.A., and Pregibon, D. 1993. Tree-based models. *In* Statistical models in S. *Edited by* J.M. Chambers, and T.J. Hastie. Chapman and Hall, London. pp. 377–419.

FEMAT (Forest Ecosystem Management Assessment Team). 1993. Forest ecosystem management: an ecological, economic, and social assessment. U.S. Forest Service, National Marine Fisheries Service, Bureau of Land Management, U.S. Fish and Wildlife Service, National Park Service, U.S. Environmental Protection Agency, Portland, Oreg., and Washington, D.C.

Frissel, C.A. 1992. Culmulative impacts of land use on salmon habitat in coastal Oregon. Ph.D. dissertation, Oregon State University, Corvallis.

Groot, C., and Margolis, L. (*Editors*). 1991. Pacific salmon life histories. University of British Columbia Press, Vancouver.

Hicks, B.J., Hall, J.D., Bisson, P.A., and Sedell, J.R. 1991. Responses of salmonids to habitat changes. *In* Influences of forest and rangeland on salmonid fishes and their habitat. *Edited by* W.R. Meehan. American Fisheries Society, Spec. Publ. 19, Bethesda, Md. pp. 483–518.

House, R.A., and Boehne, P.L. 1987. The effect of stream cleaning on salmonid habitat and populations in a coastal Oregon drainage. West. J. Appl. For. **2**: 84–87.

Keim, R.F., Skaugset, A.E., and Bateman, D.S. 2000. Dynamics of

© 2002 NRC Canada

coarse woody debris placed in three Oregon streams. For. Sci. **46**(1): 13–22.

Meehan, W.R. (*Editor*). 1991. Influences of forest and rangeland management on salmonid fishes and their habitats. Am. Fish. Soc. Spec. Publ. 19. Bethesda, Md.

Montgomery, D.R., Buffington, J.M., Smith, R.D., Schmidt, K.M., and Pess, G. 1995. Pool spacing in forest channels. Water Resour. Res. **31**: 1097–1105.

Montgomery, D.R., Abbe, T.B., Peterson, N.P., Buffington, J.M., Schmidt, K.M., and Stock, J.D. 1996. Distribution of bedrock and alluvial channels in forested mountain drainage basins. Nature (London), **381**: 587–589.

Moore, K., Jones, K., and Dambacher, J. 1998. Aquatic inventory project: methods for stream habitat surveys. Oregon Department of Fish and Wildlife, Research and Development Section, Corvallis.

Murphy, M.L., and Koski, K.V. 1989. Input and depletion of woody debris in Alaska streams and implications for streamside management. N. Am. J. Fish. Manag. **9**: 427–436.

NRC (National Research Council). 1996. Upstream: salmon and society in the Pacific Northwest. National Academy Press, Washington, D.C.

Nehlsen, W. 1997. Pacific salmon status and trends—a coastwide perspective. *In* Pacific salmon and their ecosystems: status and future options. *Edited by* D.J. Stouder, P.A. Bisson, and R.J. Naiman. Chapman and Hall, New York. pp. 41–50.

ODF (Oregon Department of Forestry). 1994. Oregon forest practice rules and statutes. Oregon Department of Forestry, Salem.

Orr, E.L., and Orr, W.N. 1999. Geology of Oregon. Kendall / Hunt Publishing, Dubuque, Iowa.

Ralph, S.C., Poole, G.C., Conquest, L.L., and Naiman R.J. 1994. Stream channel morphology and woody debris in logged and unlogged basins of western Washington. Can. J. Fish. Aquat. Sci. **51**: 37–51.

Rathert, D., White, D., and Sifneos, J.C. 1999. Environmental correlates of species richness for native freshwater fish in Oregon, U.S.A. J. Biogeogr. **26**: 257–273.

Reeves, G.H., Everest, F.H., and Sedell, J.R. 1993. Diversity of juvenile anadromous salmonid assemblages in coastal Oregon basins with different levels of timber harvest. Trans. Am. Fish. Soc. **122**: 309–317.

Rejwan, C., Collins, N.C., Brunner, L.J., Shuter, B.J., and Ridgway, M.S. 1999. Tree regression analysis on the nesting habitat of smallmouth bass. Ecology, **80**: 341–348.

Rosgen, D.L. 1994. A classification of natural rivers. Catena, **22**: 169–199.

Rot, B.W. 1995. The interaction of valley constraint, riparian landform, and riparian plant community size and age upon channel configuration of small streams of the western Cascade Mountains, Washington. M.Sc. thesis. University of Washington, Seattle.

Sedell, J.R., and Luchessa, K.J. 1982. Using the historical record as an aid to salmonid habitat enhancement. *In* Acquisition and utilization of aquatic habitat inventory information. *Edited by* N.B. Armentrout. American Fisheries Society, Bethesda, Md. pp. 210–223.

Swanson, F.J., Gregory, S.V., Sedell, J.R., and Campbell, A.G. 1982. Land–water interactions: the riparian zone. *In* Analysis of coniferous forest ecosystems in the western United States. *Edited by* R.L. Edmonds. Hutchinson Ross, Stroudsburg, Pa. pp. 267–291.

Therneau, T.M., and Atkinson, E.J. 1997. An introduction to recursive partitioning using the RPART routines. Mayo Foundation, Technical Report No. 61. (http://www.mayo.edu/hsr/techrpt/61.pdf)

Tschaplinski, P.J., and Hartman, G.F. 1983. Winter distribution of juvenile coho salmon (*Oncorhynchus kisutch*) before and after logging in Carnation Creek, British Columbia, and some implications for overwinter survival. Can. J. Fish. Aquat. Sci. **40**: 452–461.

Walker, G.W., and King, P.B. 1967. Geologic map of Oregon, scale 1 : 2 000 000. United States Geological Survey, Washington, D.C.

Walker, G.W., and MacLeod, N.S. 1991. Geologic map of Oregon, scale 1 : 500 000, two sheets. United States Geological Survey, Washington, D.C.

Wing, M., and Skaugset, A. 1998. GIS casts a line: examining salmon habitat in Oregon streams. Geo Info Systems, **8**: 36–41.

© 2002 NRC Canada

Bleaching of color of kraft pulp mill effluents and natural organic matter in lakes

Anssi V. Vähätalo, Kalevi Salonen, Eija Saski, and Mirja S. Salkinoja-Salonen

Abstract: In situ changes in the color of lake water and biologically treated kraft pulp mill effluents mixed in lake water were examined in three lakes. In 1.7 m^3 enclosures, the color (400–700 g $Pt \cdot m^{-3}$) of the mixture of pulp mill effluent and lake water remained similar for 4 months in darkness, whereas exposure to solar radiation resulted in 17–42% bleaching of color. During the summer stratification of a humic lake, the color (160 g $Pt \cdot m^{-3}$) of hypolimnetic water remained similar to that found during spring turnover, but the color of epilimnion decreased 13%. The measured rates of photochemical bleaching of color by solar radiation could explain the decrease of epilimnetic color. Attenuation of photobleaching in the water column was similar to that of blue irradiance. Measured photobleaching was well described by a model based on quantum yields. The model revealed that visible solar radiation accounted for 29% of photobleaching at the surface and 66% in the whole water column. The results indicated that solar radiation, rather than plankton, bleached color of lake water and pulp mill effluents in surface strata.

Résumé : Nous avons examiné dans 3 lacs les changements in situ de la couleur de l'eau, ainsi que celle des effluents d'usine de pâte kraft ayant subi un traitement biologique et mêlés à de l'eau de lac. Dans des enclos de 1,7 m^3, la couleur (400–700 g $Pt \cdot m^{-3}$) d'un mélange d'effluent d'usine de pâte et d'eau de lac est restée stable pendant 4 mois à l'obscurité; en revanche, un blanchiment de la couleur de l'ordre de 17–42 % a suivi une exposition à la radiation solaire. Durant la stratification estivale dans un lac humique, la couleur de l'eau de l'hypolimnion (160 g $Pt \cdot m^{-3}$) est demeurée la même que celle qui prévalait au moment du brassage du printemps, alors que la couleur de l'épilimnion a diminué de 13 %. Les taux de blanchiment photochimique de la couleur par la radiation solaire observés peuvent expliquer la diminution de la couleur de l'épilimnion. L'atténuation du blanchiment photochimique dans la colonne d'eau est semblable à celle de l'irradiance de la couleur bleue. Le blanchiment observé peut être décrit de façon adéquate par un modèle basé sur les rendements quantiques. Le modèle démontre que la radiation solaire visible est responsable de 29 % du blanchiment optique à la surface et de 66 % dans l'ensemble de la colonne d'eau. Ces observations montrent que c'est la radiation solaire, plutôt que le plancton, qui cause le blanchiment de la couleur de l'eau des lacs et des effluents d'usine de pâte dans les couches superficielles.

[Traduit par la Rédaction]

Introduction

Chromophoric dissolved organic matter (CDOM) contributes to color of water and refers to that portion of dissolved organic matter (DOM) that absorbs solar radiation. In natural waters the largest category of CDOM is humic substances. Anthropogenous sources of color may be important. For example, in 1996 Finnish kraft pulp mills discharged 550×10^6 m^3 of effluent (PME) or 1.9×10^9 grams of color in platinum units (Saski 1998). CDOM is the most important component in the absorption of solar ultraviolet (UV) and blue radiation in most fresh waters (Morris et al. 1995). This property of CDOM has several implications: (*i*) color shelters aquatic organisms from harmful solar UV radiation (Williamson 1995); (*ii*) color competes with phytoplankton for the absorption of photons at the blue and green range of spectrum (Vähätalo et al. 2000); (*iii*) color affects the upward flux of photons from water and thus interferes with remote sensing of natural waters (Del Castillo et al. 2001); (*iv*) color promotes thermal stratification of waters (e.g., Jones and Arvola 1984); and (*v*) color initiates photochemical processes in surface waters (e.g., Vähätalo et al. 2000).

Photochemical reactions and microbes are the main factors that can potentially mediate decomposition of color

Received 15 March 2001. Accepted 27 March 2002. Published on the NRC Research Press Web site at http://cjfas.nrc.ca on 14 June 2002.
J16263

A.V. Vähätalo[1,2] and K. Salonen.[3] Lammi Biological Station, University of Helsinki, FIN-16900 Lammi, Finland.
E. Saski[4] and M.S. Salkinoja-Salonen. Department of Applied Chemistry and Microbiology, P.O. Box 56, FIN-00014 University of Helsinki, Finland.

[1]Corresponding author (e-mail: anssi_vahatalo@hotmail.com).
[2]Present address: Department of Environmental Sciences and Engineering, University of North Carolina, Chapel Hill, NC 27599-7431, U.S.A.
[3]Present address: Section of Hydrobiology, Department of Biological and Environmental Sciences, University of Jyväskylä, P.O. Box 35, FIN-40351 Jyväskylä, Finland.
[4]Present address: Metsä-Serla, Packaging Group, P.O. Box 20, FIN-02020 Metsä, Finland.

 DOI: 10.1139/F02-047 © 2002 NRC Canada

(bleaching) in natural waters. Numerous studies from Whipple (1927) to recent Osburn et al. (2001) have convincingly shown that solar radiation photochemically bleaches (photobleaches) color in lakes. The rates of photobleaching in surface waters have been quantified with several methods (e.g., Reche et al. 2000; Gibson et al. 2001; Osburn et al. 2001). Most methods use quantum yield or first-order kinetics. In the latter, photobleaching has been related to incident radiation or time to calculate first-order bleaching coefficients (k_{BLE}), which have been applied later to the whole water column (Curtis and Schindler 1997; Molot and Dillon 1997*a*; Reche et al. 2000). In a quantum-yield approach, photobleaching has been related to the number of absorbed photons to calculate apparent quantum yields for photobleaching (Whitehead et al. 2000; Osburn et al. 2001; see also Miller 1998).

Several studies have assayed the contribution of solar spectral bands to photobleaching (e.g., Reche et al. 2000; Whitehead et al. 2000; Osburn et al. 2001). De Haan (1993) suggested that radiation below 320 nm was mainly responsible for photobleaching in a bog lake, whereas the same spectral band had little effect on estuarine CDOM (Whitehead et al. 2000). These contrasting results indicate that the spectral dependence of photobleaching needs to be clarified.

Microbial bleaching of color is a potentially important process, because unlike photobleaching it can also proceed in darkness. Microbes can bleach color (Hessen et al. 1994; Morris and Hargreaves 1997; Nelson et al. 1998). However, biological humification of DOM can also increase color (Shin and Lim 1996; Rochelle-Newall and Fisher 2002). Because of this dual relationship and the lack of in situ studies, the impact of microbes on color of lake water is not well known.

The purposes of this study were to compare photobleaching to bleaching by plankton in lakes and PME recipients in a time scale of months, to compare modeling with first-order and quantum-yield approaches, to provide a quantum-yield model that predicts photobleaching at a desired depth and in the whole water column, and to determine spectral dependence of photobleaching.

Materials and methods

Enclosures were set up in polyhumic Lake Mekkojärvi (61°13′N, 25°09′E, area 0.004 km^2, elevation 136 m; Jones and Arvola 1984) and in clear-water Lake Valkea Mustajärvi (61°13′N, 25°07′E, area 0.139 km^2, elevation 136 m; Table 1; details in Saski et al. 1995). Changes in color were monitored and photobleaching was measured in quartz vials placed in Lake Valkea-Kotinen (61°14′N, 25°04′E, area 0.04 km^2, elevation 156 m, mean depth 3 m; Keskitalo et al. 1998; Table 1). Water was sampled with a 1-m tube sampler. In the enclosures, only the uppermost metre of the water column was sampled. Lake Valkea-Kotinen was sampled at its deepest point from the surface to the maximum depth of 6 m. Samples were taken weekly during the ice-free period and monthly during the period of ice cover.

Biologically treated PMEs were obtained on 23–24 May 1991 from two kraft mills that pulped Scots pine (*Pinus sylvestris*) and Norway spruce (*Picea abies*; Table 1). Mill A bleached pulp with a sequence of D-EO-D-E-D and mill C used a sequence of O-C(85)-D(15)-EO-D-E-D, where D = chlorine dioxide, E = alkali, O = oxygen, and C = chlorine. The waste waters of mill A were biologically treated in an activated sludge plant with a 20-h hydraulic retention time (HRT). Mill C treated waste water in an anaerobic lagoon (HRT = 2.4 days), followed by an aerobic lagoon (HRT = 6.4 days; details in Jokela et al. 1993).

For an enclosure experiment, 16 cylindrical enclosures (diameter 1.2 m, depth 1.7 m, volume 1.73 m^3) of clear or black polyethylene film were attached to a floating wooden frame and placed in the open water of the two lakes (details in Saski et al. 1995). On 3 June 1991 (day 0), the enclosures were filled with PME and lake water. Two enclosures in each lake contained only lake water, while the others contained 2% to 10% PME from two mills. To prevent entrance of solar radiation, four black enclosures with 8–10% PME were covered with black polyethylene film. Enclosures were exposed to ambient conditions for 142 days unless terminated earlier because of leakage.

Determinations of absorption, color, and respiration

After filtration of water through Millipore GS filters (pore size 0.2 μm), the absorbance of CDOM ($A_{CDOM,\lambda}$, cm^{-1}·nm^{-1}) was measured with a Shimadzu UV-2100 spectrophotometer from 300 to 700 nm. The absorbance at 420 nm in a 10-mm cuvette (coefficient of variation 2%) was converted to color (g Pt·m^{-3}) according to platinum–cobalt standards (APHA 1998). Absorption coefficient ($a_{CDOM,\lambda}$, m^{-1}·nm^{-1}) was calculated according to $a_{CDOM,\lambda} = 2.303A_{CDOM,\lambda}\ 0.01^{-1}$. Spectral measurements from 300 to 700 nm showed that the exponential relationship between the wavelength and the absorption of CDOM (S value, Bricaud et al. 1981) was 0.0144 ± 0.0003 nm^{-1} in the three samples collected from Lake Valkea-Kotinen on 26 July 1995 and 1 and 31 July 1999. Day-long exposures to solar radiation increased the S value only slightly (<1.3%, Vähätalo et al. 2000). The spectrum of CDOM absorption was calculated for each day by

$$(1) \qquad a_{CDOM,\lambda} = a_{CDOM,420}e^{0.0144(420-\lambda)}$$

where $a_{CDOM,420}$ is the absorption of CDOM at 420 nm (m^{-1}), 0.0144 is the slope (nm^{-1}), and λ is wavelength (nm).

Total absorption ($a_{tot,\lambda}$) is the sum of absorption by CDOM, phytoplankton, tripton, and H_2O. Absorption by phytoplankton was calculated from chlorophyll *a* (Chl *a*; Keskitalo and Salonen 1996) and a model absorption spectrum for phytoplankton (Arrigo 1994). Carbon-normalized absorption spectra of tripton and CDOM were assumed to be identical, and the absorption by tripton was calculated from its concentration (details in Vähätalo et al. 2000). Absorption of H_2O was taken from literature (Arrigo 1994).

For the measurement of respiration of plankton, unfiltered water was fed through a divider into two borosilicate bottles. One bottle was immediately taken for the measurement of the initial concentration of dissolved inorganic carbon (DIC, Salonen 1981) and the other bottle was covered with aluminum foil and incubated at 16°C for 48 h. After incubation the concentration of DIC was measured and respiration was calculated as the difference between the final and initial concentrations of DIC.

© 2002 NRC Canada

Table 1. Characteristics of lake waters (0–1 m) and the pulp mill effluents (PME) used in the enclosure study.

	PME[a]		Lake		
Characteristic	Mill A	Mill C	Valkea-Kotinen[b]	Valkea Mustajärvi[a]	Mekkojärvi[a]
TOC (g C·m^{-3})	380	280	12[c]	5	21
Total N (mg·m^{-3})	3620	5050	495	235	475
Total P (mg·m^{-3})	902	1040	20	9	17
AOX (g Cl·m^{-3})	26	21	—	0.01	0.03
Alkalinity (mol·m^{-3})	7.0	6.4	0.01	0.1	0.1
Color (g Pt·m^{-3})	3930	3230	140	28	309
pH	7.6	7.6	5.3	6.4	5.8
Conduc. at 25°C (mS·m^{-1})	380	300	3	3	4

Note: The data for PME and Lakes Valkea Mustajärvi and Mekkojärvi were determined before the enclosure experiment on 3 June 1991. The data for Lake Valkea-Kotinen are the means of weekly determinations from May to September 1994. —, not determined; TOC, total organic carbon; AOX, adsorbable organic halogen; Conduc., conductivity.

[a]Saski et al. (1995).

[b]Keskitalo and Salonen (1996).

[c]Dissolved organic carbon.

Bleaching rate constants in the enclosures

Bleaching of color in the enclosures was related to incident radiation. First-order rate constant (eq. 2) was calculated by fitting logarithmically transformed color linearly to the cumulative global radiation:

$$(2) \qquad \mathrm{dCOLOR}/\mathrm{d}I = -k_{\mathrm{BLE}}\mathrm{COLOR}$$

where COLOR is given as in g Pt·m^{-3}, I is global radiation (MJ·m^{-2}), and k_{BLE} is the first-order bleaching rate constant (MJ^{-1}·m^{2}). Half-times for bleaching were calculated as $\ln 2 k_{\mathrm{BLE}}^{-1}$. These calculations also needed global radiation doses during the exposure.

Photobleaching of color in Lake Valkea-Kotinen

Photobleaching was measured weekly between 14 June to 16 August 1994 in the epilimnion of Lake Valkea-Kotinen. The water samples were taken from the surface of the lake and sterile filtered (0.2-μm Millipore Millex-GS) into quartz and borosilicate vials (16 mm × 150 mm, pre-ignited for 2 h at 450°C). The duplicate vials were filled without air bubbles, closed with glass stoppers, and placed in the center of lake at the depths of 0.01, 0.025, 0.05, and 0.1 m. The quartz vials were exposed to ambient solar radiation. The borosilicate vials were wrapped in aluminum foil (darkened vials). After 24 h, the vials were placed in crushed ice and sheltered from light, and the color was measured in the laboratory within 12 h. Photobleaching (BLE_z at each depth z) was calculated by subtracting the color in darkened vial from that of the exposed one.

Theoretical model of photobleaching

The rate of photobleaching at a depth z (BLE_z, g Pt·m^{-3}·day^{-1}) was presented as a product of three spectra

$$(3) \qquad \mathrm{BLE}_z = \int_{\lambda_{\min}}^{\lambda_{\max}} \phi_{\mathrm{BLE},\lambda}\, Q_{\mathrm{s},z,\lambda}\, a_{\mathrm{CDOM},\lambda}\, \mathrm{d}\lambda$$

where $\phi_{\mathrm{BLE},\lambda}$ is the spectrum of apparent photobleaching yield (g Pt·(mol photons)$^{-1}$·nm^{-1}), $Q_{\mathrm{s},z,\lambda}$ is the scalar photon flux density spectrum at a depth z (mol photons·m^{-2}·day^{-1}·nm^{-1}), and $a_{\mathrm{CDOM},\lambda}$ is the absorption spectrum of CDOM (m^{-1}·nm^{-1}). $\lambda_{\min}$ and $\lambda_{\max}$ are the minimum and maximum wavelengths (nm) contributing to photobleaching, respectively.

In the whole water column, the rate of photobleaching (BLE, g Pt·m^{-2}·day^{-1}) was described as

$$(4) \qquad \mathrm{BLE} = \int_{\lambda_{\min}}^{\lambda_{\max}} \phi_{\mathrm{BLE},\lambda}\, Q_{\mathrm{a},\lambda}\, a_{\mathrm{CDOM},\lambda}/a_{\mathrm{tot},\lambda}\, \mathrm{d}\lambda$$

where $Q_{a,\lambda}$ represents photons absorbed in the water column (mol photons·m^{-2}·day^{-1}·nm^{-1}) and the $a_{\mathrm{CDOM},\lambda}/a_{\mathrm{tot},\lambda}$ ratio illustrates the contribution of CDOM to total absorption. In optically deep waters, where solar radiation does not reach the bottom of water body, $Q_{a,\lambda}$ roughly equals the downward vector photon flux density just below the surface ($Q_{\mathrm{d,v},0,\lambda}$).

Apparent photobleaching yields have been reported to decrease exponentially with increasing wavelength (Kouassi and Zika 1992; Whitehead et al. 2000; Osburn et al. 2001). We described this relationship as

$$(5) \qquad \phi_{\mathrm{BLE},\lambda} = c\mathrm{e}^{-d\lambda}$$

where c (g Pt·(mol photons)$^{-1}$·nm^{-1}) and d (nm^{-1}) are positive constants and λ is a wavelength (nm). Different combinations of c and d can cover a wide range of exponential relationships between quantum yield and wavelength. Equation 5 does not specify a fixed maximum wavelength inducing photochemical reactions ($\lambda_{\max}$) but states that with increasing wavelength, $\phi_{\mathrm{BLE},\lambda}$ exponentially approaches zero. Equations 3–5 were modified from Vähätalo et al. (2000).

Irradiation measurements and calculations for photon flux densities

Global radiation was measured with an Aanderaa global radiation meter (Aanderaa Instruments, Bergen, Norway) in 1991 or with a global radiation meter equipped with a BPW 20 photodiode (Hortimic Oy (Ltd.), Turku, Finland) in 1994 at 10-min intervals at a site located about 20 km from the study lakes. Downward irradiance into Lake Valkea-Kotinen was measured on 26 July 1995 between wavelengths of 310 nm and 700 nm at intervals of 5 nm with a factory-calibrated Macam SR991 spectroradiometer (Macam Photometrics Ltd., Livingston, Scotland). Measurements were

© 2002 NRC Canada

Fig. 1. The development of temperature (*a*; °C) and color (*b*; g Pt·m^{-3}) in Lake Valkea-Kotinen in 1994. In *a*, the shaded areas represent anoxic water and black areas represent thickness of ice cover. The vertical ticks at the upper margin of *b* indicate the dates of photobleaching measurements shown in Fig. 2.

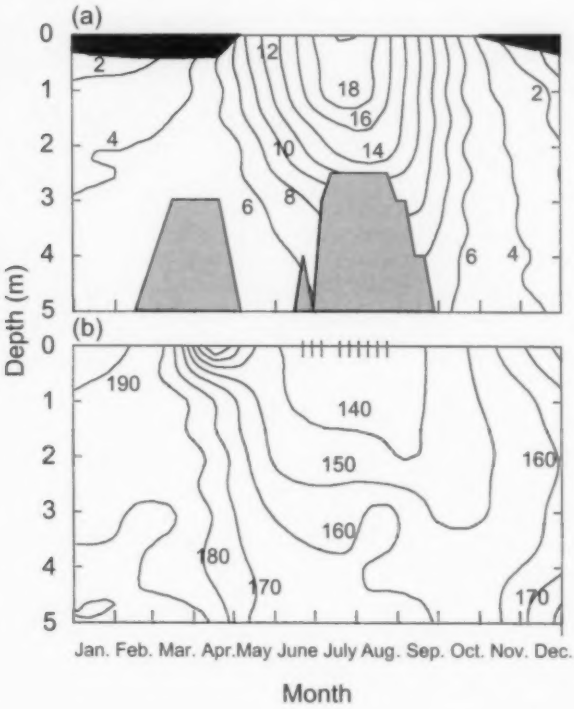

done at seven depths between 0.05 m and 0.4 m with solar zenith angles of 47° to 54°. The attenuation coefficients for downward irradiance ($K_{d,\lambda}$, m^{-1}·nm^{-1}) were determined from the slope of linear regression of the natural logarithm of downward irradiance ($I_{d,z,\lambda}$) vs. depth (*z*; Morris et al. 1995).

To obtain a close estimate of scalar photon flux density ($Q_{s,z,\lambda}$, eq. 3), we measured global radiation at 10-min intervals during the photobleaching experiments. The global radiation measurements were spectrally resolved with a model spectrum of solar radiation and taking into account variations in atmospheric ozone (details in Vähätalo et al. 2000). Solar radiation was separated into direct and diffuse parts according to the atmospheric molecular and turbidity scatter with a 5-nm resolution. Photons reflected according to Fresnel's law of reflection from the water–air interface were excluded. The mean cosine of downward photons in water was calculated according to Snell's law and the index of refraction. The radiative transfer in water took into account backscattering, absorption by H_2O, phytoplankton, CDOM, and tripton. Vector photon fluxes divided by the mean cosine of downward photons resulted in the downward scalar photon flux densities for both direct and diffuse photons. These two photon fluxes were combined to receive a spectrum of downward scalar photon flux density at the depth where the center of the vial was located ($Q_{d,s,z,\lambda}$). The above calculations were repeated at 10-min intervals and summed to obtain the $Q_{d,s,z,\lambda}$ (mol photons·m^{-2}·day^{-1}·nm^{-1} at depth *z* and wavelength λ) for the period lasting over the exposure of vials to solar radiation. $Q_{d,s,z,\lambda}$ was used as a substitute of $Q_{s,z,\lambda}$ in eq. 3. The reflectance of downward irradiance in water column was <0.3% on 31 July 1999, suggesting that $Q_{d,s,z,\lambda}$ served as a good estimate of $Q_{s,z,\lambda}$.

Fig. 2. Mean photobleaching of color (circles with standard error of mean, $n = 9$) in the top 0.15 m of Lake Valkea-Kotinen between 14 June and 16 August 1994. The curve shows the fitting according to eq. 6. Photobleaching calculated according to eq. 3 (×) is shown for comparison.

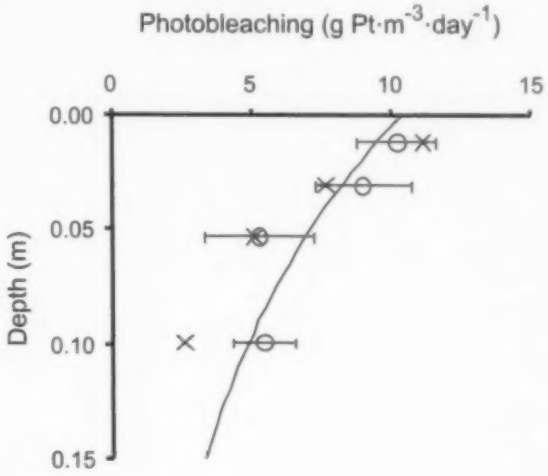

Mathematical determination of photobleaching yield

When the measured photobleaching at a depth *z* (BLE_z), $Q_{d,s,z,\lambda}$, and $a_{CDOM,\lambda}$ were applied to eq. 3, only $\phi_{BLE,\lambda}$ remained unknown. The latter (more precisely, the constants *c* and *d* of eq. 5) was optimized with the "fmins" function of the MATLAB software (The MathWorks, Inc., Natick, Mass.) so that the product of parameters on the right side of eq. 3 was as close as possible to the measured photobleaching at depth *z*. The optimization was done simultaneously for the whole data set of 36 measurements. The spectra (300–700 nm) for the parameters of eq. 3 were calculated at 5-nm steps.

Results

Seasonal dynamics of color in a Lake Valkea-Kotinen

Monitoring of seasonal dynamics of color in dimictic humic Lake Valkea-Kotinen showed that during the spring turnover (on 5 May) color was 162 g Pt·m^{-3} throughout the water column (Fig. 1). Between 14 June and 16 August, color was 136 ± 4 g Pt·m^{-3} (mean ± stardard deviation (SD), $n = 10$) in the epilimnion and less than 163 ± 4 g Pt·m^{-3} ($n = 10$) in the hypolimnion; thus hypolimnetic color did not differ in the summer from the color during the spring turnover. On 4 October, color was 146 g Pt·m^{-3} throughout the water column as a result of the autumnal turnover. The difference in colors between spring and autumnal turnovers indicated a

© 2002 NRC Canada

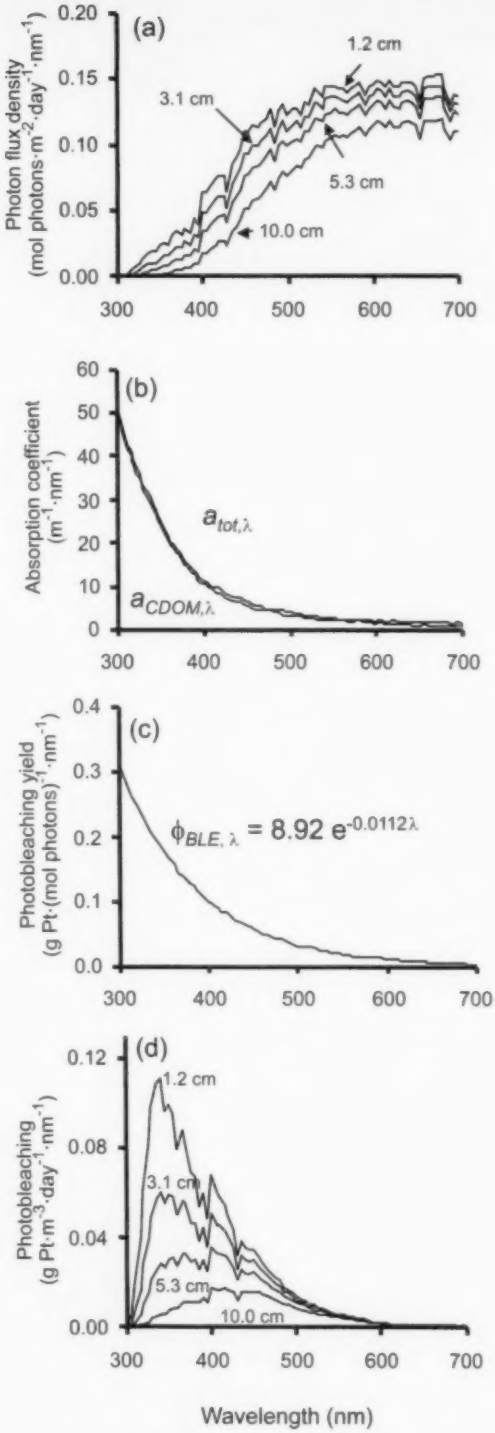

Fig. 3. Calculated photobleaching at four depths in Lake Valkea-Kotinen and parameters used for its calculation (eq. 3). The spectra are means (n = 9) between 14 June and 16 August 1994. (*a*) Downward scalar photon flux densities ($Q_{d,s,z,\lambda}$); (*b*) absorption by chromophoric dissolved organic matter ($a_{CDOM,\lambda}$) and by all absorbing components ($a_{tot,\lambda}$); (*c*) apparent quantum yield for photobleaching ($\phi_{BLE,\lambda}$); (*d*) calculated photobleaching at a depth z.

decrease of 16 g Pt·m^{-3}, which equaled 48 g Pt·m^{-2} when the mean depth of the lake (3 m) is taken into account.

Photobleaching of color in Lake Valkea-Kotinen

To test whether or not solar radiation caused the decrease in the color of the epilimnion of Lake Valkea-Kotinen (Fig. 1), photobleaching was measured in quartz vials placed in the epilimnion. At the depth of 0.01 m (with mean global radiation of 16 ± 4 MJ·m^{-2}·day^{-1} between 14 June to 16 August 1994), photobleaching was 10.2 ± 4.3 g Pt·m^{-3}·day^{-1} (mean ± SD, n = 9, Fig. 2). Linear regression between depth and logarithm of photobleaching ($F_{[1,34]}$ = 5, p < 0.05) showed that the rate decreased with increasing depth (Fig. 2) and followed the equation

$$(6) \qquad BLE_z = 10.4e^{-7.6z}$$

where 10.4 is the rate of photobleaching (g Pt·m^{-3}·day^{-1}) immediately below the surface (0 m) and 7.6 is the attenuation coefficient for photobleaching ($K_{d,BLE}$, m^{-1}). The $K_{d,BLE}$ indicated that 90% of the photobleaching occurred in the uppermost 0.3 m of the water column. Integration of eq. 6 over depths suggests that the rate of photobleaching was 1.4 g Pt·m^{-2}·day^{-1} in the whole water column. According to this rate, the half-time for photobleaching of color in the upper 1 m was 116 days (= 162 g Pt·m^{-2}/1.4 g Pt·m^{-2}·day^{-1}). Between 14 June and 16 August, solar radiation photobleached color 85 g Pt·m^{-2} (= 62 days × 1.4 g Pt·m^{-2}·day^{-1}), which was almost two times higher than the loss of color observed in the lake between spring and autumn turnovers.

Photobleaching yield and its use in modeling

The measured photobleaching (Fig. 2) was applied in eq. 3 to determine the apparent photobleaching yield ($\phi_{BLE,\lambda}$, g Pt·(mol photons)$^{-1}$·nm^{-1}). The best fit between the observed and modeled photobleaching was $\phi_{BLE,\lambda} = 8.92e^{-0.0112\lambda}$ (Fig. 3*c*). The spectral dependence of photobleaching (Fig. 3*d*) was calculated according to eq. 3 with the parameters shown in Figs. 3*a*–3*c*. Near the surface (depth of 0.012 m), the ultraviolet band of solar radiation photobleached color most effectively (Fig. 3*d*, Table 2). At this depth the solar radiation between 300 and 375 nm was responsible for 50% of the photobleaching, i.e., the median wavelength responsible for photobleaching ($\lambda_{BLE,50\%}$) was 375 nm (Fig. 3*d*, Table 2). With increasing depth, UV radiation decreased, $\lambda_{BLE,50\%}$ increased, and the relative contribution of photons at visible wavelengths to photobleaching increased (Fig. 3, Table 2).

The photobleaching integrated over the whole water column (Fig. 4*c*) was calculated according to eq. 4 using the parameters in Figs. 4*a*, 4*b*, and 3*c*. In the whole 6-m-deep water column, visible wavelengths were responsible for 66% of photobleaching and $\lambda_{BLE,50\%}$ was 425 nm (Fig. 4*c*, Table 2). At that wavelength the attenuation coefficient for the downward vector irradiance ($K_{d,425}$) was 10.8 m^{-1}. $K_{d,425}$ had similar magnitude to that of the attenuation coefficient observed for photobleaching ($K_{d,BLE}$ = 7.6 m^{-1}, eq. 7), which

© 2002 NRC Canada

Table 2. Contributions of solar UV-B, UV-A, and visible wavelengths to photobleaching and the median wavelength causing photobleaching ($\lambda_{BLE,50\%}$) at different depths and in the whole 0- to 6-m water column of Lake Valkea-Kotinen according to eq. 3 and eq. 4, respectively.

	Contribution to photobleaching (%)			
Depth (m)	300–315 nm	320–400 nm	405–700 nm	$\lambda_{BLE,50\%}$ (nm)
0.000	4.6	66.5	28.9	360
0.012	2.9	61.1	36.0	375
0.031	1.7	53.9	44.3	390
0.053	0.7	44.5	54.8	405
0.100	0.2	27.8	72.0	435
0–6.0	1.2	33.0	65.8	425

corresponded to the attenuation of downward irradiance at the wavelength of 445 nm. The observed attenuation of photobleaching ($K_{d,BLE}$ = 7.6 m^{-1}) and the $\lambda_{BLE,50\%}$ of 425 nm calculated from eq. 4 suggest that the attenuation of photobleaching followed the attenuation of blue irradiance.

By integrating the spectra shown in Fig. 3*d* over wavelengths, the modeled rates of photobleaching were in reasonable agreement with the measured photobleaching at the studied depths (Fig. 2). In the whole water column (Fig. 4*c*), the modeled photobleaching rate was 1.0 g Pt·m^{-2}·day^{-1} and close to the estimate (1.4 g Pt·m^{-2}·day^{-1}) based on eq. 6. These results indicated that modeling reproduced well the measured photobleaching.

Changes of color in the enclosures

Changes of color were also studied in enclosures build in two lakes. In highly humic (309 g Pt·m^{-3}) Lake Mekkojärvi, the depth of eplimnion was <1 m and therefore the enclosures were steeply stratified during the summer. In clear-water (28 g Pt·m^{-3}) Lake Valkea Mustajärvi, the enclosures were within the epilimnion and hence water in the enclosures was well mixed. In each lake, color of lake water decreased similarly in the two enclosures containing lake water alone (Fig. 5*b*). During over 4 months of exposure to solar radiation, decrease of color was 16 g Pt·m^{-3} in Lake Valkea Mustajärvi and 65 g Pt·m^{-3} in Lake Mekkojärvi (Fig. 5*b*). The first-order bleaching coefficients (k_{BLE}) were almost three times higher for water of Lake Valkea Mustajärvi than for water of Lake Mekkojärvi (Fig. 6*a*). In highly humic Lake Mekkojärvi, we calculated k_{BLE} for the summer only, because the autumnal turnover brought to the surface hypolimnetic water, which during the summer had been deeper than light penetration (Fig. 5*b*). In the top metre, the half-times for the bleaching of lake water color were about 120 days in Lake Valkea Mustajärvi and 455 days in Lake Mekkojärvi (Fig. 6*b*).

To study changes of color of biologically treated pulp mill effluents (PME; Table 1) in recipient lakes, PME from two kraft pulp mills was introduced into enclosures, and some enclosures were then covered with black film. In the darkened enclosures, the color did not change over the period of 4 months (Fig. 5*a*). During this time, color decreased 17–42% in the enclosures exposed to solar radiation (Fig. 5*b*).

Fig. 4. Calculated photobleaching in the whole water column (0–6 m) of Lake Valkea-Kotinen and two parameters for its calculation (eq. 4). The spectra are means (n = 9) between 14 June and 16 August 1994. (*a*) Downward vector photon flux density just below the surface (0 m, $Q_{d,v,0,\lambda}$); (*b*) the ratio of absorption by chromophoric dissolved organic matter ($a_{CDOM,\lambda}$) to total absorption ($a_{tot,\lambda}$); (*c*) calculated photobleaching in the water column (0–6 m).

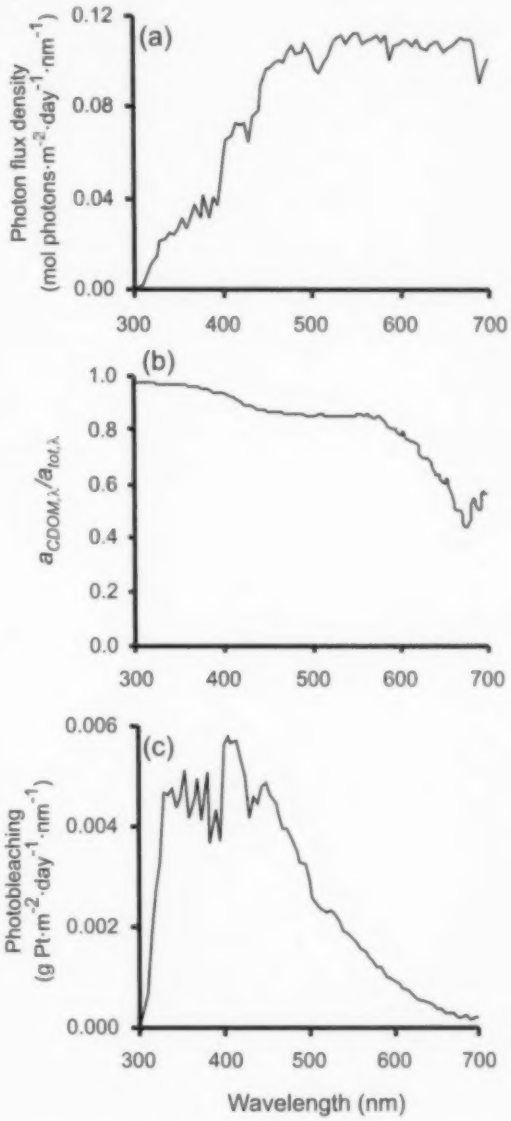

Respiration of plankton was similar in the exposed (114 ± 47 mg C·m^{-3}·day^{-1}, mean ± SD, n = 12) and the darkened (129 ± 32 mg C·m^{-3}·day^{-1}, n = 4) enclosures, which indicates that toxicity of PME was low and that heterotrophic plankton had negligible effect on bleaching of color (Fig. 5*a*). In the enclosures with PME, k_{BLE} ranged from 0.00014 to 0.00044 MJ^{-1}·m^2 and the values decreased with

© 2002 NRC Canada

Fig. 5. The development of color with or without amendments of pulp mill effluents in (*a*) darkened and (*b*) solar radiation exposed enclosures. + and ×, lake water alone; squares, with effluent from mill A; circles, with effluent from mill C; % shows the concentration of pulp mill effluent (vol./vol.). The curves in *b* show first-order kinetics fitting (eq. 2).

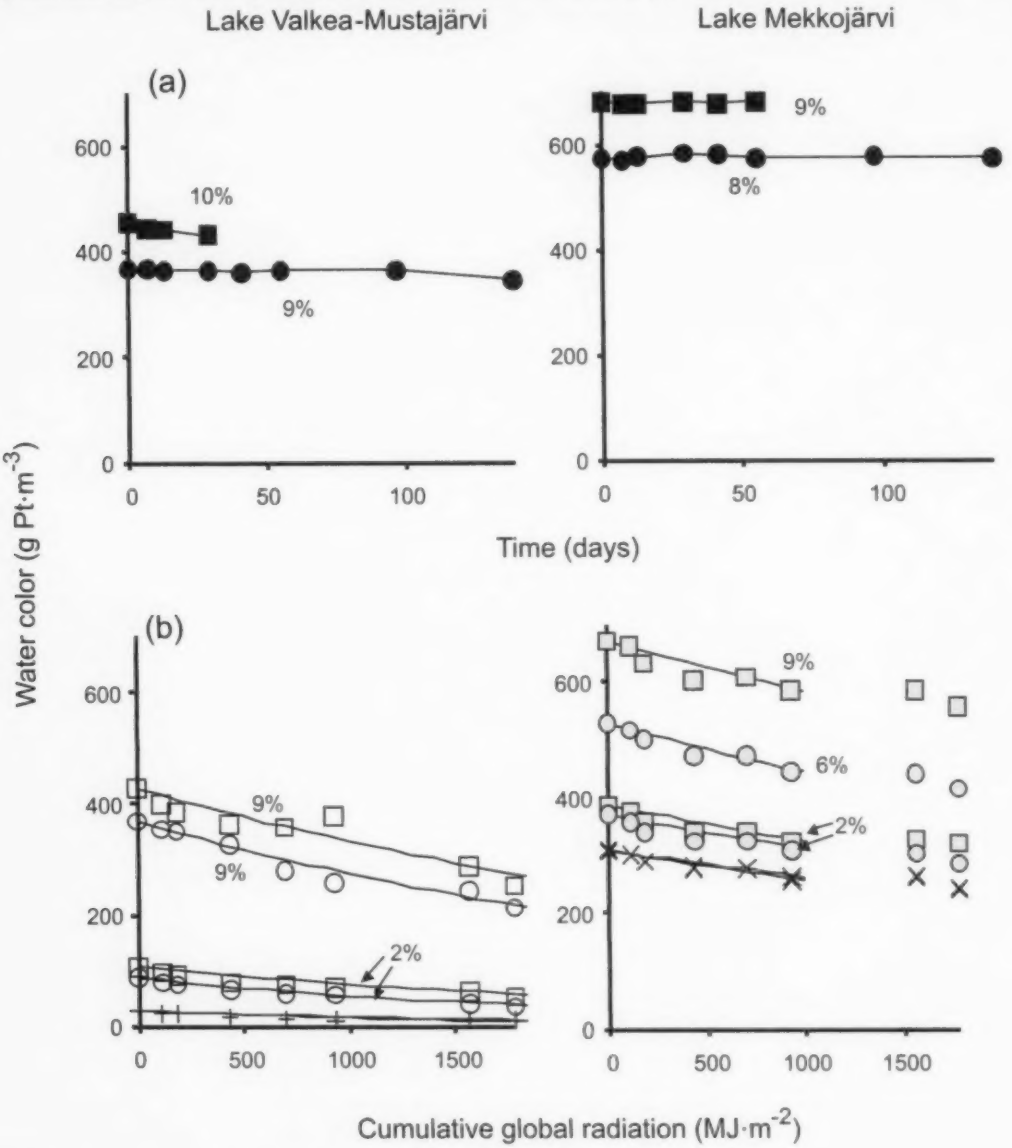

increasing initial color (Fig. 6*a*). Half-time of bleaching of color generally increased in concert with color (Fig. 6*b*).

Comparison of bleaching rates of lake water and PME

To compare bleaching rates in Lake Valkea-Kotinen and in the enclosures holding lake water with or without PME, the areal bleaching induced by an arbitrarily selected global radiation load of 100 MJ·m^{-2} was calculated (eq. 4, or by applying the bleaching coefficients in Fig. 6*a* to eq. 2; Table 3). The bleaching rates were similar in Lakes Valkea-Kotinen and Mekkojärvi (without PME, Table 3). In these cases, the color was ≥140 g Pt·m^{-3} (Table 1) and photobleaching occurred near (<0.3 m) the surface (Fig. 2). In the lake-water enclosures containing Lake Valkea Mustajärvi water, the bleaching rate was one-quarter that found in the two other lakes (Table 3). Because of the high transparency of water in Lake Valkea Mustajärvi (28 g Pt·m^{-3}, Table 1), the photobleaching capacity was not fully expressed in the 1.7-m-deep enclosures. The bleaching rates in the enclosures with 6–9% PME (colors >380 g Pt·m^{-3}, Fig. 5*b*) were about two times higher than those in Lake Valkea-Kotinen or in the lake-water enclosures of Lake Mekkojärvi (Table 3).

© 2002 NRC Canada

Fig. 6. (*a*) The first-order bleaching coefficients (k_{BLE} of eq. 2) and (*b*) half-times for bleaching in the exposed enclosures containing lake water with or without pulp mill effluents (from Fig. 5*b*). +, water of Lake Valkea Mustajärvi alone; ×, water of Lake Mekkojärvi alone; squares, with effluent from mill A; circles, with effluent from mill C. Open and shaded symbols show enclosures with pulp mill effluents in Lake Valkea Mustajärvi and Lake Mekkojärvi, respectively.

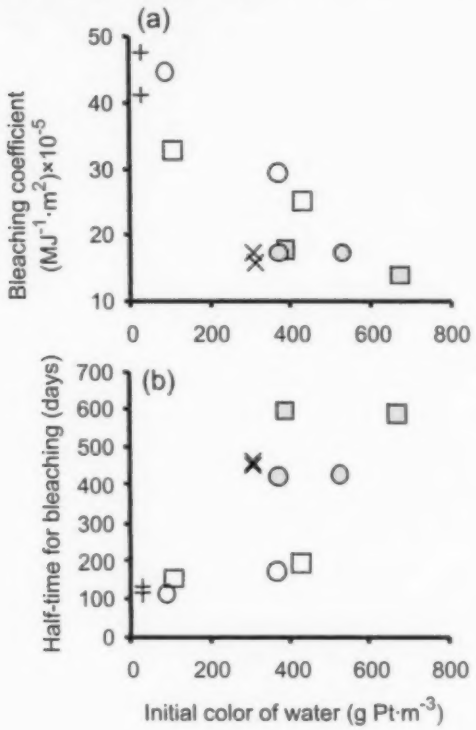

These differences in bleaching per unit of solar radiation suggested that the color of PME was more photoreactive than the water of the two studied humic lakes.

Discussion

In agreement with earlier studies (e.g., Archibald et al. 1997; Gibson et al. 2001; Osburn et al. 2001), the color of lake water and PME decreased under exposure to solar radiation and the measured photobleaching was sufficiently high to explain the observed decrease of color in the epilimnion of Lake Valkea-Kotinen. Although biological humification can increase absorptivity of dissolved organic matter (DOM; Shin and Lim 1996; Nelson et al. 1998; Rochelle-Newall and Fisher 2002), biological production of color was not observed either in the darkened enclosures with PME or in the hypolimnion of Lake Valkea-Kotinen. In this study, a large part of DOM was already humified in the catchment of Lake Valkea-Kotinen or in the wastewater treatment plants of the mills, which may explain why further biological humification was not observed.

Biological bleaching of color (Hessen et al. 1994; Morris and Hargreaves 1997; Nelson et al. 1998) may be important, especially at depths below the penetration of solar radiation. However, measurable changes in color of water could not be detected in the hypolimnion of Lake Valkea-Kotinen or in the darkened enclosures despite the presence of actively respiring plankton. Similar to Lake Valkea-Kotinen, absorption of CDOM decreased in the epilimnion but did not change in the hypolimnion in two Pennsylvanian lakes during summer stratification (Morris and Hargreaves 1997). Negligible bleaching of color in darkness suggests that plankton contributed only little to the loss of color in Lake Valkea-Kotinen and in the enclosures.

Table 3. Bleaching of color by global radiation (100 MJ·m^{-2}) in lake waters with or without amendments of pulp mill effluents (PME) from mills A and C.

	Bleaching (g Pt·m^{-2})		
Mill and concentration of PME	Lake Valkea Mustajärvi 0–1.7 m	Lake Mekkojärvi 0–1.7 m	Lake Valkea-Kotinen 0–6 m
0%	2	8	8
A, 2%	5	11	
A, 9%	16	14	
C, 2%	6	10	
C, 9% or C, 6%	16[a]	14[b]	

Note: Bleaching in the enclosures located in Lakes Valkea Mustajärvi and Mekkojärvi (Fig. 5*b*) was calculated according to eq. 2 with the bleaching coefficients shown in Fig. 6*a*. Photobleaching in Lake Valkea-Kotinen was calculated according to eq. 4 applying $\phi_{BLE,\lambda} = 8.92e^{-0.0112\lambda}$ (Fig. 3c) and assuming that chromophoric dissolved organic matter absorbed all solar radiation. The calculated values were integrated over the depth of enclosures (0–1.7 m) and Lake Valkea-Kotinen (0–6 m).

[a]9%.

[b]6%.

In this study, the measured photobleaching exceeded the observed loss of color in Lake Valkea-Kotinen, similar to the earlier findings in four North American lakes (Curtis and Schindler 1997; Morris and Hargreaves 1997). This indicated that source of color, such as inflow of CDOM, partly compensated for photochemical losses of color, e.g., in Ontario the color of inflowing water was the highest during summer (Molot and Dillon 1997*b*). Recently Gibson et al. (2001) found that an episodic inflow of CDOM even increased color despite intensive photobleaching in a subarctic lake. Therefore photobleaching may not always result in decrease of color in waters with short residence times and appreciable watershed runoff.

Depth of photolytic stratum and limitations of first-order kinetic approach

Nelson et al. (1998) modeled dynamics of CDOM in the Sargasso Sea and found that photobleaching attenuated into water column with a $K_{d,BLE}$ of 0.019 m^{-1}. This corresponded to the attenuation of radiation between 380 and 480 nm (N. Nelson, ICESS/UCSB, Santa Barbara, CA 93106, U.S.A., personal communication). Because this range includes blue radiation, photobleaching may have attenuated similar to blue radiation in Lake Valkea-Kotinen and in the Sargasso Sea. Attenuation of blue radiation, thus, may serve as a rough estimate for the penetration of photobleaching in optically different waters.

© 2002 NRC Canada

Optical conditions vary greatly among lakes, e.g., in 65 North and South American lakes, $K_{d,380}$ ranged from 0.07 to 31.7 m^{-1} and $K_{d,PAR}$ ranged from 0.10 to 5.21 m^{-1} (Morris et al. 1995). We estimated that the downward attenuation of blue irradiance ($K_{d,435}$) in these lakes was 0.10 m^{-1} in the clearest lake (Lake Schmoll with color of 0.5 g $Pt \cdot m^{-3}$) and 14.4 m^{-1} in the most optically dense lake (Lake Little Echo with color of 237 g $Pt \cdot m^{-3}$). If photobleaching attenuates downward as does blue irradiation with an areal magnitude of 1 g $Pt \cdot m^{-2} \cdot day^{-1}$, then the rate of photobleaching (refer to BLE_z of eq. 6) would attenuate according to $0.1e^{-0.1z}$ and $14.4e^{-14.4z}$ into Lake Schmoll and Lake Little Echo, respectively. In Lake Little Echo, almost all photobleaching would occur in the top 0.4 m. In Lake Schmoll, photobleaching would reach down to the depth of 40 m. Thus, even if areal photobleaching is uniform in different water bodies, the depth of photolytic stratum may vary greatly depending on optical properties.

The variation in optical properties affects the determination of first-order bleaching coefficients (k_{BLE} of eq. 2). To illustrate this we present a hypothetical example. If one determines k_{BLE} in Lakes Schmoll and Little Echo by using a vial (with an optical pathlength of 0.02 m) placed immediately beneath the surface (0–0.02 m), volumetric photobleaching would be 0.1 $Pt \cdot m^{-3} \cdot day^{-1}$ and 12.5 g $Pt \cdot m^{-3} \cdot day^{-1}$, respectively. Compared with the initial color, photobleaching would be 20% in Lake Schmoll and 5.3% in Lake Little Echo. The same fourfold difference will hold also for k_{BLE}. A vial at the depth of 0.1 m would result in 14 times higher k_{BLE} in Lake Schmoll than in Lake Little Echo. The example above illustrates that even if the areal photobleaching in lakes is the same, k_{BLE} would be higher in clear water than in optically dense water. This relationship explains why the measured values of k_{BLE} were highest in the enclosures with the lowest color of water. Thus, at their best, k_{BLE} values predict the loss of color only at a specific depth and in those optical properties of water where they were determined. Therefore, instead of k_{BLE}, we recommend the quantum-yield approach for modeling photobleaching.

Spectral dependence of photobleaching and quantum yields

In this study, UV-B radiation contributed 5% and 1% to photobleaching at the surface and in the whole water column of Lake Valkea-Kotinen, respectively. Some studies have suggested a larger contribution of UV-B to photobleaching than found in this study. For example, De Haan (1993) compared loss of absorption at 250 nm in bog water to the attenuation of UV radiation and concluded that radiation below 320 nm was mainly responsible for photobleaching. In addition, Reche et al. (2000) determined waveband-specific k_{BLE} for UV-B using quartz and borosilicate bottles and estimated that UV-B radiation photobleached 10% to 40% of color in the whole water column of a hypothetical lake. Earlier quantum-yield studies have reported spectral dependence of photobleaching similar to that found in this study (Whitehead et al. 2000; Osburn et al. 2001). Osburn et al. (2001) calculated that radiation at 280–320 nm contributed 12% (mean, range 5–22%) to photobleaching in four lake waters, bog water, and algal extract at the surface conditions. This agrees with the 9% contribution of the same spectral band at the surface of Lake Valkea-Kotinen. Whitehead et al. (2000) found that in optically deep enclosures, an approximately doubled dose of UV-B radiation did not enhance photobleaching of estuarine water, which is in agreement with low (1.2%) contribution of UV-B to photobleaching in the whole water column of Lake Valkea-Kotinen. The published spectra of quantum yields (Whitehead et al. 2000; Osburn et al. 2001) and this study suggest that in the studied waters, solar UV-B (280–315 nm) contributed 5–15% to photobleaching at the very surface but only 1–2% in the water column that completely absorbed solar radiation.

The differences in the reported spectral dependence of photobleaching depends partly on the wavelength applied for the measurement of photobleaching. Photobleaching has been measured by several methods, including loss of absorbance at single wavelengths ranging from 250 nm to 465 nm (see reviews Hongve and Åkesson 1996; Molot and Dillon 1997*b*). Absorbance at 465 nm coincides with the highest solar irradiance, whereas absorbance at 250 nm is outside the range of solar radiation on the surface of the Earth. Experiments with monochromatic irradiation have showed that marine CDOM lost absorbance most at the wavelength of irradiation (Kouassi and Zika 1992). That study suggests that, for example, visual wavelengths of solar radiation bleach more $a_{CDOM,465}$ than $a_{CDOM,250}$ and may explain why loss of $a_{CDOM,250}$ was strongly related to UV-B radiation in the study of De Haan (1993).

In the quantum-yield studies, photobleaching has been measured at different spectral regions: at several single wavelengths between 280 and 540 nm in Whitehead et al. (2000); as a mean of 280–500 nm in Osburn et al. (2001); and at 420 nm in this study. Despite these differences, the spectral dependence of published quantum yields is similar. In this study, the quantum yield for the photobleaching of color ($\phi_{BLE,\lambda}$) decreased exponentially with increasing wavelength with a slope of 0.0112 nm^{-1}, which was close to that of 0.0108 nm^{-1} determined for estuary water (estimated from fig. 5*a* of Whitehead et al. 2000). In four lakes in Argentina and the U.S.A., the spectral dependence of weighting factor for photobleaching had a slope of 0.0108 nm^{-1} (Osburn et al. 2001). The corresponding slope in Lake Valkea-Kotinen was 0.0138 nm^{-1}, calculated from the measured quantum yields and accounting for the energy of photons. Those studies of Whitehead et al. (2000) and Osburn et al. (2001) together with the present study suggest that the spectral dependence of quantum yield for photobleaching is similar among the studied natural waters.

Vähätalo et al. (2000) determined the spectral dependence of quantum yield for photomineralization of dissolved organic carbon (DOC) from the same samples used in this study. The slope of spectral dependence of quantum yield was 2.5 times higher for photomineralization than for photobleaching. The difference between slopes indicates that solar radiation photobleached color more than it mineralized DOC in Lake Valkea-Kotinen, which is in agreement with earlier studies with marine (Moran et al. 2000) and fresh (Molot and Dillon 1997*a*; Morris and Hargreaves 1997) waters as well as PMEs (Archibald and Roy-Arcand 1995). Solar radiation appears to selectively remove CDOM and decreases specific absorption of DOC (Curtis and Schindler 1997; Reche et al. 2000).

© 2002 NRC Canada

The modeled rates agreed with the measured values in photobleaching (this study) and photochemical mineralization of DOC (Vähätalo et al. 2000). The good fit between modeled and measured values suggests that the quantum-yield approach estimates photochemical rates in surface waters accurately. The quantum-yield approach is sensitive for changes in quantum yield. This study indicated a twofold difference in quantum yield between humic lake waters and PMEs. Osburn et al. (2001) found a fourfold difference in the photoreactivity between the most (bog water) and least (Argentina lakes) reactive CDOMs. The variability of quantum yields should be taken into account in modeling, and for the most accurate results, we recommend determination of quantum yield for each studied water before modeling.

Bleaching of PMEs

In this study, color of PME decreased under solar radiation, whereas negligible changes were observed in darkness despite the presence of active heterotrophic metabolism. This finding suggests that solar radiation rather than heterotrophic plankton photobleached color of PME and agrees with photobleaching of PME found in earlier studies (e.g., Roy-Arcand and Archibald 1993; Millar et al. 1996; Archibald et al. 1997) and low loss of color during and after conventional wastewater treatment (Roy-Arcand and Archibald 1993; Bajpai and Bajpai 1994). Although fungal and bacterial cultures can effectively bleach color of PME under optimal conditions (e.g., Millar et al. 1996; Jain et al. 1997), our study suggests that is not the case in the water column of recipient waters.

PMEs were about twice as sensitive as water of the two humic lakes to photobleaching. Unlike the studied lake waters, the PMEs were exposed to solar radiation for the first time. Unexposed DOM of inflowing water was more sensitive to photomineralization than DOM previously exposed to solar radiation in the epilimnion (Salonen and Vähätalo 1994). The unexposed chromophores of PME may have explained the high sensitivity of PME for photobleaching.

Archibald and Roy-Arcand (1995) observed 1.3 times higher apparent photobleaching yield for PME at 350 nm than at 400 nm. In Lake Valkea-Kotinen, the corresponding difference was larger (1.8) than in the PME studied by Archibald and Roy-Arcand (1995), which suggests that the same dose of solar radiation bleaches more PMEs than the natural DOM of humic lakes, which is in agreement with our results.

Acknowledgements

The Maj and Tor Nessling Foundation, Ministry of the Environment, University of Helsinki, and Academy of Finland funded this study. Jaakko Vainionpää and Riitta Ilola helped in the color measurements, and Jorma Keskitalo assisted in the work at Lake Valkea-Kotinen. Juhani Virta and Anne Ojala kindly provided global radiation data. Tom Frisk, Marko Järvinen, Uwe Münster, Norm Nelson, Robert G. Wetzel, and three anonymous reviewers gave valuable comments during the preparation of the manuscript.

References

APHA (American Public Health Association, American Water Works Association, and Water Pollution Control Federation). 1998. Standard methods for the examination of water and wastewater. Method 2120 C. 20th ed. American Public Health Association, Washington, D.C.

Archibald, F., and Roy-Arcand, L. 1995. Photodegradation of high molecular weight kraft bleachery effluent organochlorine and color. Water Res. **29**: 661–669.

Archibald, F., Roy-Arcand, L., and Méthot, M. 1997. Time, sunlight, and the fate of biotreated kraft mill organochlorines (AOX) in nature. Water Res. **31**: 85–94.

Arrigo, K.R. 1994. The impact of ozone depletion on phytoplankton growth in the Southern Ocean: large-scale spatial and temporal variability. Mar. Ecol. Prog. Ser. **144**: 1–12.

Bajpai, P., and Bajpai, P.K. 1994. Biological colour removal of pulp and paper mill waste waters. J. Biotechnol. **33**: 211–220.

Bricaud, A., Morel, A., and Prieur, L. 1981. Absorption by dissolved organic matter of the sea (yellow substance) in the UV and visible domains. Limnol. Oceanogr. **26**: 43–53.

Curtis, J.P., and Schindler, D.W. 1997. Hydrologic control of dissolved organic matter in low-order Precambrian Shield lakes. Biogeochemistry, **36**: 125–138.

De Haan, H. 1993. Solar UV-light penetration and photodegradation of humic substances in peaty lake water. Limnol. Oceanogr. **38**: 1072–1076.

Del Castillo, C.E., Coble, P.G., Conmy, R.N., Müller-Karger, F.E., Vanderbloemen, L., and Vargo, G.A. 2001. Multispectral in situ measurements of organic matter and chlorophyll fluorescence in seawater: documenting the intrusion of the Mississippi River plume in the West Florida Shelf. Limnol. Oceanogr. **46**: 1836–1843.

Gibson, J.A.E., Vincent, W.F., and Pienitz, R. 2001. Hydrologic control and diurnal photobleaching of CDOM in a subarctic lake. Arch. Hydrobiol. **152**: 143–159.

Hessen, D.O., Nygaard, K., Salonen, K., and Vähätalo, A. 1994. The effect of substrate stoichiometry on microbial activity and carbon degradation in humic lakes. Environ. Int. **20**: 67–76.

Hongve, D., and Åkesson, G. 1996. Spectrophotometric determination of water colour in Hazen units. Water Res. **30**: 2771–2775.

Jain, N., Shrivastava, S.K., and Shrivastava, A.K. 1997. Treatment of pulp mill wastewater by bacterial strain *Acinetobacter calcoaceticus*. Indian J. Exp. Biol. **35**: 139–143.

Jokela, J.K., Laine, M., Ek, M., and Salkinoja-Salonen, M. 1993. Effect of biological treatment on halogenated organics in bleached kraft pulp mill effluents studied by molecular weight distribution analysis. Environ. Sci. Technol. **27**: 547–557.

Jones, R.I., and Arvola, L. 1984. Light penetration and some related characteristics in small forest lakes in southern Finland. Verh. Int. Ver. Limnol. **22**: 811–816.

Keskitalo, J., and Salonen, K. 1996. Integrated monitoring studies of plankton in Valkea-Kotinen in 1994. Report 16, Finnish Environment Agency, Helsinki. [In Finnish.]

Keskitalo, J., Salonen, K., and Holopainen, A.-L. 1998. Long-term fluctuations in environmental conditions, plankton and macrophytes in a humic lake, Valkea-Kotinen. Boreal Environ. Res. **3**: 251–262.

Kouassi, A.M., and Zika, R.G. 1992. Light-induced destruction of the absorbance property of dissolved organic matter in seawater. Toxicol. Environ. Chem. **35**: 195–211.

Millar, K., Carey, J.C., Burnison, B.K., Lee, H., and Trevors, J.T. 1996. Degradation of high molecular weight fraction of bleached kraft mill effluent by biological and photochemical processes. *In* Environmental fates and effects of pulp and paper mill effluents.

© 2002 NRC Canada

Edited by M.R. Servos, K.R. Munkittrick, J.H. Carey, and G.J. Van der Kraak. St. Luice Press, Delray, Fla. pp. 239–251.

Miller, W.L. 1998. Effects of UV radiation on aquatic humus: photochemical principles and experimental considerations. *In* Aquatic humic substances. *Edited by* D.O. Hessen and L.J. Tranvik. Springer-Verlag, Berlin. pp. 125–143.

Molot, L.A., and Dillon, P.J. 1997*a*. Photolytic regulation of dissolved organic carbon in northern lakes. Global Biogeochem. Cycles, **11**: 357–365.

Molot, L.A., and Dillon, P.J. 1997*b*. Colour – mass balances and colour – dissolved organic carbon relationships in lakes and streams in central Ontario. Can. J. Fish. Aquat. Sci. **54**: 2789–2795.

Moran, M.A., Sheldon, W.M., and Zepp, R.G. 2000. Carbon loss and optical property changes during long-term photochemical and biological degradation of estuarine dissolved organic matter. Limnol. Oceanogr. **45**: 1254–1264.

Morris, D.P., and Hargreaves, B.R. 1997. The role of photochemical degradation of dissolved organic carbon in regulating the UV transparency of three lakes on the Pocono Plateau. Limnol. Oceanogr. **42**: 239–249.

Morris, D.P., Zagarese, H., Williamson, C.E., Balseiro, E.G., Hargreaves, B.R., Modenutti, B., Moeller, R., and Queimalinos, C. 1995. The attenuation of solar UV radiation in lakes and the role of dissolved organic carbon. Limnol. Oceanogr. **40**: 1381–1391.

Nelson, N.B., Siegel, D.A., and Michaels, A.F. 1998. Seasonal dynamics of colored dissolved material in the Sargasso Sea. Deep-Sea Res. I, **45**: 931–957.

Osburn, C.L., Zagarese, H.E., Morris, D.P., Hargreaves, B.R., and Cravero, W.E. 2001. Calculation of spectral weighting functions for the solar photobleaching of chromophoric dissolved organic matter in temperate lakes. Limnol. Oceanogr. **46**: 1455–1467.

Reche, I., Pace, M.L., and Cole, J.J. 2000. Modeled effects of dissolved organic carbon and solar spectra on photobleaching in lake ecosystems. Ecosystems, **3**: 419–432.

Rochelle-Newall, E.J., and Fisher, T.R. 2002. Production of chromophoric dissolved organic matter fluorescence in marine and estuarine environments: an investigation into the role of phytoplankton. Mar. Chem. **77**: 7–21.

Roy-Arcand, L., and Archibald, F.S. 1993. Effect of time, daylight, and settling pond microorganisms on the high molecular weight fraction of kraft bleachery effluents. Water Res. **27**: 873–881.

Salonen, K. 1981. Rapid and precise determination of total inorganic carbon and some gases by high temperature combustion. Water Res. **15**: 403–406.

Salonen, K., and Vähätalo, A. 1994. Photochemical mineralisation of dissolved organic matter in Lake Skervatjern. Environ. Int. **20**: 307–312.

Saski, E. 1998. Accumulation and transformation of pulp mill organic discharges in recipient lakes. Ph.D. thesis, University of Helsinki, Dissertationes Biocentri Viikki Universitatis Helsingiensis 3/1998.

Saski, E.K., Salonen, K., Vähätalo, A., and Salkinoja-Salonen, M. 1995. Degradation of the halogenated organic fraction of biologically treated bleached kraft pulp mill effluents in Finnish lake water enclosures. *In* The contaminants in the Nordic ecosystems: dynamics, processes and fate. *Edited by* M. Munwar and M. Luotola. ECOVISION, Word Monograph Series. SPB Academic Publishing, Amsterdam, The Netherlands. pp. 109–123.

Shin, H.-S., and Lim, K.-H. 1996. Spectroscopic and elemental investigation of microbial decomposition of aquatic fulvic acids in biological process of drinking water treatment. Biodegradation, **7**: 287–295.

Vähätalo, A.V., Salkinoja-Salonen, M., Taalas, P., and Salonen, K. 2000. Spectrum of the quantum yield for photochemical mineralization of dissolved organic carbon in a humic lake. Limnol. Oceanogr. **45**: 664–676.

Whipple, G.C. 1927. The microscopy of drinking water. 4th ed. John Wiley & Sons, New York.

Whitehead, R.F., de Mora, S., Demers, S., Gosselin, M., Monfort, P., and Mostajir, B. 2000. Interactions of ultraviolet-B radiation, mixing, and biological activity on photobleaching of natural chromophoric dissolved organic matter: a mesocosm study. Limnol. Oceanogr. **45**: 278–291.

Williamson, G.E. 1995. What role does UV-B radiation play in freshwater ecosystems? Limnol. Oceanogr. **40**: 386–392.

© 2002 NRC Canada

Altered body size distributions in a large river fish community enriched by sewage

Adrian M.H. deBruyn, David J. Marcogliese, and Joseph B. Rasmussen

Abstract: We used two approaches (interspecific upper bound and normalized biomass spectrum, NBS) to study size distributions in a littoral fish community across a natural gradient of epiphytic primary production and at sites enriched by primary-treated sewage. The upper bound of the interspecific density – body size relationship supported universal energetic constraints on the regional assemblage but revealed substantial variation in size distributions at a local scale. Multivariate analysis of the modes composing the NBS suggested possible mechanisms for this local variation in size distributions. Only the largest organisms had higher densities at higher levels of productivity. Densities of smaller organisms could be explained by a combination of habitat characteristics and feeding interactions.

Résumé : Deux approches, la limite supérieure interspécifique et le spectre normalisé des biomasses, nous ont permis d'étudier la distribution en taille d'une communauté de poissons littoraux le long d'un gradient naturel de productivité primaire épiphytique, ainsi qu'à des sites enrichis par des eaux d'égout qui ont subi un traitement primaire. La limite supérieure de la relation interspécifique entre la densité et la taille appuie l'existence de contraintes énergétiques globales sur la communauté régionale, mais met en lumière d'importantes variations dans la distribution en taille à l'échelle locale. L'analyse multidimensionnelle des modes qui composent le spectre normalisé des biomasses indique l'existence possible de mécanismes pour expliquer cette variation locale dans la distribution des tailles. Seuls les plus grands organismes atteignent des densités plus élevées aux taux plus hauts de productivité. Les densités des organismes plus petits peuvent peut-être s'expliquer par une combinaison de caractéristiques de l'habitat et d'interactions alimentaires.

[Traduit par la Rédaction]

Introduction

Body size is arguably the most fundamental aspect of ecology, spanning more than 21 orders of magnitude. Size determines how an organism perceives its physical environment, and size scales with biological characteristics ranging from individual metabolic rate to species richness (Peters 1983). For more than 60 years, ecologists have identified statistical patterns in the size structure of communities that seemingly reflect the operation of general principles or natural laws. These empirical investigations have followed two parallel but rarely intersecting paths. Community ecologists have focused on the negative allometric scaling of population density among species, invoking energetic constraints to explain the upper limit of density possible for a species of a given body size. Contemporary work by a number of (aquatic) ecosystem ecologists has largely foregone taxonomic distinctions, considering how the total density of organisms is distributed along a spectrum of logarithmic size-classes. These two parallel lines of investigation offer complementary insights into the factors that influence community size structure.

The interspecific relationship between population density and body size has been examined in a wide variety of taxonomic groups and in a few entire natural communities. However, there is little consensus regarding the form of the relationship or the mechanisms that generate it. Data are usually plotted on double log axes, where a linear relationship reflects an underlying power function. When a linear relation is observed, it often has an OLS (ordinary least squares) regression slope near –0.75. This is the inverse of the allometric scaling coefficient for per capita energy requirements (+0.75), and it has been suggested that energy consumption per population is therefore independent of body size, reflecting an underlying energetic constraint on population density (the "energetic equivalence rule"; Damuth 1987). Under the hypothesis that energetic constraints are most important to the most abundant species (those adjacent to the upper bound of the density – body size relationship), some authors have calculated the maximum density across log size-classes and expressed the allometric scaling of this value, the "upper-bound slope" (e.g., Lawton 1989; Blackburn et al. 1992). Often, the relation between density and body size is approximately triangular. Even if energy requirements set the upper bound of density, the effect of body size on energy acquisition and conversion processes favours medium-sized species within major taxonomic groups at both ecological and evolutionary scales (Brown et al. 1993).

Marquet et al. (1995) noted that the energy available to a species is determined both by the basal productivity of its

Received 26 July 2001. Accepted 15 April 2002. Published on the NRC Research Press Web site at http://cjfas.nrc.ca on 14 June 2002.
J16465

A.M.H. deBruyn[1] **and J.B. Rasmussen.** Department of Biology, McGill University, 1205 Docteur Penfield Avenue, Montreal, QC H3A 1B1, Canada.
D.J. Marcogliese. St. Lawrence Centre, Environment Canada, 105 McGill Avenue, Montreal, QC H2Y 2E7, Canada.

[1]Corresponding author (e-mail: adrian.debruyn@mail.mcgill.ca).

 DOI: 10.1139/F02-056 © 2002 NRC Canada

habitat and by the assemblage with which it must share this productivity. This suggests that perhaps energetic hypotheses are better addressed by the allometric scaling of total density, rather than density per species (Griffiths 1992). This has been the approach taken in aquatic ecology. The total density – body size relationship is commonly expressed as the normalized biomass spectrum (NBS), obtained by summing all biomass within $\log_2$ size-classes, then normalizing these sums to the lower bound (= width) of the size interval. This calculation estimates the total density of individuals within each size-class, irrespective of taxonomic identity. NBS slopes are commonly near –1.0, which reflects a roughly uniform distribution of biomass over logarithmically increasing size-classes. This pattern has been interpreted to mean that size structure reflects the flow of energy and matter from small to large organisms in the pelagia (Borgmann 1987), although similar slopes are observed in the benthos, where most large organisms are microphagous (Rasmussen 1993).

Both approaches to the density – body size relationship rely heavily on energetic arguments, but the effect of varying productivity on this relationship is far from clear (Blackburn and Lawton 1994; Marquet et al. 1995). It is widely recognized that species' densities are influenced by a combination of resource availability and exploitation by predators (e.g., Power 1992). Size-structured feeding relationships are common in aquatic systems (Mittelbach and Persson 1998), and this favours top-down influences on body size distributions in pelagic (Carpenter et al. 1996) and benthic (Blumenshine et al. 2000) communities. Changes in body size distributions with increasing productivity could in fact reflect cascading trophic interactions, with higher (large) predator densities in more productive systems controlling the density of smaller size-classes. If body size corresponds roughly to trophic level, food web models with consumer control (e.g., Oksanen et al. 1981) predict that increasing productivity will produce uneven increases in density across the size spectrum (Sprules 1988; Fig. 1).

Here we address the effect of productivity and compare the results obtained using the two alternative approaches outlined above. We studied size distributions in a littoral fish community across a natural gradient of epiphytic primary production and at sites enriched by primary-treated sewage (a large-scale natural experiment). The municipal wastewater treatment plant of Montreal, Quebec, has been discharging >450 tonnes (t) phosphorus and >90 000 t particulate organic matter annually into the St. Lawrence River since 1988 (Purenne 1998). High current speeds and strong vertical mixing prevent deoxygenation and net sedimentation in this reach of the river, so the primary effect of this discharge is sustained enrichment. This type of enrichment has been linked to enhanced production of benthic macroinvertebrates (King and Ball 1967) and fish (Katz and Howard 1955).

Methods

Study system

The St. Lawrence is a large, fast-flowing, temperate river. Nutrient levels are moderate (dissolved P < 30 $\mu g \cdot L^{-1}$; dissolved N < 0.5 $mg \cdot L^{-1}$) and pelagic productivity is low (median summer chlorophyll a < 2.5 $\mu g \cdot L^{-1}$; Hudon and Sylvestre 1998). Flow rates are typically 1–2 $m \cdot s^{-1}$ in the main channel, and net sedimentation of suspended material is restricted to the deepest areas outside the main channel.

The Montreal Urban Community (MUC) wastewater treatment plant is a primary treatment facility serving 1.8 million people on the Island of Montreal (Purenne 1998). This wastewater is treated to promote coagulation, passed through settling ponds, and discharged directly to the St. Lawrence River via an underwater pipe. Effluent is discharged at an average rate of $2 \cdot 10^6$ $m^3 \cdot day^{-1}$, with an average of approximately 100 mg (wet weight (w.w.)) $\cdot L^{-1}$ of suspended particulate matter, 0.5 $mg \cdot L^{-1}$ total phosphorus, and 9 $mg \cdot L^{-1}$ total nitrogen (Purenne 1998). On an annual basis, this discharge contributes 450 t phosphorus and $9 \cdot 10^4$ t (w.w.) of particulate matter to the weakly productive waters of the St. Lawrence River (Purenne 1998).

We sampled littoral fish from 12 sites downstream of the Island of Montreal, chosen to reflect a gradient of macrophyte cover, and therefore a gradient of epiphytic primary productivity. Three of these were in the discharge plume of the municipal wastewater treatment plant, within 10 km of the outfall. The remainder were reference sites, either upstream of the outfall, or downstream but hydrodynamically isolated from the plume. Lateral mixing in this reach of the St. Lawrence is very slow, and a narrow mixing zone between the Ottawa River and the Great Lakes water masses persists at least 60 km downstream of Montreal (Verrette 1990). The MUC wastewater is discharged into the middle of the mixed zone, and widens only very gradually downstream. We used stable isotope analysis of benthic invertebrates and benthivorous fish to detect entry of sewage-derived organic matter into the littoral food web (deBruyn 2001). This technique is sensitive enough to detect assimilation of sewage organic matter at sites exposed to less than 1% effluent (deBruyn and Rasmussen 2002). None of the reference sites showed any evidence of sewage organic matter in the diets of primary consumers.

Sampling and analysis

Fish were collected on two visits to each site between 17 July and 7 Sept. 2000, using a 40 × 2 m seine (0.5-cm mesh). At least three seine hauls were taken on each visit, 50–100 m apart and successively upstream. One or two additional hauls were taken if low numbers of fish were obtained. Five to 10 individuals of each species per visit (or as many as were available) were sacrificed and frozen for other studies. All other fish were measured before release, and their wet weights were calculated using length–weight relationships derived from sacrificed fish.

Size distributions

We estimated the upper bound of the interspecific density – body size relationship according to the method of Blackburn et al. (1992), with the following modification. This method effectively assumes that only the mean (or mean adult) size of a species is important in its ecological and evolutionary interactions. This may be a reasonable assumption for species that rapidly attain adult size (e.g., birds). It is probably not a good assumption for species that grow slowly, occupy

© 2002 NRC Canada

Fig. 1. Schematic representation of how the size distribution of a size-structured, three-level food chain is predicted to respond to basal enrichment, considering (*a*) only resource control and (*b*) resource and consumer control. Arrows indicate changes in density between unenriched (lower line) and enriched (upper line) states.

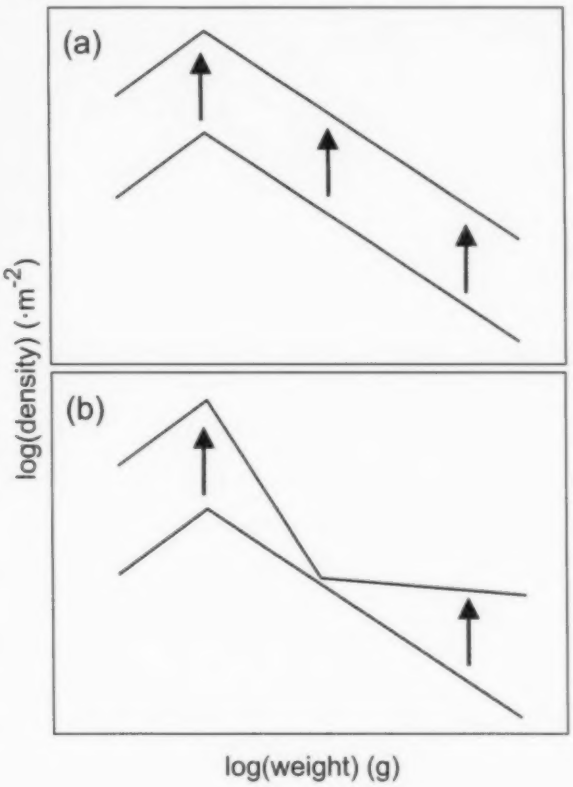

a wide range of body sizes throughout their lifespan (e.g., oviparous species), have indeterminate growth form (e.g., fish), or show plasticity of form within a population (again, fish are a good example). We therefore treated each age-class of each species as an independent datum; effectively, each age-class was considered to be ecologically equivalent to a species. If the unit of study was the complete community of a closed system, this would superimpose species survivorship curves (many small young versus few large adults) on the density – body size pattern. However, our study system is not closed. The littoral zone of temperate rivers like the St. Lawrence is recolonized each spring by fish age 1+ and older. Young-of-the-year are produced in situ by spawning adults, presumably according to the site's suitability for rearing young. Each age-class of a species independently selects its summer habitat and should thus be considered independently of other age-classes. Treating age-classes separately also at least partially accommodates the strongly size-structured nature of fish ecology (e.g., ontogenetic diet and habitat shifts, predator–prey size ratios, etc.; Mittelbach and Persson 1998). Best-fit lines were calculated for the positively and negatively sloped portions of the upper bound by OLS regression. Maximum energy use per size-class was calculated by multiplying these upper-bound densities by individual total metabolism, using an allometric scaling coefficient of 0.81 (Peters 1983).

Normalized biomass spectra were constructed by summing biomass densities of fish (g (w.w.)·m^{-2}) within the same $\log_2$ size-classes as above, regardless of taxon, and plotting $\log_{10}$(sum of biomass in each size-class/range of the size-class) against $\log_{10}$ of the maximum body size in each class (Sprules and Munawar 1986). Best-fit lines were calculated for the positively (<1 g) and negatively (>1 g) sloped portions of each distribution by OLS regression. Total energy use per size-class was calculated as above.

Effect of productivity

We performed two analyses to test for effects of productivity on size distributions. First, we used analysis of covariance (ANCOVA) to compare slopes between sewage-enriched and reference size distributions. Where slopes were similar, ANCOVA could also be used to compare intercepts. Mean NBS and upper bound lines were constructed by taking the mean value within each size-class, among either reference or sewage sites. This analysis tested for a categorical effect of sewage enrichment on the parameters of the size distribution.

Next, we used OLS regression to test for a continuous effect of productivity (among all sites) on the slopes, intercepts, and variance explained (r^2) of upper bound and NBS best-fit lines. Secondary production was estimated for each fish species at each site using the instantaneous growth rate method (Rigler and Downing 1984). Total production of benthic invertebrate primary consumers was then back-calculated from fish production to provide an overall measure of productivity for each site. We assumed conversion efficiencies of 10% for benthivorous fish and 15% for piscivorous fish, reflecting differences in assimilation efficiency (1 – fecal and urinary losses) and growth efficiency (growth/consumption) between trophic levels (Sherwood et al. 2000; Trudel et al. 2001).

Effect of site characteristics

We used principal components analysis (PCA) to examine the relationships among size-classes and between size-classes and site characteristics. Variables included in the PCA were log-transformed total densities in each size-class (log g (ww)·m^{-2}), weed cover (%), current velocity (nominal scale), sediment slope (%), and sewage contribution to the diets of primary consumers (%, deBruyn 2001). Most sites had too many empty size-classes in the interspecific density – body size upper bound, so only total densities (i.e., NBS) could be analyzed by PCA. All variables were standardized to Z scores before PCA, such that each contributes equal variance to the analysis.

Groups of NBS size-classes that covaried strongly were combined into "peaks" (Rasmussen 1993). We hypothesized that the relationships between total peak densities and site characteristics were mediated by food web interactions. We therefore subdivided each peak into three groups of species with similar prey and similar predators ("trophic species"). Most species (primarily Cyprinidae, Centrarchidae, and

© 2002 NRC Canada

Table 1. Log(weight (*W*), mean of all sites, g) and log(density (*D*), per site, g·ha^{-1}) of age-classes of fish in the St. Lawrence River.

			log(*D*) reference sites									log(*D*) sewage-enriched sites		
Species	Age	log(*W*)	0.07	0.20	0.23	0.27	0.30	0.32	0.50	0.70	0.82	0.13	0.28	0.60
Alewife	0+	−1.00	—	—	0.8	—	—	—	—	—	—	1.6	0.7	—
Blacknose shiner	0+	−0.94	—	—	—	—	—	—	1.9	2.0	1.0	—	1.9	—
Pumpkinseed	0+	−0.91	—	—	—	—	—	—	1.4	0.5	1.7	—	0.7	—
Emerald shiner	0+	−0.82	—	1.7	—	—	—	2.8	—	—	2.3	0.8	2.1	1.0
Banded killifish	0+	−0.81	—	—	0.8	—	1.1	—	1.9	2.2	1.6	—	—	—
Golden shiner	0+	−0.74	—	1.1	—	—	—	—	2.1	2.8	2.4	—	—	—
Rock bass	0+	−0.67	1.0	1.6	—	0.9	1.3	2.5	3.0	2.1	2.1	1.4	2.7	2.2
Johnny darter	0+	−0.58	2.2	1.5	1.1	2.7	2.0	1.9	3.3	1.3	1.9	1.8	2.7	3.0
Spottail shiner	0+	−0.50	0.9	2.2	—	3.3	0.5	2.1	2.1	1.4	2.6	1.3	3.2	1.4
Brown bullhead	0+	−0.30	—	—	—	0.6	—	0.7	1.1	1.0	—	1.1	—	3.4
Logperch	0+	−0.19	1.4	—	1.8	3.0	1.8	2.7	1.9	—	2.4	0.9	3.3	2.7
Troutperch	0+	−0.17	1.5	1.6	—	3.7	0.5	1.0	—	0.7	—	2.6	2.2	1.7
Blacknose shiner	1+	−0.08	2.3	—	1.3	1.5	0.5	—	1.9	—	1.5	0.9	2.2	0.7
Emererald shiner	1+	0.11	1.4	2.7	1.8	3.2	1.9	3.7	—	—	—	1.9	3.4	1.6
Suckers[a]	0+	0.16	2.8	2.0	2.1	3.6	3.0	2.3	3.7	2.4	1.6	1.9	3.9	4.3
Smallmouth bass	0+	0.19	—	—	1.1	1.6	1.1	0.7	1.1	0.6	0.7	—	—	1.0
Yellow perch	0+	0.24	—	2.1	—	3.1	0.8	2.7	1.9	1.1	1.5	—	0.7	1.6
Blacknose shiner	2+	0.24	1.9	—	—	1.7	1.6	1.6	1.6	—	—	—	—	—
Largemouth bass	0+	0.31	0.6	0.6	—	1.8	—	—	—	1.6	2.1	—	—	—
Johnny darter	1+	0.33	1.2	1.0	—	—	1.5	1.0	2.4	1.0	1.7	—	1.4	2.0
Alewife	1+	0.34	0.7	—	2.6	0.6	2.3	1.8	2.4	—	—	—	1.9	—
Banded killifish	1+	0.39	—	0.8	—	1.1	2.7	—	—	2.2	1.3	—	—	1.7
Emererald shiner	2+	0.42	—	2.3	2.9	2.5	3.0	3.0	1.1	0.5	1.1	0.8	2.8	—
Walleye	0+	0.53	—	—	—	0.6	—	2.1	—	1.1	—	1.3	1.8	1.7
Golden shiner	1+	0.54	—	2.4	—	1.7	0.8	1.5	2.7	3.0	2.1	—	1.0	—
Spottail shiner	1+	0.69	—	1.8	0.8	2.7	1.4	2.1	2.8	—	—	2.4	—	—
Troutperch	1+	0.72	0.7	—	—	0.6	—	—	—	—	—	—	—	—
Johnny darter	2+	0.75	—	—	—	—	—	—	—	—	—	—	—	0.7
Logperch	1+	0.76	1.7	0.5	0.8	1.3	—	1.4	—	—	1.8	—	1.9	0.7
Banded killifish	2+	0.80	—	1.6	—	—	—	—	—	—	—	—	—	—
Muskellunge	0	0.85	—	—	0.8	—	0.6	—	0.8	0.6	1.2	—	—	1.0
Pumpkinseed	1+	0.89	—	0.8	0.8	1.7	—	2.5	1.3	2.1	2.5	—	—	—
Rock bass	1+	0.95	0.7	0.5	—	1.8	—	1.3	1.7	1.0	1.2	—	—	1.0
Golden shiner	2+	1.19	—	1.0	—	0.9	—	—	—	0.5	—	—	—	—
Northern pike	0	1.28	0.6	—	0.8	—	—	1.3	1.4	0.9	1.9	0.8	—	1.2
Yellow perch	1+	1.39	1.8	1.8	1.5	1.9	2.0	2.6	2.8	2.6	2.7	1.7	1.6	2.4
Largemouth bass	1+	1.42	0.6	—	—	—	—	—	—	—	1.8	—	—	—
Suckers[a]	1+	1.54	—	0.8	1.5	0.6	—	1.8	—	—	—	0.9	—	—
Rock bass	2+	1.56	—	—	—	0.6	—	—	—	—	—	—	—	—
Walleye	1+	1.69	—	—	—	—	—	—	—	—	—	0.8	—	—
Pumpkinseed	2+	1.73	—	—	—	1.4	—	—	—	0.8	1.5	—	—	—
Smallmouth bass	1+	1.75	1.2	—	—	—	—	1.0	—	—	—	—	1.5	—
Yellow perch	2+	1.90	—	1.2	0.8	0.6	0.8	0.7	—	1.4	1.7	—	1.6	1.0
Walleye	2+	2.16	—	—	—	—	—	0.7	—	—	—	1.3	—	—
Northern pike	1	2.93	—	—	—	—	—	—	0.8	0.6	0.7	—	1.1	1.4
Muskellunge	1	2.97	—	—	—	—	—	—	—	—	0.7	—	—	—
Silver redhorse	2	3.00	—	—	—	—	—	1.4	—	—	—	—	—	—
Smallmouth bass	2+	3.11	—	—	—	—	—	—	—	—	—	0.8	1.1	0.7
White sucker	2+	3.14	—	—	1.1	—	—	—	—	0.5	—	2.0	1.5	0.7

Note: Sites are ranked according to the fraction of site area covered by submerged vegetation (value given at head of each column). For species names, see Results section.

[a]0+ and 1+ suckers (white sucker and silver redhorse) could not always be discriminated to species in the field.

Percidae) were considered generalist benthivores, feeding on sediment- and macrophyte-dwelling invertebrates. These species are vulnerable to predation by piscivorous fish (primarily Esocidae). Suckers (Catastomidae) were considered separately, as these fishes have mouthparts specialized to feeding only on sediment and sediment-dwelling organisms. Additionally, suckers reach large sizes and tend to avoid macrophyte beds; they are therefore less vulnerable than

© 2002 NRC Canada

Table 2. Summary statistics for the normalized biomass spectrum (NBS) and the negative upper-bound slope of the interspecific density – body size relationship for littoral fish communities at reference and sewage-enriched sites in the St. Lawrence River.

Parameter	Reference (n = 9)		Sewage-enriched (n = 3)	
NBS				
slope	–0.88 ± 0.22	(–1.25 to –0.52)	–0.55 ± 0.24	(–0.70 to –0.27)
intercept	2.28 ± 0.52	(1.57 to 3.13)	1.82 ± 0.58	(1.14 to 2.17)
r^2	0.84 ± 0.05	(0.77 to 0.93)	0.60 ± 0.19	(0.38 to 0.73)
Upper bound				
slope	–0.80 ± 0.29	(–1.15 to –0.28)	–0.41 ± 0.31	(–0.63 to –0.06)
intercept	1.83 ± 0.45	(1.06 to 2.38)	1.45 ± 0.67	(0.71 to 2.01)
r^2	0.53 ± 0.17	(0.23 to 0.74)	0.26 ± 0.28	(0.01 to 0.56)

Note: Values are mean ± standard deviation (range).

other benthivorous species to the piscivores in these habitats. We then performed a PCA of total peak density (3 peaks × 3 trophic species) and site characteristics.

Results

A total of 19 404 fish were captured, >95% of which were age 0+ to 1+ (Table 1). Generalist benthivores included johnny darter (*Etheostoma nigrum*), logperch (*Percina caprodes*), pumpkinseed (*Lepomis gibbosus*), rock bass (*Ambloplites rupestris*), troutperch (*Percopsis omiscomaycus*), banded killifish (*Fundulus diaphanus*), yellow perch (*Perca flavescens*), smallmouth bass (*Micropterus dolomieui*), largemouth bass (*Micropterus salmoides*), spottail shiner (*Notropis hudsonius*), emerald shiner (*Notropis atherinoides*), golden shiner (*Notemigonus crysoleucas*), blacknose shiner (*Notropis heterolepis*), alewife (*Alosa pseudoharengus*) and brown bullhead (*Ictalurus nebulosus*). Suckers were white sucker (*Catastomus commersoni*) and silver redhorse (*Moxostoma anisurum*). Piscivores were northern pike (*Esox lucius*), muskellunge (*Esox masquinongy*), and walleye (*Stizostedeon vitreum vitreum*).

The interspecific density – body size relationship was approximately triangular, with a peak near 1 g (Fig. 2*a*). ANCOVA revealed a significant effect of sewage enrichment on the negative (>1 g) upper-bound slope of this relationship ($F_{[1,20]}$ = 4.94; p = 0.037; Fig. 3*a*) and could not, therefore, test for an effect on the intercept. The more productive sewage-enriched sites had a relative predominance of larger individuals (Fig. 3*a*) and this resulted in a shallower negative upper-bound slope for sewage-enriched sites than for reference sites (Table 2; Fig. 4). OLS regression also detected a continuous effect of productivity on the negative upper-bound slope ($F_{[1,10]}$ = 7.36; p = 0.022), but this was weak (r^2 = 0.42; Fig. 4). ANCOVA could detect no effect of sewage enrichment on the slope ($F_{[1,2]}$ = 5.81; p = 0.073) or intercept ($F_{[1,2]}$ = 3.40; p = 0.14) of the positively sloped portion of the upper bound. Maximum population energy use at reference sites (Fig. 3*b*) increased slightly up to 1 g but remained approximately constant thereafter (slope not significantly different from zero; b = –0.13; $t_{[1,11]}$ = 1.22; p = 0.28). At sewage-enriched sites, maximum population energy use continued to increase above 1 g (b = 0.42; $t_{[1,11]}$ = 4.56; p = 0.00081).

Total density of organisms per size-class (the NBS) showed a peaked shape similar to that observed for maximum (upper-bound) density, increasing up to 1 g and declining at higher body sizes. The negative portion of the size spectrum at reference sites had a mean slope near –1 and was reasonably well described by linear regression (Table 2; Fig. 3*c*). Spectra from sewage-enriched sites were more strongly trimodal and were not well described by linear regression (Table 2; Fig. 3*c*). Mean r^2 for the negative slope of the NBS was significantly lower at sewage-enriched sites than at reference sites ($t_{[1,10]}$ = 3.88; p = 0.003).

Fig. 2. Size structure of the St. Lawrence River littoral fish community at reference (open circles) and sewage-enriched (solid circles) sites. (*a*) Density vs. body size among species year-classes (see text for details); (*b*) total biomass of all individuals in $\log_2$ size-classes.

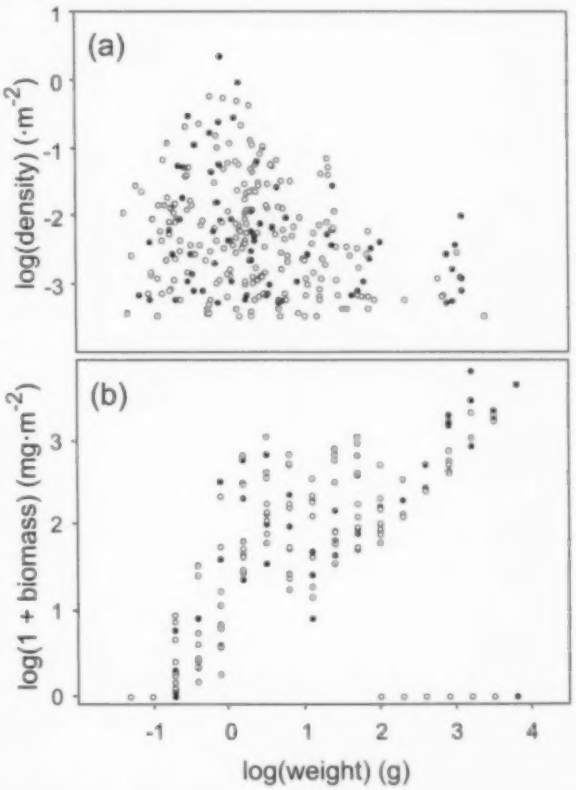

© 2002 NRC Canada

Fig. 3. Size dependence of (*a*) maximum density, (*b*) maximum energy use, (*c*) total density, and (*d*) total energy use of size-classes in the St. Lawrence River littoral fish community. Points are mean values per size-class for reference (open circles) and sewage-enriched sites (solid circles).

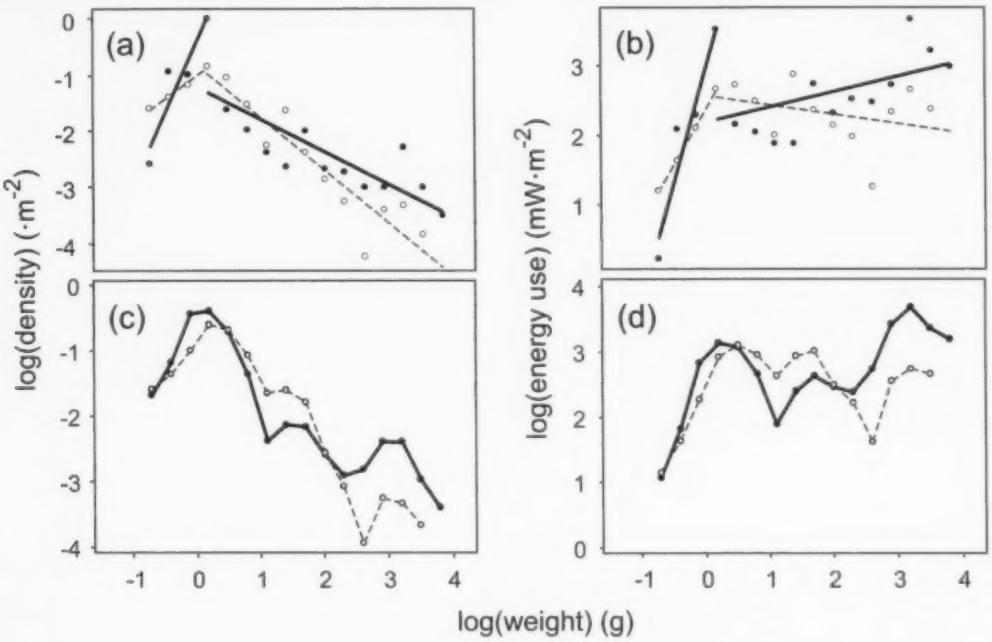

Table 3. Principal component loading scores for densities of fish in $\log_2$ size-classes and characteristics of the littoral habitat among sites in the St. Lawrence River.

	Component (variance explained)		
Variable	I (20.1%)	II (17.8%)	III (16.4%)
Weed cover	—	—	0.80
Sediment slope	—	—	—
Current	—	—	—
Sewage enrichment	—	0.83	—
Size-class, g (w.w.)			
<0.1	—	—	—
0.1–0.2	—	—	—
0.2–0.4	0.78	—	—
0.4–0.8	0.84	—	—
0.8–1.6	0.88	—	—
1.6–3.2	0.76	—	—
3.2–6.4	0.74	—	—
6.4–12.8	0.56	—	—
12.8–25.6	—	—	0.75
25.6–51.2	—	—	0.81
51.2–102.4	—	—	0.51
102.4–204.8	—	—	0.71
204.8–409.6	—	0.53	—
409.6–819.2	—	0.76	—
819.2–1638.4	—	0.88	—
1638.4–3276.8	—	0.61	—
3276.8–6553.6	—	0.50	—

Note: Only scores >0.5 are shown. w.w., weight weight.

ANCOVA revealed a significant effect of sewage enrichment on the negative slope of the NBS ($F_{[1,20]} = 6.17$; $p = 0.021$; Fig. 3*c*). The negative slope was shallower for the combined sewage-enriched sites than for combined reference sites (Table 2). OLS regression could detect no continuous effect of productivity on the NBS slope, although we did observe a weak trend toward a shallower NBS slope at more productive sites ($r^2 = 0.20$; $F_{[1,10]} = 2.43$; $p = 0.15$; Fig. 4). This trend was driven by the three sewage-enriched sites, which had shallower slopes on average than the reference sites (two-sample $t_{[1,10]} = 2.20$; $p = 0.05$). ANCOVA could detect no effect of sewage enrichment on the slope ($F_{[1,2]} = 0.001$; $p = 0.92$) or intercept ($F_{[1,2]} = 0.91$; $p = 0.13$) of the positively sloped portion of the NBS. Total size-class energy use (Fig. 3*d*) at reference sites increased slightly up to 1 g, but remained approximately constant thereafter ($b = -0.18$; slope not significantly different from zero; $t_{[1,11]} = 1.87$; $p = 0.88$). At sewage-enriched sites, maximum population energy use continued to increase above 1 g ($b = 0.28$; $t_{[1,11]} = 2.47$; $p = 0.031$).

PCA of size-classes and site characteristics identified three orthogonal components, which together expressed 54.3% of the total variance (Table 3). Each component expressed covariance in several adjacent $\log_2$ size-classes, corresponding to the peaks apparent in Fig. 3: the "small" peak comprised fish 0.2–12.8 g, the "middle" peak 12.8–205.2 g, and the "large" peak 205.2–6553.6 g. All 12 sites had biomass peaks in the lower and middle parts of the spectrum. The six most productive reference sites and all three sewage-enriched sites also had a third peak in the upper part of the size range. PCA of trophic species' densities in each peak

© 2002 NRC Canada

Fig. 4. Effect of site productivity on parameters of the normalized biomass spectrum (left panels) and the interspecific density – body size relationship (right panels) for the St. Lawrence River littoral fish community at reference (open circles) and sewage-enriched sites (solid circles).

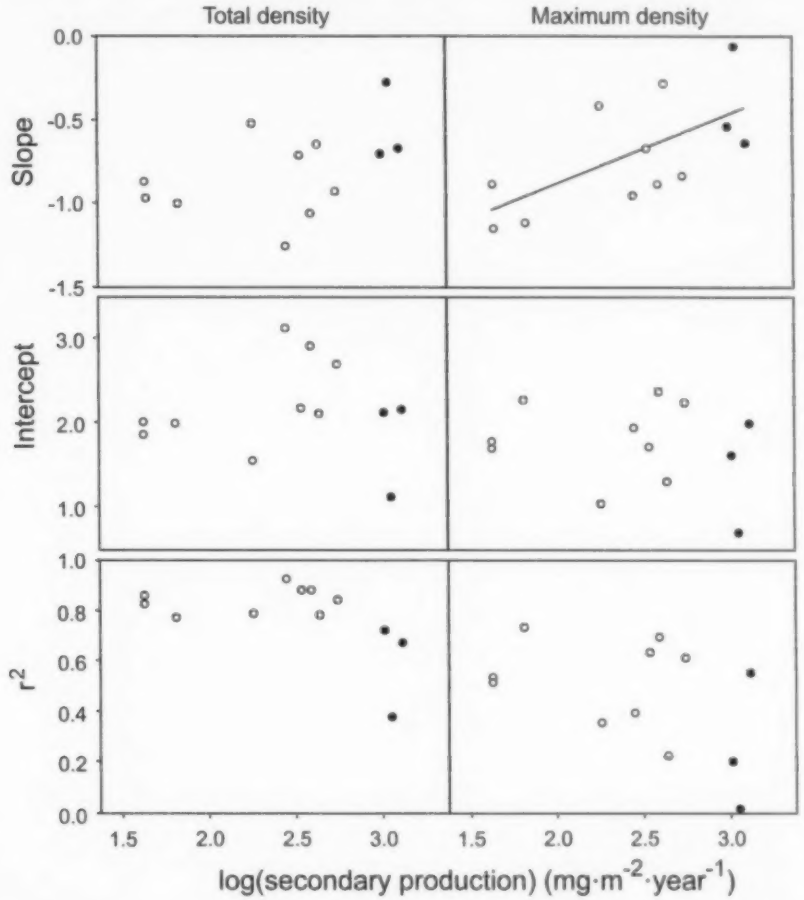

and site characteristics identified four components, expressing 72.7% of total variance (Table 4).

Discussion

Productivity and maximum density

It is generally recognized that the basal energy flux (productivity) of a habitat sets the upper bound of potential energy usage and thus the maximum possible density of species at a given body size (e.g., Maurer and Brown 1988; Cyr et al. 1997), but the effect of basal productivity on the interspecific density – body size relationship has rarely been directly tested. Leaper and Raffaelli (1999) reported that the upper bound of the density – body size relationship was insensitive to gross changes in productivity for a well-documented estuarine food web. Our results for the littoral fish community of the St. Lawrence River, on the other hand, showed that more productive (especially sewage-enriched) sites had a relative predominance of larger individuals. Despite our limited sample size and consequently low statistical power, we observed consistently shallower negative upper-bound slopes at sewage-enriched sites than at reference sites.

The mean negative upper-bound slope for all reference sites combined was comparable to those reported in the literature (Blackburn and Lawton 1994) and consistent with an approximately constant maximum population energy use across size-classes. Sewage enrichment did not increase the mean value of this maximum energy use, but the slope of the upper bound was significantly steeper, indicating a relatively higher maximum energy use for large species and a relatively lower maximum energy use for medium-sized species. This is in direct contradiction to the energetic equivalence rule (Damuth 1987). Universal energetic constraints are supported at large spatial and temporal scales, but our data suggest that other factors may be more important at a local scale.

Productivity and total density

Productivity has been directly addressed more often in studies of the interspecific upper-bound NBS. These studies typically report that more productive systems exhibit a shallower NBS slope (e.g., Sprules and Munawar 1986; Ahrens

© 2002 NRC Canada

Table 4. Principal component loading scores for densities of fish in three peaks of the normalized biomass spectrum and characteristics of the littoral habitat among sites in the St. Lawrence River.

	Component (variance explained)			
Variable	I (24.0%)	II (18.5%)	III (15.0%)	IV (15.8%)
Weed cover	—	0.89	—	—
Slope	—	0.84	—	—
Current	—	—	0.69	–0.51
Sewage enrichment	0.90	—	—	—
Secondary production	0.76	0.36	—	—
Small				
Benthivores	—	—	—	0.91
Suckers	—	—	—	0.53
Piscivores	0.56	—	—	—
Middle				
Benthivores	—	0.60	—	0.61
Suckers	—	–0.67	—	0.44
Piscivores	—	—	0.80	—
Large				
Benthivores	0.80	—	—	—
Suckers	0.82	—	—	—
Piscivores	0.42	0.79	—	—

Note: Only scores >0.5 are shown, with a few exceptions (see text for details).

and Peters 1991; Bourassa and Morin 1995), although some authors have reported no trend (Morin and Nadon 1991) or the opposite trend (Rasmussen 1993; Cyr et al. 1997). In at least two of these studies, the shallower slope resulted from an increase in density of larger size fractions (Sprules and Munawar 1986; Bourassa and Morin 1995). We found similar trends for the NBS of the St. Lawrence littoral fish community. The more productive sewage-enriched sites had a relative predominance of larger individuals and this resulted in shallower NBS slopes than at reference sites.

The poor linear fit of the NBS at sewage-enriched sites reflected an uneven distribution of biomass across the size spectrum. Nonlinear size spectra are commonly observed in aquatic systems and it has been suggested that the NBS is in fact composed of several to many small unimodal distributions (Ahrens and Peters 1991; Sprules and Goyke 1994). These component modes vary independently, respond to different environmental characteristics, and may represent major functional groups of organisms (Strayer 1991; Rasmussen 1993). As in previous studies, much of the variation in these modes among our study sites was correlated with variation in site characteristics.

Other influences on body size distributions

PCA of trophic species' densities in each peak and site characteristics suggested possible mechanisms behind these relationships, although it is important to note that this technique reveals correlations only; we can only speculate about causal relationships. Only the largest size-classes (the large peak) increased with sewage enrichment. We found better correlations of most small and medium-sized fish with site characteristics than with productivity. Small and medium nonpiscivores were primarily associated with low current, irrespective of the level of weed cover or sewage enrichment. Medium benthivores and suckers also covaried with weed cover, but in opposite directions: benthivore densities were highest at weedy sites, whereas suckers were associated with relatively bare sites. The proportion of the variance in weed cover captured by the PCA was large (component loading score 0.89) but only weakly correlated with productivity (component loading score 0.36). Therefore, the influence of weed cover on fish densities seemed to be as a physical structure of the habitat.

In addition, we observed an interaction between site characteristics and productivity. The response of the large peak to sewage enrichment depended qualitatively on weed cover: at low weed cover, the large peak comprised predominantly suckers, whereas at high weed cover it was predominantly piscivores. This may be because the most abundant piscivores in this system are esocid fishes (pikes), which are ambush predators typically associated with macrophyte beds and woody debris. Relatively bare sites provide poor habitat for this type of predator, irrespective of the density of prey fish.

The pattern of species' responses to sewage enrichment in the St. Lawrence supports the hypothesis that the NBS reflects a size-structured food web (Sprules 1988; Borgmann 1987). Large benthivores had higher densities at enriched sites at all levels of weed cover, revealing a higher rate of production of benthic invertebrate prey. Despite this, densities of medium and small benthivores did not respond to sewage enrichment. Overall, the middle peak was smaller at sewage-enriched sites, as predicted by models of consumer control. Higher densities of large piscivores at sewage-enriched sites support the hypothesis that exploitation (top-down control) is a more important determinant of benthivore densities than resource abundance. This hypothesis is consistent with recent work on the effects of enrichment on food webs with heterogeneous trophic levels: vulnerable prey are strongly controlled by exploitation, whereas protected prey are free to respond to an increase in resources (e.g., Leibold 1989; Persson et al. 2001). In aquatic systems, vulnerability

© 2002 NRC Canada

is largely a matter of predator–prey size ratios (Mittelbach and Persson 1998).

Reconciling the two approaches

The interspecific upper bound and the NBS address the relationship between density and body size in fundamentally different ways. These approaches converge when there is only one species per size-class, and one size-class per species. However, real assemblages always contain more species than size-classes, and richness is usually highest at intermediate body sizes (Hutchinson and MacArthur 1959; Maurer and Brown 1988). This sort of assemblage produces a relatively dense cluster of points in the center of an interspecific relationship, and a peak in the NBS. It is therefore inappropriate to directly compare interspecific slopes and NBS slopes (but see Griffiths 1992; Cyr et al. 1997). The two approaches may only be reconciled with careful attention to the types of hypotheses that may be addressed with each.

The form of the interspecific density – body size relationship is usually attributed to ecological constraints acting over evolutionary time. By treating each species as an independent datum, this approach implicitly assumes that each species is responding to a common, external driver in a size-dependent way. It has been suggested that this driver is energetic, and that it may be manifested through competition with other members of the community (Damuth 1987; Blackburn et al. 1994), but the underlying constraint is still external to the biota. Thus, the slope of this relationship, or at least the slope of its upper bound, should be invariant. At a coarse scale, this view is supported in the St. Lawrence. The mean upper-bound slope for all sites combined (reference and sewage enriched) is –0.82 (standard error, SE = 0.098; $r^2 = 0.87$; $F_{[1,11]} = 71$; $p = 0.0000039$), statistically indistinguishable from that predicted by the energetic equivalence rule. At a local scale, however, there is considerable variation in the upper-bound slope. The trend toward shallower slopes at more productive sites, in particular, indicates that the energetic equivalence rule may not be supported at all scales.

Interestingly, our results parallel those of a large-scale survey of birds in Britain. Blackburn et al. (1994) found that the slope of the upper bound of the density – body size relationship was shallower for breeding birds than for wintering birds in Britain, and attributed this to immigration of large, abundant species such as waterfowl and waders. Because migration is usually motivated by feeding opportunities, this could be interpreted as an effect of greater productivity in summer than winter. We found a similar increase in large-bodied fish species at enriched sites in the St. Lawrence River. This resulted in a shallower negative upper-bound slope for sewage-enriched sites combined than for reference sites combined. Our results also parallel those for British birds in the underlying mechanism: in both cases, the shallower slope resulted from larger individuals moving into highly productive patches in space (our results) or time (Blackburn et al. 1994).

The NBS, on the other hand, considers the size spectrum to represent a functionally integrated community. Whereas the area under the NBS (total community biomass) may be energetically constrained, the shape of the NBS is taken to reflect ecological processes that govern the transfer of energy among trophic groups (Sprules 1988; Borgmann 1987). Our results support a growing body of evidence against a simple linear relationship between total density and body size (e.g., Sprules and Munawar 1986; Ahrens and Peters 1991; Rasmussen 1993). Modality in the NBS was pronounced, and the response of the NBS to varying productivity was not well reflected by a linear best fit. However, we were able to explain much of the variance in the shape of the NBS with a very simplified consideration of habitat requirements and feeding relationships.

Thus, these two approaches offer complementary information on the ecological implications of body size. The interspecific density – body size relationship speaks to processes governing the size structure of assemblages on large spatial and temporal scales, whereas the NBS seems to reflect local processes acting on short time scales. We suggest that there is a hierarchy of explanations for the density – body size relationship: our data support previous evidence for universal energetic constraints on the size structure of regional assemblages, but they also highlight the importance of factors that influence the local abundance of various components of the size spectrum. We hope that these observations will help to reconcile these two largely independent approaches and to better integrate both with other aspects of ecology.

Acknowledgements

We thank Kelly W. Armstrong, Veronique Bussiers, Levi Cammack, Suresh Job, Kristin Lunn, Andrea MacLeod, Keith Martin-Smith, Kevin McCann, Jessica Meeuwig, Liz Moseman, Amy Nelson, Graham Peers, Ciara Raudsepp-Hearne, and Neil Rooney for help with fieldwork. Thanks also to Christiane Hudon, Francois Gagne, James Umbenhower, and Jen Kövecses for discussions, advice, and logistical support. Financial support was provided by Fonds pour la Formation de Chercheurs et l'Aide à la Recherche (FCAR) to the Groupe de recherche interuniversitaire en limnologie et en environnement aquatique (GRIL), a Natural Sciences and Engineering Research Council of Canada (NSERC) operating grant to J.B. Rasmussen, and a Vineberg Family Fellowship to A.M.H. deBruyn.

References

Ahrens, M.A., and Peters, R.H. 1991. Patterns and limitations in limnoplankton size spectra. Can. J. Fish. Aquat. Sci. **48**: 1967–1978.

Blackburn, T.M., and Lawton, J.H. 1994. Population abundance and body-size in animal assemblages. Philos. Trans. R. Soc. Lond. B, Biol. Sci. **343**: 33–39.

Blackburn, T.M., Lawton, J.H., and Perry, J.N. 1992. A method of estimating the slope of upper bounds of plots of body size and abundance in natural animal assemblages. Oikos, **65**: 107–112.

Blackburn, T.M., Gates, S., Lawton, J.H., and Greenwood, J.J.D. 1994. Relations between body size, abundance, and taxonomy of birds wintering in Britain and Ireland. Philos. Trans. R. Soc. Lond. B, Biol. Sci. **343**: 135–144.

Blumenshine, S.C., Lodge, D.M., and Hodgson, J.R. 2000. Gradient of fish predation alters body size distributions of lake benthos. Ecology, **81**: 374–386

© 2002 NRC Canada

Borgmann, U. 1987. Models on the slope of, and biomass flow up, the biomass size spectrum. Can. J. Fish. Aquat. Sci. **44**(Suppl. 2): 136–140.

Bourassa, N., and Morin, A. 1995. Relationships between size structure of invertebrate assemblages and trophy and substrate composition in streams. J. N. Am. Benthol. Soc. **14**: 393–403.

Brown, J.H., Marquet, P.A., and Taper, M.L. 1993. Evolution of body size: consequences of an energetic difinition of fitness. Am. Nat. **142**: 573–584.

Carpenter, S.R., Kitchell, J.F., Cottingham, K.L., Schindler, D.E., Christensen, D.L., Post, D.M., and Voichick, N. 1996. Chlorophyll variability, nutrient input, and grazing: evidence from whole-lake experiments. Ecology, **77**: 725–735.

Cyr, H., Peters, R.H., and Downing, J.A. 1997. Population density and community size structure: comparison of aquatic and terrestrial systems. Oikos, **80**: 139–149.

Damuth, J. 1987. Interspecific allometry of population density in mammals and other animals: the independence of body mass and population energy-use. Biol. J. Linn. Soc. **31**: 193–246.

deBruyn, A.M.H. 2001. Sewage and the ecology of the St. Lawrence River. Ph.D. thesis, McGill University, 1205 Dr. Penfield Ave., Montreal, Que.

deBruyn, A.M.H., and Rasmussen, J.B. 2002. Quantifying assimilation of sewage organic matter by riverine benthos. Ecol. Appl. **12**: 511–520.

Griffiths, D. 1992. Size, abundance and energy use in communities. J. Anim. Ecol. **61**: 307–315.

Hudon, C., and Sylvestre, A. 1998. Qualité de l'eau en aval de l'archipel de Montréal—1994–1996. Scientific Report ST-170 of Environment Canada—Quebec Region, Environmental Conservation, St. Lawrence Center, 105 McGill Ave., Montreal, Que.

Hutchinson, G.E., and MacArthur, R.H. 1959. A theoretical ecological model of size distributions among species of animals. Am. Nat. **93**: 145–159.

Katz, M., and Howard, W.C. 1955. The length and growth of 0-year class creek chubs in relation to domestic pollution. Trans. Am. Fish. Soc. **84**: 228–238.

King, D.L., and Ball, R.C. 1967. Comparative energetics of a polluted stream. Limnol. Oceanogr. **12**: 27–33.

Lawton, J.H. 1989. What is the relationship between population density and body size in animals? Oikos, **55**: 429–434.

Leaper, R., and Raffaelli, D. 1999. Defining the abundance body-size constraint space: data from a real food web. Ecol. Lett. **2**: 191–199.

Leibold, M.A. 1989. Resource edibility and the effects of predators and productivity on the outcome of trophic interactions. Am. Nat. **134**: 922–949.

Marquet, P.A., Navarrete, S.A., and Castilla, J.C. 1995. Body size, population density and the energetic equivalence rule. J. Anim. Ecol. **64**: 325–332.

Maurer, B.A., and Brown, J.H. 1988. Distribution of energy use and biomass among species of North American terrestrial birds. Ecology, **69**: 1923–1932.

Mittelbach, G.G., and Persson, L. 1998. The ontogeny of piscivory and its ecological consequences. Can. J. Fish. Aquat. Sci. **55**: 1454–1465.

Morin, A., and Nadon, D. 1991. Size distribution of epilithic lotic invertebrates and implications for community metabolism. J. N. Am. Benthol. Soc. **10**: 300–308.

Oksanen, L., Fretwell, S.D., Arruda, J., and Niemela, P. 1981. Exploitation ecosystems in gradients of primary productivity. Am. Nat. **118**: 240–261.

Persson, A., Hansson, L.-A., Brönmark, C., Lundberg, P., Pettersson, L.B., Greenberg, L., Nilsson, P.A., Nyström, P., Romare, P., and Tranvik, L. 2001. Effects of enrichment on simple aquatic food webs. Am. Nat. **157**: 654–669.

Peters, R.H. 1983. The ecological implications of body size. Cambridge University Press, Cambridge, U.K.

Power, M.E. 1992. Top-down and bottom-up forces in food webs: do plants have primacy? Ecology, **73**: 733–746.

Purenne, P. 1998. Annual Report 1997. Process Engineering Division, MUC Wastewater Treatment Plant, 12001 Maurice Duplessis, Montreal, Que.

Rasmussen, J.B. 1993. Patterns in the size structure of littoral zone macroinvertebrate communities. Can. J. Fish. Aquat. Sci. **50**: 2192–2204.

Rigler, F.H., and Downing, J.A. 1984. The calculation of secondary productivity. *In* A manual on methods for the assessment of secondary productivity in fresh waters. *Edited by* J.A. Downing and F.H. Rigler. Blackwell Scientific, Oxford, U.K. pp. 19–58.

Sherwood G.D., Rasmussen, J.B., Rowan, D.J., Brodeur, J., and Hontela, A. 2000. Bioenergetic costs of heavy metal exposure in yellow perch (*Perca flavescens*): in situ estimates with a radiotracer (^{137}Cs) technique. Can. J. Fish. Aquat. Sci. **57**: 441–450.

Sprules, W.G. 1988. Effects of trophic interactions on the shape of pelagic size spectra. Verh. Internat. Verein. Limnol. **23**: 234–240.

Sprules, W.G., and Goyke, A.P. 1994. Size-based structure and production in the pelagia of lakes Ontario and Michigan. Can. J. Fish. Aquat. Sci. **51**: 2603–2611.

Sprules, W.G., and Munawar, M. 1986. Plankton size spectra in relation to ecosystem productivity, size, and perturbation. Can. J. Fish. Aquat. Sci. **43**: 1789–1794.

Strayer, D.L. 1991. Perspectives on the size structure of lacustrine zoobenthos, its causes, and its consequences. J. N. Am. Benthol. Soc. **10**: 210–221.

Trudel, M., Tremblay, A., Schetagne, R., and Rasmussen, J.B. 2001. Why are dwarf fish so small? An energetic analysis of polymorphism in lake whitefish (*Coregonus clupeaformis*). Can. J. Fish. Aquat. Sci. **58**: 394–405.

Verrette, J.L. 1990. Délimitation des principales masses d'eau du St-Laurent (Beauharnois à Quebec). Les Consultants Hydriques for Environment Canada, Conservation and Protection, Quebec Region, St. Lawrence Centre, Montreal, Que.

© 2002 NRC Canada

Influence of trends in fishing power on bioeconomics in the North Sea flatfish fishery regulated by catches or by effort quotas

Clara Ulrich, Sean Pascoe, Per J. Sparre, Jan-Willem De Wilde, and Paul Marchal

Abstract: Total allowable effort quotas (TAEs) are often considered as promising alternatives to single-species total allowable catch quotas (TACs) in fisheries management. However, implementing TAEs would primarily require converting nominal effort into fishing mortality rate, i.e., developing a relevant model of the dynamics of catchability. Assuming that trends in the catchability may occur through fishing-power creeping linked to increased capital invested and technology, we compare, by stochastic and dynamic simulation modelling, the relative biological and economic benefits and drawbacks of TAEs and TACs in the North Sea sole (*Solea solea* L.) and plaice (*Pleuronectes platessa* L.) fishery. Management targets are based on the Precautionary Approach and Harvest Control Rules developed by the International Council for the Exploration of the Sea (ICES). Fishermen are assumed to set their effort at the most (TAE) or least (TAC) conservative level. Overall, the outcomes are more sensitive to the catchability model when implementing TAEs, especially in the medium and long term, but the variability in catchability has a much greater impact on stock levels than on the fisheries profit.

Résumé : Les quotas d'effort par unité de pêche (TAEs) sont souvent considérés comme une alternative prometteuse aux quotas de captures par espèce (TACs) traditionnellement employés en gestion des pêches. Mais la mise en place de TAEs requiert au préalable de pouvoir convertir l'effort nominal en taux de mortalité par pêche, c'est-à-dire de développer un modèle mathématique adéquat de la dynamique de la capturabilité. On suppose ici que la capturabilité croît du fait de la dérive des puissances de pêche, issue d'un accroissement régulier de l'investissement et de la technologie. On compare alors, par un modèle de simulation stochastique et dynamique, les avantages et inconvénients relatifs des TACs et TAEs, d'un point de vue à la fois biologique et économique. Le modèle est appliqué à la pêcherie de sole (*Solea solea* L.) et de plie (*Pleuronectes platessa* L.) en Mer du Nord. Les objectifs de gestion sont calqués sur l'Approche de précaution et les Règles de captures du Conseil International pour l'Exploration de la Mer (CIEM). Les pêcheurs sont supposés fixer leur activité au niveau le plus (TAE) ou le moins (TAC) conservatif. Globalement, les résultats sont plus sensibles au modèle de capturabilité dans le cas des quotas d'effort, surtout à moyen et long terme. Mais la variabilité de la capturabilité a plus d'impact sur le niveau des stocks que sur la rentabilité de la pêcherie.

Introduction

The management of the fisheries in the European Union (EU) is currently based on the use of a combination of tools, foremost of which are technical measures (minimum landing size, mesh size, fisheries area, or season closure) and the use of single-species total allowable catch (TAC). There have been criticisms on the implementation of such TACs as a tool to achieve fisheries management objectives (Holden 1994). First, the use of TACs represents a way to control the outputs (yield) of a fishery but does not allow direct regulation of the level of input (e.g., fishing effort). A reduction in TAC without an equivalent reduction in inputs results in an imbalance between the harvesting capacity of the fleet and the available catch. Apart from the economic inefficiencies this imposes, the excess capacity of the fleet may act as an incentive to misreport catches, thereby exceeding the TAC. Second, TACs are usually calculated on a single-species basis and ignore the presence of technical interactions that occur when several species are caught by the same fleet. Fishing for one species may then lead to discards of another species with exceeded quota. Moreover, as TACs are set on the basis of multiple management objectives, they may not correspond to those recommended by scientists and thereby not achieve their conservation objectives (Holden 1994).

Received 25 July 2001. Accepted 28 March 2002. Published on the NRC Research Press Web site at http://cjfas.nrc.ca on 14 June 2002.
J16463

C. Ulrich,[1] **P.J. Sparre, and P. Marchal.**[2] Danish Institute of Fisheries Research (DIFRES), Charlottenlund Castle, 2920 Charlottenlund, Denmark.
S. Pascoe. CEMARE, University of Portsmouth, Locksway Road, Southsea PO4 8JF, U.K.
J.-W. De Wilde. LEI-DLO, P.O. Box 29703, 2502 LS, The Hague, The Netherlands.

[1]Corresponding author (e-mail: clu@dfu.min.dk).
[2]Present address: IFREMER, 150 quai Gambetta, BP 699, 62321 Boulogne-sur-mer, France.

 DOI: 10.1139/F02-057 © 2002 NRC Canada

The main alternative to TAC is to limit the total allowable fishing effort (TAE). This could be achieved by controlling the level of physical inputs used in fishing (e.g., boat numbers, engine power, etc.) and the number of days at sea. Although not always easier to control and enforce than TACs, the use of TAE as a management measure is believed to confer two main advantages. First, TAEs should not induce overquota discards. Second, although no model has yet accurately quantified the effective pressure exerted on fish stocks by fishing fleets, it is obvious that the smaller the number and size of the vessels, the smaller the pressure exerted on the harvested stocks. Ultimately, if a vessel does not exist, it cannot catch any fish. The application of TAEs, however, may also be subject to several drawbacks. First, if TAEs are to be implemented by means of a limitation of days at sea, then the fixed costs of the fleet will not decrease and only variable costs such as fuel are reduced (provided that input prices do not increase at the same time). As a result, the fishing activity may become economically inefficient (Crutchfield 1979; Waters 1991). Second, the control of one input in a fishery may lead to the substitution of uncontrolled inputs (e.g., Townsend 1985; Campbell 1991; Pascoe and Robinson 1998). This may result in the conservation benefits being dissipated and the industry operating at a higher cost than it might otherwise operate if unrestricted. The potential effectiveness of an effort-limitation program depends on the potential for input substitution (Campbell and Lindner 1990), which varies fishery by fishery. Finally, implementing TAEs would primarily require having a mathematical model to convert nominal fishing effort into an equivalent fishing mortality rate, i.e., a model of the catchability dynamics.

These dynamics are commonly disregarded in studies dealing with fisheries management (e.g., Overholtz et al. 1995; Marchal 1997), in theory allowing the management of fishing mortality through direct input control. However, catchability is probably never constant but is prone to complex random and nonrandom variations. In particular, there is increasing evidence that the fishing power of a number of fisheries has increased (Millischer et al. 1999; Marchal et al. 2001*a*). Pascoe et al. (2001) showed that this creep could be related to both physical inputs (such as days fished and boat size) and nonmeasurable inputs (such as skipper skill and level of technology). The nonphysical inputs have been captured through the measurement of technical efficiency. Such changes in technical efficiency change the relationship between physical inputs and output, resulting in a change in the catchability. Both fish stock assessment and fisheries management would benefit from a better understanding of the dynamics of the fishing power (Pope and Shepherd 1985; Holden 1994).

Many theoretical investigations have examined the relative properties of some fisheries management tools. The economic implications of implementing effort quotas have been quantified in Campbell and Lindner (1990) and Overholtz et al. (1995). Other studies have compared, by simulation, the relative properties and, more particularly, the amount of discards generated by fisheries management strategies implemented by different tools of management (Gillis et al. 1995; Vestergaard 1996). During the 1990s, an increased need for evaluating alternative management processes led to the development of improved fishery management systems and procedures (McAllister et al. 1999). A variety of technically and conceptually different modelling approaches have emerged from this research (e.g., Pelletier and Laurec 1992; Marchal 1997; Kell et al. 1999). However, most deal with improving management targets and strategies more than implementation tools, or they ignore catchability dynamics. We are not aware of any of these models evaluating management procedures in relation to trends in fishing power and catchability in a multispecies–multifleet context.

The scope of the present study is to analyze, through the use of a simulation model, different properties of TAEs and TACs with particular focus on the sensitivity of their expected biological and economic benefits given existing trends in catchability as the result of fishing-power creep. The performances of each combination of catchability model and management tool are appraised in relation to biological and economic returns. The above methodology is applied to the flatfish multifleet fishery in the southern North Sea (ICES Statistical Division IVbc).

Materials and methods

Approach adopted and case study

The methodological framework of this study is made up of various stochastic and non-Bayesian modules describing biological dynamics, the harvesting process, catchability dynamics, the economic analysis, the estimation procedure, fisheries management, the implementation of the management tools, and fishing strategies. The model used here is a bioeconomic extension of a multispecies–multifleet dynamic model developed for the biological comparison of quota and effort management scenarios (P. Sparre, unpublished data).

Various nonstandard features are used in the model: (*i*) a trend in fishing power based on economic parameters; (*ii*) the implementation of the Precautionary Approach and Harvest Control Rules (HCR) of the ICES (International Council for the Exploration of the Sea); (*iii*) a predictive model of costs and profits; (*iv*) a simple illustration of fishermen's fishing and discarding behaviour; and (*v*) a two-step approach, where the first step is a deterministic analysis over a known period (1991–1999), and the second, some stochastic predictions over a future period (2000–2009). The biological and harvest models are both length- and age-based. The catchability is prone to both stochastic and deterministic variations. The observational model is used to simulate stock assessments and estimate fishing mortality. The fisheries management model is based on outcomes of the stock assessment and sets short-term fishing mortality targets following the harvest control rules. These targets are spread among fleets depending on their relative fishing mortality rate, considered constant across fleets in the simulations. Finally, the fishing strategy is made simple. When TAEs are implemented, fishermen are assumed to set their effort at the most conservative level, i.e., in order not to fish over the minimum authorized fishing mortality across stocks. Conversely, when TACs are implemented, fishermen are assumed to set their effort in order to reach the maximal TAC across stocks, over-TAC for other stocks being discarded. Simulations are carried out over a *Y*-year management period, assuming annual random fluctuations in recruitment,

© 2002 NRC Canada

Fig. 1. The components of the simulation model: SIM, simulation; FOR, forecast; *N*, population number; *C*, catches; *y*, year index; TAC, total allowable catch quota; *E*, effort; *F*, fishing mortality.

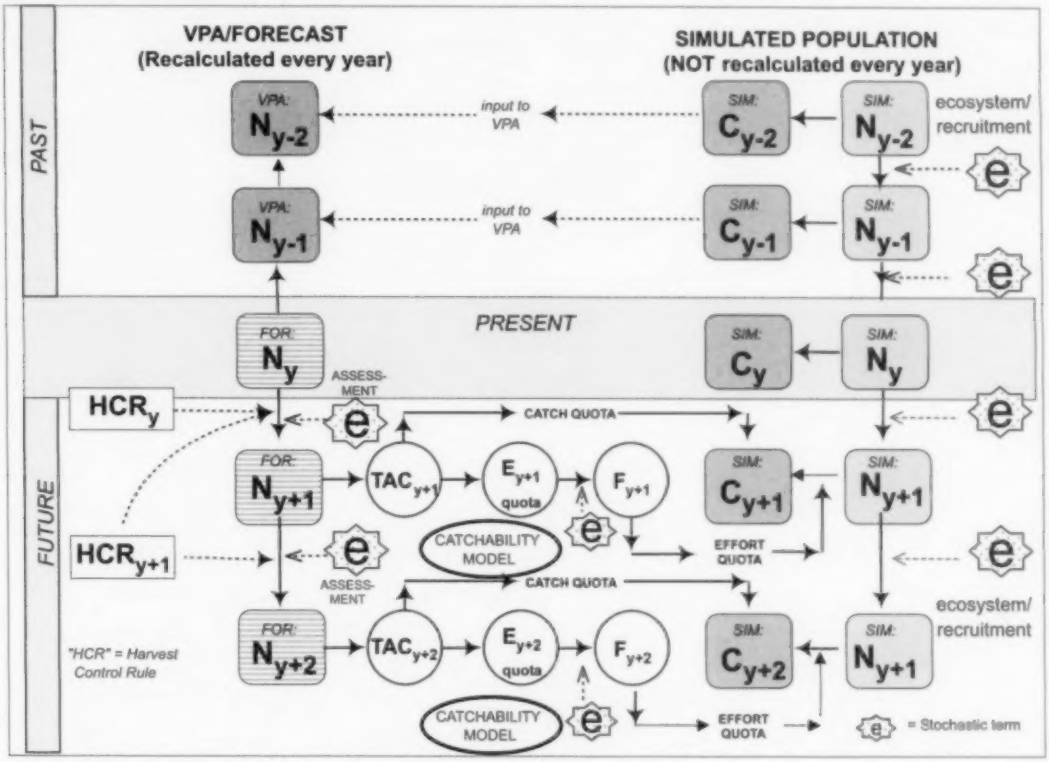

growth, catchability, and market prices and uncertainty in estimated numbers at age. The model is written in Visual Basic Applications under Excel software (see Fig. 1).

This model has been applied to the flatfish (sole (*Solea solea* L.) and plaice (*Pleuronectes platessa* L.)) fishery of the North Sea. This fishery is thought to be an appropriate case study because (*i*) the dynamics of the fishing power has been already widely investigated from both a biological (Marchal et al. 2001*b*) and economic (Pascoe et al. 2001) point of view, (*ii*) many socioeconomic data are available, and (*iii*) assessment data for sole and plaice are available for the single area IV, without aggregation within a larger assessment area (ICES 2000).

By focusing on the relationship between catchability and capital invested, the outcomes from Pascoe et al. (2001) allow some predictions on the future trends in fishing power to be made based on trends in fleet investment behaviour. Conversely, the biological analysis showed that trends in fishing power could be different among fleets and stocks and thus provides valuable information on how to distribute these predicted future trends over stocks. For these reasons, the bioeconomic model, in particular the catchability and cost modules, is fairly case specific, although it was initially built as a generic modelling tool (and can be readily adapted to other fisheries provided appropriate comparable information is available).

Three Dutch beam-trawler fleets (NL_small, <300 HP; NL_medium, 300–2000 HP; and NL_big, > 2000 HP) and one Danish gillnetter fleet have been identified and parameterized. Other fleets have been aggregated in the "Others" category, and only their fishing mortality is provided. However, the specific model of costs and catchability in relation to capital invested could be made available for the three Dutch fleets only. In the absence of more information about the Danish fleet, we assume that cost structure and catchability for this fleet are constant over the simulation period. For this reason, the results are displayed and analyzed only for the Dutch fleets.

Biological, harvest, and operational models

A general length- and age-structured biological model was developed for a multifleet and mixed-species fishery so as to calculate the "true" state of the stocks (Appendix A, eqs. A1 and A2). Biological parameters are estimated from usual length-based growth equations (i.e., Von Bertalanffy growth model, length–weight relationships, logistic curve of maturity at length) with annual fluctuations simulated by normally distributed positive stochastic parameters (Table 1). Given the variability of the recruitment and the growing evidence that for a large majority of worldwide stocks, choosing any of the traditional stock–recruitment models is rather arbitrary (Myers et al. 1990; Power 1996), the recruitment is modelled through a simple Beverton–Holt equation (Appendix A, eq. A3) with lognormal random fluctuations based on the ICES assessment (ICES 2000). The fishing mortality generated by the fleets is related to fishing effort,

© 2002 NRC Canada

Table 1. Biological parameters by stocks.

Type of parameter	Parameter	Sole		Plaice	
		Value	CV	Value	CV
Relative fishing mortality rate by fleet	F_{rel}(NL_small)	0.05		0.02	
	F_{rel}(NL_medium)	0.34		0.25	
	F_{rel}(NL_big)	0.31		0.18	
	F_{rel}(DK_gillnet)	0.05		0.15	
	F_{rel}(Others)	0.25		0.4	
Growth and natural mortality parameters	L_∞	37.4		46.0	
	K	0.31	0.1	0.20	0.1
	t_0	−1		−1.6	
	Condition factor	0.000 004	0.1	0.000 005	0.1
	Condition expon.	3.26		3.20	
	M	0.1		0.1	
Maturity ogive	$L_{50\%}$	26		27	
	$L_{75\%}$	27		29	
Stock–recruitment relationship	BH1	676 643		3 492	
	BH2	7.179	0.8	0.009 9	0.4
Harvest control rules (HCR)	B_{lim}	25 000		210 000	
	B_{pa}	35 000		300 000	
	F_{pa}	0.4		0.3	
	Age F_{bar}	2–8		2–10	
ICES assessment	$\epsilon_{TF\text{-}Year}$(St,y)		0.1		0.1
	$\epsilon_{TF\text{-}Age}$(St,y)		0.1		0.1
	$W_{\epsilon\text{-}Year}$		2		2

Note: NL, Netherlands; DK, Denmark; CV, coefficient of variation (%); expon., exponential condition parameter b in the length–weight relationship $W = aL^b$; ICES, International Council on the Exploration of the Sea.

catchability, and age-specific selection ogives (Appendix A, eq. A4). The random fluctuations of the catchability are simulated by a normally distributed positive stochastic parameter. Selection ogives are calculated from the Von Bertalanffy model and length-based and gear-specific selectivity equations (logistic curve for trawling fleets, lognormal curve for gillnetters). The fishing mortality by fleet is composed of landing mortality and discard mortality arising from the catches of undersized fish (and not included the overquota discards in the case of a TAC-based management simulation; see below). The discard mortality is modelled by the logistic curve (Appendix A, eqs. A5 and A6).

The virtual population analysis (VPA), as implemented by ICES, contains a tuning component by which an index of effort or an index of stock abundance is used to estimate the fishing mortalities in the last data-year. The tuning process is crucial as it produces the estimate of the current stock size, but it is also a problematic step in the stock assessment, which is subject to process error as well as measurement error. For many simulation models, the variability in the estimation of stock abundance is generated by (*i*) adding a truncated normally distributed error term in the "true" stock size (Horwood et al. 1990; Frederick and Peterman 1995; Marchal 1997) or (*ii*) running a VPA assuming error-prone estimation in catch and weight data (Pelletier and Laurec 1992) or natural mortality (Restrepo et al. 1992). Considering the time required to run simulations, the simplest way of generating error in the stock assessment, that is *i*, has therefore been chosen (Appendix A, eq. A7).

Catchability model

In the harvest model, catch is a function of the level of effort (expressed in days fished), stock size, and the catchability coefficient (Appendix A, eq. A8). Assuming that availability varies without trends over time, the relationship between catch and effort will vary if the factors producing the effort also vary. An increase in the average boat size would be assumed to result in an increase in average catch per day. Similarly, improvements in skipper skill or on-board technology (i.e., changes in technical efficiency) will also increase catch per unit of nominal effort. As a result, catchability is not constant over time. A model was derived to allow for changes in catchability, through changes in fishing power, as a function of both average boat characteristics (represented by the level of investment) and trends in technical efficiency. The econometric analyses and associated tests that underpin the catchability model are presented in Pascoe et al. (2001), but the present model has been restricted to slightly fewer parameters.

The direct effect of a change in the average level of investment on the catchability coefficient was derived from the translog production frontier estimated by Pascoe et al. (2001). The key inputs used in the production frontier were the level of capital invested in the vessel (representing the total physical inputs into the fishery such as boat size, engine size, and level of technology used), days fished (representing capital utilization), and a composite stock index. Capital value has been used to represent a composite measure of physical inputs in a number of studies of fisheries

© 2002 NRC Canada

production functions and frontiers (e.g., Squires 1987; Kirkley et al. 1995, 1998). The effect, estimated as elasticity, was dependent also on the number of days fished. The elasticity δ_q represents the percentage change in catchability from a 1% change in capital investment and is evaluated at a given level of investment and days fished. The total impact on catchability is then this elasticity × the percentage change in investment. These two relationships are given by

$$(1)\quad \begin{cases} \delta_q = \alpha_0 + \alpha_{\text{capital}} \ln(\text{INV}(\text{fl}, y)) + \alpha_{\text{days}} \ln(N_{\text{days}}(\text{fl}, y)) \\ q_{\text{fleet}}(\text{fl}, y) = q_{\text{fleet}}(\text{fl}, y-1) \dfrac{\text{INV}(\text{fl}, y) - \text{INV}(\text{fl}, y-1)}{\text{INV}(\text{fl}, y-1)} 100 e^{\delta_q} \end{cases}$$

where α_0, α_{capital}, and α_{days} are fixed coefficients, and $q_{\text{fleet}}(\text{fl},y)$, $\text{INV}(\text{fl},y)$, and $N_{\text{days}}(\text{fl},y)$ represent the catchability by boat (all stocks combined) and year, the mean annual capital invested per boat, and the number of days at sea per boat respectively within a fleet. This accounts for the fact that the fishing units spending the most time beam trawling, preferentially to other gears, are also the most skilled ones and thus the ones with the highest catchability.

Changes in technical efficiency also affect the catchability coefficient. Pascoe et al. (2001) identified several factors that affected technical efficiency and hence catchability. The introduction of bigger boats with larger crews increases the average fishing power of the vessels. The elasticity δ_{crew} of crew change ((d(crew)/d(capital))/(crew/capital)) with respect to change in capital was evaluated at the mean levels and found to be different for all fleets. Decreasing the average vintage (i.e., the age and year of construction) of the boats $\text{VINT}(\text{fl},y)$ also increases the fishing power. Both crew and vintage effects are considered as constant in the model. Combining the two effects, the final equation for change in catchability in the model is

$$(2)\quad \begin{cases} q_{\text{fleet}}(\text{fl}, y) \\ \quad = q_{\text{fleet}}(\text{fl}, y-1) \left[\left(\dfrac{\text{INV}(\text{fl}, y) - \text{INV}(\text{fl}, y-1)}{\text{INV}(\text{fl}, y-1)} 100 e^{\delta_{\text{crew}}} \right) \right. \\ \quad \left. + q_{\text{constant}}(\text{fl}, y) \right] \\ q_{\text{constant}}(\text{fl}, y) \\ \quad = \left(\dfrac{\overline{\text{INV}(\text{fl}, y) - \text{INV}(\text{fl}, y-1)}}{\text{INV}(\text{fl}, y-1)} 100 e^{\delta_{\text{crew}}} \right) \\ \quad + \dfrac{\overline{\text{VINT}(\text{fl}, y) - \text{VINT}(\text{fl}, y-1)}}{\text{VINT}(\text{fl}, y-1)} 100 \end{cases}$$

This model links the catchability to the capital invested and the mean vintage of boats within a fleet, all stocks included. However, the trends in the catchability of the Dutch beam-trawler fleets would only be detected in relation to sole fishing (Marchal et al. 2001*b*). As a result, the whole catchability increase calculated above is applied on the sole stock only. The catchability of plaice is assumed constant.

Economic model

The economic model estimates the revenue and cost in each year given the estimated fleet activity and stock conditions. The parameters of the model were derived from an analysis of the costs of the Dutch fleet in the North Sea (Tables 2 and 3). The gross revenue by fleet and year, $\text{REV}(\text{fl},y)$, is derived from the landings and prices by stock, fleet, and year, increased by a percentage $\alpha_{\text{bycatch}}(\text{fl},y)$ as a result of the catch of other species not modelled directly (Appendix A, eq. A9). Previous analyses of the price–quantity relationships for the two key species (sole and plaice) found that prices were generally highly inflexible (<0.31 for both species in absolute terms; Jaffry et al. 1999). Given this, prices are not expected to vary substantially with changes in quantity landed and were assumed to fluctuate stochastically following a normally distributed function truncated to zero.

The costs are divided into four groups: (*i*) fuel costs, proportional to the number of days at sea; (*ii*) landings costs, depending on the value landed; (*iii*) crew costs; and (*iv*) fixed costs. Fuel and oil costs, $\text{COST}_{\text{fuel}}(\text{fl},y)$, are estimated as a function of fuel use per day by fleet, total effort by fleet, $E(\text{fl},y)$, and the average price of fuel, P_{fuel}, considered as constant. A linear model of fuel use per day as a function of average capital per vessel was developed. Landings costs, $\text{COST}_{\text{land}}(\text{fl},y)$, are calculated as a fixed percentage, $\alpha_{\text{land}}(\text{fl})$, of the total value landed. Crew costs, $\text{COST}_{\text{crew}}(\text{fl},y)$, are also calculated as a fixed percentage, $\alpha_{\text{crew}}(\text{fl})$, of the net revenue, i.e., the gross revenue minus the fuel and landings costs. Finally, cash and noncash (depreciation) fixed costs, $\text{COST}_{\text{fixed}}(\text{fl},y)$, are estimated as a fixed percentage, $\alpha_{\text{fixed_costs}}(\text{fl})$, of the capital invested:

$$(3)\quad \begin{cases} \text{COST}_{\text{fuel}}(\text{fl}, y) = [\alpha_{\text{fuel1}} + \alpha_{\text{fuel2}} \text{INV}(\text{fl}, y)] E(\text{fl}, y) P_{\text{fuel}} \\ \text{COST}_{\text{land}}(\text{fl}, y) = \alpha_{\text{land}}(\text{fl}) \text{REV}(\text{fl}, y) \\ \text{COST}_{\text{crew}}(\text{fl}, y) = \alpha_{\text{crew}}(\text{fl}) [\text{REV}(\text{fl}, y) - \text{COST}_{\text{fuel}}(\text{fl}, y) \\ \qquad - \text{COST}_{\text{land}}(\text{fl}, y)] \\ \text{COST}_{\text{fixed}}(\text{fl}, y) = \alpha_{\text{fixed_costs}}(\text{fl}) \text{INV}(\text{fl}, y) N_{\text{boats}}(\text{fl}, y) \\ \text{COST}_{\text{total}}(\text{fl}, y) = \text{COST}_{\text{fuel}} + \text{COST}_{\text{land}}(\text{fl}, y) \\ \qquad + \text{COST}_{\text{crew}}(\text{fl}, y) + \text{COST}_{\text{fixed}}(\text{fl}, y) \end{cases}$$

where α_{fuel1} and α_{fuel2} are the parameters of the linear regression between fuel use and capital and $N_{\text{boats}}(\text{fl},y)$ is the number of boats by fleet.

The profit of the fleet is estimated as the difference between gross revenue and costs. A key feature of the model is that costs change with changes in the level of investment. This directly affects fuel and fixed costs and indirectly affects crew and landing costs through the effects of catchability increases on catch (and hence revenue). For the Dutch fleets, the average real level of capital invested (i.e., after removing cost increases due to general inflationary pressures) has increased at a fairly constant rate $[1 + \alpha_{\text{inv}}(\text{fl})]$ over the last decade.

Management and fishermen behaviour models

We assume here that management advice is based on the HCR, setting mean target fishing mortality F_{HCR} depending on the spawning biomass and the limit and precautionary approach reference points B_{lim}, B_{pa}, and F_{pa} (ICES 2001). The forecast is made after the VPA at the beginning of year y (the current year of the simulation) for the following year, $y + 1$, based on data in the previous data-year, $y - 1$. $F_{\text{HCR}}(\text{St},y+1)$ is defined as follows:

© 2002 NRC Canada

Table 2. Deterministic 1991–1999 parameters by Dutch fleet.

Fleet	Parameters	1991	1992	1993	1994	1995	1996	1997	1998	1999
NL_small (<300 HP)	N_{boats}	57	45	42	45	31	36	35	30	34
	Effort	96	110	125	130	144	134	128	142	135
	Fuel costs·day^{-1}	0.157	0.160	0.160	0.174	0.171	0.195	0.198	0.195	0.201
	Landings costs (%)	6.8	6.7	6.7	7.1	6.9	6.9	7.0	6.7	6.8
	Fixed costs	357.1	409.1	393.2	426.6	424.6	422.1	431.6	451.1	419.3
	Crew share (%)	44	43	42	42	42	43	41	41	41
	Investment	1875.9	1904.8	1907.6	2027.7	1998.7	2206.2	2233.0	2212.8	2257.0
	Price sole	14.8	16.3	13.4	12.5	13.8	17.7	24.1	16.7	16.4
	Price plaice	4.5	3.3	3.3	3.5	3.4	3.9	4.0	4.4	4.1
	Catchability sole ($\times 10^{-6}$)	4.85	5.17	5.74	5.21	7.17	7.96	7.29	7.93	5.74
	Catchability plaice ($\times 10^{-6}$)	1.54	1.78	1.69	1.57	1.88	1.81	2.05	1.64	1.39
NL_medium (300–2000 HP)	N_{boats}	140	123	127	124	124	114	96	95	94
	N_{days}	142	156	172	189	192	166	183	187	189
	Fuel costs·day^{-1}	1.904	2.048	2.079	2.352	2.450	2.777	2.926	3.067	3.010
	Landings costs (%)	6.5	6.4	6.6	6.7	6.5	6.5	6.6	6.6	6.5
	Fixed costs	851.1	839.9	796.3	930.6	956.1	996.6	1036.2	1084.2	965.4
	Crew share (%)	38	38	37	37	37	37	37	37	37
	Investment	4810.2	5016.2	5060.2	5449.3	5588.6	6053.5	6266.8	6467.8	6385.2
	Price sole	14.6	16.0	13.3	12.1	13.8	17.7	23.4	16.6	16.6
	Price plaice	4.1	3.1	3.2	3.4	3.2	3.8	4.0	4.2	4.5
	Catchability sole ($\times 10^{-6}$)[a]	9.13	9.01	9.34	8.79	9.17	1.38*	1.26*	1.29*	1.01*
	Catchability plaice ($\times 10^{-6}$)	5.32	5.71	5.06	4.88	4.42	5.76	6.53	4.91	4.5
NL_big (>2000 HP)	N_{boats}	82	80	76	75	69	67	68	64	61
	N_{days}	152	169	187	193	203	180	190	192	186
	Fuel costs·day^{-1}	3.205	3.259	3.349	3.628	3.615	3.996	4.080	4.038	4.072
	Landings costs (%)	6.6	6.6	6.6	6.9	6.8	6.6	6.5	6.6	6.6
	Fixed costs	1505.1	1464.7	1344.9	1304.6	1167.1	1141.1	1180.5	1118.7	992.8
	Crew share (%)	37	36	35	36	36	36	36	36	37
	Investment	6663.4	6740.0	6868.6	7265.7	7247.4	7789.7	7910.5	7850.2	7898.9
	Price sole	14.6	15.9	13.6	12.3	13.7	17.5	22.9	17.2	16.8
	Price plaice	4.1	3.1	3.1	3.4	3.3	3.8	3.9	4.2	4.4
	Catchability sole ($\times 10^{-5}$)	1.32	1.17	1.31	1.3	1.42	1.97	1.56	1.7	1.44
	Catchability plaice ($\times 10^{-6}$)	6.07	5.84	5.6	5.68	5.39	6.49	6.39	5.1	5.07

Note: Costs are in 10^3 NGL·boat^{-1}, effort is in days at sea, and prices are in NGL·kg^{-1} (NGL = Netherlands Guilders).
[a]Values in this row marked with an asterisk (*) are $\times 10^{-5}$.

$$(4)\quad F_{HCR}(St,y+1) = \begin{cases} 0 \text{ if } SSB(St,y-1) \le B_{lim}(St) \\ F_{pa}(St)\dfrac{SSB(St,y-1) - B_{lim}(St)}{B_{pa}(St) - B_{lim}(St)} \\ \qquad \text{if } B_{lim}(St) < SSB(St,\ y-1) \le B_{pa}(St) \\ F_{pa}(St) \text{ if } SSB(St,\ y-1) > B_{pa}(St) \end{cases}$$

Consistent with ICES analyses, the forecast model predicts the stock and the fishery of all combined fleets for the two years. F_{HCR} is distributed among fleets by using partial fishing mortalities and selection ogives. The conversion of the F_{HCR} by stock into effort by fleet is made possible through the introduction of the theoretical concept of "stock-dependent effort" $E^{*}_{HCR}(St,fl,y+1)$, i.e., the effort you need to apply to produce a given fishing mortality on a given stock, disregarding all other activities of the fleet:

$$(5)\quad E^{*}_{HCR}(St,fl,y+1) = \text{Max}_a[F_{catch}(St,fl,y+1,a)]/q(St,fl,y+1)$$

where $F_{catch}(St,fl,y,a)$ and $q(St,fl,y)$ represent the total fishing mortality (landings plus discards) by stock, fleet, year, and age and the catchability by stock, fleet, and year, respectively. The predicted yield is based on $F_{HCR}(St,y+1)$. Given selection and discards ogives, total forecast landings and discards are estimated. The TAC is counted against the forecast landings.

The overall effort by fleet E_{HCR} depends on the regulation used. If the fishery is regulated by fishing effort quotas (TAEs), it is assumed that the multispecies regulation is set to the most overexploited stocks. The F_{HCR} cannot be exceeded for any of the stocks, and thus the fishery is stopped or reduced as soon as the precautionary approach is exceeded for one stock. Conversely, if the fishery is regulated by catches quotas (TACs), it is assumed that fishermen will fish at the highest level authorized, i.e., that they will set their effort to fish the highest quota and will discard overquota catches for other stocks. In that case, the fishery is stopped or reduced only when the precautionary approach is exceeded for all stocks. In both cases, the effort by fleet is limited by the user-defined maximal capacity of the fleet $E_{capacity}$, i.e., the number of boats × the maximum number of days at sea per boat and at year $y + 1$:

$$(6)\quad \begin{cases} E_{HCR}(fl,y+1) = \text{Min}_{St}\left[E^{*}_{HCR}(St,fl,y+1)\right] \text{ if TAE} \\ E_{HCR}(fl,y+1) = \text{Max}_{St}\left[E^{*}_{HCR}(St,fl,y+1)\right] \text{ if TAC} \\ \text{if } E_{HCR}(fl,y+1) > E_{capacity}(fl,y+1), \\ \qquad \text{then } E_{HCR}(fl,y+1) = E_{capacity}(fl,y+1) \end{cases}$$

Once effort by the fleet is defined, fishing mortality coeffi-

© 2002 NRC Canada

Table 3. Constant and stochastic parameters by Dutch fleet.

		NL_small		NL_medium		NL_big	
Type of parameter	Parameter	Value	CV	Value	CV	Value	CV
Capacity and costs	Maximum number of days	144		192		203	
	$\alpha_{bycatch}$ (%)	20		20		20	
	α_{fuel1}	–162		–4033		–4033	
	α_{fuel2}	0.000 315		0.001 922		0.001 922	
	P_{fuel} (NGL·litre^{-1})	0.365 26		0.365 26		0.365 26	
	α_{land} (%)	7		7		7	
	α_{crew} (%)	42		37		36	
	α_{fixed_costs} (%)	20		17		16	
	α_{inv} (%)	2.4		3.6		2.2	
Gear selection (cm)	$L_{50\%}$ sole	25		25		25	
	$L_{75\%}$ sole	27		27		27	
	$L_{50\%}$ plaice	19		19		19	
	$L_{75\%}$ plaice	20.7		20.7		20.7	
Discard ogive (cm)	$L_{50\%Disc}$ sole	23		23		23	
	$L_{75\%Disc}$ sole	24		24		24	
	$L_{50\%Disc}$ plaice	26		26		26	
	$L_{75\%Disc}$ plaice	27		27		27	
Catchability	$q_{constant}$	1.01241		1.00975		1.00753	
Sole	q(2000)	6.08×10^{-6}	0.2	1.07×10^{-5}	0.2	1.51×10^{-5}	0.2
Plaice	q(plaice)	1.71×10^{-6}	0.1	5.23×10^{-6}	0.1	5.74×10^{-6}	0.1
Mean price (NGL·kg^{-1})	Sole	16.2	0.2	16.0	0.2	16.1	0.2
	Plaice	4.1	0.1	4.5	0.1	4.4	0.1

Note: CV, coefficient of variation (%); NGL = Netherlands Guilders.

cients by stock, fleet, and age are recalculated for year y+1. If the fishery is regulated by TAC, then the amount of "kept" yield (yield minus undersized discarded fish) is compared with the TAC. If it exceeds this latter, then the surplus is transferred from landings to discards.

Validation and simulations

The model was run in two consecutive stages. To validate the model, it was run over the past period 1991–1999, with fixed parameters and no stochasticity. We run the rules corresponding to a TAC management simulation but impose the actual TACs set by the EU (rather than those derived from the HCR). Initial stock numbers, recruitment, and real TAC parameters are found in ICES (2000, 2001). Dutch economic and effort data come from the LEI-DLO databases (Agricultural Economics Research Institute, The Hague, The Netherlands), and catchability inputs were calculated by the ratio between the mean fishing mortality by stock and the nominal effort by fleet. In addition, the series is simulated with the HCR to compare the expected evolution of the fishery if the HCR had been set in the early 1990s instead of the real TACs. Both the TAE and TAC versions of the HCR were examined.

The second step of the analysis involves stochastic simulations of the future development of the fishery, investigating the consequences of changes in the catchability of sole stock on management results over a given predicting period. The stochastic period was set at 10 years (i.e., 2000–2009) from the starting values based on the output from the preceding deterministic simulation using the real TACs. Catchability was initialized for the year 2000 as the mean over observed 1991–1999 data. The maximum effort by boat was set at the maximum observed during the previous decade. HCR were implemented at the beginning of simulated year 2000.

Various scenarios were explored, with 1000 model runs for each. Changes were tracked in relation to two major parameters: (*i*) catchability (influence of an error on the catchability model) and (*ii*) choice of management tool (respective drawbacks and benefits of TAC and TAE, and particularly in relation to assumptions on catchability). Parameter *i* was investigated by running, for the same set of stochastic parameters and management choices, three simulations. First, catchability increases, but this increase is known and taken into account in management (run "q trend"). Second, the catchability does not increase anymore and remains constant at the year 2000 level, and this is also taken into account (run "q cst"). Finally, the catchability increases over time, but this is not known and not taken into account in management. The level of effort used is that estimated as if the catchability was constant (run "q bias"). Parameter *ii* was investigated by running both management scenarios with the same initial set of parameters.

Results

Validation of the model—the deterministic simulation

The deterministic simulation over the 1991–1999 time period is analyzed from both the biological and economic aspects (Figs. 2 and 3). The simulation results with the real TACs are compared with the actual observed values (ICES assessment data).

© 2002 NRC Canada

In general, the simulation model correctly fits the ICES assessment for the sole stock but is less satisfactory for the plaice stock, both landings and spawning stock biomass (SSB) being underestimated (Fig. 2). This could be due to a misspecification of the length-based growth and harvest models (in particular, the weight-at-age calculated in the model underestimates slightly the weight at the ages 2 to 4, which represents an important part of the stock biomass) and to a likely underestimation of the catchability owing to the major discards occurring on that stock, especially on the young ages. However, major trends observed by ICES are also observed in the simulated fishery. Both SSB and landings decreased sharply over the decade, and a slight stabilization and increase occurred after 1997. This coherence between observed and simulated data gives consistency to the model and relevancy for stochastic prediction analyses.

For the same simulated population, implementing the HCR at the beginning of the decade would have had immediate positive effects on stock biomass, maintaining the sole stock around its 1991–1993 level and keeping the plaice stock above B_{lim} (Fig. 2). It would have also stabilized the exploitation pattern, maintaining the fishing mortality around F_{pa}. TAE appears to be an efficient tool to limit discards. Discarding would have remained high and variable with TAC, especially following strong recruitment years (1997–1998). However, implementing the HCR would also have had immediate negative effects on fleets activity and economic results (Fig. 3). During the first 3 years following the implementation, activity would have been limited and landings reduced. Positive returns on the individual fisherman's profit would have been expected only in the medium term, after at least 6 years of implementation. Furthermore, a management by HCR would not have led to a stabilization of effort, especially with TAE.

Stochastic prediction simulations

Considering the annual biological statuses of both stocks, the most striking results are the strong differences arising from the choice of the management tools (Fig. 4). On average, both management tools safeguard the stocks. The mean sole biomass remains always over B_{pa}. The mean plaice biomass, which was below B_{lim} in 1999, increases above this limit in the short term. However, both measures also imply an initial drastic reduction of the fishing mortality to first get the stocks into the safe biological limit. This is particularly true when simulating TAE, which requires a reduction in fishermen's activity in the short term to rebuild the plaice stock over B_{lim}. TAE are in all cases more conservative than TAC, the levels of biomass being always higher. Conversely, TAC management induces more stability over time and less uncertainty in both biomass and fishing mortality levels. It is worth noting also that after the few years of transition following the implementation of HCR, the TAE level is mainly driven and limited by the dynamics of the sole stock, whereas the TAC policy is mainly determined by the dynamics of the plaice stock (fishing mortality stable and close to F_{pa}).

Besides these differences resulting from the management tools and arising mainly from the fact that the simulations begin with a stock being outside safe biological limits, a major result is the evidence of the influence of the catchability model on the biological status of stocks. The catchability average trends are estimated to increase by 6% per year for the small boats, 7.8% for the medium boats, and 4.9% for the larger boats. No contrast could be observed in the short term, as differences in catchability are low, but in the medium and long term (2004 and later), increasing differences occur between the various runs. For sole stock, little difference exists when the catchability trend is correctly known and integrated in management (runs "q trend" and "q cst"). However, differences exist between these two runs for the plaice stock, which has a constant catchability. A constant catchability for sole implies higher allowable effort levels and thus higher fishing mortality coefficients for the plaice stock. Furthermore, the bias induced by a misspecification of the catchability (i.e., the allowable effort levels are set by considering that the catchability was constant, whereas it had increased) leads to major underestimation of fishing mortality coefficients and lower levels of biomass. TAEs are more sensitive to this bias than TACs. The probability of having the sole SSB falling below B_{pa} in the medium and long term is three to four times higher when underestimating the trend in catchability under a TAE policy, whereas this probability is less than twice higher with TAC.

Mean fleet activity and economic results rely also on the hypothesis made on catchability and on the choice of management tools (Fig. 5). After the first few years following the implementation of HCR, the assumed fishing mortality (i.e., run "q bias" excluded) by stock and fleet reaches an equilibrium level. Thus, the total effort by fleet allowed by managers (TAE) or reached by fishermen (TAC) is constant if the catchability is assumed to be constant, or decreases inversely proportionally to the increase of catchability if this is considered to increase over time. Consequently, if the number of boats remains constant, the individual effort remains stable if the catchability is constant. However, effort has to be decreased continuously to adjust for catchability trends when they exist, and particularly in the case of TAE.

In the medium and long term, the mean individual expected profit is always higher with TAEs than with TACs. This is partly due to the fact that the stock sizes and thus the catches are higher, whereas the effort and thus the variable costs are lower, but the main reason for such a difference in expected profit is the level of discards. The TAC simulations lead to major quantities of overquota discards of valuable fish. The estimated level of discard is on average 6 to 10 times lower in the TAE simulations, and the revenue is thus higher. However, it is to be noted that the profits in the TAC simulations are likely to be underestimated, as the model is likely to overestimate the level of effort employed. In reality, fishermen would not attempt to fill every TAC and would stop fishing once the marginal cost of fishing exceeded the marginal value of the catch, even if the TAC for some species remained unfilled. Hence, the estimated costs are higher than what would be truly expected under a TAC regime. The TAC policy leads to a great stability of landings and profit, whereas profits under the TAE are more variable over time and follow the same trends as the sole stock biomass. The bias induced by an error on the catchability model is also, as observed for the stocks dynamics, more important in the case of TAE than with TAC. It would lead to higher profit in the medium term when the biomass is high, but to sharper

© 2002 NRC Canada

Fig. 2. ICES assessment (◆) and biological results of the deterministic simulation for the sole (left) and plaice (right) stocks between 1991 and 1999 for three different management options: real total allowable catch quotas (TAC) (□), harvest control rules (HCR) with TAC (▲), and HCR with total allowable effort quotas (TAE) (×). (*a* and *b*) Spawning stock biomass (SSB)/B_{pa}; (*c* and *d*) fishing mortality (F)/F_{pa}; (*e* and *f*) landings; (*g* and *h*) discards; dotted line, B_{lim}/B_{pa}.

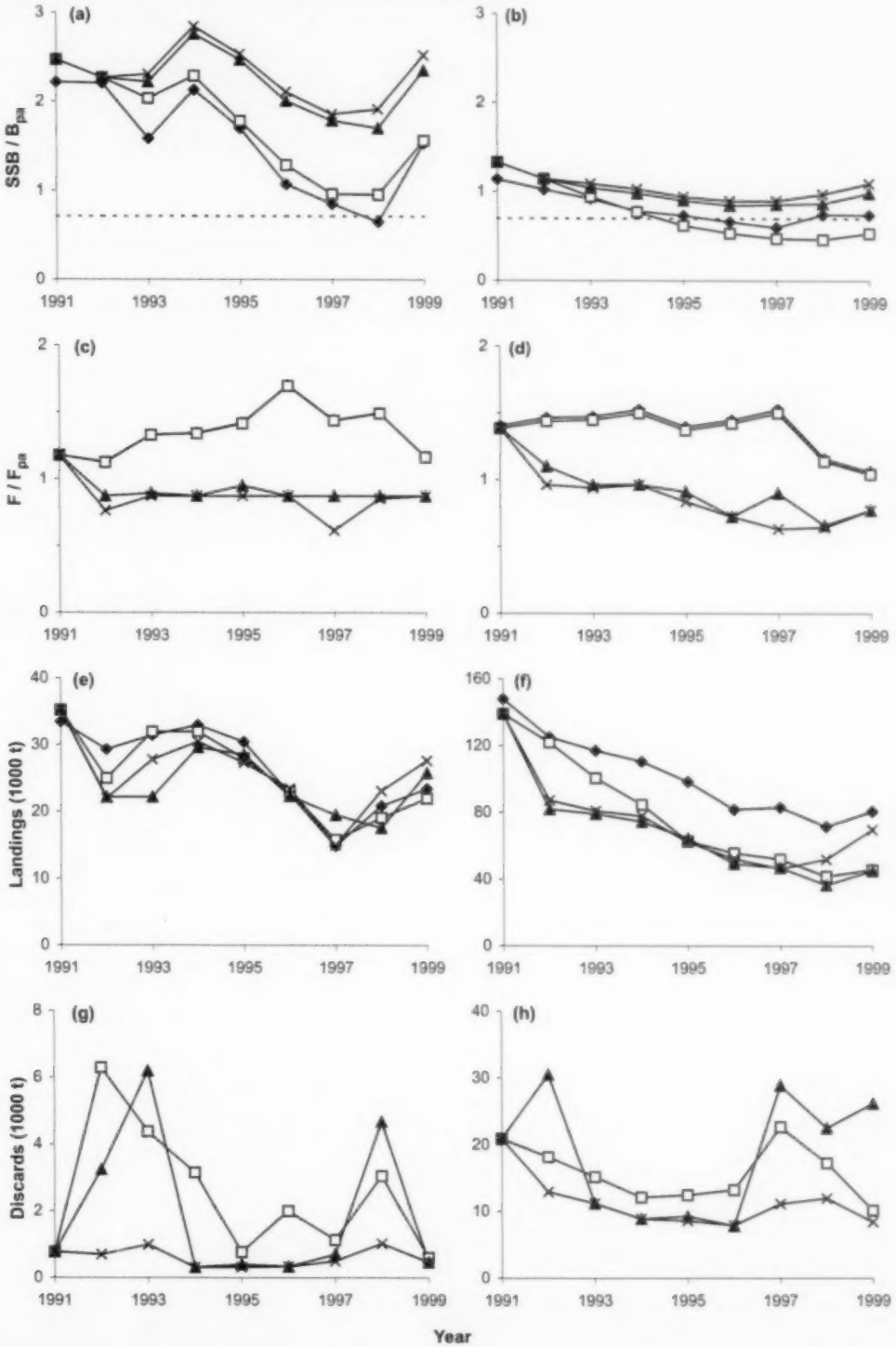

© 2002 NRC Canada

Fig. 3. Simulated annual effort per boat (left) and individual cumulated discounted profit (right) between 1991 and 1999 for the three Dutch fleets and three different management options: real total allowable catch, TAC (□); harvest control rules (HCR) with TAC (▲); and HCR with total allowable effort (TAE) (×). (*a* and *b*) NL_small; (*c* and *d*) NL_medium; (*e* and *f*) NL_big.

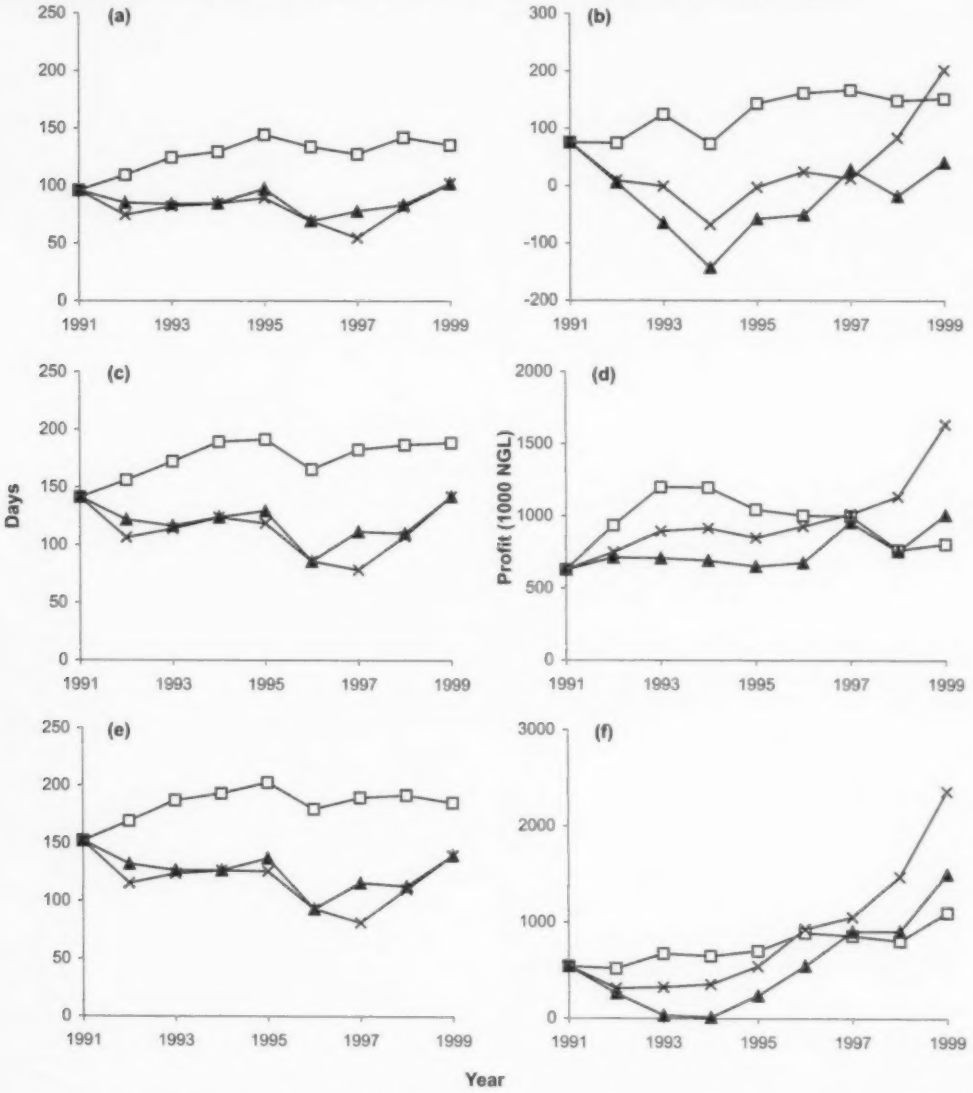

decrease in the long term. The simulated profits are mostly negative. Generally, it appears that the HCR, which are fairly conservative and restrictive, are not economically viable with the current number of boats in the fishery.

Discussion

First, the results of this study suggest that in a multispecies–multifleet fishery, there are wide biological and economic differences expected when implementing the same management rules with different management tools. In the case of the fisheries being examined (Dutch beam-trawlers harvesting sole and plaice in the North Sea), effort limitations have the following advantages over TACs: (*i*) they do not induce overquota discarding (as initially defined in the model configuration); and (*ii*) they may lead to enhanced biological statuses and higher profit in the long term. It should also be noted that the assumptions underlying the catchability model have consequences for the biological dynamics of the stocks, but not for the profit raised by the related fisheries. TACs have the following advantages over effort control: (*i*) they give more stability to the fishery; (*ii*) they do not require closing the fishery in the short term, and (*iii*) they are less sensitive to the assumptions underlying the catchability model. Overall, our HCR appear inapplicable, whatever the management tool is, because short-term (TAE) or long-term (TAC) losses could not been sustained for several years by any fishery. However, alternatives are not easy to define, as

© 2002 NRC Canada

Fig. 4. (*a* and *b*) Mean 1999–2009 SSB–*F* trajectories for sole (left) and plaice (right) stocks managed with total allowable catch (TAC, triangles) or total allowable effort (TAE, squares): solid symbols, scenario "q cst"; open symbols, scenario "q trend"; shaded symbols, scenario "q bias". (*c* and *d*) Annual probability of spawning stock biomass (SSB) falling below B_{pa} for sole (left) and plaice (right) stocks.

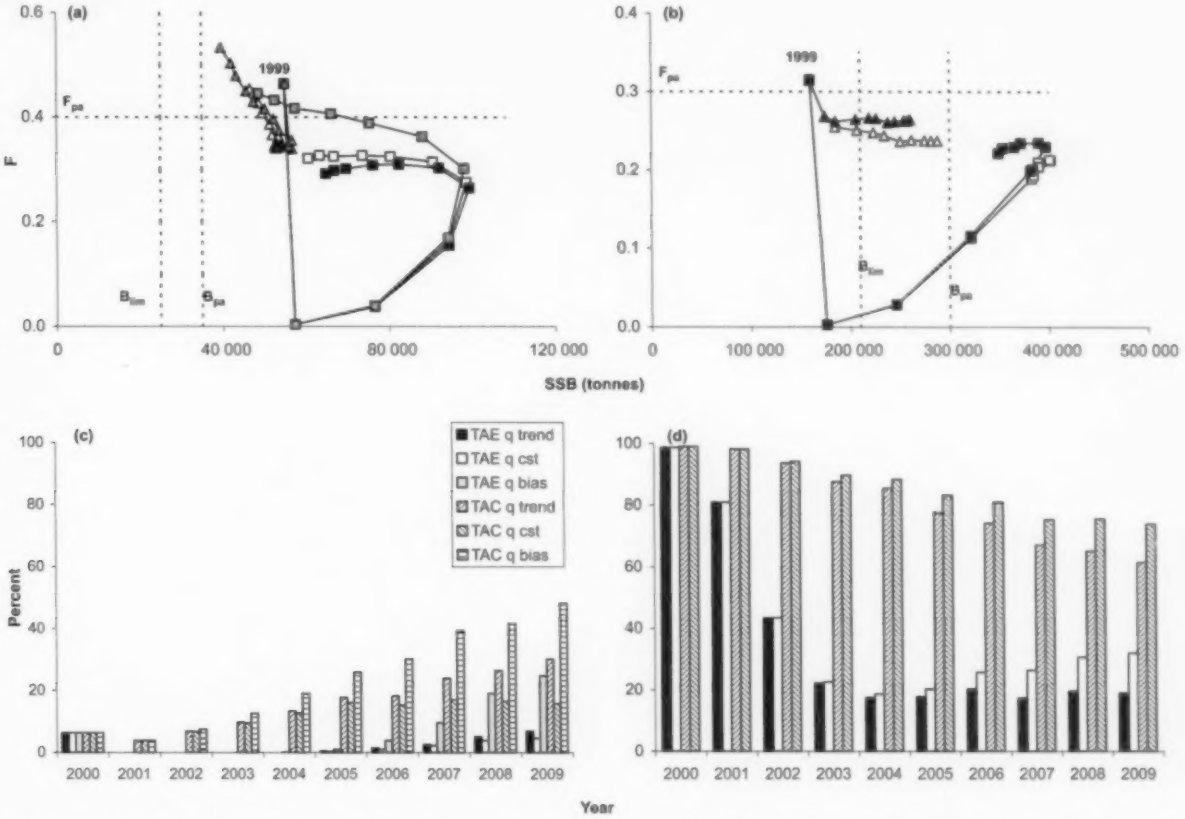

management objectives are variable and set to a year-to-year basis in the North Sea (ICES 2001). It is worth noting also that some of these drawbacks linked to HCR, and in particular the short-term losses when implementing TAE, are specific to the fishery investigated here, which was already partly below safe biological limits at the beginning of the simulation. Another case study with different initial conditions might lead to different results. In ICES areas, however, most stocks are already below B_{pa}.

Second, this study provides valuable information on dynamics of catchability and its influence on management models and forecast. The economic parameters used for prediction (increase in capital invested and mean age and technology of the boat) have proven to be rather stable, although the fishery experienced many changes in stocks biomass and management during the past decades (Pascoe et al. 2001). Linking the observed past trend in catchability to these parameters with little interannual variability allows making fairly coherent and reliable predictions on future expected dynamics, which would not have been possible with only a biological analysis. With similar slow increase of investment and technology, the Dutch fleet catchability should go on increasing 5–8% per year, which is a level high but consistent with that observed during the 1990s (Marchal et al. 2001*b*). Although the catchability is only one of the various parameters subject to uncertainty in the fisheries forecast model, we showed that an error in its specification would lead to major fishing mortality underestimates and biomass overestimates, especially when managing a fishery with TAE. Additionally, the sensitivity to the catchability model increases with time. However, the variability in catchability has a much greater impact on stock levels than on the fisheries profit. Overall, the effects of the assumptions underlying the catchability model are more than offset by the choice of a management strategy (catch or effort quotas) and of an HCR.

The outcomes of this study may only be contrasted with theoretical views, because to our knowledge, no study to date has compared the bioeconomic performances of management regimes based on catch or effort quotas in relation to different assumptions underlying catchability dynamics. Gillis et al. (1995) explicitly contrasted the expected outcomes of management strategies based on catch or effort control. However, compared to our investigation, these authors used a different HCR, a different fishermen behaviour model, and different performance indices, and more importantly, they did not explicitly account for the dynamics of catchability. In our results, TACs represent a practical and species-specific management tool that is expected to provide

© 2002 NRC Canada

Fig. 5. Mean annual effort per boat (left) and individual profit (right) between 1999 and 2009 for the three Dutch fleets managed with total allowable catch (TAC, triangles) or total allowable effort (TAE, squares): solid symbols, scenario "q cst"; open symbols, scenario "q trend"; shaded symbols, scenario "q bias". (*a* and *b*) NL_small; (*c* and *d*) NL_medium; (*e* and *f*) NL_big.

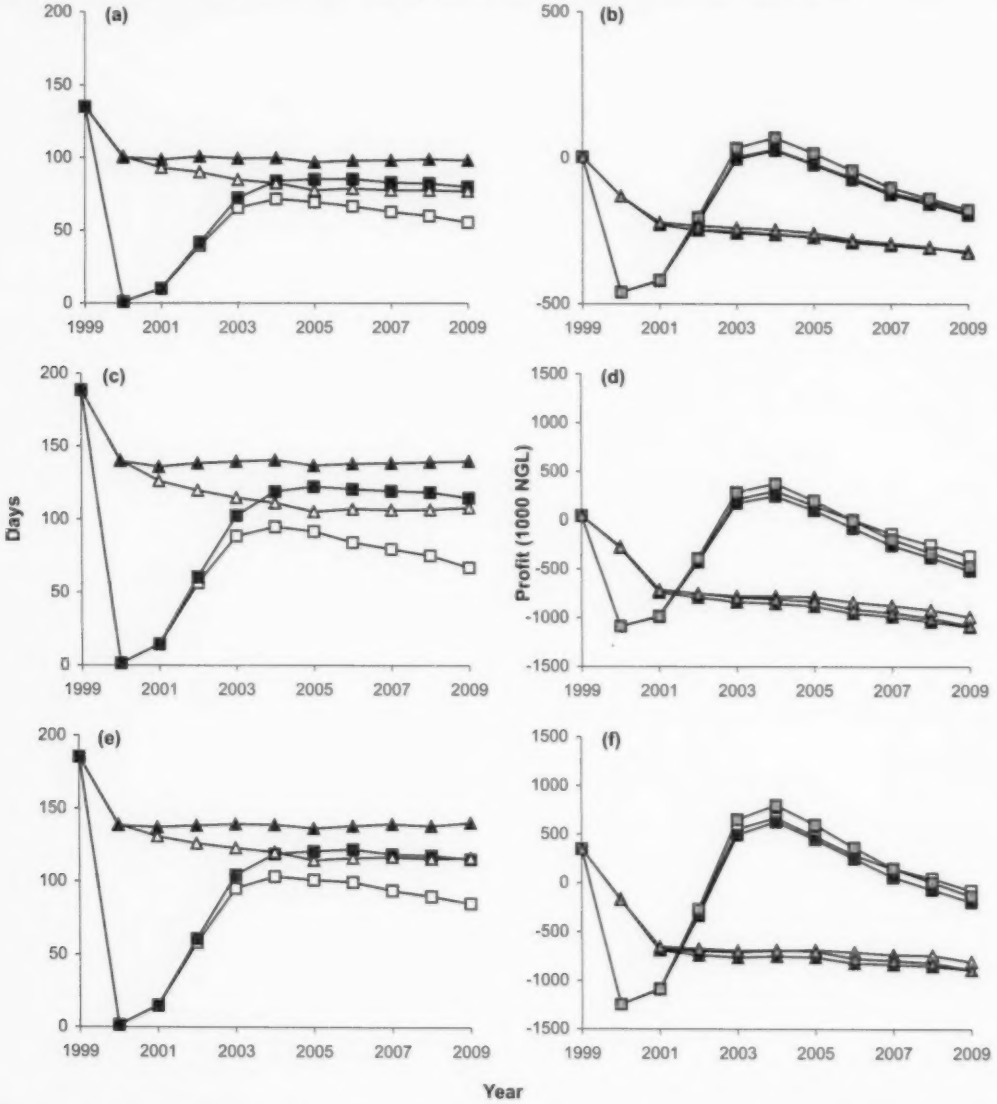

some stability to the fishing industry by allowing direct control on the yields. However, single-species TACs have been increasingly criticized because their enforcement is cumbersome and they may give incentives to overquota discarding. General perception on fishing effort limits is that despite preventing overquota discards, their implementation is undermined by (*i*) imperfect information on the link between fishing mortality and effort; (*ii*) their lack of biological specificity; (*iii*) the potential for input substitution that can offset, to some degree, the effectiveness of the measure in controlling fishing mortality (Campbell 1991; Pascoe and Robinson 1998); and (*iv*) their resultant economical inefficiency (Holden 1994; Sutinen 1999).

All conclusions drawn from this study should in any case be interpreted cautiously, because they are limited by the assumptions underlying the simulation models being used. Some of the biological relationships used (growth model, Beverton–Holt stock–recruitment relationships, etc.) may not reflect perfectly the true dynamics of the stocks, especially as interannual variability is high (e.g., the sole stock recruitment). Similarly, the description of the catches with length-based gear selection and discard ogives allows simulating the "real" harvest process but also leads to some inconsistency with the ICES age- and landings-based recruitment and catchability data. This problem is not of great importance for sole stock because very few age-1 fish are caught (6% of the simulated population) and the overall level of discards is low (less than 15% for age-2 fish). How-

© 2002 NRC Canada

ever, it may introduce a bias in the plaice stock dynamics, with a major underestimation of age-1 catches (simulated gear selection is 80% for age-1, almost completely discarded) and high age-2 discards (55%). This feature is probably the main reason of the mismatch between observed and simulated data over 1991–1999.

The continuously negative profits obtained suggest that either the behaviour assumptions are not reliable or that the costs and capacity module was misspecified. It is likely that the behaviour rule under the TAC simulation would lead to an overestimate of the level of effort expended in the fishery, and this could be contributing to the negative profits in the simulation results. Further, the trends in cost of effort might have been overestimated. In particular, major variations in costs arise from the fluctuations in fuel price, which is highly variable and rather unpredictable. Negative profits may also arise from a misspecification of the number of boats. It is unlikely that this stays constant if such negative profits are generated.

The HCR implemented here are simplified shortcuts to the management advice provided by ICES and based on the Precautionary Approach (ICES 1998, 2001). This choice has been made regarding the fact that the stocks investigated here are all evaluated by ICES. However, HCR could have been implemented in many other ways (e.g., Kell et al. 1999; Restrepo and Powers 1999). The search for "optimal" HCR or management strategies has been widely investigated through simulation models (e.g., Pelletier and Laurec 1992; Marchal 1997), but results are strongly related to model design, parameters estimation, and case study and little generalization can be made on the optimal configuration (McAllister et al. 1999). The scope of the present study was, however, not to investigate the optimal HCR that could be applied in the North Sea, but to simulate the one currently underlying ICES advice, although further analysis could be conducted later.

The implementation of the management tools used to regulate the fishery is dependent upon two conditions. First, it is assumed that fisheries management is based on scientific advice. Although there have been several examples in the history of fisheries where legally binding TACs were inconsistent with TACs recommended by ICES (Holden 1994), this source of uncertainty is notoriously difficult to appraise, and in the absence of more descriptive information, it has been neglected. Second, it is assumed that total catch quota is shared on a fixed basis at the beginning of the fishing year among all the fleets on the basis of their mean relative yield and that all fleets reduce their effort by the same proportions when the quota is reduced. This is a sharing procedure that is neither unreasonable nor unfair. It respects the "principle of relative stability" that is at the core of the Common Fisheries Policy. Alternative ways of sharing the quota could have been performed. In particular, some individual transferable quotas (ITQs) are currently in force in Dutch fisheries, implying moving shares among fleets. However, Pascoe et al. (2001) showed that ITQs on their own do not significantly influence catchability dynamics and thus do not appear as a major source of bias in this model.

The behaviour of fishermen has been modelled through their fishing activity and discarding practice. Fishermen are assumed conservative with respect to their choice of target species and fishing ground. Alternative strategies could have been set. Effort could have been defined as a mean or weighted mean (by value, or price, or yield, etc.) of the "stock-dependent efforts" by fleet, especially under the quota regime. Fishermen could also have been assumed to maximize their gross or net revenues, or their profit, but such a choice would have required additional and somehow complex maximization modules in the model, which would not be supported by available data anyway. It is also likely that given the expected contrasted trajectories of the stocks considered, the fishermen show large-scale adaptations of unknown direction. The extent to which any violation to this assumption could adversely affect the conclusions stated above could not be accurately evaluated. More over, this issue is probably of not so major importance in the particular case study investigated here: simulations deal with only two stocks, considered as fairly stable and with comparable levels of exploitation (ICES 2000). The range of "acceptable" effort is thus limited, and the simulations show consistent effort levels (the difference of fishing effort between the two options is always around 20% after the first years of recovery). A fishery involving a greater number of stocks with more heterogeneous dynamics would require a more thorough investigation of the fleet's behaviour. It has also been assumed that under a TAC policy, fish were discarded when their related quota was exceeded. This assumption is somehow problematic when dealing with stocks having so different market values as sole and plaice. It is not likely that in reality all valuable overquota sole will be discarded. More generally, this issue calls for the assumption that management rules are strictly applied and respected. However, in the absence of more descriptive information, potential illegal behaviours or major changes in fishing strategies or adaptations to new management rules have not been modelled.

Despite all these limitations inherent to any complex model, the model presented here has proven to be a rather innovative and useful framework for the bioeconomic analysis of some aspects of great importance for fisheries management. It matched reasonably the simulated populations with the observed data and could be parameterized without requiring any specific data other than the usual ones commonly provided by biological and economic fisheries databases. Thus, although some parts of it are strongly related to the fishery under investigation (e.g., the catchability model), this model can easily be adapted to any other case study. There is a wide scope for further development of some parts of the model (HCR, fleet behaviour, quota share, etc.), but this lies outside the objectives of the present investigation.

Acknowledgements

The study was undertaken as part of the EU-funded project "On the applicability of economic indicators to improve the understanding of the relationship between fishing effort and mortality. Examples from the flat- and round-fish fisheries of the North Sea" (DGXIV 98/027). It does not necessarily reflect its views and in no way anticipates the Commission's future policy in this area. Former and further development of the bioeconomic simulation model was funded by the Danish Ministry of Food, Agriculture and

© 2002 NRC Canada

Fisheries (Effort Regulation Project/TEMAS project). This support is gratefully acknowledged.

References

Campbell, H.F. 1991. Estimating the elasticity of substitution between restricted and unrestricted inputs in a regulated fishery: a probit approach. J. Environ. Econ. Manag. **20**: 262–274.

Campbell, H.F., and Lindner, R.K. 1990. The production of fishing effort and the economic performance of licence limitation programs. Land Econ. **66**: 56–66.

Crutchfield, J.A. 1979. Economic and social implications of the main policy alternatives for controlling fishing effort. J. Fish. Res. Board Can. **36**: 742–752.

Frederick, S.W., and Peterman, R.M. 1995. Choosing fisheries harvest policies: when does uncertainty matter? Can. J. Fish. Aquat. Sci. **52**: 291–306.

Gillis, D.M., Peterman, R.M., and Pikitch, E.K. 1995. Implications of trip regulations for high-grading: a model of the behaviour of fishermen. Can. J. Fish. Aquat. Sci. **52**: 402–415.

Holden, M. 1994. The Common Fisheries Policy. Origin, evaluation and future. Fishing News Books, Trustees, The Buckland Foundation, London, U.K., 1994.

Horwood, J.W., Jacobs, O.L.R., and Balance, D.J. 1990. A feed-back control law to stabilize fisheries. J. Cons. Int. Expl. Mer, **47**: 57–64.

ICES (International Council for the Exploration of the Sea). 1998. Report of the study group on the precautionary approach to fisheries management, Copenhagen, Denmark, 3–6 February 1998. ICES CM 1998/ACFM.

ICES. 2000. Report of the Working Group on the assessment of demersal stocks in the North Sea and Skagerrak, Copenhagen, Denmark, 11–20 October 1999. ICES CM 2000/ACFM:7.

ICES. 2001. Report of the ICES Advisory Committee on the Fisheries Management, 2000. ICES Coop. Res. Rep. 242.

Jaffry, S., Pascoe, S., and Robinson, C. 1999. Long run flexibilities for high valued UK fish species: a cointegration systems approach. Appl. Econ. **31**: 473–481.

Kell, L.T., O'Brien, C.M., Smith, M.T., Stokes, T.K., and Rackham, B.D. 1999. An evaluation of management procedures for implementing a precautionary approach in the ICES context for North Sea plaice (*Pleuronectes platessa* L.). ICES J. Mar. Sci. **56**: 834–845.

Kirkley, J.E., Squires, D., and Strand, I.E. 1995. Assessing technical efficiency in commercial fisheries: the mid-Atlantic sea scallop fishery. Am. J. Agric. Econ. **77**: 686–97.

Kirkley, J.E., Squires, D., and Strand, I.E. 1998. Characterizing managerial skill and technical efficiency in a fishery. J. Prod. Anal. **9**: 145–160.

Marchal, P. 1997. Managing growth overfishing with multiannual compromise strategies. Can. J. Fish. Aquat. Sci. **54**: 2255–2276.

Marchal, P., Nielsen, J.R., Hovgård, H., and Lassen, H. 2001*a*. Time changes in fishing power in Baltic Sea cod fisheries. ICES J. Mar. Sci. **58**: 298–310.

Marchal, P., Ulrich, C., Andersen, J., Pastoors, M., Poos, J.J., De Wilde, J.W., Korsbrekke, K., Casey, J., O'Brien, C., Rackham, B., and Pascoe, S. 2001*b*. On the applicability of biological and economic indicators to improve the understanding of the relationship between effort and mortality. Examples from the flat- and round-fish fisheries of the North Sea. Final Report of the EU study no. 98/027. DFU (Denmark), SJFI (Denmark), RIVO (The Netherlands), LEI (The Netherlands), IMR (Norway), CEFAS (U.K.), CEMARE (U.K.).

McAllister, M.K., Starr, P.J., Restrepo, V.R., and Kirkwood, G.P. 1999. Formulating quantitative methods to evaluate fishery-management systems: what fishery processes should be modelled and what trade-offs should be made? ICES J. Mar. Sci. **56**: 900–916.

Millischer, L., Gascuel, D., and Biseau, A. 1999. Estimation of the overall fishing power: a study of the dynamics and fishing strategies of Brittany's industrial fleets. Aquat. Liv. Res. **12**: 89–103.

Myers, R.A., Blanchard, W., and Thompson, K.R. 1990. Summary of North Atlantic fish recruitment 1942–1987. Can. Tech. Rep. Fish. Aquat. Sci. No. 1743.

Overholtz, W.J., Edwards, S.F., and Brodziak, K.T. 1995. Effort control in the New England groundfish fishery: a bio-economic perspective. Can. J. Fish. Aquat. Sci. **52**: 1944–1957.

Pascoe, S., and Robinson, C. 1998. Input controls, input substitution and profit maximisation in the English Channel beam trawl fishery. J. Agr. Econ. **48**: 16–30.

Pascoe, S., Andersen, J., and de Wilde, J.W. 2001. The impact of management regulation on the technical efficiency of vessels in the Dutch beam trawl fishery. Eur. Rev. Agr. Econ. **28**: 187–206.

Pelletier, D., and Laurec, A. 1992. Management under uncertainty: defining strategies for reducing overexploitation. ICES J. Mar. Sci. **49**: 389–401.

Pope, J.G., and Shepherd, J.G. 1985. A comparison of the performance of various methods for tuning VPAs using effort data. J. Cons. Int. Expl. Mer, **42**: 129–151.

Power, M. 1996. The testing and selection of recruitment distributions for North Atlantic fish stocks. Fish. Res. **25**: 77–95.

Restrepo, V.R., and Powers, J.E. 1999. Precautionary control rules in US fisheries management: specification and performance. ICES J. Mar. Sci. **56**: 846–852.

Restrepo, V.R., Hoenig, J.M., Powers, J.E., Baird, J.W., and Turner, S.C. 1992. A simple simulation approach to risk and cost analysis, with applications to swordfish and cod fisheries. Fish. Bull. **90**: 736–748.

Squires, D. 1987. Fishing effort: its testing, specification, and internal structure in fisheries economics and management. J. Environ. Econ. Manag. **14**: 268–282.

Sutinen, J.G. 1999. What works well and why: evidence from fishery-management experiences in OECD countries. ICES J. Mar. Sci. **56**: 1051–1058.

Townsend, R.E. 1985. On capital stuffing in regulated fisheries. Land Econ. **61**: 195–97.

Vestergaard, N. 1996. Discard behaviour, highgrading and regulation: the case of the Greenland shrimp fishery. Mar. Res. Econ. **11**: 247–266.

Waters J.R. 1991. Restricted access versus open access methods of management: toward more effective regulation of fishing effort. Mar. Fish. Rev. **53**: 1–10.

© 2002 NRC Canada

Appendix A

Definitions

St	Stock
S	Total number of stocks
y	Year
a	Age
A	Total number of age-classes for stock St
fl	Fleet
BH1(St), BH2(St)	Parameters of the Beverton–Holt stock–recruitment relationship
$C(\mathrm{St,fl},y,a)$	Catch in number by stock, fleet, age, and year
$E(\mathrm{fl},y)$	Fishing effort by fleet and year
$F_{\mathrm{catch}}(\mathrm{St,fl},y,a)$	Total fishing mortality by stock, fleet, age, and year
$F_{\mathrm{disc}}(\mathrm{St,fl},y,a)$	Discard fishing mortality by stock, fleet, age, and year
$F_{\mathrm{land}}(\mathrm{St,fl},y,a)$	Landing fishing mortality by stock, fleet, age, and year
$F_{\mathrm{VPA}}(\mathrm{St},y,a)$	Total fishing mortality assessed in the Virtual Population Analysis by stock, year, and age
$L(\mathrm{St},y,a)$	Body length-at-age by stock and year
$L_{50\%\mathrm{Disc}}(\mathrm{St})$	Body length at which 50% of the fish caught are discarded by stock
$L_{75\%\mathrm{Disc}}(\mathrm{St})$	Body length at which 75% of the fish caught are discarded by stock
$\mathrm{Mat}(\mathrm{St},y,a)$	Proportion of fish mature by stock, year, and age
$N(\mathrm{St},y,a)$	Population number by stock, year, and age
$P(\mathrm{St,fl},y)$	Sale price by stock, fleet, and year
$q(\mathrm{St,fl},y)$	Catchability by stock, fleet, and year
$R(\mathrm{St},y)$	Recruitment by stock and year
$\mathrm{REV}(\mathrm{fl},y)$	Revenue by fleet and year
$\mathrm{SEL}(\mathrm{St,fl},y,a)$	Gear selection by stock, fleet, year, and age
$\mathrm{SSB}(\mathrm{St},y)$	Spawning stock biomass by stock and year
$W(\mathrm{St},y,a)$	Mean weight of fish by stock, year, and age
$Y(\mathrm{St,fl},y)$	Catch in weight by stock, fleet, and year
$Y_{\mathrm{land}}(\mathrm{St,fl},y)$	Landings in weight by stock, fleet, and year
$Z(\mathrm{St},y,a)$	Total mortality by stock, age and year
$\alpha_{\mathrm{bycatch}}(\mathrm{fl},y)$	Percentage of revenue due to other stocks not modelled by fleet and year
$\epsilon_{\mathrm{p}}(\mathrm{St,fl},y)$	Normally distributed positive factor depicting random variability in sale price by stock, fleet, and year
$\epsilon_{\mathrm{q}}(\mathrm{St,fl},y)$	Normally distributed positive factor depicting random variability in catchability by stock, fleet, and year
$\epsilon_{\mathrm{SR}}(\mathrm{St},y)$	Lognormally distributed positive factor depicting random variability in recruitment by stock and year
$\epsilon_{\mathrm{TF\text{-}Year}}(\mathrm{St},y)$	Normally distributed positive factor depicting the year effect in terminal F in VPA by fleet and year
$\epsilon_{\mathrm{TF\text{-}Age}}(\mathrm{St},y)$	Normally distributed positive factor depicting the age group effect in terminal F in VPA by fleet and year
$W_{\epsilon\text{-Year}}$	Weight of the year effect in the terminal F in VPA

Additional equations of the biological, harvest, and operational models

$$\text{(A1)}\quad \begin{cases} N(\mathrm{St},y,0) = R(\mathrm{St},y) \\ N(\mathrm{St},y,a) = N(\mathrm{St},y-1,a-1)\exp[-Z(\mathrm{St},y-1,a-1)], \\ \qquad\qquad \text{for } a \in [2,\ A-1] \\ N(\mathrm{St},y,A) = N(\mathrm{St},y-1,\ A-1)\exp[-Z(\mathrm{St},y-1,A-1)] \\ \qquad\qquad + N(\mathrm{St},y-1,\ A)\exp[-Z(\mathrm{St},y-1,A)] \end{cases}$$

$$\text{(A2)}\quad \mathrm{SSB}(\mathrm{St},y) = \sum_{a=1}^{A} \mathrm{Mat}(\mathrm{St},y,a)W(\mathrm{St},y,a)N(\mathrm{St},y,a)$$

$$\text{(A3)}\quad R(\mathrm{St},y) = \frac{\mathrm{BH1(St)}}{1 + \mathrm{BH2(St)} \times \mathrm{SSB}(\mathrm{St},y-1)}\epsilon_{\mathrm{SR}}(\mathrm{St},y)$$

$$\text{(A4)}\quad F_{\mathrm{catch}}(\mathrm{St,fl},y,a) = E(\mathrm{fl},y)\mathrm{SEL}(\mathrm{St,fl},y,a) \times q(\mathrm{St,fl},y) \times \epsilon_q(\mathrm{St,fl},y)$$

$$\text{(A5)}\quad \begin{cases} \mathrm{Dis}(\mathrm{St,fl},y,a) = 1 - \dfrac{1}{1+\exp(\mathrm{Dis1(St)} + \mathrm{Dis2(St)}L(\mathrm{St},y,a))} \\ F_{\mathrm{disc}}(\mathrm{St,fl},y,a) = F_{\mathrm{catch}}(\mathrm{St,fl},y,a)\mathrm{Dis}(\mathrm{St,fl},y,a) \\ F_{\mathrm{land}}(\mathrm{St,fl},y,a) = F_{\mathrm{catch}}(\mathrm{St,fl},y,a) - F_{\mathrm{disc}}(\mathrm{St,fl},y,a) \end{cases}$$

with

$$\text{(A6)}\quad \begin{cases} \mathrm{Dis1(St)} = \ln(3)L_{50\%\mathrm{Disc}}(\mathrm{St}) \,/\, (L_{75\%\mathrm{Disc}}(\mathrm{St}) - L_{50\%\mathrm{Disc}}(\mathrm{St})) \\ \mathrm{Dis2(St)} = \ln(3) \,/\, (L_{75\%\mathrm{Disc}}(\mathrm{St}) - L_{50\%\mathrm{Disc}}(\mathrm{St})) \end{cases}$$

$$\text{(A7)}\quad F_{\mathrm{VPA}}(\mathrm{St},y-1,a) = F(\mathrm{St},y-1,a) \times \frac{\epsilon_{\mathrm{TF-Year}}(\mathrm{St},y-1)\mathrm{W}_{\epsilon\text{-year}} + \epsilon_{\mathrm{TF-Age}}(\mathrm{St},a,y-1)}{(\mathrm{W}_{\epsilon\text{-year}} + 1)}$$

$$\text{(A8)}\quad \begin{cases} C(\mathrm{St,fl},y,a) = \dfrac{F_{\mathrm{catch}}(\mathrm{St,fl},y,a)}{Z(\mathrm{St,fl},y,a)} \\ \qquad\qquad \times [1 - \exp(-Z(\mathrm{St,fl},y,a)]N(\mathrm{St},y,a) \\ Y(\mathrm{St,fl},y) = \displaystyle\sum_{a=1}^{A} C(\mathrm{St,fl},y,a)W(\mathrm{St},y,a) \end{cases}$$

$$\text{(A9)}\quad \mathrm{REV}(\mathrm{fl},y) = \left(\sum_{\mathrm{St}=1}^{S} Y_{\mathrm{land}}(\mathrm{St,fl},y)P(\mathrm{St,fl},y)\epsilon_{\mathrm{p}}(\mathrm{St,fl},y)\right) \times [1 + \alpha_{\mathrm{bycatch}}(\mathrm{fl},y)]$$

© 2002 NRC Canada

Diffusion of fish from a single release point

Claus R. Sparrevohn, Anders Nielsen, and Josianne G. Støttrup

Abstract: In a field experiment, 3529 turbot (*Psetta maxima*) were released in order to estimate and describe the movements of hatchery-reared fish by applying diffusion theory. After liberation, the development of the population density was estimated during the following 9 days, and from that, the rate of diffusion and the advection were determined. Two approaches were followed to describe the data: a normal distribution approximation (NDA) model and a partial differential equation (PDE) model. In the latter, it was possible to include the effect of sampling. The two models gave similar results, indicating that the sampling of fish during the experiment did not have any detectable effect on the population density. The activity of the released turbot resulted in an individual daily displacement of 151 m·day^{-1}, except for the first 2 days at liberty, where the displacement was estimated to be considerably lower. Advection was significant and was related to the displacement of the water body. Further, it was possible to estimate the postrelease mortality as 14%·day^{-1} and the catchability of the turbot when caught with a young fish trawl as 28%.

Résumé : Dans une expérience sur le terrain, 3529 turbots (*Psetta maxima*) ont été relâchés dans le but d'estimer et de décrire les déplacements de poissons élevés en pisciculture d'après la théorie de la diffusion. Après la libération, l'évolution de la densité de la population a été suivie pendant 9 jours; par la suite, le taux de diffusion et l'advection ont été déterminés. Deux approches ont été utilisées pour décrire les données, un modèle d'approximation de la distribution normale (NDA) et un modèle d'équation différentielle partielle (PDE); il a été possible d'inclure dans ce second modèle les effets de l'échantillonnage. Les deux modèles donnent des résultats similaires et indiquent que l'échantillonnage des poissons durant l'expérience est resté sans effet décelable sur la densité de la population. L'activité des turbots relâchés a produit un déplacement journalier individuel de 151 m·jour^{-1}, sauf pendant les deux premiers jours de liberté où le déplacement estimé a été beaucoup moindre. L'advection était importante et variait en fonction du déplacement de la masse d'eau. De plus, il a été possible d'évaluer la mortalité après la libération à 14 %·jour^{-1} et la capturabilité des turbots par un chalut pour jeunes poissons à 28 %.

[Traduit par la Rédaction]

Introduction

When releasing cultured fish into a natural habitat, it is crucial to analyze the speed and direction at which these newly released individuals colonize the habitat. This is important because the dispersal into the area will influence the density as well as the numbers of prey and predators that the introduced fish will encounter. In addition, one might want to know which factors (i.e., the hydrographic environment or migratory behavior) influence advection.

One very successful way of modeling movements of living organisms has been to apply diffusion theory. A central parameter in diffusion models is the rate at which the population diffuses into the environment (D), which can be interpreted as a result of movements made by each single organism following a Brownian motion. One way of deriving the Brownian motion is as the limit of a random walk. Let τ be the time between two steps and δ be the length of each step in a random walk. If we let $\tau,\delta \to 0$ in such a way that $(\delta^2/\tau) \to (\sigma^2/4)$, then we get a Brownian motion with variance parameter σ^2. The resulting diffusion model at population level will have a diffusion coefficient of $D = \sigma^2/2$. If the probability of stepping in one direction is ε greater than the probability of stepping in the other direction and $\lim_{\delta,\tau,\varepsilon\to 0} \varepsilon\delta/\tau = \alpha$, then we get a Brownian motion with advection α. The assumption that each individual organism follows a Brownian motion can be relaxed in several ways without losing the application of the diffusion model at the population level (Okubo 1980). For instance, whether the steps of each individual are correlated in short time intervals is of minor importance, the key assumption is that the individuals move independently of each other.

When analyzing movement of individuals and applying diffusion models, it is crucial to address the problem of spatial scaling (Levin 1992). One can view the movement on a small spatial scale and analyze the nature and dispersal range of individual organisms (e.g., Kareiva and Shigesada 1983; Viswanathan et al. 1996). Another approach is to look at a larger spatial scale and analyze the diffusion of populations (Kareiva 1983; Andow et al. 1990; Sibert et al. 1999), where a major part of the work on the application of diffusion theory to natural events has been to analyze the speed at which invading animals colonize new habitats (e.g., Skellam 1951; Lubina and Levin 1988).

In fisheries biology, the main interest concerning move-

Received 25 October 2001. Accepted 15 April 2002. Published on the NRC Research Press Web site at http://cjfas.nrc.ca on 14 June 2002.
J16590

C.R. Sparrevohn.[1] Danish Institute for Fisheries Research, North Sea Centre, Postbox 101, DK-9850 Hirtshals, Denmark.
A. Nielsen. Department of Mathematics and Physics, The Royal Veterinary and Agricultural University, Thorvaldsensvej 40, DK-1871 Frederiksberg C, Denmark.
J.G. Støttrup. Danish Institute for Fisheries Research, Charlottenlund Castle, DK-2920 Charlottenlund, Denmark.

[1]Corresponding author (e-mail: crs@dfu.min.dk).

 DOI: 10.1139/F02-059 © 2002 NRC Canada

ments of marine fish has been on a large scale, where the focus has been on migrating species and the mobility of exploited stocks. Much effort has been devoted to a descriptive approach of evaluating the migratory behavior of fish and fish stocks in order to identify spawning, nursery, and feeding areas. Some studies, though, have been dealing with complex models, such as the advection–diffusion–reaction model applied to data on tagged skipjack tuna (*Katsuwounus pelamis*) (Sibert et al. 1999). Further, most studies have been based on data from traditional capture–recapture experiments, but in recent years experiments have also been based on data gathered from data storage tags (DST) (e.g., Metcalfe and Arnold 1997).

Most work focusing on large scale movements of fish and fish stocks has been based on capture–recapture experiments where the time and distance between release and recapture typically is big. As a consequence of that, although known to be an important factor in the coexistence of species (Levin et al. 1984) and the interactions between fish stocks (Rose and Leggett 1990; Neuenfeldt 2002), small scale movement has been neglected.

In this study we present an investigation on small scale diffusion in a natural environment. In mid-May 2001, a total of 3529 turbot (*Psetta maxima*) between 7 and 8 cm in length were released in a homogeneous coastal area. For the following 9 days, the released turbot were recaptured in order to estimate the resulting population density. We decided to sample and analyze our data in one dimension only, i.e., only the distance parallel to the shore was considered. This unique dataset carried the foundation for present analysis, where the primary objective was to estimate the rate at which the released turbot dispersed into the habitat in addition to analyzing the interaction between hydrographic properties and advection. Further, as a result of the experimental design, we were able to estimate the mortality and in addition the catchability of the released turbot when caught with a young fish trawl. Two models were applied to describe the data: an easily implemented normal distribution approximation (NDA) model and a more complex partial differential equation (PDE) model. With the latter, it was possible to include any effect from sampling on the distribution.

Materials and methods

Location and experimental design

Begtrup Vig, a small bay located near Århus, Denmark, was the chosen site for this experiment. This bay was found to be suitable because the bottom was exclusively sand to a depth of approximately 4 m, which corresponded to 400 m from the shoreline, and therefore it was easy to fish with a young fish trawl. Further, the bay was a natural habitat for turbot with a small wild population. The release position was central in the bay (Fig. 1). In the western direction, the sand area stretched to 1300 m from the release point. Beyond this point, a large eelgrass (*Zostera marina*) belt made it impossible to fish. In the eastern direction, larger stones at a distance approximately 1100 m from the release site delimited the survey area.

Turbot of an average size between 7 and 8 cm were purchased from a commercial fish farm. Fifteen days before liberation, turbot were sorted at the fish farm to ensure as narrow a length distribution as possible and were tagged with external individually identifiable T-bar tags. They were not fed for 2 days before release to ensure empty stomachs. The turbot were transported at 11.5°C from the fish farm to the release site by truck. At the time of release the temperature in Begtrup Vig was 17°C. A total of $N_{0,0} = 3529$ was released at 18:00 ($t = 0$) at 0.5 m depth. Fishing for the released turbot started the next morning and continued for the next 9 days with a varying number of hauls per day. Every fishing day started with one haul parallel to the coast at the 6 m bathometer line. The duration of these parallel hauls was 10 min with equal time devoted east and west of the release site. The purpose of this haul was to ensure that it was appropriate to end the following hauls, which were perpendicular to the coast at a depth of 6 m. For the rest of the day, only hauls perpendicular to the coast were conducted. These hauls all started at the shore or as close to the shore as possible and were towed to a depth of 6 m. The intention was to maintain a towing speed of 0.8 knots, but problems with maintaining the direction were encountered when the wind was stronger than 5 $m \cdot s^{-1}$, from either the east or the west. Thus, on a few occasions a compromise was made between increasing the speed to 1 knot and deviating from a 90° angle from the coastline. This was only a problem towards the end of the survey, i.e., days 8 and 9. The trawl used was a young fish trawl with a total opening of 4.5 m. For a more detailed description see Støttrup et al. (2002).

The distance of the haul from the release position was not chosen at random but was fixed to sampling distances, about 0, 1, and 2 times the predicted standard deviation of the population density. This strategy was chosen to optimize the information about the population density with a limited number of hauls (see Appendix A). Additional hauls were chosen at random but within the area where 90% of the released turbot were expected.

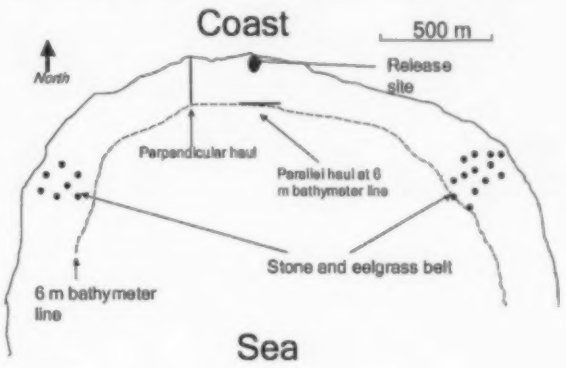

Fig. 1. A schematic representation of the investigation area. As no turbot were caught in the perpendicular hauls at the 6 m depth, they were mainly assured to spread out parallel to the coast. The data used in the analysis were collected with the perpendicular hauls. The investigation area was delimited by stone and eelgrass belts in the eastern and western direction.

Stomach analysis

A subsample of the total catch of tagged turbot was taken for later stomach analysis in the laboratory. The remaining

© 2002 NRC Canada

fish were liberated at a depth of 1 m in the middle of the trawl track. Towards the end of the survey the entire catch was sampled because of low catches. In the laboratory, stomachs were analyzed to determine if the fish had begun feeding on natural prey. All fish with traces of food items in their stomach were defined as fish that had started feeding.

Model and data handling

Let $x_t^{(i)}$ denote the x position of the ith fish at time $t > 0$. Assuming that the fish are independent and that the movement of each fish can be approximated by a biased Brownian motion, where $B_t^{(i)}$ is a normalized Brownian motion, then

$$(1) \quad x_0^{(i)} = 0 \text{ and } \mathrm{d}x_t^{(i)} = \alpha \mathrm{d}t + \sigma \mathrm{d}B_t^{(i)}$$

The key assumption of independent movement is difficult to confirm, but to our knowledge, social behavior, schooling, or synchronization in the swimming activity of turbot has never been observed or reported except during the spawning season.

Normal distribution approximation

Assuming that the effect of fishing is negligible, the density of the stock at some time $t > 0$ can be described as the density of a normal distribution $\varphi_{\alpha t,\sigma^2 t}$ with mean αt and variance $\sigma^2 t$. The expected number of tagged fish in a trawl width w around a position p at time $t > 0$ is denoted as follows:

$$(2) \quad \overline{N}_{w,p,t} = E(N_{w,p,t}) = N_{0,0}\int_{p-w/2}^{p+w/2} \varphi_{\alpha t,\sigma^2 t}(u)\mathrm{d}u = N_{0,0}\left(\Phi\left(\frac{p+w/2-\alpha t}{\sqrt{\sigma^2 t}}\right) - \Phi\left(\frac{p-w/2-\alpha t}{\sqrt{\sigma^2 t}}\right)\right)$$

where Φ is the distribution function of a normal distribution and $N_{0,0}$ is the number of fish initially released. The expected catch ($\overline{C}$) is the fraction $q \in (0,1)$ of the expected number of fish that has survived to time t that can be caught:

$$(3) \quad \overline{C}_{w,p,t} = q\overline{N}_{w,p,t}$$

If the standard deviation of the distribution of the tagged fish $\sqrt{\sigma^2 t}$ is large compared to the trawl width, then we can assume that the number of caught fish follow a Poisson distribution:

$$(4) \quad C_{p,t} \sim \mathrm{Pois}(q\overline{N}_{w,p,t}(\alpha,\sigma))$$

Another approximation that is also valid if the standard deviation is large compared to the trawl width is

$$(5) \quad \overline{N}_{w,p,t} \approx N_{0,0} w \varphi_{\alpha t,\sigma^2 t}(p)$$

This can be useful if it is too time consuming to evaluate Φ.

The negative log likelihood function of the observed catches (c) given the parameter values is given by

$$(6) \quad l(\underline{c};q,\alpha,\sigma) = \sum_{(p,t)} (\log(c_{p,t}!) + q\overline{N}_{w,p,t}(\alpha,\sigma) - c_{p,t}\log(q\overline{N}_{w,p,t}(\alpha,\sigma))) \propto \sum_{(p,t)} (q\overline{N}_{w,p,t}(\alpha,\sigma) - c_{p,t}\log(q\overline{N}_{w,p,t}(\alpha,\sigma)))$$

Partial differential equation

Let us again assume the x position of each fish to follow eq. 1 and to be independent. The development of the stock density can be described by a partial differential equation (Okubo 1980):

$$(7) \quad \frac{\partial}{\partial t} N_{x,t} = -\alpha \frac{\partial}{\partial x} N_{x,t} + \frac{\sigma^2}{2} \frac{\partial^2}{\partial x^2} N_{x,t}$$

and $N_{\cdot,0} = 1_{\{0\}} N_{0,0}$. This model is exactly the same as the NDA model if we simply solve the equation.

Besides solving the PDE model analytically where the solution is the NDA model, an equation like eq. 7 can be solved numerically by iterating forward in time from the initial condition $N_{\cdot,0} = 1_{\{0\}} N_{0,0}$. This way of solving a PDE model can be used to incorporate the effect of fishing into the solution. Each time the solution scheme passes a time point where catch–release takes place, we simply update the solution accordingly. If a large fraction of the total number of fish are caught each day, we should include this information in the model, even though we re-release the fish we catch at the same position. From the solution of eq. 7, the expected number of tagged fish in a trawl width w around a position p at time $t > 0$ can be estimated. This number is denoted $\tilde{N}_{w,p,t}$.

The negative log likelihood is derived as before:

$$(8) \quad l(\underline{c};q,\alpha,\sigma) \propto \sum_{(p,t)} (q\tilde{N}_{w,p,t}(\alpha,\sigma) - c_{p,t}\log(q\tilde{N}_{w,p,t}(\alpha,\sigma)))$$

Numerical solution of the PDE model

Because the numerical solution scheme is needed as part of an optimization routine, it is very important that it is efficient. It may be necessary to evaluate the solution hundreds of times. A relatively fine spatial resolution of $\Delta x = 1$ m was chosen because the trawl is only 4.5 m wide. The time resolution was chosen to be 1 min.

Finite-difference schemes are frequently used to solve differential equations like eq. 7 (e.g., Sibert et al. 1999) and are efficient if the (approximate) solution is needed for every grid point. Several finite-difference schemes were implemented, but it became evident that it was too time consuming with the desired resolution. Fortunately, the solution in every grid point is not necessary. To optimize the likelihood, it is sufficient to know the solution in catch points at catch times. This is used in the following solution scheme.

The solution scheme needs to keep track of every single discrete impact to the system, denoted as impulses. An impulse is a set of three parameters $\mathrm{I} = \{n,p,t\}$, where n is the number of fish added to the system (catches are negative), p is the position, and t is the time. The first impulse is the release of the $N_{0,0}$ tagged fish at position $p = 0$ at time $t = 0$, or in other words $\mathrm{I}_0 = \{N_{0,0},0,0\}$. If this impulse was the

© 2002 NRC Canada

only one, we could calculate the solution in every future point from formula 2. This is not the case in our experiment because the catches are additional impacts on the system. The first catch results in a number of impulses equal to the number of spatial grid points covered by the trawl. Each of these impulses is a fraction of the catch proportional to a fraction of the trawl width, which covers the interval multiplied by the population density, known from previous impulses. This implies that the impulses can only be calculated forward in time. After the impulses from the first catch follow the impulses from the first re-release, and so on.

Each of these impulses contributes to the total solution, in any future points, in exactly the same way as the first impulse. The total solution is found as the sum of the contributions from each of the previous impulses. Given the set of impulses I_0, I_1,..., I_I we can calculate the numerical solution in any grid point (p,t) from

$$(9)\qquad \tilde{N}_{\Delta x,p,t} = \sum_{\{i:t>t_i\}} n_i \left(\Phi\left(\frac{(p+\Delta x/2) - p_i + \alpha(t-t_i)}{\sqrt{\sigma^2(t-t_i)}} \right) - \Phi\left(\frac{(p-\Delta x/2) - p_i + \alpha(t-t_i)}{\sqrt{\sigma^2(t-t_i)}} \right) \right)$$

This solution scheme dramatically reduces the calculation time in this example, and the gain will be even greater if the spatial dimension was 2 or higher. The only drawback is that a bit more bookkeeping is required.

Parameterization

For simplicity, in the previous presentation of the models the parameters q,α,σ are assumed to be constant during the 9-day sampling period. This is not a realistic assumption because the hydrographic parameters change during the experimental period and the released turbot adapt to their new environment.

Therefore, to allow changes in these parameters, an NDA model where each of the three parameters is assumed constant during 24-h intervals (counting from release time) was fitted to the data. Hence q_t, α_t, and σ_t are estimated, where $t = 1,...,9$ equals days at liberty. The resulting model, called the full model, corresponds to estimating one normal distribution from each of the 9 days' catches, which produces a total estimation of 27 parameters.

From this full model the goal was to find another model with fewer parameters needed to describe the density distributions. This reduced model was found by testing the hypotheses that advection was zero ($\alpha_t = 0$) and that the variance was the same all (or some) days ($\sigma_1 = \cdots = \sigma_9$). The recaptured part ($q_t$) being connected to the trawl catchability (ρ) and the total mortality (Z) as

$$(10)\qquad q_t = \rho e^{-Zt}$$

was also analyzed, where it was assumed that mortality and catchability are constant. All hypotheses were tested by standard likelihood ratio tests.

Normal distribution approximation vs. partial differential equation

To evaluate if the two models gave identical results, the parameter estimates were compared. This comparison was done only for the reduced model but for all parameters (α_t, σ_t, ρ_t, and Z_t).

Because the NDA model is the solution to the PDE, the differences between these two models does not lie in the basic assumption about diffusion. The main difference is that the PDE model incorporates our interference with the population density. To make the NDA model even simpler, we assumed that the population density does not change between catches taken on the same day. This assumption was not necessary to make the NDA model work, but it made the model very simple and intuitive. Unfortunately, this assumption makes it difficult to compare the estimates from the two models because the population density (and the resulting parameters) estimated from the NDA actually represents an average of several population densities. Therefore, to facilitate a comparison, we chose simply to compare the daily population estimates from the NDA to the population estimates from the PDE at 18:00 each day.

Wind data

Wind data, consisting of eight measurements per day, were purchased from the Danish Institute of Metrology, and from those, the water body displacement (WBD_t) in the east–west direction parallel to this coast was calculated. Because the thickness of the Ekman layer was much larger than the depth at the location, Coriolis forces could be excluded. Hence WBD_t could be calculated as the steady state balance between wind stress and bottom friction with the surface and bottom drag coefficients set equal:

$$(11)\qquad WBD_t = \int_0^t \lambda \sqrt{v^2(s) \cdot |\sin(u(s))| \cdot \rho_a / \rho_w}\, ds$$

Where $\lambda = -1$ or 1 for western and eastern wind, respectively, ρ_a and ρ_w represent the density of the air and water, 1.22 kg·m^{-3} and 1028 kg·m^{-3}, respectively. Wind velocity is v, and wind direction is u. Each wind measurement is denoted by s. The integral was estimated by summing the average between two subsequent wind measurements. Two different estimates of water body displacements were calculated: one using the wind data from the entire day and one using only the wind in the period from 21:00 to 06:00, i.e., during the night. These data were compared with the advection estimates found in the NDA.

Results

No released turbot were caught in any of the hauls towed parallel to the coast at the 6-m depth. During the sampling period, 332 catches were accomplished distributed on 105 hauls perpendicular to the coastline. Fewer than 10 wild turbot of the same length class were caught, which were easily recognized by their darker pigmentation, aside from the lack of a T-bar tag. Out of the total recaptures, 136 were frozen for stomach content analysis in the laboratory. One haul on day 7 where two turbot were recaptured 1030 m west of the release position was excluded in the data analysis. The maximum catch was obtained on the first day, when more than

© 2002 NRC Canada

Fig. 2. Recaptured turbot per day (○) with the density distribution estimated from the full NDA model (solid line). Solid vertical line is the release position. Distance between small broken vertical lines represents 100 m, whereas distance between large broken lines represents 1 km. Day is days at liberty.

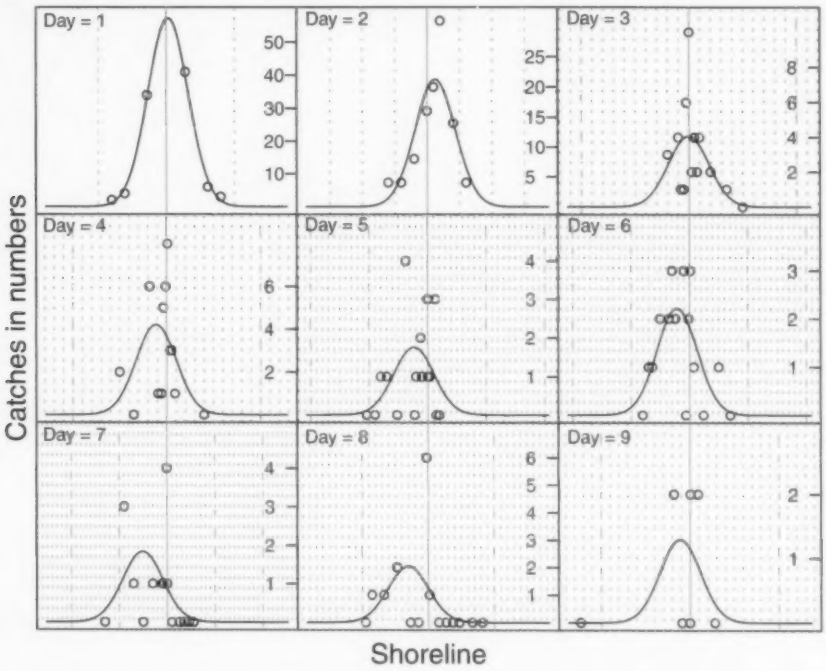

Fig. 3. Estimated values and 95% confidence limits for the parameters describing the normal distribution curves seen in Figs. 2 and 4. The parameters are (*a*) the cumulated standard deviation (σ_t), (*b*) the advection (α_t), and (*c*) the recaptured part (q_t). In the full model, parameters describing one normal distribution curve for each single day were estimated. In the reduced model, σ_t and q_t were restricted as described in the text.

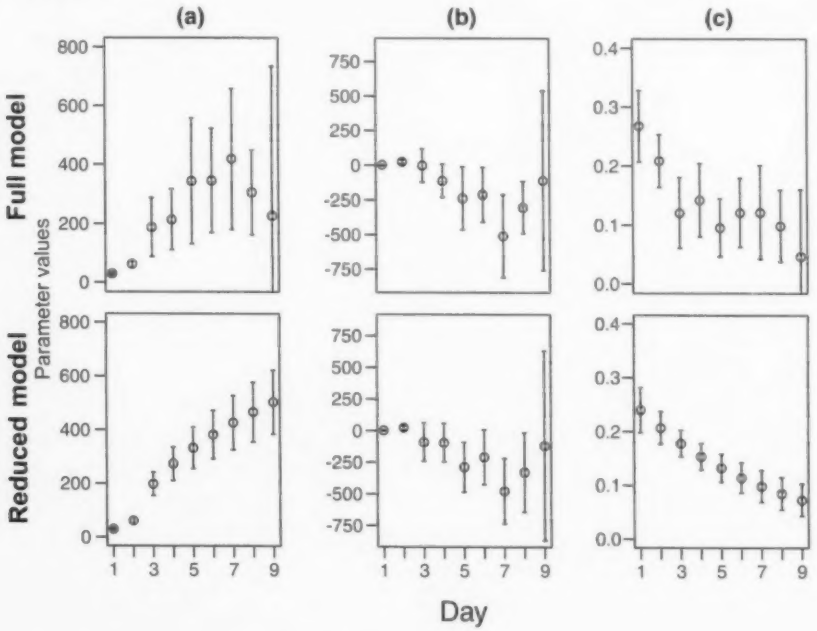

© 2002 NRC Canada

Fig. 4. Recaptured turbot per day (○) with the density distribution estimated from the reduced NDA model (solid line). Solid vertical line is the release position. Distance between small broken vertical lines represents 100 m, whereas distance between large broken lines represents 1 km. Day is days at liberty.

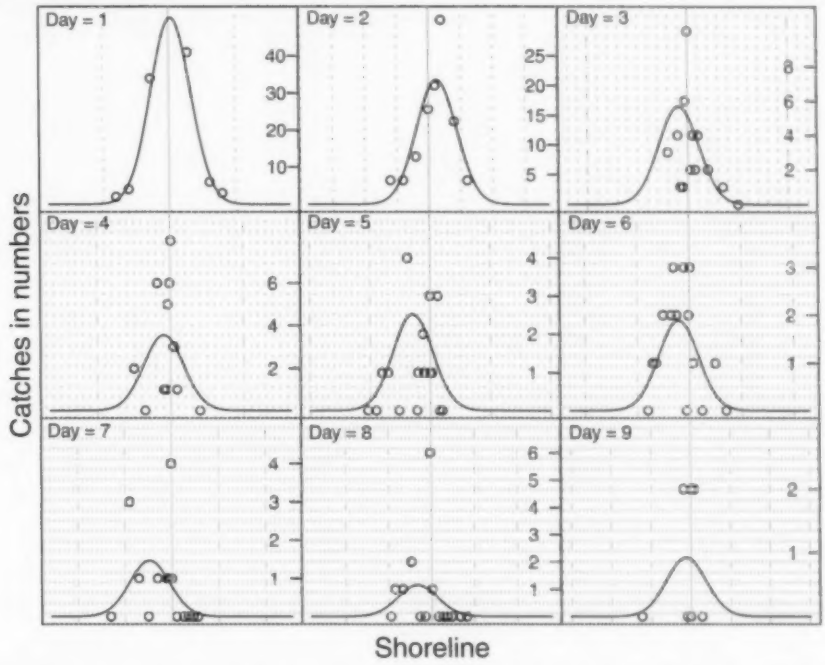

40 individuals were caught in a single haul. During the following period, the daily catches gradually decreased to a minimum on day 9.

The first attempt to analyze the catch data was to fit a full NDA model, meaning that one normal distribution curve was fitted to the recaptures from each day and thus for each day one set of parameters describing a normal distribution curve was estimated (Fig. 2). These parameters are σ_t (m·day$^{-1/2}$), α_t (m·day^{-1}), and q_t (as a fraction) (Fig. 3).

The full model (Fig. 4) was reduced to a model with fewer parameters where the fit was not significantly reduced (likelihood ratio test with p value = 47%). It was possible to describe the spreading of the released turbot using one single σ value for each day from days 3 to 9 (Table 1). It was reasonable to describe q_t with one constant mortality (Z) and one constant catchability (ρ). The catchability was found to be 28%, indicating that 72% had escaped a direct contact with the trawl. The mortality was estimated to be 14%·day^{-1}, which means that at the end of the experimental period only 900 individuals of the initial 3529 would still be alive.

In Table 1, the parameter estimates from both the reduced NDA and PDE are shown. The estimates for mortality (Z) and catchability (ρ) derived from the two models were similar. Further, these two estimates are also determined with the same precision and the two models produced identical values for the standard deviation (σ_t). For the advection estimated, minor differences were found between the two models, but it should be noted that the precision at which this parameter is estimated is quite low and that it is mainly during the last day of sampling that differences are present.

From the model, we estimated the daily average movement for the released turbot (see Appendix B). The average distance moved was estimated to be 24 m·day^{-1} on the first day, 44 m·day^{-1} on the second day, and 151 m·day^{-1} in the remaining days. These values correspond to 320, 587, and 2013 body lengths·day^{-1}, respectively.

The proportion of fish that had started to feed was constant around 22% during the first 2 days at liberty (Fig. 5). After day 2 the percentage that had started to feed increased abruptly to approximately 95% and remained constant during the following days, except during day 8 when only 75% of the recaptured fish had traces of food in their stomachs.

It appears that displacement calculated using night wind only agrees better with the advection found in the reduced NDA model than when displacement is calculated using wind data from the entire day (Fig. 6). However, one should note that the difference between the two estimated WBD_t is a result of an eastern wind during the 2 first days; after that, the trend is similar, independent of whether wind data was taken all day or only during night for the calculation of WBD_t.

Discussion

No released turbot were caught in any of the hauls towed parallel to the coast at the 6 m depth. During the first period after release, liberated turbot are known to remain in shallow waters (Støttrup et al. 2002) and natural turbot of this small size group have only been observed at depths shallower than 2 m (Gibson 1973). Thus, the experimental design with fishing to the 6 m depth bathometer line is considered sufficient to cover the entire depth distribution of the released turbot

© 2002 NRC Canada

Table 1. Daily standard deviation (σ_i), advection (α_i), mortality (Z), and catchability (ρ) estimates from both the normal distribution approximation (NDA) and the partial differential equation (PDE) models.

Parameter name	NDA estimate (95% CI)	PDE estimate (95% CI)
ρ	0.28 (0.22; 0.34)	0.26 (0.2; 0.31)
Z	0.15 (0.09; 0.21)	0.15 (0.08; 0.22)
σ_1	30.20 (26.26; 34.15)	37.04 (32.37; 41.71)
σ_2	54.66 (39.84; 69.47)	59.22 (39.18; 79.26)
$\sigma_3 = \cdots = \sigma_9$	188.85 (143.49; 234.21)	192.03 (107.15; 276.91)
α_1	2.86 (–2.27; 8.0)	5.95 (–1.8; 13.7)
$\alpha_1 + \alpha_2$	25.04 (9.39; 40.69)	30.96 (8.26; 53.66)
$\alpha_1 + \cdots + \alpha_3$	–88.67 (–239.73; 62.38)	–41.49 (–976.45; 893.47)
$\alpha_1 + \cdots + \alpha_4$	–93.44 (–245.44; 58.55)	–127.61 (–509.05; 253.83)
$\alpha_1 + \cdots + \alpha_5$	–286.51 (–482.47; –90.55)	–336.89 (–630.45; –43.33)
$\alpha_1 + \cdots + \alpha_6$	–208.04 (–424.78; 8.7)	–171.57 (–465.85; 122.71)
$\alpha_1 + \cdots + \alpha_7$	–476.91 (–734.45; –219.37)	–571.48 (–981.7; –161.26)
$\alpha_1 + \cdots + \alpha_8$	–329.00 (–641.86; –16.14)	–193.37 (–765.07; 378.33)
$\alpha_1 + \cdots + \alpha_9$	–118.04 (–866.46; 630.38)	–47.29 (–1331.89; 1237.31)

Note: The 95% confidence intervals (CI) are given in parentheses.

Fig. 5. The percentage of turbot with food or traces of food items in their stomach. Day is days after release, and all catches during the day are pooled.

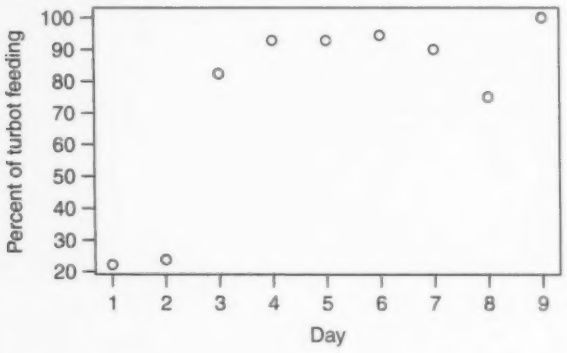

Fig. 6. Water body displacement (WBD) was calculated from wind data. The solid line indicates the displacement when only night wind was included in the calculation and the broken line indicates displacement calculated from the wind for the entire day. Open circles are the advection (α) estimated from the normal approximation model.

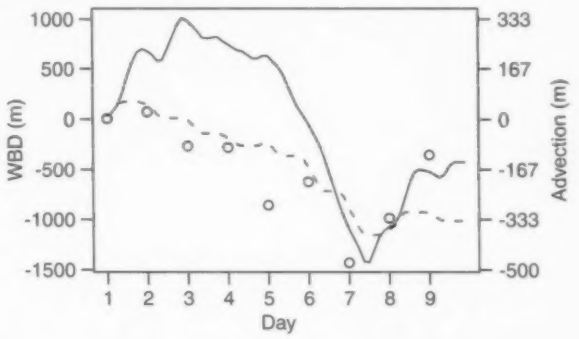

and provides the opportunity to analyze dispersal in one dimension only.

One single haul was treated as an outlier and was excluded from the data analysis. This was a haul from day 7, where two tagged turbot were caught 1030 m west of the release position. A large eelgrass belt located 1300 m from the release position limited the investigation area in that direction and the high catch may have been the result of an accumulation of turbot at the boundary of the sand area.

During the first days after liberation, it was clear that there was a good and highly significant agreement between the normal distribution curve estimated by the full NDA model and the observed data. As time at liberty increased, the visual presentation could give the impression of a decreasing fit of the model, but this was a result of the fact that only integer number of turbot could be caught. The model still described the low catches well.

The reduced model was not significantly worsened compared with the full model, as seen from the likelihood ratio test, but the number of parameters estimated was reduced from 27 to 14. This model revealed a catchability of turbot of 28% when using a young fish trawl. However, the last column on Fig. 3 indicates that the reduced model overestimates the mortality during the last days and underestimates the mortality during the first days.

In this experiment the daily mortality was estimated to be 14%·day^{-1}, which would result in no fish surviving beyond a year. That released turbot do survive beyond a year and can be recaptured in subsequent years has been demonstrated in a previous study (Støttrup et al. 2002). In that study, the mortality estimated from the year following the release and over the subsequent years was 0.15%·day^{-1}. Although the study by Støttrup et al. (2002) was conducted on slightly larger fish, i.e., 15 cm compared with 7–8 cm in this study and size-at-release has been demonstrated to be important for postrelease mortality (Yamashita et al. 1994), the size difference does not account for the large differences in the estimated mortality. These results suggest that there may be

© 2002 NRC Canada

an initial "adaptation" period when the released fish are highly vulnerable and suffer high mortality rates. This is supported by the study of Furuta et al. (1997), who estimated mortality rates of approximately 10%·day^{-1} for juvenile Japanese flounder (*Paralichthys olivaceus*) within the first week after release. Thus, measures to improve survival immediately following the release may help improve the outcome of fish releases.

It appears from this study that the mortality provided by the model is overestimated during the last 6 days at liberty and underestimated during the first 3 days. Apart from this apparent repetitive change in mortality rate with days at liberty, there were other indications that pointed towards the possibility that what was actually observed was a mixture of two different activity levels and hence two different diffusion patterns. This was indicated by the fact that the model was not able to describe the diffusion using one single estimate on σ, but could only reduce the model down to having the same σ from day 3. One other indication of a switch in behavior and diffusion pattern was the sudden increase in the percentage of turbot that had started to feed between the 2nd and the 3rd days of liberty. At this time, a change to a steady diffusion pattern is observed, which could be described by one σ. The event of feeding, the mortality, and the diffusion rate are not necessarily connected but they seem to occur simultaneously.

Advection estimated from the reduced NDA was three times lower than the estimated displacement of the water body. Turbot, being a flatfish, spends a large proportion of its time inactive at the bottom, and during that inactive period, the current will not have any effect on the position of the fish. Hence if the advection of the released fish is a result of the current, it would mean that the fish is only present in the water column one-third of the day. Whether the better fit using the night wind alone to describe the WBD is a result of the turbot being more active during night or a result of a lower activity level during the first 2 days is difficult to tell. It is known that other flatfish species increase their activity level during dusk and dawn (Gibson et al. 1998), but the difference might well be a result of lower postrelease activity caused by stress. The constant speed at which the turbot dispersed after day 3 would, under the assumption that they were active one-third of the day, be 0.07 body lengths·s^{-1} if they had moved in a straight line between release and recapture position. This is not a realistic swimming speed, because flatfish are negatively buoyant and the energy needed to lift the body from the bottom results in uneconomical swimming speeds below 0.6 body lengths·s^{-1} (Priede and Holliday 1980). Further, Priede and Holliday (1980) estimated the optimal swimming speed to be around 1.2 and 1.6 body lengths·s^{-1} at 5 and 15°C, respectively. Hence, assuming a swimming speed of 1 body length·s^{-1} and that turbot move in a straight line, the resulting daily time spent in the water column from day 3 would be approximately 35 min. Juvenile Japanese flounder of the same size class as the turbot used in this experiment fed on mysis, which was also the main diet for turbot in our release. They were observed to increase their swimming activity as the level of hunger increased by swimming for a longer period in the water column after an attack on a prey (Miyazaki et al. 2000).

There were only minor differences between the ρ and Z values estimated from the NDA and the PDE models. So even though approximately 10% of the released turbot were caught within a 9-day period, this relatively high recapture rate did not result in any detectable effect on the distribution of the released turbot.

This study has shown that applying diffusion theory is a very successful method for modeling movements of living organisms even when applied to small-scale migration experiments. Further, it has been shown that even though the sampling intensity in this experiment was fairly high, it was sufficient to fit an NDA model instead of using the more complex PDE model. It seems as if the dispersal took place in two steps and that the change from one dispersal rate to another happened simultaneous to a change in mortality and to the event of feeding. The current is one factor that may have determined the direction of turbot displacement. These results provide more information needed to ensure a successful stocking of marine fish species. In addition, this type of experiment provides knowledge on postrelease mortality and the catchability of the implemented gear. In the near future, improvements in the capability of data storage tags may provide us with valuable additional knowledge that could be prosperous when combined with data obtained from studies similar to this.

Acknowledgments

A special thanks to Dr. Andy Visser, Dr. Peter Lewy, Dr. Uffe Høgsbro Thygesen, and Professor Ib Michael Skovgaard for valuable discussions. Further, the authors would like to thank Claus Petersen, Jesper Knudsen, and Birtha M. Nielsen for technical assistance.

References

Andow, D.A., Kareiva, P.M., Levin, S.A., and Okubo, A. 1990. Spread of invading organisms. Landscape Ecol. **4**: 177–188.

Furuta, S., Watanabe, T., Yamada, H., Nishida, T., and Miyanaga, T. 1997. Changes in distribution, growth and abundance of hatchery-reared Japanese flounder *Paralichtys olivaceus* released in the costal area of Tottori prefecture. Nippon Suisan Gakkaishi, **63**: 877–885. [In Japanese.]

Gibson, R.N. 1973. The intertidal movements of young fish on a sandy beach with special reference to the plaice (*Pleuronectes platessa* L.). J. Exp. Mar. Biol. Ecol. **12**: 79–102.

Gibson, R.N., Pihl, L., Burrows, M.T., Modin, J., Wennhage, H., and Nickell, L.A. 1998. Diel movements of juvenile plaice *Pleuronectes platessa* in relation to predators, competitors, food availability and abiotic factors on a microtidal nursery ground. Mar. Ecol. Prog. Ser. **165**: 145–159.

Kareiva, P.M. 1983. Local movements in herbivorous insects: applying a passive diffusion model to mark–recapture field experiments. Oceologia, **57**: 322–327.

Kareiva, P.M., and Shigesada, N. 1983. Analyzing insect movements as correlated random walk. Oceologia, **56**: 234–238.

Levin, S.A. 1992. The problem of pattern and scale in ecology. Ecology, **73**: 1943–1967.

Levin, S.A., Cohen, D., and Hastings A. 1984. Dispersal strategies in patchy environments. Theor. Popul. Biol. **26**: 165–191.

© 2002 NRC Canada

Lubina, J.A., and Levin, S.A. 1988. The spreading of a reinvading species: range expansion in the california sea otter. Am. Nat. **131**: 526–543.

Metcalfe, J.D., and Arnold, G.P. 1997. Tracking fish with electronic tags. Nature (London), **387**: 665–666.

Miyazaki, T., Masuda, R., Furuta, S., and Tsukamoto, T. 2000. Feeding behaviour of hatchery-reared juveniles of the Japanese flounder following a period of starvation. Aquaculture, **190**: 129–138.

Neuenfeldt, S. 2002. The influence of oxygen saturation on the distributional overlap of predator (cod, *Gadus morhua*) and prey (herring, *Clupea harengus*) in the Bornholm Basin of the Baltic Sea. Fish. Oceanogr. **11**: 11–17.

Okubo, A. 1980. Diffusion and ecological problems: mathematical models. Springer-Verlag, Berlin, Germany.

Priede, I.G., and Holliday, F.G.T. 1980. The use of a new tilting tunnel respirometer to investigate some aspects of the metabolism and swimming activity of the plaice (*Pleuronectes Platessa* L.). J. Exp. Biol. **85**: 295–309.

Rose, G.A., and Leggett, W.C. 1990. The importance of scale to predator–prey spatial correlations: an example of Atlantic fishes. Ecology, **71**: 33–43.

Sibert, J.R., Hampton, J., Fournier, D.A., and Bills, P.J. 1999 An advection–diffusion–reaction model for the estimation of fish movement parameters from tagging data, with application to skipjack tuna (*Katsuwonus pelamis*). Can. J. Fish. Aquat. Sci. **56**: 925–938.

Skellam, J.G. 1951. Random dispersal in theoretical populations. Biometrika, **38**: 196–218.

Støttrup, J.G., Sparrevohn, C.R., Modin, J., and Lehmann, K. 2002. The use of reared fish to enhance natural populations. A case study on turbot *Psetta maxima* (Linné, 1758). Fish. Res. **1361**: 1–20.

Viswanathan, G.M., Afanasyev, V., Buldyrev, S.V., Murphy, E.J., Prince, P.A., and Stanley, H.E. 1996. Lévy flight search patterns of wandering albatrosses. Nature (London), **381**: 413–415.

Yamashita, Y., Nagahora, S., Yamada, H., and Kitagawa, D. 1994. Effects of release size on the survival and growth of Japanese flounder *Paralichthys olivaceus* in coastal waters off Iwate Prefecture, northeastern Japan. Mar. Ecol. Prog. Ser. **105**: 269–276.

Appendix A

Optimizing the fishing effort

The obvious question is where should we trawl to get most information about the model parameters? In other words, we wish to estimate (q,σ) and need to decide on a number of positions $p_1,\ldots,p_m$.

Frequentist approach

We start by assuming that we know the true parameter values (q_0,σ_0). This may seem unreasonable, but as the experiment progresses we will improve our knowledge about the true parameter values.

To make calculations simple, we used the following approximation to the log likelihood for some fixed time point t_0:

$$\log L(\underline{c}; q, \sigma) \overset{\text{app.}}{\propto} \sum_p (c_{p,t_0} \log(q\varphi_{0,\sigma^2 t_0}(p)) - qN_{0,0} w \varphi_{0,\sigma^2 t_0}(p))$$

We calculate the Fisher information I by

$$I = -E_{q_0,\sigma_0}(D^2_{q,\sigma} \log L(\underline{c}; \theta, p)) = -\sum_p E_{q_0,\sigma_0} \begin{pmatrix} \dfrac{c_{p,t_0}}{q^2} & N_{0,0} w \varphi'_{0,\sigma^2 t_0}(p) \\ \star & \dfrac{c_{p,t_0}(\varphi'_{0,\sigma^2 t_0}(p))^2}{(\varphi_{0,\sigma^2 t_0}(p))^2} + qN_{0,0} w \varphi''_{0,\sigma^2 t_0}(p) - \dfrac{c_{p,t_0}\varphi''_{0,\sigma^2 t_0}(p)}{\varphi_{0,\sigma^2 t_0}(p)} \end{pmatrix}$$

In this case, it is simple to evaluate the mean because I is a linear function of c. We get

$$I = -\sum_p \begin{pmatrix} \dfrac{N_{0,0} w \varphi_{0,\sigma^2 t_0}(p)}{q} & N_{0,0} w \varphi'_{0,\sigma^2 t_0}(p) \\ \star & qN_{0,0} w \dfrac{(\varphi'_{0,\sigma^2 t_0}(p))^2}{\varphi_{0,\sigma^2 t_0}(p)} \end{pmatrix}$$

The covariance V of the parameter estimate is estimated by the inverse of the Fisher information $V = I^{-1}$. Hence we should choose the positions $p_1,\ldots,p_m$ that minimize (some scalar extracts of) V. For instance, if we want to get the most precise estimate of σ, we should choose the points that minimize $V_{2,2}$. For overall optimization, it is often chosen to minimize $|V|$.

Bayesian approach

As seen above, the covariance V is a function of the positions and the parameter values. In the frequentist approach, we simply assumed to know the true parameter values (q_0,σ_0) and then minimized V with respect to the positions.

In the Bayesian approach, we try to express our knowledge (uncertainty) about the parameters in terms of a prior distribution and then minimize the expected variance

© 2002 NRC Canada

$$E_{\text{prior}}\{V(\underline{p}, (q,\sigma))\}$$

with respect to the positions.

As we do not really know the true values of the parameters, this approach may seem more reasonable, but we must keep in mind that we do not know the true distribution of our knowledge either. A more pragmatic view is that the frequentist approach is the special case of the Bayesian approach where the variance of the prior distribution is (close to) zero.

Parameterization

If we try to minimize $|V|$ without any restrictions on $\underline{p}$ we will not be able to find a unique minimum, as any permutation of the elements in $\underline{p}$ will result in the same value of $|V|$. We have to find a different parameterization of the problem.

To further simplify the problem, we will only consider symmetric designs containing the point zero. We choose the following parameterization:

$$p_{\lceil m/2 \rceil} = 0, p_{\lceil m/2 \rceil+1} = \tilde{p}_1, p_{\lceil m/2 \rceil+2} = \tilde{p}_1 + \tilde{p}_2, \ldots, p_m = \sum_{i=1}^{\lfloor m/2 \rfloor} \tilde{p}_i$$

where $\tilde{p}_i > 0$ and $p_{\lceil m/2 \rceil+i} = -p_{\lceil m/2 \rceil-i}$

Appendix B

Calculation of average daily movement

The daily average movement is calculated from the daily standard deviation σ_t under the assumption that the daily advection α_t is zero. Biologically this assumption means that any advection, if present, is caused by passive movement, hence the average movement that we calculate equals the movement caused by active swimming.

The daily average movement is calculated as the mean of absolute distance from the center of the normal distribution with standard deviation equal to the daily standard deviation. In other words, the daily average movement (in metres) is calculated as

$$\int_{-\infty}^{\infty} |x| \varphi_{0,\sigma_t^2 \cdot 1\text{day}}(x)\mathrm{d}x = \sqrt{2/\pi}\,\sigma_t \approx 0.8\sigma_t$$

© 2002 NRC Canada

Measurement error and bias in the maximum reproductive rate for the Ricker model

Daniel G. Kehler, Ransom A. Myers, and Christopher A. Field

Abstract: We investigated the consequences of measurement errors in spawner abundance on the estimation of $\tilde{\alpha}$, the maximum lifetime reproductive rate, in the Ricker spawner–recruit model. This rate is equivalent to the slope at the origin for the Ricker model, which is crucial for the estimation of management reference points. Simulation results indicate that measurement error in spawner abundance does not lead, in general, to an overestimate of $\tilde{\alpha}$, as had been previously thought. Instead, the direction, and to some extent the magnitude, of the bias is related to the range of spawner values, and we provide an analytical explanation for this phenomenon. For stocks that have been heavily exploited and have low spawner values, measurement error tends to result in an overestimate of $\log\tilde{\alpha}$, usually by ≤5%. Less exploited stocks with large spawner values will have their $\log\tilde{\alpha}$ underestimated, commonly by –15 to –25%. Results from data-based simulations indicate that under certain conditions, empirical Bayes estimates for the distributions for $\tilde{\alpha}$ among stocks, i.e., the prior distribution, can still be relatively unbiased in the presence of measurement error.

Résumé : Notre étude analyse les conséquences des erreurs de mesure dans l'abondance des reproducteurs sur l'estimation de $\tilde{\alpha}$, le taux maximum de reproduction durant toute la vie, dans le modèle reproducteurs-recrues de Ricker. Ce taux équivaut à la pente à l'origine du modèle de Ricker, qui est une donnée essentielle pour l'estimation des critères utilisés en gestion. Des résultats de simulations indiquent qu'une erreur de mesure dans l'abondance des reproducteurs ne conduit pas, en général, à une surestimation de $\tilde{\alpha}$, comme on le croyait jusqu'à maintenant. Au contraire, la direction et, jusqu'à un certain point, l'importance de l'erreur sont en relation avec l'étendue des données d'abondance des reproducteurs. Nous fournissons une analyse explicative de ce phénomène. Chez les stocks qui ont subi une forte exploitation et qui ont présentement des abondances de reproducteurs faibles, les erreurs de mesure ont tendance à causer une surestimation de $\log\tilde{\alpha}$, normalement de ≤5 %. Les stocks moins exploités à abondance de reproducteurs plus élevée verront l'estimation de leur $\log\tilde{\alpha}$ sous-estimée de –15 % à –25 %. Les résultats de simulations faites sur des données réelles indiquent que, dans certaines conditions, les estimations empiriques bayésiennes des distributions de $\tilde{\alpha}$ parmi les stocks, i.e. la distribution a priori, peuvent s'avérer relativement peu faussées en présence d'erreurs de mesure.

[Traduit par la Rédaction]

Introduction

In fisheries science, a key problem is predicting recruits (R) from spawners (S). Commonly, a spawner–recruitment relationship is used to model the population dynamics of a fish stock. However, estimated parameters from spawner–recruitment models can be biased if, for example, spawner sizes are not independent of previous spawner–recruit observations (time series bias) (Walters 1990), spawner values are measured with error (Walters and Ludwig 1981), or interannual variability is not random (Armstrong and Shelton 1988). Using biased parameter estimates to make decisions about the management of a fish stock can have serious economic and (or) biological consequences. Time series bias has been explored both empirically (Myers and Barrowman 1995) and analytically (Walters 1990), but bias resulting from measurement error in spawner values is less well understood, and no accepted solution to the problem exists (Quinn and Deriso 1999).

Bias in parameter estimates resulting from measurement error in the independent variable is a well-known problem in regression analysis (Fuller 1987). Methods for generating asymptotically unbiased parameter estimates or estimates with low small sample bias have been developed but require some knowledge of the variance of the measurement error (Stefanski 1985; Fuller 1987). For fisheries data, this information is rarely available.

Our purpose here is to investigate bias resulting from measurement error in the context of the Ricker spawner–recruitment model (Ricker 1954). The Ricker model can be linearized, and assuming lognormal errors, parameter estimation can proceed using ordinary least squares. Let R_t be the recruits

Received 26 November 2001. Accepted 8 May 2002. Published on the NRC Research Press Web site at http://cjfas.nrc.ca on 29 June 2002.
J16628

D.G. Kehler[1] **and C.A. Field.** Department of Mathematics and Statistics, Dalhousie University, Halifax, NS B3H 3J5, Canada.
R.A. Myers. Department of Biology, Dalhousie University, Halifax, NS B3H 4J1, Canada.

[1]Corresponding author (e-mail: kehler@mscs.dal.ca).

 DOI: 10.1139/F02-060 © 2002 NRC Canada

resulting from spawners at time t (S_t). The linearized Ricker function is

$$(1) \qquad \log\left(\frac{R_t}{S_t}\right) = \log\alpha - \beta S_t + \varepsilon_t \quad \text{where} \quad \varepsilon_t \sim N(0,\sigma^2)$$

If we assume that measurement errors in spawner abundance are also lognormally distributed, then the measurement error in S_t enters the model both additively and nonadditively. Thus, results obtained for ordinary regression are unlikely to apply.

Walters and Ludwig (1981) investigated the measurement error problem in the Ricker model in some detail. They dealt with the special case of semelparous life histories when all individuals mature at the same age, typical of some Pacific salmon species. Walters and Ludwig (1981) developed consistent (asymptotically unbiased) estimators for the parameters in the Ricker stock–recruitment function for cases where either the measurement error variance or more simply the ratio of process (environmental) to measurement error variance is known (Ludwig and Walters 1981). There are two main problems with these estimators that restrict their usefulness. First, the estimators performed poorly for short, and hence realistic, time series (less than 20 years). Second, in practice, the measurement error variance is not known for most stocks and the ratio of variances can only be guessed. The biases observed by Walters and Ludwig (1981) may also have been unrealistically high, as the authors realized later that the bias that they observed in the Ricker parameters was partly a time series bias (Caputi 1988). In addition, recruits in year y were estimated as the sum of the catch in that year plus the escapement, i.e., spawners, that produce the next generation of recruits. Thus, measurement errors in spawner stock size affect the estimates of recruitment as well. This may overemphasize the effect of measurement error for most stocks, where spawners are estimated independently of recruits.

Here, we consider the case that is more typical of species other than Pacific salmon, where recruits are estimated from a research survey or from a catch-at-age analysis. In this case, the estimation errors of recruits are completely, or largely, independent of the estimation errors of spawners. We also focus exclusively on the bias that results from measurement error by generating data, where observations in one year are independent of observations in previous years. Note that our model is appropriate for Pacific salmon if the recruits are estimated during a pre-adult life history stage.

Our interest is bias in the α parameter, which describes the slope of the spawner–recruitment curve at the origin and gives the maximum reproductive rate. This slope is used to calculate important management parameters (Myers and Mertz 1998), including steepness, which is commonly used in stock assessments (Hilborn and Walters 1992). However, calculating most management parameters requires a standardization of α into maximum lifetime reproductive rate, $\tilde{\alpha}$. The data on recruitment we use will be standardized to be in the same units as the spawners (Myers et al. 1999). For example, if recruits are originally in units of age-3 recruits and spawners in units of kilograms of spawners, we multiply the recruits by the biomass of spawners produced by one age-3 recruit in the absence of fishing mortality, i.e., $SPR_{F=0}$. Thus, $\tilde{\alpha}$ represents the number of spawners produced by each spawner over its lifetime at low abundance in the absence of fishing. This standardization also allows the units of $\tilde{\alpha}$ to be directly comparable among stocks, permitting the meta-analyses carried out in, for example, Myers et al. (1999) and Myers et al. (2001). For notational convenience, we hereafter refer to $\tilde{\alpha}$ as simply α.

We investigate the problem of bias in α resulting from measurement error using simulations and develop an analytic explanation for the observed bias. We will examine the effect of measurement error bias independently of time series bias (Walters 1985). We return to the important issue of time series bias in the Discussion. Simulating realistic data, however, is not a trivial task. The results of theoretical simulations can be difficult to translate into practical terms, whereas data-based simulations do not always allow the problem to be studied with sufficient generality. We thus used a combination of data-based and theoretical simulations to address the practical import of bias resulting from measurement errors and to examine what attributes of data sets affect this bias.

Methods

Data-based simulations

For the data-based simulations, we used existing spawner and recruit data from 259 stocks comprising 57 species and explored the consequences of adding lognormal and nonrandom measurement error to spawner values. Data sets and their descriptions can be obtained from http://www.fish.dal.ca/welcome.html and are the same data sets used in previous studies (Myers et al. 1999). For a particular stock, s, we added random normal measurement error to log (S):

$$(2) \qquad \log(S) = \log(S) + \delta_t \quad \text{where} \quad \delta_t \sim N(0, \tau_s^2)$$

The difficulty lies in determining an appropriate level for the measurement error variance τ_s^2 for each stock. As we did not know the true measurement error for each stock, we used the residual error variance ($\hat{\sigma}_s^2$) estimated from individual Ricker fits to each of the 259 populations as an upper limit. There are several reasons for believing that $\hat{\sigma}_s^2$ is, on average, the extreme upper limit of the possible measurement error variance. First, the estimated σ_s^2 represents the total unaccounted variability in log(R/S), including both process (environmental) and measurement error. Second, recruitment is often more poorly estimated than spawner abundance, since adult abundance is usually better estimated than juvenile abundance from research surveys (Myers and Cadigan 1993). Third, for longer lived species, there will be several potential estimates of spawner abundance because it will change relatively slowly, while recruitment in one year is often very weakly related to recruitment in previous years. At the extreme, $\tau_s^2 = \sigma_s^2$ if all of the variability in log(R/S) is due to measurement error in log(S) alone. This situation is highly improbable. Instead, τ_s^2 is more likely to be some fraction of σ_s^2. For each stock, four levels of random normal measurement error (τ_s^2) were added to log(S): low ($\tau_s/\hat{\sigma}_s = 0.1$), medium ($\tau_s/\hat{\sigma}_s = 0.3$), high ($\tau_s/\hat{\sigma}_s = 0.6$), and extreme ($\tau_s/\hat{\sigma}_s = 1.0$).

We examined stock assessments for which the standard deviation of the measurement error in spawner abundance (on a log scale) had been estimated (Table 1). These esti-

© 2002 NRC Canada

Table 1. Summary of stock assessments where the standard deviation of the estimation errors of spawner abundance, $\hat{\tau}_s$, could be estimated.

Species	Stock	$\hat{\tau}_s$	$\hat{\sigma}$	Ratio	Method	Source
Herring	North Sea	0.02	0.61	0.033	b	ICES CM 2001ACFM:12
Herring	Irish Sea	0.1	0.41	0.21	m	ICES CM 2001/ACFM:12
Whiting	North Sea	0.056	0.53	0.10	m	ICES CM 2002/ACFM:01
Cod	West of Scotland	0.06	0.52	0.11	m	ICES CM 2002/ACFM:02
Haddock	West of Scotland	0.058	0.873	0.067	m	ICES CM 2002/ACFM:02
Whiting	West of Scotland	0.063	0.394	0.16	m	ICES CM 2002/ACFM:02
Whiting	Irish Sea	0.1	0.436	0.23	m	ICES CM 2002 ACFM:02
Walleye pollock	Eastern Bering Sea	0.14	0.405	0.34	m	Ianelli and Fritz 2001
Walleye pollock	Gulf of Alaska	0.35	1.12	0.31	m	Dorn et al. 2000
Pacific cod	Eastern Bering Sea	0.09	0.616	0.15	s	Thompson and Dorn 2000
Pacific hake	California – British Columbia	0.15	1.29	0.12	m	Dorn et al. 1999

Note: Also given is the standard deviation of the log residuals from the spawner–recruit relationship, $\hat{\sigma}$, and the ratio of the two. The method used to estimate the $\hat{\tau}_s$ is also given, i.e., bootstrap (b), model based (m), or standard error from the sampling statistics of the trawl survey (s) (see text for details). For the analyses from International Council for the Exploration of the Sea (ICES) assessments, we provide the ID number; the assessments may be found at http://www.ices.dk/committe/acfm/acfm.htm.

mates were usually presented as standard errors for the estimated spawner abundances on a yearly basis from which we estimated the median τ_s. Most of the estimates were based on models where the spawning stock biomass is a derived parameter and its standard error is calculated from the covariance matrix of the estimated parameters. These model-based estimates of the measurement error variance depend upon the assumptions of the model being met and are likely to be underestimates of the true measurement error variance. If we use these few stocks as an approximate and conservative guide, the medium ratio of measurement error to residual error appears typical, with the high ratio being a reasonable upper bound.

Assuming that there is normal error in $\log(S)$ is equivalent to assuming lognormal error in S. However, by so doing, we change the expected value of S. If $S = Se\delta$ where $\delta \sim N(0, \tau_s^2)$, then $E[S] = S(e^{\tau_s^2/2})$. If we solve this problem by letting $\delta \sim N(-\tau_s^2/2, \tau_s^2)$, then we are no longer adding zero-mean measurement error on the $\log(S)$ scale. We thus modeled error both ways, where the addition of each level of error was repeated 5000 times for each stock and the relative bias of log α was calculated.

Measurement errors may also be nonrandom if spawner abundances are consistently over- or under-estimated owing to technological or statistical assessment methods. To reflect this possibility, we changed all spawner values by ±5 and ±10%.

Theoretical simulations

For the theoretical simulations, we randomly generated spawner values. Corresponding random recruitment values were generated by adding a lognormal error term to the Ricker model with a fixed α and β. We examined the effects of six factors on the bias in log α resulting from measurement errors in spawner abundance. We considered the effect of log α (six levels), the amount of residual error, σ (six levels), the length of the time series, n (six levels), the range of spawner values (three ranges), the degree of autocorrelation in the measurement errors, ρ (six levels), and four levels for the magnitude of the measurement errors added to spawner values. We chose values of log α and σ to cover the range of the bulk of the observed values from fitting the Ricker model to the 259 stocks used in the data-based simulations. Values for n and ρ were chosen to reflect both worst-case (e.g., $\rho = 0.9$ or $n = 5$) and best-case scenarios (e.g., $\rho = 0$ or $n = 100$) one might expect to see in a fisheries context. The magnitude of measurement error variability was varied by using the same ratios of measurement error standard deviation to residual error standard deviation as in the data-based simulations.

Spawner values were generated from uniform distributions whose ranges were chosen to represent three general scenarios for spawner and recruitment data. In the first case, spawner values were drawn from between 0 and S_{max}; S_{max} is the spawner abundance that results in the maximum possible recruitment in the Ricker model and is given by $1/\beta$ (Hilborn and Walters 1992). This situation represents an exploited population, and one might expect α to be estimated well. Second, spawner values were drawn from between S_{max} and S^*; S^* is the equilibrium spawner biomass where one spawner, over its lifetime, will produce one spawner equivalent and is given by $(\log \alpha)/\beta$ (Hilborn and Walters 1992). In this case, the stock is relatively unexploited, and little information exists to estimate α. Third, we used spawner values between 0 and S^* to represent a stock that has, over time, experienced both heavy and light fishing pressure. Since the range of spawner values is defined in terms of β, the latter becomes a scaling factor and its effect on the bias is not explored.

Measurement errors may be correlated if a mistake in one year's estimate of spawner abundance affects estimates of spawner biomass in subsequent years, as in some age-structured models (Lapointe et al. 1989; Hilborn and Walters 1992) or as a result of errors in estimating natural mortality (Mertz and Myers 1997). To recreate this situation, we let the measurement error be a first-order autoregressive process

$$\delta_t = \rho\delta_{t-1} + Z_t, \quad \text{where} \quad Z_t \sim N(0, \tau_{s,c}^2) \tag{3}$$

with values of ρ (the lag 1 correlation coefficient) between 0.4 and 0.9. As the variance of δ is given by $\tau_{s,c}^2/(1-\rho^2)$, to ensure that the correlated and uncorrelated errors have the same variance ($\tau_{s,c}^2$ and $\tau_{s,uc}^2$, respectively), we let $\tau_{s,c}^2 = (\sqrt{1-\rho^2})\tau_{s,uc}$.

It has been suggested that the degree of measurement error bias is related to the fluctuation in spawner stock size from lowest to highest value (Hilborn and Walters 1992). To

© 2002 NRC Canada

Fig. 1. Relationship between relative bias in log α for an individual stock across different levels of measurement error. Results for (*a*) low (*x*-axis) versus medium (*y*-axis), (*b*) medium (*x*-axis) versus high (*y*-axis), and (*c*) high (*x*-axis) versus extreme (*y*-axis) levels of measurement error are displayed. To ease comparison, the line of equality (45°) and the zero-line on the *x*-axis are displayed.

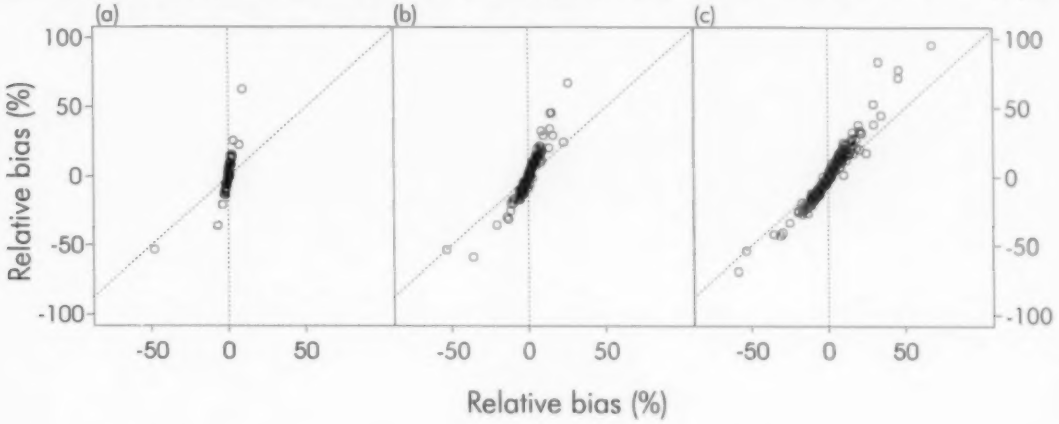

Table 2. Relative bias in $\widehat{\log\alpha}$ estimated from 5000 data-based simulations adding random measurement error to spawner values from 259 stocks as a function of the assumed ratio of the assumed standard deviation of the measurement error to the standard deviation of the log residuals from the Ricker spawner–recruit function.

Ratio	Mean bias	Median bias	% of stocks with bias less than ±5%	% of stocks with bias less than ±10%	% of stocks with bias less than ±20%
Low	–0.1	0.1	98.4	99.6	99.6
Medium	0.6	0.5	81.5	93.4	97.5
High	1.9	1.7	47.3	72.8	92.8
Extreme	3.0	2.4	30.0	50.6	82.7

Note: These estimates provide the correct direction but underestimate the magnitude of the bias; see the Theoretical simulations section for the interpretation of these results.

examine in more detail the role played by the range of spawner values in determining the measurement error bias, we generated data to cover different fractions of the three initial ranges of spawner abundance. Only one value of log α (2.3), σ (0.66), and number of observations (20) was used. In this first case, we generated spawner values between 0 and *p*% of *S**, where *p* ranges from 0 to 100. In the second case, we generated data from *p*% of *S** to *S**, and in the third case, we generated data in the interval $S^*/2 \pm p\%$ of $S^*/2$. We used increments of 10% for *p* in all cases. The third case (and parts of the second) represents a situation where the numbers of spawners have been kept constant, for example, via a fixed escapement policy, as has been used for certain types of Pacific salmon (Quinn and Deriso 1999).

Finally, we used the theoretical simulations to address a potentially serious concern with the data-based simulations. The actual data may already be contaminated by measurement error, and it is not clear whether reliable inferences can be made in this situation. To answer this question, we recreated the addition of measurement error to data already containing measurement error. Using the median values for $\widehat{\log\alpha}$ (2.3) and $\hat{\sigma}$ (0.66) from the 259 stocks, we reran the simulations at the three spawner ranges and four levels of measurement error under four starting conditions: spawner values had already been contaminated with either low, medium, high, or extreme levels of measurement error. To calculate bias, we compared estimates of log α from fits to data where measurement error had been added twice with estimates from data where measurement error had been added once.

For both the data-based and theoretical simulations, relative bias in $\widehat{\log\alpha}$ was calculated as

$$(4) \qquad \frac{\widehat{\log\alpha} - \log\alpha_{true}}{|\log\alpha_{true}|}$$

where $\widehat{\log\alpha}$ is the mean log α estimated from 5000 simulations and $\log\alpha_{true}$ is either (*i*) the parameter value obtained from the Ricker model fit for each stock with no measurement error for the data-based simulations or (*ii*) the predetermined value for the theoretical simulations.

Results

Results for zero-mean additive error on the log scale and mean of 1 multiplicative error on the original scale were almost identical, and we present the former.

© 2002 NRC Canada

Fig. 2. Relative bias in $\widehat{\log \alpha}$ resulting from the addition of measurement error across four ratios of measurement error variance (τ^2) to residual variance (σ^2). The four ratios were low ($\tau/\sigma = 0.1$), medium ($\tau/\sigma = 0.3$), high ($\tau/\sigma = 0.6$), and extreme ($\tau/\sigma = 1.0$). Simulations were carried out while varying four factors for data at each of three spawner ranges: (*a–d*) 0–S^*, (*e–h*) S_{max}–S^*, and (*i–l*) 0–S_{max}. The plotted symbols are numbers corresponding to increasing levels of (*a*, *e*, *i*) log α, (*b*, *f*, *j*) σ, (*c*, *g*, *k*) *n*, and (*d*, *h*, *l*) ρ. Levels for log α were 1.6, 2.3, 2.7, 3.0, 3.21, and 3.55. Levels for σ were 0.16, 0.33, 0.50, 0.66, 0.83, and 1.0. Levels for *n* were 5, 10, 20, 30, 50, and 100. Levels for ρ were 0.4, 0.5, 0.6, 0.7, 0.8, and 0.9.

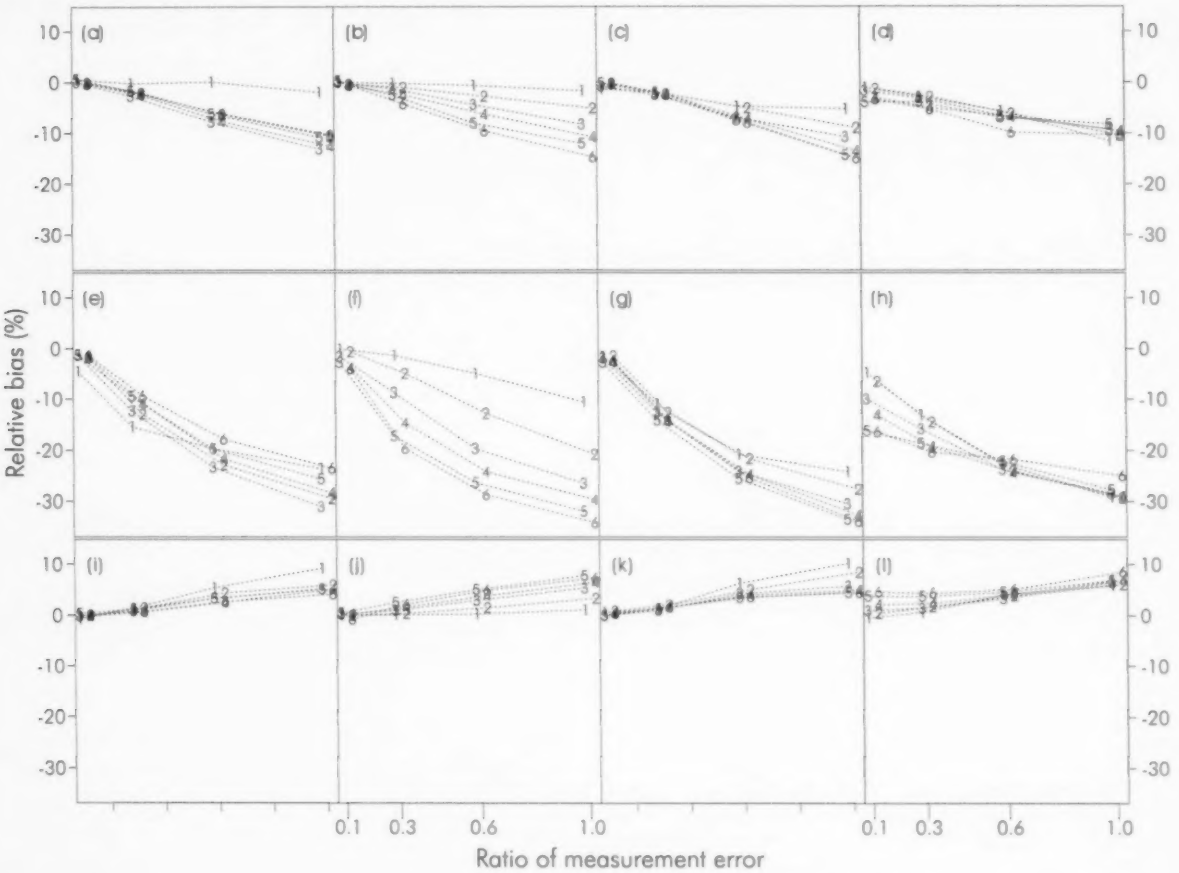

Data-based simulations

Of the 259 stocks used initially, 16 were omitted, as the Ricker model fits resulted in a negative estimate of β and estimates of log α near zero. These estimates are biologically unreasonable, since recruitment approaches infinity as spawner abundance increases. Surprisingly, the direction of the bias in log α was not consistent across stocks. For a particular stock, the estimates of log α were consistently biased positively or negatively across levels of measurement error, with the magnitude of this bias increasing with the error variance. The relative increase in bias was highest when moving from low to medium error and lowest when moving from high to extreme error (Fig. 1). The mean and median bias across all stocks appeared to be near zero or slightly positive for all levels of measurement error (Table 2). To evaluate the seriousness of bias resulting from measurement error, we examine the range of relative biases in log α experienced at each level of measurement error. At low levels of measurement error, the bias in most stocks is negligible. At the medium level, most stocks experience a small bias (±5%). Only at higher levels of measurement error does the bias in more stocks become serious.

If spawner abundances are consistently over- or underestimated by a fixed percentage (nonrandom measurement error), the resulting biases in log α are of roughly the same magnitude. Adding 5 and 10% (on a log scale) to all spawner values resulted in mean biases of –3.8 and –7.4%, respectively (medians were –7.6 and –15.0%). Consistently underestimating spawner abundances by –5 and –10% resulted in mean and median biases of similar magnitude but opposite direction.

Two questions remain. Why do some stocks have a positive bias and others a negative bias in log α? Can results from data-based simulations be used if data are already contaminated by measurement error?

Theoretical simulations

Interestingly, the direction of the bias in log α appears to

© 2002 NRC Canada

Fig. 3. Relative bias in $\widehat{\log\alpha}$ for varying ranges of spawner abundance and four levels of the ratio of measurement error standard deviation to residual error standard deviation. The four ratios were low ($\tau/\sigma = 0.1$) (solid line), medium ($\tau/\sigma = 0.3$) (dotted line), high ($\tau/\sigma = 0.6$) (short-dashed line), and extreme ($\tau/\sigma = 1.0$) (long-dashed line). The three cases are (*a*) $0 - (1 - p)\%$ of S^*, (*b*) $S^*/2 \pm (1 - p)\%$ of $S^*/2$, and (*c*) $p\%$ of S^* to S^*. Points were displaced slightly on the horizontal axis to increase clarity.

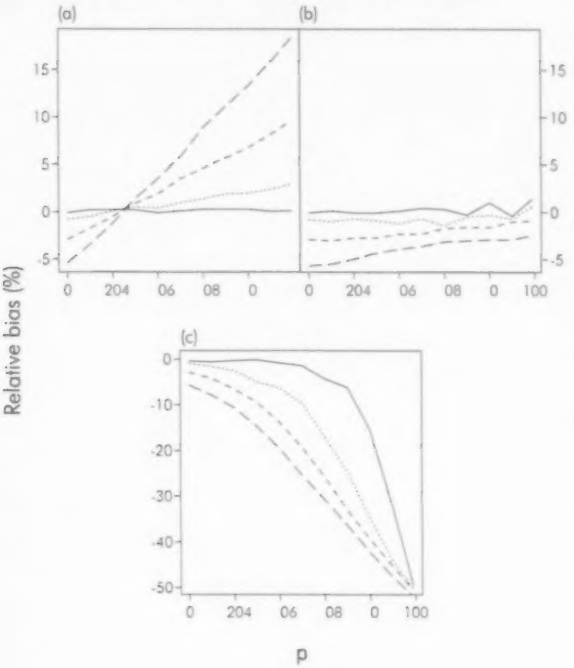

depend upon the range of spawner values (Fig. 2). Across all values of log α, σ, ρ, and *n*, the bias was negative for data in the 0–S^* and S_{max}–S^* ranges and positive in the 0–S_{max} range. There was little variation in the bias across levels of log α, ρ, and *n* (excepting the extreme level of error) relative to the variation in bias across different spawner ranges (Fig. 2). As one might expect, varying σ had the largest effect on the relative biases, since σ determines how much measurement error is actually added. For data in the 0–S^* and S_{max}–S^* ranges, there is no indication that the biases had reached a plateau, and thus, an additional increase in σ would result in even larger biases. For the remaining factors that were varied, there was little difference in bias among the highest levels of these factors, suggesting that the maximum bias had been reached (e.g., Figs. 2*a* or 2*g*). Contrary to expectations, the data sets with fewer observations tended to have smaller biases, with the exception of data with spawner values in the 0–S_{max} range. For data in the 0–S^* and S_{max}–S^* ranges, having between 20 and 100 observations resulted in very similar biases, but sample sizes of 5 and 10 resulted in biases up to half as small. Varying log α and ρ had relatively little effect on the bias in log α, except in two cases. The smallest value of log α resulted in a substantially lower bias for data with spawner values in the 0–S^* range (Fig. 2*a*). This is likely because S^* and S_{max} are very similar when log α is small, and thus, biases for data in the 0–S^* range are closer to biases observed in the 0–S_{max} range. Having a high degree of autocorrelation in the measurement error made little difference except for the low levels of error in the S_{max}–S^* range (Fig. 2*h*). Large negative biases with increasing ρ are possible here, unlike all other simulations with a low ratio of measurement error where biases were very small.

It is clear that the most serious biases occur for data with spawner values in the S_{max}–S^* range, where log α can be underestimated by up to –25% (and up to –35% for the extreme level). Biases also tended to increase at the greatest rate across levels of measurement error for this range of spawner values. For data with spawner values in the 0–S^* and 0–S_{max} ranges, biases were greater than –10 or less than 5%, respectively, for all but the extreme level of measurement error, where biases reached –15 and 11%, respectively.

We also examined all two-way interactions between *n*, log α, ρ, and σ across the three ranges of spawner abundance. In general, the biases across levels of ρ, *n*, and log α increased with increasing σ. Other factors had little effect upon each other and results are not presented.

If we examine the role of the range of spawner abundances more closely, several interesting patterns emerge. The small negative bias present when data are in the 0–S^* range changes to a positive bias once the data are constrained to be between 0 and 80% of S^* (Fig. 3*a*). As a greater proportion of the data are clustered close to the zero spawner abundance, the bias becomes increasingly positive, and the rate of this increase depends upon the magnitude of the measurement error present. When the spawner values are clustered close to S^*, then the bias for all levels of measurement error approaches an apparent maximum bias, for the values of log α and σ used, of approximately –50%, although the rate at which the maximum is approached depends upon the level of measurement error. Interestingly, having spawner values clustered around $S^*/2$ results in relatively small negative biases, with a maximum of –6% for the extreme level of measurement error. It does not appear that the lack of range in the spawner ranges leads to large biases in log α in this situation.

Adding measurement error to data that are already contaminated with measurement error results in an underestimate of the true bias (Fig. 4). There were only a few cases when the initial contamination was relatively unimportant. First, if the initial contamination was small (low ratio of measurement error to residual error), then the underestimate of the true bias was very small. Second, if only a low ratio of measurement error was added subsequent to the contamination, then similarly, the effect of the initial contamination, regardless of the magnitude, was minimal. Third, for data in the 0–S^* range, where σ is low (2/6), the underestimate of the true bias was relatively small, except at the extreme (Fig. 4*a*). For most other cases, however, the underestimate of the true bias was large. The underestimate tended to be larger with increasing σ and for data with spawner values in the S_{max}–S^* range, where the reported bias could be as small as 1/20 of the true bias. For the most likely levels of measurement error (medium to high), observed biases tend to be, on average, roughly half of the true bias.

© 2002 NRC Canada

Fig. 4. Relative bias in $\widehat{\log\alpha}$ resulting from adding measurement error to spawner values already contaminated by varying degrees of measurement error. Results are displayed for data at each of three spawner ranges: (*a–c*) 0–S^*, (*d–f*) S_{max}–S^*, and (*g–i*) 0–S_{max}. Simulations were also run at three levels of residual error σ, (*a*, *d*, *g*) 0.33, (*b*, *e*, *h*) 0.5, and (*c*, *f*, *i*) 1, with log α = 2.3, *n* = 20, and ρ = 0. In each panel, the true relative bias (bias resulting from adding measurement error to uncontaminated spawner values) is indicated by circles. Also indicated are biases resulting from adding four levels of measurement error to data already containing low (l), medium (m), high (h), and extreme (e) levels of measurement error. These levels of measurement error correspond to ratios of measurement error to residual error used in other simulations (see Fig. 2). Points were displaced slightly on the horizontal axis to increase clarity.

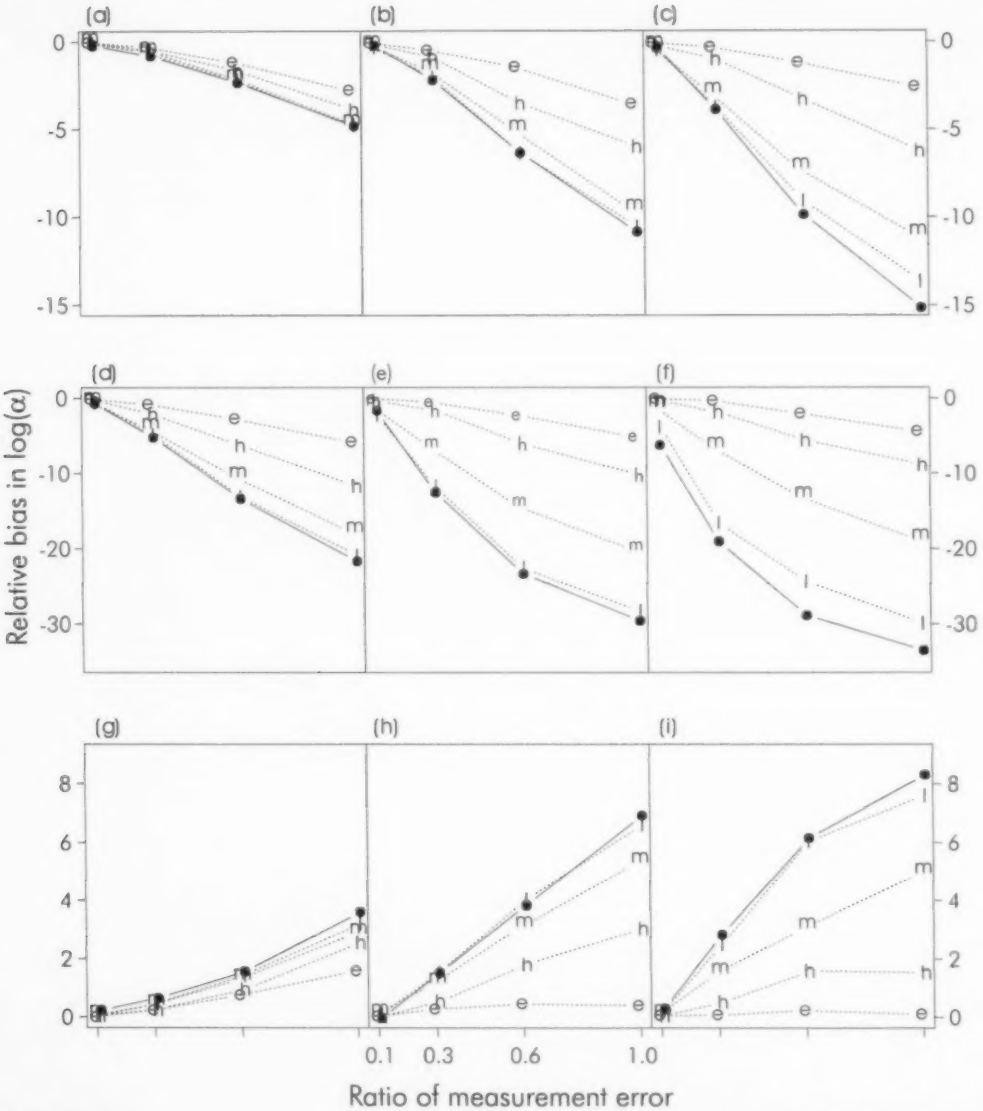

Analytical explanation

Why does the range of spawner values appear to be important in determining both the magnitude and direction of the bias in α? The nature of the bias can be understood by plotting log survival against spawner abundance and examining the effect of the addition of measurement error (Fig. 5). Points at low spawner abundance are translated more vertically, whereas points at high spawner abundance tend to be translated more horizontally. The slope of the translation is a function of the spawner value (S) and the measurement error added (δ) and can be expressed as

$$\text{slope} = -\frac{1}{S\left(1+\frac{1}{2}\delta^2+\frac{1}{6}\delta^3+\right)} \quad (5)$$

(see Appendix A for details).

Thus, a first-order approximation of the slope of the trans-

© 2002 NRC Canada

Fig. 5. Translation of simulated data points (solid circles) after addition of a high level of measurement error (open circles) for three ranges of data: (*a*) 0–S^*, (*b*) S_{max}–S^*, and (*c*) 0–S_{max}. The fitted lines for the log Ricker model for the original data (solid line) and data with measurement error added (dotted line) are also indicated.

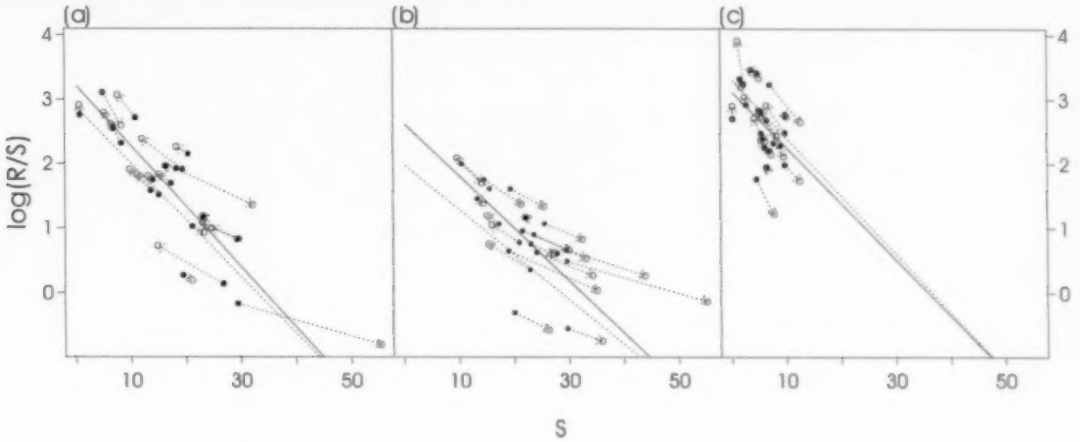

Fig. 6. Plot of the approximate slope of the translation of points (on the log survival scale) due to the addition of measurement error in spawner values. The Ricker function can be reparameterized so that the slope on this scale is equal to $-\log\alpha$ and S_{max} is equal to $1/\log\alpha$. An example is shown where the stock has a log α value of 3. Note that lines drawn from the slope ($-\log\alpha$) and S_{max} will intersect at the approximate slope of the translation.

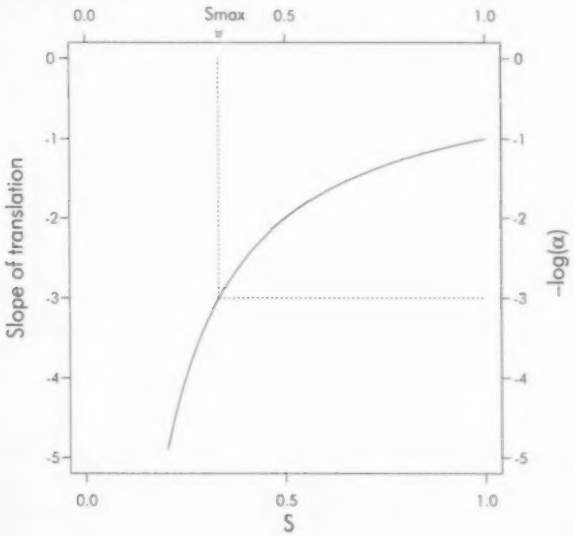

lation is given by $-1/S$. To clarify matters, we rescale the Ricker function to eliminate β by letting $S^* = 1$, i.e., without loss of generality, we can scale spawners as a fraction of S^*, giving

$$(6) \qquad S^* = \frac{\log\alpha}{\beta} = 1, \quad \text{or } \beta = \log\alpha$$

The Ricker model then becomes

$$(7) \qquad R = \alpha S e^{-(\log\alpha)S} \quad \text{and} \quad \log\left(\frac{R}{S}\right) = \log\alpha - (\log\alpha)S$$

Thus, on the log survival scale, the line still has an intercept at $\log\alpha$ but also has a slope of $-\log\alpha$. We can now plot the slope of the Ricker line on the log survival scale and the approximate slope of the translation on the same graph. Recalling that $S_{max} = 1/\beta$, with the above rescaling, S_{max} becomes $1/\log\alpha$.

We can expect that most stocks, if managed for maximum recruitment, or maximum yield, will have spawner abundances close to S_{max}. If all spawner abundances were exactly at S_{max}, then all points would be translated with an approximate slope equal to the true slope ($-\log\alpha$) (Fig. 6). Obviously, to the first-order approximation, this would affect neither the estimate of the slope nor the intercept. However, if spawner values are less than S_{max}, then the slope of the translation will exceed the true slope in magnitude, and the resulting estimate of the intercept ($\log\alpha$) will be biased positively. Similarly, if points are greater than S_{max}, then the slope of the translation will be smaller than the true slope, and the resulting estimate of the intercept will be biased negatively.

Returning to the original formulation of the Ricker model, we express this by observing that points with low S values are translated with a slope greater than β, while points with large S values are translated with a slope less than β. Thus, the direction and, in great part, the magnitude of the bias are determined by where the spawner abundances lie relative to S_{max}. We observed this pattern in the 259 stocks by plotting the relative bias against the proportion of data points that falls in the 0–S_{max} range (Fig. 7). When the proportion of data points in this range is low, the bias tends to be negative and vice versa. Note that the variability in bias appears to be greater at the extremes, when either all or no points are in this range.

Discussion

Our results suggest that measurement error in spawner

© 2002 NRC Canada

Fig. 7. Relative bias in $\widehat{\log\alpha}$ plotted against the proportion of data points in the 0–S_{max} range for (*a*) low, (*b*) medium, (*c*) high, and (*d*) extreme levels of measurement error. Stocks where a negative β was estimated have been removed.

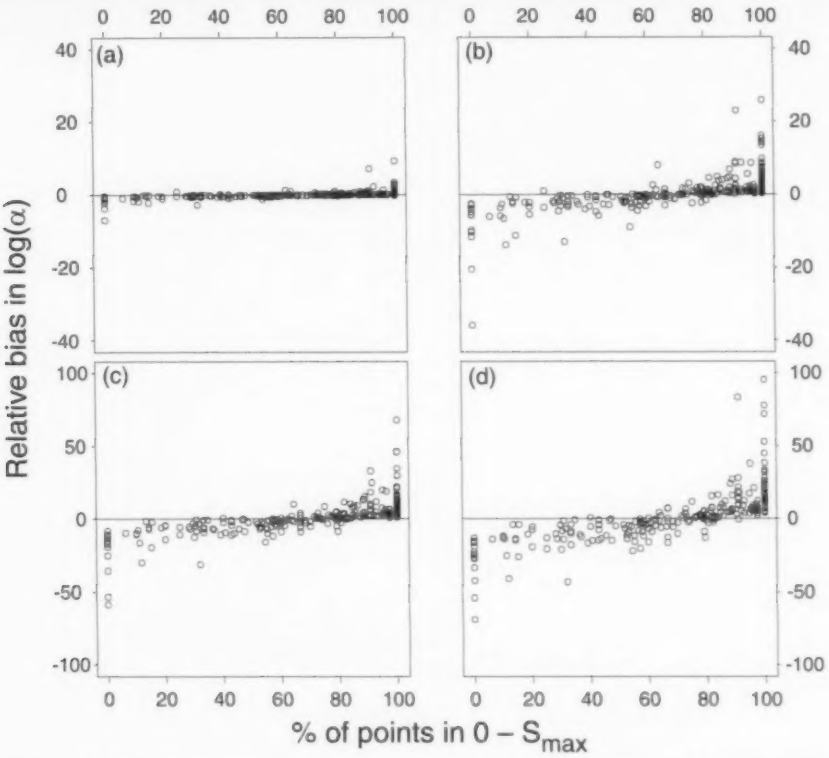

abundance does not generally lead to an overestimate of the maximum reproductive rate, as had been previously thought (Caputi 1988; Quinn and Deriso 1999). Instead, the bias is determined by the specifics of an individual data set, as is common in nonlinear models (Ratkowsky 1983). The spawner abundance of a particular data point will determine the slope of the translation (on the *S* versus log(*R*/*S*) axes) of that point after the addition of measurement error. It is the relative difference between the slope of the translation and the true slope of the spawner–recruitment function that determines the magnitude and direction of the bias. Points with low spawner values induce a positive bias, whereas points with high spawner values induce a negative bias in log α. Thus, the range of spawner abundances, or rather the proportion of spawner abundances in different ranges, plays a central role in determining both the magnitude and the direction of the bias. Hilborn and Walters (1992) suggested that the range of spawner stock sizes affects the magnitude of the measurement error bias, but this statement is somewhat misleading, as we demonstrate that the relationship between spawner stock fluctuations and bias is more complicated. It is possible to have very little measurement eror bias with only slight fluctuations in stock size (when observations are close to *S**/2) and vice versa (when observations are close to zero). These important subtleties, combined with the result that the measurement error bias can be both positive and negative, appear to be previously unknown, and have some important consequences for fisheries management. Stocks that have been fished heavily will have data points close to the origin and estimates of the maximum reproductive rate derived from these stocks will tend to be overly optimistic (usually less than 5%). Conversely, stocks that have not been fished heavily will have data points further away from the origin and close to *S**, and resulting estimates of the maximum reproductive rate will tend to be conservative (usually less than –25%).

Of the other factors we examined, only the degree of measurement error added played an important role in determining the magnitude of the bias. The degree of measurement error added depended upon both the ratio of measurement error standard deviation to residual error standard deviation (τ_s/σ_s) used and the value of the residual error standard deviation (σ_s).

We also examined the use of data-based simulations to assess the extent of measurement error bias. In these simulations, error was added to a sample data set in many replications, and the resulting "biases" from the initial estimates were calculated. We found that this approach successfully identified the direction of the bias but usually underestimated the magnitude of the bias, particularly if the original data were in the S_{max}–*S** range. Only if the initial or subsequent contamination is low will the data-based simulations give reliable estimates of the magnitude of the bias. Otherwise, the true bias will be underestimated by about 50% for medium to high levels of initial contamination. Data-based simulations can thus be used to determine the direction, and as a rough guide to the magnitude, of the bias.

It is interesting to note that for the data-based simulations, the mean of the biases across all stocks appeared to be close

© 2002 NRC Canada

to zero. This result should still hold as long as the initial contamination by measurement error was equally prevalent for stocks that displayed both negative and positive biases or if initial contamination was small. In these cases, we can expect little or no bias caused by measurement errors of spawner abundance in the estimation of the mean of the distribution of maximum reproductive rate when many populations are examined, as recommended as a general method by Myers et al. (2002).

Use of the results of the data-based and theoretical simulations would be greatly aided by actual estimates of measurement error from trawl surveys or other means. Obtaining such estimates, in most cases, requires considerable effort, which may explain their relative paucity.

We have focused on random and nonrandom errors in the estimation of spawner abundance. We can also compare our findings with those for bias introduced because the "independent" variable, spawning population size, is not independent of the interannual variation in the stock–recruitment relationship: for a given spawning population, above-average recruitment tends to result in higher spawning populations, while below-average recruitment tends to result in lower spawning populations (Walters 1985). This bias appears to be very difficult to correct for in practice (Korman et al. 1995). However, the magnitude of this bias was studied for a large number of fish stocks by Myers and Barrowman (1995). Although the results were given in terms of the density-dependent parameter, β, we summarize here their unpublished results for the maximum reproductive rate. They found that for the maximum reproductive rate, the bias would typically cause an overestimate of approximately 10% (this bias will be greater for extremely overexploited stocks). Thus, for most stocks, it would appear that bias resulting from measurement error in spawner abundance is similar in magnitude to time series bias. It should be remembered that our simulated data were generated so as to study the bias resulting from measurement error in isolation. In reality, biases resulting from time series, nonrandom environmental variation, and measurement error may interact (Caputi 1988). In this analysis, we have assumed that estimation errors in spawner abundance are independent from the errors in the estimation of the resulting recruits.

One potential cause for concern is that many of the data sets collected by Myers et al. (1995) contain estimates of spawners and recruits derived from age-structured assessment models. The correlational structure of these estimates can be complex for certain models, and there may be cases where our assumption that the estimation error in spawners and recruits is independent may be violated. Were this to be true, further simulations would be required to determine the effect of this correlation on the bias resulting from measurement error. Such an analysis, although important, is beyond the scope of this work. Nonetheless, because spawners and recruits come from different cohorts, and the lag between spawning and recruitment to the fishery can be several years, we feel that for most cases, estimation errors in spawners are unlikely to be correlated with estimation errors in recruits. Thus, this issue is not likely to play a major role in influencing the results presented here.

In conclusion, it appears that bias resulting from measurement error will be relatively small for exploited stocks and moderate for stocks that have undergone a range of fishing pressures. Relatively unexploited stocks will have their maximum reproductive rate underestimated considerably. It is important to consider, however, that bias gives the average distance between the estimate and the true value. An estimate for an individual stock may be further from or closer to the true value. Using data-based simulations, as described here, will provide a useful guide to the direction and magnitude of the bias in α, particularly if combined with an estimate of the measurement error variance.

References

Armstrong, M.J., and Shelton, P.A. 1988. Bias in estimation of stock–recruit function parameters caused by nonrandom environmental variability. Can. J. Fish. Aquat. Sci. **45**: 554–557.

Caputi, N. 1988. Factors affecting the time series bias in stock–recruitment relationships and the interaction between time series and measurement error bias. Can. J. Fish. Aquat. Sci. **45**: 178–184.

Dorn, M.W., Saunders, M.W., Wilson, C.D., Guttormsen, M.A., Cooke, K., Kieser, R., and Wilkins, M.E. 1999. Status of the coastal Pacific whiting stock in US and Canada in 1998. *In* Status of the Pacific Coast groundfish fishery through 1997 and recommended acceptable biological catches in 1999. Appendix. North Pacific Fishery Management Council, 605 West 4th, Suite 406, Anchorage, AK 99501-2252, U.S.A.

Dorn, M.W., Hollowed, A.B., Brown, E., Megrey, B., Wilson, C., and Blackburn, J. 2000. Walleye pollock. Available from http://www.afsc.noaa.gov/assessments.html. Alaska Fisheries Science Center, Seattle, Wash.

Fuller, W.A. 1987. Measurement error models. John Wiley & Sons, New York.

Hilborn, R., and Walters, C.J. 1992. Quantitative fisheries stock assessment: choice, dynamics and uncertainty. Chapman and Hall, New York.

Ianelli, J., and Fritz, L. 2001. Eastern Bering Sea walleye pollock stock assessment. Available from http://www.afsc.noaa.gov/assessments.html. Alaska Fisheries Science Center, Seattle, Wash.

Korman, J., Peterman, R.M., and Walters, C.J. 1995. Empirical and theoretical analyses of correction of time-series bias in stock–recruitment relationships of sockeye salmon (*Oncorhynchus nerka*). Can. J. Fish. Aquat. Sci. **52**: 2174–2189.

Lapointe, M.F., Peterman, R.M., and MacCall, A.D. 1989. Trends in fishing mortality rate along with errors in natural mortality rate can cause spurious time trends in fish stock abundances estimated by virtual population analysis (VPA). Can. J. Fish. Aquat. Sci. **46**: 2129–2139.

Ludwig, D., and Walters, C.J. 1981. Measurement errors and uncertainty in parameter estimates for stock and recruitment. Can. J. Fish. Aquat. Sci. **38**: 711–720.

Mertz, G., and Myers, R.A. 1997. Influence of errors in natural mortality estimates in cohort analysis. Can. J. Fish. Aquat. Sci. **54**: 1608–1612.

Myers, R.A., and Barrowman, N.J. 1995. Time series bias in the estimation of density-dependent mortality in stock–recruitment models. Can. J. Fish. Aquat. Sci. **52**: 223–232.

Myers, R.A., and Cadigan, N.G. 1993. Density-dependent juvenile mortality in marine demersal fish. Can. J. Fish. Aquat. Sci. **50**: 1576–1590.

Myers, R.A., and Mertz, G. 1998. The limits of exploitation: a precautionary approach. Ecol. Appl. **8**(Suppl. 1): S165–S169.

Myers, R.A., Bridson, J., and Barrowman, N.J. 1995. Summary of worldwide stock and recruitment data. Can. Tech. Rep. Fish. Aquat. Sci. No. 2024.

© 2002 NRC Canada

Myers, R.A., Bowen, K.G., and Barrowman, N.J. 1999. The maximum reproductive rate of fish at low population sizes. Can. J. Fish. Aquat. Sci. **56**: 2404–2419.

Myers, R.A., MacKenzie, B.R., Bowen, K.G., and Barrowman, N.J. 2001. What is the carrying capacity for fish in the ocean? A meta-analysis of population dynamics of North Atlantic cod. Can. J. Fish. Aquat. Sci. **58**: 1464–1476.

Myers, R.A., Barrowman, N.J., Hilborn, R., and Kehler, D.G. 2002. Inferring the Bayes priors with limited direct data with applications for risk analysis and reference points. N. Am. J. Fish. Manag. **22**: 351–364.

Quinn, T.J.I., and Deriso, R.B. 1999. Quantitative fish dynamics. Oxford University Press, New York.

Ratkowsky, D.A. 1983. Nonlinear regression modeling. Marcel Dekker, Inc., New York.

Ricker, W.E. 1954. Stock and recruitment. J. Fish. Res. Board Can. **11**: 559–623.

Stefanski, L.A. 1985. The effects of measurement error on parameter estimation. Biometrika, **72**: 583–592.

Thompson, G.G., and Dorn, M.W. 2000. Assessment of the Pacific cod stock in the eastern Berring Sea and the Aleutian Islands area. Available from http://www.afsc.noaa.gov/assessments.html. Alaska Fisheries Science Center, Seattle, Wash.

Walters, C.J. 1985. Bias in the estimation of functional relationships from time series data. Can. J. Fish. Aquat. Sci. **42**: 147–149.

Walters, C.J. 1990. A partial bias correction factor for stock–recruitment parameter estimation in the presence of autocorrelated environmental effects. Can. J. Fish. Aquat. Sci. **47**: 516–519.

Walters, C.J., and Ludwig, D. 1981. Effects of measurement errors on the assessment of stock–recruitment relationships. Can. J. Fish. Aquat. Sci. **38**: 704–710.

Appendix A

The slope of the translation of a point plotted on the log R/S versus S axes after the addition of measurement error δ is given by

$$\text{(A1)}\quad \text{slope} = \frac{\log\left(\frac{R}{S}\right) - \log\left(\frac{r}{Se^{\delta}}\right)}{S - Se^{\delta}}$$

Rearranging and observing that e^{δ} can be expressed as a Maclaurin series

$$\text{(A2)}\quad e^{\delta} = \sum_{n=0}^{\infty} \frac{\delta^n}{n!}$$

we get

$$\text{(A3)}\quad \text{slope} = -\frac{\delta}{S\left(\delta + \frac{1}{2}\delta^2 + \frac{1}{6}\delta^3 + \right)} = -\frac{1}{S\left(1 + \frac{1}{2}\delta + \right)}$$

Thus, a first-order approximation (ignoring squared and higher order terms) to the slope of the translation is $-1/S$.

© 2002 NRC Canada

Nitrogen and phosphorus relationships to benthic algal biomass in temperate streams

Walter K. Dodds, Val H. Smith, and Kirk Lohman

Abstract: Knowledge of factors limiting benthic algal (periphyton) biomass is central to understanding energy flow in stream ecosystems and stream eutrophication. We used several data sets to determine how water column nutrients and nonnutrient factors are linked to periphytic biomass and if the ecoregion concept is applicable to nutrient–periphyton relationships. Literature values for seasonal means of biomass of periphyton, nutrient concentrations, and other stream characteristics were collected for almost 300 sampling periods from temperate streams. Data for benthic chlorophyll and nutrient concentrations from a subset of 620 stations in the United States National Stream Water-Quality Monitoring Networks were also analyzed. The greatest portion of variance in models for the mean and maximum biomass of benthic stream algae (about 40%) was explained by concentrations of total N and P. Breakpoint regression and a two-dimensional Kolmogorov–Smirnov statistical technique established significant breakpoints of about 30 μg total $P \cdot L^{-1}$ and 40 μg total $N \cdot L^{-1}$, above which mean chlorophyll values were substantially higher. Ecoregion effects on nutrient–chlorophyll relationships were weak. Ecoregion effects were cross-correlated with anthropogenic effects such as percent urban and cropland area in the watershed and population density. Thus, caution is necessary to separate anthropogenic effects from natural variation at the ecoregion level.

Résumé : La connaissance des facteurs qui limitent la biomasse des algues benthiques (périphyton) est essentielle à la compréhension de l'eutrophisation des cours d'eau et du passage de l'énergie dans les écosystèmes d'eau courante. L'utilisation de plusieurs séries de données nous a servi à déterminer comment les nutriments et d'autres facteurs non-nutritionnels de la colonne d'eau sont reliés à la biomasse des algues et de voir si le concept d'écorégion peut s'appliquer aux relations nutriments–périphyton. Des données de la littérature ont été colligées, représentant presque 300 périodes de récolte sur des cours d'eau tempérés et traitant de biomasse moyenne saisonnière de périphyton, de concentrations de nutriments et d'autres caractéristiques. Nous avons aussi pu analyser des mesures de concentrations de chlorophylle benthique et de nutriments provenant d'un sous-ensemble de 620 stations du United States National Stream Water-Quality Monitoring Networks. Dans les modèles décrivant les biomasses moyennes et maximales des algues benthiques en eau courante, la plus grande partie de la variance (environ 40 %) s'explique par les concentrations totales de N et de P. Des méthodes de régression avec points de rupture et des techniques statistiques bidimensionnelles de Kolmogorov–Smirnov ont permis d'identifier des points de rupture significatifs à environ 30 $\mu g \cdot L^{-1}$ P total et 40 $\mu g \cdot L^{-1}$ N total, au dessus desquels les concentrations sont considérablement plus élevées. Les effets de l'écorégion sur les relations nutriments–chlorophylle sont faibles. Les effets de l'écorégion sont en corrélation croisée avec les effets anthropiques, tels que le pourcentage de terres agricoles ou de surfaces urbanisées dans le bassin versant et la densité de la population. Il faut donc prendre soin de distinguer les effets anthropiques de la variation naturelle à l'échelle de l'écorégion.

[Traduit par la Rédaction]

Introduction

Nitrogen and phosphorus are often the primary limiting nutrients for aquatic algal production because they are frequently in short supply relative to cellular growth requirements. Accrual of algal biomass, and thus overall ecosystem productivity, may be controlled by the type and intensity of nutrient limitation. Understanding links between nutrient concentration and algal biomass is also important in efforts to manage eutrophication in streams (Smith et al. 1999; Biggs 2000; Dodds and Welch 2000) and in efforts to delineate stream trophic state (Dodds et al. 1998).

Nutrient enrichment typically stimulates periphyton growth in flowing waters (e.g., Blum 1956). For example, nutrient enrichment bioassays in a variety of streams have demonstrated that benthic algal biomass can be stimulated by the addition of N, P, or both nutrients (Francouer 2001). Thus, we know that nutrients can stimulate growth when

Received 20 August 2001. Accepted 13 May 2002. Published on the NRC Research Press Web site at http://cjfas.nrc.ca on 4 July 2002.
J16498

W.K. Dodds.[1] Division of Biology, Kansas State University, Manhattan, KS 66506, U.S.A.
V.H. Smith. Department of Ecology and Evolutionary Biology, University of Kansas, Lawrence, KS 66045, U.S.A.
K. Lohman. National Park Service, 2525 Gambell St., Anchorage, AK 99503, U.S.A.

[1]Corresponding author (e-mail: wkdodds@ksu.edu).

 DOI: 10.1139/F02-063 © 2002 NRC Canada

added in excess and that N or P can be in short supply. However, nutrient limitation assays do not provide the predictive relationships between nutrient concentrations and algal biomass that we need to manage eutrophication in streams over broad geographic regions or to understand ecosystem-level relationships between nutrient loading and biomass of algal primary producers.

Empirical regression models that link algal biomass and water column nutrients have been used with great success worldwide in the eutrophication management of freshwater lakes and reservoirs (Cooke et al. 1993; Smith 1998; Smith et al. 1999). Attempts to derive similar relationships for nutrients and periphyton biomass in streams are less advanced and have been primarily regional in nature (e.g., Lohman et al. 1992; Biggs 2000). Generally, relationships between nutrients and chlorophyll are weaker in streams than in lakes, and this may explain why such models are not as highly developed for streams. The development of equivalent eutrophication models for streams is a pressing need, however, because these quantitative relationships can provide an objective framework for stream water quality management and because they can also be extended to predict key ecosystem properties that are important to the structure and function of lotic food webs.

Several important questions remain about the relationship between nutrient availability and periphyton biomass in streams. These questions include which nutrient(s) are limiting and how much of the observed variation in algal biomass can be explained by nutrient availability. In addition, it is still unclear whether distinct ecoregions (Omernik 1977) alter these nutrient–periphyton relationships. It is not clear if ecoregions based on terrestrial vegetation and land use have any influence on nutrient loading and nutrient–periphyton relationships in spite of the fact that regulatory agencies (e.g., U.S. Environmental Protection Agency) are attempting to set ecoregion-specific nutrient criteria.

Our approach to creating general models to predict benthic chlorophyll in streams was to construct a large database derived from a wide variety of temperate zone streams and then to use this database to quantify the relationships between key environmental variables and periphyton biomass. The aims of our study were to clarify links between water column nutrient concentrations and periphyton biomass and to identify other nonnutrient factors that may influence this relationship. We compared data taken from several different sources to expand the geographic coverage of our modeling efforts and to evaluate potential biases in our data collection.

Methods

We compiled data from the literature on periphyton biomass, nutrient concentrations, and abiotic variables from almost 300 distinct sites located in more than 200 rivers in North America and New Zealand (hereafter referred to as the "literature data set"). A detailed description of a major portion of this literature data set and its sources has been published elsewhere (Dodds et al. 1997). Additional literature data were added from a Spanish river (four seasons, Romaní and Sabater 1999), an Australian stream (one season, Mosisch et al. 1999), 12 streams from Quebec (Bourassa and Cattaneo 1998), a river in British Columbia (two sites, two seasons, Dubé et al. 1997), nine Quebec streams (Cattaneo et al. 1997), eight Oklahoma streams (Toetz et al. 1999), two groups of sites on the St. Lawrence River (Vis et al. 1998), and 13 streams in Ontario and Quebec (Chétlat et al. 1999).

Annual mean values were used in our analyses when possible (except for maximum chlorophyll concentrations); otherwise, seasonal means (at least 2 months) were used. Arithmetic means were used when available, but occasionally, only geometric means were reported by the original investigators. The entire data set for mean chlorophyll included 362 values composed of 110 values from the central United States, 68 from New Zealand, 82 from the northwestern United States and southwestern Canada, 77 from the northeastern United States and southeastern Canada, seven from the southeastern United States, five from alpine or Alaskan sites, 11 from Europe, and one each from Australia and the southwestern United States. A wide range of river sizes was included in the data set, ranging from large rivers such as navigation pools in the upper Mississippi and the St. Lawrence River to small first- or second-order streams, although more small streams were included than large rivers.

Where values were reported, we entered total P (TP), dissolved inorganic N (DIN), soluble reactive P (SRP), total N (TN), temperature, latitude, substrate type (natural or artificial), stream gradient, mean discharge, maximum discharge, minimum discharge, stream width, and stream order in the literature data set.

Three other data sets were also constructed to use for these analyses. Additional data for stream periphyton and nutrients were obtained from the United States Geological Survey National Stream Water-Quality Monitoring Networks (Alexander et al. 1996) (hereafter referred to as the "USGS data set"). Two subsets of stream data were derived from the original USGS data set. The first subset initially contained all dates for all sampling stations that contained no missing values for chlorophyll (determined spectrophotometrically), TN, or TP. This trimmed database was further refined to include only stations having more than four values for chlorophyll, resulting in a working USGS subset containing 2870 chlorophyll measurements from 314 stations. Values were taken from these stations for percent cropland, farmland, forest, pasture, range, and urban area in the watershed. Values were also retained for ammonium, conductivity, dissolved oxygen, drainage area, instantaneous discharge, latitude, nitrate, human population in the watershed (as of 1990), SRP, temperature, and turbidity.

Mean chlorophyll values from each site in the USGS data set were coupled with ecoregions derived from maps produced by the National Health and Environmental Effects Research Laboratory of the United States Environmental Protection Agency for levels I, II, and III (Omernik 1987; Commission for Environmental Cooperation 1997). The ecoregion at the sampling point was used. Three subsets of data (one for each ecoregion level) were created for analysis by ecoregion; only ecoregions at each level were considered with 10 or more sampling stations within the ecoregion. Potential errors associated with watershed boundaries that cross ecoregions are explored in the discussion.

A second USGS data subset that contained values for both TN and TP was also created. This data set was used to eval-

© 2002 NRC Canada

uate distribution of TN and TP values. The means for each station with more than 10 values were obtained, resulting in mean TN and TP values from 658 stations (means calculated from a total of 84 934 sampling events). All data from all years for each single station were averaged to lower the amount of variance and allow comparison with the other literature values.

A lake data set containing values for growing season mean TN, TP, and chlorophyll *a* concentrations for 300 lakes as derived from table 1 in Smith (1982) was used to compare stream chlorophyll–nutrient relationships with those derived from lakes.

Both nonparametric and parametric methods were used to explore the relative importance of chemical and physical factors that regulate stream periphyton biomass. An initial screening for significant relationships among the candidate variables was made with Kendall's τ-b multiple comparison correlation procedure. This nonparametric method accounts for unequal and nonnormal distributions based on the number of concordant and discordant pairs of observations and uses a correction for tied pairs. Correlations were determined for all factors associated with chlorophyll in the literature and USGS data sets.

Predictive empirical models were then constructed using multiple regression analysis. When multiple regressions were used to develop statistical relationships between TN, TP, and chlorophyll, only those cases in the data sets that simultaneously contained values of both TN and TP were used in the analysis. For both nonparametric and parametric comparisons between artificial versus natural substrates using the literature data set, the substrate type was coded as a dummy variable in which the substrate was coded as 0 for artificial substrates and 1 for natural substrates.

Different subsets of the literature and USGS data sets were also used for the regression analyses. In most cases, not all values were present for all potential independent variables along with chlorophyll. For example, DIN and SRP values were not always available when chlorophyll *a*, TN, and TP were because not all sites had all types of data. Few chlorophyll values in the literature data set had all of the variables (i.e., TP, DIN, SRP, TN, temperature, latitude, substrate type (natural or artificial), stream gradient, mean discharge) present. The more variables that we included, the smaller the complete data set. Thus, we could not construct more complex predictive regression models (e.g., stepwise regression, path analysis) using multiple variables. Therefore, we only report regression models using TN, TP, DIN, or SRP to predict chlorophyll. Analysis of variance (ANOVA) was used to assess potential influences of ecoregions within the USGS data set. If the overall ANOVA gave a significant result, then pairwise comparisons were made with Fisher's least significant difference method.

Analysis for breakpoints in the chlorophyll–TN and chlorophyll–TP data were conducted on the literature data set using two techniques. Breakpoint regression is a nonlinear regression procedure that uses quasi-Newton search methods to find two linear relationships that describe the highest proportion of the variance and was analyzed with Statistica software (StatSoft, Tulsa, Okla.). Two-dimensional Kolmogorv–Smironov tests were used to test for breaks in variance in bivariate data (Garvey et al. 1998).

Table 1. Significant nonparametric correlations among mean chlorophyll (chl), maximum chlorophyll, TN, TP, DIN, SRP, stream gradient, latitude, water temperature, substrate type (natural or artificial), and maximum discharge for the literature data set (Kendall's τ-b procedure).

Factor 1	Factor 2	*r*	*p*	*N*
Mean chl	Max. chl	0.67	<0.0001	186
	TP	0.32	<0.0001	259
	Gradient	–0.32	0.001	49
	DIN	0.28	<0.0001	233
	SRP	0.23	<0.0001	200
	TN	0.20	<0.0001	209
	Temperature	0.18	0.01	91
	Latitude	–0.17	0.00005	267
	Substrate type	0.15	0.0001	300
	TN:TP	–0.11	0.05	148
Max. chl	Mean chl	0.67	<0.0001	186
	TN	0.32	<0.0001	109
	Gradient	–0.29	0.004	46
	DIN	0.21	0.00003	181
	TP	0.20	0.003	145
	DIN:SRP	0.20	0.005	93
	Latitude	–0.20	0.002	149
	TN:TP	–0.18	0.008	104
	Substrate type	0.16	0.02	170
	Max. discharge	–0.16	0.03	77

Note: TN, total nitrogen; TP, total phosphorus; DIN, dissolved inorganic nitrogen; SRP, soluble reactive phosphorus; max, maximum.

Results

Correlation analyses

Analyses of the literature data set (Table 1) revealed that benthic chlorophyll was significantly correlated with water column nutrients. Both mean and maximum concentrations of benthic chlorophyll were positively correlated with TN and TP concentrations. Mean and maximum concentrations of benthic chlorophyll were more weakly correlated with total DIN concentrations relative to TN and TP concentrations, and SRP was significantly correlated only with maximum benthic chlorophyll.

Of the nonnutrient factors in the literature data set that could be related to benthic chlorophyll, stream gradient appeared to be most important, with lower chlorophyll concentrations occurring in steeper gradient systems. High water temperatures and lower latitudes were also correlated with higher mean benthic chlorophyll levels, although more weakly than with nutrient concentrations. Both mean and maximum chlorophyll were positively correlated with the dummy variable for substrate in the literature data, indicating that benthic chlorophyll values were typically higher on natural than on artificial substrates.

Correlation analyses of the USGS data set (Table 2) confirmed the results obtained from the literature data. TN and TP were positively correlated, temperature was positively correlated, and latitude was negatively correlated with benthic chlorophyll concentrations. Three indicators of human impacts that were not available in the literature data set

© 2002 NRC Canada

Table 2. Significant correlations among mean chlorophyll, TN, TP, ammonium, nitrate, latitude, temperature, mean discharge, and human influence variables for the USGS data set.

Factor	*r*	*p*	*N*
Nitrate	0.29	<0.0001	256
TN	0.25	<0.0001	314
Latitude	–0.18	<0.0001	314
TP	0.17	<0.0001	314
Temperature	0.17	<0.0001	314
% urban	0.17	<0.0001	314
Ammonium	0.16	0.002	233
% cropland	0.12	0.001	314
Dissolved oxygen	–0.11	0.002	302
Drainage area	0.11	0.002	314
Conductivity	0.11	0.002	314
% pasture	0.10	0.01	314
Discharge	0.09	0.02	307

Note: Nonsignificant correlations were found for percent forest, percent rangeland, turbidity, suspended solids, and SRP (Kendall's τ-b procedure). TN, total nitrogen; TP, total phosphorus.

but were in the USGS data set (percentage of watershed in urban, cropland, and pasture) were also positively correlated with benthic chlorophyll.

Comparative analyses of nutrient limitation status in streams and lacustrine ecosystems

Nitrogen to P ratios are commonly used as empirical criteria for the assessment of nutrient limitation status in aquatic ecosystems, so we used three data sets to compare the relative frequencies of potential N and P limitation in stream versus lacustrine ecosystems (Fig. 1). The range of TN:TP ratios in the literature data set was somewhat greater than that in the much larger USGS data set, and the literature data set also contained lower TN:TP values than did either the lake or the USGS data set. The mean TN:TP values were 14.2, 17.6, and 22.4 by mass for the USGS, literature, and lake data sets, respectively. These three statistical distributions also differed significantly from each other ($p < 0.001$, Kolmogorov–Smirnov test).

Testing factors that may influence chlorophyll yield per unit nutrient

Mean chlorophyll levels were divided by water column TN to provide an index of chlorophyll yield per unit nutrient. The resulting ratio was subjected to nonparametric correlation analyses using both the literature and the USGS data sets (Table 3). There was a significant positive effect of TP in both data sets, indicating that the chlorophyll yield per unit N is greater when TP is greater. In the USGS data set, there was also a trend towards a higher yield of benthic chlorophyll per unit N at higher water temperatures, lower latitudes, larger drainage basin areas, and higher percentage of watershed in cropland.

The chlorophyll yield per unit water column N was also tested by ecoregion (Table 4). Ecoregion level III had the only significant effects of ecoregion on chlorophyll:TN. This was driven primarily by high chlorophyll yield in the

Fig. 1. TN:TP (total nitrogen : total phosphorus) mass ratios for (*a*) streams in the USGS stream data set, (*b*) streams in the literature stream data set, and (*c*) north-temperate lakes (data from Smith 1982). The distributions of TN:TP were significantly different from each other ($p < 0.001$) using the nonparametric Kolmogorov–Smirnov analysis to test for differences in mean values as well as skew (Press et al. 1986).

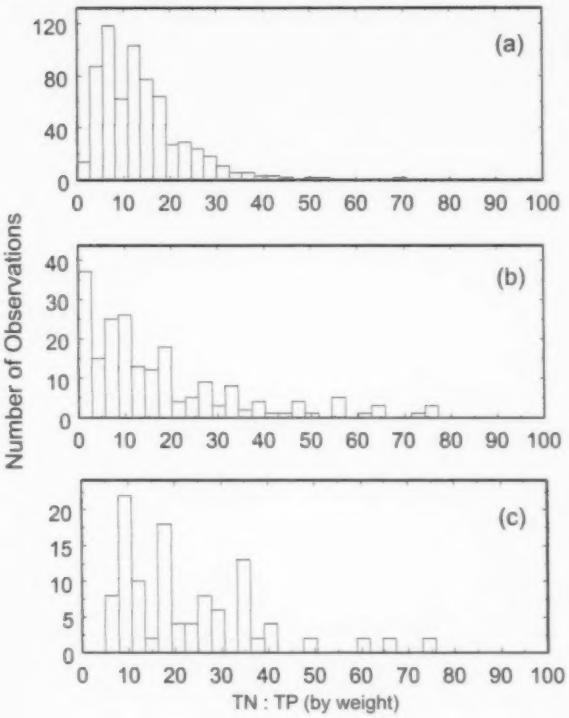

Table 3. Significant correlations of environmental factors with the chlorophyll:TN for the literature and USGS data sets (Kendall's τ-b procedure).

Factor	*r*	*p*	*N*
Literature data set			
TN:TP	–0.53	<0.000001	201
TP	0.37	<0.000001	201
Max. chlorophyll	0.34	0.002	109
Order	–0.20	0.01	136
USGS data set			
Population	0.29	<0.000001	314
Latitude	–0.25	0.000005	314
% urban	0.24	0.00002	314
Temperature	0.24	0.00002	314
TP	0.18	0.001	314
Drainage area	0.16	0.004	314
Dissolved oxygen	–0.15	0.009	302
% cropland	0.14	0.01	314
Conductivity	0.12	0.03	314

Note: TN, total nitrogen; TP, total phosphorus.

© 2002 NRC Canada

Table 4. Results of analysis of variance (ANOVA) of TN, TP, chlorophyll, and chlorophyll:TN from USGS data by ecoregion.

Independent variable	Dependent variable	*N*	*F*	*p*
Ecoregion level I	TN	6	3.98	0.0017
	TP	6	1.65	0.1457
	Chlorophyll	6	5.51	0.0001
	Chlorophyll:TN	6	1.00	0.4173
Ecoregion level II	TN	16	3.82	<0.0001
	TP	16	0.81	0.6684
	Chlorophyll	16	2.78	0.0005
	Chlorophyll:TN	16	1.20	0.2756
Ecoregion level III	TN	7	6.97	0.0000
	TP	7	1.53	0.1773
	Chlorophyll	7	3.73	0.0025
	Chlorophyll:TN	7	3.01	0.0113

Note: TN, total nitrogen; TP, total phosphorus.

Southern Coastal Plain (most of Florida and some Gulf and Atlantic low coastal areas to the north and west of Florida). Very high N values were found in the Central U.S. Plains classified in ecoregion level II, an ecoregion that encompasses most of Illinois, Indiana, and western Ohio (data not shown). At ecoregion level I, there were low TN values in forested regions and the highest TN values in the Mediterranean California ecoregion.

Regression analyses

Multiple regression analysis was used to develop quantitative relationships between benthic chlorophyll and water column nutrients using data separately from both the literature and the USGS data sets (Table 5). For mean and maximum chlorophyll concentrations in the literature data set, mean stream water TN and TP concentrations described 40 and 31% of the total variance, respectively. However, an interaction between TN and TP in the literature data set is evident (Fig. 2), which indicates that low TN:TP values typically result in a lower yield of chlorophyll at any single value of TP relative to higher stream water TN:TP values. Comparable regression models for the USGS data set were similar in structure but were typically weaker; for example, TN and TP together only described 12% of the variance in mean chlorophyll. Although the relationships between chlorophyll and water column nutrients were more variable in the USGS data set than in the literature data set (Table 5; Fig. 2), a TN–TP interaction was still evident in the USGS data set (Fig. 2). In all regression analyses, TP explained more variance in benthic chlorophyll concentrations than did SRP. Similarly, DIN explained far less variance in chlorophyll than did TN.

Analysis of the chlorophyll–TN and chlorophyll–TP relationships by two statistical methods revealed significant breakpoints with agreement between the two methods except in the case of maximum chlorophyll as a function of TP (Table 6). In general, breakpoints were higher when considering maximum chlorophyll–nutrient relationships as compared with mean chlorophyll–nutrient relationships and higher for chlorophyll–TN than for chlorophyll–TP relationships. The breakpoints provide evidence for a saturation effect of nutrients on periphyton biomass accrual.

Fig. 2. Relationships between total phosphorus and mean benthic chlorophyll *a* as a function of the TN:TP mass ratio in stream water for the (*a*) literature data set and (*b*) USGS data set. Lowess curve fitting was used to fit points in this plot to illustrate how chlorophyll yield varies with TN:TP. Circles and dotted lines are for points with TN:TP less than 15 by mass, and triangles and solid lines represent points with TN:TP greater than 15.

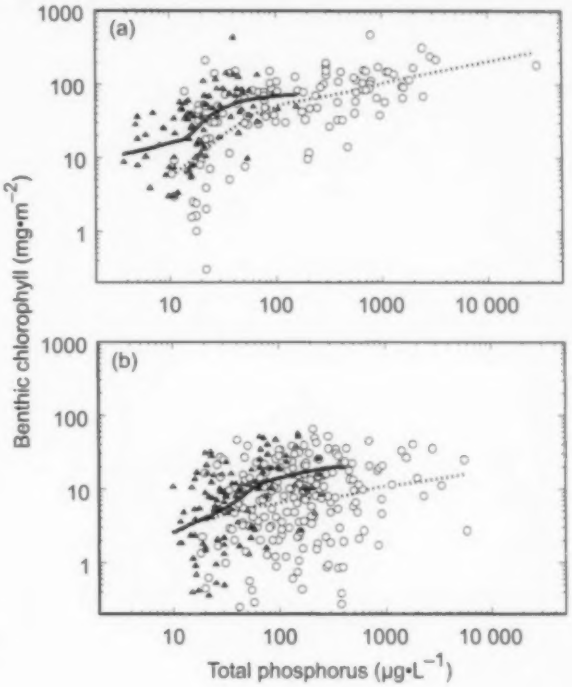

Discussion

Nitrogen and P limitation

Although the occurrence of N limitation in streams is inconsistent with the early view that P is generally the primary limiting factor in inland freshwaters, experimental nutrient enrichment bioassays have confirmed N limitation in a variety of different stream ecosystems (Francouer 2001; also see relevant citations in Smith et al. 1999). The data reveal a significant N–P interaction in streams and suggest that it is necessary to consider both N and P as potentially limiting nutrients for periphyton biomass accrual in lotic ecosystems.

The hyperbolic relationship between TN or TP and chlorophyll reported in an earlier, more limited version of the literature data set (Dodds et al. 1997) could be interpreted as an indication of lack of nutrient limitation at high water column nutrient concentrations. This saturation effect was not evident in the literature or the USGS data set using the statistical method employed by Dodds et al. (1997) to assess a saturation effect (a test for significance of the squared term of the second-order polynomial). However, the two statistical techniques used in this paper are more appropriate for determining if breakpoints occur in data, and they did

© 2002 NRC Canada

Table 5. Regression models for mean and maximum benthic chlorophyll in streams using the literature and the USGS data sets as a function of TN, TP, DIN, and SRP.

Dependent variable	Intercept	Independent variable 1	Independent variable 2	N	Adjusted r^2 or R^2
Literature data set					
log(mean chl)	1.101***	log(TN) 0.182**		209	0.05
log(mean chl)	0.847***	log(TP) 0.364***		259	0.20
log(mean chl)	0.155	log(TN) 0.236***	log(TP) 0.443***	200	0.40
log(mean chl)	0.676***	log(DIN) 0.367***		233	0.19
log(mean chl)	0.981***	log(SRP) 0.368***		200	0.13
log(mean chl)	0.298	log(DIN) 0.388***	log(SRP)	141	0.27
log(max. chl)	0.653*	log(TN) 0.546***		109	0.24
log(max. chl)	1.391***	log(TP) 0.339***		145	0.11
log(max. chl)	0.714*	log(TN) 0.372*	log(TP) 0.223*	103	0.31
log(max. chl)	1.385***	log(DIN) 0.263***		181	0.09
log(max. chl)	1.721***	log(SRP) 0.115		97	0.01
USGS data set					
log(mean chl)	–0.804***	log(TN) 0.544***		314	0.12
log(mean chl)	0.374***	log(TP) 0.241***		314	0.05
log(mean chl)	–0.923***	log(TN) 0.632***	log(TP) –0.074	313	0.12
log(mean chl)	–0.130	log(DIN) 0.388***		230	0.16
log(mean chl)	0.729***	log(SRP) 0.103		49	0.01
log(mean chl)	–0.409	log(DIN) 0.576***	log(SRP) –0.091	41	0.18

Note: Mean and maximum stream chlorophyll (mean chl and max. chl, respectively) in mg·m^{-2}; total phosphorus (TP), total nitrogen (TN), dissolved inorganic nitrogen (DIN), and soluble reactive phosphorus (SRP) in mg·m^{-3}. Significance levels for regression coefficients: *$p < 0.05$, **$p < 0.01$, ***$p < 0.001$.

Table 6. Analysis of breakpoints from regression and two-dimensional Kolmogorov–Smirnov (2DKS) in TP, TN, and mean and maximum chlorophyll relationships using the literature data set.

Dependent variable	Independent variable	Breakpoint from regression (μg·L^{-1})	Breakpoint from 2DKS
log(mean chl)	log(TP)	31	29
log(mean chl)	log(TN)	36	41
log(max. chl)	log(TP)	100	27
log(max. chl)	log(TN)	147	145

Note: Mean and maximum chlorophyll, mean chl and max. chl, respectively; total phosphorus (TP), total nitrogen (TN). $p < 0.0002$ for all 2DKS determinations.

indicate saturation breakpoints in the literature data set. Hyperbolic relationships have been documented for TP and phytoplankton in lakes (McCauley et al. 1989; Prairie et al. 1989) and for TP and seston in rivers and streams (Van Nieuwenhuyse and Jones 1996). Such saturation may be an important effect; nutrient control strategies should take into account the possibility that it is less likely that there will be a decrease in benthic algal biomass unless water column nutrients are lowered below some threshold value.

We suggest that a pattern of colimitation will become evident as has been broadly observed in lakes (Elser et al. 1990) when more flowing waters are tested for nutrient deficiency and that a shifting balance between N and P limitation of algal growth will be observed along strong N:P supply gradients (Smith 1982). This pattern of nutrient colimitation in lakes has been explained by the presence of nonequilibrium conditions and mixed phytoplankton species assemblages (Dodds et al. 1989); these two conditions are major characteristics of stream periphyton communities.

We also found nutrient data for streams that may indicate a greater degree of N limitation than lakes where nutrient data were available. The water column TN:TP values were lower in both the stream literature and the USGS stream data sets than in Smith's (1982) lake data set. A similar pattern documenting lower particulate N:P in stream seston than in lacustrine phytoplankton has been reported for the Experimental Lakes Area of Canada (Hecky et al. 1993).

Variance in nutrients and benthic chlorophyll

Nonequilibrium conditions are clearly important in lotic systems, and we conclude that this environmental noise results in a markedly higher statistical variance in algal–nutrient relationships in temperate streams than is observed for lakes. For example, our best regressions using TN and TP to estimate benthic chlorophyll had R^2 values of 40%, whereas models to estimate planktonic chlorophyll in lakes using TN and TP published by Smith (1982) had R^2 values ranging from 69 to 76%, and regressions between TP and chlorophyll on regional lake

© 2002 NRC Canada

data sets commonly yield R^2 values greater than 90% (Cooke et al. 1993).

There also may be lower variance in relationships between water column nutrients and suspended (sestonic) chlorophyll in rivers than we observed for benthic chlorophyll in streams. Data analyses published for suspended chlorophyll in streams demonstrate that the relationship between TP and suspended algal biomass yields higher R^2 values, about 70% (Van Nieuwenhuyse and Jones 1996), than the similar comparison with our benthic chlorophyll data. This progressive decoupling of nutrients from chlorophyll from lake phytoplankton to river seston to benthic river algae could be in part because suspended P must be high when suspended chlorophyll is high because algal cells contain both chlorophyll and P. River seston is probably more likely to contain suspended nonliving particles that contain N and P from the benthos than many lakes because streams have greater turbulent energy.

Data for chlorophyll–nutrient relationships from the USGS data set were even more variable than those from the literature data set. This is consistent with our earlier attempts to synthesize literature data. We needed at least several points within each season to minimize variance in the data, and most data points in the literature data set are composed of several points per season. The USGS chlorophyll data are not taken frequently enough in most cases to provide seasonal averages (i.e., only four times over a year) and thus probably encompass more variation.

A number of factors may account for the large proportion of across-system variance that remains unexplained in our relationships. The hydrological parameters that we used were crude, but better data were not available for a wide variety of systems. Hydraulic disturbance and flow can be important determinants of periphyton biomass. Considerably more variance was accounted for in two detailed studies of benthic stream chlorophyll (Lohman et al. 1992; Biggs 1995) where hydrological and land use parameters were more closely monitored, locale was more restricted, and procedures remained consistent within studies. Lohman et al. (1992) were able to explain between 47 and 60% of the variance in periphyton with TN and TP models for Ozark streams (Missouri, U.S.A.), respectively, and were also able to relate the length of time since the last flood to periphyton biomass. Similarly, Biggs (1995) analyzed 16 New Zealand stream sites and was able to explain 89% of the variance with a model that considered flood frequency, land use, and geology. These studies show that regional relationships likely will provide a greater degree of predictive ability. We sacrifice predictive power for generality by including more studies done with a variety of procedures in a wider range of habitat types.

In the literature data set, there was more benthic chlorophyll on natural than on artificial substrates. However, multiple regression analysis demonstrated that including substrate type only improved R^2 by 1% (data not shown). Artificial versus natural substrates have been previously shown to alter estimates of benthic chlorophyll (Cattaneo and Amireault 1992). This could be an important observation because many scientists use artificial substrates to assess algal biomass in natural streams, although our regression analysis suggests that the effect is minor.

Light availability can also influence algal biomass in streams, and nutrient limitation can be influenced by light (Triska et al. 1983). Two possible variables related to light in this study were turbidity and suspended solids data from the USGS data set, and neither of these parameters was correlated with benthic chlorophyll or with chlorophyll:TN. However, it is likely that researchers are biased against measurement of algal biomass in highly shaded, deep, or highly turbid streams, so our data cannot be used to rule out differences in light regime increasing variance in nutrient – benthic chlorophyll relationships. The higher chlorophyll at low latitudes could be related to greater light.

Grazing was not considered, and interactions may exist among parameters that we could not assess in this study. For example, hydrodynamic scouring can interact with grazing by invertebrates to create an extremely variable habitat for periphyton, and these factors and others may influence biomass simultaneously. The interaction between limitation by grazers and nutrients was not assessed here, but such relationships are expected to increase observed variance in the chlorophyll–nutrient relationships and should receive attention in future studies.

Relevance of our data analysis to eutrophication problems in streams

Regardless of the existence of factors that decouple relationships between algal biomass and nutrients, eutrophication of lotic systems is an important issue. Benthic chlorophyll from 100 to 150 mg·m^{-2} has been considered excessive (Welch et al. 1988). In the literature data set, 22% of the mean benthic chlorophyll and 56% of the maximum chlorophyll values exceeded 100 mg·m^{-2} (Fig. 3). Even if it is only possible to explain a limited amount of variance in benthic algal biomass using water column nutrients, most other factors (e.g., light, flooding, grazing) cannot be controlled, leaving management of nutrient loading as the most likely method to control excessive algal biomass in streams.

Methods of applying equations such as those in this study to controlling eutrophication in streams have been published elsewhere (Dodds et al. 1997) using an earlier subset of the literature data set. Adding values from other systems altered the regression equations, substantially in some cases. For example, TN alone was less able to explain variance when the new data were added. This change in regression equations, combined with the variance in the relationships between nutrients and chlorophyll, indicates that care should be taken in using any specific set of published equations for management decisions.

The USGS data set was much more variable and contained no chlorophyll values that were in excess of 100 mg·m^{-2}. There may be a number of reasons why the USGS data set had lower chlorophyll than the literature data set, including different methods, sampling turbid rivers, sampling deeper waters, and more winter (low light) samples collected. Because our experience suggests that at least some of the waters sampled should have mean chlorophyll values in excess of 100 mg·m^{-2}, and the USGS data set was more variable, we are more confident in models constructed from the literature data set. However, the USGS data set correlations followed those obtained from the literature data set, so

© 2002 NRC Canada

Fig. 3. Cumulative frequency distributions for (*a*) mean and (*b*) maximum benthic chlorophyll from the literature data set.

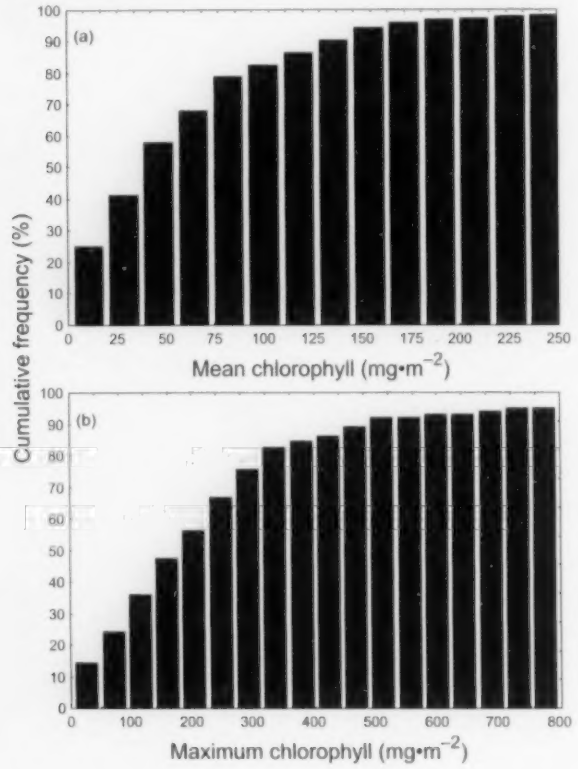

the overall trends resulting from the USGS data set (e.g., the ecoregion analysis) seem reliable.

The literature data set included breakpoints that may provide important guidance. They suggest that there is little probability of low benthic algal chlorophyll above the breakpoint value for TN or TP. If TN or TP is below the breakpoint, there is more likely to be low chlorophyll (but not in all cases). Probably the most prudent method for establishing nutrient criteria to control benthic chlorophyll is to use regression equations (best from the regions of interest, alternatively those published here for the literature data set), keep in mind a potential breakpoint effect, and also use a reference site approach wherever reasonably pristine sites are available to employ as a baseline.

Ecoregions and benthic chlorophyll–nutrient relationships

The concept of ecoregions has been considered for setting nutrient criteria. Ecoregions had little discernable influence on chlorophyll yield related to TP in European lakes (Seip et al. 2000). Pan et al. (1999) demonstrated a possible ecoregion effect using periphyton samples taken in the mid-Atlantic region of the United States. TP was correlated weakly, but significantly, with algal biomass expressed as chlorophyll but not TN across the entire region. However, subregions varied, with N, P, or neither correlating significantly with algal biomass. This suggests a potential existence of chlorophyll–nutrient ecoregions.

We did see an ecoregion effect on chlorophyll yield (chlorophyll:TN) but only in the Southern Coastal Region. This ecoregion effect is consistent with correlation analysis that demonstrated that low-latitude (high-light) and high-temperature sampling stations had higher chlorophyll. The Southern Coastal Region was the furthest southern ecoregion that had sufficient data (10 or more sampling stations) to be analyzed by ANOVA. However, this difference in chlorophyll yield only occurred at one ecoregion level. This is in spite of the fact that TN and chlorophyll values varied significantly with ecoregion.

Our data do not rule out an ecoregion approach. For example, correlation analyses suggest that stream gradient, temperature, and latitude may have altered benthic chlorophyll. There are reasonable physical explanations for these correlations; growth rates are greater with higher temperature, light and temperature are higher at lower latitudes, and higher gradient systems may have more intense floods that remove algal biomass. However, high-gradient systems may be less likely to receive nutrient pollution, and high temperatures may be associated with lowland streams with greater anthropogenic input. In addition, anthropogenic effects that we were able to test (e.g., percent urban and cropland watershed area) were all correlated with increased chlorophyll. This suggests that any attempts to establish ecoregions should clearly identify and separate anthropogenic effects from basic ecological characteristics.

The ecoregion approach is difficult to apply to large watersheds. This is because watersheds can span several ecoregions (Omernik and Bailey 1997). However, chlorophyll yield could be more specific to local effects such as light, grazers, and flood history. Consideration of ecoregions may assist in water quality management (Griffith et al. 1999), but a more detailed approach is necessary than that taken here.

Better data are required to establish the validity of the ecoregion approach with regard to benthic chlorophyll–nutrient relationships. This would mean establishing pristine reference streams within each ecoregion and then using those systems as a baseline to compare within and between ecoregions. Currently, it would not be prudent to assume that ecoregion-specific stream eutrophication models will be useful in management of nutrient pollution, particularly because chlorophyll:TN did not vary over most of the United States according to our analysis.

We can draw several important conclusions from this data analysis: (*i*) nutrient availability (bottom-up control) can explain about 40% of the variation in autotrophic biomass in a wide variety of temperate streams, (*ii*) both N and P should be considered as potential limiting nutrients, (*iii*) the exact regression coefficients depend on the data set being considered; extending the scale of the observations may require more data (collected with carefully controlled methods) than are currently available and a geographic approach similar to that of Omernik (1977) may improve results, (*iv*) there are breakpoints such that when TN and TP in the water column exceed certain levels, low benthic chlorophyll values are unlikely, (*v*) there may be some basis for natural ecoregions with regard to chlorophyll–nutrient relationships, but these

© 2002 NRC Canada

may be difficult to separate from human-instigated land use changes, and (*vi*) nonequilibrium conditions and multiple limiting factors are more likely to predominate in streams than in lakes and lead to inherently high variability of primary producer biomass.

Acknowledgments

We thank D. Gudder, M. Smith, and G. Henebry for technical assistance and B.J.F. Biggs, J. Chétlat, and J.R. Jones for kindly providing data. W.S. Baillargeon assisted with a portion of the data collection. This research was supported in part by U.S. NSF Konza LTER to W.K.D. and by a General Research Fund grant to V.H.S. from the University of Kansas. This is contribution no. 95-551-J from the Kansas Agricultural Experiment Station.

References

Alexander, R.B., Ludtke, A.S., Fitzgerald, K.K., and Schertz, T.L. 1996. Data from selected U.S. Geological Survey National Stream Water – Quality Monitoring Networks (WQN) on CD-ROM. U.S. Geol. Surv. Open-File Rep. 96-337.

Biggs, B.J.F. 1995. The contribution of flood disturbance, catchment geology and land use to the habitat template of periphyton in stream ecosystems. Freshwater Biol. **33**: 419–438.

Biggs, B.J.F. 2000. Eutrophication of streams and rivers: dissolved nutrient – chlorophyll relationships for benthic algae. J. North Am. Benthol. Soc. **19**: 17–31.

Blum, J.L. 1956. The ecology of river algae. Bot. Rev. **22**: 291–331.

Bourassa, N., and Cattaneo, A. 1998. Control of periphyton biomass in Laurentian streams (Québec). J. North Am. Benthol. Soc. **17**: 420–429.

Cattaneo, A., and Amireault, M.C. 1992. How artificial are artificial substrata for periphyton? J. North Am. Benthol. Soc. **11**: 244–256.

Cattaneo, A., Kerimian, T., Roberge, M., and Marty, J. 1997. Periphyton distribution and abundance on substrata of different size along a gradient of stream trophy. Hydrobiologia, **354**: 101–110.

Chétlat, J., Pick, F., Morin, A., and Hamilton, P. 1999. Periphyton biomass and community composition in rivers of different nutrient status. Can. J. Fish. Aquat. Sci. **56**: 560–569.

Commission for Environmental Cooperation. 1997. Ecological regions of North America: toward a common perspective. Map (scale 1 : 12 500 000). Commission for Environmental Cooperation, Montreal, Que.

Cooke, G.D., Welch, E.B., Peterson, S.A., and Newroth, P.R. 1993. Restoration and management of lakes and reservoirs. 2nd ed. Lewis Publishers, Boca Raton, Fla.

Dodds, W.K., and Welch, E. 2000. Establishing nutrient criteria in streams. J. North Am. Benthol. Soc. **19**: 186–196.

Dodds, W.K., Johnson, K.R., and Priscu, J.C. 1989. Simultaneous nitrogen and phosphorus deficiency in natural phytoplankton assemblages; theory, empirical evidence, and implications for lake management. Lake Reservoir Manage. **5**: 21–26.

Dodds, W.K., Smith, V.H., and Zander, B. 1997. Developing nutrient targets to control benthic chlorophyll levels in streams: a case study of the Clark Fork River. Water Res. **31**: 1738–1750.

Dodds, W.K., Jones, J.R., and Welch, E.B. 1998. Suggested classification for stream trophic state: distributions of temperate stream types by chlorophyll, total N and P. Water Res. **32**: 1455–1462.

Dubé, M.G., Culp, J.M., and Scrimgeour, G.J. 1997. Nutrient limitation and herbivory: processes influenced by bleached kraft pulp mill effluent. Can. J. Fish. Aquat. Sci. **54**: 2584–2595.

Elser, J.J., Marzolf, E.R., and Goldman, C.R. 1990. Phosphorus and nitrogen limitation of phytoplankton growth in the freshwaters of North America: a review and critique of experimental enrichments. Can. J. Fish. Aquat. Sci. **47**: 1468–1477.

Francouer, S.N. 2001. Meta-analysis of lotic nutrient amendment experiments: detecting and quantifying subtle responses. J. North Am. Benthol. Soc. **20**: 358–368.

Garvey, J.E., Marschall, E.A., and Wright, R.A. 1998. From star charts to stoneflies: detecting relationships in continuous bivariate data. Ecology, **79**: 442–447.

Griffith, G.E., Omernik, J.M., and Woods, A.J. 1999. Ecoregions, watershed, basins, and HUCs: how state and federal agencies frame water quality. J. Soil Water Conserv. **54**: 666–677.

Hecky, R.E., Campbell, P., and Hendzel, L.L. 1993. The stoichiometry of carbon, nitrogen, and phosphorus in particulate matter of lakes and oceans. Limnol. Oceanogr. **38**: 709–724.

Lohman, K., Jones, J.R., and Perkins, B.D. 1992. Effects of nutrient enrichment and flood frequency on periphyton biomass in Northern Ozark streams. Can. J. Fish. Aquat. Sci. **49**: 1198–1205.

McCauley, E., Downing, J.A., and Watson, S. 1989. Sigmoid relationships between nutrient and chlorophyll among lakes. Can. J. Fish. Aquat. Sci. **46**: 1175.

Mosisch, T.D., Bunn, S.E., Davies, P.M., and Marshall, C.J. 1999. Effects of shade and nutrient manipulation on periphyton growth in a subtropical stream. Aquat. Bot. **64**: 167–177.

Omernik, J.M. 1977. Nonpoint source – stream nutrient level relationships: a nationwide study. EPA-600/3-77-105. Corvallis Environmental Research Laboratory, Office of Research and Development, U.S. Environmental Protection Agency, Corvallis, Oreg.

Omernik, J.M. 1987. Ecoregions of the conterminous United States. Map (scale 1 : 7 500 000). Ann. Assoc. Am. Geogr. **77**: 118–125.

Omernik, J.M., and Bailey, R.G. 1997. Distinguishing between watersheds and ecoregions. J. Am. Water Res. Assoc. **33**: 935–949.

Pan, Y.R., Stevenson, J., Hill, B.H., Kaufmann, P.R., and Herlihy, A.T. 1999. Spatial patterns and ecological determinants of benthic algal assemblages in mid-Atlantic streams, U.S.A. J. Phycol. **35**: 460–482.

Prairie, Y.T., Duarte, C.M., and Kalff, J. 1989. Unifying nutrient–chlorophyll relationships in lakes. Can. J. Fish. Aquat. Sci. **46**: 1176–1182.

Press, W.H., Flannery, B.P., Teukolsky, S.A., and Vetterling, W.T. 1986. Numerical recipes. Cambridge University Press, Cambridge, Mass.

Romaní, A.M., and Sabater, S. 1999. Epilithic ectoenzyme activity in a nutrient-rich Mediterranean river. Aquat. Sci. **61**: 122–132.

Seip, K.L., Jeppsen, E., Jensen, J.P., and Faafeng, B. 2000. Is trophic state or regional location the strongest determinant for Chl-*a*/TP relationships in lakes? Aquat. Sci. **62**: 195–204.

Smith, V.H. 1982. The nitrogen and phosphorus dependence of algal biomass in lakes: an empirical and theoretical analysis. Limnol. Oceanogr. **27**: 1101–1112.

Smith, V.H. 1998. Cultural eutrophication of inland, estuarine, and coastal waters. *In* Successes, limitations and frontiers in ecosystem science. *Edited by* M.L. Pace and P.M. Groffman. Springer-Verlag, New York. pp. 7–49.

© 2002 NRC Canada

Smith, V.H., Tilman, G.D., and Nekola, J.C. 1999. Eutrophication: effects of excess nutrient inputs on freshwater, marine, and terrestrial ecosystems. Environ. Pollut. **100**: 179–196.

Toetz, D., Tang, L., Storm, D.E., Mihuc, T., and Smolen, M.D. 1999. Assessment of predictors from stream eutrophication potential. J. Am. Water Res. Assoc. **35**: 853–865.

Triska, F.J., Kennedy, V.C., Avanzino, R.J., and Reilly, B.N. 1983. Effect of simulated canopy cover regulation of nitrate uptake and primary production by natural periphyton assemblages. *In* Dynamics of lotic ecosystems. *Edited by* T.D. Fontaine III and S.M. Bartell. Ann Arbor Science Publishers, Ann Arbor, Mich. pp. 129–160.

Van Nieuwenhuyse, E.E., and Jones, J.R. 1996. Phosphorus–chlorophyll relationship in temperate streams and its variation with stream catchment area. Can. J. Fish. Aquat. Sci. **53**: 99–105.

Vis, C., Cattaneo, A., and Hudon, C. 1998. Periphyton in the clear and colored water masses of the St. Lawrence River (Quebec, Canada): a 20-year overview. J. Gt. Lakes Res. **24**: 105–117.

Welch, E.B., Jacoby, J.M., Horner, R.R., and Seeley, M.R. 1988. Nuisance biomass levels of periphytic algae in streams. Hydrobiologia, **157**: 161–168.

© 2002 NRC Canada

Using reproductive values to define optimal harvesting for multisite density-dependent populations: example with a marine reserve

Elizabeth N. Brooks

Abstract: A new method for determining optimal harvest from age-structured populations with a density-dependent stock–recruit relationship is presented. The theoretical optimal harvest comes from removing the age-class with the smallest ratio of reproductive value to weight. The method is derived from considering the sensitivity of equilibrium egg production to harvest using results for density-dependent Leslie matrices. The method holds in both single- and multi-site contexts and is derived for both Ricker and Beverton–Holt recruitment functions. I illustrate the method for a one-site model of Arcto-Norwegian cod (*Gadus morhua*) and obtain the same optimal strategy as previous methods, namely that age-class 6 should be harvested 45%. Including age-specific selectivities, the best constrained yields occur at a harvest rate of 11% on ages 5–12. This yield is 73% of the theoretical optimum. I considered the same model when a reserve is established and found that high transfer rates out of the reserve (where spawners attain a higher fecundity) produced greater yields that were 86% of the one-site (no reserve) yield. Also, if overfishing occurs at 1.5 and 2.0 times the optimal level in the one-site case, then most yields from the reserve model are greater than those from the one-site model.

Résumé : On trouvera ici une nouvelle méthode pour déterminer la récolte optimale chez des populations structurées selon l'âge dont la relation entre le stock et le recrutement est dépendante de la densité. La récolte optimale théorique s'obtient en retirant la classe d'âge qui possède le rapport le plus faible entre la valeur reproductive et la masse. La méthode est dérivée de la prise en compte à l'aide de matrices de Leslie dépendantes de la densité de la sensibilité de la production d'œufs à l'équilibre à la récolte. La méthode fonctionne dans les situations où il y a un ou plusieurs sites et elles est issue à la fois des fonctions de recrutement de Ricker et de Beverton–Holt. En guise d'illustration, la méthode est utilisée comme modèle à un seul site de la population arcto-norvégienne de la morue franche (*Gadus morhua*) et elle génère la même stratégie optimale que les modèles précédents, soit que la classe d'âge 6 devrait être récoltée à 45 %. Lorsqu'on inclut les sélectivités propres à chacun des âges, les meilleurs rendements forcés se réalisent aux taux de récolte de 11 % des classes d'âge 5–12. Ce rendement correspond à 73 % de l'optimum théorique. Si on établit une réserve, les forts taux de transfert hors de la réserve où les reproducteurs atteignent une fécondité supérieure, produisent des rendements accrus qui correspondent à 86 % du rendement à un site (sans réserve). De plus, si la surpêche se produit à un taux qui correspond à 1,5 ou 2,0 fois le niveau optimal dans le cas du site unique, alors la plupart des rendements du modèle avec réserve sont plus élevés que ceux prédits par le modèle à un site.

[Traduit par la Rédaction]

Introduction

The first analytical treatments of optimal harvesting were presented by Beddington and Taylor (1973), Doubleday (1975), and Rorres and Fair (1975), although the subject of maximizing harvesting had been present in the literature since at least Baranov (1918) (translated in Vilim 1977). For a density-independent age-structured matrix model (i.e., the "Leslie" matrix (Leslie 1945)), Beddington and Taylor (1973) and Rorres and Fair (1975) demonstrated analytically that the optimal solution involved harvesting at most two age-classes: the complete harvest of one age-class and a partial harvest of a second (younger) age-class. Doubleday (1975) showed that the optimal harvest problem could be easily solved by linear programming. The two age-class solution results directly from linear programming theory (Getz and Haight 1989). Dynamic programming was introduced into the fishery literature by Walters (1975) and Hilborn (1976). Other optimization techniques have been used, including graphical approaches and numeric searches where various potential strategies are explored and the resulting maximum sustainable yield (MSY) is compared (Hilborn 1979; Hightower and Lenarz 1989; Jensen 1996). Hilborn and Walters (1992) reviewed some of these techniques.

The methods cited above rely on numeric computations and (or) simulations to identify the optimal strategy without necessarily revealing the underlying biological reasons that

Received 15 October 2001. Accepted 30 April 2002. Published on the NRC Research Press Web site at http://cjfas.nrc.ca on 9 July 2002.
J16569

E.N. Brooks.[1] Department of Statistics, Biomathematics Program, North Carolina State University, Raleigh, NC 27695-8203, U.S.A.

[1]Present address: National Marine Fisheries Service, Southeast Fisheries Center, 75 Virginia Beach Drive, Miami, FL 33149, U.S.A. (e-mail: Liz.Brooks@noaa.gov).

 DOI: 10.1139/F02-058 © 2002 NRC Canada

make them optimal. In addition, this work pertained to single-site populations. A new method for determining optimal harvest (or minimum cost) in multisite, stage-structured matrix models was derived in Brooks and Lebreton (2001). They showed that yield would be maximized by harvesting the stage with the smallest ratio of reproductive value to harvest value and that harvest rate could be estimated from sensitivity analysis (e.g., Caswell 2001). This method provided a biological interpretation of the optimal solution, but density dependence was not included.

Reed (1980) demonstrated how the density-dependent, nonlinear harvesting problem could be solved by repeated application of a linear optimization. He found that the optimal strategy involved the harvest of at most two age-classes, the same result as for the density-independent models.

In this paper, the optimization methodology of Brooks and Lebreton (2001) is developed in a density-dependent context. I show that the criterion for selecting the optimal age-class is the same, although the estimation of optimal harvest level differs. This method is illustrated for Arcto-Norwegian cod (*Gadus morhua*) using the same model and parameter values as Reed (1980). I first develop a one-site age-structured matrix model and estimate the optimal harvesting strategy, which is seen to be equivalent to that found by Reed (1980) with linear programming. I then develop a two-site model to predict optimal harvesting strategies when only a part of the population is available to the fishery as a result of a marine reserve being established. For both models, the optimal strategies can be interpreted as a theoretical MSY, since implementation problems (e.g., gear selectivity) guarantee a lower observed yield. I therefore address constrained harvesting scenarios and demonstrate how alternative strategies can be ranked a priori using the same criterion.

Model development

One-site density-independent Leslie matrix

For populations that exhibit an annual birth pulse, and where annual survival and reproduction are similar among individuals of a given age, the Leslie matrix (Leslie 1945) is an appropriate model. Reproduction is assumed to occur as a "pulse", or at least in a short enough period of time that no mortality occurs contemporaneously. The number of individuals in each age-class at time t is given by the population vector, N_t. Given the Leslie matrix, L,

$$(1)\qquad \begin{bmatrix} f_1 & f_2 & \dots & f_n \\ s_1 & 0 & \dots & 0 \\ 0 & s_2 & 0 & \dots 0 \\ 0 & 0 \dots & \dots s_n & \dots 0 \end{bmatrix}$$

with age-specific fecundity (f_i) in the first row and age-specific survival (s_i) on the first subdiagonal, the size of the population at any time can be calculated by $N_{t+1} = LN_t$.

Well-known asymptotic results for matrix models have been derived elsewhere (Caswell 2001), so I summarize only a few essential details. Population growth rate, λ, is the dominant eigenvalue of L. The population increases or decreases exponentially for $\lambda > 1$ or $\lambda < 1$, respectively; $\lambda = 1$ indicates a stable population. Associated with λ are a right eigenvector, **w**, and left eigenvector, **v**; **w** gives the stable age structure, where $w_i = \frac{\prod_{j=1}^{j=i-1} s_j}{\lambda^{i-1}} = \frac{w_{i-1}s_{i-1}}{\lambda}$, and **v** gives the age-specific reproductive value, where $v_i = \frac{f_i}{\lambda} + \frac{f_{i+1}s_i}{\lambda^2} + \dots + \frac{f_n s_i s_{i+1} s_{i+2} \dots s_{k-1}}{\lambda^k}$ (assuming that k is the maximum age) and $v_1 = 1$. The sensitivity of λ to perturbation of entry l_{ij} in L is given by $\frac{\partial\lambda}{\partial l_{ij}} = \frac{v_i w_j}{< \mathbf{vw} >}$; **<vw>** is the scalar product.

One-site density-dependent matrix models

When one or more entries in L are a function of one or more age-classes in the population vector, N_t, the matrix is density dependent, and we have $N_{t+1} = L_{N_t}N_t$. The population size increases to an equilibrium value, $\bar{N}$, which may or may not be stable. As described above for density-independent models, one is generally interested in measuring sensitivity of λ (population growth rate). However, in a density-dependent model, $\lambda = 1$ at equilibrium. Perturbing matrix elements will shift the equilibrium value, but λ will return to 1, and thus, the sensitivity of λ is 0. Takada and Nakajima (1992) developed a method for calculating sensitivity of quantities other than λ in a density-dependent Leslie model. For example, if κ is a density-dependent factor in a matrix model, L (with entries l_{ij}), then the sensitivity of κ to a change in l_{ij} is given by (Takada and Nakajima 1992)

$$(2)\qquad \frac{\Delta\kappa}{\Delta l_{ij}} \approx \frac{\partial\kappa}{\partial l_{ij}} = \frac{v_i w_j}{-\sum_{i,j} v_i w_j \left[\frac{\mathrm{d}l_{ij}(\kappa)}{\mathrm{d}\kappa}\right]_{\kappa=\bar{\kappa}}}$$

In eq. 2, the sensitivity of κ to l_{ij} is proportional to the sensitivity of λ to l_{ij}, with the denominator containing the derivative of all l_{ij} that contain κ, weighted by the corresponding elements of the left and right eigenvectors. This derivative is evaluated at $\bar{\kappa}$, the equilibrium value associated with the unperturbed matrix.

In the matrix models that follow, density dependence is only incorporated into first-year survival, following a Ricker equation, so that the number of 1-year-olds alive at the end of one time step is given by $n_1 = Ee^{\alpha-\beta E}$, where E is total egg production given by $E = \sum_i f_i n_i$, where f_i is age-specific fecundity and n_i is the number of age i individuals (Ricker 1954; Reed 1980). The stability of the equilibrium for various forms of density-dependent first-year survival is discussed in Getz and Haight (1989, pp. 76–79). For the Ricker equation used in this model, Reed (1980) proved its stability.

Generalization to multiple sites

I briefly sketch the extension of Leslie matrices to multiple sites and refer readers to Lebreton (1996) and Brooks and Lebreton (2001) for a more thorough presentation. In one-site models, all entries in L are scalars. The multisite Leslie matrix, M, can be visualized from L as follows. For a

© 2002 NRC Canada

model of p sites and n age-classes, each entry in L becomes a $p \times p$ submatrix in M

$$(3) \quad M = \begin{bmatrix} M_{1,1} & M_{1,2} & M_{1,3} & \cdots & M_{1,n} \\ M_{2,1} & 0 & & \cdots & 0 \\ 0 & M_{3,2} & 0 & \cdots & 0 \\ \cdots & 0 & \cdots & 0 & \cdots \\ 0 & 0 & \cdots & M_{n,n-1} & 0 \end{bmatrix}$$

For each submatrix ($M_{i,j}$) in M, sites are nested within age-classes. For example, the first p rows of M contain age-specific submatrices $M_{1,a}$ with fecundity entries f_{ij}^a, representing an age a mother in site j who produces offspring in site i. In general, each $p \times p$ matrix of age-specific fecundities is considered diagonal, thus containing entries f_{ii}^a (Lebreton 1996)

$$(4) \quad M_{1,a} = \begin{bmatrix} f_{1,1}^a & 0 & \cdots & 0 \\ 0 & f_{2,2}^a & 0 & \cdots \\ \cdots & 0 & \cdots & 0 \\ 0 & \cdots & 0 & f_{p,p}^a \end{bmatrix}$$

On the first subdiagonal of M are $p \times p$ submatrices ($M_{a,a-1}$) with entries representing the product of annual probability of survival and migration from age $a - 1$ to age a

$$(5) \quad M_{a,a-1} = \begin{bmatrix} s_{1,1}^{a-1} & s_{1,2}^{a-1} & \cdots & s_{1,p}^{a-1} \\ s_{2,1}^{a-1} & s_{2,2}^{a-1} & \cdots & s_{2,p}^{a-1} \\ \cdots & & & \cdots \\ s_{p,1}^{a-1} & \cdots & & s_{p,p}^{a-1} \end{bmatrix}$$

For example, entries in $M_{a,a-1}$ are s_{ij}^{a-1} for an age $a - 1$ individual that began the year in site j, survived, and was present in site i at the start of the next time interval. In representing the process of survival and dispersal in an annual matrix, an assumption has to be made about the timing of migration. Traditionally, one forces the migration event to occur at the beginning or at the end of the survival process. For this model, I assume that the timing of annual events is reproduction, migration, and then survival. This is a simplification of the migration process that can have important implications for the model (Brooks 2000).

As in the one-site case, λ, the dominant eigenvalue of M, gives the overall growth rate of the system. The associated eigenvectors $\mathbf{w}$ and $\mathbf{v}$ give stable age-by-site structure and age-by-site reproductive value, respectively.

Optimal harvesting

The total yield, Y, achieved in a given year is

$$(6) \quad Y = \sum_{i,j} \text{weight}_{i,j} n_{i,j} h_{i,j}$$

where $\text{weight}_{i,j}$ is the weight of an age i individual in site j, $n_{i,j}$ is the number of age i individuals in site j, and $h_{i,j}$ is the proportion harvested from age i in site j. The optimum strategy will maximize Y for all possible h, i.e., it will give MSY. The only density-dependent term is survival in the first age-class, so the number of individuals in age-classes >1 at a given site can be calculated as the product of the number of 1-year-olds at the harvested equilibrium value for that site ($\bar{n}_{1(h),j}$) and the cumulative survival from harvesting to age i in that site ($\ell_{i(h),j}$) for the remaining age-classes ($\ell_{1(h),j}$ is defined to be 1). Consider harvesting age a in site 1 only

$$(7) \quad Y_{a,1} = \text{weight}_{a,1} \bar{n}_{1(h),1} \ell_{a,1} h_{a,1}$$

where $\ell_{a,1}$ is the cumulative survival to age a in site 1 in the absence of harvesting.

A multisite Ricker function is

$$(8) \quad n_{1,j} = E_j e^{\alpha_j - \beta_j E_j} = \varphi_j(E_j)$$

where $E_j = \sum_i f_{i,j} n_{i,j}$ is total egg production at site j and α_j and β_j are site-specific Ricker parameters. Thus, $\varphi_j(E_j)$ provides the number of recruits that survive for a given number of eggs produced in a year at site j, E_j.

Returning to eq. 7, there is a dependence between $h_{a,1}$ and $\bar{n}_{1(h),1}$ because the level of harvest will reduce the number of spawners, which in turn will alter E_1. Suppose we have a two-site system ($j = 1$ or 2). The $h_{a,1}$ will occur in matrix entries $m_{2a-1,2a-3}$ and $m_{2a-1,2a-2}$, which are $(1 - h_{a,1}) s_{1,1}^{a-1}$ and $(1 - h_{a,1}) s_{1,2}^{a-1}$. Using the chain rule for differentiating in conjunction with the density-dependent formula for sensitivity from eq. 2, the sensitivity of E_1 with respect to $h_{a,1}$ is

$$(9) \quad \frac{\Delta E_1}{\Delta h_{a,1}} \approx \frac{\partial E_1}{\partial h_{a,1}} = \frac{-v_{a,1} w_{a-1,1} s_{1,1}^{a-1} - v_{a,1} w_{a-1,2} s_{1,2}^{a-1}}{-\sum_{i,j} v_{i,1} w_{i,1} \left[\dfrac{\mathrm{d}m_{ij}(E_1)}{\mathrm{d}E_1} \right]_{E_1 = \bar{E}_1}}$$

Recalling that E_1 appears in only the first row of matrix M (in entries of the form $f_{1,1}^i \varphi_1(E_1)$ for all ages i) and that $w_{a,1} = w_{a-1,1} s_{1,1}^{a-1} + w_{a-1,2} s_{1,2}^{a-1}$ when $\lambda = 1$, eq. 9 simplifies to

$$(10) \quad \frac{\Delta E_1}{\Delta h_{a,1}} \approx \frac{-v_{a,1} w_{a,1}}{-v_{1,1} \sum_i w_{i,1} f_{1,1}^i \varphi_1'(\bar{E}_1)}$$

where $v_{a,1}$ is the reproductive value of an age a individual in site 1 and $w_{a,1}$ is the proportion of individuals age a in site 1.

Given that $\Delta h_{a,1} = 0 - h_{a,1} = -h_{a,1}$, an estimate of $h_{a,1}$ is then

$$(11) \quad \hat{h}_{a,1} = \frac{-\Delta E_1 \left(v_{1,1} \sum_i w_{i,1} f_{1,1}^i \varphi_1'(\bar{E}_1) \right)}{v_{a,1} w_{a,1}}$$

In eq. 11, $\varphi_1'(\bar{E}_1)$ is a constant and $\sum_i w_{i,1} f_{1,1}^i$ is also a constant and will be similar to P_{unfished} (defined below; see Goodyear 1993). However, migration between sites and the fact that density dependence is tacitly incorporated into the stable age-by-site vector $\mathbf{w}$ complicate a direct comparison with P_{unfished}.

The expression for yield when only one age is harvested was

$$(12) \quad Y_{a,1} = \text{weight}_{a,1} \bar{n}_{1(h),1} \ell_{a,1} h_{a,1}$$

© 2002 NRC Canada

Substituting $\hat{h}_{a,1}$ and $\bar{n}_{1(h),1} = \varphi_1(E_{1(h_a)})$, where $E_{1(h_a)}$ is egg production in site 1 when age a is harvested by proportion h, the expression for yield becomes

$$(13)\quad Y_{a,1} = \frac{\text{weight}_{a,1}\varphi_1(E_{1(h_a)})\ell_{a,1}(-\Delta E_1)\varphi_1'(\bar{E}_1)v_{1,1}\sum_i w_{i,1}f_{1,1}^i}{v_{a,1}w_{a,1}}$$

Lastly, recognizing $\ell_{a,1} = w_{a,1}$, we have

$$(14)\quad \hat{Y}_{a,1} = \frac{\varphi_1(E_{1(h_a)})(-\Delta E_1)\varphi_1'(\bar{E}_1)v_{1,1}\sum_i w_{i,1}f_{1,1}^i}{v_{a,1}/\text{weight}_{a,1}}$$

For the Ricker curve, there is one level of stock size where production of recruits beyond replacement is greatest (see Ricker 1975). There will be many harvesting strategies that can reduce the stock to this level. Thus, regardless of the age-class(es) harvested, $\varphi_1(E_{1(h)})$ and ΔE_1 will be constant. However, we want to know which one of those strategies gives the overall maximum yield. Examining eq. 14, the only age-dependent terms are reproductive value in site 1 ($v_{a,1}$) and age-specific weight in site 1 ($\text{weight}_{a,1}$); all remaining terms are constants. Thus, yield will increase as this ratio ($v_{a,1}/\text{weight}_{a,1}$) decreases, and the optimal harvesting strategy will be to harvest the age- and site-class with the smallest ratio of reproductive value to weight. (The development above is presented in a multisite context but will clearly hold for a one-site model. Also, because the Beverton–Holt curve possesses a unique point of maximum surplus production, the result will hold for that case as well.)

This is precisely the result obtained in the density-independent case by Brooks and Lebreton (2001). The interpretation is analogous also: if all age-classes were of the same economic value, the greatest number of individuals could be removed from the least reproductively valuable age-class; when economic value (weight in this example) varies with age and site, then an individual's reproductive value is "weighted" by its weight.

Estimation of proportion to harvest ($h_{a,1}$)

Having identified the optimum age-class to harvest, one might look to eq. 11 above to estimate $h_{a,1}$. All quantities are known except $E_{1(h_a)}$, which is the egg production of the harvested population. It is also the point where replacement is maximized. However, because the Ricker function is transcendental, $E_{1(h_a)}$ cannot be found analytically. Instead, one can vary $h_{a,1}$ from 0 and 1 and compare the resulting yields to identify the level of harvest producing the MSY. (But see appendix III in Ricker (1975) and Hilborn (1985) for a solution when both E and $\varphi(E)$ have the same units.)

In one-site models, the optimal solution involves harvesting at most two age-classes. That would be detected from this method as follows. First, the optimal age- and site-class, $n_{a,j}$, is identified from the vector **v/weight**; next, one varies $h_{a,j}$ from 0 to 1 and examines the resulting yield. If the yield increases monotonically, then the predicted MSY will occur for $h_{a,j} = 1$. There are two possibilities at this point: either the MSY involves complete harvest of age a at site j and no additional harvest or a second (younger) age-class will be harvested partially. To determine which possibility is correct, one returns to the original **v/weight** vector and selects the age-class with the second smallest value, e.g., age b at site k ($b < a$ necessarily). By fixing $h_{a,j}$ at 1.0 and varying $h_{b,k}$ from 0 to 1, MSY will either increase from the value when only age a was harvested completely or it will not. If it increases, the optimal harvesting strategy involves two age-classes; if it does not, then only age a should be harvested.

The reason for the two-age strategy in a one-site model is simple: complete harvest of one age-class effectively reduces the maximum age. Therefore, at any given time, only one age-class can be harvested completely and a second age-class partially. However, as Brooks and Lebreton (2001) showed, this result is particular to one-site models. In a multisite model, migration from unharvested sites can "replenish" age-classes beyond the one completely exploited at the harvested site. Therefore, it is possible to obtain optimal solutions involving the harvest of more than two age-classes in multisite models. The method for identifying successive ages to harvest remains the same.

Finite versus instantaneous rates

The model parameters s and h have been implicitly assumed to be finite rates (h is akin to u, the finite annual exploitation in the fisheries literature). In the absence of fishing, instantaneous age-specific natural mortality, M_i, is

$$(15)\quad M_i = -\ln(s_i) \quad (\text{or } s_i = e^{-M_i})$$

The model development assumes that age-specific (and site-specific in a multisite case) survivals and fecundities are known. However, the timing of the fishery will affect the estimate of h_i and hence of F_i (instantaneous fishing mortality). If a pulse fishery is assumed, then h_i can be estimated as described above, and F_i is

$$(16)\quad F_i = -\ln(1-h_i) \quad \text{or} \quad F_i = -\ln(1-h_i e^{M_i})$$

for a pulse at the start or end of the year, respectively. If fishing occurs continuously throughout the year or for only a fraction, Δt, of the year, then there is no direct relationship between h and s, and F_i cannot be estimated as before (see Pollock et al. (1991) and Brooks et al. (1998) for instantaneous rate formulations for these cases). Whereas $h_i = 1$ implies no survival beyond age i, in an instantaneous formulation, survival only approaches zero asymptotically. One way to resolve this is to select an instantaneous rate beyond which one assumes zero survival. For example, for $Z_i = F_i + M_i \geq 5$, e^{-Z_i} is effectively zero. Thus, $5 - M_i$ could be used as an upper bound for the estimate of F_i. To test whether the optimal strategy involves harvesting more than one age, the process is similar to that outlined above: if MSY increases monotonically for F_i in $[0, 5 - M_i]$, then fix F_i at $5 - M_i$ and vary F_j from 0 to $5 - M_j$, where j corresponds to the age-class with the second smallest ratio of reproductive value to weight.

Robustness of method

Determination of natural mortality is notoriously difficult in practice. I explored how the optimal strategy varied if the assumed level of natural mortality was biased by assuming that all age-specific natural mortality was under- or overestimated by 10 or 50%. I reran the model with each set of

© 2002 NRC Canada

biased survival rates and recalculated the vector **v/weight** to see if the ranking of elements changed.

Illustration: Arcto-Norwegian cod

One-site case (no reserve)

A 12-age-class, density-dependent matrix model was constructed using parameter values (Table 1) presented in Reed (1980) (the data trace to Walters (1969) and ultimately to Garrod (1967)). Following Reed (1980), I assume that survival probability beyond age 12 is zero. Fecundity is given as the proportion mature at age multiplied by average weight at age (Walters 1969). For the Ricker relationship, $\bar{n}_1 = Ee^{\alpha-\beta E}$, $\alpha = 2.895$, and $\beta = 0.0174$ (Reed 1980).

Given an arbitrary initial population structure, the model was projected until it reached equilibrium (Table 2). At equilibrium, I calculated the left eigenvector, **v**, which gives age-specific reproductive value, and then found the ratio of age-specific reproductive value to age-specific weight (Table 1). From this new vector (**v/weight**), it was possible to identify the age-class (a) that had the smallest ratio, making it the optimal age-class to harvest. I then allowed h_a to vary between 0 and 1 and compared the resulting yields to identify the harvest level giving maximum yield.

Since implementing a single age-class harvest would be impossible in practice, I considered alternative (constrained) harvesting strategies by looking at the pattern of **v/weight** values. This vector allows one to evaluate a priori how different combinations of minimum and maximum size restrictions will impact expected MSY. Perhaps the most realistic harvesting strategy to implement involves specifying only a minimum age (this could be translated to a minimum size limit by an age–length relationship). Walters (1969) pointed out that it was not appropriate to assume knife-edge mesh selection. Therefore, I used age-specific selectivities for ages 3–6 of 0.05, 0.38, 0.62, and 0.85, respectively, assuming that ages 7 and older were fully recruited (Walters 1969), and calculated yield for all possible minimum sizes between ages 3 and 12.

Two-site case (reserve and nonreserve area)

A two-site density-dependent matrix model was constructed using the same age-specific survival, fecundity, and weight values as for the one-site case (Table 1). Assuming that the reserve site made up 25% of the total area and that the fish were uniformly distributed, site-specific Ricker functions were created by adjusting α and β until the unfished equilibrium population size in the reserve (R) was 25% of $\bar{N}$ (the one-site equilibrium population size) and in the nonreserve (NR) was 75% of $\bar{N}$ (Table 2). These adjusted values were $\alpha_R = 2.39$, $\beta_R = 0.0357$, $\alpha_{NR} = 2.82$, and $\beta_{NR} = 0.0215$.

To allow interaction between the reserve and nonreserve, parameter values for migration are needed. This parameter will be difficult to measure in practice but could be estimated from tagging studies (Hilborn 1990; Brownie et al. 1993; Schwarz et al. 1993). Migration is expected to vary with the size of the closed area and could vary for different age groups. I considered a fixed reserve size (25% of the total area) and evaluated three simple transfer rate scenarios assuming that all age-classes migrate with the same probability: (*i*) transfer rates correspond directly to reserve proportion (25% of the fish population move into the reserve and 75% of the fish population move into the nonreserve area annually), (*ii*) equal migration of 50% between sites annually, and (*iii*) limited, unequal migration of 10% moving from reserve to nonreserve and 15% moving from nonreserve to reserve annually. These transfer rates were chosen to give a wide range of movement probabilities and also to cover the three possible outcomes for movement bias (higher probability to move into the reserve, higher probability to move out of the reserve, equal probability to move into or out of the reserve). My objective was not to estimate the optimal reserve size but rather to illustrate how the introduction of a closed area could affect yield and optimal harvesting strategies. In addition, I explored how constrained optimal harvesting strategies could vary between a no-reserve versus a reserve system.

The equipment employed for harvesting fish can be very destructive to the habitat (e.g., bottom trawling devices). Closing an area to fishing could lead to a higher quality habitat in the reserve, which could positively influence survival and (or) fecundity. I explored a situation where fish in the reserve are 10% more productive by increasing the Ricker parameters: $\alpha_{R(HF)} = 2.6$ and $\beta_{R(HF)} = 0.035$ (where HF is high fecundity) (Fig. 1). In the absence of harvesting, this additional fecundity brought the equilibrium population size to $\bar{N} = 1396.5$ (with no migration). I compare optimum yields from constrained harvesting for one-site and two-site models with normal or high fecundity.

Lastly, I consider how creating a reserve compares with a no-reserve case where the level of fishing exceeds the optimum. The yields calculated at the optimum harvest level in the no-reserve case are almost surely unattainable because it requires that all fisheries harvest at the exact mandated level. As many stocks are overexploited, it is unrealistic to compare yields with a reserve with yields that assume strict compliance. Therefore, I compare yields with a reserve with yields obtained without a reserve but where fishing level is 1.5 or 2.0 times the optimal harvest level.

For all simulations, calculations for spawner potential ratio (SPR) are made. This quantity represents the ratio of fished to unfished lifetime reproductive potential and has become a standard biological reference point for fisheries management (Goodyear 1993; Mace and Sissenwine 1993). SPR was calculated as

$$\text{(17)} \quad \text{SPR} = \frac{P_{\text{fished}}}{P_{\text{unfished}}}$$

where (Goodyear 1993)

$$\text{(18)} \quad P = \sum_{i=1}^{n} f_i \prod_{j=0}^{i-1} s_j$$

In these equations, P is the average lifetime reproductive potential and is calculated with and without fishing, f_i is fecundity at age i (density dependence ignored), and s_j is survival from age j to $j + 1$ (Goodyear 1993). Because this calculation is presented for each MSY harvesting strategy, we are in fact calculating SPR_{MSY}.

© 2002 NRC Canada

Table 1. Age-specific annual survival probability, weight at age, annual fecundity rates, and age-specific reproductive value (v_i) divided by weight (weight$_i$) for Arcto-Norwegian cod.

Age	Survival	Weight	Fecundity	v_i/weight$_i$
1	Density dependent	—	—	—
2	0.72	—	—	—
3	0.72	0.20	—	9.65
4	0.72	0.53	—	5.06
5	0.72	1.01	—	3.68
6	0.70	1.60	—	**3.32**
7	0.60	2.35	0.10	3.77
8	0.50	2.91	0.38	5.65
9	0.50	3.58	0.94	7.83
10	0.61	4.22	1.76	8.55
11	0.68	4.82	3.05	7.57
12	0.61	5.37	4.36	5.19

Note: Age-class 6 has the lowest v_i/weight$_i$ value (in bold) and is therefore the optimum age-class to harvest. Fecundity is average age-specific weight multiplied by proportion mature.

Table 2. Equilibrium values for unharvested population in one-site and two-site models.

Parameter	Description	Equilibrium value
One-site model		
$\bar{N}$	Total population size	1261.50
$\bar{n}_1$	Recruitment	382.04
$\bar{E}$	Egg production	59.74
$\varphi(\bar{E})$	Ricker function	6.39
Two-site model		
$\bar{N}$	Total population size	1263.50
$\bar{N}_R$	Population size in reserve	316.16
$\bar{N}_{NR}$	Population size in nonreserve	947.30
$\bar{n}_1$	Total recruitment	382.63
$\bar{n}_{1R}$	Recruits in reserve	95.75
$\bar{n}_{1NR}$	Recruits in nonreserve	286.88

Note: R, reserve; NR, nonreserve.

Results

One-site case (no reserve)

Age 6 is the optimal age-class to harvest, as it has the smallest ratio of reproductive value to weight (Table 1). By varying h_6 from 0 to 1 (by increments of 0.01), I found that the maximum yield occurred when h_6 = 0.45 (MSY = 39.98). This agrees with Reed (1980). Examining the vector **v/weight**, one can predict a priori that the best maximum yield for constrained harvesting strategies (where both minimum and maximum age exploited can be controlled) will involve harvesting ages 5 and 6 (because age 5 has the second smallest ratio) and will decrease for other strategies in the order listed in Table 3 (knife-edge selectivity assumed). This is consistent with fig. 2 in Reed (1980).

As more age-classes were exploited, the level of sustainable harvest decreased from a high of 0.45 when only age 6 was targeted to 0.07 when ages 3–12 were caught (Table 3). This harvest rate can be interpreted as an annual exploitation rate (u in fisheries literature). For simplicity, a pulse fishery was assumed. Yield per recruit (YPR) decreased monotonically, while equilibrium population size and number of recruits varied slightly (although unsystematically). SPR_{MSY} was 0.55.

Incorporating selectivity, I found that the MSY for a minimum age control occurs for a low level of harvest for ages 5–12 (MSY = 29.00, h = 0.11). This value is about 73% of the theoretical MSY (when only age 6 is harvested). Increasing the minimum age causes MSY to decrease, with the sharpest decline when changing from a minimum age of 7 to 8 (Table 4). Harvesting ages 7–12 would achieve 62% of the theoretical MSY.

When optimal fishing levels (h values in Table 4) for a minimum age control are 1.5 times the optimal h, yields are 46–56% less than the optimal MSY, and the harvested population size ($\bar{N}_h$) is 25–30% the unharvested size for many of the harvest strategies (Table 5). When harvesting at twice the optimal h, yields are negligible, and so is the harvested population size. This precipitous drop is associated with SPR levels below 35%.

Two-site case (reserve and nonreserve)

The ratios for age-specific reproductive value to weight were exactly the same as for the one-site case. Thus, regardless of migration pattern, age-class 6 is still the optimal class to exploit when a reserve equal to 25% of the total fished area is created. The theoretical unconstrained MSY for migration pattern *i* is 84% that of the one-site case, while for migration patterns *ii* and *iii*, it is 86 and 70% of the one-site value, respectively (Table 6).

MSY for constrained harvesting follows the same age category rankings as in the one-site case. MSY decreases (as do harvest level and YPR) as transfer rates from reserve to nonreserve decrease. In general, MSY values from the two-site constrained scenarios (Table 6) were less than the one-site values (Table 3). The harvested equilibrium population size and number of recruits (total in both sites) was in approximately the same range as that found in the one-site case (Tables 3 and 4), although for migration pattern *iii*, it was about 12–20% lower. The level of harvest is similar to the level of harvest in the one-site model for migration pattern *i* and is slightly higher than the one-site levels for migration patterns *ii* and *iii*.

© 2002 NRC Canada

Fig. 1. Ricker curves used in the models. The solid line corresponds to the one-site Ricker curve, the open circles are the nonreserve curve (for the two-site model), and the dashed line is the reserve curve (for the two-site model). The curve with the plus signs refers to the two-site model when it was assumed that fish in the reserve obtained a higher fecundity. E is a proxy for total egg production given by $E = \sum_i f_i n_i$, where f_i is relative reproductive potential (calculated as proportion mature at age i multiplied by weight at age i) and n_i is the number of age i individuals. $\phi(E) = Ee^{\alpha-\beta E}$ and gives the number of age-1 fish that results from a given level of E.

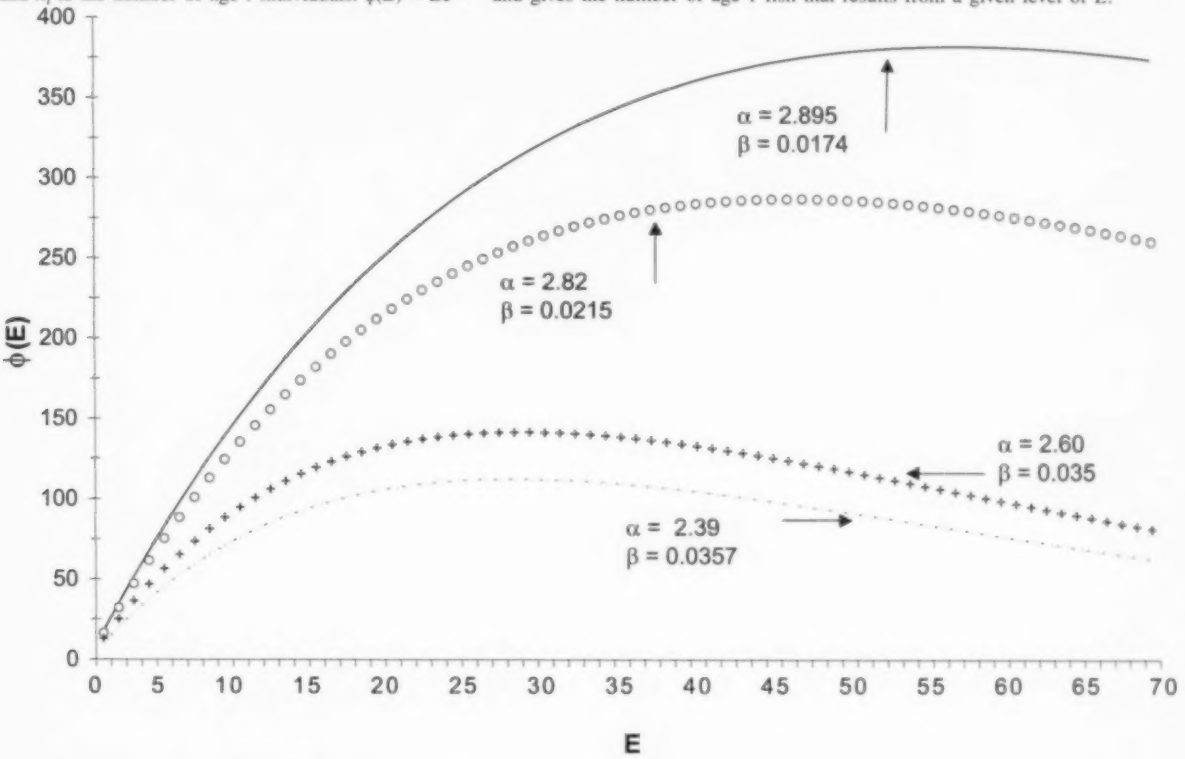

Table 3. One-site constrained MSY for different combinations of harvested age-classes.

Ages harvested	MSY	Harvest level	Equilibrium population	Number at age 1	YPR	SPR
6	**39.98**	**0.45**	**918.58**	**295.14**	**0.14**	**0.55**
5–6	37.71	0.26	892.66	293.50	0.13	0.55
5–7	37.12	0.18	914.04	296.07	0.13	0.55
4–7	33.75	0.14	880.91	293.09	0.12	0.55
4–8	32.35	0.11	927.95	303.82	0.11	0.56
4–9	30.79	0.10	903.22	294.14	0.10	0.55
4–10	29.67	0.09	916.74	296.71	0.10	0.55
4–11	28.98	0.09	872.56	282.50	0.10	0.53
4–12	28.93	0.08	946.31	304.29	0.10	0.56
3–12	26.39	0.07	923.64	304.53	0.09	0.56

Note: When more than one age-class is harvested, it is assumed that harvest is applied equally to all harvested age-classes (i.e., full selectivity assumed). The row for age-class 6 is in bold, indicating the theoretical MSY. YPR, yield per recruit; SPR, spawner potential ratio.

Calculation of SPR in the multisite model is not straightforward, given that there is not a reliable measure of net multisite reproductive rate: the one-site measure is corrupted by the fact that progeny may migrate to different sites where survival and fecundity differ, thus causing slight differences in generation times by site (Lebreton 1996). For the sake of this paper, site-specific SPR was calculated as the ratio of site-specific egg production with and without harvesting: $\mathrm{SPR}_j = \overline{E}_{j(h)}/\overline{E}_j$. This prevents direct comparison with SPR values in the one-site case but at least provides a comparison within the two-site models. SPR levels in the nonreserve ranged from 0.40 to 0.55 and from 0.43 to 0.61 in the reserve when both a minimum age control and a maximum age control were implemented. When only the minimum age can be controlled, SPR in the nonreserve varied from 0.38 to 0.48 and from 0.42 to 0.75 in the reserve, and for the cases

© 2002 NRC Canada

Table 4. One-site constrained MSY assuming that control of only the minimum age-class recruited is possible.

Ages harvested	MSY	Harvest level	Equilibrium population	Number of recruits	YPR	SPR
3–12	28.51	0.10	924.48	293.96	0.10	0.55
4–12	28.68	0.10	932.49	295.84	0.10	0.55
5–12	**29.00**	**0.11**	**917.77**	**288.79**	**0.10**	**0.54**
6–12	27.99	0.12	951.98	296.31	0.09	0.55
7–12	24.72	0.15	938.22	289.63	0.09	0.54
8–12	19.77	0.20	958.67	294.02	0.07	0.55
9–12	17.03	0.29	986.66	301.50	0.06	0.56
10–12	16.59	0.49	996.40	303.89	0.05	0.56
11–12	17.52	0.94	1042.10	317.33	0.06	0.59
12	14.38	1.00	1236.10	375.14	0.04	0.80

Note: Ages 7–12 were assumed to be fully recruited to the fishery, whereas for ages 3–6, age-specific harvest was scaled by age-specific selectivity (0.05, 0.38, 0.62, and 0.85, respectively). The row with ages 5–12 is in bold, indicating overall MSY.

Table 5. One-site constrained MSY when the level of fishing is 1.5 times the optimal h (from Table 4).

Ages harvested	MSY	Harvest level	Equilibrium population	Number of recruits	YPR	SPR
3–12	15.28	0.15	358.00	116.30	0.13	0.40
4–12	16.09	0.15	377.50	122.20	0.14	0.40
5–12	13.47	0.165	307.90	98.50	0.14	0.39
6–12	15.85	0.18	388.40	122.30	0.13	0.40
7–12	11.80	0.225	325.30	101.20	0.12	0.39
8–12	11.22	0.30	405.80	125.10	0.09	0.41
9–12	11.96	0.435	537.10	164.65	0.07	0.43
10–12	13.06	0.735	644.00	196.80	0.06	0.45
11–12	**17.45**	**1.00**	**1015.70**	**309.40**	**0.06**	**0.57**
12	14.38	1.00	1236.10	375.14	0.04	0.80

Note: I assume that control of only the minimum age-class recruited is possible. Ages 7–12 were assumed to be fully recruited to the fishery, whereas for ages 3–6, age-specific harvest was scaled by age-specific selectivity (0.05, 0.38, and 0.85, respectively). The row with ages 11–12 is in bold, indicating overall MSY. For the last two rows, harvest level is not 1.5 times optimal h because h cannot be increased beyond 1.0.

Table 6. MSY for different combinations of harvested age-classes in the nonreserve area.

Ages harvested	MSY[a]	Harvest level[a]	YPR[a]	MSY[b]	Harvest level[b]	YPR[b]	MSY[c]	Harvest level[c]	YPR[c]
6	**33.44**	**0.52**	**0.17**	**34.37**	**0.67**	**0.20**	**23.66**	**0.59**	**0.18**
5–6	30.23	0.29	0.14	29.11	0.35	0.16	22.02	0.35	0.16
5–7	29.53	0.20	0.14	28.08	0.24	0.16	21.02	0.24	0.16
4–7	26.65	0.15	0.12	25.04	0.18	0.14	18.97	0.18	0.14
4–8	25.54	0.12	0.11	24.08	0.15	0.13	17.84	0.14	0.13
4–9	24.40	0.11	0.11	22.98	0.13	0.13	16.66	0.12	0.12
4–10	23.56	0.10	0.11	22.21	0.12	0.12	15.78	0.11	0.12
4–11	23.10	0.09	0.10	21.82	0.11	0.12	15.25	0.10	0.11
4–12	23.12	0.09	0.10	21.79	0.11	0.12	15.07	0.10	0.11
3–12	20.96	0.08	0.10	19.57	0.09	0.10	13.73	0.09	0.10

Note: When more than one age-class is harvested, it is assumed that harvest is applied equally to all harvested age-classes (i.e., full selectivity assumed). The row for age-class 6 is in bold, indicating theoretical MSY.

[a]Transfer rate from reserve to nonreserve was 0.75; transfer rate from nonreserve to reserve was 0.25.

[b]Transfer rate from reserve to nonreserve was 0.5; transfer rate from nonreserve to reserve was 0.5.

[c]Transfer rate from reserve to nonreserve was 0.10; transfer rate from nonreserve to reserve was 0.15.

when only the oldest ages are harvested, $SPR_{nonreserve}$ was 0.72–0.78 and $SPR_{reserve}$ was 0.90–0.98.

When only the minimum age harvested in the nonreserve can be controlled, the maximum yield occurs for harvesting ages 5–12 (Fig. 2). MSY decreases as migration rates out of the reserve decrease. The sharpest decline within each migration pattern occurs between harvesting ages 7–12 versus ages 8–12. Compared with constrained harvests from the one-site model (Table 4), yields from the reserve model were generally less. However, nearly all two-site constrained yields were greater than one-site yields for "overfished" scenarios. (This comparison excludes the last two entries in Table 5 because h could not be increased sufficiently.)

When fish in the reserve realize a higher fecundity, yields for migration pattern *i* are approximately 87% the one-site yields, while for migration patterns *ii* and *iii*, yields are 74–89 and 51–62% that of one-site models. When the level of fishing in the one-site model exceeded the optimal level,

© 2002 NRC Canada

Fig. 2. MSY for alternative management scenarios. The transfer rates are abbreviated T1, T2, and T3, reserve+HF are the cases where fish reproducing in the reserve obtain higher fecundity, and the overfished scenarios are given by 1.5×*h* and 2.0×*h*. Yield is in relative biomass.

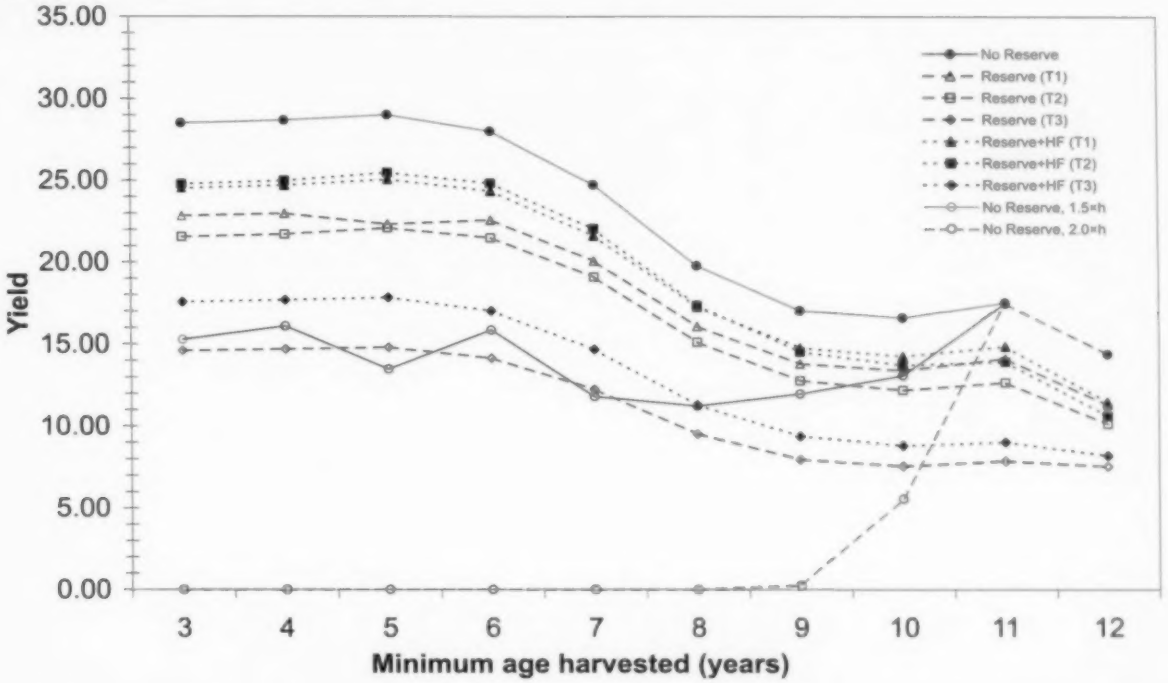

yields from the high-fecundity reserve model were higher for nearly all migration patterns.

Overall, the best yields are obtained with no reserve, assuming perfect compliance with the minimum age (Fig. 2). The next best yields were obtained with a reserve for migration patterns *i* and *ii* when fish in the reserve obtain higher fecundity followed by the same migration patterns assuming normal fecundity.

If natural mortality rate of all age-classes is over- or underestimated by the same proportion, the ranking of elements in the vector **v/weight** is unchanged, and thus the optimal age-class can still be identified.

Discussion

A very simple, biologically intuitive method for determining optimal harvesting strategies has been developed for density-dependent matrix models. Because matrix models have been in the literature for more than 50 years (density-independent case: Leslie 1945; density-dependent case: Leslie 1948), their construction and the calculation of their asymptotic properties (eigenvalues and eigenvectors) are assumed to be routine. (The availability of mathematical software with linear algebra packages, such as MATLAB® or MAPLE®, makes this trivial.) The optimal age-class to harvest can be determined simply by examining age-specific lifetime reproductive value (the left eigenvector at unharvested equilibrium) divided by age-specific weight. Yield will be maximized by harvesting the age-class with the smallest ratio. If a second age-class is to be harvested to attain MSY, it will be the age-class with the second smallest ratio. Furthermore, by inspection of the vector **v/weight**, various age-specific harvesting strategies can be ranked.

Many management reference points involve calculation of the reproductive potential of the spawning stock, either SPR or spawning stock biomass (SSB). Katsukawa and Matsumiya (1998) used the concept of Fisher's reproductive value to calculate age-specific expected lifetime spawning values, which are precisely the same quantities as the elements of the left eigenvector, **v**. They demonstrated that management decisions based on total reproductive value are more robust to errors in stock size than calculations based on SSB. Their work supports the criterion developed herein, where age-specific reproductive values play a central role. This criterion for selecting the optimal age-class encapsulates the inherent harvesting trade-off between the value of a given age-class to the population (given by its expected lifetime reproductive value) versus its value to a fishery (in terms of weight). This conclusion is general, without respect to life history, and holds for multisite models as well (both density independent and density dependent). Unlike the one-site case, however, the multisite solution may involve harvesting more than two age-classes.

While other methods exist for determining MSY, they are essentially numeric and lack a clear, biological motivation in their approach. The methodology of this paper, based on sensitivity of equilibrium egg production ($\bar{E}$) to harvest, was biologically driven. First-year survival is a density-

© 2002 NRC Canada

dependent function of stock size (and the quantity of eggs that they produce). Therefore, the sensitivity of $\overline{E}$ to harvest is expected to play a role in determining the optimal strategy because survival (and hence, recruitment to the fishery) depends on egg production.

Garrod (1988) stated that the life history of cod is such that the pattern of YPR shows a maximum at low F values when the minimum age harvested is low, with the maximum shifting to higher F values when the minimum age harvested is increased. This was found to be true in both one- and two-site models. However, analysis of YPR values is not sufficient to identify the optimal strategy because YPR does not account for the effect of harvest on subsequent recruitment.

In summarizing some general characteristics of maximum yield policies, Walters (1969, pp. 511–512) stated that they would be "most strongly determined by growth rates and reproductive parameters (relative fecundities, reproduction curve constants)..." and that "the best policy is to harvest each cohort close to the age when biomass loss through numbers decline balances biomass gain through growth...". Reed showed analytically that for increasing recruitment functions (i.e., no overcompensation), the optimal strategy would not occur before the age where natural biomass (defined as age-specific weight multiplied by cumulative survival-to-age) reaches a maximum. Getz (1980) proved the same result for a more general class of recruitment functions (Getz and Haight 1989). These authors verbalized or analytically proved an MSY "guideline", i.e., they identified an age-class that served as a lower bound for optimal harvesting strategies. However, a simple and explicit method for determining which age (or ages) should be harvested had been lacking.

Prager et al. (1987) suggested that lifetime reproductive values be used as a guideline for evaluating alternative management strategies aimed at rebuilding fish stocks. This is similar to the criterion developed herein, when the vector of weights (or economic value) is equal for all age-classes. However, the values that he used for lifetime reproduction actually correspond to net-maternity values (see Caswell 2001), which will only be equivalent to elements of the left eigenvector if $\lambda = 1.0$ (which is true for density-dependent populations).

In this analysis, $SPR_{MSY} = 55\%$ and the population declined dramatically when SPR dropped below 35%. Traditionally, SPR in the range of 30–40% has served as a management threshold. My results suggest that perhaps higher SPR values should be considered.

When confronted with the need to introduce new management controls to reduce exploitation, there are two main options. The first is to try to decrease harvesting levels (either through increasing the minimum age harvested or decreasing total fishing pressure). This was the primary method used for most of the last century. The current status of many fish stocks indicates that this approach has not been successful. One reason is that implementation is not perfect. As the minimum age is increased, at-sea discards of underaged fish may increase as well, which would mitigate the expected gain in protection from the new size limit. Also, bycatch mortality is difficult to control and may not have been accurately accounted for when new fishing recommendations were created. An alternative control is to close certain areas to fishing. Implementation may be limited by enforcement (but see Murawski et al. (2000), who reported the use of ship and aircraft patrol as well as a requirement that all vessels carry a satellite receiver–transmitter). The effect on yields depends on the size of the reserve, the transfer rates into and out of the reserve, and the quality of the reserve habitat and its effects on survival and reproduction of fish located within its boundaries. Intuitively, if fish live longer in a reserve, they will attain a greater size and should have higher fecundity.

It remains to be determined what an appropriate reserve size is and what transfer rates could be expected. Also, deciding on reserve placement will surely have social or political components factored into the decision. This simple model indicates that reasonable yields are still obtainable when a reserve is created. And when a stock is being overfished, creating a reserve led to higher sustainable yields.

Several important factors are ignored in this development. First, the model is deterministic, although high recruitment variability is a common feature of many fisheries. This would affect realized yields but would probably not have much effect on the **v/weight** vector. Second, release mortality is ignored. This could significantly reduce realized yields as the minimum age is raised. Third, the method derived equilibrium yield, but it is probably unreasonable to expect that equilibrium conditions can be attained, let alone maintained. In this respect, transient (short term) yields may be more important criteria for deciding on an appropriate management strategy. Transient analysis of the harvesting strategies presented here indicates that the more age-classes that are harvested, the faster the model converged and the less severe the annual fluctuations in yield (Brooks 2000). This supports a strategy with light harvesting and a fairly young minimum age (which would also cut down on release mortality). The theoretical optimum will rarely be obtainable, but it provides an upper bound against which alternative yields can be compared. Nevertheless, by providing a direct connection with the biology, the selection criterion for determining the optimal strategy reinforces the notion that reproduction is a key factor to consider in the management of fish stocks.

Acknowledgements

Drs. K.H. Pollock, J.E. Hightower, and G.R. Hess provided valuable suggestions for improving this manuscript. The author also acknowledges the comments of Dr. D. Vaughan and an anonymous referee, which helped improve the final manuscript.

References

Baranov, T.I. 1918. On the question of the biological basis of fisheries. Nauch. Issledov. Iktiol. Inst. Izv. I, (1), Moscow. pp. 81–128.

Beddington, J.R., and Taylor, D.B. 1973. Optimum age specific harvesting of a population. Biometrics, **29**: 801–809.

Brooks, E.N. 2000. Dynamics and management of sub-divided populations. Ph.D. thesis, North Carolina State University, Raleigh, N.C.

Brooks, E.N., and Lebreton, J.-D. 2001. Optimizing removals to control a metapopulation: application to the yellow legged herring gull (*Larus cachinnans*) Ecol. Model. **136**: 269–284.

© 2002 NRC Canada

Brooks, E.N., Pollock, K.H., Hoenig, J.M., and Hearn, W.S. 1998. Estimation of fishing and natural mortality from tagging studies on fisheries with two user groups. Can. J. Fish. Aquat. Sci. **55**: 2001–2010.

Brownie, C., Hines, J.E., Nichols, J.D., Pollock, K.H., and Hestbeck, J.B. 1993. Capture–recapture studies for multiple strata including non-Markovian transitions. Biometrics, **49**: 1173–1187.

Caswell, H. 2001. Matrix population models. 2nd ed. Sinauer, Sunderland, Mass.

Doubleday, W.G. 1975. Harvesting in matrix population models. Biometrics, **31**: 189–200.

Garrod, D.J. 1967. Population dynamics of the Arcto-Norwegian cod. J. Fish. Res. Board Can. **24**: 145–190.

Garrod, D.J. 1988. North Atlantic cod: fisheries and management to 1986. *In* Fish population dynamics. 2nd ed. *Edited by* J.A. Gulland. John Wiley & Sons, New York. pp. 185–218.

Getz, W.M. 1980. The ultimate sustainable yield problem in nonlinear age-structured populations. Math. Biosci. **48**: 279–292.

Getz, W.M., and Haight, R.G. 1989. Population harvesting. Princeton University Press, Princeton, N.J.

Goodyear, C.P. 1993. Spawning stock biomass per recruit in fisheries management: foundation and current use. *In* Risk evaluation and biological reference points for fisheries management. *Edited by* S.J. Smith, J.J. Hunt, and D. Rivard. Can. Spec. Publ. Fish. Aquat. Sci. No. 120. pp. 67–81.

Hightower, J.E., and Lenarz, W.H. 1989. Optimal harvesting policies for the widow rockfish fishery. Am. Fish. Soc. Symp. **6**: 83–91.

Hilborn, R. 1976. Optimal exploitation of multiple stocks by a common fishery: a new methodology. J. Fish. Res. Board Can. **33**: 1–5.

Hilborn, R. 1979. Comparison of fisheries control systems that utilize catch and effort data. J. Fish. Res. Board Can. **36**: 1477–1489.

Hilborn, R. 1985. Simplified calculation of optimum spawning stock size from Ricker's stock recruitment curve. Can. J. Fish. Aquat. Sci. **42**: 1833–1834.

Hilborn, R. 1990. Determination of fish movement patterns from tag recoveries using maximum likelihood estimators. Can. J. Fish. Aquat. Sci. **47**: 635–643.

Hilborn, R., and Walters, C.J. 1992. Quantitative fisheries stock assessment. Chapman and Hall, New York.

Jensen, A.L. 1996. Density-dependent matrix yield equation for optimal harvest of age-structured wildlife populations. Ecol. Model. **88**: 125–132.

Katsukawa, T., and Matsumiya, Y. 1998. Fisheries management based on reproductive potential: an example for chub mackerel. *In* Fishery stock assessment models. *Edited by* F. Funk, T.J. Quinn II, J. Heifetz, J.N. Ianelli, J.E. Powers, J.F. Schweigert, P.J. Sullivan, and C.-I. Zhang. Alaska Sea Grant College Program Rep. No. AK-SG-98-01, University of Alaska Fairbanks. pp. 999–1012.

Lebreton, J-D. 1996. Demographic models for subdivided populations: the renewal equation approach. Theor. Popul. Biol. **49**: 291–313.

Leslie, P.H. 1945. On the use of matrices in certain population mathematics. Biometrika, **35**: 183–212.

Leslie, P.H. 1948. Some further notes on the use of matrices in population mathematics. Biometrika, **35**: 213–245.

Mace, P., and Sissenwine, M.P. 1993. How much spawning per recruit is enough? *In* Risk evaluation and biological reference points for fisheries management. *Edited by* S.J. Smith, J.J. Hunt, and D. Rivard. Can. Spec. Publ. Fish. Aquat. Sci. No. 120. pp. 101–118.

Murawski, S.A., Brown, R., Lai, H.-L., Rago, P.J., and Hendrickson, L. 2000. Large-scale closed areas as a fishery-management tool in temperate marine systems: the Georges Bank experience. Bull. Mar. Sci. **66**: 775–798.

Pollock, K.H., Hoenig, J.M., and Jones, C.M. 1991. Estimation of fishing and natural mortality when a tagging study is combined with a creel survey or port sampling. Am. Fish. Soc. Symp. **12**: 423–434.

Prager, M.H., O'Brien, J.F., and Saila, S.B. 1987. Using lifetime fecundity to compare management strategies: a case history for striped bass. N. Am. J. Fish. Manag. **7**: 403–409.

Reed, W.J. 1980. Optimum age-specific harvesting in a nonlinear population model. Biometrics, **36**: 579–593.

Ricker, W.E. 1954. Stock and recruitment. J. Fish. Res. Board Can. **11**: 559–623.

Ricker, W.E. 1975. Computation and interpretation of biological statistics of fish populations. Bull. Fish. Res. Board Can. No. 191.

Rorres, C., and Fair, W. 1975. Optimal harvesting policy for an age-specific population. Math. Biosci. **24**: 31–47.

Schwarz, C.J., Schweigert, J.F., and Arnason, A.N. 1993. Estimating migration rates using tag-recovery data. Biometrics, **49**: 177–193.

Takada, T., and Nakajima, H. 1992. An analysis of life history evolution in terms of the density-dependent Lefkovitch matrix model. Math. Biosci. **112**: 155–176.

Vilim, E. 1977. Theory of fishing. *In* Selected works on fishing gear. Vol. 3. *Edited by* P. Greenburg. Keter Publishing House, Jerusalem. pp. 2–41.

Walters, C.J. 1969. A generalized computer simulation model for fish population studies. Trans. Am. Fish. Soc. **98**: 505–512.

Walters, C.J. 1975. Optimal harvest strategies for salmon in relation to environmental variability and uncertain production parameters. J. Fish. Res. Board Can. **32**: 1777–1784.

© 2002 NRC Canada

Among- and within-species variability in fatty acid signatures of marine fish and invertebrates on the Scotian Shelf, Georges Bank, and southern Gulf of St. Lawrence

Suzanne M. Budge, Sara J. Iverson, W. Don Bowen, and Robert G. Ackman

Abstract: The fat and fatty acid compositions of 28 species of fish and invertebrates (n = 954) from the Scotian Shelf, Georges Bank, and the Gulf of St. Lawrence were determined. Discriminant analysis of the 16 most numerous species ($n \geq 18$ each), using 17 major fatty acids, classified species with greater than 98% accuracy and grouped species into three general clusters (gadids, flatfish, and planktivores) with similar fatty acid compositions, and likely, similar diets. A number of species exhibited changes in fatty acid signatures with increasing size (multivariate analysis of variance), which corresponded with known dietary shifts reported from stomach contents analyses. Location effects were also observed among the three major geographical regions and were probably due to broad-scale variations in prey assemblages and phytoplankton composition in the northwestern Atlantic. Despite these effects, within-species variation was still substantially less than among-species variation. Thus, fatty acid signatures can be used to distinguish and characterize fish and invertebrate species in a given ecosystem, as well as to study finer-scale trophic interactions of these species. These data also have applications at higher trophic levels and will serve as a prey database for studying the diets of other fish and marine mammal predators using fatty acid signatures.

Résumé : On trouvera ici une analyse de la composition en graisses et en acides gras de 28 espèces de poissons et d'invertébrés (n = 954) de la plate-forme néo-écossaise, du banc George et du golfe du Saint-Laurent. Une analyse discriminante des 16 espèces les plus abondantes (nombre d'individus $\geq$ 18) basée sur 17 acides gras principaux classifie correctement les espèces avec une précision de 98 % et les rassemble en trois groupes généraux (les gadidés, les poissons plats et les planctonophages) qui possèdent des compositions en acides gras et probablement des régimes alimentaires similaires. Plusieurs espèces affichent un changement dans leurs signatures d'acides gras en fonction de la taille (analyse multidimensionnelle de variance), ce qui correspond à des variations du régime alimentaire déjà observées par l'analyse des contenus stomacaux. Il existe aussi des variations spatiales dans les trois principales régions géographiques, variations qui sont probablement dues à des différences à grande échelle dans les communautés de proies et la composition du phytoplancton dans le nord-ouest de l'Atlantique. Malgré ces effets, la variation intraspécifique est considérablement plus faible que la variation interspécifique. Les signatures d'acides gras peuvent donc être utilisées pour reconnaître et caractériser les espèces de poissons et d'invertébrés dans un écosystème donné, ainsi que pour étudier les interactions trophiques détaillées de ces espèces. Ces données peuvent s'appliquer aussi aux niveaux trophiques plus élevés et servir d'information de base sur les proies dans l'étude des régimes alimentaires d'autres poissons et mammifères marins prédateurs à l'aide des signatures d'acides gras.

[Traduit par la Rédaction]

Introduction

The decline or collapse of many commercial fisheries around the world has underscored the need for alternatives to single-species assessments (Pauly et al. 1998). Among the alternative approaches is an attempt to understand stock dynamics within a broader ecosystem context (e.g., Christensen et al. 1996; Köster et al. 2001). These approaches recognize that the interrelationships among predators and prey, as well as changes in the physical environment, can influence the population dynamics of commercial stocks. Fish and marine mammals are significant consumers of commercially harvested species in a number of marine ecosystems (Bax 1991; Bowen 1997). In eastern Canada, attempts to understand bottom-up

Received 3 August 2001. Accepted 8 March 2002. Published on the NRC Research Press Web site at http://cjfas.nrc.ca on 9 July 2002.
J16482

S.M. Budge[1] **and S.J. Iverson.** Department of Biology, Dalhousie University, Halifax, NS B3H 4J1, Canada.
W.D. Bowen. Marine Fish Division, Bedford Institute of Oceanography, Department of Fisheries and Oceans, Dartmouth, NS B2Y 4A2, Canada.
R.G. Ackman. Canadian Institute of Fisheries Technology, DalTech, Dalhousie University, Halifax, NS B3J 2X4, Canada.

[1]Corresponding author (e-mail: budges@is.dal.ca).

 DOI: 10.1139/F02-062 © 2002 NRC Canada

or top-down trophic interactions of commercial fish stocks have been sporadic, with few long-term studies of the diets of the fish stocks of interest or of their fish or marine mammal predators (Lilly 1986; Albikovskaya et al. 1991). Determining the diet composition of predators is clearly fundamental to delineating food webs. The predominant methods that have been used to estimate the diets of marine predators are based on the recovery of prey structures resistant to digestion from stomachs and faeces (e.g., Popova 1978; Pierce and Boyle 1991). These methods have proved useful, and in fact, most of our understanding of fish and marine mammal diets has been derived from such studies. Nevertheless, these methods are subject to known biases, some of which can be corrected, whereas others continue to limit the value of estimated diets (e.g., Jobling and Breiby 1986). For example, prey without hard structures or with readily degradable structures may be underrepresented in diet reconstructions.

It has been known for some time that lipids, and especially fatty acids, can be used as biological markers and general diet indicators in marine ecosystems (e.g., Sargent et al. 1987). Fatty acids are components of the more general group of lipids and are ubiquitous in nature. They have a variety of structures but, in marine organisms, commonly contain from 14 to 24 carbon atoms and have varying degrees of unsaturation. Because of biochemical properties and limitations, many dietary fatty acids are incorporated into marine animals with little or no modification of the original structure, making these fatty acids useful as indicators or markers of the dietary source. Combinations of these markers, or the whole suite of fatty acids present, are referred to as the fatty acid signature of an organism (Iverson 1993).

Early studies recognized that the fatty acid composition of zooplankton lipids influenced the fatty acid composition of the blubber lipids of the baleen whales that fed on them (e.g., Ackman and Eaton 1966). However, Sargent et al. (1987) were among the first groups to suggest the use of marker fatty acids in the study of trophic relationships. Since that time, numerous studies have demonstrated that fatty acid signatures can be passed from prey to predator, both at the bottom (e.g., Fraser et al. 1989; Graeve et al. 1994) and near the top (e.g., Iverson 1993; Kirsch et al. 1998; Kirsch et al. 2000) of the food web. Once fatty acid patterns are characterized in prey, they can be used to trace food webs and diets of predators. For example, fatty acids have been used to study the diets of fish and copepods (e.g., Sargent et al. 1989; Fraser et al. 1989; St. John and Lund 1996). Fatty acids have also been used to indicate the presence of fish and other prey in the diets of terrestrial and aquatic carnivores (e.g., Rouvinen et al. 1992; Colby et al. 1993), the degree to which plants have been consumed by terrestrial carnivores (Iverson et al. 2001), and spatial or temporal differences in diets both within and between marine mammal species (Iverson et al. 1997*a*, 1997*b*; Smith et al. 1997).

Thus, the fatty acid signatures of marine fish and invertebrates can be used to study their ecology and trophic interactions (i.e., bottom-up) but can also be characterized to study the diets of their fish or marine mammal predators. To use fatty acids to estimate the diets of apex marine carnivores, we need to understand the degree to which prey species can be distinguished on the basis of their fatty acid signatures and how stable these signatures are with respect to ecological variability. We expect marine fish and invertebrate fatty acid signatures to vary predominantly with the diets characteristic of the species, but also with changes in primary and secondary production related, in turn, to temporal and spatial variability in the physical environment. Changes in the diet of a fish can result in a significant change in its fatty acid signature in as little as 3 weeks (Kirsch et al. 1998); thus we can expect to rapidly detect shifts in diet. Fatty acid composition is also influenced to varying degrees by the biochemistry of the organism and its reproductive status (i.e., the presence of lipid-rich eggs prior to spawning) (Sargent et al. 1989; Sargent 1995). Lastly, for some fish species, including gadids, diets change with increasing body size such that fatty acid signatures may vary among age groups within a species (e.g., Iverson et al. 1997*b*).

The objectives of this study were (*i*) to determine the fatty acid composition of selected commercial and noncommercial marine fishes and invertebrates from the Scotian Shelf, Georges Bank, and Gulf of St. Lawrence that are known or potential prey of marine mammals; (*ii*) to determine whether species can be reliably differentiated on the basis of their fatty acids; and (*iii*) to examine the effects of geographic location and body size on fatty acid signatures within prey species.

Materials and methods

Sample collection

Fish and invertebrate samples were collected during stratified-random bottom-trawl surveys conducted in the spring, summer, or fall on the Scotian Shelf (Northwest Atlantic Fisheries Organization (NAFO) subareas 4V, 4W, and 4X), and on Georges Bank (5Z) in 1993, 1994, 1995, and 1996, and in the southern Gulf of St. Lawrence (4T) in 1999 (Fig. 1; Table 1). Additional invertebrate samples were obtained from research cruises and commercial fisheries on the Scotian Shelf. As our initial interest was to determine the fatty acid signatures of potential prey of marine mammals, we restricted the length of fish collected to between 10 and 40 cm (Bowen et al. 1993). No restriction was placed on the size of invertebrates collected. Although we would have preferred to collect species in all seasons, locations, and years, this was not possible because of constraints associated with collection and sampling. At collection, individuals or groups of individuals of each species were stored frozen at –20°C in airtight plastic bags until analysis (<6 months).

Lipid and fatty acid analysis

Individual fishes and invertebrates were thawed and fork length or carapace width of each individual was measured to the nearest 0.1 cm; body mass was measured to the nearest 0.1 g. Each individual was then homogenized in a blender or food processor. Although it may have increased within-species variability, we made no attempt to remove stomach contents of individuals before homogenization because our objective was to characterize them as prey, which are generally eaten whole by fish and marine mammal predators. Lipids were quantitatively recovered in duplicate from samples of the homogenized tissue using a modified Folch et al. (1957) method. Briefly, 1.5-g tissue aliquots were extracted with 30 mL 2:1 chloroform–methanol and the entire lower

© 2002 NRC Canada

Fig. 1. Northwest Atlantic Fisheries Organization (NAFO) fishing zones surrounding Nova Scotia, Canada, referred to in the present study.

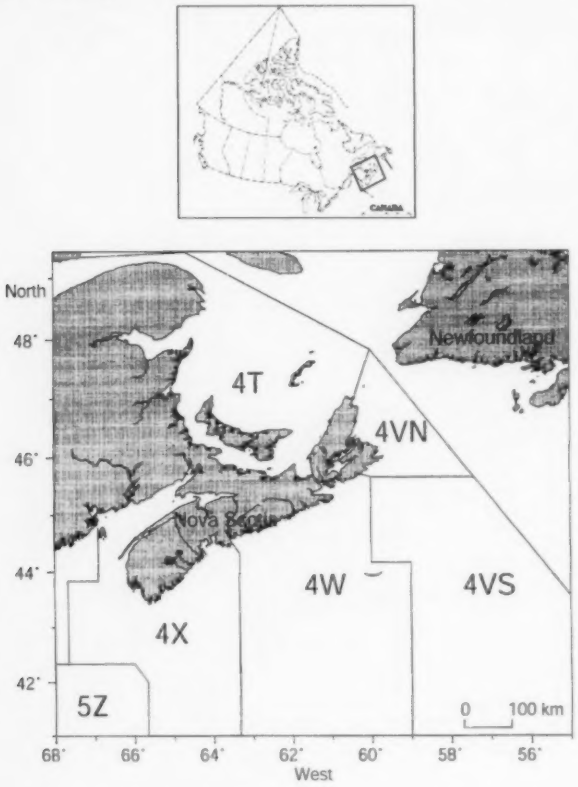

phase was collected. This fraction was then washed, filtered through anhydrous sodium sulphate, evaporated under nitrogen, and vacuum sonicated to obtain total lipid weight. Fatty acid methyl esters (FAME) were prepared and analyzed in duplicate according to Iverson et al. (1997*b*) using a Perkin-Elmer Autosystem II capillary gas chromatograph (GC) (Norwalk, Conn.) with a flame ionization detector (ID) using a flexible fused silica column (30 × 0.25 mm ID) coated with 50% cyanopropyl polysiloxane (0.25 μm film thickness; J&W DB-23; Folsom, Calif.). Helium was used as the carrier gas and the gas line was equipped with an oxygen scrubber. The following temperature program was used: 153°C for 2 min, hold at 174°C for 0.2 min after ramping at 2.3°C·min^{-1}, and hold at 220°C for 3 min after ramping at 2.5°C·min^{-1}. Up to 66 FAME were identified according to Iverson et al. (1997*b*, 2001) and reported as weight percent of total fatty acids. Each fatty acid was described using the shorthand nomenclature of *A*:*Bn*–*X*, where A represents the number of carbon atoms, *B* the number of double bonds, and *X* the position of the double bond closest to the terminal methyl group.

Data analysis and interpretation

Fatty acid data were analyzed using a combination of classification and regression trees (CART), discriminant function analysis, and multivariate analysis of variance (MANOVA). Most multivariate methods require that the data meet several requirements. With discriminant analysis and MANOVA, the number of samples must exceed the number of variables to offer some assurance that the covariance matrices are homogeneous (Stevens 1986). In this study, we have set the number of fatty acid variables to 17 allowing all species with sample numbers of 18 or greater to be included in the analysis. We used the 17 fatty acids that were either most abundant and (or) exhibited the greatest average variance across all species, accounting for approximately 86% of total fatty acids identified. In addition, for both discriminant analysis and MANOVA, the data were normalized using a log transformation according to the following equation: $x_{trans} = \ln(x_i/c_r)$, where x_i is a given fatty acid expressed as percent of total fatty acids, x_{trans} is the transformed fatty acid data, and c_r is the percentage of a reference fatty acid, in this case, 18:0 (Aitchison 1986).

We also investigated differences in the fatty acid compositions of samples with CART, which has been used previously to classify fatty acid signatures (Iverson et al. 1997*a*, 1997*b*; Smith et al. 1997). CART has the advantage of making fewer assumptions than most other multivariate methods. Homogeneous covariance matrices are not required, the number of variables is not limited by sample size, and variables need not be normally distributed, so that untransformed percentage data may be used. This permitted us to use all fatty acids and a greater number of species in the analysis. CART analyses were conducted with the S-PLUS 4.0 software (Statsci Division, Mathsoft Inc., Seattle, Wash.). All other analyses were carried out with SPSS 9.0 (SPSS Inc., Chicago, Ill.). The standard deviations (SD) are given as a measure of variability about the mean.

Results

A total of 954 samples representing 28 species were analyzed for total fat content and fatty acid composition (Tables 1 and 2). Scientific names of species referred to in the text are given in Table 1. We also present average lipid concentration, length, body mass, and fatty acid composition of all species (Table 2). (Note that individual data from all 954 samples are available from the authors.) Data from all 28 species (i.e., $n \geq 5$) were used in classifications with CART (classification success given in Table 2). Of these, 16 species had sample sizes ≥18 and were examined in more detail using discriminant analysis and MANOVA.

Among-species variation in fatty acid composition

Major fatty acid characteristics

Of the 66 fatty acids identified, 14:0, 16:0, 16:1*n*–7, 18:1*n*–9, 20:1*n*–9, 22:1*n*–11, 20:5*n*–3, and 22:6*n*–3 made up 60–80% of total fatty acids in the 28 species (Table 2). Other fatty acids, including 18:0, 18:1*n*–7, 20:1*n*–11, 22:1*n*–9, 18:2*n*–6, 18:4*n*–3, 20:4*n*–6, and 22:5*n*–3 were often present in amounts >1%. A preliminary examination of the average fatty acid compositions among different species (Table 2) revealed some obvious similarities and differences. For example, in the Gadidae species (cod, haddock, pollock, red hake, silver hake, and white hake), levels of 22:6*n*–3 tended to be

© 2002 NRC Canada

Table 1. Distribution of species collected with respect to location (NAFO subarea; see Fig. 1) and season.

Species	4VsW	4Vs	4Vn	4W	4X	5Z	4T	Unknown	Total
American plaice (*Hippoglossoides platessoides*)	—	25sp	—	3sp	29s	24sp	18f	—	99
Argentine (*Argentina silus*)	—	—	—	—	10s	—	—	—	10
Butterfish (*Peprilus triacanthus*)	—	—	—	10sp	—	—	—	—	10
Capelin (*Mallotus villosus*)	—	6s	—	29sp	—	—	21f	—	56
Cod (*Gadus morhua*)	23u	—	—	9sp, 16s	—	15sp	21f	—	84
Gaspereau (*Alosa pseudoharengus*)	—	—	—	19sp	—	—	22f	—	41
Haddock (*Melanogrammus aeglefinus*)	—	3sp	—	10sp, 6s	28s	7sp	—	—	54
Halibut (*Hippoglossus hippoglossus*)	—	—	—	8sp	—	—	—	—	8
Herring (*Clupea harengus*)	—	—	—	38s	—	—	21f	15f	74
Lobster (*Homarus americanus*)	—	—	9u	—	—	—	—	—	9
Longhorn sculpin (*Myoxocephalus octodecemspinosus*)	—	10sp	—	10sp	—	—	—	—	20
Mackerel (*Scomber scombrus*)	—	—	—	10sp	—	—	—	—	10
Northern sand lance (*Ammodytes dubius*)	—	27sp	—	44s	—	—	—	—	71
Ocean pout (*Macrozoarces americanus*)	—	—	—	11sp	7s	—	—	—	18
Pollock (*Pollachius virens*)	—	—	10sp	4s	7s	4sp	—	—	25
Red crab (*Geryon quinquedens*)	—	—	—	—	14u	—	—	—	14
Red hake (*Urophycis chuss*)	—	—	—	7sp	—	—	—	—	7
Redfish (*Sebastes* sp.)	—	—	8s	3s	8s	—	30f	—	49
Rock crab (*Cancer irroratus*)	—	—	10u	—	—	—	—	—	10
Sea raven (*Hemitripterus americanus*)	—	—	—	4sp	2s	—	—	—	6
Shrimp (*Pandalus borealis*)	—	—	25sp	21f	—	—	—	—	46
Silver hake (*Merluccius bilinearis*)	—	—	—	18sp	15s	5sp	—	—	38
Smooth skate (*Raja senta*)	—	5sp	—	—	—	—	—	—	5
Thorny skate (*Raja radiata*)	—	12sp	—	—	—	—	—	—	12
White hake (*Urophycis tenuis*)	—	11sp	—	5sp	—	—	30f	—	46
Winter flounder (*Pseudopleuronectes americanus*)	—	—	—	4sp, 10s	11s	—	—	—	25
Winter skate (*Raja ocellata*)	—	—	—	15sp	—	—	—	—	15
Yellowtail flounder (*Limanda furruginea*)	5sp, 26s	—	—	15sp, 10s	4s	12sp	20f	—	92
Total	54	99	62	339	135	67	183	15	954

Note: NAFO, Northwest Atlantic Fisheries Organization; sp, spring; s, summer; f, fall; u, unknown.

higher than in most other species, whereas 20:1*n*–9 and 22:1*n*–11 were more abundant in planktivores such as capelin, herring, and sandlance.

CART analysis

We initially investigated variation in fatty acid signatures of the 28 species using all 66 fatty acids. A tree using 20:5*n*–3 at the root node generated 65 terminal nodes and an overall classification success rate of 89% (Table 2). Although the tree was complex, the root node generally separated species according to feeding patterns and life histories with, for instance, all capelin and sand lance classified into the left branch and all invertebrates and most of the flatfish into the right branch of the tree. Tenfold cross-validation with forcing of 20:5*n*–3 at the root node produced a reduced classification success of 73%, as would be expected (see below). Selection of other fatty acids for the root node generated trees with similar separation of species along each branch but with poorer classification success.

Despite the overall high classification success of nearly 90%, there was considerable variation in the proportion correctly classified among species. In 18 of the 28 species, ≥80% of individuals were correctly classified (12 species >90% correct; Table 2). However, in the other 10 species, classification percentage generally varied from 40 to 73%, with one case of 0% in the sea ravens ($n = 6$). We expected that one source of this variability in success might be sample size, which ranged from 5 to 99 among species. Species represented with data from <20 individuals were significantly more likely to have a classification rate <80% than species represented by a larger number of samples ($\chi^2 = 11.9$, df = 1, $P = 0.001$).

Discriminant analysis

To investigate among-species variation in greater detail, we conducted a discriminant function analysis of the 16 most numerous species. Fifteen discriminant functions, or linear combinations of variables, were generated with the first five functions accounting for 88% of the variance. A plot of the average scores of the first two discriminant functions, representing 57% of the variance, showed three major groups of species that tended to have similar fatty acid compositions (Fig. 2). The first discriminant function separated species into two groups, roughly representing flatfish and gadids in the upper and lower right quadrants and the planktivores (including sand lance, herring, and capelin) in the upper left quadrant. The second discriminant function separated Gadidae species and shrimp from the flatfish. Al-

© 2002 NRC Canada

Table 2. Fat and fatty acid composition of fish and invertebrate species from the Scotian Shelf, Georges Bank, and the Gulf of

	American plaice (n = 99)	Argentine (n = 10)	Butterfish (n = 10)	Capelin (n = 56)	Cod (n = 84)	Gaspereau (n = 41)	Haddock (n = 54)
Length (cm)	27.4 ± 8.5	26.2 ± 1.2	15.5 ± 1.9	13.3 ± 2.2	36.5 ± 6.7	22.8 ± 3.4	27.0 ± 5.8
Mass (g)	217.8 ± 201.9	180.1 ± 27.0	73.1 ± 29.8	12.4 ± 5.9	481.1 ± 264.4	126.3 ± 48.2	202.2 ± 133.2
Lipid content (%)	2.2 ± 1.3	6.6 ± 2.7	7.2 ± 3.1	8.3 ± 4.4	2.1 ± 1.0	12.6 ± 6.7	1.4 ± 0.6
Saturated fatty acids (%)							
14:0	3.52 ± 1.46	6.56 ± 0.44	5.00 ± 0.96	6.26 ± 1.17	2.06 ± 0.84	5.17 ± 1.04	1.97 ± 0.94
16:0	14.35 ± 2.03	11.90 ± 0.89	16.48 ± 1.00	12.48 ± 3.10	14.32 ± 1.79	16.83 ± 1.02	14.39 ± 1.13
18:0	3.73 ± 1.15	2.13 ± 0.19	4.84 ± 0.77	1.14 ± 0.42	3.63 ± 0.95	2.87 ± 0.72	4.08 ± 0.73
Subtotal	21.61 ± 2.31	20.59 ± 0.82	26.32 ± 1.26	19.88 ± 3.98	20.00 ± 2.12	24.87 ± 1.05	20.44 ± 0.93
Monounsaturated fatty acids (%)							
16:1n–7	6.29 ± 3.88	4.77 ± 0.56	3.11 ± 0.74	9.96 ± 2.67	5.19 ± 3.10	3.85 ± 0.56	3.07 ± 1.20
18:1n–9	8.42 ± 1.62	7.40 ± 1.65	22.69 ± 5.37	7.26 ± 3.63	10.14 ± 1.67	15.46 ± 3.47	8.82 ± 1.91
18:1n–7	4.18 ± 1.09	2.04 ± 0.33	2.10 ± 0.32	2.87 ± 1.54	4.71 ± 1.33	3.28 ± 0.66	4.13 ± 0.86
20:1n–11	1.02 ± 0.79	0.65 ± 0.11	0.23 ± 0.22	0.46 ± 0.16	0.71 ± 0.30	0.83 ± 0.20	0.72 ± 0.24
20:1n–9	3.26 ± 2.02	13.52 ± 1.60	4.50 ± 1.27	12.42 ± 4.72	3.96 ± 2.49	5.91 ± 1.28	3.10 ± 1.94
20:1n–7	1.44 ± 0.86	0.56 ± 0.13	1.25 ± 0.31	0.74 ± 0.29	0.74 ± 0.45	0.56 ± 0.17	0.83 ± 0.30
22:1n–11	2.71 ± 2.61	17.67 ± 3.09	2.70 ± 2.65	15.34 ± 6.59	2.64 ± 2.30	5.80 ± 2.93	1.65 ± 1.58
22:1n–9	0.56 ± 0.42	1.69 ± 0.20	3.07 ± 0.84	1.40 ± 0.57	0.48 ± 0.28	0.75 ± 0.43	0.49 ± 0.24
24:1	1.09 ± 0.44	0.43 ± 0.12	0.72 ± 0.28	0.91 ± 0.31	1.06 ± 0.68	0.53 ± 0.22	1.17 ± 0.41
Subtotal	28.96 ± 8.30	48.73 ± 2.92	40.37 ± 3.42	51.36 ± 9.24	29.62 ± 7.99	36.97 ± 3.52	23.98 ± 3.62
Polyunsaturated fatty acids (%)							
18:2n–6	0.93 ± 0.32	0.96 ± 0.12	0.75 ± 0.23	1.19 ± 0.32	0.78 ± 0.20	1.36 ± 0.37	0.76 ± 0.16
18:4n–3	0.84 ± 0.63	1.77 ± 0.42	0.76 ± 0.42	1.34 ± 0.45	0.83 ± 0.47	1.63 ± 0.72	0.75 ± 0.51
20:4n–6	2.51 ± 1.18	0.70 ± 0.07	1.63 ± 0.39	0.34 ± 0.19	1.83 ± 0.81	0.86 ± 0.29	2.54 ± 0.67
20:5n–3	13.90 ± 2.76	7.61 ± 1.13	5.06 ± 0.84	7.39 ± 2.56	13.81 ± 2.23	7.48 ± 0.87	14.77 ± 2.34
22:5n–3	2.65 ± 0.76	1.40 ± 0.24	2.35 ± 0.20	0.74 ± 0.13	1.44 ± 0.30	1.64 ± 0.32	1.90 ± 0.37
22:6n–3	17.03 ± 5.76	9.60 ± 1.72	10.76 ± 2.26	9.65 ± 4.53	22.77 ± 7.50	15.04 ± 3.13	24.77 ± 4.69
Subtotal	37.86 ± 7.17	22.04 ± 2.58	21.31 ± 2.87	20.66 ± 6.10	41.47 ± 6.66	28.00 ± 3.16	45.49 ± 3.92
Total	88.43 ± 1.65	91.36 ± 0.39	88.00 ± 0.79	91.91 ± 0.69	91.09 ± 0.99	89.84 ± 1.00	89.91 ± 1.15
CART Classification	92.9%	100.0%	80.0%	96.4%	90.5%	92.7%	83.3%

Note: Values are mean ± standard deviation of the 17 fatty acids (and 18:0 reference) used in discriminant analysis and MANOVA. Complete data, including individuals correctly classified to species (89.3% overall).

Fig. 2. Discriminant analysis of the 16 species represented by ≥18 individuals and using the 17 fatty acids that exhibited the greatest average variance (see Table 2). Plot shows the average scores of the first 2 of 15 discriminant functions that classified individuals to species with a 98% success rate. Ellipses surrounding the three major clusters of groups are based on the data point clouds of individuals, rather than just the average scores.

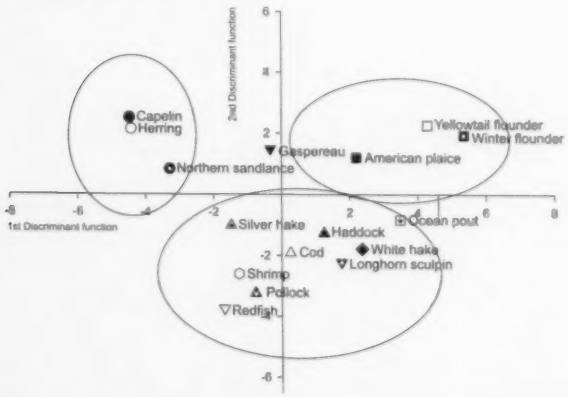

though shrimp were grouped with the Gadidae species using only the first two discriminant functions, they separated from those species when the eighth and ninth functions were considered. Similarly, capelin and herring, while grouped closely together on the first two functions, separated well on the fourth and fifth discriminant functions (Fig. 3). Based on both the function coefficients and function-variable correlations, discriminant function 1 was primarily defined by 22:1n–11 and 20:1n–9, whereas function 2 mainly represented the influence of 16:0. Together, the 15 discriminant functions classified species with a 98% success rate using a quadratic classification rule (Fig. 2). Tenfold cross-validation using discriminant analysis, like CART, also resulted in a reduced classification success of 88%. These lower percentages from cross-validation of results of both CART and discriminant analyses are expected simply because the data being classified are not used to create the classification function. Cross-validation gives a more realistic estimate of the classification success that can be expected when the function is applied to a new data set (Stevens 1986).

Within-species variation in fatty acid composition

Size

As fish grow, especially in species with a large body size range, they often change their diet. To investigate within-species variation in fatty acid composition as a function of fish length, data for each species were divided into two groups based on either median length in our sample or a length from the literature at which significant changes in diet might be ex-

© 2002 NRC Canada

St. Lawrence (n = 954). Table 2 continues on following pages.

Halibut (n = 8)	Herring (n = 74)	Lobster (n = 9)	Longhorn sculpin (n = 20)	Mackerel (n = 10)	Northern sand lance (n = 71)	Ocean pout (n = 18)	Pollock (n = 25)	Red crab (n = 14)
30.2 ± 4.3	26.0 ± 4.2	19.7 ± 0.8	25.0 ± 3.1	32.5 ± 2.2	18.5 ± 5.0	26.6 ± 6.1	24.8 ± 9.8	10.2 ± 0.9
245.0 ± 139.2	196.0 ± 91.1	243.7 ± 23.5	166.4 ± 72.0	280.5 ± 73.8	14.5 ± 10.1	81.0 ± 57.7	221.1 ± 256.5	354.8 ± 102.4
1.1 ± 0.3	7.7 ± 3.9	2.0 ± 0.6	1.4 ± 1.0	3.4 ± 2.0	5.6 ± 4.3	2.0 ± 1.0	3.0 ± 1.9	1.8 ± 0.4
0.99 ± 0.28	5.33 ± 1.35	2.65 ± 0.51	2.63 ± 0.89	3.59 ± 1.19	5.43 ± 1.49	2.46 ± 1.06	2.89 ± 1.37	1.95 ± 0.32
17.58 ± 0.56	13.65 ± 2.18	11.41 ± 0.67	12.46 ± 1.27	16.41 ± 0.95	13.44 ± 1.69	12.95 ± 1.20	14.53 ± 2.32	10.15 ± 0.71
5.65 ± 0.61	1.39 ± 0.54	3.16 ± 0.28	3.78 ± 0.84	4.58 ± 1.03	2.04 ± 0.81	4.69 ± 1.08	4.26 ± 0.44	2.40 ± 0.50
24.21 ± 0.87	20.37 ± 2.47	17.22 ± 0.78	18.88 ± 1.54	24.59 ± 0.90	20.92 ± 2.20	20.10 ± 0.85	21.68 ± 3.46	14.51 ± 0.69
3.32 ± 1.45	6.24 ± 2.60	6.52 ± 0.43	6.71 ± 2.38	2.96 ± 0.79	6.23 ± 2.12	6.14 ± 2.73	3.53 ± 0.97	6.17 ± 1.00
7.34 ± 1.18	7.25 ± 3.48	10.40 ± 1.50	11.26 ± 1.19	10.99 ± 2.57	5.88 ± 1.59	10.61 ± 3.16	10.77 ± 1.98	15.28 ± 2.11
4.37 ± 0.77	2.34 ± 0.50	6.53 ± 0.73	4.77 ± 0.91	3.46 ± 0.58	2.47 ± 0.64	5.79 ± 1.15	3.51 ± 0.58	4.84 ± 1.01
0.30 ± 0.25	0.96 ± 0.36	1.68 ± 0.37	0.63 ± 0.17	0.66 ± 0.23	0.49 ± 0.16	1.32 ± 0.66	0.71 ± 0.32	1.78 ± 0.37
0.82 ± 0.28	11.09 ± 3.41	4.53 ± 1.55	3.87 ± 1.48	4.92 ± 1.94	7.50 ± 3.02	1.42 ± 0.26	4.40 ± 1.76	6.65 ± 1.22
0.60 ± 0.32	0.50 ± 0.28	1.69 ± 0.20	0.46 ± 0.18	0.52 ± 0.12	0.45 ± 0.23	1.65 ± 0.82	0.40 ± 0.16	0.92 ± 0.38
0.19 ± 0.22	17.27 ± 5.68	3.51 ± 2.26	1.88 ± 1.36	6.07 ± 3.44	9.39 ± 4.20	0.53 ± 0.24	2.68 ± 1.45	6.69 ± 2.04
0.16 ± 0.06	1.23 ± 0.65	0.71 ± 0.21	0.41 ± 0.11	0.99 ± 0.36	1.11 ± 1.06	0.29 ± 0.09	0.49 ± 0.23	1.00 ± 0.21
1.18 ± 0.34	0.75 ± 0.39	0.18 ± 0.05	1.20 ± 0.51	1.25 ± 0.21	1.34 ± 0.33	1.10 ± 0.60	1.01 ± 0.38	0.44 ± 0.11
18.27 ± 3.76	47.61 ± 8.90	35.76 ± 2.91	31.19 ± 3.92	31.81 ± 6.72	34.84 ± 7.70	28.84 ± 4.54	27.51 ± 5.84	43.78 ± 2.92
0.61 ± 0.15	1.15 ± 0.34	0.84 ± 0.08	1.27 ± 0.40	1.49 ± 0.17	1.49 ± 0.50	0.86 ± 0.11	1.00 ± 0.18	0.83 ± 0.06
0.17 ± 0.08	1.51 ± 0.80	0.83 ± 0.18	0.67 ± 0.36	1.44 ± 0.70	1.98 ± 1.17	0.43 ± 0.26	1.35 ± 0.39	0.25 ± 0.05
5.43 ± 0.84	0.42 ± 0.28	6.33 ± 1.17	3.00 ± 1.20	1.50 ± 0.68	0.59 ± 0.31	4.06 ± 1.29	1.11 ± 0.44	3.04 ± 0.74
9.59 ± 1.04	7.77 ± 1.57	17.04 ± 1.10	13.78 ± 1.84	8.03 ± 1.21	12.96 ± 1.87	15.07 ± 2.76	11.03 ± 2.19	12.13 ± 1.32
2.56 ± 0.27	0.83 ± 0.13	1.29 ± 0.20	1.66 ± 0.32	1.58 ± 0.27	1.03 ± 0.32	1.98 ± 0.51	1.00 ± 0.36	2.25 ± 0.99
30.60 ± 4.38	12.46 ± 6.89	7.69 ± 1.06	19.86 ± 3.14	19.34 ± 5.89	16.17 ± 4.90	14.32 ± 4.58	25.58 ± 8.39	11.93 ± 2.46
48.95 ± 3.97	24.15 ± 7.71	34.01 ± 2.27	40.24 ± 4.01	33.37 ± 6.98	34.23 ± 6.09	36.71 ± 6.87	41.08 ± 8.91	30.42 ± 2.18
91.44 ± 0.83	92.13 ± 1.05	86.99 ± 0.85	86.21 ± 1.57	89.76 ± 0.84	89.99 ± 1.70	85.64 ± 3.57	90.26 ± 0.70	88.70 ± 2.19
50.0%	98.6%	100.0%	70.0%	70.0%	94.4%	50.0%	80.0%	42.9%

all 66 fatty acids quantified among individuals, are available on request from the corresponding author. CART classification is the percentage of

Fig. 3. Plot of scores for capelin and herring fatty acids based on the fourth and fifth discriminant functions (see Fig. 2) (solid circles, capelin; open circles, herring).

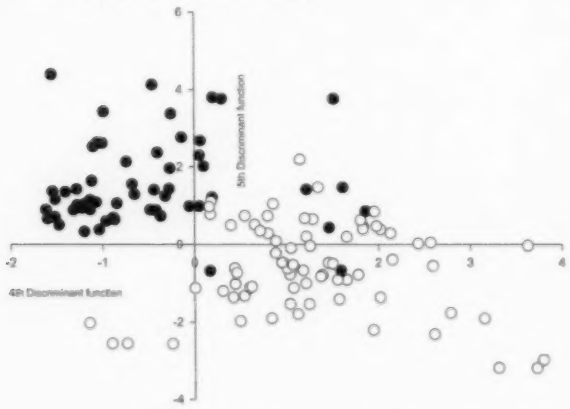

pected (i.e., for American plaice, cod, redfish, winter flounder, and yellowtail flounder). Confounding of length with geographic location of sampling was a concern with most species. Thus, we conducted a MANOVA on the main effects of both length and location, as well as their interaction, for each species (Table 3). For some species, the number of fatty acids (i.e., 17) exceeded the number of samples in the subsets; thus, fatty acids accounting for the greatest variance were retained with the constraint that the number of fatty acids was less than the number of samples within each length or area class.

Nine species exhibited a significant effect of length on fatty acid signature ($P < 0.05$) and two others were close to significance ($P < 0.06$; Table 3). Of all of the fish species considered, only longhorn sculpin displayed a significant length effect without a concurrent significant interaction with location. For this species, Tukey's test identified 22:1n–11 as the only univariately significant fatty acid (Table 3). To examine some of the variation in fatty acid composition with length in other species, we selected only a single area, each with the largest sample size, for illustration (Fig. 4). Redfish and sand lance had the greatest number of significantly different fatty acids among the two size classes, including 16:1n–7, 22:1n–11, and 20:5n–3, as well as several other fatty acids not shown. Fewer differences were apparent among size classes of capelin and herring with only 16:1n–7, 22:1n–11, and 22:6n–3 being significantly different in capelin and 14:0 and 18:4n–3 being significantly different in herring. To further illustrate the variation with size, significant correlations of selected fatty acid levels with fish length may be shown (Fig. 5). In the examples shown, there were clear decreases in levels of the indicated fatty acid with increasing size. However, among all four species, there were no consistent trends in variation of fatty acid levels with size. For example, in capelin, redfish, and sandlance, levels

© 2002 NRC Canada

Table 2 (*concluded*).

	Red hake (n = 7)	Redfish (n = 49)	Rock crab (n = 10)	Sea raven (n = 6)	Shrimp (n = 46)	Silver hake (n = 38)	Smooth skate (n = 5)	Thorny skate (n = 12)
Length (cm)	29.3 ± 5.1	27.6 ± 9.2	8.1 ± 0.6	27.2 ± 5.5	11.5 ± 1.0	22.8 ± 6.9	29.7 ± 8.2	33.0 ± 3.0
Mass (g)	183.7 ± 102.8	405.6 ± 339.3	184.4 ± 44.5	389.9 ± 238.8	10.5 ± 4.1	88.9 ± 74.4	120.7 ± 91.1	297.1 ± 64.4
Lipid content (%)	1.7 ± 0.8	6.3 ± 2.9	0.8 ± 0.2	0.8 ± 0.3	2.6 ± 0.7	2.2 ± 1.4	1.4 ± 0.4	1.1 ± 0.2
Saturated fatty acids (%)								
14:0	1.32 ± 0.40	3.74 ± 0.74	1.69 ± 0.55	1.20 ± 0.74	2.89 ± 0.43	2.34 ± 0.96	1.66 ± 0.60	1.77 ± 0.56
16:0	15.08 ± 1.14	9.39 ± 1.84	10.44 ± 0.72	13.88 ± 1.85	11.42 ± 0.94	16.80 ± 1.25	16.65 ± 2.16	16.82 ± 0.65
18:0	5.87 ± 0.45	2.43 ± 0.51	3.18 ± 0.27	5.31 ± 1.55	1.93 ± 0.33	3.72 ± 1.06	4.23 ± 1.16	4.04 ± 0.59
Subtotal	22.27 ± 1.10	15.56 ± 2.67	15.31 ± 1.15	20.40 ± 2.63	16.24 ± 1.10	22.86 ± 1.32	22.54 ± 2.69	22.63 ± 0.74
Monounsaturated fatty acids (%)								
16:1n–7	2.87 ± 1.37	7.63 ± 2.23	5.93 ± 0.78	6.71 ± 3.77	8.74 ± 1.59	3.20 ± 1.54	7.60 ± 2.52	6.57 ± 1.74
18:1n–9	12.13 ± 2.63	8.66 ± 3.34	8.16 ± 1.39	13.29 ± 1.20	11.76 ± 2.63	11.29 ± 1.81	10.68 ± 0.48	12.63 ± 1.63
18:1n–7	5.59 ± 1.34	3.33 ± 0.63	7.45 ± 1.83	7.28 ± 0.69	6.83 ± 1.93	3.23 ± 0.76	6.99 ± 0.26	6.40 ± 0.54
20:1n–11	0.52 ± 0.15	1.07 ± 0.43	1.37 ± 0.35	0.48 ± 0.27	1.40 ± 1.03	1.02 ± 0.32	0.49 ± 0.18	0.73 ± 0.19
20:1n–9	1.94 ± 0.58	14.91 ± 3.05	3.85 ± 1.49	1.77 ± 0.87	4.85 ± 1.45	5.16 ± 2.36	1.08 ± 0.39	1.92 ± 0.49
20:1n–7	0.46 ± 0.19	1.37 ± 0.63	1.84 ± 0.62	0.74 ± 0.32	1.53 ± 0.32	0.33 ± 0.12	0.86 ± 0.41	1.03 ± 0.15
22:1n–11	0.81 ± 0.33	15.91 ± 3.70	3.63 ± 2.01	0.50 ± 0.49	6.74 ± 2.35	4.16 ± 3.07	0.24 ± 0.19	0.66 ± 0.59
22:1n–9	0.26 ± 0.06	3.02 ± 1.74	0.61 ± 0.23	0.24 ± 0.05	1.56 ± 0.71	0.54 ± 0.36	0.30 ± 0.07	0.45 ± 0.11
24:1	1.29 ± 0.46	0.87 ± 0.41	0.30 ± 0.08	0.72 ± 0.16	0.30 ± 0.21	1.48 ± 0.73	0.27 ± 0.09	0.31 ± 0.09
Subtotal	25.86 ± 4.94	56.76 ± 7.66	33.15 ± 2.81	31.73 ± 5.57	43.71 ± 2.30	30.40 ± 6.52	28.50 ± 3.62	30.69 ± 2.23
Polyunsaturated fatty acids (%)								
18:2n–6	0.79 ± 0.20	0.90 ± 0.22	1.00 ± 0.13	0.91 ± 0.31	1.00 ± 0.18	1.05 ± 0.22	1.50 ± 0.29	1.41 ± 0.10
18:4n–3	0.44 ± 0.23	1.07 ± 0.41	0.42 ± 0.13	0.48 ± 0.42	0.71 ± 0.29	0.70 ± 0.38	0.90 ± 0.50	0.65 ± 0.31
20:4n–6	2.59 ± 0.96	0.57 ± 0.39	4.05 ± 1.11	4.40 ± 1.63	1.66 ± 0.72	1.45 ± 0.51	3.09 ± 0.48	3.46 ± 0.74
20:5n–3	9.90 ± 3.16	7.39 ± 1.81	20.74 ± 2.19	12.44 ± 1.53	15.26 ± 1.30	9.66 ± 2.56	10.02 ± 2.24	8.30 ± 1.45
22:5n–3	2.25 ± 0.44	0.79 ± 0.14	2.06 ± 0.40	2.32 ± 1.00	0.74 ± 0.21	1.11 ± 0.23	1.75 ± 0.25	2.35 ± 0.25
22:6n–3	25.16 ± 7.13	8.23 ± 3.10	10.35 ± 1.74	18.73 ± 3.57	11.37 ± 1.99	23.64 ± 6.28	20.87 ± 3.20	21.89 ± 2.14
Subtotal	41.13 ± 4.79	18.95 ± 4.60	38.62 ± 3.12	39.27 ± 4.14	30.75 ± 2.27	37.61 ± 6.28	38.14 ± 1.37	38.06 ± 1.71
Total	89.26 ± 1.14	91.27 ± 0.96	87.08 ± 0.87	91.40 ± 1.14	90.70 ± 1.86	90.87 ± 0.69	89.18 ± 0.51	91.39 ± 0.54
CART Classification	57.1%	100.0%	70.0%	0.0%	100.0%	89.5%	40.0%	91.7%

of 22:1n–11 were greater in the larger size class, but in herring, the opposite effect was observed, likely reflecting different types of diet shifts in the species considered.

Geographic location

Given that there are broad-scale geographic differences in prey assemblages, and therefore, in the diets of fishes, we also investigated the effect of sampling location on fatty acid composition within species. Species with <4 samples from one area were dropped from the analysis and the number of fatty acids included was chosen as described above, based on maximizing retained variance. All species had a significant Wilks' Lambda, indicating differences among geographic locations, but only six of these did not exhibit a significant interaction between fish length and area (Table 3). To illustrate some of these differences, discriminant analysis was carried out on three of the better-represented species (i.e., American plaice >25 cm in length, cod, and yellowtail flounder), again adjusting the number of fatty acids used (Fig. 6). In each species, there was evidence that different stocks differed in fatty acid composition. In American plaice, there was some overlap of samples from subareas 5Z and 4Vs, indicating similarity in the composition of the fatty acids that are most closely related to those two discriminant functions (20:5n–3 and 16:1n–7 on the first function and 20:1n–9 and 22:1n–11 on the second function). Nevertheless, a plot of individual scores for these and other selected species according to subarea and placed in the original discriminant analysis plot for all 16 species (Fig. 7) illustrates that despite the clear separation among stocks on a fine scale, members of each species were more similar to each other in fatty acid signature than to the other species.

Discussion

The results of this study demonstrate that fatty acid signatures of fish and invertebrate species can be used not only to distinguish and characterize species in a given ecosystem, but also to study finer-scale within-species variation with size, and possibly, within regional food webs. In general, individuals were accurately classified to their species based on fatty acid signature. As stated earlier, we made no attempt to remove stomach contents of the individuals we analyzed because we wished to characterize them as prey that would be eaten whole by a predator. However, this may have increased variability within species, resulting in a more conservative classification success.

When all 66 fatty acids were considered, CART successfully classified 89% of the samples, demonstrating the information contained within fatty acid signatures. These signatures were distinctive for most species, with 18 of the 28 species having a classification success rate greater than 80% (12 of which were >90%). In the 10 more poorly classified species with sample sizes of <20, the within-species variance in the fatty

© 2002 NRC Canada

White hake (n = 46)	Winter flounder (n = 25)	Winter skate (n = 15)	Yellowtail flounder (n = 92)
32.9 ± 5.3	27.0 ± 6.6	35.6 ± 4.0	26.8 ± 6.1
281.1 ± 142.8	274.8 ± 189.8	262.2 ± 112.3	189.8 ± 138.6
1.3 ± 0.8	1.9 ± 0.8	1.5 ± 0.6	2.7 ± 1.3
1.49 ± 0.61	1.96 ± 0.69	1.58 ± 1.09	2.72 ± 0.87
14.39 ± 1.05	15.04 ± 0.86	16.94 ± 2.20	14.01 ± 1.53
5.37 ± 0.92	4.51 ± 0.85	3.98 ± 0.90	3.56 ± 0.96
21.26 ± 1.40	21.51 ± 0.91	22.50 ± 2.02	20.30 ± 1.78
3.59 ± 1.52	5.21 ± 2.92	4.30 ± 1.20	6.47 ± 2.90
12.08 ± 2.82	7.31 ± 1.61	9.30 ± 0.73	9.75 ± 2.57
5.69 ± 1.08	3.61 ± 0.86	5.24 ± 0.96	4.25 ± 0.75
0.72 ± 0.35	0.55 ± 0.27	0.59 ± 0.35	0.76 ± 0.32
3.18 ± 2.37	1.27 ± 0.30	2.10 ± 2.10	1.34 ± 0.38
0.66 ± 0.24	2.52 ± 1.57	0.81 ± 0.36	1.65 ± 0.74
1.75 ± 1.80	0.23 ± 0.09	1.19 ± 2.18	0.49 ± 0.28
0.36 ± 0.22	0.35 ± 0.11	0.37 ± 0.15	0.25 ± 0.11
0.90 ± 0.46	0.61 ± 0.49	0.54 ± 0.27	0.69 ± 0.41
28.92 ± 7.25	21.67 ± 5.72	24.44 ± 4.47	25.65 ± 4.83
0.80 ± 0.17	0.60 ± 0.17	1.34 ± 0.24	1.03 ± 0.24
0.43 ± 0.27	0.48 ± 0.28	0.64 ± 0.41	0.95 ± 0.57
2.29 ± 0.94	3.58 ± 0.99	3.24 ± 1.22	2.55 ± 1.25
9.61 ± 1.54	14.43 ± 2.14	7.78 ± 1.91	15.02 ± 3.32
2.69 ± 0.61	3.82 ± 0.97	2.93 ± 0.75	3.31 ± 0.97
24.83 ± 5.90	20.10 ± 4.26	26.06 ± 4.61	18.73 ± 4.84
40.66 ± 6.67	43.01 ± 5.65	41.99 ± 3.71	41.59 ± 4.19
90.84 ± 0.89	86.19 ± 2.32	88.93 ± 2.24	87.53 ± 2.07
91.3%	84.0%	73.3%	89.1%

acid signature was too large to allow accurate identification. There were several exceptions where species with only 9–12 samples (e.g., argentine, lobster, and thorny skate) were nevertheless accurately classified (92–100%), perhaps because these species had fatty acid signatures that were particularly unusual or relatively invariant. One limitation of CART is that it is based on the calculation of greatest deviation among samples remaining at each node, and such dichotomous splits provide no indication of the overall relationships of fatty acid composition among species. In this study, with the exception of the crabs, the 10 poorly classified species tended to be randomly misidentified rather than misidentified as a related species. For example, the three misclassified smooth skates (n = 5) were classified as cod and longhorn sculpin rather than thorny or winter skates.

Discriminant analysis of the 16 most numerous species resulted in high (98%) classification success. Plots of these analyses also serve to illustrate the relationships between species' fatty acid signatures. For instance, all of the Gadidae species (cod, haddock, pollock, silver hake, and white hake) grouped together, whereas the Pleuronectidae species (American plaice, winter flounder, and yellowtail flounder) formed a separate group. Certainly, some similarity in fatty acid composition among such closely related species may be expected because of shared patterns in life histories and feeding strategies. However, ocean pout, redfish, and sculpin were also included in the Gadidae cluster,

Table 3. Results of MANOVA of fish species ($n \geq 18$ individuals) showing main effects of body length and location (NAFO subarea; see Fig. 1), as well as their interaction, on fatty acid composition.

			Variation with length		Variation with location		
	$P_{interaction}$	Median length (cm)	P_{length}	Univariately significant fatty acids	Locations	$P_{location}$	Univariately significant fatty acids
American plaice	<0.001	25[b]	<0.001	20:1*n*–11, 20:1*n*–7, 22:6*n*–3	4Vs, 4X, 5Z, 4T	<0.001	All
Capelin	ND	13	0.008	22:6*n*–3	4Vs, 4W, 4T	<0.001	16:0, 20:1*n*–9, 22:6*n*–3
Cod	0.052	35[a]	0.056	—	4W, 5Z, 4T	<0.001	All
Gaspereau	<0.001	23	0.003	18:1*n*–9, 20:1*n*–7, 22:6*n*–3	4W, 4T	<0.001	20:4*n*–3, 22:5*n*–3, 22:6*n*–3
Haddock	<0.001	27	<0.001	14:0, 16:1*n*–7, 20:5*n*–3	4X, 4W	<0.001	14:0, 20:1*n*–9, 22:1*n*–11
Herring	ND	27	<0.001	16:0, 20:5*n*–3, 24:1	4W, 4T	<0.001	16:0, 22:1*n*–7, 22:5*n*–3
Longhorn sculpin	0.48	25	0.035	22:1*n*–11	4Vs, 4W	<0.001	18:1*n*–9, 20:4*n*–6
Northern sand lance	0.013	17	<0.001	18:2*n*–6, 20:4*n*–6, 22:6*n*–3	4Vs, 4W	<0.001	18:1*n*–7, 18:2*n*–6, 20:5*n*–3
Ocean pout	0.48	28	0.33	——	4X, 4W	0.001	18:1*n*–9, 18:1*n*–7, 22:6*n*–3
Pollock	ND	17	0.75	——	4Vn, 4X	0.006	16:0, 20:1*n*–9, 22:6*n*–3
Redfish	<0.001	27[c]	<0.001	18:1*n*–9, 22:1*n*–11	4Vn, 4X, 4T	<0.001	16:1*n*–7, 22:1*n*–11, 22:1*n*–9
Silver hake	<0.001	23	<0.001	16:0, 18:1*n*–9, 18:4*n*–3	4W, 4X	<0.001	18:1*n*–7, 20:5*n*–3, 24:1
White hake	0.62	33	0.13	——	4Vs, 4T	0.044	None
Winter flounder	0.26	25[b]	0.088	——	4W, 4X	0.002	16:1*n*–7, 18:1*n*–9, 20:1*n*–7
Yellowtail flounder	0.097	25[b]	0.055	——	4W, 5Z, 4T	0.003	18:1*n*–9, 18:4*n*–3, 20:5*n*–3

Note: Significant diet changes were expected in species at the length denoted by a superscript based on [a]Bundy et al. (2000), [b]Martell and McClelland (1994), and [c]Cannalejo et al. (1989). Univariate significance was determined using Tukey's test. ND, not determined.

© 2002 NRC Canada

Fig. 4. Variation in selected fatty acids with body length within one major location for (*a*) capelin (4W), (*b*) herring (4W), (*c*) northern sand lance (4W), and (*d*) redfish (4T). For each species, the median length for that specific location was used to classify species as small and large. The fatty acids illustrated included those that were the most univariately significant (e.g., Table 3) across the four species. Asterisks indicate statistically significant differences. A greater number of fatty acids are univariately significant in this plot than indicated in Table 3 because only data from a single area were considered, removing constraints placed on the number of fatty acids that could be used in the analyses. Use of a single location also eliminates any potential interaction of length and area.

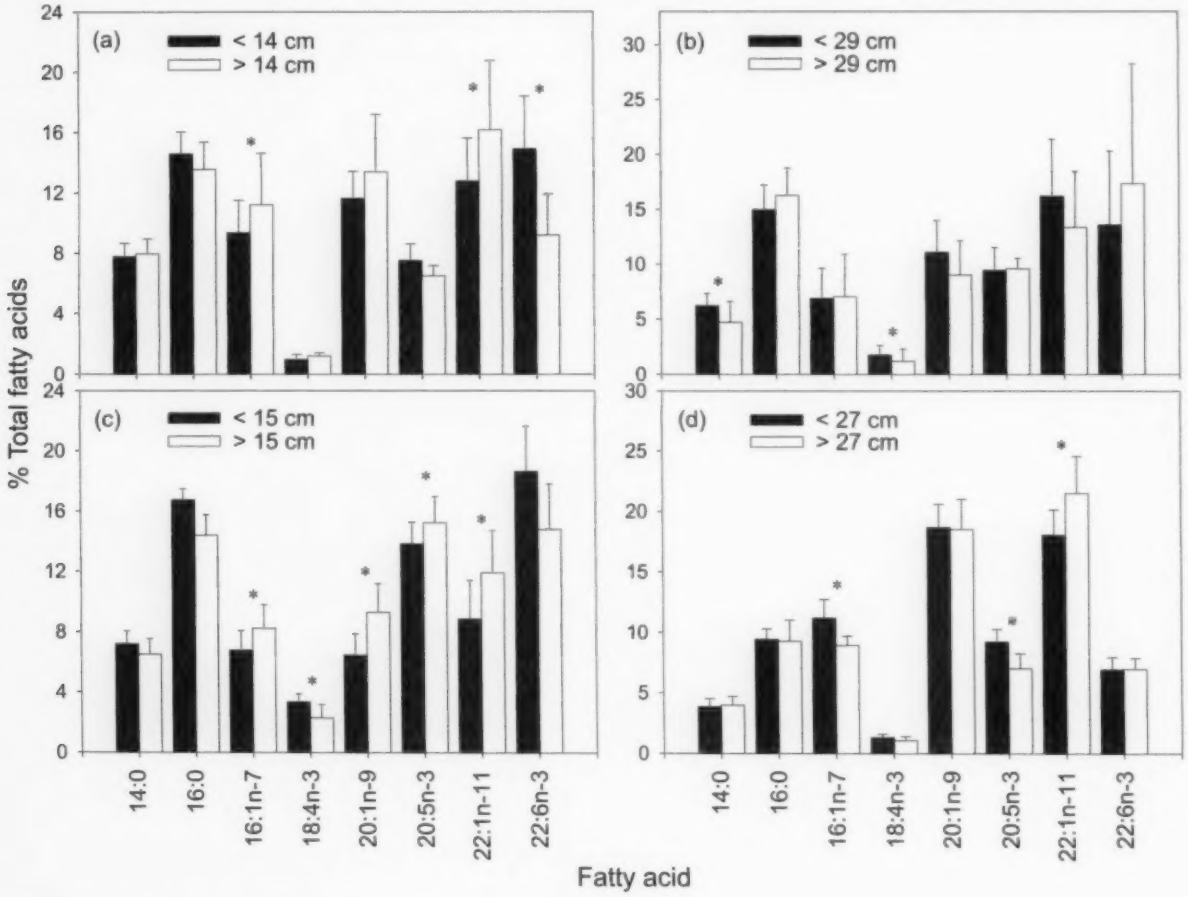

indicating that factors other than phylogeny, i.e., diet, play an important role in fatty acid composition (e.g., Kirsch et al. 1998). That is, unrelated species with similar diets would be expected to share similar patterns in fatty acid signatures. For instance, capelin, herring, and sand lance, members of three different families that share a similar and predominantly planktivorous diet (Scott and Scott 1988), were located in a third separate group, further illustrating the influence of diet on fatty acid composition. The classification of shrimp with the Gadidae cluster was somewhat unexpected, particularly because shrimp and gadids have very different diets. However, gadids eat shrimp. In fact, shrimp may compose up to 20% by weight of the diet of Gadidae species (Bundy et al. 2000). Thus, if the gadids that we analyzed were consuming diets high in shrimp, this could explain the similarity in some of the signatures displayed in the first two discriminant functions. However, without analyses of stomach contents, we can only speculate as to the diets of the gadids analyzed. Gaspereau was the only species that was not included in any group, suggesting that its fatty acid signature was unusual, possibly because of its anadromous nature. For instance, lipids from freshwater fish typically contain higher proportions of saturated fatty acids, C18 polyunsaturated fatty acids (PUFA) and *n*–6 PUFA than marine fish owing to consumption of different diets (Henderson and Tocher 1987). In our data set, Gaspereau did contain elevated levels of both saturated fatty acids and C18 PUFA.

The 17 fatty acids with greatest variance across all species were selected for the multivariate analyses based on the assumption that the fatty acids with the largest fluctuations in levels would provide the most useful information in differentiating among species. It is possible that a different subset of fatty acids may generate a better classification scheme. For example, the use of only dietary fatty acids excludes such major fatty acids as 16:0 and 18:1*n*–9 (which can be readily biosynthesized) and produces a less accurate classification

© 2002 NRC Canada

Fig. 5. Correlation of the indicated fatty acid with body length within one major location for (*a*) capelin (4W), (*b*) herring (4W), (*c*) northern sand lance (4W), and (*d*) redfish (4T). The fatty acids illustrated were both univariately significant (see Fig. 4) and significantly correlated with length.

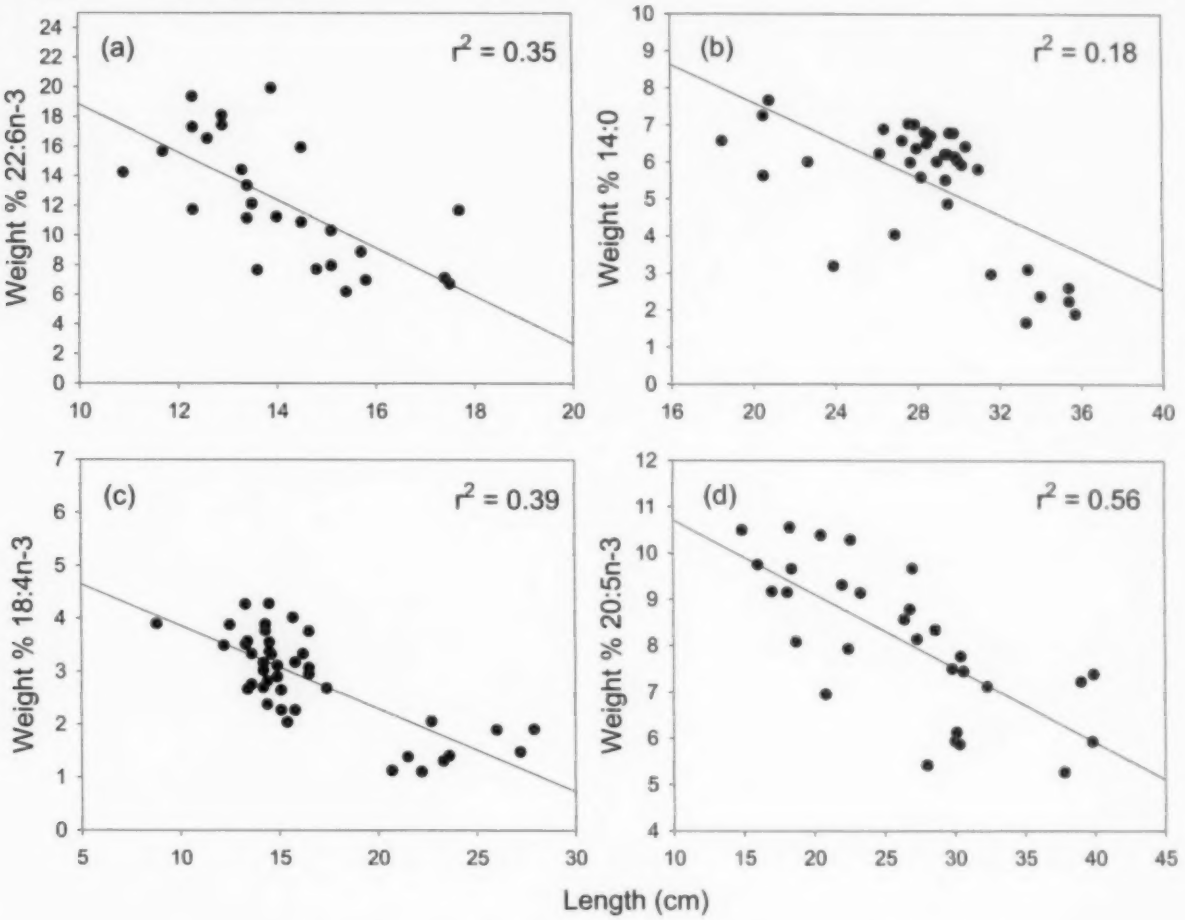

scheme, but one that more clearly represents fish with similar diets. Thus, it may still be useful in supplementing stomach content analyses when determining fish diets. It is also possible that using a larger number of fatty acids would result in better resolution, for instance, in the separation of shrimp from the Gadidae species. This would be possible with a greater number of samples for each species collected and would avoid subjective variable selection.

A number of investigations have reported variation in diet with fish size (Lilly 1986; Canalejo et al. 1989; Martell and McClelland 1994); thus, it is not surprising that we found differences in fatty acid composition as a function of fish length. Both capelin and herring are planktonic feeders, but at larger body sizes, they are known to consume other small fish (Gerasimova 1994). Similarly, changes in the diet of redfish with body size are well documented in stomach content analyses (Canalejo et al. 1989). Thus, dietary fatty acid intake and deposition should differ in fish consuming these differing diets. For instance, the fatty acids 20:1*n*–9 and 22:1*n*–11 are associated with zooplankton, specifically copepod lipids (Graeve et al. 1994), and variation in levels of these two fatty acids likely reflects varying amounts of zooplankton in their diets. However, the variation in fatty acid composition in northern sand lance (*Ammodytes dubius*) was unexpected. The diet of sand lance is reported to be exclusively planktonic (Scott 1973), so a shift in diet to small fish species with increasing body size, as seen in capelin and herring, seems unlikely. Nonetheless, the significant differences observed in the fatty acid composition of the larger sand lance (with lengths up to 28 cm) indicate consumption of diets that are different than those of the smaller fish.

More detailed information is available on diets from stomach content analyses in American plaice, winter flounder, and yellowtail flounder. In both flounders, Martell and McClelland (1994) found shifts in the diet of small fish to large fish. Although small flounder consumed mainly small cumaceans, amphipods, and tunicates, large flounder consumed larger infauna such as polychaetes and tubaceous amphipods. The diets of American plaice have also been found to vary markedly with length (Martell and McClelland 1994),

© 2002 NRC Canada

Fig. 6. Discriminant analyses displaying geographic effects on fatty acid composition within single species for (*a*) American plaice (>25 cm), (*b*) cod, and (*c*) yellowtail flounder. Discriminant scores on the first and second functions for three separate analyses are plotted. The species selected were sampled in at least three areas and did not exhibit a significant interaction between area and length, or in the case of American plaice, only samples from one size class were used.

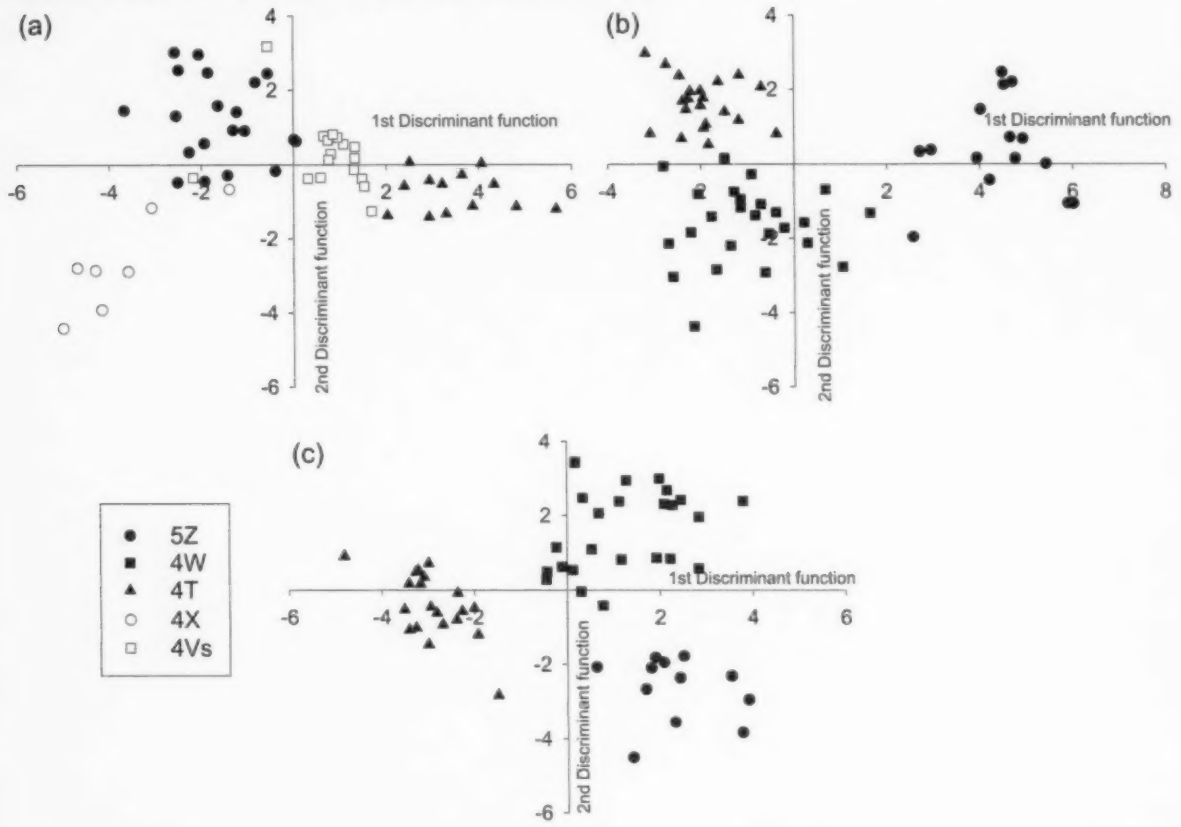

with small fish ingesting small invertebrates, such as amphipods and mysids, and larger fish consuming decapods, echinoderms, and fish. In American plaice and yellowtail flounder, the previously described diet shifts occurred primarily at 20–30 cm (Martell and McClelland 1994), which agreed well with our results from fatty acid analyses.

The diets of Atlantic cod and redfish also vary with fish length (Canalejo et al. 1989). In cod, at lengths greater than 50 cm, a dramatic increase in the amount of teleosts and a decrease in the amount of invertebrates were reported in the diet. At 30 cm, a more subtle change was apparent with more shrimp and molluscs consumed and fewer polychaetes, euphausiids, and mysids. Similarly, it was reported that in redfish at lengths greater than 27 cm, more chaetognaths and finfish and fewer invertebrates were consumed. The fatty acid data are consistent with this information, with differences in composition being observed at 35 and 27 cm for cod and redfish, respectively. The average length of cod in our data set was 37 cm, with only one sample exceeding 50 cm. Had we sampled larger cod (>50 cm), perhaps a significant change in fatty acid composition would also have been apparent. The agreement of changes in fatty acid signatures with changes in diets as reported from stomach content analysis in flatfish, cod, and redfish suggests that the differences in fatty acid composition for the other species considered in this study likely indicate general dietary differences with size. Larger fish are capable of consuming larger prey, and it has been suggested that changes in mouth morphology are responsible for diet variation (Hacunda 1981).

Variability in fatty acid composition among geographic locations may also reflect changes in fish diet. There are known to be broad-scale differences in prey assemblages in the Northwest Atlantic, and some variation may exist among the regions we sampled. Additionally, phytoplankton composition at the base of the food web fluctuates seasonally (Parrish et al. 1995), and the fatty acid composition varies among classes of phytoplankton (Volkman et al. 1989; Viso and Marty 1993) and with characteristic water temperature, salinity, incident light, and available nutrients, all of which may differ geographically. This can result in differences in the fatty acid signatures of phytoplankton in a study area, and thus, the fatty acid composition of food available to higher trophic levels. For instance, Fraser et al. (1989) documented changes in zooplankton fatty acids corresponding to changes in phytoplankton fatty acids. Such changes in fatty

© 2002 NRC Canada

Fig. 7. Plot of individual scores for six selected species according to sampling location from discriminant analyses of all 16 species (see Fig. 2). Ellipses represent point clouds as drawn in Fig. 2.

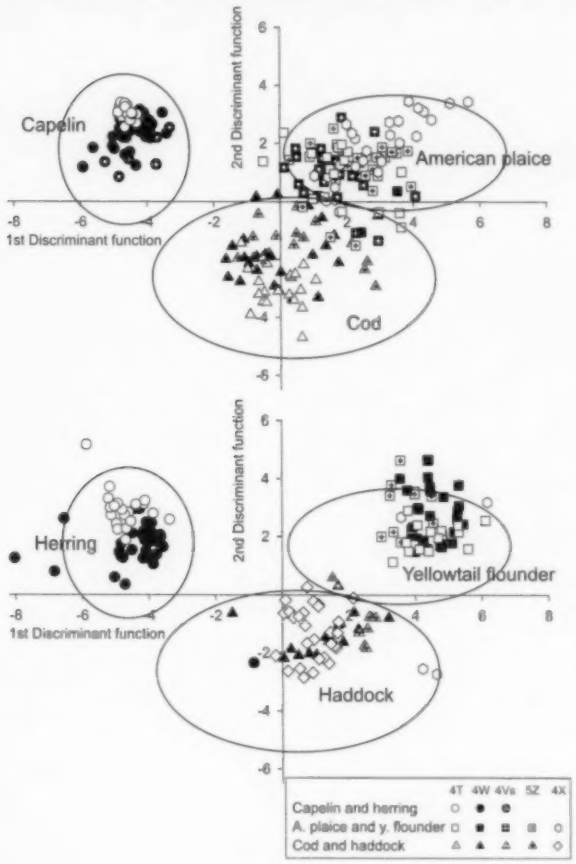

acid composition in zooplankton are, in turn, expected to influence the fatty acid signature of fish consuming that zooplankton (St. John and Lund 1996). Although we might not expect differences in prey assemblages and primary production to be particularly great across the Scotian Shelf, some differences in fatty acid signatures within species were evident. In the species most broadly sampled, it appeared that the largest differences within species occurred between the three major regions of the Scotian Shelf (4V, 4W, 4X), Georges Bank (5Z), and the Gulf of St. Lawrence (4T), where we would expect different water temperatures, salinities, and nutrient-supplying currents. However, despite these broad-scale and more subtle geographical differences, within-species variation in fatty acid composition was still less than between-species variation.

Although our main objective was to demonstrate the value of using fatty acid signatures to differentiate among fish species, there exist many potential uses of fatty acids in understanding trophic dynamics and predator–prey interactions. In addition to identifying species with similar diets, it may be possible to determine interannual changes in the diets of separate stocks of fish. In migratory fish, like mackerel, fatty acid signatures may provide information on spawning and feeding locations. Furthermore, the fatty acid data reported here will have applications at higher trophic levels. If fish and other prey species from a given geographic region can be distinguished by their fatty acid signatures, then they can be used to estimate the prey composition in the diet of predators like marine mammals (S.J. Iverson, C. Field, W.D. Bowen, and W. Blanchard, unpublished data). This paper represents the first step toward documenting differences in fish and invertebrate fatty acid compositions on the Scotian Shelf, Georges Bank, and Gulf of St. Lawrence. These data, combined with other techniques, will be valuable in investigating ecological relationships at a number of trophic levels.

Acknowledgements

We thank S. Lang, E. MacPherson, D. Muise, L. Smith, G. Thiemann, A. Bowen, and J. Lassner for assistance with sample analyses. This study was supported by Natural Sciences and Engineering Research Council of Canada (NSERC) Research and Equipment grants to S.J.I. and by an NSERC Strategic grant (No. STRO133825).

References

Ackman, R.G., and Eaton, C.A. 1966. Lipids of the fin whale (*Balaenoptera physalus*) from north Atlantic waters. III. Occurrence of eicosenoic and docosenoic fatty acids in the zooplankter *Meganyctiphanes norvegica* (M. Sars) and their effect on whale oil composition. Can. J. Biochem. **44**: 1561–1566.

Aitchison, J. 1986. The statistical analysis of compositional data. Chapman and Hall, New York.

Albikovskaya, L.K., Gerasimova, O.V., and Kotlyarov, S.M. 1991. Estimates of consumption of major food objects by cod in Grand Bank areas in spring–summer 1990. NAFO SCR Doc. 91/121.

Bax, N.J. 1991. A comparison of the fish biomass flow to fish, fisheries, and mammals in six marine ecosystems. ICES Mar. Sci. Symp. **193**: 217–224.

Bowen, W.D. 1997. Role of marine mammals in aquatic ecosystems. Mar. Ecol. Prog. Ser. **158**: 267–274.

Bowen, W.D., Lawson, J.W., and Beck, B. 1993. Seasonal and geographic variation in the species composition and size of prey consumed by grey seals (*Halichoerus grypus*) on the Scotian Shelf. Can. J. Fish. Aquat. Sci. **50**: 1768–1778.

Bundy, A., Lilly, G.R., and Shelton, P.A. 2000. A mass balance model of the Newfoundland–Labrador Shelf. Can. Tech. Rep. Fish. Aquat. Sci. No. 2310.

Canalejo, F.J.P., Alvarez, F.J.V., Arroyo, A.F., Sanchez, J.M.C., and de Cardenas, E. 1989. The feeding of American plaice (*Hippoglossoides platessodies*), redfish (*Sebastes marinus*) and cod (*Gadus morhua*) in the Flemish Cap during July 1988. NAFO SCR Doc. 89/45.

Christensen, N., Bartuska, A.M., Brown, J.H., Carpenter, S., D'Antonio, C., Francis, R., Franklin, J.F., MacMahon, J.A., Noss, R.F., Parsons, D.J., Peterson, C.H., Turner, M.G., and Woodmansee, R.G. 1996. Report of the Ecological Society of America Committee on the Scientific Basis for Ecosystem Management. Ecol. Appl. **6**: 665–691.

Colby, R.H., Mattacks, C.A., and Pond, C.M. 1993. The gross anatomy, cellular structure and fatty acid composition of adipose tissue in captive polar bears (*Ursus maritimus*). Zoo Biol. **12**: 267–275.

© 2002 NRC Canada

Folch, J., Lees, M., and Sloane Stanley, G.H. 1957. A simple method for the isolation and purification of total lipids from animal tissues. J. Biol. Chem. **226**: 497–509.

Fraser, A.J., Sargent, J.R., Gamble, J.C., and Seaton, D.D. 1989. Formation and transfer of fatty acids in an enclosed marine food chain comprising phytoplankton, zooplankton and herring (*Clupea harengus*) larvae. Mar. Chem. **27**: 1–18.

Gerasimova, O.V. 1994. Peculiarities of spring feeding by capelin (*Mallotus villosus*) on the Grand Bank in 1987–90. J. Northw. Atl. Fish. Sci. **17**: 59–67.

Graeve, M., Hagen, W., and Kattner, G. 1994. Herbivorous or omnivorous? On the significance of lipid compositions as trophic markers in Antarctic copepods. Deep-Sea Res. I, **41**: 915–924.

Hacunda, J.S. 1981. Trophic relationships among demersal fishes in a coastal area of the Gulf of Maine. Fish. Bull. **79**: 775–788.

Henderson, R.J., and Tocher, D.R. 1987. The lipid composition and biochemistry of freshwater fish. Prog. Lipid Res. **26**: 281–347.

Iverson, S.J. 1993. Milk secretion in marine mammals in relation to foraging: can milk fatty acids predict diet? Symp. Zool. Soc. Lond. **66**: 263–291.

Iverson, S.J., Arnould, J.P.Y., and Boyd, I.L. 1997*a*. Milk fatty acid signatures indicate both major and minor shifts in the diet of lactating Antarctic fur seals. Can. J. Zool. **75**: 188–197.

Iverson, S.J., Frost, K.J., and Lowry, L.F. 1997*b*. Fatty acid signatures reveal fine scale structure of foraging distribution of harbor seals and their prey in Prince William Sound, Alaska. Mar. Ecol. Prog. Ser. **151**: 255–271.

Iverson, S.J., McDonald, J.E., and Smith, L.K. 2001. Changes in the diet of free-ranging black bears in years of contrasting food availability revealed through milk fatty acids. Can. J. Zool. **79**: 2268–2279.

Jobling, M., and Breiby, A. 1986. The use and abuse of fish otoliths in studies of feeding habits of marine piscivores. Sarsia, **71**: 265–274.

Kirsch, P.E., Iverson, S.J., Bowen, W.D., Kerr, S.R., and Ackman, R.G. 1998. Dietary effects on the fatty acid signature of whole Atlantic cod (*Gadus morhua*). Can. J. Fish. Aquat. Sci. **55**: 1378–1386.

Kirsch, P.E., Iverson, S.J., and Bowen, W.D. 2000. Effect of diet on body composition and blubber fatty acids in captive harp seals (*Phoca groenlandica*). Physiol. Biochem. Zool. **73**: 45–59.

Köster, W.F., Möllmann, C., Neuenfeldt, S., St. John, M.A., Plikshs, M., and Voss, R. 2001. Developing Baltic cod recruitment models. I. Resolving spatial and temporal dynamics of spawning stock and recruitment for cod, herring, and sprat. Can. J. Fish. Aquat. Sci. **58**: 1516–1533.

Lilly, G.R. 1986. A synopsis of research related to recruitment of cod and redfish on Flemish Cap. NAFO SCR Doc. 86/101.

Martell, D.J., and McClelland, G. 1994. Diets of sympatric flatfishes, *Hippoglossoides platessoides*, *Pleuronectes ferrugineus*, *Pleuronectes americanus*, from Sable Island Bank, Canada. J. Fish Biol. **44**: 821–848.

Parrish, C.C., McKenzie, C.H., MacDonald, B.A., and Hatfield, E.A. 1995. Seasonal studies of seston lipids in relation to microplankton species composition and scallop growth in South Broad Cove, Newfoundland. Mar. Ecol. Prog. Ser. **129**: 151–164.

Pauly, D., Trites, A.W., Capuli, E., and Christensen, V. 1998. Diet composition and trophic levels of marine mammals. ICES J. Mar. Sci. **55**: 467–481.

Pierce, G.J., and Boyle, P.R. 1991. A review of methods for diet analysis in piscivorous marine mammals. Oceanogr. Mar. Biol. Annu. Rev. **29**: 409–486.

Popova, O.A. 1978. The role of predaceous fish in ecosystems. *In* Ecology of freshwater fish production. *Edited by* S.D. Gerking. Blackwell Scientific, London. pp. 215–249.

Rouvinen, K., Jaakko, M., Kiiskinen, T., and Nummela, S. 1992. Accumulation of dietary fish fatty acids in the body fat reserves of some carnivorous fur-bearing animals. Agric. Sci. Finland, **1**: 483–489.

Sargent, J.R. 1995. Origins and functions of egg lipids: nutritional implications. *In* Broodstock management and egg and larval quality. *Edited by* N.R. Bromage and R.J. Roberts. Blackwell Science, Oxford. pp. 353–372.

Sargent, J.R., Parkes, R.J., Mueller-Harvey, I., and Henderson, R.J. 1987. Lipid biomarkers in marine ecology. *In* Microbes in the sea. *Edited by* M.A. Sleigh. Wiley and Sons, New York. pp. 119–138.

Sargent, J.R., Henderson, R.J., and Tocher, D.R. 1989. The lipids. *In* Fish nutrition. *Edited by* J.E. Halver. Academic Press, Washington, D.C. pp. 153–218.

Scott, J.S. 1973. Food and inferred feeding behavior of northern sand lance (*Ammodytes dubius*). J. Fish. Res. Board Can. **30**: 451–454.

Scott, W.B., and Scott, M.G. 1988. Atlantic fishes of Canada. Can. Bull. Fish. Aquat. Sci. No. 219.

Smith, S.J., Iverson, S.J., and Bowen, W.D. 1997. Fatty acid signatures and classification trees: new tools for investigating the foraging ecology of seals. Can. J. Fish. Aquat. Sci. **54**: 1377–1386.

St. John, M.A., and Lund, T. 1996. Lipid biomarkers: linking the utilization of frontal plankton biomass to enhanced condition of juvenile North Sea cod. Mar. Ecol. Prog. Ser. **131**: 75–85.

Stevens, J. 1986. Applied multivariate statistics for the social sciences. Lawrence Erlbaum Associates, Mahwah, N.J.

Viso, A., and Marty, J. 1993. Fatty acids from 28 marine microalgae. Prog. Lipid Res. **32**: 1521–1533.

Volkman, J.K., Jeffrey, S.W., Nichols, P.D., Rogers, G.I., and Garland, C.D. 1989. Fatty acid and lipid composition of 10 species of microalgae used in mariculture. J. Exp. Biol. Ecol. **128**: 219–240.

© 2002 NRC Canada

Simulations of the impact of different temporal and spatial allocations of fishing effort on fishing mortality in a lobster (*Homarus americanus*) fishery

Louise Gendron and Jean-Claude Brêthes

Abstract: A spatially explicit model is proposed to assess the impact on fishing mortality of modifying effort patterns for an American lobster (*Homarus americanus*) fishery. A two-box (offshore and inshore grounds) model is developed for the 1995 lobster fishery season in the Magdalen Islands (Quebec). It considers lobster migration and fisher's temporal and spatial effort dynamics to estimate within-season catchability patterns and exchange rates between the two spatial units. Different management scenarios are simulated: reducing nominal fishing effort and changing its temporal (season's length) and spatial (area closures) allocations. Catchability showed a strong temporal trend, being highest during the first 3 weeks and declining regularly afterwards. The model indicated a continuous migration toward the inshore during the fishing season and that a significant amount of biomass remained offshore. As a result, reducing fishing effort at the beginning of the season would have the greatest impact on exploitation rate. Allowing less effort in the offshore area would also reduce the exploitation rate significantly. Restricting effort to the inshore area, as it was 25 years ago, reduced substantially the exploitation rate. This model represents the first attempt to analyze in-season fishery dynamics and should be useful to further assess the impact of management measures.

Résumé : Un modèle spatial est proposé pour évaluer l'impact de modifications d'allocation d'effort sur la mortalité par pêche dans une pêcherie de homard d'Amérique (*Homarus americanus*). Un modèle à deux compartiments (zones du large et côtière) a été développé pour la saison de pêche au homard 1995 aux îles de la Madeleine (Québec). Il prend en compte la migration de l'espèce et la dynamique spatiale et temporelle de l'effort de pêche pour estimer la capturabilité en cours de saison et les taux d'échange entre les deux unités spatiales. Différents scénarios de gestion ont été simulés : réduction de l'effort nominal et modification dans le temps (durée de la saison) et dans l'espace (fermeture de zones) de l'allocation de l'effort. La capturabilité montre un fort patron temporel, étant plus élevée durant les trois premières semaines et diminuant régulièrement ensuite. Le modèle montre une migration continue du large vers la côte en cours de saison et qu'une fraction significative de la biomasse reste au large. De ce fait, réduire l'effort au début de la saison devrait avoir le maximum d'effet sur le taux d'exploitation. Diminuer l'effort au large réduirait aussi significativement ce taux d'exploitation. Concentrer l'effort à la côte, comme cela se passait il y a 25 ans, diminuerait substantiellement le taux d'exploitation. Ce modèle est une première tentative pour analyser la dynamique de la pêcherie au cours d'une saison et pourrait être utile pour évaluer plus en détail l'impact de mesures de gestion.

Introduction

Like many crustacean fisheries, the American lobster (*Homarus americanus*) fishery has been traditionally managed by input controls. Controls on fishing effort and fishing activity are presently being used to limit fishing mortality, in addition to escapement measures such as size limits and protection of berried females. All those measures are expected to prevent growth overfishing and maintain an acceptable level of egg-per-recruit production to prevent recruitment overfishing. Despite those measures, it was recently recognized that Atlantic Canadian lobster remains heavily exploited and that more stringent conservation measures, including reductions in fishing effort, should be implemented (FRCC 1995).

Fishing effort controls are implemented under the assumption that fishing mortality (F) is proportional to fishing effort (f), according to the relation $F = qf$, where q is the catchability coefficient, i.e., the fraction of a fish stock

Received 8 June 2001. Accepted 13 May 2002. Published on the NRC Research Press Web site at http://cjfas.nrc.ca on 9 July 2002.
J16398

L. Gendron.[1] Department of Fisheries and Oceans, Maurice-Lamontagne Institute, 850, route de la Mer, Mont-Joli, QC G5H 3Z4, Canada.
J.-C. Brêthes. Institut des sciences de la mer de Rimouski, Université du Québec à Rimouski, 310, Allée des Ursulines, Rimouski, QC G5L 3A1, Canada.

[1]Corresponding author (e-mail: gendronl@dfo-mpo.gc.ca).

 DOI: 10.1139/F02-068 © 2002 NRC Canada

caught by a unit of fishing effort (Ricker 1975). If q were constant, the impact on fishing mortality of reductions in fishing effort could be easily predicted. However, in practice, q is rarely constant and is influenced by a number of factors affecting the vulnerability of lobster to traps, as well as by the effectiveness of the fishing gear (see Miller 1990). Catchability can vary over time, because of life cycle, and in space, because of spatial distribution, and will also depend on the behaviour of the fishers and their ability to target resource concentrations (Hilborn and Walters 1992). The impact of those various factors (animal behaviour and fisher behaviour) on the actual effectiveness of effort control has never been fully assessed.

In this paper, we present a deterministic model that can be used as a tool to assess the impact of reductions in fishing effort on fishing mortality within a fishing season and that incorporates the temporal variability of lobster catchability. The model is based on the lobster fishery in the Magdalen Islands (Quebec). This model is spatially explicit and accounts for spatiotemporal trends in the fishery resulting from both lobster migration (Munro and Therriault 1983) and fishers' behaviour (Gendron and Archambault 1997). It is a two-box spatial model that represents the inshore and offshore fishing grounds.

Spatially explicit models applied to lobster are rather scarce in the literature. Fogarty (1998) has developed a spatial box model comprising two subpopulations to investigate the possible causes of the resilience of the coastal populations of the American lobster of the Gulf of Maine to high exploitation. The model was developed in the context of the inshore–offshore system in the Gulf of Maine lobster metapopulation. Spatial models exist for the Western Australian rock lobster (*Panulirus cygnus*; Walters et al. 1993; Hall 1994) and the rock lobster fishery (*Jasus edwardsii*) in Southern Australia (McGarvey and Prescott 1998; Walters et al. 1998) and in Tasmania (Punt and Kennedy 1997), where ontogenic distributions and migrations as well as spatial changes in fishing effort are well recognized and documented. These models are presently used as management and conservation tools. The model developed in this paper is intended to be a tool to help managers in their choice of measures to control fishing effort. With the objective of reducing global exploitation rate, the model estimates the possible effect of the most often suggested measures (reduction of number of traps per fisher, reduction of the fishing season), as well as the effect of alternative measures like closing fishing areas during a period of the fishing season.

Material and methods

Description of the fishery

The model was developed based on the 1995 Magdalen Islands lobster fishery (Quebec; Fig. 1). We concentrated the study on the fishing port of Grande-Entrée, which represents the largest fishing community on the Magdalen Islands with approximately 100 fishers out of the 325 lobster fishers and where about 30% of the total lobster catches of the archipelago are landed each year. It is a spring fishery that lasts 9 weeks (63 days), opening in May after the ice breakup. In 1995, lobster traps were set in the water on Saturday, 12 May. Each fisher is allowed to fish 300 traps. Traps are hauled each day, except on Sundays.

Lobsters are mostly found on offshore grounds at the start of the season and move closer to shore as season progresses (Munro and Therriault 1983). Most fishers have adapted their fishing strategy to take into account this movement through a so-called pursuit strategy: fishers will move offshore at the beginning of the fishing season to target lobsters in their wintering grounds and then move their traps inshore to follow concentrations (Gendron and Archambault 1997). A minority of fishers still use an interception strategy in which traps are set for the whole season in areas that lobsters will eventually reach. Lobster catchability is known to increase at the beginning of the season as temperature rises and to decrease by the end of the fishing season because of the molting period (Miller 1990; Tremblay and Eagles 1997).

Modeling in-season dynamics

Description of the model

A two-box spatial model was used to describe the dynamics of the resource and the fishery within a fishing season. The model described here was first developed by Beverton and Holt (1957) and is further detailed in Maury (1998). From data on catch, effort, and initial stock abundance, this model allows an estimation of lobster biomass and fishing mortality in each spatial unit at each time step from which the within-season pattern of catchability and exchange rates between the spatial units are derived. Catchability values and exchange rates are then used later for simulations of different scenarios of fishing effort. In this work, the model was developed using a 1-day time step.

At each time step, population abundance diminishes through fishing mortality and varies through migration between areas. Considering two spatial units, the abundance in each unit at the period $t + 1$ can be expressed as follows:

$$(1) \qquad B_{1,t+1} = B_{1,t}e^{-F_{1,t}}(1 - T_{12,t}) + B_{2,t}e^{-F_{2,t}}T_{21,t}$$

$$(2) \qquad B_{2,t+1} = B_{2,t}e^{-F_{2,t}}(1 - T_{21,t}) + B_{1,t}e^{-F_{1,t}}T_{12,t}$$

where $B_{1,t+1}$ (and $B_{2,t+1}$) is the abundance on the spatial unit 1 (and 2) at the beginning of the period $t + 1$, $B_{1,t}$ (and $B_{2,t}$) is the abundance on the spatial unit 1 (and 2) at the beginning of the period t, $F_{1,t}$ (and $F_{2,t}$) is the fishing mortality on unit 1 (and 2) during the period t, and $T_{12,t}$ (and $T_{21,t}$) is the exchange rate from the unit 1 (and 2) to the unit 2 (and 1) at the end of the period t. At each time period t, $B_t = B_{1,t} + B_{2,t}$.

Computations begin with the calculation of fishing mortality. At each time step t, the fishing mortality rate in a given spatial unit ($F_{1,t}$ and $F_{2,t}$) is derived from the fishing mortality (F_t) and catchability (q_t) estimated for the whole area. Fishing mortality over the whole area is obtained from the ratio

$$(3) \qquad F_t = C_t/B_t$$

where C_t is the catch over the whole area during the period t and B_t is the total biomass at the beginning of the same period. Given B_0, the total standing stock at the beginning of the season, F_t is then deduced from the total catches at each time step. Knowing the fishing mortality and fishing effort

© 2002 NRC Canada

Fig. 1. Map of the Magdalen Islands in the southern Gulf of St. Lawrence showing the study area off Grande-Entrée and the two spatial units roughly separated by the 20-m isobath.

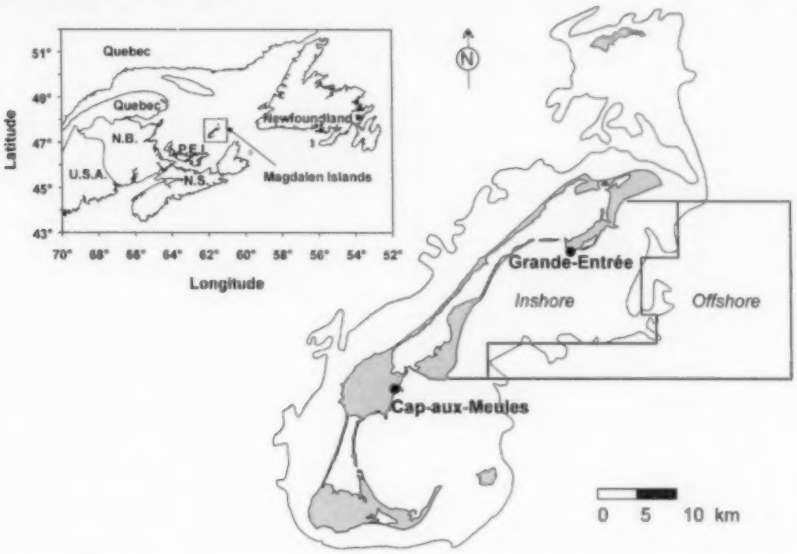

(f_t) at each time step, catchability is then computed as the ratio F_t/f_t.

Total fishing mortality is then partitioned between the two spatial units, at each time step, from data on catchability, respective surfaces of each spatial unit, and fishing effort in each spatial unit ($f_{1,t}$ and $f_{2,t}$)

$$F_{1,t} = \left(q_t \times \frac{S_{\text{total}}}{S_1} \right) \times f_{1,t} \quad (4)$$

$$F_{2,t} = \left(q_t \times \frac{S_{\text{total}}}{S_2} \right) \times f_{2,t} \quad (5)$$

where S_1, S_2, and S_{total} are the surfaces occupied by the stock in units 1, 2, and over the whole area, respectively. Expressions in parentheses correspond to the surface catchability in each spatial unit. A similar approach was used by Pelletier and Magal (1996).

Exchange between the two areas may occur in the form of migration or dispersion. Migration is directional from one spatial unit to the other. Dispersion is a random movement between the two areas and can occur at any time in any direction. The migration rate from unit 1 to unit 2 is expressed from eq. 2 as

$$T_{12,t} = \frac{B_{2,t+1} - B_{2,t} e^{-F_{2,t}} (1 - T_{21,t})}{B_{1,t} e^{-F_{1,t}}} \quad (6)$$

$$T_{21,t} = D_t$$

where D_t is the dispersion rate. For the present study, dispersion was considered negligible compared to migration. The exchange from area 2 to area 1 can be expressed in a symmetric way. Knowledge of lobster movements (Munro and Theriault 1983) indicates that at the period of the fishing season, the inshore to offshore migration was negligible and was thus set to zero. The offshore to inshore migration was further averaged on a weekly basis.

Model assumptions

The model is based on the assumption that both the resource and the fishing effort were distributed homogeneously inside each spatial unit. It is also based on the assumption of constant catchability inside each spatial unit. We know that local aggregations can occur that will translate into modifications of local catchability. However, this spatial scale is much narrower that the scale used in this study. Even if it generates some noise in the data, we consider that it should not affect the general trend.

We assumed that natural mortality was negligible during the fishing season. The fishing period is short and occurs before the molting period, when the large part of the natural mortality is assumed to take place. We also assumed that there was no recruitment to the population during the period. The study covered most of the fishing grounds off Grande-Entrée, and recruitment from further offshore or from north of the study area was considered unlikely. Some recruitment from the south may, however, be possible but probably over a longer period than the one considered in this study (Dubé 1984). The spatial domain was considered more or less as a closed system, although we know that some fishers from neighboring wharves may sometimes fish on the offshore grounds during the first part of the season. However, we assume that this should not affect the general trend.

Data

Data were obtained from four different sources. Daily catches (in weight), fishing effort, and fishing location (on a grid of 2′ latitude × 2′ longitude) were recorded by fishers participating on a voluntary basis to an index-fishers (IF) program. In 1995, 7 of the 100 fishers participated in data collection. Fishing strategies (pursuit and interception) and

© 2002 NRC Canada

the spatiotemporal patterns of allocation of fishing effort were derived from a survey on fishing practices conducted in 1996 among Magdalen Islands lobster fishers (Gendron and Archambault 1997). Weekly landings in weight for each of the 12 fishing wharves of the Magdalen Islands were obtained from official statistics of the Department of Fisheries and Oceans (DFO), which are generally considered reliable and not severely underestimated by misreporting or poaching. Finally, sampling at sea, done on a regular basis since 1985, provided data on demographic structure from which annual fishing mortality rates were estimated (Gendron 1996; Gendron and Savard 2000).

The fishing area was divided into two units, the offshore area and the inshore area, separated roughly by a 20-m isobath (Fig. 1). The surface of each area was defined in relative units, corresponding to the number of squares exploited by the IF (from the grid). The offshore surface was estimated at 48 units, and the coastal surface at 33 units. We derived the effort in each unit and at each time step from the IF data and from the proportion of fishers off Grande-Entrée using the pursuit and interception fishing strategies. According to the survey, 50% of the 100 fishers fishing off Grande-Entrée use a pursuit strategy, starting offshore and moving gradually inshore as season progresses (type 1); 35% use an interception fishing strategy in the offshore area (type 2), whereas 15% use the interception strategy in the inshore area (type 3). Among the 7 IF, 4, 1, and 2 fishers were associated with type 1, type 2, and type 3 fishing strategies, respectively. The percentage of effort devoted to the offshore area on a daily basis was computed as follows: offshore effort = [(% of traps offshore for the IF using type 1 fishing strategy) 0.50 + (% of traps offshore for the IF using type 2 fishing strategy)0.35] × total effort. The total effort was based on 100 fishers using 300 traps each (30 000 traps/day). The inshore effort was obtained from the difference between the total effort and the offshore effort (Fig. 2).

The total catch over the whole area was obtained by multiplying the average catch-per-unit-effort (CPUE) of the IF by total effort. Catch in each spatial unit over each time step was estimated using the average daily catch rates (CPUE) from the IF of each spatial unit multiplied by the effort in each spatial unit computed above. The validity of the model was tested by comparing the overall catches derived from the calculation with the official landings database. Traps are never hauled on Sundays; therefore, based on the observed ratio of $CPUE_{48h}$ to $CPUE_{24h}$ just before and after the 48-h period (i.e., Saturday and Monday), 0.625 of the catch recorded on Monday was attributed to Sunday and 0.375 to Monday.

The standing stock biomass at the beginning of the fishing season (B_0) was determined from an estimation of fishing mortality (F) of the lobster population of the southern part of the Magdalen Islands based on the size composition of the catch (Gendron 1996; Gendron and Savard 2000). Mortality was calculated according to the equation presented in Miller et al. (1987): $Z = -\ln S$. Survival (S) was estimated by measuring the change in abundance of the first molt group recruited to the fishery (76–86 mm carapace length, CL) compared with the second molt group (87–99 mm CL) 1 year later under the assumption that all animals have the same probability of capture (Tremblay et al. 1998). Natural mortality (M) was assumed to be 0.15. Therefore, $F = Z - 0.15$. In 1995, estimated F reached 1.29, which corresponds to an exploitation rate (u) of 72% ($u = 1 - e^{-F}$; Ricker 1975).

Fig. 2. Pattern of fishing effort allocation in the inshore (dashed line) and offshore (solid line) areas off Grande-Entrée, Magdalen Islands, described for the 1995 season and then used in the simulations.

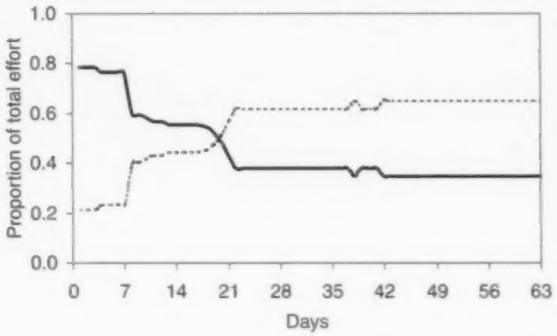

Simulations

Daily catchability coefficients and daily migration rates derived from the model were used to simulate the impact of scenarios of fishing effort that could possibly be implemented by managers to reduce fishing mortality (Table 1). Five possibilities were simulated: a reduction in the nominal effort (number of traps) from 300 traps per fisher to 250; a reduction in the length of the fishing season to 8 weeks either by opening the season 1 week later or by closing 1 week earlier; the implementation of area closure by closing the offshore area the first 3 weeks of the season or the inshore area the last 4 weeks of the fishery, a measure that would protect females that move inshore to mate, spawn, or hatch their eggs. The patterns of fishing allocation retained in the simulations include a reaction of fishers to the management measures. In delaying the opening of the season by 7 days, the fishing season started with 60% of the total effort offshore compared with 80% in the basic situation, considering that fishers would assume the inshore lobster migration already started. After the 3-week offshore closure, we allowed only the fishers using an offshore interception strategy to go offshore. In that simulation we considered that the pursuit fishers would have remained inshore, assuming the bulk of lobster migration would be achieved.

We also simulated the case where fishing would be allowed on Sundays to assess the benefits of closing the fishery for 1 day during the week. Finally, we simulated a fishery totally restricted to an inshore interception strategy to mimic the way it was 25 years ago.

Except for the case where a reduction in the number of traps was simulated, we used constant individual fishing effort of 300 traps/day and a total of 100 fishers fishing 6 days/week in all scenarios. For each scenario, the exploitation rate (ratio of total catches during the fishing season to the initial standing biomass) was calculated and compared to the exploitation rate (simulated value) of the reference situation (1995 current management regime).

© 2002 NRC Canada

Table 1. Fishing effort (number of traps, season duration, and spatiotemporal allocation) characterizing the different management scenarios simulated with the spatial model.

			Beginning – end of season	
	Number of traps	Number of weeks	Effort offshore	Effort inshore
Basic pattern under the 1995 management regime	300	9 without Sundays	80%–35%	20%–65%
New management scenarios[a]				
Reduction in the nominal fishing effort	250	9	80%–35%	20%–65%
Reduction in the length of the fishing season—delay in opening	300	8	80%–35%	20%–65%
Reduction in the length of the fishing season—early closure	300	8	80%–35%	20%–65%
Area closure (offshore) (weeks 1–3)	300	9	0%–35%	100%–65%
Area closure (inshore) (weeks 6–9)	300	9	80%–100%	20%–0%
Historic fishing strategy				
Sunday fishing	300	9	80%–35%	20%–65%
100% inshore interception strategy	300	9	0%–0%	100%–100%

[a]Simulations were done using three levels of exploitation rates and a hypothetical seasonal catchability pattern (see text).

Sensitivity analysis

To account for our uncertainty in the value of exploitation rate used to determine initial standing biomass (B_0), the model was also run for exploitation rates of 65% and 80%, which represent roughly a 10% variation around the estimated value of 72%. The resulting patterns of seasonal catchability and migration rates were used to simulate the same management scenarios as above. Additionally, all five management scenarios were simulated using a hypothetical in-season catchability pattern characterized by low values at the opening of the fishing season increasing linearly during the first 14 days and then following the observed pattern for the rest of the season (see Fig. 3). We used the starting biomass and migration rates obtained with a 72% exploitation rate from the previous calculation.

Results

Daily catchability coefficients, calculated from the model for the 1995 lobster fishery off Grande-Entrée, showed a strong temporal pattern (Fig. 3), and coefficients were higher in the inshore than in the offshore area because of the smaller surface of the inshore area. The highest values were observed at the beginning of the fishing season. Catchability remained more or less stable during the first 3 weeks (days 1 to 21). An important decrease was observed during the 4th week, between days 21 and 28. It increased at the beginning of the 5th week and then decreased regularly until the end of the season, consistent with a lessened responsiveness to bait. Patterns of catchability showed similar general trends for the three different exploitation rates. At the higher exploitation rate, catchability values were higher, as could be expected, but also showed a lower rate of decrease during the season. Between the beginning and the end of the fishing season, catchability decreased by a factor of 2 at the higher exploitation rate (80%) compared with 3.5 at the lower exploitation rate (65%). At the higher exploitation rate, catchability at the end of the season remained relatively high, twice as high as what was observed at 65%.

Fig. 3. Daily surface catchability coefficients for (*a*) inshore and (*b*) offshore areas estimated for the 1995 fishing season using three different values of exploitation rates: 65% (open circles), 72% (solid line), and 80% (solid triangles). The hypothetical values of catchability for days 1–14 used in the simulations are also presented (broken line).

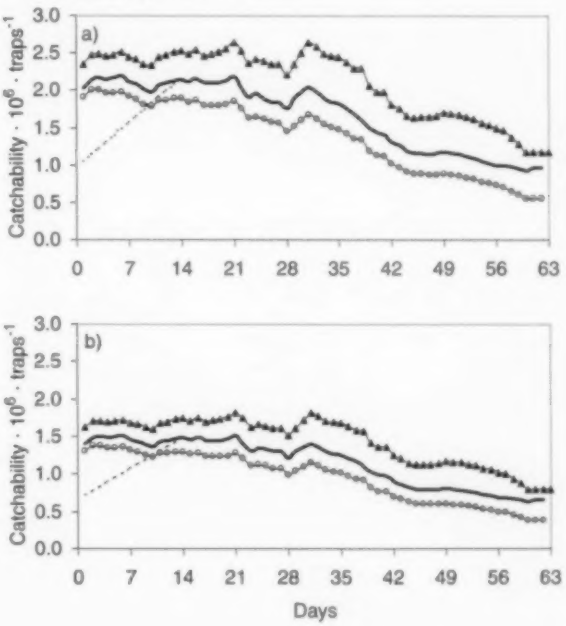

The model shows a continuous migration of lobsters in-

© 2002 NRC Canada

Fig. 4. Net migration rates (averaged over 1 week) from the offshore to the inshore area estimated from the spatial model for three different levels of exploitation rates: 65% (open circles), 72% (solid line), and 80% (solid triangles).

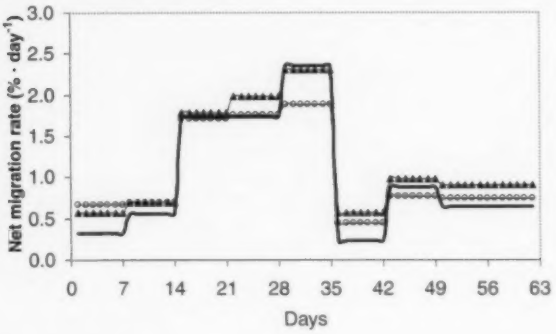

shore during the fishing season (Fig. 4). Migration was more intense during weeks 3 to 5 (days 14 to 35). Migration slowed down during the 6th week, increased slightly during the 7th week, and then remained constant until the end of the fishing season. The important migration observed in the middle of the fishing season is realistic and is a known phenomenon on which fishers build their strategy of fishing effort allocation between inshore and offshore. No major differences were observed in the general migration pattern derived with the different levels of exploitation rate.

The model was first used to reproduce the seasonal pattern of catches and biomass made inshore and offshore during the 1995 fishing season under the present management regime. Identical catch patterns were derived using the three different levels of exploitation rates. At the beginning of the fishing season, catches were maximal in the offshore area, mainly because of heavy fishing pressure but also because of high catchability and high biomass (Fig. 5*a*). A larger proportion of the biomass was located in the offshore area at the beginning of the fishing season (Fig. 5*c*). This offshore biomass declined rapidly during the first 3 weeks resulting from heavy fishing pressure when catchability was high and also from the inshore migration. In the inshore area, catch increased slowly to reach a peak at the end of the 3rd week, when it exceeded the offshore catch (Fig. 5*b*). This augmentation is explained by the reallocation of effort and the inshore migration of lobster. The inshore biomass, which represented roughly one third of the total biomass at the beginning of the season, declined slowly (Fig. 5*d*). Inshore biomass depletion due to fishing is partially compensated for by the arrival of lobsters from offshore. At the end of the season, the total remaining biomass was roughly equal in the two spatial components. Even if the inshore movement is substantial in the middle of the season, a large part of the remaining biomass is still located offshore at the end of the season. The effect of fishing in an area adds up to the natural changes in biomass caused by migration. For instance, in a situation where no fishing occurs, the offshore biomass is constantly decreasing (Fig. 5*c*) because of the net migration of lobsters inshore, where the biomass increases (Fig. 5*d*). However, at the end of the simulation period, 33% of the biomass still remains offshore. As expected, biomass depletion offshore and inshore was more severe at the higher exploitation rate, but trends were similar.

Total catches obtained from the simulations of the current 1995 management regime (650–670 t (tonnes)) reflect the value obtained from the IF data extrapolated to the entire area (660 t), which gives some confidence in the simulations. Also, IF data extrapolated to the entire area are close to the DFO official statistics recorded in 1995 for Grande-Entrée (667 t), which gives some confidence that the index fishers adequately represent the fleet. However, spatial distribution of the catches between the inshore and offshore areas was slightly different, and approximately 14% more catches were attributed to the inshore area in the simulated data compared with the original IF data.

The various scenarios of fishing effort reduction modeled showed visible but rather small impacts in the reduction of the exploitation rate. Reductions were generally less than 10% (Table 2; Fig. 6*a*). For example, exploitation rates obtained for the different scenarios tested ranged from 63% to 70% compared with the initial situation of 72%, corresponding to reductions ranging from 2% to 9%. The reduction in the number of traps from 300 to 250 had a visible effect, reducing the exploitation rate by 6% on the whole. Simulation was made, however, under the assumption of no increase in efficiency of the remaining fishing effort. Reduction in the duration of the fishing season yielded different exploitation rates whether the season was opened with a 1-week delay or whether it was closed 1 week earlier. Earlier closure of the fishing season had a lesser impact than a late opening because of the lower catchability at the end of the season. Reductions were around 2–3% compared with 5–6% for the delay in the opening. Prohibiting fishing on Sundays also showed some benefits, although marginal, because fishing 7 days/week would cause the exploitation rate to increase by 2% (Table 2).

Adopting area closures for short periods of time in the context of a 9-week fishery showed interesting results (Table 2; Fig. 6*a*). On the whole, the spatial closures tested appeared more efficient in reducing the exploitation rate than temporal closures. By closing the offshore area at the beginning of the season (first 3 weeks) and then allowing only a small part of the fleet to fish in the offshore area, exploitation rate was reduced by 8–9%. Total closure of the inshore area towards the end of the fishing season (last 4 weeks) reduced exploitation rate by 6–7%. The effect of offshore closure at the beginning of the fishing season was larger because of the higher catchability and higher biomass offshore at that period.

The fact that fishers did not gather to fish offshore in the past created a spatial refuge where a large part of the biomass was protected from the fishery. This strict inshore interception strategy (100% effort inshore) was prevalent some 25 years ago. Simulation according to this scenario showed much lower exploitation rates (53%, 55%, and 62%) compared with that from the present management regime (66%, 72%, and 81%, respectively; Table 2).

Results of the simulations obtained at different exploitation rates reflect the differences in the respective seasonal catchability patterns. At the higher exploitation rate, reduction in the length of the fishing season by opening 1 week

© 2002 NRC Canada

Fig. 5. Daily catch (*a* and *b*) and biomass (*c* and *d*) in the inshore and offshore areas derived from the spatial model using three different values of exploitation rates: 65% (open circles), 72% (solid line), and 80% (solid triangles) and under a scenario without fishing (broken line).

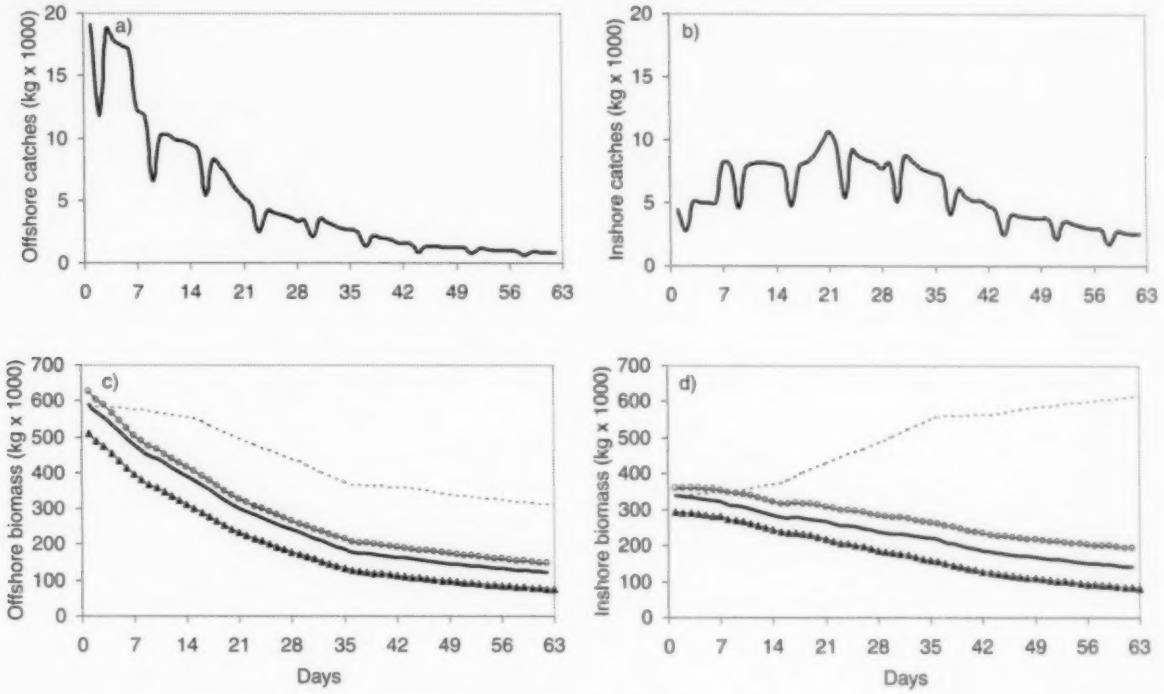

later or closing 1 week earlier reduced exploitation rate by 5% and 3%, respectively (Fig. 6*a*). At the lower exploitation rate, the difference between the two scenarios was greater and reductions calculated were 6% and 2%, respectively. At the high exploitation rate, catchability remains relatively high even at the end of the season and therefore attenuates the difference between the two scenarios, shortening the fishing season. For the same reason, closing the inshore area at the end of the season when biomass builds up has a stronger effect in reducing exploitation rate. Simulations performed using a seasonal pattern of catchability characterized by lower values at the beginning of the fishing season showed that the previously observed benefits of delaying the opening of the fishing season by 1 week compared with closing 1 week later were less obvious. As well, benefits of the offshore area closure are reduced, although they still remain important (Fig. 6*b*).

Despite the fact that scenarios of area closure generate similar catches, area closures translate into different patterns of biomass distribution between inshore and offshore grounds and different levels of abundance in the two areas at the end of the fishing season (Fig. 7). For example, closing the inshore area during the last part of the fishing season leaves up to twice as much biomass inshore (172–288 t) at the end of the fishing season compared with the offshore closure situation (89–185 t) (Figs. 7*a*, 7*c*). Inshore closure could therefore protect a larger proportion of lobsters that succeeded to migrate inshore in the course of the fishing season (fast migrants). On the other hand, closure of the offshore area leaves two to three times more biomass offshore (137–232 t) compared with inshore closure (42–107 t) (Figs. 7*b*, 7*d*). This measure could increase the protection of those lobsters that have not yet left the area for the inshore migration (slow migrants).

Discussion

The work presented here describes and analyses a fishery on a fine temporal scale and explores the spatial dynamics of both the resource and the fishing fleet. The model developed provides a tool that allows the assessment of short-term benefits of different measures of controlling fishing effort. The model can be used to simulate changes in the spatiotemporal allocation of different levels of fishing effort between the inshore and offshore grounds. It also proved its usefulness in recreating fishing practices used in the past.

One of the main results of this work is the identification of a seasonal pattern in the catchability coefficient. This seasonal pattern is important and governs the outcome of the management measures taken to reduce fishing effort, especially those dealing with temporal allocation. According to the pattern of catchability observed in 1995, a greater reduction in exploitation rate would have been possible by delaying the opening of the fishing season by 1 week. Closing 1 week earlier would only have had a marginal effect, because catchability was already at its lowest.

Catchability is related to the lobster behaviour (see Miller 1990) and environmental factors such as temperature. There-

© 2002 NRC Canada

Table 2. Catches and exploitation rates resulting from different scenarios of spatial and temporal allocation of fishing effort as estimated from the spatial model for three values of exploitation rates used to determine initial biomass and for an hypothetical seasonal catchability pattern.

	65%		72%		80%		72% hypothetical catchability pattern	
	Total catch (× 1000 kg)	Exploitation rate	Total catch (× 1000 kg)	Exploitation Rate	Total catch (× 1000 kg)	Exploitation rate	Total catch (× 1000 kg)	Exploitation rate
Basic pattern under the 1995 management regime (simulation)	650	66.0%	671	72.2%	650	80.9%	651	70.1%
New management scenarios								
Reduction from 300 traps to 250 traps	586	59.4%	611	65.8%	591	73.6%	591	63.7%
Reduction in the length of the fishing season—delay in opening	588	59.7%	617	66.5%	612	76.2%	616	66.4%
Reduction in the length of the fishing season—early closure	627	63.6%	647	69.7%	628	78.2%	625	67.3%
Area closure(offshore) (weeks 1–3)	573	58.1%	588	63.4%	581	72.4%	584	62.9%
Area closure (inshore) (weeks 6–9)	593	60.1%	613	66.1%	591	73.6%	590	63.6%
Historic fishing strategy								
Sunday fishing	672	68.2%	692	74.5	665	82.8	—	—
100% inshore interception strategy	517	52.5%	512	55.2%	494	61.5%	—	—

Fig. 6. Reduction of the exploitation rate following the implementation of different management measures calculated for (*a*) three different values of exploitation rate: 65% (open bars), 72% (solid bars), and 80% (shaded bars), and (*b*) for the observed (solid bars) and hypothetical (hatched bars) seasonal catchability patterns.

fore, the general seasonal trend in catchability presented here may be specific to the 1995 fishing season. In other years, for example, 1993 and 1994, unlike 1995, the fishing season started with low catches, with water temperature below 1°C (L. Gendron, unpublished data), suggesting very low catchability values in the first 1 or 2 weeks. The hypothetical catchability pattern used here in the simulations could mimic such situations. In those cases, the difference between closing later or opening earlier was lower. This suggests that the extent of the benefits of the management measures examined here could vary from year to year, depending on the water temperature at the opening of the fishing season. In the recent years, however, fishers from Grande-Entrée area have asked for a close monitoring of the water temperature during the winter to help them determine the proper time to open the season. Their objective is to avoid fishing in conditions of low catchability. Their target is to have the season opened when the water temperature is near 2°C. The situation described using the hypothetical catchability pattern could also represent what can be seen on the northern side of the Magdalen Islands where water temperature is known to increase later in the season.

Because of the uncertainties concerning within-season trends in catchability, reducing the number of traps would therefore appear more efficient and more straightforward for reducing exploitation rates, as suggested by our results. In the simulation exercise, however, we did not incorporate any factor taking into account an increase in effort efficiency, which

© 2002 NRC Canada

Fig. 7. In-season trends in lobster biomass in the inshore and offshore areas following (*a* and *b*) offshore area closure and (*c* and *d*) inshore area closure calculated for three different values of exploitation rate: 65% (open circles), 72% (solid line), and 80% (solid triangles).

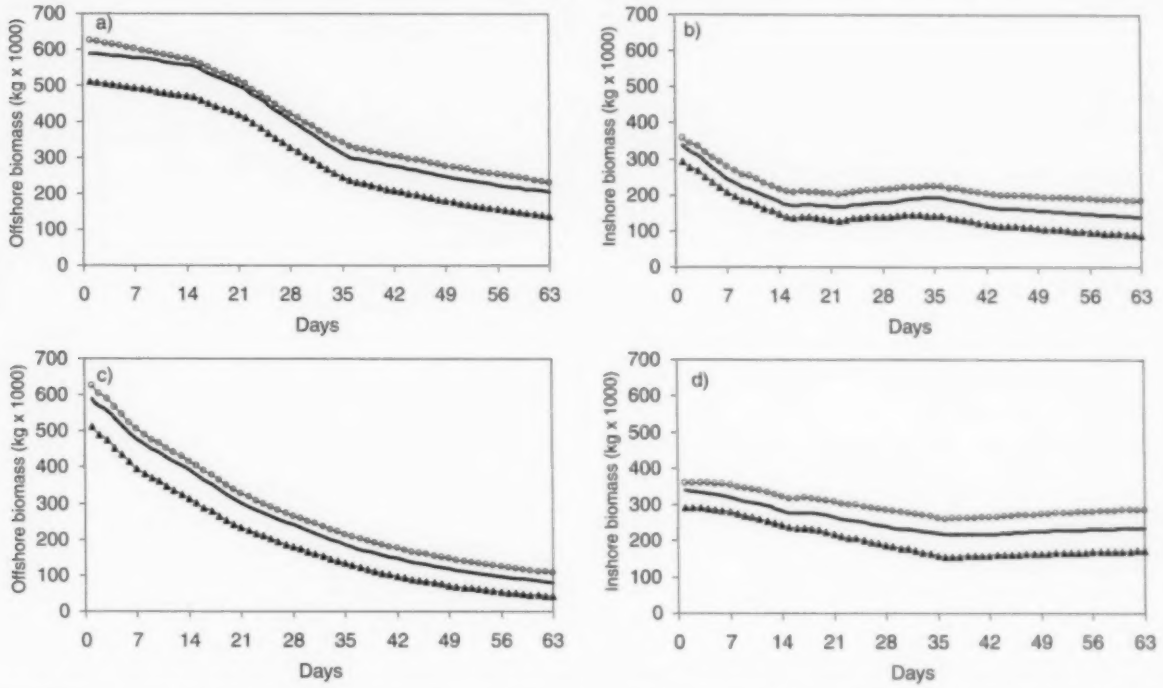

would likely occur if this measure were implemented. The benefit might then be lower than computed.

The spatial model showed that not all lobsters migrate inshore during the fishing season and that a significant amount of biomass remains in the offshore sector. This result explains why the interception strategy in the offshore area remains a valid option for some fishers, despite the higher travel costs. Biomass distribution between inshore and offshore grounds during the fishing season is strongly dependant on lobster movement. This means that the impact of area closures on reduction of exploitation rates will strongly depend on the rate and timing of lobster movement. For example, slower migration would tend to reduce the benefits of inshore closure. For now, however, it is difficult to speculate on alternative migration patterns to the one described here, as the factors governing this movement are not yet well known.

Although there were no major differences in total catches between the two scenarios involving area closures, there could, however, be a difference in the catch composition, because a fishery that operates inshore will target the fastest migrants, whereas a fleet operating offshore will mainly fish the animals that tend to be sedentary or migrate inshore later in the season. It would be interesting to characterize the reproductive status of the slow and fast migrants to see if area closures could have a conservation value. From the fishers' point of view, it would certainly be worth looking into if the reductions in catches caused by the offshore closure would be compensated for by a reduction in the cost of travel offshore.

Given the fact that migration to the inshore area affects only part of the lobster population, it is not surprising to observe a big change when effort is focused on the inshore area only. This result is interesting because the tested scenario mimics the historical period, when only the inshore interception strategy existed. The emergence of a pursuit strategy was concomitant with technological developments that started in the early 1980s (Gendron and Archambault 1997). Fishing efficiency has increased in the recent past, and the offshore spatial refuge for the population no longer exists. These results provide an explanation for the past resilience of the Magdalen Islands lobster population. At the same time, it calls for caution in the future management of the resource.

The model developed here relies on the knowledge of the standing stock biomass at the beginning of the fishing season. Initial biomass was obtained by dividing catches reported for the area by the exploitation rate. The estimate of the exploitation rate over the entire season was based on population size structure from the whole southern area, whereas our model is restricted to the area off Grande-Entrée. If there is spatial heterogeneity in the levels of exploitation and in population structure, the exploitation rate calculated may not be fully representative of the Grande-Entrée area. These uncertainties could not be quantified, and to account for a possible over- or under-estimation of the value of the exploitation rate, two additional values were used to determine standing stock biomass. Catchability patterns were sensitive to the different values of exploitation rate, causing slight variations in the effect of the different

© 2002 NRC Canada

management measures on the reduction of the exploitation rate, but without modifying the general conclusions.

We recognize that the whole work is based on a rather unusually small sample of index fishers. However, we believe that they properly represent the fishing fleet. The fact that the extrapolated values of catches match the observed landings gives some confidence to the exercise. We further believe that official landings reflect the catches made in the Grande-Entrée area, given the usual fidelity of the fishers to their wharf and the territoriality of fishers, which limits to a certain extent the activity of other wharves' fishers in the study area.

The work presented here constitutes a first attempt to introduce a spatial approach in the management of American lobster fishery. It is now recognized that the knowledge of stocks' spatial structures becomes necessary both to understand population dynamics and to design management methods (Freire and Garcia-Allut 2000). Spatial harvesting policies are seen as a viable approach to resource management (Fogarty et al. 1997). The model developed here allows us to analyze those spatial harvesting strategies in conjunction with the spatial dynamics of the resource. Coupling biological research with fishers' behaviour was profitable and outlines the importance of having good knowledge of fishing strategies and patterns to properly describe the spatial dynamics of the fishery (Gendron et al. 2000).

Unlike common fisheries dynamic models, such as those of Walters et al. (1993), Pelletier and Magal (1996), and Maury (1998), this study focuses specifically on in-season dynamics. The intent was not to define the current state of the lobster resource compared with a theoretical level, or the optimum exploitation rate, which cannot be estimated at the present time, as is the case for several invertebrate coastal stocks (Freire and Garcia-Allut 2000). We took as a baseline that exploitation rates are too high and should be reduced to enhance eggs-per-recruit production (FRCC 1995). Therefore, we made the assumption that any reduction in the exploitation rate in the short term might be beneficial in the long term. We chose then to analyze the in-season fishery dynamics to assess the effect of management measures for a single season. This approach is of immediate interest for both managers and fishers who can better visualize the impact of measures of effort control on the dynamics of a fishery and better understand why there is uncertainty in effectiveness of such measures.

The model was based on a number of assumptions. We recognize that the assumption of homogeneity inside each spatial compartment should eventually be addressed in more detail. The approach developed here is deterministic and is based on constant parameters. Although such models have often provided robust approximations to the processes under study, despite their reductionist approach (Gordon et al. 1994), it would be interesting to further develop the model to account for random variation in the different parameters. Considering its simplifications and specificity to the 1995 fishing season, even if it included a sensitivity analysis, the model presented here can be seen as a starting point for further investigations.

Unlike many invertebrate coastal fisheries, which are complex with several targeted species and several gears and varying in time and space, the lobster fishery under study is simple. This fishery is not far from a closed system, including a fixed number of fishers, a fixed number of a single gear type, and a limited season duration. This allows the use of a simple model like the one described here. We can believe, then, that the effect of management scenarios tested here are likely to be valid in relative terms, at least in the short term. The same type of approach could be used in other lobster fishing areas in Canadian Atlantic where a similar management system prevails. It could also be used for other small-scale invertebrate fisheries where daily effort and catches can be sampled over constant steps in time and space.

Acknowledgements

This work was funded by a High Priority Research Program from the Department of Fisheries and Oceans under the Canadian Lobster Atlantic-Wide Study program. We thank Dr. O. Maury for his clear advice and ideas. We also want to thank the Magdalen Islands' fishers: without their participation in the survey and in the index-fishers program, this work would not have been possible. The manuscript benefitted from the review and comments of Drs. Dominique Pelletier, Ian McQuinn, and Hugo Bourdages and an anonymous referee.

References

Beverton, R.J.H., and Holt, S.J. 1957. On the dynamics of exploited fish populations. U.K. Min. Agric. Fish. Food Fish. Invest. (Ser. 2) No. 19.

Dubé, P. 1984. Analyse des déplacements du homard (*Homarus americanus*) sur les côtes des Îles-de-la-Madeleine, à partir des données de marquage et de recaptures, de 1978 à 1983. Canadian Atlantic Fisheries Scientific Advisory Committee Res. Doc. 84/37.

Fogarty, M.J. 1998. Implications of migration and larval interchange in American lobster (*Homarus americanus*) stocks: spatial structure and resilience. *In* Proceedings of the North Pacific Symposium on Invertebrate Stock Assessment and Management. *Edited by* G.S. Jamieson and A. Campbell. Can. Spec. Publ. Fish. Aquat. Sci. 125. pp. 273–283.

Fogarty, M.J., Hilborn, R., and Gunderson, D. 1997. Chaos and parametric management. Marine Policy, **21**: 187–194.

FRCC (Fisheries Resource Conservation Council). 1995. A conservation framework for Atlantic lobster. (http://www.ncr.dfo.ca/frcc/index.htm)

Freire, J., and Garcia-Allut, A. 2000. Socioeconomic and biological causes of management failures in European artisanal fisheries: the case of Galicia (NW Spain). Marine Policy, **24**: 375–384.

Gendron, L. 1996. État des stocks de homard des côtes du Québec en 1995 et analyse des mesures de conservation. Department of Fisheries and Oceans Atlantic Fisheries Res. Doc. 96/123.

Gendron, L., and Archambault, J. 1997. Change in fishing capacity in the American lobster (*Homarus americanus*) fishery of the Magdalen Islands (Québec) from 1975 to 1995. Can. Tech. Rep. Fish. Aquat. Sci. 2189.

Gendron, L., and Savard, G. 2000. État des stocks de homard des côtes du Québec en 1999 et suivi des impacts de l'augmentation de la taille minimale de capture. Canadian Stock Assessment Secretariat. Res. Doc. 2000/115.

Gendron, L., Camirand, R., and Archambault, J. 2000. Knowledge-sharing between fishers and scientists: towards a better understanding of the status of lobster stocks in the Magdalen Islands. *In* Finding our sea legs: linking fishery poeple and their knowl-

© 2002 NRC Canada

edge with science and management. *Edited by* B. Neis and L. Felt. ISER Press, St. John's. pp. 56–71.

Gordon, G.N.G., Andrew, N.L., and Montgomery, S.S. 1994. A compartment model of the eastern king prawn fishery. *In* Population dynamics for fisheries management. Australian Society for Fish Biology Workshop Proceedings, Perth, 24–25 August 1993. *Edited by* D.A. Hanckock. Australian Society for Fish Biology, Perth. pp.144–154.

Hall, N.G. 1994. Modelling the western rock lobster fishery. *In* Population dynamics for fisheries management. Australian Society for Fish Biology Workshop Proceedings, Perth, 24–25 August 1993. *Edited by* D.A. Hanckock. Australian Society for Fish Biology, Perth. pp. 155–159.

Hilborn, R., and Walters, C.J. 1992. Quantitative fisheries stock assessment: choice, dynamics and uncertainty. Chapman and Hall, London.

Maury, O. 1998. Modélisation spatiale en halieutique. Approche par simulateur sous SIG. Application à la modélisation hiérarchique de la population de thons albacore (*Thunnus albacares*) de l'Atlantique tropical. Ph.D. thesis, École Nationale Supérieure Agronomique de Rennes, France.

McGarvey, R., and Prescott, J.H. 1998. A model for assessing season closure management options in the south Australian rock lobster (*Jasus edwardsii*) fishery. *In* Proceedings of the North Pacific Symposium on Invertebrate Stock Asssessment and Management. *Edited by* G.S. Jamieson and A. Campbell. Can. Spec. Publ. Fish. Aquat. Sci. 125. pp. 335–340.

Miller, R.J. 1990. Effectiveness of crab and lobster traps. Can. J. Fish. Aquat. Sci. **47**: 1228–1251.

Miller, R.J., Moore, D.S., and Pringle, J.D. 1987. Overview of the inshore lobster resources in the Scotia–Fundy region. Canadian Atlantic Fisheries Scientific Advisory Committee Res. Doc. 87/85.

Munro, J., and Therriault, J.-C. 1983. Migrations saisonnières du homard (*Homarus americanus*) entre la côte et les Îles-de-la-Madeleine. Can. J. Fish. Aquat. Sci. **40**: 905–918.

Pelletier, D., and Magal, P. 1996. Dynamics of a migratory population under different fishing effort allocation schemes in time and space. Can. J. Fish. Aquat. Sci. **53**: 1186–1199.

Punt, A.E., and Kennedy, R.B. 1997. Population modelling of Tasmanian rock lobster, *Jasus edwardsii*, resources. Mar. Freshw. Res. **48**: 967–989.

Ricker, W.E. 1975. Computation and interpretation of biological statistics of fish populations. Bull. Fish. Res. Board Can. 191.

Tremblay, M.J., and Eagles, M.D. 1997. Molt timing and growth of the lobster, *Homarus americanus*, off northeastern Cape Breton Island, Nova Scotia. J. Shellfish Res. **16**: 383–394.

Tremblay, M.J., Eagles, M.D., and Black, G.A.P. 1998. Movements of the lobster, *Homarus americanus*, off northeastern Cape Breton Island, with notes on lobster catchability. Can. Tech. Rep. Fish. Aquat. Sci. 2220.

Walters, C.J., Hall, N., Brown, R., and Chubb, C. 1993. Spatial model for the population dynamics and exploitation of the western Australian rock lobster, *Panulirus cygnus*. Can. J. Fish. Aquat. Sci. **50**: 1650–1662.

Walters, C.J., Prescott. J., McGarvey, R., and Prince, J. 1998. Management options for the South Australian rock lobster (*Jasus edwardsii*) fishery: a case study of co-operative assessment and policy design for fishers and biologists. *In* Proceedings of the North Pacific Symposium on Invertebrate Stock Asssessment and Management. *Edited by* G.S. Jamieson and A. Campbell. Can. Spec. Publ. Fish. Aquat. Sci. 125. pp. 377–384.

© 2002 NRC Canada

PERSPECTIVE

Evolutionary individual-based model for the recruitment of anchovy (*Engraulis capensis*) in the southern Benguela

Christian Mullon, Philippe Cury, and Pierrick Penven

Abstract: Evolutionary simulations are developed to explore environmental constraints that select observed spatial and temporal spawning patterns for anchovy (*Engraulis capensis*) in the southern Benguela. They couple a realistic three-dimensional hydrodynamic model with an individual-based model in which an evolutionary-based reproductive strategy for adult fish and a passive transport for early life stages are implemented. The evolutionary success of spawning is quantified when patterns at the population level emerge after many generations from constraints at the individual level through a selective process. As a result, several self-sustaining populations are identified considering different sets of selective constraints. Simulated spawning patterns better match the observed mean spawning pattern when two selective environmental constraints are associated: a threshold temperature of 14°C, above which the development of early life stages is ensured, and the avoidance of offshore currents that constitute a loss of spawning products. Simulated recruitment patterns are more realistic when considering the constraint of reaching the nursery area. This modeling experience can help to identify, temporally and spatially, environmental factors important for fish recruitment and to establish a hierarchy of these factors. The probable coexistence in nature of several self-sustaining populations of pelagic fishes is shown to be important for recruitment studies.

Résumé : Nous avons mis au point des simulations évolutives pour étudier les contraintes environnementales qui agissent sur la sélection des comportements de ponte que l'on observe chez l'anchois (*Engraulis capensis*) dans le sud Benguela. Les simulations associent un modèle hydrodynamique 3-D avec un modèle centré sur l'individu; elles représentent les effets évolutifs du couplage entre la stratégie de reproduction des adultes et le transport passif lors des jeunes stades (oeufs et larves). Nous nous intéressons à l'apparition au niveau de la population de patterns spatio-temporels de ponte causés par un processus de sélection dans lequel des contraintes s'exercent au niveau individuel pendant plusieurs générations. Plusieurs populations autosuffisantes, correspondant à ces patterns, peuvent être identifiées et associées à différentes séries de contraintes évolutives. Les patterns de ponte simulés s'accordent mieux avec le pattern de ponte observé lorsque deux contraintes sélectives de l'environnement sont associées: un seuil de température de 14°C et l'évitement des courants au large. Les patterns de recrutement simulés sont plus réalistes si on tient compte de la nécessité d'atteindre la zone de nourricerie. Une telle expérience de modélisation aide à identifier dans le temps et l'espace les facteurs environnementaux les plus importants pour le recrutement et à les hiérarchiser. Il nous apparaît alors que la coexistence probable en nature de plusieurs populations autosuffisantes de poissons pélagiques est un facteur important à considérer dans les études sur le recrutement.

[Traduit par la Rédaction]

Introduction

The marine fish egg and larvae studies carried out under the direction of Committee A of the International Council for the Exploration of the Sea between 1902 and 1907 generated a paradigm shift that is still highly influential today (Sinclair 1997). The results of studies on the geography of spawning led to a new working hypothesis in evolution

Received 19 September 2001. Accepted 31 March 2002. Published on the NRC Research Press Web site at http://cjfas.nrc.ca on 9 July 2002.
J16536

C. Mullon.[1] Oceanography Department, University of Cape Town, Rondebosch 7701, South Africa, and IRD GEODES Research Unit, Bondy, France.
P. Cury. Oceanography Department, University of Cape Town, Rondebosch 7701, Marine and Coastal Management, Cape Town, South Africa, and IRD IDYLE Research Unit, Paris, France.
P. Penven. Institute of Geophysics and Planetary Physics, University of California at Los Angeles, 405 Hilgard Avenue, Los Angeles, CA 90095-1567, U.S.A., and IRD IDYLE Research Unit, Paris, France.

[1]Corresponding author (e-mail: cmullon@physci.uct.ac.za).

 DOI: 10.1139/F02-064 © 2002 NRC Canada

(Sinclair 1988) because patterns in spawning locations and the geographical scale of the larval distributions provided a new image of species. This new interpretation was dependent on the recognition that species comprise self-sustaining stocks or populations (Wyatt et al. 1991; Sinclair 1997). In fact, spawning occurs in very restricted and distinct areas relative to the distribution of the species as a whole. Moreover, fish spawn once or several times every year but generally over a limited period of time (see www.fishbase.org for further details). This reproductive strategy in marine fishes is thought to have evolved as a mechanism to synchronize the occurrence of larval stages with environmental conditions that are optimal for their survival (Roy et al. 1992). Food availability is an obvious factor that determines larval survival (Cushing 1996). However, microscale and mesoscale oceanographic events, related to retention, concentration, and enrichment processes, have been identified more recently as playing a major role in recruitment success (Bakun 1996).

Given the difficulties in assembling all of the temporally flexible physical attributes and biological processes into a single spatially explicit framework (Boisclair 2001), it is scientifically challenging to estimate environmental risks with different habitats during the various early life stages of pelagic fish (Hutchings et al. 1998). The potential of considering spatial and temporal dynamics in ecological studies to explain recruitment variability in fish populations is promising (Frank and Leggett 1994; Hinckley et al. 1996; Rose et al. 1999). However, this presents new methodological difficulties such as how to evaluate the relative beneficial or detrimental effects of several environmental factors acting simultaneously or independently during the different phases of larval life histories. Moreover, theoretical difficulties in the study of the variability of fish populations have underlined the necessity of taking into account the evolutionary process that they derive from (Frank and Leggett 1994). An integrated approach is needed that would conciliate evolutionary and ecological constraints.

In this paper, we explore the viability of self-sustaining spawning populations under selective environmental constraints. For this purpose, we develop evolutionary simulations that associate environmental constraints with spatial and temporal spawning patterns for anchovy (*Engraulis capensis*) in the southern Benguela. A realistic three-dimensional hydrodynamic model is coupled with an individual-based model (IBM) in which an evolutionary-based reproductive strategy for adult fish and passive transport for early life stages are modeled. Finally, a methodology is derived from this modeling study to identify sets of environmental factors that are important for self-sustaining populations and fish recruitment.

Background and hypotheses

Pelagic fish reproductive strategy in the Benguela ecosystem and environmental constraints

Pelagic fish usually spawn in the nursery area. In two known cases, the Canary and Benguela ecosystems, anchovy spawn in an area from which the eggs are jetted to a distinct nursery area in which the larvae develop further (Wyatt et al. 1991). In the southern Benguela, anchovy spawn on the Agulhas Bank between September and December (Fig. 1) with a peak season during mid-November (Huggett et al. 1998). Eggs and larvae are then advected by a strong jet current to a nursery habitat on the west coast of South Africa where they grow as larvae and juveniles (Fig. 1*b*). Transport of anchovy eggs and larvae from the western Agulhas Bank

Fig. 1. (*a*) Spawning patterns for anchovy as depicted by spatial egg distribution. The map is a composite calculated from the egg distribution obtained during scientific surveys conducted during November between 1983 and 2000 (van der Lingen et al. 2001); 100- and 200-m isobaths are shown. (*b*) Empirical model of anchovy eggs and larvae dynamics in the southern Benguela derived from field studies. The eggs and larvae are transported by a strong jet current from the spawning area in the western Agulhas Bank to the nursery area located on the west coast (from Hutchings 1992).

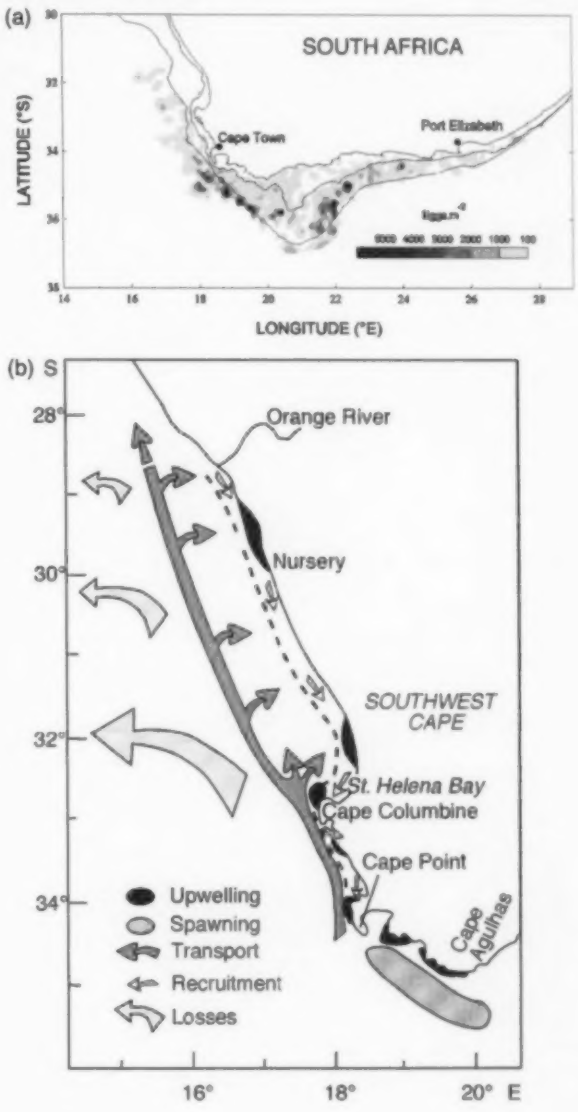

© 2002 NRC Canada

Fig. 2. Temporal pattern of anchovy recruitment in the Benguela. (*a*) Biomass X_t from 1984 to 2001 derived from acoustic estimates (Barange et al. 1999, M&CM data); (*b*) rate of recruitment, i.e., $X_{t+1}/X_t \times 100$.

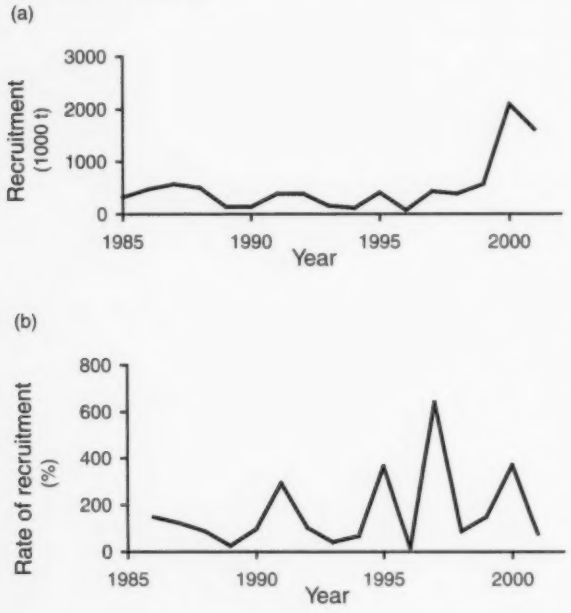

to the nursery grounds on the Cape West Coast has been investigated in numerous field, empirical, and modeling studies. All of these studies aimed at trying to understand and predict the observed large fluctuations of anchovy recruits (Fig. 2). The predominant role of environmental factors on the early life stages has long been noticed (Hutchings 1992).

Multiple factors affect the early life stages of South African anchovy in the spawning, transport, and nursery areas in which environmental constraints to larval survival appear to be different (Hutchings et al. 1998). For anchovy in the Benguela, we will focus on two environmental factors known to have direct effects on eggs or larvae and regarded as surrogates for ecological factors that are strongly linked to environmental fluctuations (Hutchings et al. 1998). These are wind (direction, intensity, and frequency, all related to transport and enrichment processes) and temperature (related to spawner biomass, development, and growth, food availability, and spawning intensity). These two factors have many biological and ecological consequences that can be tested for fish larval survival.

In the southern Benguela, strong southerly winds produce stronger upwelling, currents, and offshore transport, resulting in an increased loss of eggs and larvae from the coastal upwelling system (Shannon et al. 1992; Huggett et al. 1998). Empirical studies revealed a strong negative correlation between southeasterly winds and anchovy recruitment success in the transport area off the east coast, indicating that such winds were not conducive to good recruitment during the 1980s and 1990s (Hutchings et al. 1998). Strong southeasterly winds (Boyd et al. 1998) and advective losses as a result of an Agulhas ring (Duncombe-Rae et al. 1992) could account for the reduced recruitment in 1988–1989 (see Fig. 2). Losses during the transport phase may be significant (Hutchings et al. 1998), and the extension offshore of the 16°C isotherm has been used as a proxy for evaluating transport success (Cochrane and Hutchings 1995).

Incubated eggs of anchovy survived experimentally a temperature of 11–31°C, but the minimal temperature for anchovy normal development in Cape waters was found to be above 14°C (King et al. 1978). The optimum temperature range for spawning has been determined to be between 16 and 19°C in the upper mixed layers (Anders 1965). This temperature range also constitutes a suitable spawning habitat for adult fish, associated with optimal production of large copepods on the western Agulhas Bank (Richardson et al. 1998). High gonad atresia was also observed in anchovy found in cool, inshore waters in January 1994 (Hutchings et al. 1998).

These studies were dedicated to identifying key environmental factors to explain distribution or patterns of abundance of pelagic fish. The impacts of spawning distributions and advection processes on larval survival were modeled by Shannon (1998).

In our study, we would like to extend this exploration to better understand the selective pressures imposed by the environment on spawning dynamics. Therefore, we implement a model that simulates the reproductive strategy in relation to the physical environment.

An evolutionary reproductive strategy to relate spawning and the environment in the Benguela

Pelagic fishes are thought to have developed opportunistic reproductive strategies, i.e., they spawn when environmental conditions are favourable. This seems a tautological definition, as one might question what "favourable" means at an individual level. From an ecological point of view, favourable could mean a favourable food environment for the larvae, a suitable temperature for egg development, or a suitable retention area to avoid losses, factors that were discussed previously. From an evolutionary point of view, it means not only life history survival, survival from birth to adulthood, but also survival over the generations that face environmental changes or evolutionary success (Michod 1999). Using evolutionary and ecological arguments, Cury (1994) proposed an extended homing strategy within which homing is viewed as part of a continuum of reproductive strategies, all relying on imprinting. This Darwinian way of looking at the "imprinting" mechanism provides, at the individual level, a basic mechanism for coupling adult fish reproductive strategy to the surrounding environment (Le Page and Cury 1997). Using the concept of "extended homing", Cury (1994) generalized this reproductive strategy for marine fish species (in particular pelagic fish) and its importance for the viability of self-sustaining populations.

In the Benguela, if location, timing, and duration of anchovy spawning have a strong ecological meaning, then one may consider that spawning in another place at a different time is detrimental and has been counterselected by one or more environmental factors. Recurrent spawning patterns for anchovy are observed in restricted areas (Hutchings et al. 1998) and their apparent slight spatial changes do not appear to be related to environmental changes (van der Lingen et al. 2001). Therefore, one may consider that individuals "home" to specific locations at particular times to spawn. This re-

© 2002 NRC Canada

Fig. 3. Hydrodynamic model. Examples of model outputs: sea surface temperature (°C) on 1 November for year 5 (left) and year 7 (right). Notice the presence of cold water owing to upwelling along the west coast, the plumes and filaments extending offshore, the mesoscale eddies, and the warm Agulhas Current flowing along the eastern Agulhas Bank. Also notice the differences between the two years regarding shapes of the eddies appearing in the central part of the area and the jet intensity.

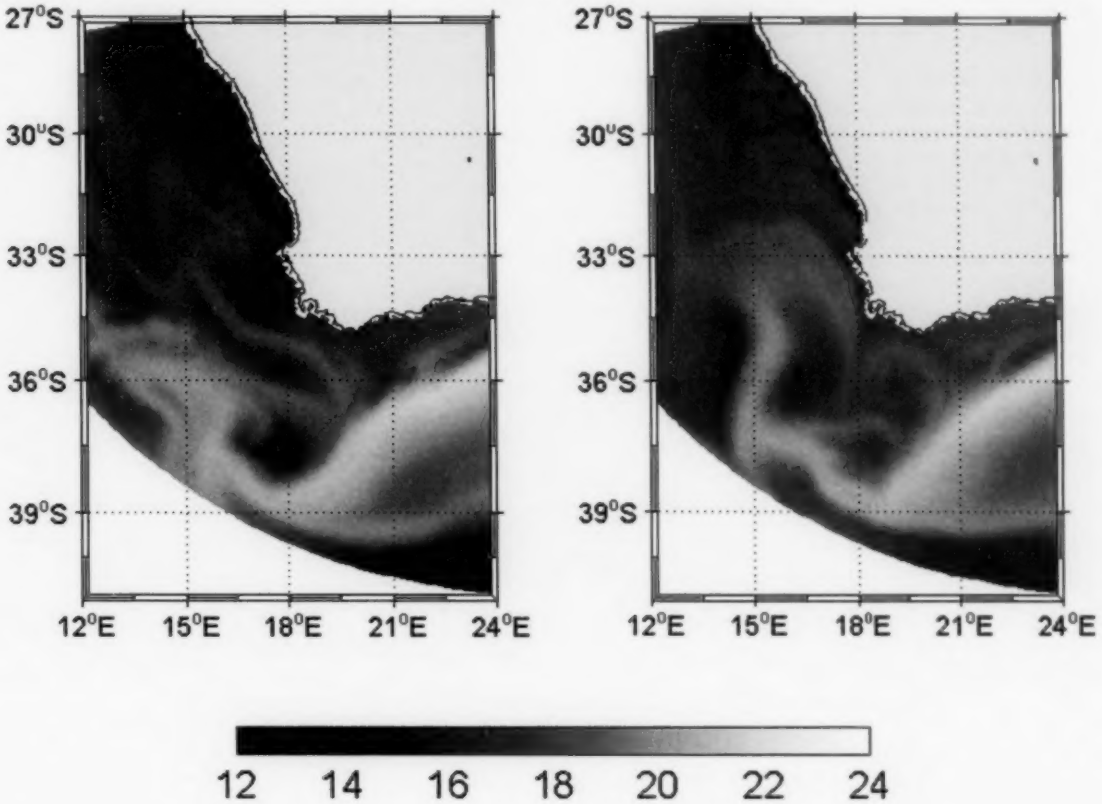

mains a hypothesis, as we do not know what determines the spawning process at the individual level. However, we consider it useful for assigning spatial and temporal coordinates in a dynamical way to spawning individuals.

Considering this reproductive strategy in the present modeling framework can help to identify the environmental factors that determine the timing and location of the observed spawning and its renewal through successive generations. It is thus necessary to integrate this reproductive strategy into a realistic and dynamical environment.

Materials and methods

A realistic three-dimensional hydrodynamic model is coupled with an IBM by considering an evolutionary-based reproductive strategy for adult fish and passive transport for early life stages. It is implemented to understand the spawning strategy of anchovy in the southern Benguela upwelling system. The evolutionary success of spawning is quantified when patterns at the population level emerge after many generations from constraints at the individual level through a selective process.

A hydrodynamic model to simulate a realistic and dynamical environment

A numerical oceanic model of the dynamics in the southern Benguela has been set up in the coastal area between 28 and 40°S and 10 and 26°E (Penven 2000; Penven et al. 2001*b*). It relies on the regional ocean modeling system (ROMS) developed at the State University of Rutgers (New Brunswick, N.J.) and at the University of California at Los Angeles. It resolves the hydrostatic primitive equations with a variable free surface. A specific open-boundary scheme has been developed for long-term integration of the model on limited size regional domains (Marchesiello et al. 2001; Penven et al. 2001*a*). The model uses a horizontal curvilinear coordinates system and a variable vertical coordinates system that is able to keep a high vertical resolution in the boundary layers (e.g., at the surface of the ocean). The horizontal grid is pie-shaped to follow the southwestern corner of the African continent (Fig. 3). The horizontal resolution ranges linearly from 9 km at the coast to 16 km offshore. Twenty vertical levels preserve a high vertical resolution near the surface. These modeling choices (spatial extension, spatial resolution, and time resolution) have been made to generate mesoscale circulation features important for the transport and retention of pelagic fish (Bakun 1996).

© 2002 NRC Canada

The model is integrated for 10 years, using yearly climatologic data for the surface-forcing and open-boundary conditions. After a spinup of 2 years, the model results are stored at 2-day intervals to provide a high temporal sampling for the IBM. The model develops an important mesoscale activity produced by intrinsic instability processes of the ocean dynamics (Penven 2000; Penven et al. 2001*a*): it provides realistic patterns in the Benguela system like the coastal upwelling, coastal jet, eddies, filaments, and plumes extending from the major capes (Fig. 3). It also generates a realistic circulation in the Agulhas Current area (Penven 2000). Despite being forced by the same averaged conditions every year, the model generates an important year-to-year variability (Fig. 3). For example, simulated temperature depth distributions exhibit interannual variability comparable with the one observed in several points of measurements on the shelf of the Agulhas Current. It affects, both in time and space, the hydrodynamic structures (jets, filaments, and eddies) of interest for eggs or larvae transport.

An evolutionary IBM: a reproductive strategy evolving in a physical environment under different selective constraints

An IBM is a bottom-up approach that starts with the parts (i.e., individuals) of a system (i.e., population) and then tries to understand how the properties of a system emerge from the interactions between the parts (Grimm 1999). An evolutionary approach attempts to express how patterns at the population level emerge from constraints at the individual level through a Darwinian selective process (i.e., relative selective advantages).

In our model, individuals are particles released and advected in the currents of the hydrodynamic model. They can be considered eggs, larvae, or juveniles. They have a memory that encodes their spawning strategy, i.e., date and location. Individuals are subject to a set of constraints under which they survive or die. The surviving individuals are able to spawn again at the place where they were born and in the same time period. These dynamics generate a new population. This algorithm can be viewed as a simple genetic algorithm (Mitchell and Taylor 1999) where the "genotype" is an encoded spawning strategy and the "fitness" corresponds to the recruitment success. This is an elementary IBM: the individuals only differ by their spawning strategy, date, and location.

The algorithm for the IBM is implemented as follows. (*i*) Choose a set of selective environmental constraints for survival, expressed in terms of offshore advection, sensitivity to temperature, reaching of the recruitment area, etc. (*ii*) Create a population of N_I individuals with random spawning strategies. (*iii*) Repeat during N_G generations (each generation equals 1 year): (*a*) randomly choose one year among the seven years of the three-dimensional hydrodynamic model output, (*b*) allow the individuals to be passively advected in the currents and temperature fields corresponding to that particular year during 60 days after their birth date, (*c*) observe which ones have fulfilled the constraints, (*d*) create a new population of N_I individuals by allowing successful individuals to spawn eggs in the neighbourhood of their natal spawning area (around N_K km) at the same date of their birth (within plus or minus N_D days) (the number of eggs per recruit is then N_I/S, where S is the number of successful individuals; this ensures a constant population level), and (*e*) visualize the spawning pattern after each generation. (*iv*) Plot the results of the simulation: the spatial distribution of spawning locations at generation 60 is plotted. The recruitment index during the first N_G generations is defined as the number of eggs and larvae that survived under the chosen constraints.

Assumptions

The assumptions of the evolutionary IBM are as follows. (*i*) The output of the three-dimensional hydrodynamic model provides realistic dynamics of the environment: they present sufficient seasonal and interannual variability to test the environmental changes experienced by eggs and larvae. (*ii*) We can consider eggs and larvae to be analogous to passive drifters (particle tracking without diffusion) in this virtual environment; other abilities (swimming) and biological processes (feeding and predation) are assumed to be negligible for recruitment success. (*iii*) An extended homing mechanism drives the spawning process: this implies that successful adults try to spawn in the same place and at the same time of the year in which they were born.

Design of the simulations

The present model is aimed at illustrating how a combination of environmental constraints can explain recruitment variability. The following procedure ensures that hypotheses, model population dynamics, and model results are the following. (*i*) Observable: visualization of the hypotheses, of the different dynamics, and of the results is an important outcome of the approach; hypotheses, selective constraints, and the resulting dynamics are observable and easily interpreted from graphical displays and outputs. (*ii*) Comparable: we start by enunciating a null hypothesis; this allows comparison of any simulation using environmental selective constraints with a null hypothesis where no selective constraints are imposed. (*iii*) Testable: we follow a pattern-oriented approach (Grimm et al. 1996; Grimm 1999). First, a set of observed patterns is defined at the global level. Subsequently, alternative models are compared according to their ability to produce matching patterns. This constitutes a powerful way to infer the mechanisms by which individuals respond to their environment. (*iv*) Believable: we follow a KISS principle (keep it simple stupid) after A. Okubo (Slobodkin 1999), adopting simple and tractable rules and hypotheses. This is the way to compare and learn from hypotheses and simulations to make a model understandable and believable.

We have chosen two specific patterns derived from the field surveys to be compared with the output of the simulations: spawning pattern and recruitment pattern. The spawning pattern has a spatial component that is compared with the observed egg distribution (Fig. 1*a*). It also has a temporal component, i.e., spawning dates. Simulated spawning patterns are compared with the results of surveys that indicate summer (i.e., November–December) as the most probable period for spawning. The number of surviving eggs or larvae at the end of each generation can be considered as a recruitment-like pattern that is compared with the observed recruitment time series (Fig. 2*b*).

© 2002 NRC Canada

Fig. 4. Example of a simulation showing how anchovy spawning patterns emerge through time. Each dot represents the spawning location of an individual. The colour indicates the month of spawning according to the legend on the figure. The solid area corresponds to our definition of the nursery grounds. In some of the forthcoming simulations, eggs and larvae are considered to be recruited when they reach this area. (*a*) At time = 0, eggs are randomly spread over the grid; (*b*) spawning pattern after two generations; (*c*) spawning pattern after five generations; (*d*) spawning pattern after 60 generations.

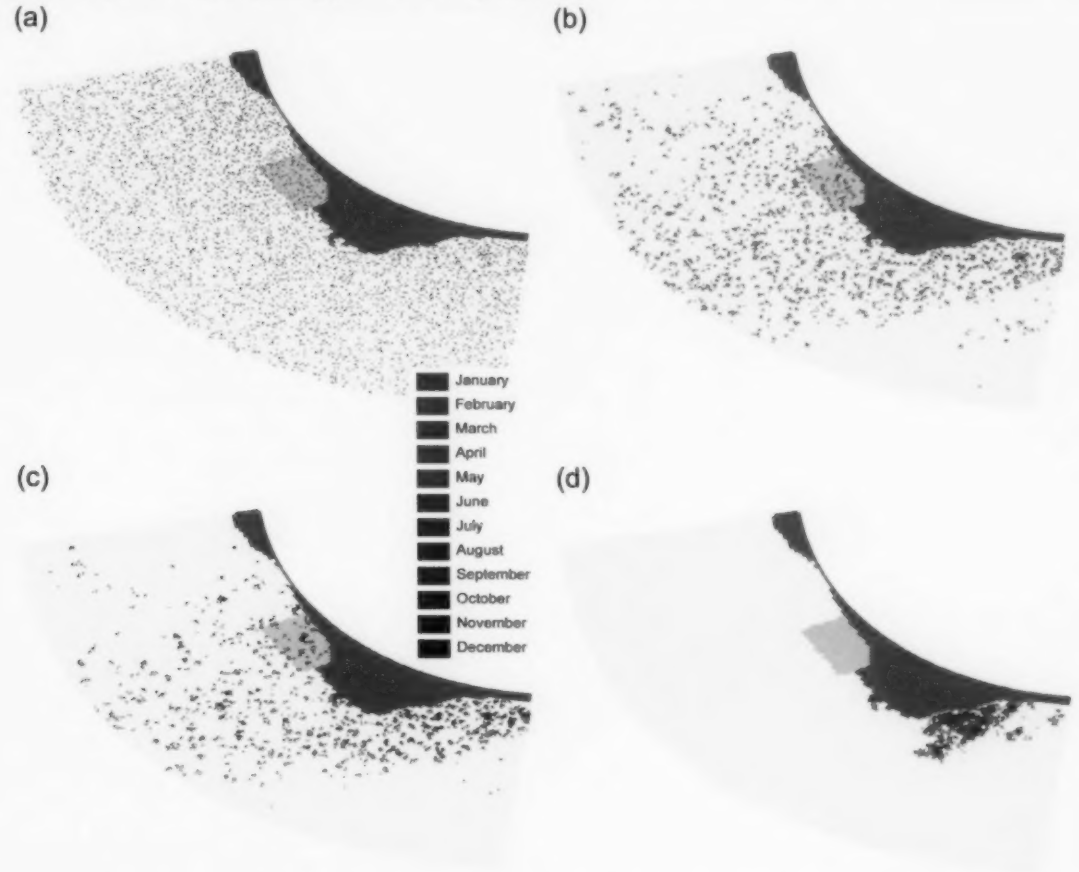

This approach results in a series of experiments. Each one simulates dynamics associated with one or a set of environmental constraints that have been previously recognized to have an effect on recruitment. Tested environmental constraints are as follows: (*i*) no environmental constraint: the null hypothesis, (*ii*) avoiding offshore advection, (*iii*) avoiding offshore advection and being successively transported, (*iv*) avoiding offshore advection and staying in temperatures greater than 14°C, (*v*) avoiding offshore advection, staying in temperatures greater than 14°C, and being successively transported, and (*vi*) avoiding offshore advection, staying in temperatures between 16 and 19°C, and being successively transported.

Results

Assigning values to the parameters

As for any genetic algorithm, a compromise has to be found between the size of population, the selective pressure, and the number of generations according to limitations imposed by computer time for simulations. After many preliminary attempts, we have chosen the following for use in this study: N_I (number of individuals) = 5000, N_K (distance from natal and spawning locations) < 5 km, N_D (difference between birth and spawning anniversary dates) < 10 days, and N_G (number of generations) = 60. It appears that the resulting patterns do not change substantially after 60 generations. Using this algorithm, we are able to observe how patterns emerge spatially and temporally under chosen selective constraints (Fig. 4).

Checking the stability of the algorithm

There are three sources of stochasticity in the algorithm: (*i*) the random initial distribution of spawners in time and space, (*ii*) at each generation, the random choice of a particular year of the output of the hydrodynamic model, and (*iii*) the spawning positions randomly chosen close to the natal site. To deal with this stochasticity and test the robustness

© 2002 NRC Canada

Fig. 5. Resulting anchovy spawning patterns for four trials of simulation 6: individuals do not reproduce when advected offshore, experience water temperatures below 14°C, or do not reach the nursery area after 30 and before 60 days.

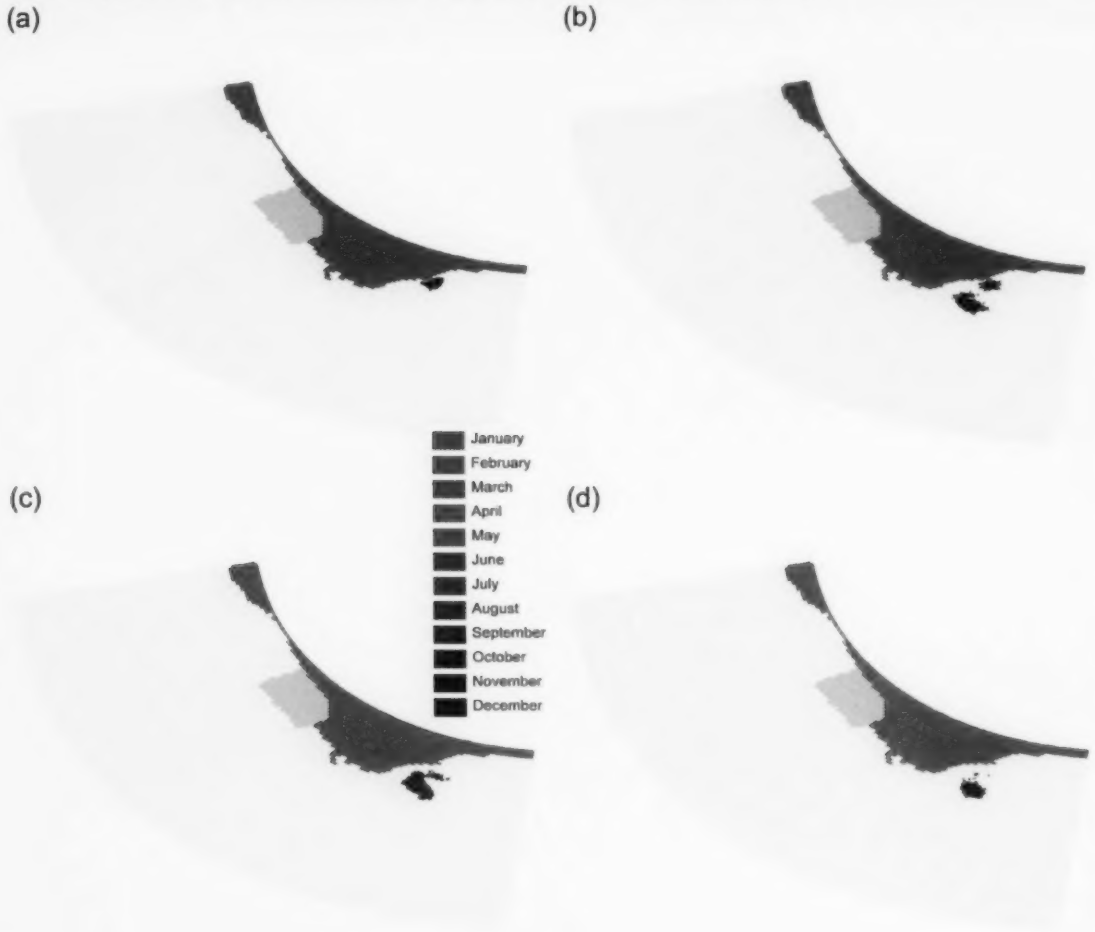

of the resulting patterns, we proceed for each simulation with four independent runs of the algorithm. Different patterns can emerge from the same set of constraints (Fig. 5). However, most emerging patterns appear to be robust to stochasticity, as indicated by the four replicates that were performed for each simulation. We only present one output of each simulation in forthcoming figures of the spawning patterns.

Simulation 1. Null hypothesis: no environmental constraint on larval survival

In this first simulation, we consider that the environment has no selective effects on egg or larval survival. There are no constraints on advection or temperature and no criteria for recruitment success. The probability of being able to spawn is 50%. Spawning patterns are "structured" by homing behaviour, but no realistic spawning patterns emerged (see Fig. 6*a*). This special situation of "genetic drift" illustrates that a neutral Darwinian process can create patterns. The recruitment index is almost constant at the defined probability level of 50% (Fig. 7*a*).

Simulation 2. Where should anchovy spawn to avoid offshore advection?

This simulation explores where spawning should occur to avoid offshore advection. Individuals do not reproduce when advected offshore (i.e., distance from the coast greater than 400 km). No other criterion is considered here as an environmental constraint. The probability of being able to spawn is 75% for individual surviving to reproductive age.

This simulation (see Fig. 6*b*) gives a realistic spatial spawning pattern in comparison with the observed one (Fig. 1*a*). However, the simulation results in spawning activity during winter (May–July), which is not realistic. Moreover, the recruitment pattern (Fig. 7*b*) appears to be much less variable than the observed one (Fig. 2*b*). During the first several years, the recruitment index steadily increases and finally reaches a plateau with a value of about 70% (Fig. 7*b*).

© 2002 NRC Canada

Fig. 6. Simulated anchovy spawning patterns produced by the evolutionary model considering the following environmental constraints: (*a*) simulation 1: null hypothesis where individuals that reproduce are randomly chosen; (*b*) simulation 2: individuals do not reproduce when advected offshore; (*c*) simulation 3: individuals do not reproduce when advected offshore or do not reach the nursery area after 30 and before 60 days; (*d*) simulation 4: individuals do not reproduce when advected offshore or experience water temperatures below 14°C; (*e*) simulation 5: individuals do not reproduce when advected offshore, experience water temperatures below 14°C, or do not reach the nursery area after 30 and before 60 days; (*f*) simulation 6: individuals do not reproduce when advected offshore, experience water temperatures below 14°C, or do not reach the nursery area after 30 and before 60 days.

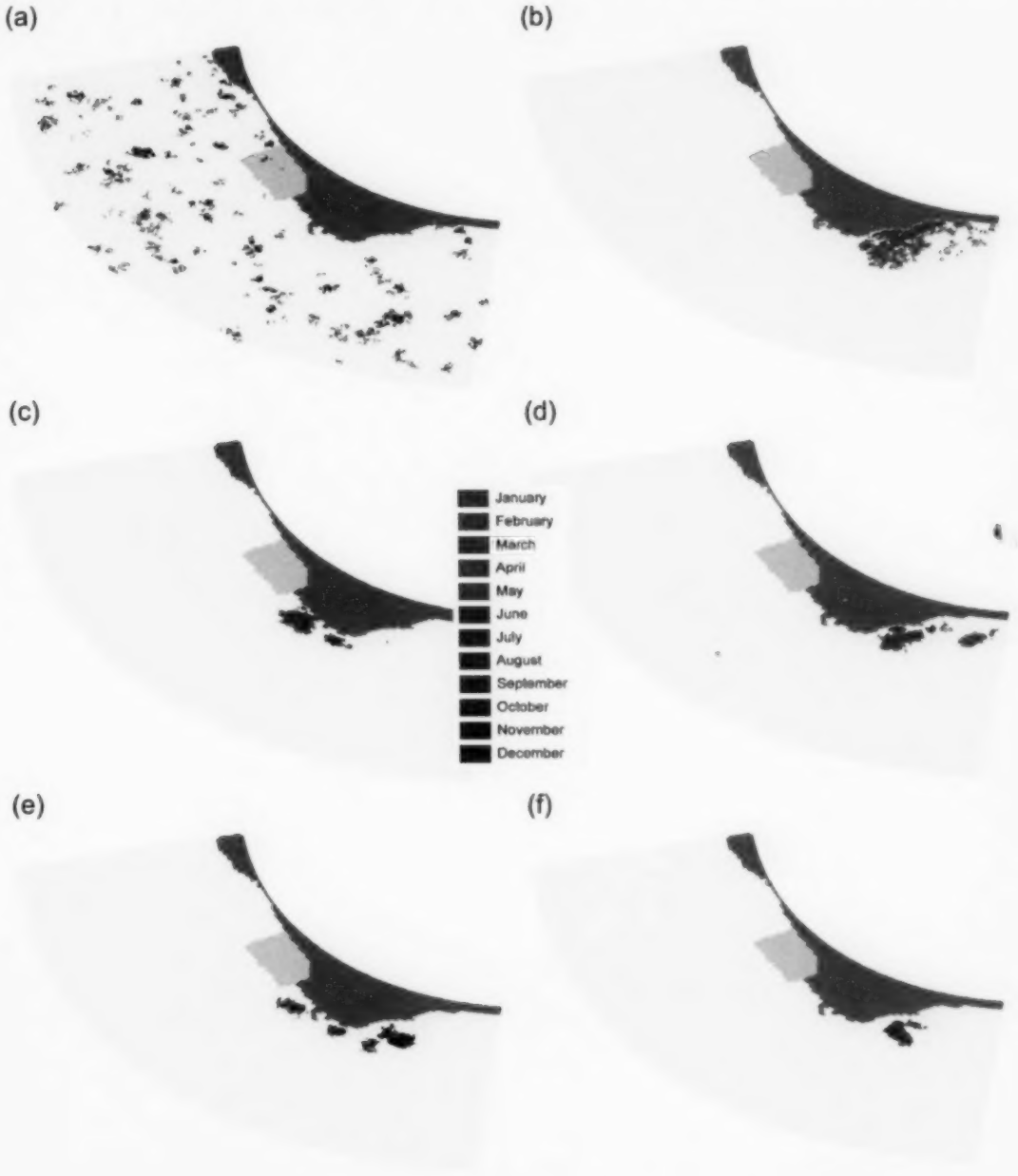

© 2002 NRC Canada

Fig. 7. Simulated anchovy recruitment variability measured as the number of surviving eggs and larvae at the end of each generation: (*a*) simulation 1; (*b*) simulation 2; (*c*) simulation 3; (*d*) simulation 4; (*e*) simulation 5; (*f*) simulation 6.

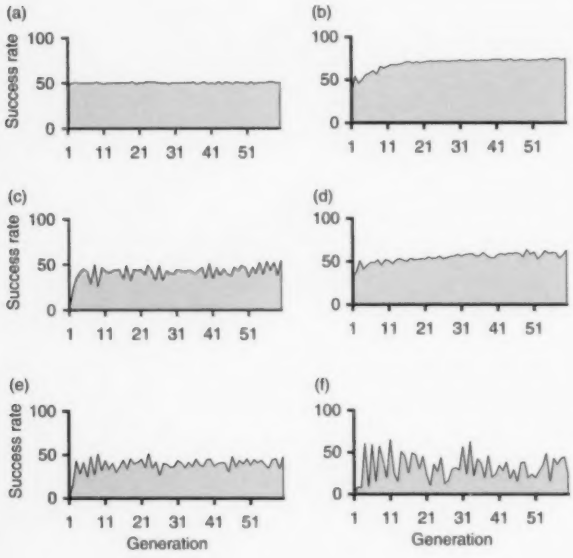

In fact, the population progressively adapts itself to environmental constraints through generations and finally finds an appropriate spawning location under this selective constraint. Thus, it seems that the evolutionary process results from an effective trial-and-error strategy at the population level.

Simulation 3. Where should anchovy spawn to avoid offshore advection and to reach the nursery area?

In this simulation, the individuals are considered successful when they avoid offshore advection and when they reach the nursery area between 30 and 60 days. If those two conditions are fulfilled, then they become adults and reproduce again at the same location and in the same time period during which they were produced.

The resulting spawning patterns are not stable. According to the different replicates, they correspond to a small confined area located off Cape Point for replicates 1, 2, and 3 (Fig. 6*c*) or in the nursery area in St. Helena Bay for replicate 4. In addition, in all four replicates, some spawning occurs in winter. The fourth replicate suggests a possible persistent spawning area within the nursery area, which is something that has not been observed in field surveys (Fig. 1*a*). As stressed in the Introduction, spawning and nursery areas of anchovy are distinct and remote from one another in the Benguela. The discrepancy between the evolutionary model and the observed pattern tells us that the environmental constraint "to avoid offshore advection" should not be the only one that controls anchovy spawning. Another factor must also be important, for example, temperature, which is explored in simulation 4.

Simulated recruitment shows quite high variability, but variation (standard deviation/mean) is low when compared with the observed recruitment. In this simulation, the population progressively detects a spawning habitat that is subject to high environmental variability. This is detrimental to recruitment, which varies from 30 to 65% (Fig. 7*c*). In this case, the population finds a spawning pattern that ensures its persistence through time. However, it is not then able to detect any environmental patterns that will improve its fitness, as a trial and error strategy is no longer effective.

Simulation 4. Where should anchovy spawn to avoid offshore advection and cool waters (<14°C)?

In simulation 4, individuals do not reproduce when advected offshore or encountering a temperature below 14°C. Then the probability of spawning for an individual that is still alive after 30 days is 0.75.

The resulting spawning pattern appears to be realistic (see Fig. 6*d*) according to the observed egg distribution (Fig. 1*a*). Two groups that spawn at two different time periods can be identified (Fig. 7*d*): on the eastern Agulhas Bank during January–February and on the western Agulhas Bank during November–December. This corroborates the observed temporal pattern of spawning for anchovy in the Benguela (Hutchings et al. 1998).

The resulting pattern of recruitment variability shows a slow but progressive convergence to optimal conditions (Fig. 7*d*). This observed pattern of recruitment variability is different from the observed one, which appears more erratic (Fig. 2*b*). Here again, it seems that the evolutionary process results from an effective trial-and-error strategy at the population level.

Simulation 5. Where should anchovy spawn to avoid offshore advection and cool waters (<14°C) and to reach the nursery area?

To the constraints of simulation 4, we add now the constraint of reaching the nursery area within 30–60 days (see Fig. 6*e*). This simulation appears quite unstable, as replicates produce slightly different patterns. As a common feature, the resulting spawning pattern is a set of confined areas off the Cape peninsula. For some of these areas, the corresponding spawning dates are in spring (September) and autumn (April), which is not in agreement with field studies (van der Lingen 2001). The resulting pattern of recruitment variability exhibits erratic fluctuations (Fig. 7*e*). Because of environmental variability, recruitment is highly variable, but here again, variation is low when compared with the observed recruitment.

Simulation 6. Where should anchovy spawn to avoid offshore advection, to stay in waters between 16 and 19°C, and to reach the nursery area?

Here, we consider a small interval of temperatures (16–19°C) according to ecological arguments that were discussed in the Introduction and are related to food availability on the Agulhas Bank. Offshore advection and being able to reach the nursery area are additional constraints.

© 2002 NRC Canada

Table 1. Summary of the results of the six simulations for anchovy regarding their stability and their fit to observed data.

	Environmental constraints: eggs and larvae randomly die when	Stability of convergence of the algorithm	Simulated vs. observed spawning pattern	Simulated vs. observed recruitment pattern
1	there are no environmental constraints		Grounds: no fit Dates: no fit	No fit
2	they are advected offshore	High	Grounds: good fit Dates: poor fit	No fit
3	they are advected offshore they do not reach the nursery area after 30 and before 60 days	Low	Grounds: no fit Dates: no fit	Poor fit
4	they are advected offshore they experience water temperatures below 14°C	High	Grounds: good fit Dates: good fit	Poor fit
5	they are advected offshore they experience water temperatures below 14°C they do not reach the nursery area after 30 and before 60 days	Medium	Grounds: poor fit Dates: good fit	Poor fit
6	they are advected offshore they experience water temperatures between 16 and 19°C they do not reach the nursery area after 30 and before 60 days	Medium	Grounds: poor fit Dates: good fit	Good fit

Table 2. Anchovy recruitment strength (percentage of successfully transported individuals) according to the different hydrodynamic years considered in the simulations.

Year	Simulation 1	Simulation 2	Simulation 3	Simulation 4	Simulation 5	Simulation 6
3	49	70	42	57	43	13
4	50	63	42	54	38	34
5	49	71	37	53	41	32
6	49	71	38	53	31	33
7	49	72	43	56	37	55
8	50	67	35	54	44	26
9	49	64	43	53	39	30

The resulting spawning pattern that emerges from these selective constraints is a small area located in the central Agulhas Bank around mid-December (Fig. 6*f*). This spawning pattern has not been extensively sampled during this time period in field studies. Therefore, it would be interesting to explore if this pattern is real.

Associated with this pattern is high recruitment variability, which can be compared with the observed one (Fig. 7*f*). When compared with simulation 2, this simulation does not constitute an optimal spawning area, as recruitment variability is always very high (Fig. 7*f*). However, this may be viewed as a persistent spawning area, as the population maintains itself through time (for every generation, recruitment is good enough to ensure the survival of the population).

Summary of the results

We summarize results of the six simulations according to their characteristics in terms of stability and their ability to reproduce the observed spawning and recruitment patterns (Table 1). It appears that none of these simulations gives a "perfect" fit to both the spawning and recruitment patterns observed in the field. Considering avoidance of offshore advection and cold waters results in fairly realistic spawning patterns in time and space. Attempting to reach the recruitment area results in highly variable recruitment, similar to the observed one.

We compute for each simulation the mean recruitment success according to the hydrodynamic year (Table 2). It appears that recruitment strength depends on the hydrodynamic year when taking into account the constraint of reaching the nursery area (simulations 3, 5, and 6), especially when a temperature constraint is added (simulations 5 and 6).

Discussion

Tools from individual-based modeling provide new and refreshing views in recruitment studies (Rose et al. 1999). For example, Hermann et al. (1996) have considered individuals advected in the currents of an oceanic model and differing by many biological and ecological attributes. We have used concepts from evolutionary ecology, which are efficient for considering the adaptation of organisms to their environment (Frank and Leggett 1994; Fox et al. 2001), and have carried out an IBM with very simple individuals, but in an evolutionary perspective.

The proposed evolutionary model, which is not predictive but exploratory in essence, illustrates how selective constraints can affect spawning and recruitment patterns. It is aimed at promoting transfer between two different scales:

© 2002 NRC Canada

the individual in its surrounding environment and the emerging spawning pattern of a pelagic fish in an upwelling area. We believe that this modeling experience can help to identify environmental factors important for fish recruitment and establish a hierarchy for these factors.

A hierarchy for the selective environmental constraints

The results, especially those from simulation 6, suggest some independence between two types of constraints, namely (*i*) avoiding offshore advection and cold waters, and (*ii*) being successfully transported to the nursery area. To survive, anchovy must satisfy the first set of constraints, which apparently drives their spawning behaviour, and then the recruitment success largely depends on the specific hydrodynamic features of the current year.

Concerning the nature of effective selective constraints, a paradox should be discussed when comparing results from simulations 2 and 3. Environmental constraint for simulation 2 is a subset of the constraints of simulation 3. In that case, as a result, one would expect to observe the resulting spawning pattern of simulation 3 to be found among the solutions obtained with simulation 2. This is not the case: adding one constraint to another drastically modifies the emerging pattern. Adding one environmental constraint means defining new viable spawning patterns, as it changes the hierarchy of the relative advantages of the spawning strategies. In other words, spawning location and timing result from specific interactions between environmental and ecological processes. Adding one selective constraint to another means changing the whole functional relationship between the environment and the ability of the species to evolve.

Identifying self-sustaining populations

As Lewontin (1983) noticed, "by its behaviour—its genetically determined use of habitats and resources—an animal largely defines the selective pressures to which it is subject". The choice of a spawning location has major consequences for recruitment success and evolution, as it defines the choice of the present and future habitats for the eggs and early life stages, and consequently, associated selective constraints. Simulated persistent spawning patterns can be viewed as virtual self-sustaining populations. Several of them were identified, and when related to observed spawning and recruitment patterns, some of them appeared to be more realistic than others. A simulated spawning pattern was found to match better the mean observed pattern when two selective environmental constraints were associated: a threshold temperature of 14°C, above which the development of early life stages is ensured, and the avoidance of offshore currents that constitute a loss of spawning products. Thus, two environmental constraints seem to have shaped the main reproductive pattern of anchovy in the southern Benguela. On the other hand, the recruitment variability is related to the constraint of reaching the nursery area and facing interannual environmental changes.

Systematic acoustic surveys have shown that from one year to another, observed spawning patterns exhibit recurrent patterns and also slow and consistent spatial changes. Thus, it appears that in recent years, more anchovies are spawning on the eastern Agulhas Bank (van der Lingen et al. 2001). The dynamics at the whole-population level can then be seen as the result of the dynamics of numerous self-sustaining subpopulations that react differently to given environmental conditions. Our modeling experiment can provide a framework for understanding changing spawning patterns. Observed spawning patterns might be viewed as a combination of several self-sustaining populations, like the ones emerging in simulations 4, 5, and 6. Thus, recognizing differences in spawning strategy (location and date) between individuals and considering their adaptation to environmental constraints may explain some diversity (i.e., coexistence of self-sustaining populations) and some population dynamics features. For certain years, in a certain environmental context, one or the other self-sustaining population is selected in a differential way, which will lead to varying strength in recruitment.

Self-sustaining populations have long been recognized in marine fish populations (Hjort 1914). Their importance for fish population dynamics and fisheries management is only recent (Sinclair 1997; Page et al. 1999). To recognize their importance emphasizes the need for promoting recruitment studies that will focus on spawning patterns and their spatial dynamics. According to Sinclair (1988), geographical differences in the retention of eggs and larval distribution areas are key processes in the regulation of fish abundance. However, temporal changes in spawning patterns are mostly seen as anecdotal, and the link between recruitment strength and spatial dynamics is rarely addressed. A recurrent topic in the fisheries literature is to question empirical relationships between recruitment and environmental indices that fail through time (Myers 1998). However, recognizing the heterogeneous character of fish populations could help to understand the changing nature of such relationships. Recognizing the diversity and coexistence of persistent spawning patterns can potentially have major consequences for recruitment studies and fish exploitation.

Our modeling experience can help to better understand the role of diversity for fish spawning dynamics. Recognizing diversity, the essence of life, as the basic principle for recruitment studies can also stimulate our imagination and provide new and refreshing views to old problems.

Acknowledgements

This work is a contribution to a joint South African – French program, which is associated with the IRD (Institut de Recherche pour le Développement) research unit IDYLE, the University of Cape Town, and the Marine and Coastal Management and which involves the IRD research unit GEODES. We especially thank Lynne Shannon and Penny Krohn for their help in correcting the manuscript. We thank Carl van der Lingen, Claude Roy, Larry Hutchings, Andy Bakun, Carolina Parada, and John Field for stimulating discussions. We also thank Pierre Fréon, Mike Sinclair, and the anonymous referees for numerous constructive comments.

References

Anders, A.S. 1965. Preliminary observations on anchovy spawning off the South African coast. S. Afr. Shipping News Fish. Ind. Rev. **20**: 103–107.

© 2002 NRC Canada

Bakun, A. 1996. Patterns in the ocean: ocean processes and marine population dynamics. University of California Sea Grant, San Diego, Calif., in cooperation with Centro de Investigaciones Biolgicas de Noroeste, La Paz, Baja California Sur, Mexico.

Barange, M., Hampton, I., and Roel, B.A. 1999. Trends in the abundance and distribution of anchovy and sardine on the South Africa continental shelf in the 1990s, deduced from acoustic surveys. S. Afr. J. Mar. Sci. **21**: 349–366.

Boisclair, D. 2001. Fish habitat modeling: from conceptual framework to functional tools. Can. J. Fish. Aquat. Sci. **58**: 1–9.

Boyd, A.J., Shannon, L.J., Schulein, F.H., and Taunton-Clark, J. 1998. Food, transport and anchovy recruitment in the southern Benguela upwelling system of South Africa. *In* From local to global changes in upwelling systems. *Edited by* M.H. Durand, P. Cury, R. Mendelssohn, C. Roy, A. Bakun, and D. Pauly. Orstom Editions, Paris. pp. 267–274.

Cochrane, K.L., and Hutchings, L. 1995. A structured approach to using biological and environmental parameters to forecast anchovy recruitment. Fish. Oceanogr. **4**: 102–127.

Cury, P. 1994. Obstinate nature: an ecology of individuals: thoughts on reproductive behavior and biodiversity. Can. J. Fish. Aquat. Sci. **51**: 1664–1673.

Cushing, D.H. 1996. Towards a science of recruitment in fish populations. *In* Excellence in ecology. Vol. 7. *Series Editor* O. Kinne. Ecology Institute, D21386 Oldendorf/Luhe, Germany.

Duncombe-Rae, C.M., Boyd, A., and Crawford, R.J.M. 1992. "Predation" of anchovy by an Agulhas ring: a possible contributory cause of the very poor year-class of 1989. *In* Benguela dynamics. *Edited by* S.C. Pillar, C.L. Moloney, A.I.L. Payne, and F.A. Shillington. S. Afr. J. Mar. Sci. **19**: 167–174.

Fox, C.W., Roff, D.A., and Fairbairn, D.J. 2001. Evolutionary ecology. Concepts and case studies. Oxford University Press, New York.

Frank, K.T., and Leggett, W.C. 1994. Fisheries ecology in the context of ecological and evolutionary theory. Annu. Rev. Ecol. Syst. **25**: 401–422.

Grimm, V. 1999. Ten years of individual-based modelling in ecology: what have we learned and what could we learn in the future? Ecol. Model. **115**: 129–148.

Grimm, V., Frank, K., Jelsch, F., Brandl, R., Uchmanski, J., and Wiseel, C. 1996. Pattern oriented modelling in population ecology. Sci. Total Environ. **183**. 151–166.

Hermann, A.J., Hinckley, S., Megrey, B.A., and Stabeno, P.J. 1996. Interannual variability of the early life history of walleye pollock near Shelikof Strait as inferred from a spatially explicit, individual-based model. Fish. Oceanogr. **5**: 39–57

Hinckley, S., Hermann, A.J., and Megrey, B. 1996. Development of a spatially explicit individual based model of marine fish early life history. Mar. Ecol. Prog. Ser. **139**: 47–68.

Hjort, J. 1914. Fluctuations in the great fisheries of northern Europe. Rapp. p.-v. Réun. Cons. Perm. Int. Explor. Mer, **20**: 1–228.

Huggett, J.A., Boyd, A.J., Hutchings, L., and Kemp, A.D. 1998. Weekly variability of clupeoid eggs and larvae in the Benguela jet current: implications for recruitment. *In* Benguela dynamics. *Edited by* S.C. Pillar, C.L. Moloney, A.I.L. Payne, and F.A. Shillington. S. Afr. J. Mar. Sci. **19**: 197–210.

Hutchings, L. 1992. Fish harvesting in a variable, productive environment—searching for rules or searching for exceptions? *In* Benguela trophic functioning. *Edited by* A.I.L. Payne, K.H. Brink, K.H. Mann, and R. Hilborn. S. Afr. J. Mar. Sci. **12**: 297–318.

Hutchings, L., Barange, M., Bloomer, S.F., Boyd, A.J., Crawford, R.J.M., Huggett, J.A., Kerstan, M., Korrubel, J.L., De Oliveira, J.A.A., Painting, S.J., Richardson, A.J., Shannon, L.J., Schulein, F.H., van der Lingen, C.D., and Verheye, H.M. 1998. Multiple factors affecting South African anchovy recruitment in the spawning, transport and nursery areas. *In* Benguela dynamics. *Edited by* S.C. Pillar, C.L. Moloney, A.I.L. Payne, and F.A. Shillington. S. Afr. J. Mar. Sci. **19**: 211–225.

King, D.P.F., Robertson, A.A., and Shelton, P.A. 1978. Laboratory observations on the early development of the anchovy *Engraulis capensis* from the Cape Peninsula. Fish. Bull. S. Afr. **10**: 37–45.

Le Page, C., and Cury, P. 1997. Population viability and spatial fish reproductive strategies in constant and changing environments: an individual-based modelling approach. Can. J. Fish. Aquat. Sci. **54**: 2235–2246.

Lewontin, R.C. 1983. The organism as the subject and object of evolution. Scientia, **118**: 65–82.

Marchesiello, P., McWilliams, J.C., and Shchepetkin A. 2001. Open boundary condition for long-term integration of regional oceanic models. Ocean Model. **3**: 1–20.

Michod, R.E. 1999. Darwinian dynamics. Evolutionary transitions in fitness and individuality. Princeton University Press, Princeton, N.J.

Mitchell, M., and Taylor, C. 1999. Evolutionary computation: an overview. Annu. Rev. Ecol. Syst. **20**: 593–616.

Myers, R.A. 1998. When do environment–recruitment correlations work? Rev. Fish Biol. Fish. **8**: 285–304.

Page, F.H., Sinclair, M., Naimie, C.E., Loder, L.W., Losier, R.J., Berrien, P.L., and Lough, R.G. 1999. Cod and haddock spawning on Georges Bank in relation to water residence times. Fish. Oceanogr. **8**: 212–226.

Penven, P. 2000. A numerical study of the Southern circulation with an application to fish recruitment. Ph.D. thesis, Université de Bretagne Occidentale, Brest, France.

Penven, P., Lutjeharms, J.R.E., Marchesiello, P., Roy, C., and Weeks, S.J. 2001*a*. Generation of cyclonic eddies by the Agulhas Current in the lee of the Agulhas Bank. Geophys. Res. Lett. **28**: 1055–1058.

Penven, P., Roy, C., Bundrit, G.B., Colin de Verdière, A., Fréon, P., Johnson, A.S., Lutjeharms, J.R.E., and Shillington, F.A. 2001*b*. A regional hydrodynamic model of upwelling in the Southern Benguela. S. Afr. J. Sci. **97**: 472–475.

Richardson, A.J., Mitchell-Innes, B.A., Fowler, J.L., Bloomer, S.F., Verheye, H.M., Field, J.G., Hutchings, L., and Painting, S.J. 1998. The effect of sea temperature and food availability on the spawning success of cape anchovy *Engraulis capensis* in the southern Benguela. *In* Benguela dynamics. *Edited by* S.C. Pillar, C.L. Moloney, A.I.L. Payne, and F.A. Shillington. S. Afr. J. Mar. Sci. **19**: 275–290.

Rose, K.A., Cowan, J.H., Jr., Clark, M.E., Houde, E.D., and Wang, S.B. 1999. An individual-based model of bay anchovy population dynamics in the mesohaline region of Chesapeake Bay. Mar. Ecol. Prog. Ser. **185**: 113–132.

Roy, C., Cury, P., and Kifani, S. 1992. Pelagic fish recruitment success and reproductive strategy in upwelling areas: environmental compromises. *In* Benguela trophic functioning. *Edited by* A.I.L. Payne, K.H. Brink, K.H. Mann, and R. Hilborn. S. Afr. J. Mar. Sci. **12**: 135–146.

Shannon, L. 1998. Modelling environmental effects on the early life history of the South African anchovy and sardine: a comparative approach. *In* Benguela dynamics. *Edited by* S.C. Pillar, C.L. Moloney, A.I.L. Payne, and F.A. Shillington. S. Afr. J. Mar. Sci. **19**: 291–304.

Shannon, L.V., Crawford, R.J.M., Pollock, D.E., Hutchings, L., Boyd, A.J., Taunton-Clark, J., Badenhorst, A., Melville-Smith, R., Augustin, C.J., Cochrane, K.L., Hampton, I., Nelson, G., Japp, T.W., and Tarr, R.J.Q. 1992. The 1980s—a decade of

© 2002 NRC Canada

change in the Benguela ecosystem. *In* Benguela trophic functioning. *Edited by* A.I.L. Payne, K.H. Brink, K.H. Mann, and R. Hilborn. S. Afr. J. Mar. Sci. **12**: 271–296.

Sinclair, M. 1988. Marine populations: an essay on population regulation and speciation. Washington Sea Grant Program, University of Washington Press, Seattle, Wash.

Sinclair, M. 1997. Prologue. Recruitment in fish populations: the paradigm shift generated by ICES Committee A. *In* Early life history and recruitment in fish populations. *Edited by* R.C. Chambers and E.A. Trippel. Chapman and Hall, London. pp. 1–27.

Slobodkin, L.B. 1999. Akira Okubo and the theory of blooms. Oceanography, **12**: 9–14.

van der Lingen, C.D., Hutchings, L., Merkle, D., van der Westhuizen, J.J., and Nelson, G. 2001. Comparative spawning habitats of anchovy (*Engraulis capensis*) and sardine (*Sardinops sagax*) in the Southern Benguela upwelling ecosystem. *In* Spatial processes and management of marine populations. *Edited by* G.H. Kruse, N. Bez, T. Booth, M. Dorn, S. Hills, R. Lipcius, D. Pelletier, C. Roy, S. Smith, and D. Witherell. University of Alaska Sea Grant, AK-SG-00-04, Fairbanks, Alaska.

Wyatt, T., Cushing, D.H., and Junquera, S. 1991. Stock distinctions and evolution of European sardine. *In* Long term variability of pelagic fish population and their environment. *Edited by* T. Kawazaki, S. Tanaka, Y. Toba, and A. Taniguchi. Pergamon Press, Oxford. pp. 229–238.

© 2002 NRC Canada

ERRATUM

Erratum: Otolith sulfur isotope method to reconstruct salmon (*Oncorhynchus tshawytscha*) life history

Peter K. Weber, Ian D. Hutcheon, Kevin D. McKeegan, and B. Lynn Ingram

Ref: Can. J. Fish. Aquat. Sci. **59**: 587–591 (2002).

On p. 590, in Fig. 3, the scale should read Distance from centre (μm).

Accepted 30 May 2002. Published on the NRC Research Press Web site at http://cjfas.nrc.ca on 9 July 2002.
J16683E

P.K. Weber.[1] Department of Geography, University of California, Berkeley, CA 94720, U.S.A.
I.D. Hutcheon. Analytical & Nuclear Chemistry Division, Lawrence Livermore National Laboratory, Livermore, CA 94551, U.S.A.
K.D. McKeegan. Department of Earth and Space Sciences, University of California, Los Angeles, CA 90095, U.S.A.
B.L. Ingram. Department of Earth and Planetary Science, University of California, Berkeley, CA 94720, U.S.A.

[1]Corresponding author (email: pweber@socrates.berkeley.edu).

 DOI: 10.1139/F02-901 © 2002 NRC Canada

The Canadian Conference for Fisheries Research

Ottawa, Ontario, Canada
2–5 January 2003

Where

Westin Hotel
11 Colonel By Drive, Ottawa, ON K1N 9H4
Telephone: 613-560-7000 or 800-WESTIN-1

Themes

1. Protecting Canada's aquatic resources (CCFFR/SCL)
2. Impact of invasive species (CCFFR/SCL)
3. Impacts of multiple stressor interactions on aquatic ecosystems (CCFFR/SCL)
4. Studies of aquatic biodiversity at a landscape scale (CCFFR)
5. Improvements in sampling methods (CCFFR)
6. Percid biology in a changing environment (CCFFR)

Call for papers

Abstracts in electronic form must be submitted to the program chair (jgunn@laurentian.nickel.ca) by 15 September 2002 (at the latest).

Funding

Graduate students may apply to the Clemens-Rigler Travel Fund.

Web site

For further information on the conference, registration details, program schedules, and updates, visit the CCFFR Web site (http://www. phys.ocean.dal.ca/ccffr/).

Note

The deadline for the special rate at the hotel is 3 December 2002. Early submission of abstract/poster for acceptance will ensure adequate time for hotel booking. To avoid CCFFR and SCL being charged an extra service fee, please plan to stay at the Westin Hotel while attending the conference.

La Conférences canadienne sur la recherche des pêches

Ottawa, Ontario, Canada
2 au 5 janvier 2003

Endroit

Westin Hotel
11 Colonel By Drive, Ottawa, ON K1N 9H4
Téléphone : 613-560-7000 ou 800-WESTIN-1

Thèmes

1. La protection des resources aquatiques (CCRP/SCL)
2. L'impacte des espèces non indigènes (CCRP/SCL)
3. L'impacte des stresses muliples sur les systèmes aquatiques (CCRP/SCL)
4. L'étude de la biodiversité aquatique au niveau du paysage (CCRP)
5. L'amélioration des méthodes d'échantillonege (CCRP)
6. La biologie des *Percidae* par rapport aux changements environmentaux (CCRP)

Appel pour contributions

Les résumés en format électronique doivent êtres soumis au directeur du programme (jgunn@laurentian.nickel.ca) par le 15 septembre 2002 (au dernier).

Financement

Les élèves aux études supérieures peuvent faire une demande de financement auprès des bourses de voyage Clemens-Rigler.

Site web

Pour obtenir de plus amples renseignements sur la conférence, l'inscription, l'horaire et les mises à jour, veuillez consulter le site Web de la CCRP (http://www.phys.ocean.dal.ca/ccffr/).

Nota

La date limite pour le taux spécial à l'hôtel est le 3 décembre 2002. Si l'abstrait / l'affiche est soumis à temps (avant le 15 septembre), et accepté, vous pourrez réserver une chambre à l'hôtel avant la date limite. Pour éviter que la CCRP et la SCL soient obligé de débourser des frais des services additionnels, essayez de réserver vos chambres à l'hôtel Westin.

Elizabeth N. Brooks	**875–885**	Using reproductive values to define optimal harvesting for multisite density-dependent populations: example with a marine reserve
Suzanne M. Budge, Sara J. Iverson, W. Don Bowen, and Robert G. Ackman	**886–898**	Among- and within-species variability in fatty acid signatures of marine fish and invertebrates on the Scotian Shelf, Georges Bank, and southern Gulf of St. Lawrence
Louise Gendron and Jean-Claude Brêthes	**899–909**	Simulations of the impact of different temporal and spatial allocations of fishing effort on fishing mortality in a lobster (*Homarus americanus*) fishery
PERSPECTIVE		PERSPECTIVE
Christian Mullon, Philippe Cury, and Pierrick Penven	**910–922**	Evolutionary individual-based model for the recruitment of anchovy (*Engraulis capensis*) in the southern Benguela
ERRATUM		ERRATUM
Peter K. Weber, Ian D. Hutcheon, Kevin D. McKeegan, and B. Lynn Ingram	**923**	Erratum: Otolith sulfur isotope method to reconstruct salmon (*Oncorhynchus tshawytscha*) life history

National Research Council Canada
Ottawa, Canada K1A 0R6

Conseil national de recherches Canada
Ottawa, Canada K1A 0R6

Postage paid at Ottawa
Publications mail
Registration No. 1240579

Port payé à Ottawa
Poste-publication
Enregistrement n° 1240579

USPS periodical postage paid at Champlain, N.Y.

Canadian Journal of Fisheries and Aquatic Sciences

Volume 59, Number 5, May 2002

Journal canadien des sciences halieutiques et aquatiques

Volume 59, numéro 5, mai 2002

RAPID COMMUNICATION		COMMUNICATION RAPIDE
Rögnvaldur Hannesson	**755–758**	The economics of fishing down the food chain
ARTICLES		ARTICLES
Susan C.H. Grant and William M. Tonn	**759–767**	Effects of nutrient enrichment on recruitment of age-0 fathead minnows (*Pimephales promelas*): potential impacts of environmental change on the Boreal Plains
H.A. Campbell, R.D. Handy, and D.W. Sims	**768–777**	Increased metabolic cost of swimming and consequent alterations to circadian activity in rainbow trout (*Oncorhynchus mykiss*) exposed to dietary copper
C.D. Allen and R.E.H. Smith	**778–786**	The response of planktonic phosphate uptake and turnover to ultraviolet radiation in Lake Erie
Thomas P. Hurst and David O. Conover	**787–795**	Effects of temperature and salinity on survival of young-of-the-year Hudson River striped bass (*Morone saxatilis*): implications for optimal overwintering habitats
Michael G. Wing and Arne Skaugset	**796–807**	Relationships of channel characteristics, land ownership, and land use patterns to large woody debris in western Oregon streams
Anssi V. Vähätalo, Kalevi Salonen, Eija Saski, and Mirja S. Salkinoja-Salonen	**808–818**	Bleaching of color of kraft pulp mill effluents and natural organic matter in lakes
Adrian M.H. deBruyn, David J. Marcogliese, and Joseph B. Rasmussen	**819–828**	Altered body size distributions in a large river fish community enriched by sewage
Clara Ulrich, Sean Pascoe, Per J. Sparre, Jan-Willem De Wilde, and Paul Marchal	**829–843**	Influence of trends in fishing power on bioeconomics in the North Sea flatfish fishery regulated by catches or by effort quotas
Claus R. Sparrevohn, Anders Nielsen, and Josianne G. Støttrup	**844–853**	Diffusion of fish from a single release point
Daniel G. Kehler, Ransom A. Myers, and Christopher A. Field	**854–864**	Measurement error and bias in the maximum reproductive rate for the Ricker model
Walter K. Dodds, Val H. Smith, and Kirk Lohman	**865–874**	Nitrogen and phosphorus relationships to benthic algal biomass in temperate streams

Continued on inside back cover / Suite au verso

Canada

Printed in Canada by / Imprimé au Canada par
University of Toronto Press Inc.
Typesetting by / Typographie par
NRC Research Press / Presses scientifiques du CNRC

0706-652X(200205)59:5;1-8